NEW INSIGHTS INTO EXTRACELLULAR VESICLES IN CARDIOVASCULAR DISEASE: MOLECULAR BASIS, DIAGNOSIS AND THERAPY

EDITED BY: Xiaoheng Liu, Youhua Tan, Bingmei M. Fu and Yang Shen

PUBLISHED IN: Frontiers in Cell and Developmental Biology

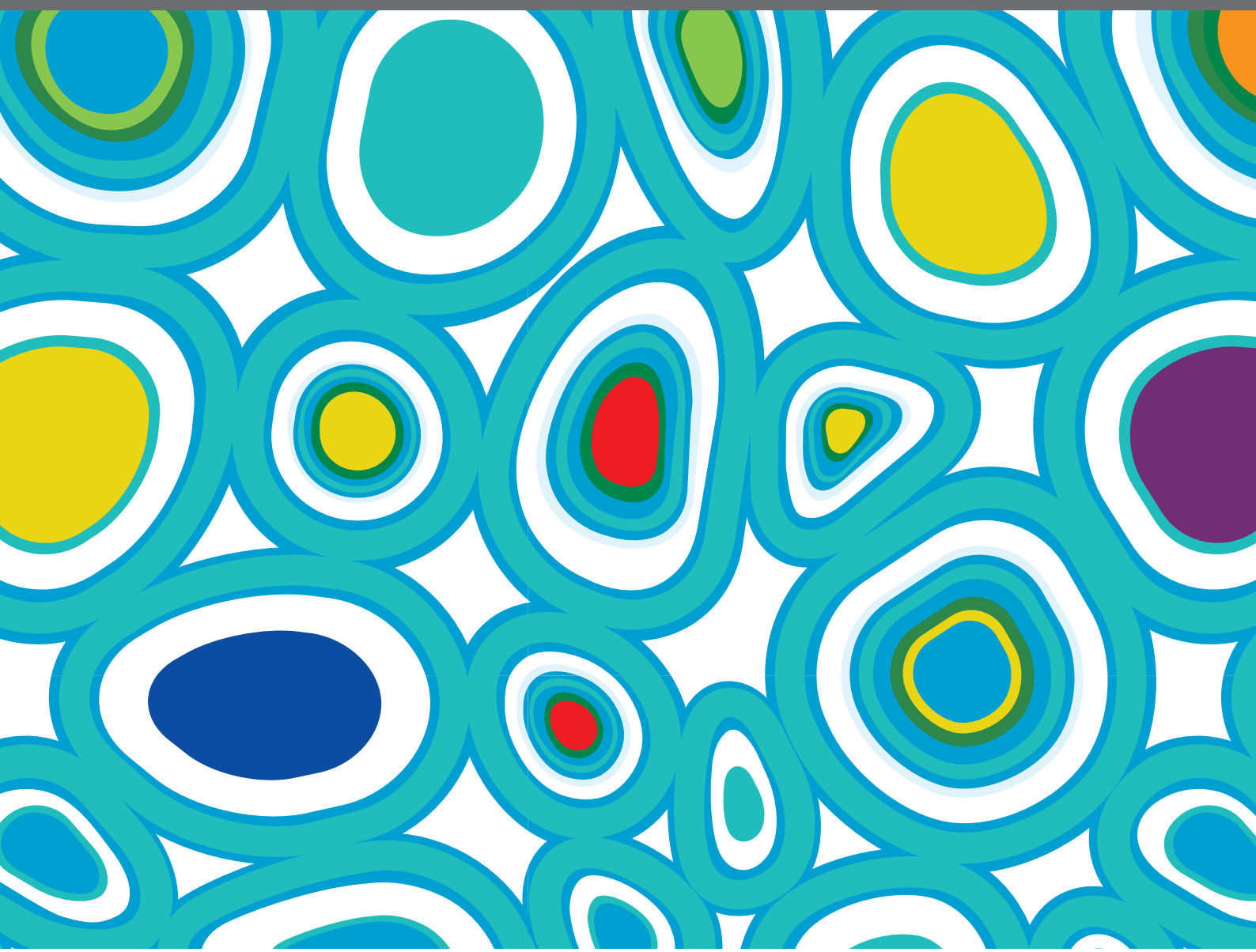

frontiers Research Topics

frontiers

ISSN 1664-8714
ISBN 978-2-83250-162-7
DOI 10.3389/978-2-83250-162-7

About Frontiers

Frontiers is more than just an open-access publisher of scholarly articles: it is a pioneering approach to the world of academia, radically improving the way scholarly research is managed. The grand vision of Frontiers is a world where all people have an equal opportunity to seek, share and generate knowledge. Frontiers provides immediate and permanent online open access to all its publications, but this alone is not enough to realize our grand goals.

Frontiers Journal Series

The Frontiers Journal Series is a multi-tier and interdisciplinary set of open-access, online journals, promising a paradigm shift from the current review, selection and dissemination processes in academic publishing. All Frontiers journals are driven by researchers for researchers; therefore, they constitute a service to the scholarly community. At the same time, the Frontiers Journal Series operates on a revolutionary invention, the tiered publishing system, initially addressing specific communities of scholars, and gradually climbing up to broader public understanding, thus serving the interests of the lay society, too.

Dedication to Quality

Each Frontiers article is a landmark of the highest quality, thanks to genuinely collaborative interactions between authors and review editors, who include some of the world's best academicians. Research must be certified by peers before entering a stream of knowledge that may eventually reach the public - and shape society; therefore, Frontiers only applies the most rigorous and unbiased reviews.
Frontiers revolutionizes research publishing by freely delivering the most outstanding research, evaluated with no bias from both the academic and social point of view. By applying the most advanced information technologies, Frontiers is catapulting scholarly publishing into a new generation.

What are Frontiers Research Topics?

Frontiers Research Topics are very popular trademarks of the Frontiers Journals Series: they are collections of at least ten articles, all centered on a particular subject. With their unique mix of varied contributions from Original Research to Review Articles, Frontiers Research Topics unify the most influential researchers, the latest key findings and historical advances in a hot research area! Find out more on how to host your own Frontiers Research Topic or contribute to one as an author by contacting the Frontiers Editorial Office: frontiersin.org/about/contact

NEW INSIGHTS INTO EXTRACELLULAR VESICLES IN CARDIOVASCULAR DISEASE: MOLECULAR BASIS, DIAGNOSIS AND THERAPY

Topic Editors:
Xiaoheng Liu, Sichuan University, China
Youhua Tan, Hong Kong Polytechnic University, Hong Kong, SAR China
Bingmei M. Fu, City College of New York (CUNY), United States
Yang Shen, Sichuan University, China

Citation: Liu, X., Tan, Y., Fu, B. M., Shen, Y., eds. (2022). New Insights Into Extracellular Vesicles in Cardiovascular Disease: Molecular Basis, Diagnosis and Therapy. Lausanne: Frontiers Media SA. doi: 10.3389/978-2-83250-162-7

Table of Contents

frontiers | Frontiers in Cell and Developmental Biology

TYPE Editorial
PUBLISHED 25 August 2022
DOI 10.3389/fcell.2022.989150

OPEN ACCESS

EDITED AND REVIEWED BY
Ramani Ramchandran,
Medical College of Wisconsin,
United States

*CORRESPONDENCE
Xiaoheng Liu,
liuxiaohg@scu.edu.cn

SPECIALTY SECTION
This article was submitted to Molecular and Cellular Pathology, a section of the journal Frontiers in Cell and Developmental Biology

RECEIVED 08 July 2022
ACCEPTED 27 July 2022
PUBLISHED 25 August 2022

CITATION
Shen Y and Liu X (2022), Editorial: New insights into extracellular vesicles in cardiovascular disease: Molecular basis, diagnosis and therapy.
Front. Cell Dev. Biol. 10:989150.
doi: 10.3389/fcell.2022.989150

Editorial: New insights into extracellular vesicles in cardiovascular disease: Molecular basis, diagnosis and therapy

Yang Shen and Xiaoheng Liu*

Institute of Biomedical Engineering, West China School of Basic Medical Sciences & Forensic Medicine, Sichuan University, Chengdu, China

KEYWORDS

extracellular vesicles, matrix vesicles, cardiovascular disease, cell and molecular biology, bioengineering

Editorial on the Research Topic
New insights into extracellular vesicles in cardiovascular disease: Molecular basis, diagnosis and therapy

Extracellular vesicles (EVs) are a heterogeneous group of membranous structures released by cells under physiological and pathological conditions (Guillaume et al., 2018). According to the density, size and subcellular origin, EVs are generally divided into three categories: apoptotic body (100–5000 nm), microvesicles (100–1000 nm), and exosomes (50–150 nm) (Mathieu et al., 2019). Noteworthy, Matrix vesicles (MVs, 100–300 nm) are now considered a specific type of EVs secreted by mineral-forming cells (Kirsi et al., 2019). So far, EVs attract widespread attention due to their diverse roles in intercellular and intracellular communication (Graça and Stahl, 2019; Guillaume et al., 2022). EVs are associated with immune responses, viral pathogenicity, cardiovascular diseases and cancer progression (Cheng and Hill, 2022). In cardiovascular research, EVs present a promising therapeutic strategy for the treatment of cardiovascular diseases or blockage of disease progression (Susmita et al., 2021). The Research Topic "*New insights into extracellular vesicles in cardiovascular disease: Molecular basis, diagnosis and therapy*" of Frontiers in Cell and Developmental Biology aims to pick exciting and noteworthy works related to the mechanistic investigation of EVs and their translational applications in cardiovascular disease. Collectively, this Research Topic comprises three original research articles and six review articles for a total of nine original contributions, articulating the roles of EVs in atherosclerosis, vascular calcification, and other cardiovascular diseases. These articles not only highlight the molecular basis, diagnosis and therapeutic potential of EVs, but reveal a field of research moving forward at an incredible pace.

This Research Topic includes three original research articles demonstrated the role and mechanism of EVs in cardiovascular disease. Liu et al. investigated the contribution of

platelet-derived microvesicles (PMVs) in phenotypic switch of vascular smooth muscle cells (VSMCs) during vascular remodeling. This work revealed that PMVs secreted by activated platelets promoted VSMC dedifferentiation *via* Src/Lamtor1/mTORC1 signaling pathway, suggesting that Lamtor1 may be a potential therapeutic target for intimal hyperplasia after injury. The study by Yaker et al. showed that EVs derived from lipopolysaccharide-treated macrophages can aggravate vascular calcification through activation of pro-inflammatory and pro-oxidative responses in VSMCs. Comarița et al. found the therapeutic potentiality of stem cell-derived EVs secreted from subcutaneous adipose tissue stem cells (ADSCs) and bone marrow mesenchymal stem cells (MSCs) on atherosclerosis-induced vascular dysfunction. Stem cell-derived EVs were identified contributing to the regression of atherosclerosis-induced endothelial dysfunction by improving the structure and function of the vascular wall. In combination with Smad2/3siRNA, the ability of ADSCs or MSCs-derived EVs was significantly amplified to regress the inflammation-mediated atherosclerotic process.

Additionally, six comprehensive review articles discussed the multifaceted functions of EVs in cardiovascular health. EVs act as extracellular biological information carriers that transfer a variety of functional transcripts and lipids to target cells to mediate cell-cell communication. Moreover, the inherent properties of EVs have great potentials to be used as biomarkers for diagnosis and prognosis of cardiovascular disease, and to play a therapeutic role as a drug or drug carrier.

Martin-Ventura et al. reviewed the role of EVs as potential diagnostic and prognostic biomarkers in chronic cardiovascular diseases, including atherosclerosis, aortic stenosis and aortic aneurysms. And they further summarized the pathological mechanisms of EVs-mediated vascular and valvular calcification, involving calcium accumulation and osteogenic phenotypic transition of VSMCs or valvular interstitial cells. Similarly, MVs are especially critical in extracellular matrix mineralization and the development of vascular calcification (Kapustin et al., 2011). Li et al. discussed the detailed roles of MVs in the regulation of vascular calcification, the possible mechanism of which involves mineral deposits, osteogenic transdifferentiation of VSMCs, and microRNAs transport.

Exosomes are small EVs (30–150 nm) coated with bi-lipid membranes and contain numerous bioactive molecules (Kalluri and LeBleu, 2020). Germena et al. summarized the current knowledge on the role of exosomes as mediators of cardiovascular diseases in atherosclerosis and diabetes. Moreover, they described evidence of intercellular connection among multiple cell types (cardiac, vasculature, immune cells) as well as the challenge of their *in vivo* analysis. Burtenshaw et al. generalized exosomal composition, biogenesis and profiling, and discussed how key exosomal signatures in liquid biopsies may act as early pathological indicators of adaptive lesion formation and arteriosclerotic disease progression.

The review by Wen et al. discussed the great potential of EV-derived circular RNAs (EV-circRNAs) as diagnostic biomarkers of atherosclerosis. And they depicted the mechanism of EV-circRNAs in regulating atherosclerosis formation and development, including EC dysfunction, phenotypic switching of VSMCs, inflammatory response, lipid deposition, and formation of foam cells. Thus, EV-circRNAs are expected to be used as novel therapeutic strategies for atherosclerosis.

Recent studies have highlighted that excess activation of NLRP3 inflammasome led to inflammation and the progression of atherosclerosis (Sharma and Kanneganti, 2021). Lu et al. reviewed the recently described mechanisms of the NLRP3 inflammasome activation, and discuss emphatically the pharmacological interventions using statins and natural medication for atherosclerosis associated with NLRP3 inflammasome. Thus, continuously developing the specific NLRP3 inhibitors may be promising therapeutic remedies to solve atherogenesis.

In summary, this Research Topic covers the broadest possible aspects of EVs and highlights the vital role of EVs in cardiovascular diseases. Based on the research findings and currently known key points, we hope to make a further understanding and better characterization of this promising but not yet well-understood field.

The success of this Research Topic is the joint efforts of everyone. We would like to thank all the authors for their contribution to the Research Topic. At the same time, we would like to appreciate the efforts of all the reviewers and editors.

Author contributions

YS and XL wrote and edited this Editorial.

Funding

YS was supported by National Natural Science Foundation of China (31870939 and 32071312), XL was supported by National Natural Science Foundation of China (11932014 and 31971239).

Acknowledgments

We would like to thank to all the authors and reviewers that contributed to this Research Topic of Frontiers in Cell and Developmental Biology.

Conflict of interest

The authors declare that the research was conducted in the absence of any commercial or financial relationships that could be construed as a potential conflict of interest.

Publisher's note

References

Cheng, Lesley, and Hill, Andrew F. (2022). Therapeutically harnessing extracellular vesicles. *Nat. Rev. Drug Discov.* 21 (5), 379–399. doi:10.1038/s41573-022-00410-w

Graça, Raposo, and Stahl, Philip D. (2019). Extracellular vesicles: a new communication paradigm? *Nat. Rev. Mol. Cell Biol.* 20 (9), 509–510. doi:10.1038/s41580-019-0158-7

Guillaume, van Niel, Carter, David R. F., Clayton, Aled, Lambert, Daniel W., Raposo, Graça, and Vader, Pieter (2022). Challenges and directions in studying cell-cell communication by extracellular vesicles. *Nat. Rev. Mol. Cell Biol.* 23 (5), 369–382. doi:10.3389/fcell.2022.892303

Guillaume, van Niel, D'Angelo, Gisela, and Raposo, Graça (2018). Shedding light on the cell biology of extracellular vesicles. *Nat. Rev. Mol. Cell Biol.* 19 (4), 213–228. doi:10.1038/nrm.2017.125

Kalluri, Raghu, and LeBleu, Valerie S. (2020). The biology, function, and biomedical applications of exosomes. *Science* 367 (6478), eaau6977. doi:10.1126/science.aau6977

Kapustin, Alexander N., Davies, John D., Reynolds, Joanne L., McNair, Rosamund, Jones, Gregory T., Sidibe, Anissa, et al. (2011). Calcium regulates key components of vascular smooth muscle cell-derived matrix vesicles to enhance mineralization. *Circ. Res.* 109 (1), e1–12. doi:10.1161/CIRCRESAHA.110.238808

Kirsi, Rilla, Anne-Mari, Mustonen, Uma, Thanigai Arasu, Härkönen, Kai, Matilainen, Johanna, and Nieminen, Petteri (2019). Extracellular vesicles are integral and functional components of the extracellular matrix. *Matrix Biol.* 75-76, 201–219. doi:10.1016/j.matbio.2017.10.003

Mathieu, Mathilde, Martin-Jaular, Lorena, Lavieu, Grégory, and Théry, Clotilde (2019). Specificities of secretion and uptake of exosomes and other extracellular vesicles for cell-to-cell communication. *Nat. Cell Biol.* 21 (1), 9–17. doi:10.1038/s41556-018-0250-9

Sharma, Bhesh Raj, and Kanneganti, Thirumala-Devi (2021). NLRP3 inflammasome in cancer and metabolic diseases. *Nat. Immunol.* 22 (5), 550–559. doi:10.1038/s41590-021-00886-5

Susmita, Sahoo, Marta, Adamiak, Prabhu, Mathiyalagan, Franziska, Kenneweg, Sabine, Kafert-Kasting, and Thomas, Thum (2021). Therapeutic and diagnostic translation of extracellular vesicles in cardiovascular diseases: Roadmap to the clinic. *Circulation* 143 (14), 1426–1449. doi:10.1161/CIRCULATIONAHA.120.049254

frontiers in Cell and Developmental Biology

ORIGINAL RESEARCH
published: 16 September 2021
doi: 10.3389/fcell.2021.744320

Platelet-Derived Microvesicles Promote VSMC Dedifferentiation After Intimal Injury via Src/Lamtor1/mTORC1 Signaling

Ji-Ting Liu[1], Han Bao[1], Yang-Jing Fan[1], Zi-Tong Li[1], Qing-Ping Yao[1], Yue Han[1], Ming-Liang Zhang[2], Zong-Lai Jiang[1]* and Ying-Xin Qi[1]**

[1] Institute of Mechanobiology and Medical Engineering, School of Life Sciences and Biotechnology, Shanghai Jiao Tong University, Shanghai, China, [2] Department of Endocrinology and Metabolism, Shanghai Jiao Tong University Affiliated Sixth People's Hospital, Shanghai Diabetes Institute, Shanghai Clinical Center for Diabetes, Shanghai Key Laboratory of Diabetes Mellitus, Shanghai Key Clinical Center for Metabolic Disease, Shanghai, China

OPEN ACCESS

Edited by:
Yang Shen,
Sichuan University, China

Reviewed by:
Juhui Qiu,
Chongqing University, China
Shun Li,
University of Electronic Science and Technology of China, China

***Correspondence:**
Ming-Liang Zhang
zml820119@126.com
Zong-Lai Jiang
zljiang@sjtu.edu.cn
Ying-Xin Qi
qiyx@sjtu.edu.cn

Specialty section:
This article was submitted to Molecular and Cellular Pathology, a section of the journal Frontiers in Cell and Developmental Biology

Received: 20 July 2021
Accepted: 26 August 2021
Published: 16 September 2021

Citation:
Liu J-T, Bao H, Fan Y-J, Li Z-T, Yao Q-P, Han Y, Zhang M-L, Jiang Z-L and Qi Y-X (2021) Platelet-Derived Microvesicles Promote VSMC Dedifferentiation After Intimal Injury via Src/Lamtor1/mTORC1 Signaling. Front. Cell Dev. Biol. 9:744320. doi: 10.3389/fcell.2021.744320

Phenotypic switch of vascular smooth muscle cells (VSMCs) is important in vascular remodeling which causes hyperplasia and restenosis after intimal injury. Platelets are activated at injured intima and secrete platelet-derived microvesicles (PMVs). Herein, we demonstrated the role of PMVs in VSMC phenotypic switch and the potential underlying mechanisms. *In vivo*, platelets were locally adhered and activated at intimal injury site, while Lamtor1 was promoted and VSMCs were dedifferentiated. PMVs, collected from collagen-activated platelets *in vitro* which mimicked collagen exposure during intimal injury, promoted VSMC dedifferentiation, induced Lamtor1 expression, and activated mTORC1 signaling, reflected by the phosphorylation of two downstream targets, i.e., S6K and 4E-BP1. Knockdown of Lamtor1 with small interfering RNA attenuated these processes induced by PMVs. Based on the previously published proteomic data, Ingenuity Pathway Analysis revealed that Src may participate in regulating effects of PMVs. Src inhibitor significantly reversed the effects of PMVs on VSMC dedifferentiation, Lamtor1 expression and mTORC1 activation. Furthermore, in SMC-specific *Lamtor1* knockout mice, intimal hyperplasia was markedly attenuated after intimal injury compared with the wild type. Our data suggested that PMVs secreted by activated platelets promoted VSMC dedifferentiation *via* Src/Lamtor1/mTORC1 signaling pathway. Lamtor1 may be a potential therapeutic target for intimal hyperplasia after injury.

Keywords: intimal hyperplasia, platelet-derived microvesicles, vascular smooth muscle cells, dedifferentiation, Lamtor1

INTRODUCTION

Vascular endothelium, which plays crucial roles in maintaining vascular homeostasis and modulating vasomotor tone, is a monolayer of cells that lines the inner luminal surface of vascular tubes and provides a barrier between blood and tissues. Endothelial injury occurs in a number of vascular pathologies, including atherosclerosis, coronary artery bypass grafting surgery,

percutaneous coronary intervention, angioplasty or stenting (Wu et al., 2017). The denudation of endothelial cell during injury exposes the underlying collagen, leading to a rapid deposition and activation of platelets, and promotes pathological proliferation and migration of vascular smooth muscle cells (VSMCs) to form neointimal hyperplasia, which ultimately leads to restenosis (Wu et al., 2017). The phenotypic switching of VSMCs is a fundamental step for proliferation and migration. VSMCs are physiologically in contractile phenotype and can dedifferentiate to synthetic state under various pathological conditions, which are characterized as repressed expression of contractile proteins including α-smooth muscle actin (SMA), SM-22α, calponin and SM myosin heavy chains (Sinha et al., 2014).

Numerous groups have reported that shortly after neointimal injury, platelets, activated by subendothelial collagen and characterized with expressed CD62P (also known as P-Selectin), release not only platelet-derived growth factor but also platelet-derived microvesicles (PMVs). Microvesicles (MVs), a kind of extracellular vesicles (EVs), are typically around 100–1000 nm in size (Akers et al., 2013). PMVs, the most abundant MVs in the circulation, are important regulators during hemostasis (Webber and Johnson, 1970), inflammation (Boilard et al., 2010), and angiogenesis (Lukasik et al., 2013).

Elevated levels of PMVs are observed in various cardiovascular diseases (Suades et al., 2015). Previous studies have demonstrated that the increased numbers of PMV is correlated with the thickness of carotid artery intima and the lipid-rich atherosclerotic plaques (Csongrádi et al., 2011). PMVs can facilitate leukocyte accumulation at the site of endothelial injury and enhance leukocyte infiltration to the intima *via* P-Selectin expressed on PMVs (Forlow et al., 2000). Interestingly, PMVs have been proved to trigger VSMC proliferation and migration from the media to the intima thereby enhancing intimal hyperplasia (Weber et al., 2000). However, the molecular mechanisms underlying this process remains largely unclear.

The late endosomal/lysosomal adaptor MAPK and mTOR activator 1 (Lamtor1), also named as p18, is a highly conserved lysosome-anchored protein for activation of mTOR complex 1 (mTORC1) (Bar-Peled et al., 2012). Lamtor1 plays a pivotal role in cell growth, membrane protein transport, and lysosome biogenesis. Previous studies showed that Lamtor1 deficiency results in enhancing of autophagy flux and apoptosis (Nowosad et al., 2020), and disrupting the osteoblast differentiation *via* reduction of YAP nuclear localization (Block et al., 2020). Moreover, ablation of Lamtor1 is fatal in the embryo (Filipek et al., 2017). Although numerous studies revealed the importance of Lamtor1 in cell homeostasis and dysfunctions, the role of Lamtor1 in intimal hyperplasia caused by injury, and whether Lamtor1 is regulated by PMVs are still unknown.

In our present study, using intimal injury model and smooth muscle cell-specific (SMC-specific) *Lamtor1* knockout (KO) mice, the effects of Lamtor1 in VSMC differentiation and intimal injury were investigated, and then the potential roles of PMVs in this process were further detected.

MATERIALS AND METHODS

SMC-Specific *Lamtor1*-KO Mice

To generation of SMC-specific *Lamtor1* KO mice with a C57BL/6J background, *Lamtor1*$^{fl/fl}$ mice were crossed with α-*SM22α-Cre*$^{+}$ mice which purchased from the Shanghai Model Organisms Center. The generated *Lamtor1*$^{fl/fl}$*SM22αCre*$^{+}$ mice were genotyped by PCR, and littermate mice were used as controls. The SMC-specific *Lamtor1* KO mice and C57BL/6J background littermate controls were maintained on a light/dark (12/12 h) cycle at 25°C, and received food and water *ad libitum*.

The animal care and experimental protocols were conducted in accordance with the Animal Management Rules of China (Documentation 55, 2001, Ministry of Health, China), and the animal study was approved by the Animal Research Committee of Shanghai Jiao Tong University.

Wire Injury Mouse Model

The carotid wire injury mouse model was constructed to mimic post-angioplasty restenosis in human (Berk et al., 1989). The left common carotid artery of each mouse was used as the experimental group, and the right one was the autologous control. In briefly, 10- to 12-week male C57BL/6J, SMC-specific *Lamtor1* KO mice or littermate control mice were anesthetized by 2% isoflurane at 1 L/min oxygen flow using an isoflurane vaporizer (Matrx VIP 3000). The left carotid artery was separated and the bifurcation area was exposed. The occipital artery, the internal carotid artery, and the external carotid artery were sequentially ligated using a surgical suture. Then a 0.3-mm diameter guide-wire (Advanced Cardiovascular Systems) was used to establish vascular intimal injury at the common carotid artery *via* the transverse arteriotomy of the external carotid artery.

Van Gieson and Immunofluorescence Staining

Tissues were fixed in 4% paraformaldehyde, dehydrated in 30% sucrose and crossed into 6 μm sections (LEICA, RM2265). For Elastin Van-Gieson staining, sections were stained with Weigert Solution for 5 min, directly immerged into Differentiation Solution (1% hydrochloric acid alcohol), and then flushed with water. Van-Gieson Dye Solution was used to re-stain the sections for 5–6 min. A microscope (Olympus IX71) was used to observe images.

For immunofluorescent staining, sections or cells were fixed with 4% paraformaldehyde for 15 min, permeabilizated with 0.2% Triton X-100 for 3 min, and incubated with blocking buffer containing 10% goat serum for 1 h at room temperature. Antibody against CD62P (Biolegend, 1:100), Lamtor1 (CST, 1:200), phosphor-p70S6K (Thr389) (CST, 1:200), or p-Src (CST, 1:200) was diluted in blocking buffer and incubated overnight at 4°C. Sections or coverslips were washed with TBS three times and incubated with secondary antibody (Alexa Fluor 568-conjugated goat anti-rabbit IgG, 1:1000, Invitrogen) and α-SMA-FITC antibody (Sigma, 1:500) for 2 h at room temperature. Nuclei were stained with 4, 6-diamidino-2-phenylindole (DAPI)

for 10 min. The images were obtained using a confocal laser scanning microscope (Fluoview 1000, Olympus).

Carotid VSMCs Culture and Treatment

VSMCs were cultured from the carotid artery of male Sprague-Dawley (SD) rats (150–180 g) via an explant method (Berk et al., 1989). Briefly, the carotid artery was cut into small pieces and cultured in Dulbeco's Modified Eagle medium (DMEM, Gibco) with 10% fetal bovine serum (FBS, Gibco), in a humidified incubator at 37°C, 5% CO_2. Upon enrichment in 80–90% confluence, cells were trypsinized and seeded at required density for further assays.

For PMV treatment, cells were serum-starved for 24 h and then treated with PMVs (10^9/mL) for 1 or 24 h at 37°C, 5% CO_2. For Src inhibitor experiment, VSMCs were pre-incubated with Src inhibitor (Sigma, 10 μM) for 1 h and then treated with PMVs (10^9/mL) for 24 h.

Platelet Activation and PMVs Purification

Whole blood from abdominal aorta of anesthetized SD rats was collected into syringes containing 100 μL/mL anticoagulant (2.94% sodium citrate, 0.1 g/mL PGE1 and 1 U apyrase). Platelet-rich plasma was then obtained by centrifugation at 600 *g* for 15 min, and platelets were sedimented at 2000 *g* for 15 min. Platelet activation was induced with 1 U/ml collagen (Sigma-Aldrich) for 60 min at 37°C with gentle agitation. PMVs were then collected from the remaining supernatant with centrifugation at 20500 *g* for 90 min at 4°C as shown in the schematic diagrams (**Supplementary Figure I**; Bao et al., 2018). The obtained PMVs were quantified with NanoSight module (NanoSight NS300, United Kingdom) and 10^9/mL PMVs were used for stimulation. The platelets treated with blank medium were used as the control group.

Fluorescent Labeling of PMVs

PKH26 (MINI26, Sigma) was used to track PMVs according to the manufacturer's protocol. Briefly, PKH26 prepared in Dilute C at a final concentration of 1×10^{-6} mol/L was used to incubate PMVs (final concentration was 1×10^7 PMVs/mL) for 5 min at room temperature. The labeled PMVs (10^9/mL) were incubated with VSMCs for 24 h. Then the samples were fixed with 4% paraformaldehyde for 15 min and counterstained with α-SMA-FITC antibody (Sigma, 1:500) for 2 h. Nuclei were stained with DAPI for 10 min. The images were obtained using a confocal laser scanning microscope (Fluoview 1000, Olympus).

siRNA Transfection

For the RNA interference experiment, VSMCs were transfected with Lamtor1 siRNA or negative control siRNA (GenePharma, Shanghai, China) for 48 h with Lipofectamine 2000 in Opti-MEM (Thermo Fisher Scientific, Waltham, MA, United States) according to the manufacturer's instructions. The sequences of siRNA oligos targeting Lamtor1 were: GCCG AGCC CAGC UACC AUAT T (5′–3′), UAUG GUAG CUGG GCUC GGCT T (5′–3′). The sequences of the negative control were: UUCU CCGA ACGU GUCA CGUT T (5′–3′), ACGU GACA CGUU CGGA GAAT T (5′–3′).

Western Blot Analysis

Samples were lysed at 4°C for 10 min with RIPA lysis buffer containing 1 mM PMSF, and were centrifuged at 12000 *g* for 5 min. Then, the protein concentration in the supernatant was quantified with BCA kit (23227, Thermo Fisher). After being isolated by PAGE, the protein was transferred onto the polyvinylidene fluoride (PVDF) membrane and blocked with 5% no-fat milk at room temperature for 1 h. The membrane was subsequently incubated with diluted primary antibodies, respectively: phosphor-Src (Tyr416, 1:1000, CST), total Src (1:1000, CST), Lamtor1 (1:1000, CST), phosphor-p70S6K (Thr389, 1:1000, CST), phosphor-4E-BP1 (Thr37/46, 1:1000, CST), phosphor-mTORC1 (Ser2448, 1:1000, CST), total mTORC1 (1:1000, CST), α-SMA (1:1000, Proteintech), SM22 (1:1000, Proteintech), calponin (1:1000, Sigma), and GAPDH (1:5000, Proteintech). Protein bands were visualized by ECL kit (Beyotime) and the intensity was quantified by Quantity One (Bio-Rad).

Ingenuity Pathway Analysis (IPA)

The Gene Ontology (GO) enrichment and Canonical Pathways of the published PMVs proteomic data (Dean et al., 2009) was analyzed by IPA software (Qiagen, content version: 39480507, https://www.qiagenbioinformatics.com/products/ingenuity-pathway-analysis). In addition, the possible molecules and transduction networks connected with Lamtor1 were obtained. IPA integrates the available knowledge on genes, drugs, chemicals, protein families, processes, and pathways, based on the interactions and functions derived from the Ingenuity Pathways Knowledge Database Literature (Dai et al., 2009).

Statistics

All experiments were performed with at least three biological replicates, and the data were presented as the mean ± standard deviation (SD). Statistical analysis was performed using GraphPad Prism (version 8.1, GraphPad, San Diego, CA). Student's *t* test was used for comparisons between two groups. $P < 0.05$ was regarded as statistically significant.

RESULTS

PMVs Induce Lamtor1 Expression and Promote VSMC Dedifferentiation Both *in vivo* and *in vitro*

The carotid wire injury mouse model which mimics post-angioplasty restenosis in human was constructed to investigate the expression and function of Lamtor1 in the intimal hyperplasia. Elastin Van-Gieson staining showed that compared with the autologous artery control, the neointimal hyperplasia after 1-week injury was significantly thickened (**Figure 1A**), and the area of neointimal hyperplasia in the grafted vein was markedly increased (**Supplementary Figure IIA**). Immunofluorescence demonstrated that the expression of Lamtor1 was increased in the neointima (**Figure 1B** and **Supplementary Figure IIB**), and the co-expressed

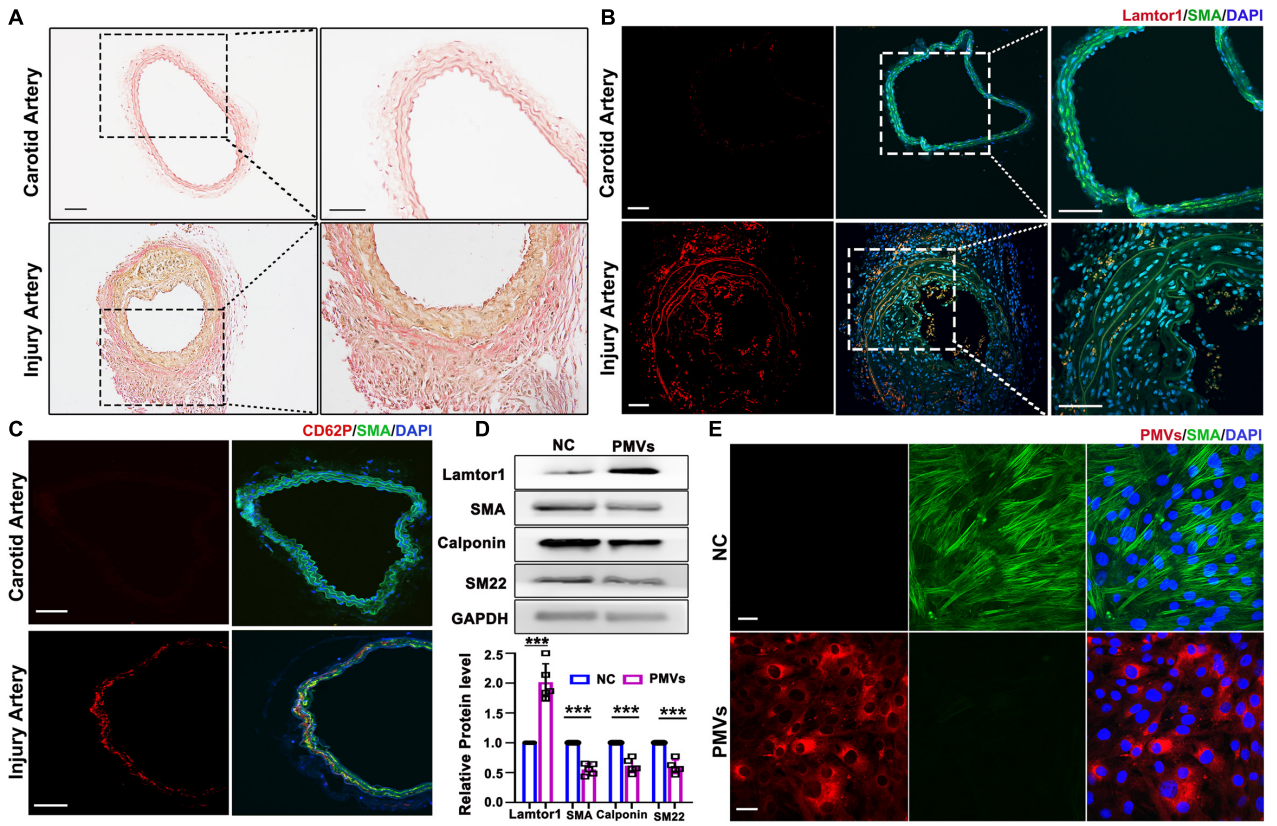

FIGURE 1 | PMVs induced Lamtor1 expression and promoted VSMC dedifferentiation both *in vivo* and *in vitro*. **(A)** Representative images of Elastin Van-Gieson staining showed that the intimal hyperplasia was significantly thickened after 1-week wire injury in mouse model. Scale bars: 100 μm. **(B)** Representative images of immunostaining showed that Lamtor1 (red) was expressed in the injured intima after 1-week surgery. Green fluorescence was SMA, nuclei were counterstained with DAPI (blue). Scale bars: 100 μm. **(C)** Immunofluorescence staining showed the activated platelet signal labeled with CD62P (red) at the injury site 3 h after intimal injury surgery. Green fluorescence was SMA, nuclei were counterstained with DAPI (blue). Scale bars: 100 μm. **(D)** Western blot revealed that Lamtor1 expression was significantly increased and differentiated markers of VSMCs, including SMA, Calponin, and SM22 were decreased after incubating with PMVs for 24 h ($n = 5$). Data represent mean ± *SD*. $P < 0.001$. **(E)** Immunofluorescence staining indicated that PMVs (red) markedly decreased the expression of SMA (green) a differentiation marker. Nuclei were counterstained with DAPI (blue). Scale bars: 50 μm.

SMA, a contractile marker, was decreased (**Figure 1B** and **Supplementary Figure IIC**).

To explore the potential role of PMVs in VSMCs, the local adhesion of platelets at injured intima was then detected. Three hours after intimal injury, immunofluorescence staining showed that CD62P, the marker of activated platelet, was accumulated at the inner wall of injured blood vessels and contacted with the internal elastic membrane (**Figure 1C** and **Supplementary Figure IID**), which suggested the local activation of platelet after intimal injury. Furthermore, collagen I was used to activate platelets *in vitro* which simulated collagen exposure after vascular intimal injury *in vivo*, and the roles of PMVs in VSMC dedifferentiation and Lamtor1 expression were demonstrated.

Western blot revealed that protein expression of Lamtor1 was dramatically increased and the expressions of differentiation markers, i.e., SMA, calponin and SM22 were all significantly repressed in VSMCs treated with PMVs for 24 h compared with the negative control (**Figure 1D**).

To confirm the effect of PMVs on VSMC dedifferentiation, PMVs were labeled with PKH26, and treated VSMCs for 24 h. The immunofluorescence staining showed that PKH26 labeled PMVs adhered to VMSCs and markedly decreased the expression of SMA (**Figure 1E**).

These results suggested that neointima was obviously formed after carotid intimal injury, where Lamtor1 was increased and VSMCs were dedifferentiated, which may be caused by the PMVs released from the activated platelets.

PMVs Promote VSMC Dedifferentiation via Lamtor1/mTORC1 Signaling

Lamtor1 has been reported to play a vital role in activating mTORC1 which controls cell growth and differentiation (Nowosad et al., 2020). Hence the responses of mTORC1 activation to Lamtor1 induced by PMVs were then investigated.

Western blot results showed that the phosphorylations of mTORC1 and the main substrates of mTORC1, i.e., S6 kinase-1 (S6K1) which stimulates the initiation of translation (Magnuson et al., 2012), and eukaryotic translation initiation factor 4E (eIF4E)-binding protein-1 (4E-BP1) which promotes the release

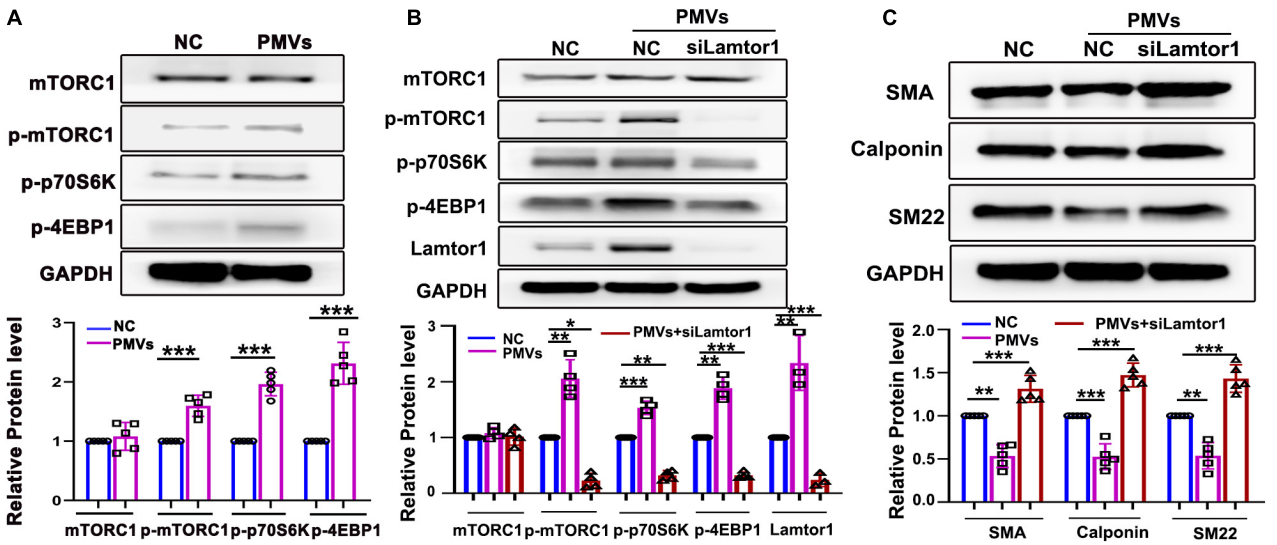

FIGURE 2 | Specific knockdown of Lamtor1 reversed the effects of PMVs on mTORC1 activation and VSMC dedifferentiation. **(A)** Western blot showed that the phosphorylations of mTORC1, 4EBP1 and p70S6K in VSMCs were increased by PMVs, while the total mTORC1 level did not change ($n = 5$). Data represent mean ± SD. $^{***}P < 0.001$. **(B)** Specific siRNA transfection significantly reversed the effects of PMVs on expression of Lamitor1 and phosphorylations of mTORC1, 4EBP1 and p70S6K ($n = 4$). Data represent mean ± *SD*. $^{*}P < 0.05$, $^{**}P < 0.01$, $^{***}P < 0.001$. **(C)** Specific Lamtor1 siRNA increased the expressions of VSMC differentiation markers, including SMA, calponin and SM22 under PMV stimulation ($n = 5$). Data represent mean ± *SD*. $^{**}P < 0.01$, $^{***}P < 0.001$.

of 4E-BP from its inhibitory binding of eIF4E at the 5′-cap of mRNAs (Wang et al., 2019), were all significantly increased (**Figure 2A**).

To further investigate whether VSMC dedifferentiation induced by PMVs is dependent on Lamtor1, VSMCs were transfected with small interfering RNA (siRNA) specifically targeting at Lamtor1 and then treated with PMVs. Western blot results indicated that the Lamtor1 expression level was significantly suppressed by Lamtor1 siRNA in comparison with the negative control group (**Figure 2B**). The increased expressions of p-mTORC1 and the substrates, i.e., p-p70S6K and p-4EBP1 induced by PMVs was markedly reversed by Lamtor1 siRNA transfection (**Figure 2B**). Furthermore, the VSMC differentiation revealed similar negative correlation with Lamtor1 expression (**Figure 2C**).

PMVs Induce Phosphorylation of Src

To explore the possible mechanism by which PMVs regulated Lamtor1 expression and VSMC dedifferentiation, Ingenuity Pathway Analysis (IPA, QIAGEN, Dusseldorf, Germany) was used to analyze the proteomic data of PMVs released by activated platelets which has been published in NCBI database (Dean et al., 2009; **Figure 3A**). Gene Ontology analysis revealed that 556 proteins expressed in PMVs were enriched into a series of important biological processes (**Supplementary Figure III**). Ingenuity Canonical Pathways Analysis revealed that these 556 proteins mainly contributed to actin cytoskeleton signaling and integrin signaling (**Supplementary Figure IV**). Further pathway analysis revealed that Src may be the upstream molecule of Lamtor1 and participate in actin cytoskeleton in differentiation (**Figure 3A**).

Western blot was used to confirm the regulating effect of PMVs on Src expression or activation in VSMCs, and the result showed that the phosphorylation of Src was significantly increased by PMV treatment (**Figure 3B**), meanwhile the total level of Src was not changed (**Figure 3B**). The immunofluorescence staining verified the increased phosphorylation of Src in cytoplasm of VSMCs (**Figure 3C**).

Src Phosphorylation Participates in VSMC Dedifferentiation, Lamtor1 Expression and mTORC1 Activation Induced by PMVs

Data described above suggested that PMVs phosphorylated Src and induced VSMC dedifferentiation. To confirm whether the effect of PMVs on VSMC dedifferentiation and Lamtor1 expression was Src dependent, specific Src inhibitor was used to pre-incubate VSMCs 1 h before PMV stimulation. Western blot result showed that Src inhibitor significantly reversed the phosphorylation of Src induced by PMVs (**Figure 4A**), but there was no significant change in the expression of total Src (**Figure 4A**). Immunofluorescence staining confirmed the decreased phosphorylation of Src in cytoplasm of VSMCs (**Figure 4B**).

Western blot also showed that Lamtor1 expression was significantly decreased by pretreatment of specific Src inhibitor (**Figure 4C**). The phosphorylations of mTORC1 and its substrates 4E-BP1 and p70S6K were all repressed by Src inhibitor (**Figure 4D**) under PMVs treatment. Moreover, Src inhibitor promoted the expression of VSMC differentiation markers, i.e., SMA, calponin, and SM22 (**Figure 4E**), and immunofluorescence staining also showed that the contractile fibers of SMA were

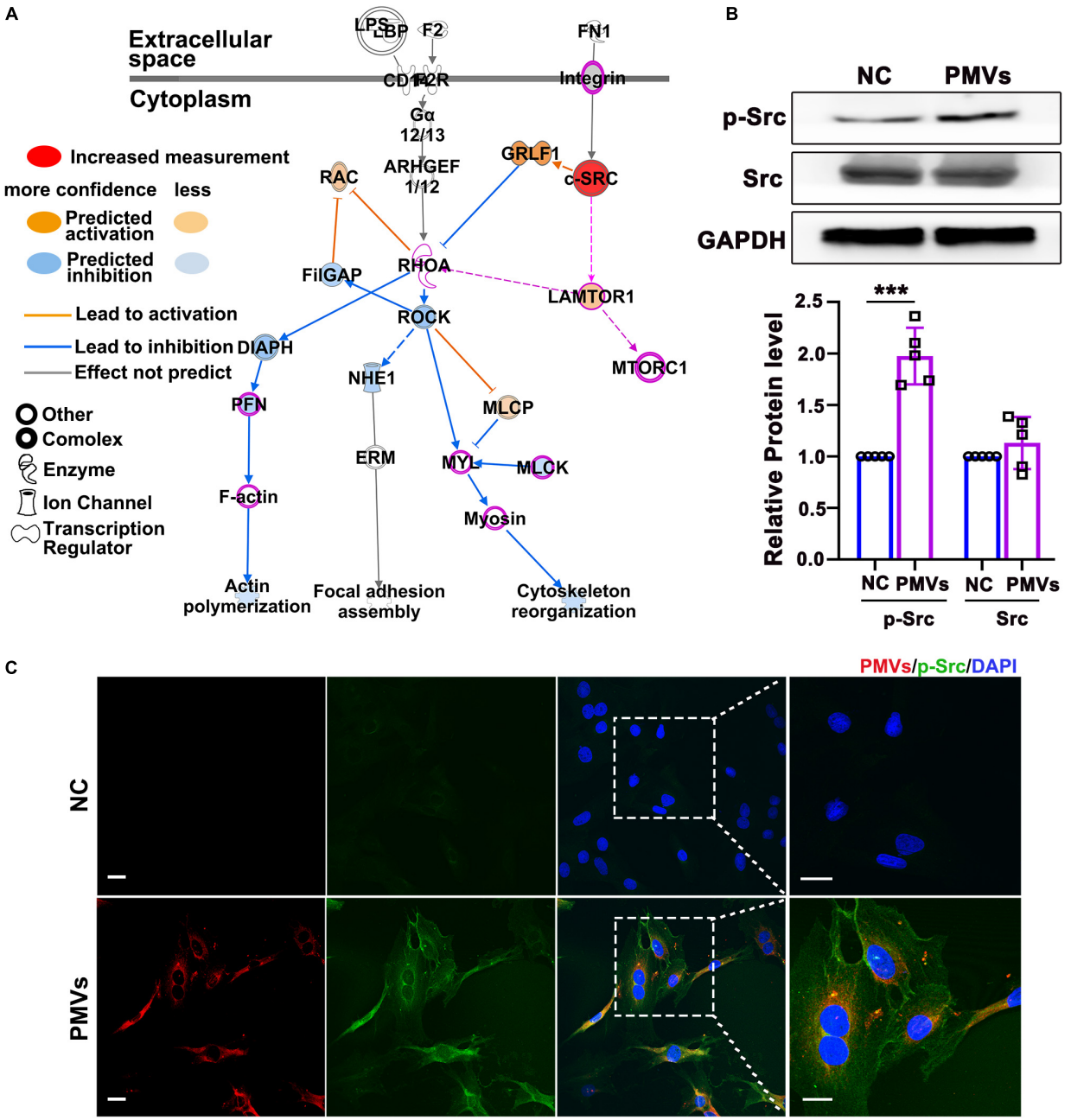

FIGURE 3 | PMVs induced Src phosphorylation. **(A)** Based on previously published proteomic data of PMVs, IPA bioinformatic analysis indicated that PMVs may induce Src activation, which may be the potential upstream molecule of Lamtor1 and participated in VSMC dedifferentiation. Solid lines for direct association and dotted lines for indirect or predicted association. **(B)** Western blot revealed that PMVs significantly increased the phosphorylation of Src, while did not change the expression of total Src ($n = 5$). Data represent mean ± *SD*. ***$P < 0.001$. **(C)** Immunofluorescence staining indicated that the expression of p-Src (green) was significantly increased after incubated with PMVs (red). Nuclei were counterstained with DAPI (blue). Scale bars: 50 μm.

increased dramatically (**Figure 4F**). Whereas, Src inhibitor revealed no significant effect on the adherent level of PMVs to VSMCs (**Supplementary Figure V**).

These data demonstrated that Src phosphorylation, in response to PMV treatment, modulated Lamtor1 expression and mTORC1 activation, which subsequently promoted VSMC dedifferentiation *in vitro*.

SMC-Specific *Lamtor1* KO Inhibits mTORC1 Activation and Represses Intima Hyperplasia *in vivo*

To assess the role of Lamtor1 in neointimal formation after intimal injury, SMC-specific *Lamtor1* KO mice combined with intimal injury was generated. Immunostaining revealed that

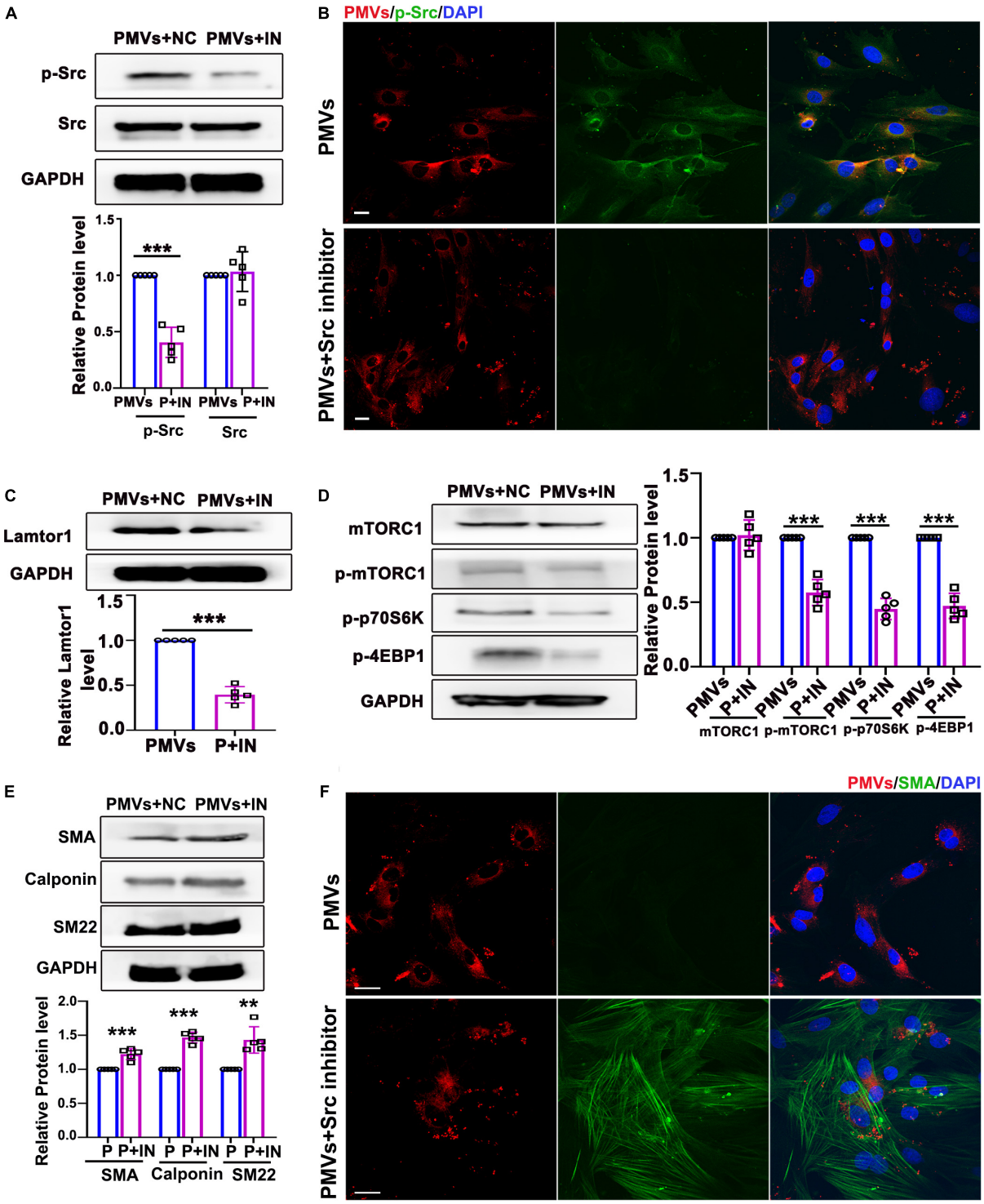

FIGURE 4 | Inhibition of p-Src repressed VSMC dedifferentiation *via* decreasing Lamtor1 expression and mTORC1 activity. **(A)** Src inhibitor (IN) decreased the phosphorylation of Src induced by PMVs, while did not change the expression of total Src ($n = 5$). Data represent mean ± *SD*. ***$P < 0.001$. **(B)** Immunofluorescence staining confirmed that the phosphorylation of Src (green) was decreased after incubated with Src IN. Nuclei were counterstained with DAPI (blue). Scale bars: 50 μm. **(C)** Src IN suppressed the protein expression of Lamtor1 induced by PMV stimulation ($n = 5$). Data represent mean ± *SD*. ***$P < 0.001$. **(D)** Src IN inhibited phosphorylations of mTORC1, 4EBP1 and p70S6K induced by PMVs, while the expression of total mTORC1 was not changed ($n = 5$). Data represent mean ± *SD*. ***$P < 0.001$. **(E)** Western blot revealed that Src IN increased the expressions of VSMC differentiation markers, i.e., SMA, calponin and SM22, ($n = 5$). Data represent mean ± *SD*. **$P < 0.01$, ***$P < 0.001$. **(F)** Immunofluorescence staining confirmed that Src inhibitor increased the expression of SMA (green). Nuclei were counterstained with DAPI (blue). Scale bars: 50 μm.

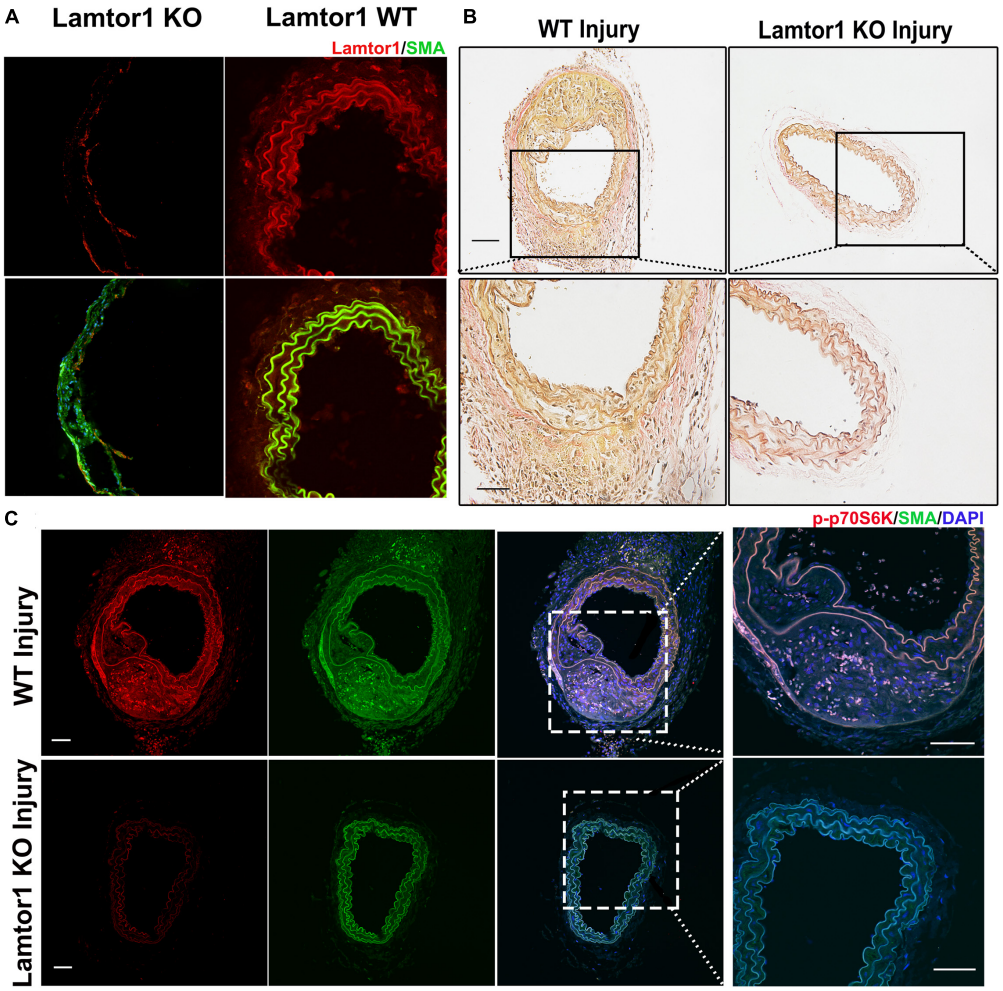

FIGURE 5 | SMC-specific *Lamtor1* KO repressed mTORC1 activation and intima hyperplasia after injury. **(A)** Representative images of immunostaining showed that in SMC-specific *Lamtor1* KO mice, Lamtor1 (red) was rarely expressed in VSMCs which was stained with SMA (green) in the wire injured carotid artery after 1-week surgery. Scale bars: 20 μm. **(B)** Representative images of Elastin Van-Gieson staining revealed that neointimal formation was significantly reduced in SM-specific *Lamtor1* KO mice after 1-week surgery. Scale bars: 100 μm. **(C)** Representative images of immunostaining showed that p-p70S6K (red) was greatly repressed in the wire injured carotid artery of SMC-specific *Lamtor1* KO mice after 1-week surgery. Nuclei are counterstained with DAPI (blue). Scale bars: 20 μm.

the expression of Lamtor1 was abolished in the media layer of carotid artery of SMC-specific *Lamtor1* KO mice compared with littermate control (**Figure 5A**). SMC-specific *Lamtor1* KO significantly reduced the neointima after intimal injury for 1 week compared to the littermate wild type (WT) mice (**Figure 5B**). Meanwhile, immunostaining revealed a decrease of p-p70S6K in SMC-specific *Lamtor1* KO mice after intimal injury in comparison with WT mice (**Figure 5C**). These data suggested that specific repression of Lamtor1 in VSMCs *in vivo* attenuated mTORC1 signaling activation and may contribute to neointimal formation after intimal injury.

DISCUSSION

Our present study demonstrated that Lamtor1 in VSMC was crucial in intimal remodeling and its repressed expression markedly attenuated intima hyperplasia after carotid injury. It has been reported that Lamtor1 suppresses the activation of mTORC1 on the lysosomal surface, and subsequently regulates cell growth and homeostasis *via* various signaling pathways (Bar-Peled et al., 2012). For example, Lamtor1 interacts with p27 in lysosomes during starvation and prevents mTORC1 activation, which promotes autophagy (Nowosad et al., 2020). Nada S et al. revealed that Lamtor1-mTORC1 is involved in the macromolecule biosynthesis, which contributes to autophagy and cell growth (Nada et al., 2009). Furthermore, dysregulation of mTORC1 signaling pathway occurs in Alzheimer's disease and cancer (Laplante and Sabatini, 2012). In cardiovascular system, loss of mTOR activity represses endothelial proliferation and angiogenesis as well as the proliferation of endothelial progenitor cells, which limits tissue repair and regeneration after cardiac injury (Humar et al., 2002; Miriuka et al., 2006). Rapamycin, the specific inhibitor of mTORC1, effectively reduces restenosis

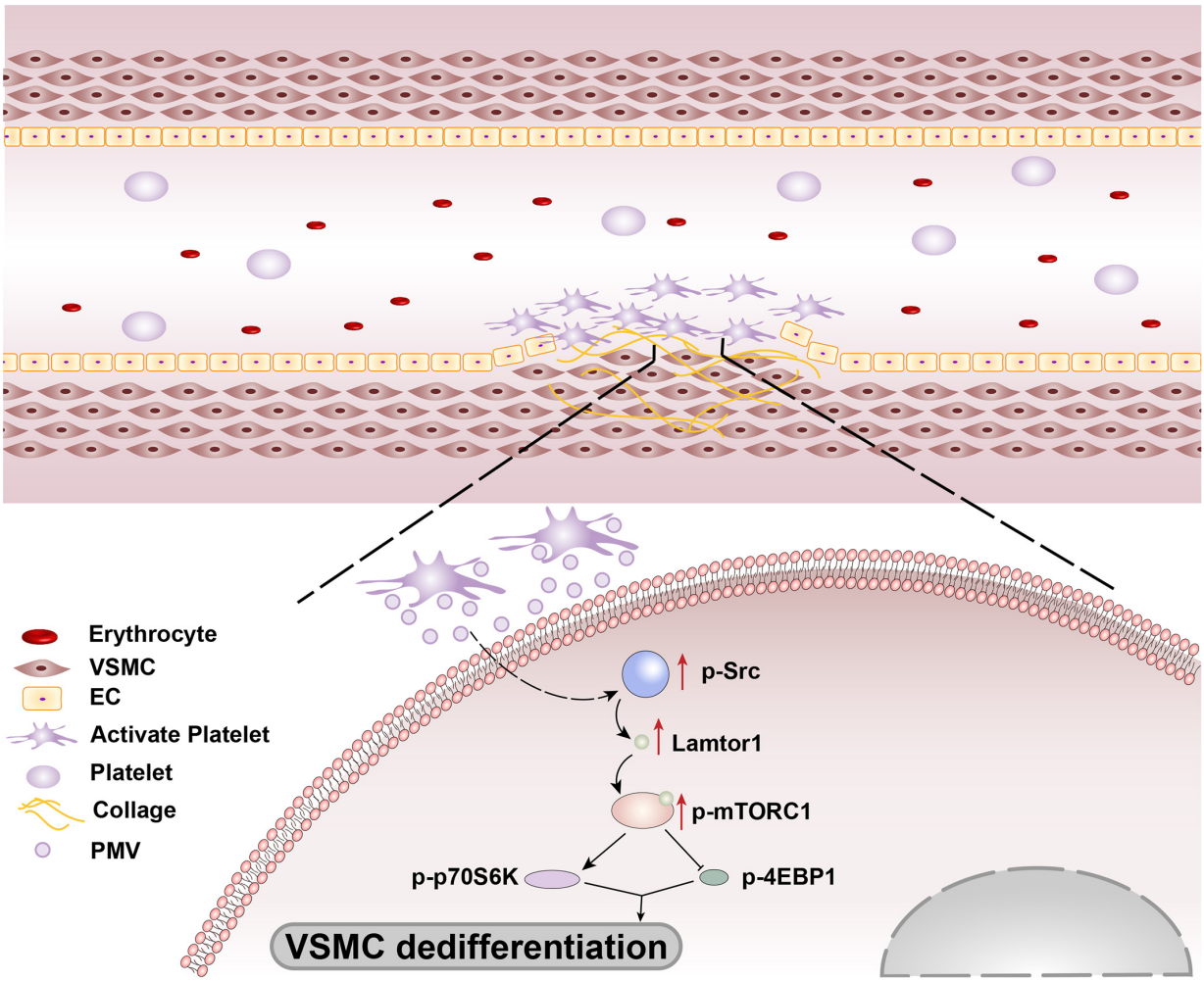

FIGURE 6 | Schematic drawing of the mechanisms of Lamtor1 in intimal hyperplasia after intimal injury.

by inhibiting the growth of VSMCs and has been approved by the FDA for clinical application after angioplasty (Stefanini and Holmes, 2013). Additionally, our present study suggested that Lamotr1 may also be a potential target for neointima formation after injury. It has been reported that complex cell responses are induced after vessel injury. The rapid proliferation and migration of endothelial cells are necessary for the repair of blood vessel damage, while the consistent proliferation, migration and dedifferentiation of VSMCs contribute to the intimal hyperplasia and the long-term patency (Tesfamariam, 2016). How to spatial and temporal adjust Lamtor1 to help blood vessel reconstruction is very important and interesting, which needs more researches in the future.

Recently, Block et al. (2020) revealed that Lamtor1 regulates Src localization on late endosome, and correlates Src trafficking toward the plasma membrane specifically at focal adhesion sites, which facilitates YAP nuclear translocation and activation. Furthermore, silencing Lamtor1 dephosphorylates Src at Tyr-416 thus attenuates Src catalytic activity (Block et al., 2020). Interestingly, in our present study, based on previously published proteomic data of PMVs, IPA bioinformatics analysis indicated that Src may also act as upstream molecule of Lamtor1.

The protein tyrosine kinase Src is a highly homologous prototype of non-receptor type tyrosine kinases, which ubiquitously expresses in various cell types and is intimately involved in many diseases, such as oncogenesis, cardiovascular diseases, and so on (Li et al., 2020). Phosphorylation of Src at tyrosine 419 is crucial to full kinase activation (Chiang and Sefton, 2000), which plays important roles in cellular proliferation, survival, adhesion and migration.

In cardiovascular system, Src kinase is highly expressed in VSMCs, endothelial cells, and myocytes (Kim et al., 2009; Wang and Aikawa, 2015), and its activity is associated with the physiological and pathological status of cells. In vascular morphogenesis, Src kinase plays critical roles in creating and decorating the endothelial cell apical membrane surface during early and late stages of lumen and tube formation (Kim et al., 2017). Inhibition of Src activity reduces oxidative stress, improves endothelial function, and normalizes ERK1/2 signaling hyper-activation, which result in attenuation of hypertension

development (Callera et al., 2016). It has been reported that Src mediates Ang-II dependent VSMC proliferation through the ERK2 and/or Ca^{2+} signaling in pathological conditions (Touyz et al., 2001; Sayeski and Ali, 2003). All these studies have demonstrated a key role of Src in promoting proliferation and migration of VSMC, while our results further indicate that Src was activated by PMVs secreted from recruited and activated platelets at injured intima, which subsequently promoted VSMC dedifferentiation *via* Lamtor1/mTORC1 pathway.

In normal adult, VSMCs maintains a contractile phenotype which proliferates slowly and expresses a range of contractile proteins for functional contraction. In response to vascular injury or local environmental alteration, contractile VSMCs dedifferentiate to synthetic phenotype (Allahverdian et al., 2018), characterized as repressed contractile proteins, altered morphology from elongated/spindle-like to thomboid/epitheloid-like, increased proliferation, and facilitated migration (Li et al., 2017). In healthy vascular wall, individual VSMC dedifferentiation occurs at a low event rate which participates in vascular wall repair. However, persistent pathological VSMC dedifferentiation significantly contributes to cardiovascular disease, such as atherosclerosis, hypertension, or graft failure (Owens et al., 2004). Therefore, VSMC phenotypic switch is an important step which leads to vascular remodeling. However, the mechanisms underlying VSMC dedifferentiation in intimal injury are poorly understood. It has been reported that inhibition of mTORC1stabilized GATA-6, which then activates transcription of promoters encoding contractile proteins, represses VSMC dedifferentiation (Xie et al., 2015). Our study suggested an important role of PMVs in VSMC dedifferentiation *via* modulating Lamtor1 expression and mTORC1 activation. Interestingly, immunofluorescent result of **Figure 1E** showed that although some VSMCs adhered less PMVs, the cell dedifferentiation was still strong, which suggested that after reach an appropriate range, PMVs probably revealed a similar regulation on VSMC functions. Since VSMC dedifferentiation is a long-term effect after PMV adhesion and PMVs adhesion may trigger a series of continuous and amplified signaling cascade, the efficient concentration of PMVs on VSMC functions needs systematic researches.

IPA analysis also predicts that PMVs may trigger the integrins family on the membrane of VSMCs which then modulate Src activation (**Figure 3A** and **Supplementary Figure IV**). It will be intriguing to examine the mechanisms by which PMVs modulate integrins on the membrane of VSMCs in the recent future.

In summary, our findings revealed that the platelets are recruited and activated at the injured intima and then secrete bulk of PMVs. The PMVs significantly phosphorylated Src in VSMCs to promote Lamtor1 expression and activate mTORC1 signaling pathway, thus induced VSMC dedifferentiation (**Figure 6**). Intriguingly, SMC-specific *Lamtor1* KO obviously attenuated intima hyperplasia in injury model, which suggested that Lamtor1 and the related molecules may provide potential therapeutic targets to ameliorate intimal hyperplasia after vascular interventional surgery.

DATA AVAILABILITY STATEMENT

The original contributions presented in the study are included in the article/**Supplementary Material**, further inquiries can be directed to the corresponding author/s.

ETHICS STATEMENT

The animal study was reviewed and approved by Animal Research Committee of Shanghai Jiao Tong University.

AUTHOR CONTRIBUTIONS

Y-XQ and J-TL designed and guided the work. J-TL and HB participated in data collection, data processing, program implementation, and manuscript writing. Y-JF and Z-TL contributed to statistical analysis. Y-XQ, Q-PY, and M-LZ contributed to manuscript writing and article publication. Z-LJ and YH revised the manuscript critically. Y-XQ and Z-LJ provided funding acquisition. All authors provided critical advice for the final manuscript.

FUNDING

This study was supported by the National Natural Science Foundation of China (Grant Nos. 11972232 and 12032003).

ACKNOWLEDGMENTS

We thank professor Sheng-Cai Lin at Xiamen University for sharing *Lamtor1*$^{flox/flox}$ mice.

SUPPLEMENTARY MATERIAL

The Supplementary Material for this article can be found online at: https://www.frontiersin.org/articles/10.3389/fcell.2021.744320/full#supplementary-material

REFERENCES

Akers, J. C., Gonda, D., Kim, R., Carter, B. S., and Chen, C. C. (2013). Biogenesis of extracellular vesicles (EV): exosomes, microvesicles, retrovirus-like vesicles, and apoptotic bodies. *J. Neurooncol.* 113, 1–11. doi: 10.1007/s11060-013-1084-8

Allahverdian, S., Chaabane, C., Boukais, K., Francis, G. A., and Bochaton-Piallat, M. L. (2018). Smooth muscle cell fate and plasticity in atherosclerosis. *Cardiovasc. Res.* 114, 540–550. doi: 10.1093/cvr/cvy022

Bao, H., Chen, Y. X., Huang, K., Zhuang, F., Bao, M., Han, Y., et al. (2018). Platelet-derived microparticles promote endothelial cell proliferation in hypertension via miR-142-3p. *FASEB J.* 32, 3912–3923. doi: 10.1096/fj.201701073r

Bar-Peled, L., Schweitzer, L. D., Zoncu, R., and Sabatini, D. M. (2012). Ragulator is a GEF for the rag GTPases that signal amino acid levels to mTORC1. *Cell* 150, 1196–1208. doi: 10.1016/j.cell.2012.07.032

Berk, B. C., Vallega, G., Muslin, A. J., Gordon, H. M., Canessa, M., and Alexander, R. W. (1989). Spontaneously hypertensive rat vascular smooth muscle cells in culture exhibit increased growth and Na+/H+ exchange. *J. Clin. Invest.* 83, 822–829.

Block, M. R., Brunner, M., Ziegelmeyer, T., Lallemand, D., Pezet, M., Chevalier, G., et al. (2020). The mechano-sensitive response of β1 integrin promotes SRC-positive late endosome recycling and activation of Yes-associated protein. *J. Biol. Chem.* 295, 13474–13487. doi: 10.1074/jbc.ra120.013503

Boilard, E., Nigrovic, P. A., Larabee, K., Watts, G. F., Coblyn, J. S., Weinblatt, M. E., et al. (2010). Platelets amplify inflammation in arthritis via collagen-dependent microparticle production. *Science* 327, 580–583. doi: 10.1126/science.1181928

Callera, G. E., Antunes, T. T., He, Y., Montezano, A. C., Yogi, A., Savoia, C., et al. (2016). c-Src Inhibition Improves Cardiovascular Function but not Remodeling or Fibrosis in Angiotensin II-Induced Hypertension. *Hypertension* 68, 1179–1190. doi: 10.1161/hypertensionaha.116.07699

Chiang, G. G., and Sefton, B. M. (2000). Phosphorylation of a Src kinase at the autophosphorylation site in the absence of Src kinase activity. *J. Biol. Chem.* 275, 6055–6058. doi: 10.1074/jbc.275.9.6055

Csongrádi, É, Nagy, B. Jr., Fulop, T., Varga, Z., Karányi, Z., Magyar, M. T., et al. (2011). Increased levels of platelet activation markers are positively associated with carotid wall thickness and other atherosclerotic risk factors in obese patients. *Thromb. Haemost.* 106, 683–692. doi: 10.1160/th11-01-0030

Dai, L., Li, C., Shedden, K. A., Misek, D. E., and Lubman, D. M. (2009). Comparative proteomic study of two closely related ovarian endometrioid adenocarcinoma cell lines using cIEF fractionation and pathway analysis. *Electrophoresis* 30, 1119–1131. doi: 10.1002/elps.200800505

Dean, W. L., Lee, M. J., Cummins, T. D., Schultz, D. J., and Powell, D. W. (2009). Proteomic and functional characterisation of platelet microparticle size classes. *Thromb. Haemost.* 102, 711–718. doi: 10.1160/th09-04-243

Filipek, P. A., de Araujo, M., Vogel, G. F., De Smet, C. H., Eberharter, D., Rebsamen, M., et al. (2017). LAMTOR/Ragulator is a negative regulator of Arl8b- and BORC-dependent late endosomal positioning. *J. Cell Biol.* 216, 4199–4215. doi: 10.1083/jcb.201703061

Forlow, S. B., McEver, R. P., and Nollert, M. U. (2000). Leukocyte-leukocyte interactions mediated by platelet microparticles under flow. *Blood* 95, 1317–1323. doi: 10.1182/blood.v95.4.1317.004k30_1317_1323

Humar, R., Kiefer, F. N., Berns, H., Resink, T. J., and Battegay, E. J. (2002). Hypoxia enhances vascular cell proliferation and angiogenesis in vitro via rapamycin (mTOR)-dependent signaling. *FASEB J.* 16, 771–780. doi: 10.1096/fj.01-0658com

Kim, D. J., Norden, P. R., Salvador, J., Barry, D. M., Bowers, S., Cleaver, O., et al. (2017). Src- and Fyn-dependent apical membrane trafficking events control endothelial lumen formation during vascular tube morphogenesis. *PLoS One* 12:e0184461. doi: 10.1371/journal.pone.0184461

Kim, M. P., Park, S. I., Kopetz, S., and Gallick, G. E. (2009). Src family kinases as mediators of endothelial permeability: effects on inflammation and metastasis. *Cell Tissue Res.* 335, 249–259. doi: 10.1007/s00441-008-0682-9

Laplante, M., and Sabatini, D. M. (2012). mTOR signaling in growth control and disease. *Cell* 149, 274–293. doi: 10.1016/j.cell.2012.03.017

Li, H., Zhao, C., Tian, Y., Lu, J., Zhang, G., Liang, S., et al. (2020). Src family kinases and pulmonary fibrosis: a review. *Biomed. Pharmacother.* 127:110183. doi: 10.1016/j.biopha.2020.110183

Li, Q., Wu, X., Liu, Y., Zhang, M., Bai, X., and Chen, C. (2017). The effect of anagliptin on intimal hyperplasia of rat carotid artery after balloon injury. *Mol. Med. Rep.* 16, 8003–8010. doi: 10.3892/mmr.2017.7667

Lukasik, M., Rozalski, M., Luzak, B., Michalak, M., Ambrosius, W., Watala, C., et al. (2013). Enhanced platelet-derived microparticle formation is associated with carotid atherosclerosis in convalescent stroke patients. *Platelets* 24, 63–70. doi: 10.3109/09537104.2011.654292

Magnuson, B., Ekim, B., and Fingar, D. C. (2012). Regulation and function of ribosomal protein S6 kinase (S6K) within mTOR signalling networks. *Biochem. J.* 441, 1–21. doi: 10.1042/bj20110892

Miriuka, S. G., Rao, V., Peterson, M., Tumiati, L., Delgado, D. H., Mohan, R., et al. (2006). mTOR inhibition induces endothelial progenitor cell death. *Am. J. Transplant.* 6, 2069–2079. doi: 10.1111/j.1600-6143.2006.01433.x

Nada, S., Hondo, A., Kasai, A., Koike, M., Saito, K., Uchiyama, Y., et al. (2009). The novel lipid raft adaptor p18 controls endosome dynamics by anchoring the MEK-ERK pathway to late endosomes. *EMBO J.* 28, 477–489. doi: 10.1038/emboj.2008.308

Nowosad, A., Jeannot, P., Callot, C., Creff, J., Perchey, R. T., Joffre, C., et al. (2020). p27 controls Ragulator and mTOR activity in amino acid-deprived cells to regulate the autophagy-lysosomal pathway and coordinate cell cycle and cell growth. *Nat. Cell Biol.* 22, 1076–1090.

Owens, G. K., Kumar, M. S., and Wamhoff, B. R. (2004). Molecular regulation of vascular smooth muscle cell differentiation in development and disease. *Physiol. Rev.* 84, 767–801. doi: 10.1152/physrev.00041.2003

Sayeski, P. P., and Ali, M. S. (2003). The critical role of c-Src and the Shc/Grb2/ERK2 signaling pathway in angiotensin II-dependent VSMC proliferation. *Exp. Cell Res.* 287, 339–349. doi: 10.1016/s0014-4827(03)00154-x

Sinha, S., Iyer, D., and Granata, A. (2014). Embryonic origins of human vascular smooth muscle cells: implications for in vitro modeling and clinical application. *Cell Mol. Life Sci.* 71, 2271–2288. doi: 10.1007/s00018-013-1554-3

Stefanini, G. G., and Holmes, D. R. Jr. (2013). Drug-eluting coronary-artery stents. *N. Engl. J. Med.* 368, 254–265.

Suades, R., Padró, T., Alonso, R., Mata, P., and Badimon, L. (2015). High levels of TSP1+/CD142+ platelet-derived microparticles characterise young patients with high cardiovascular risk and subclinical atherosclerosis. *Thromb. Haemost.* 114, 1310–1321. doi: 10.1160/th15-04-0325

Tesfamariam, B. (2016). Endothelial Repair and Regeneration Following Intimal Injury. *J Cardiovasc Transl Res.* 9, 91–101. doi: 10.1007/s12265-016-9677-1

Touyz, R. M., Wu, X. H., He, G., Park, J. B., Chen, X., Vacher, J., et al. (2001). Role of c-Src in the regulation of vascular contraction and Ca2+ signaling by angiotensin II in human vascular smooth muscle cells. *J. Hypertens.* 19, 441–449. doi: 10.1097/00004872-200103000-00012

Wang, J. G., and Aikawa, M. (2015). Toll-like receptors and Src-family kinases in atherosclerosis – focus on macrophages. *Circ. J.* 79, 2332–2334. doi: 10.1253/circj.cj-15-1039

Wang, Z., Feng, X., Molinolo, A. A., Martin, D., Vitale-Cross, L., Nohata, N., et al. (2019). 4E-BP1 Is a Tumor Suppressor Protein Reactivated by mTOR Inhibition in Head and Neck Cancer. *Cancer Res.* 79, 1438–1450. doi: 10.1158/0008-5472.can-18-1220

Webber, A. J., and Johnson, S. A. (1970). Platelet participation in blood coagulation aspects of hemostasis. *Am. J. Pathol.* 60, 19–42.

Weber, A., Köppen, H. O., and Schrör, K. (2000). Platelet-derived microparticles stimulate coronary artery smooth muscle cell mitogenesis by a PDGF-independent mechanism. *Thromb. Res.* 98, 461–466. doi: 10.1016/s0049-3848(00)00192-4

Wu, B., Mottola, G., Schaller, M., Upchurch, G. R. Jr., and Conte, M. S. (2017). Resolution of vascular injury: Specialized lipid mediators and their evolving therapeutic implications. *Mol. Aspects Med.* 58, 72–82. doi: 10.1016/j.mam.2017.07.005

Xie, Y., Jin, Y., Merenick, B. L., Ding, M., Fetalvero, K. M., Wagner, R. J., et al. (2015). Phosphorylation of GATA-6 is required for vascular smooth muscle cell differentiation after mTORC1 inhibition. *Sci. Signal.* 8:ra44. doi: 10.1126/scisignal.2005482

Conflict of Interest: The authors declare that the research was conducted in the absence of any commercial or financial relationships that could be construed as a potential conflict of interest.

Publisher's Note: All claims expressed in this article are solely those of the authors and do not necessarily represent those of their affiliated organizations, or those of the publisher, the editors and the reviewers. Any product that may be evaluated in this article, or claim that may be made by its manufacturer, is not guaranteed or endorsed by the publisher.

frontiers in Cell and Developmental Biology

REVIEW
published: 21 January 2022
doi: 10.3389/fcell.2022.825622

Matrix Vesicles as a Therapeutic Target for Vascular Calcification

Tiantian Li[1†], Hongchi Yu[1†], Demao Zhang[1], Tang Feng[1], Michael Miao[2], Jianwei Li[3] and Xiaoheng Liu[1]**

[1]Institute of Biomedical Engineering, West China School of Basic Medical Sciences & Forensic Medicine, Sichuan University, Chengdu, China, [2]Division of Oral & Craniofacial Health Sciences, University of North Carolina Adams School of Dentistry, Chapel Hill, NC, United States, [3]Department of Endocrinology and Metabolism, West China Hospital, Sichuan University, Chengdu, China*

Vascular calcification (VC) is linked to an increased risk of heart disease, stroke, and atherosclerotic plaque rupture. It is a cell-active process regulated by vascular cells rather than pure passive calcium (Ca) deposition. In recent years, extracellular vesicles (EVs) have attracted extensive attention because of their essential role in the process of VC. Matrix vesicles (MVs), one type of EVs, are especially critical in extracellular matrix mineralization and the early stages of the development of VC. Vascular smooth muscle cells (VSMCs) have the potential to undergo phenotypic transformation and to serve as a nucleation site for hydroxyapatite crystals upon extracellular stimulation. However, it is not clear what underlying mechanism that MVs drive the VSMCs phenotype switching and to result in calcification. This article aims to review the detailed role of MVs in the progression of VC and compare the difference with other major drivers of calcification, including aging, uremia, mechanical stress, oxidative stress, and inflammation. We will also bring attention to the novel findings in the isolation and characterization of MVs, and the therapeutic application of MVs in VC.

Keywords: vascular calcification, matrix vesicles, extracellular vesicles, exosomes, vascular smooth muscle cells

OPEN ACCESS

Edited by:
Roland Wohlgemuth, Lodz University of Technology, Poland

Reviewed by:
Tzongshi Lu, Brigham and Women's Hospital and Harvard Medical School, United States
Miriam Zacchia, University of Campania Luigi Vanvitelli, Italy

****Correspondence:***
Jianwei Li
jerryli678@yahoo.com
Xiaoheng Liu
liuxiaohg@scu.edu.cn

†These authors have contributed equally to this work

Specialty section:
This article was submitted to Molecular and Cellular Pathology, a section of the journal Frontiers in Cell and Developmental Biology

Received: *30 November 2021*
Accepted: *04 January 2022*
Published: *21 January 2022*

Citation:
Li T, Yu H, Zhang D, Feng T, Miao M, Li J and Liu X (2022) Matrix Vesicles as a Therapeutic Target for Vascular Calcification. Front. Cell Dev. Biol. 10:825622. doi: 10.3389/fcell.2022.825622

INTRODUCTION

Vascular calcification (VC) is a prominent clinical pathology of atherosclerosis, diabetes mellitus, hypertension, aging, and chronic kidney disease (CKD), resulting in abnormal calcium phosphate accumulation in the intimal and medial layers of the vessel wall (Xu et al., 2020). After vascular calcification, the stiffness of the vascular wall is increased, and the compliance is decreased, which results in myocardial ischemia, left ventricular hypertrophy, and heart failure (Nitta and Ogawa, 2015). At present, vascular calcification is still lacks effective treatment methods, and the pathogenesis mechanism remains unclear (Herrmann et al., 2020). Therefore, it is necessary to uncover its specific mechanisms and develop therapeutic strategies.

The phenotype switching of the VSMCs has been regarded as the principal driver in the calcification of intimal and medial layers. VSMCs undergo the phenotypic transformation from a differentiated "contractile" into a dedifferentiated "synthetic" proliferative phenotype in the process of vascular calcification. During this phenotypic switching, VSMCs show decreased expression of the contractile markers smooth muscle α-actin (α-SMA), smooth muscle 22α (SM22α), smooth muscle myosin heavy chain 11 (SM-MHC), CNN1, calponin, leiomodin, smoothelin (SMTN), myosin light chain (MYL) and an increase in synthetic marker S100A4, KLF4, vimentin, osteopontin (OPN) (Furmanik et al., 2020). The phenotypic switching VSMCs

express higher osteoblast-like markers, such as runt-related transcription factor 2 (Runx2), zinc finger transcription factor (Osterix), muscle segment homeobox 2 (MSX2) (Qi et al., 2019), and is associated with increased proliferation and migration ability (Kapustin and Shanahan, 2016). The osteoblast-like phenotype of VSMCs is regarded as the cellular characteristic factor of vascular calcification. Many factors such as oxidative stress damage, hyperphosphatemic environment, and inflammation increase the indices related to bone formation in VSMCs and promote their transformation into osteoblasts (Voelkl et al., 2018a). On the other hand, a variety of biochemical factors are involved in the phenotype switching of VSMCs, i.e., the growth factors platelet-derived growth factor (PDGF-BB) and transforming growth factor-β1 (TGF-β1) could promote the phenotype switching of VSMCs (Jain et al., 2021).

Matrix vesicles (MVs), one kind of extracellular matrix-derived EVs, are membrane-bound microparticles released by cells, containing various cargo, including proteins, carbohydrates, lipids, DNA and mRNAs, and species of small RNAs, such as microRNAs (miRNAs). The origin and composition of MVs determine their calcification potential (Zazzeroni et al., 2018). Recent evidence showed that extracellular MVs serve as nucleating foci to initiate microcalcification (Demer and Tintut, 2014). MV nanofragments obtained by mechanical rupture could induce rapid mineralization *in vitro* (Kunitomi et al., 2019). The formation and secretion of MVs and the increase of intracellular alkaline phosphatase (ALP) activity are also involved in the phenotypic transformation and osteoblast-like phenotype transformation of VSMCs (Lin et al., 2016). However, the specific mechanisms and functions of MVs regulating vascular calcification have not been fully elucidated. For example, what is the originating cell that releases MVs in vascular calcification, and how do the pro-calcification MVs get into the recipient cell? On the other hand, increasing evidence shows that EVs have potential therapeutic applications for many diseases. For example, overexpressing a high-affinity variant human PD-1 protein (havPD-1) EVs has been used to reduce cancer cell proliferation and induce apoptosis (Chen et al., 2022). Another therapeutic role of EVs is dependent on their proteins and/or non-coding RNAs, in particular miRNAs delivery ability (de Abreu et al., 2020). It has also been shown that MVs carry miR-199a-3p, which, by regulating GATA-binding 4 acetylation, were able to rescue electric function in engineered and *in vivo* atria (Aday et al., 2017). Alginate-based microreactors that were loaded with MVs as support for bone-like osteoblast cells were shown to enhance biomineralization in a co-assembled 3D spheroid (Itel et al., 2018). Therefore, engineered MVs have emerged as a potential therapeutic method to treat vascular calcification. In this review, targeted interventions based on MVs to treat vascular calcification are also discussed (New et al., 2013).

VASCULAR CALCIFICATION

Physiological calcification is a normal process that occurs in bones and teeth; however, pathological calcification occurs in soft tissue such as blood vessels, joints, and tumors, in association with aging, advanced atherosclerosis, diabetes, and chronic kidney disease (Jing et al., 2019). The classification of vascular calcification is divided into intimal calcification, media calcification and cardiac valve calcification **Figure 1** (Viegas and Simes, 2018). Vascular intimal calcification often occurs in atherosclerotic diseases. Intimal calcification is related to the stability of atherosclerotic plaque and the microcalcifications that contribute to plaque rupture by concentrating mechanical forces within the fibrous cap (Blaser and Aikawa, 2018). After calcification is formed, it is scattered on the inner wall of the blood vessel in the form of a spot or patch (Nakahara et al., 2017). The early-stage shows microcalcification (range: ≥0.5 to <15 μm) and then develops a spot-like calcification (Nakahara et al., 2017). Vascular media calcification often occurs in the internal elastic lamina and is more common in small and medium arteries such as the femoral artery, tibial artery and radial artery, also known as Monckeberg's medial sclerosis, which is more common in patients with advanced aging, diabetes and CKD (Zazzeroni et al., 2018). Medial calcification decreases vessel compliance, increases pulse wave velocity and systolic hypertension. The occurrence of cardiac valve calcification is related to mechanical stress and inflammation and is commonly seen in metabolic diseases such as diabetes, dyslipidemia, uremia, etc. When cardiac valve calcification occurs, spotted calcium salts are deposited, accompanied by valve fibrosis and inflammatory cell infiltration (Shekar and Budoff, 2018).

The main cause of vascular calcification is the ectopic deposition of hydroxyapatite crystals in blood vessel wall cells and extracellular matrix (ECM) (Viegas and Simes, 2018). During the last few decades, vascular calcification had been regarded as a process of accumulating insoluble precipitates of Ca phosphate without a specific cellular biological response. In recent years, increasing evidence shows that vascular cells actively regulate the calcification process (Proudfoot, 2019).

THE CONTRIBUTION OF MATRIX VESICLES TO VASCULAR CALCIFICATION

Many risk factors such as calcium and phosphorus metabolism disorder, inflammation, oxidative stress, apoptosis, autophagy and aging can contribute to vascular calcification. They can also intersect or interact with each other, thereby affecting the occurrence and development of vascular calcification (Pescatore et al., 2019). Vascular calcification is a major complication of CKD patients. This may be due to the decline of renal function, leading to calcium and phosphorus metabolism disorders, which in turn leads to hyperphosphatemia and hypercalcemia. Both hypercalcemia and hyperphosphatemia may promote intimal and media calcification. Hyperphosphatemia may increase the activity of the sodium-dependent cotransporters, PIT-1 and PIT-2, and up-regulate genes associated with matrix mineralization, which eventually leads to vascular calcification (Cozzolino et al., 2019). Interestingly, hypercalcemia and hyperphosphatemia both increase the release of MVs, leading to the deposition of hydroxyapatite in the extracellular matrix (Reynolds et al., 2004).

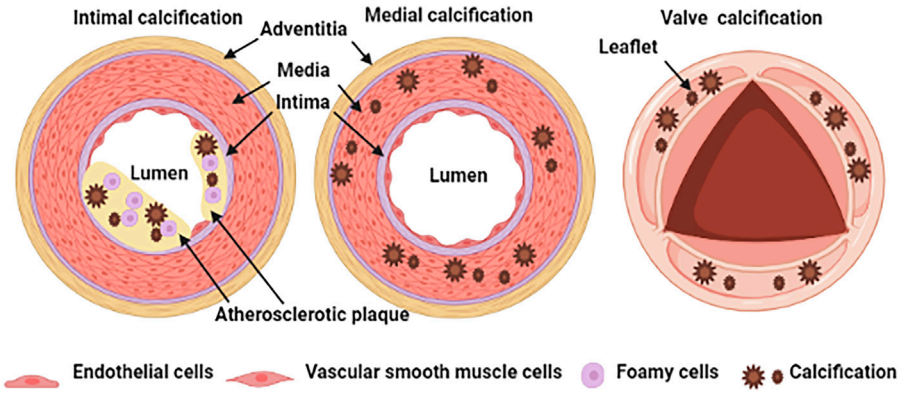

FIGURE 1 | Schematic representation of vascular calcification classification.

Inflammatory cells such as macrophages promote vascular calcification by secreting inflammatory cytokines such as TNF-a, IL-1β, and IL-6 (Henaut et al., 2016). Inflammatory cytokines directly promote calcification in VSMCs by down-regulating VSMC-specific genes and up-regulating osteoblastic genes such as BMP2 and ALP. They also indirectly reduce circulating Fetuin-A, MGP, and Klotho levels, further promoting vascular calcification procession in VSMCs (Henaut et al., 2016; Zhang et al., 2018). MVs secreted by pro-inflammatory cells also play pivotal roles in the procession of vascular calcification. These MVs participate in vascular calcification by forming the phosphatidylserine (PS)-annexin A5-S100A9 membrane complex involved in mineralization or by mediating the transport of miRNAs such as miRNA-153 and miRNA-223 (Henaut et al., 2016; Zhang et al., 2018).

Oxidative stress-induced by intracellular calcium and phosphate overloading promotes vascular calcification *via* inducing signal activation and VSMCs osteogenic phenotype transition (Nguyen et al., 2020). Pro-mineralizing MVs induced calcification of recipient VSMCs by stimulating reactive oxygen species (ROS) production (Chen et al., 2021). Apoptotic cells form a nidus for calcification, releasing apoptotic bodies loaded with calcium that participate in the calcification process by deposition of hydroxyapatite in the extracellular matrix (Cozzolino et al., 2019).

Emerging evidence has demonstrated that autophagy is directly related to vascular calcification. Crucially, autophagy maintains the physiological function of VSMCs by regulating Ca^{2+} homeostasis (Phadwal et al., 2020). Autophagy-related proteins and protein complexes play important roles in exosome biogenesis (Xu et al., 2018). It has been shown that MVs are rich in annexin-A5, which is also known to have an important role in the formation of mature autophagosomes (Ghislat and Knecht, 2012). Autophagic proteins including LAMP1, LAMP2, and LAMTOR1 were found in MVs released from rat VICs (Cui et al., 2016). In the progression of vascular calcification, MVs may be entwined with the network of autophagic vesicles during the formation or release stage (Cui et al., 2016). Cell autophagy has a special pro-calcification effect than cell apoptosis. It increases the inorganic phosphate (Pi)-induced MVs release with increased ALP activity (Dai et al., 2013). Therefore, inhibiting the autophagy pathway may help to prevent Pi-induced vascular calcification by reducing MVs release (Dai et al., 2013; Cui et al., 2016).

Vascular calcification is associated with aging, which is commonly seen in older adults or in middle-aged subjects affected by premature vascular aging. MVs released from senescent ECs and elderly subjects' plasma promote calcification of VSMCs, and MV carriage of increased quantities of annexins A2 and A6, BMP2, and Ca (Alique et al., 2017). EVs released from senescent cells can also drive the senescence of neighboring cells in a paracrine manner (Blaser and Aikawa, 2018).

The above-mentioned studies underscore the essential role of MVs, which are totally dependent on their cellular source, in regulating the vascular calcification process. Therefore, the origin of MVs is briefly described below.

THE ORIGIN OF MATRIX VESICLES

EVs encompass a wide variety of vesicles with a lipid bilayer membrane structure released by various kinds of cells in either resting or stress states (Goettsch et al., 2013). The main characteristics of various EVs are described in **Table 1**. According to the route of biogenesis, size, density, and protein markers, EVs are categorized into exosomes (50–150 nm), microvesicles (100–500 nm), and apoptotic bodies (1,000–5,000 nm) (Mathivanan et al., 2010; Goettsch et al., 2013; Blaser and Aikawa, 2018) (**Figure 2**). Exosomes are released through the endosomal-sorting complex, where intraluminal vesicles formed by the inward budding of the endosomal membrane are packaged within multivesicular bodies (MVBs). These MVBs then fuse with the plasma membrane to release their enclosed exosomes in a Rab GTPase-dependent manner (Blaser and Aikawa, 2018). Microvesicles are formed by direct budding and fission of the plasma membrane (Mathivanan et al., 2010; Blaser and Aikawa, 2018). Apoptotic bodies are formed by apoptotic cells due to the breakdown of the cytoskeleton, which induces the plasma

TABLE 1 | Main characteristics of exosomes, matrix vesicles, microvesicles, and apoptotic bodies.

	Exosomes	Matrix vesicles	Microvesicles	Apoptotic bodies	References
Size	50–150 nm	30–300 nm	100–1,000 nm	1–5 μm	Blaser and Aikawa (2018)
Origin	Intraluminal vesicles within multivesicular bodies	Plasma membrane or intraluminal vesicles within multivesicular bodies	Plasma membrane and cellular content	Plasma membrane, cellular fragments	Shapiro et al. (2015), Stahl et al. (2019)
Mechanism of formation	Fusion of multivesicular bodies with the plasma membrane	Budding of the cell plasma membrane or fusion of multivesicular bodies with the plasma membrane	Outward blebbing of the plasma membrane	Cell shrinkage and programmed cell death	Shapiro et al. (2015), Stahl et al. (2019)
Release	Constitutive and/or cellular activation	Constitutive and/or cellular activation	Constitutive and/or cellular activation	Apoptosis	Stahl et al. (2019)
Pathways	Endosomal Sorting Complex Required for Transport (ESCRT)-dependent Tetraspanin-dependent Ceramide-dependent	ESCRT-dependent tetraspanin-dependent ceramide-dependent stimuli- and cell-dependent	Ca^{2+}-dependent stimuli- and cell-dependent	Apoptosis-related	Stahl et al. (2019)
Markers	Tetraspanins (CD9, CD63, CD81,CD82, CD53, CD37, etc), MHC I, MHC II, Hsp70, Hsp90, Alix, TSG101, etc	Tetraspanins (CD9, CD81, CD63, etc), MHC I, LAMP-1, LAMP-2, TSG101, HSP90, HSP70, etc	Tetraspanins (CD40, CD83, CD31, CD34, etc), TSG101, phosphatidylserine, antigens from parent cells, ARF6, integrin VCAMP3, selectins, etc	Phosphatidylserine, propidum iodide positive, annexin V, TSP, C3b, caspase 3, histones, etc	Nabhan et al. (2012), Kapustin et al. (2015), Shapiro et al. (2015), Melki et al. (2017), Todorova et al. (2017), Zhang et al. (2017), Kubo (2018)
Contents	Proteins (MHC molecules, signal transduction, enzymes, etc.), nucleic acids (mRNA, microRNA, non-coding RNAs, ssDNAs, dsDNAs, etc.), lipids, etc	Proteins (MHC molecules, signal transduction, enzymes, etc.), nucleic acids (mRNA, microRNA, non-coding RNAs, ssDNAs, dsDNAs, etc.), lipids, etc	Nucleic acids (mRNA, microRNA, non-coding RNAs, ssDNAs, dsDNAs, mitochondrial DNA, etc.), cytoplasmic and membrane proteins (tissue factors, cytokines, enzymes, etc.), lipids, etc	Cell organelles, proteins, nuclear fractions, DNA, coding and non-coding RNA, lipids	Kubo (2018)
Functions	Progression, metastasis, and formation of the microenvironment of tumor, angiogenesis, antigen presentation, apoptosis, coagulation, cellular homeostasis, inflammation, intercellular signaling, etc	Sites of provisional mineralization	Pro-inflammatory and anti-inflammatory effects, cellular homeostasis, intercellular signaling, etc	Maintain homeostasis of the immune system, progression, metastasis, and formation of the microenvironment of tumor	Shapiro et al. (2015), Boulanger et al. (2017), Gurunathan et al. (2019)

membrane to bulge, leading to the separation of the plasma membrane (Mathivanan et al., 2010; Blaser and Aikawa, 2018).

In the process of vascular calcification, EVs that are released by macrophages are 30–300 nm in diameter and originate as membranous protrusions in the intima layer (Blaser and Aikawa, 2018). Besides this, VSMCs-derived EVs, with a diameter of 100–150 nm, originating from an exosomal pathway in the media layer, are processed by multivesicular bodies and are enriched in members of the Rab GTPase family (Blaser and Aikawa, 2018). Previous advances have shown that a common mechanism may mediate both intimal and medial vascular calcification, that is, a substantial increase of EVs in the vascular interstitial space, in particular, the small EVs (sEVs, with a size of 40–100 or to 140 nm) which are mainly produced and secreted from arterial VSMCs. These sEVs facilitate the formation of nucleate Ca phosphate (Ca/P) crystals in the form of Hydroxyapatite (Bhat et al., 2020a). Valve homeostasis also depends on appropriate intercellular interactions between valvular endothelial cells (VECs) and valvular interstitial cells (VICs) (Bakhshian Nik et al., 2017). EVs are released by VICs can influence VECs, and transfer of VIC-derived EVs containing perinuclear proteins to VECs cultures reveals intercellular vesicle transfer through the endosomal pathway (Krohn et al., 2016a; Bakhshian Nik et al., 2017).

MVs, another kind of EVs, are approximately 100–300 nm in diameter, membrane-invested particles, and can be located in the ECM (Bottini et al., 2018). Under physiological conditions, MVs can be released from hypertrophic chondrocytes, osteoblasts, odontoblasts, and tenocytes. In addition, some non-skeletal tissue cells such as VSMCs, in dead or dying macrophages, and VICs also release pathological MVs (Bakhshian Nik et al., 2017). Pro-vascular calcification MVs contain reactive oxygen species and pro-inflammatory cytokines. While inhibiting vascular calcification MVs secret anti-inflammatory factors and retards VSMCs to differentiate into osteoblast-like cells (Li et al., 2020). Macrophage-derived MVs express exosomal

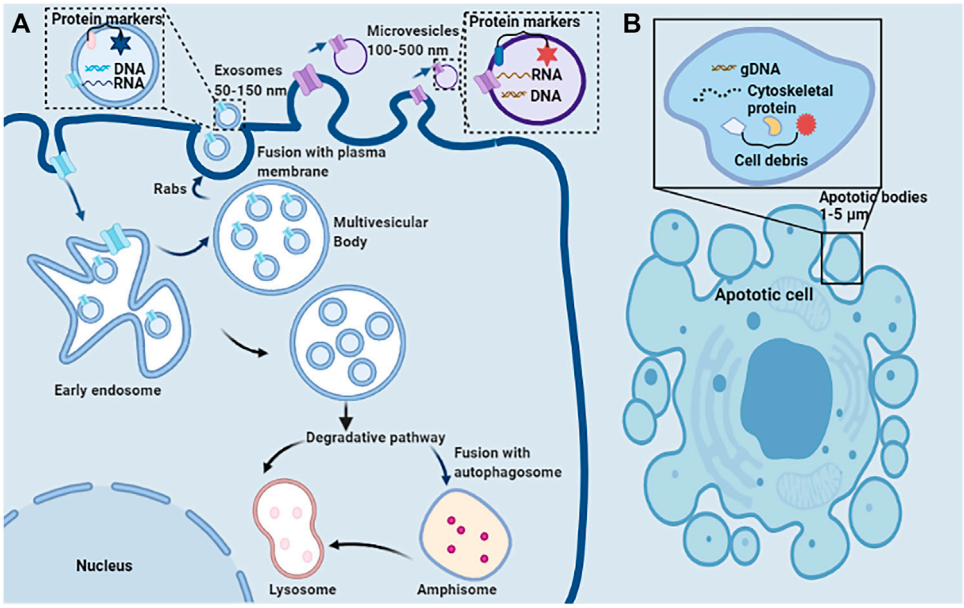

FIGURE 2 | Schematic representation of the release, structure, and composition of extracellular vesicles. **(A)** Direct sprouting and splitting of the plasma membrane deformed into microvesicles (100–500 nm in diameter). In early endosomes, proteins are sequestered in intraluminal vesicles of the larger MVBs. The inward budding of endosomal membranes forms intraluminal vesicles of MVBs. MVBs bud inward and then fuse with the plasma membrane results in the release of their enclosed exosomes (~50–150 nm) from the cell into the microenvironment. Due to its biophysical properties, MVBs can be degraded by entering the lysosome directly or fusing with autophagosome and then entering the lysosome. **(B)** Apoptotic or dying cells shrink to produce apoptotic bodies (ABs) (1,000–5,000 nm). ABs are condensed remnants of the apoptotic cell, with nuclear and cytoplasmic components.

markers (CD9 and TSG101) and contain PS-annexin A5-S100A9 membrane complex, which promotes hydroxyapatite nucleation and directly contributes to microcalcification in chronic renal disease (New et al., 2013). MVs derived from macrophages enhance ectopic mineralization in the high Ca/Pi environment (Zhang et al., 2018). VSMCs-derived MVs ranging in size from 50 to 500 nm respond by disturbing intracellular calcium homeostasis and enhance mineralization by releasing the key mineralization inhibitor matrix Gla protein loading, enhancing matrix metalloproteinase-2 activity, and forming annexin A6/PS nucleation complexes (Kapustin et al., 2011). On the other hand, circulating EVs could be taken up by recipient VSMCs, which contribute to vascular calcification in CKD, through calcification/osteogenic differentiation and inflammatory status, leading to increased mineral deposition (Viegas et al., 2018).

In calcified aortic valve disease (CAVD), the phenotypic changes of VICs play a vital role in ECM remodeling and mineral deposition (Bakhshian Nik et al., 2017). Under pathological conditions, such as hyperphosphatemia, VICs can differentiate into two distinct phenotypes: an activated myofibroblast-like VIC (aVIC) or an osteoblast-like VIC (oVIC), which are responsible for the active deposition of Ca in CAVD (Hjortnaes et al., 2015). In this calcifying milieu, pro-calcific VIC-derived EVs are similar to MVs from chondrocytes and VSMCs, showing elevated annexins A2, A5 and A6 (Bakhshian Nik et al., 2017). In the standard Ca/Pi calcification environment, the expression of vascular calcification-associated protein annexin A6 and Ca content were significantly up-regulated in rat VICs derived MVs (Cui et al., 2017). Through bioinformatics analysis techniques, MVs from calcified VICs were analyzed to reveal calcification regulators and exosome markers, including CD9, CD63, LAMP-1, and LAMP-2 (Cui et al., 2017).

Based on the above content, MVs should not be confused with microvesicles according to their different biogenesis type, particle size, and functional location.

STRATEGIES AND OPPORTUNITIES TO MODIFY MATRIX VESICLES TO TREAT VASCULAR CALCIFICATION

Nucleation and Crystallization of Minerals

Under pathological conditions, such as inflammation or hyperlipidemia, the increased expression and activity of ALP will promote calcification, stimulating the release of phosphate from biological sources (for example, ATP) for mineral nucleation (Blaser and Aikawa, 2018). In this process, the multiligand sorting receptor sortilin in EVs regulates the release of EVs and drives the activated ALP to load into calcifying EVs in a Rab11-dependent manner (Blaser and Aikawa, 2018). Importantly, MVs are a cell product that can be used as sites for hydroxyapatite crystal precipitation. The origin and content of MVs are essential factors in determining their mineralization potential (Kapustin et al., 2011). MVs can obtain mineral compounds to maintain intracellular mineral

metabolic homeostasis and participate in the process of vascular calcification by promoting mineral deposition sites formation (Zhang et al., 2018). Elevated extracellular Ca and cytosolic Ca alterations are necessary to produce the mineralization-competent MVs (Kapustin et al., 2011). In the presence of high Ca, VSMCs can release more mineralization-competent MVs, which are filled with microspicules of crystalline mineral, predominantly composed of Ca, which would lead to matrix mineralization (Reynolds et al., 2004). Unlike the cell membrane composition, MVs are rich in annexins, sphingomyelins, and PS, which are vital mineral nucleation sites on the MVs membrane (Genge et al., 2007). Upon the stimulation of Ca and phosphate, calcification inhibitor is suppressed, and annexins/PS nucleation complexes is formed, providing hydroxyapatite nucleation sites (Kapustin et al., 2011; New et al., 2013). Meanwhile, the MVs membrane also contains calcification inhibitors such as fetuin-A and MGP, which prevent mineral nucleation (Reynolds et al., 2004). In calcifying EVs, the homeostasis between calcification inhibitors and promoters is broken, resulting in a loss of mineralization inhibition.

MiRNAs in Matrix Vesicles Regulate the Process of Vascular Calcification

For the reason that the lipid bilayer of EVs can protect the small RNAs from degradation by extracellular ribonuclease and proteases (Blaser and Aikawa, 2018), small RNAs such as ribosomal RNA (rRNA), miRNAs, and transfer RNA (tRNA) are enriched in EVs. Interestingly, the total miRNA contained in EVs is higher, while the total RNA is less than the donor cells (Chaturvedi et al., 2015). MiRNAs in EVs could be transported and regulate the proliferation and differentiation of recipient cells. Furthermore, it also mediates intercellular communication during the vascular calcification process (Goettsch et al., 2013). In uraemic rats EVs, the expression of miR-221 and miR-222 were significantly enhanced, and the levels of miR-143 and miR-145 were significantly reduced. These EVs can participate in the phenotypic switch and the calcification of VSMCs *via* enhanced AKT signaling and PiT-1 expression (Freise et al., 2021). Endothelial cell-derived EVs are selectively loaded with miR-126, miR-143, and miR-145, which participate in VSMCs phenotype regulation by mediating paracrine signaling across cells within the vessel wall (Krohn et al., 2016a). Bone marrow mesenchymal stem cells derived exosomes inhibited high P-induced calcification in VSMCs through modifying miRNA profiles. The mTOR, MAPK, and Wnt signaling pathways were involved in this process (Guo et al., 2019). On the other hand, many miRNAs in EVs are also involved in inhibiting the function of vascular calcification. MiR-30, miR-125-b, miR-143, miR-145 and miR-155 loaded into calcifying VSMCs-derived EVs can influence the expression of a specific set of osteogenic markers such as Smad1, RUNX-2, ALP, and osterix, and change in the concentrations of these miRNAs in EVs lead to shifts in Ca and MAPK signaling pathways implicated in SMC-mediated calcification (Krohn et al., 2016a). Melatonin-induced exosomes miR-204 and miR-211 inhibit the osteogenic differentiation of VSMCs by reducing RUNX2 and BMP2 expression and ALP activity (Xu et al., 2020). Exosome-derived miR-324-3p regulate the expression levels of the IGF1R, MAP2K1 and PIK3CA proteins in the mouse smooth muscle cell line (MOVAS-1) and inhibit coronary artery calcification (Pan et al., 2020).

In the mineralization environment, especially the vascular calcification process, some miRNAs in MVs facilitate deposition of Ca orthophosphate, which can change Ca phosphate structure from an amorphous form to more crystalline structures, such as hydroxyapatite; some miRNAs have the opposite effect, inhibiting mineral deposition (Krohn et al., 2016a). In VMSCs from CKD rats, miR-667, miR-702, miR-3562, miR-3568, and miR-3584 are highly concentrated in MVs (Chaturvedi et al., 2015). Some miRNAs contained in MVs can regulate the phenotype of recipient cells. These studies indicate that the dysregulation of miRNAs in MVs may promote vascular calcification by causing abnormal mineral deposits, promoting hydroxyapatite's formation, or by driving the transformation of VSMCs phenotype from a contractile to a synthetic and osteochondrogenic phenotype. MVs also act as carriers to transfer dysregulated miRNAs from cell to cell to induce changes in the function of the recipient cells, which leads to vascular calcification.

Proteins Associated With Vascular Calcification in Matrix Vesicles

MVs contain a large number of proteins, each of which has specific characteristics and performs its specific functions in mineral deposits. The endogenous protein in MVs could be divided into three groups, inhibitors, promoters, and other proteins. The inhibitors in MVs, such as MGP, Gla-rich protein (GRP), and fetoglobulin A (fetuin-A) (Kapustin et al., 2015), suppress the calcification, while the promoters in MVs such as annexin family, sortilin, and S100 protein family aggregate the calcification. Finally, other proteins functionally regulate MVs secretion.

Inhibitors in Matrix Vesicles

MGP is a 15-kDa vitamin K-dependent mineral binding protein, which is widely expressed in VSMCs and chondrocytes (Bjorklund et al., 2020). MGP is known as an effective inhibitor of Ca phosphate precipitation, which can inhibit aortic and cartilage calcification (Xiao et al., 2021). The reason why MGP exerts an anti-calcfication role is that carboxylated and phosphorylated MGP could eliminate the calcification effect of various bone morphogenetic proteins (BMPs) such as BMP-2 and BMP-4 (Houben et al., 2016; Bjorklund et al., 2020; Khan et al., 2021). In addition, MGP-fetuin-A complex inhibits ectopic mineralization by combining with alkaline Ca phosphate crystals (Xiao et al., 2021). MGP is a potent inhibitor of ECM mineralization; deficiency of MGP initiates arterial calcification (Khavandgar et al., 2014). Deposits of hydroxyapatite minerals were shown in the arterial wall of MGP-deficient ($Mgp^{-/-}$) mice, which died within 2 months (Khavandgar et al., 2014). The anti-calcification function of MGP is most likely related to the formation of MVs (Bjorklund et al., 2020). The elevated Ca

concentration decreases the MGP expression in MVs, while a similar result is not observed upon high concentration of phosphate (Houben et al., 2016).

GRP (Gla-rich protein) is an inhibitor of vascular calcification involved in Ca homeostasis, and γ-carboxylated GRP could inhibit calcification and osteochondrogenic differentiation by α-SMA upregulation and osteopontin downregulation (Viegas et al., 2015). GRP was expressed at protein and mRNA levels in EVs released by macrophages, which may act as vehicles for ECM transport and information transmission (Viegas et al., 2017). It prevents Ca-induced signaling pathways and directly binds to minerals to inhibit crystal formation (Viegas et al., 2015). Ucma/GRP (Upper zone of growth plate and cartilage matrix-associated protein/Gla-rich protein) can directly interact with BMP2 and regulate phosphate-induced mineralization of VSMCs by participating in BMP-2-SMAD1/5/8 osteo/chondrogenic signaling pathway *in vitro* (Willems et al., 2018). GRP can form a large complex with MGP and fetuin-A, which is loaded in noncalcified EVs; the ratio of the complex is decreased in the high Ca-loaded vesicles (Xiao et al., 2021). Additionally, they can also combine with minerals to form a fetuin-mineral complex called colloids calciprotein particles (CPP), which greatly affects the stability of minerals (Xiao et al., 2021). Circulating CPPs and EVs, which contain lower levels of fetuin-A and GRP, are determinants of vascular calcification in CKD, with the capacity to modulate VSMCs responses through increased osteochondrogenic differentiation and inflammation, leading to increased mineral deposition (Viegas et al., 2018).

Fetuin-A is a plasma glycoprotein from the family of cystatin protease inhibitors with a TGF-β cytokine-binding motif and a Ca phosphate-binding site that can inhibit the precipitation of basic calcium phosphate *in vitro* (Khan et al., 2021). Fetuin-A is one of the biomarkers acting as calcification inhibitors, and it plays an important role in ectopic calcification. The possible mechanisms of fetuin-A involved in ectopic vascular calcification include inhibiting spontaneous mineral nucleation and growth and inhibiting the formation of hydroxyapatite crystals; combining clusters of Ca and phosphate to stabilize these ions and preventing cellular uptake; mediating the formation of protein mineral CPP (Icer and Yildiran, 2021). Fetuin-A can be loaded into MVs, which maintains the phenotype of healthy VSMCs and also binds minerals and stabilizes them against further growth, preventing vesicles from mineralizing (Chen and Moe, 2015; Kapustin et al., 2015).

Osteoprotegerin (OPG) is known to be a soluble tumor necrosis factor (TNF) superfamily receptor that inhibits the actions of the cytokine receptor activator of nuclear factor kappa-B ligand (RANKL) (Montanez-Barragan et al., 2014). OPG was also detected in VSMCs- derived MVs and co-located with annexin A6 (Cui et al., 2016). Under physiological conditions, OPG can be secreted by vesicles released from viable or apoptotic VSMCs and directly inhibit VSMCs mineralization by limiting MVs driven mineral nucleation and hydroxyapatite deposition in the vascular wall (Cui et al., 2016).

Promoters in Matrix Vesicles

As the membrane factors of MVs, the annexin family members A2, A5, and A6 mediate Ca influx into MVs and are well-known calcification promoters (Kapustin et al., 2011). The massive enrichment of various annexins in calcifying MVs may be a key factor in regulating MVs release and calcification potential in the cardiovascular system. For example, annexin A2 could bind to fetuin-A at the cell membrane of VSMCs in the presence of high calcium and contribute to MVs-mediated calcification. Additionally, the high level of annexin A2 might also be one of the reasons that end-stage renal disease-exosomes promote VSMCs calcification (Lin et al., 2020). Annexin A6 was enriched in calcifying VIC-derived MVs, and these MVs may promote aortic valve calcification in end-stage renal disease (Cui et al., 2017). Most importantly, annexin A6, the largest member of the annexin family, is present highly in MVs. Biochemical analyses revealed annexin A6 could have three different localizations in MVs during physiological mineralization. They are Ca^{2+}-bound annexin A6 interacting with the inner leaflet of the MVs membrane; annexin A6 localized on the surface of the outer leaflet; and annexin A6 inserted in the membrane's hydrophobic bilayer and co-localized in lipid domains enriched in cholesterol (Veschi et al., 2020). Moreover, annexin A6 and Ca induced PS exposure on the MVs surface and formed of annexin A6/PS nucleation complexes, thus providing hydroxyapatite nucleation sites (Hjortnaes et al., 2015).

Sortilin is a sorting receptor that directs target proteins, including growth factors, signaling receptors, and enzymes, to the secretary or endocytic compartments of cells. Sortilin expression levels are atypically high in calcified arteries in CKD and atherosclerosis disease. Moreover, sortilin deficiency reduces vascular but not skeletal calcification *in vivo,* indicating that sortilin might be a key regulator of vascular calcification (Goettsch et al., 2016). Sortilin plays a direct role in ectopic calcification and has become a potential cardiovascular risk biomarker and a drug target for cardiovascular disease (Gebraad et al., 2018). In older men aged ≥50 years, higher serum sortilin levels are associated with a higher risk of major adverse cerebrovascular and cardiovascular events (MACCE) and severe abdominal aortic calcification (AAC) (Goettsch et al., 2017). The receptors for AGEs (RAGE) down-regulated sortilin and mediated the formation of microcalcification, whereas galectin-3 up-regulated sortilin and induced macrocalcification (Sun et al., 2019).

Sortilin could traffic and load the calcification protein TNAP into VSMC-derived EVs, conferring its calcification potential (Itoh et al., 2018). Sortilin forms homodimers in the extracellular and intracellular domains with intermolecular disulfide bonds, which likely facilitate the trafficking of sortilin to the EVs (Itoh et al., 2018). Sortilin could accelerate the formation of MVs aggregates in the early stage of calcification and affect the microcalcification signals (Sun et al., 2019). In a diabetic apolipoprotein E-deficient background ($ApoE^{-/-}$) mouse model, mouse tail vein injection of Nε-Carboxymethyl-lysine (CML)-induced MVs originated from VSMCs-derived obviously aggravated diabetic atherosclerotic calcification (Jing et al., 2020). High concentrations of CML significantly promoted

the release of MVs from VSMCs and the recruitment of sortilin to MVs (Jing et al., 2020).

The S100 protein family has 21 members, which can be released from monocytes, VSMCs, and ECs in response to cellular stress stimuli. Some members of the S100 proteins family, such as S100A8, S100A9, and S100A12 have homologous structures and functions, commonly known as S100/calgranulins, and are closely related to cardiovascular disease (Xiao et al., 2020). These proteins bind with their receptors, such as advanced glycation end products (RAGE), scavenger receptors (CD36), and toll-like receptor 4 (TLR-4), contributing to the cellular response in vascular inflammation, vascular oxidative stress, and vascular calcification progression (Xiao et al., 2020). Among the S100 protein family, S100A9 is closely related to cardiovascular calcifying MVs. S100A9 is the Ca^{2+}-binding neutrophil cytosolic protein, which is strongly expressed in calcifying areas, the surrounding extracellular matrix, and calcifying MVs (McCormick et al., 2005). S100A9 in atherosclerotic plaque and calcifying MVs may be involved in the pathogenesis of atherosclerosis and dystrophic calcification by influencing redox- and Ca^{2+}-dependent processes (McCormick et al., 2005). Macrophage S100A9 plays an important role in vascular calcification in diabetes mellitus. When exposed to high glucose, pro-inflammatory macrophages-derived calcific EVs through the S100A9-RAGE axis contribute to the excessive microcalcification formation within plaques (Kawakami et al., 2020).

MMP-2, also known as gelatinase A, was involved in the process of vascular calcification. MMP-2 facilitates vascular calcification by catalyzing matrix degradation (Kapustin and Shanahan, 2016). The active form of MMP-2 is also found in VSMCs derived MVs, and elevated levels of extracellular Ca can induce enhanced MMP-2 activity. Inhibiting the activity of MMP-2 loaded in MVs can prevent vascular calcification (Kapustin and Shanahan, 2012).

Transglutaminase 2 (TG2) is a Ca-dependent enzyme that can facilitate cell-ECM interaction through integrins (Chen et al., 2013). TG2 becomes the core of inducing the arterial calcification program by promoting VSMCs transdifferentiation to osteoblasts and chondrocytes (Johnson et al., 2008). The expression of TG2 is increased in both VSMCs and MVs isolated from CKD rats. The cross-linking of the ECM with TG2 leads to enhanced cell-ECM and MVs-ECM attachment, induced phenotypic switch of VSMCs to contractile "osteoblast-like" cells, and reduced function of calcification inhibitors (Chen et al., 2013).

The phosphatase orphan 1 (PHOSPHO1), contained in MVs, as an additional inorganic phosphate (Pi) supplier was involved in the first step of MVs-mediated initiation of mineralization (Kiffer-Moreira et al., 2013; Bobryshev et al., 2014).

The Regulator Controlling Matrix Vesicles Secretion

Sphingomyelin phosphodiesterase-3 (SMPD3) is not only a key signal molecule in the process of biomineralization but also a regulator of exosomal biogenesis. In VSMCs, elevated extracellular Ca increased SMPD3 expression. In turn, the up-regulation of SMPD3 could regulate exosome secretion and fetuin-A recycling (Kapustin et al., 2015). Increased ceramide in cell membrane or cytoplasm through the SMPD3 pathway may induce sEVs biogenesis, initiating arterial calcification (Bhat et al., 2020a). Lysosomal overexpression of *Smpd1* gene specifically in VSMCs may reduce lysosome-MVB interactions, which may reduce lysosome degradation of MVBs and increase the fusion of MVBs with the plasma membrane to release sEVs, and consequently leading to medial arterial calcification (Bhat et al., 2020a).

High mobility group box 1 (HMGB1), a nuclear protein that binds to chromatin, is usually released into the extracellular space as a damage-associated molecular pattern (DAMP) when cells are activated, damaged, or die (Chen et al., 2017). HMGB1 is also a cytokine associated with biological mineralization and could induce macrophages to secrete MVs through the RAGE/p38MAPK/nSMase2 signaling pathway to enhance ectopic mineralization (Chen et al., 2016). BMSC-derived exosomes alleviate high phosphate-induced aortic calcification and ameliorate vascular function *via* the SIRT6–HMGB1 deacetylation (Wei et al., 2021).

Microtubule stabilization inhibited hyperphosphatemia-induced vascular calcification by down-regulation of osteogenic signal and attenuation of MVs release (Lee et al., 2014). *Mucolipin 1* Gene deletion in mice increased sEVs secretion by inhibiting lysosomes and MVB interactions in arterial stiffening and medial calcification. The expression of exosome/sEVs markers, CD63, and annexin A2 were significantly increased in the coronary arterial wall of $Mcoln1^{-/-}$ mice (Bhat et al., 2020b). Endoplasmic reticulum (ER) stress induces calcification of VSMCs *in vitro* and modifies VSMCs phenotype by increasing the release of Grp78-loaded calcifying EVs (Furmanik et al., 2021).

The interaction between EVs and ECM accelerates the extracellular accumulation and aggregation of calcifying EVs. In human atherosclerotic plaque formation, a large amount of disorganized collagen will accumulate before calcification begins. However, the content of collagen is inversely proportional to the size of microcalcifications: when collagen is degraded, EVs can aggregate, nucleate hydroxyapatite and form microcalcifications (Blaser and Aikawa, 2018). Many high levels of collagen-binding proteins such as ALP, proteoglycan link proteins, hyaluronic-acid binding regions, and annexins are also found in calcifying EVs (Blaser and Aikawa, 2018). It indicated that the collagen protein inhibits the accumulation of EVs. The MVs secreted by VSMCs can locate close to collagen fibrils and interact with collagen type I (COL1) in VSMCs under calcifying conditions (Tyson et al., 2003). Fetuin-A, MGP, S100A9, and annexins have emerged as active regulators of this interaction (Reynolds et al., 2004). 8-degree-polymerized oligogalacturonic acid prevents vascular calcification development by inhibiting the osteogenic marker expression and dissociating the direct interaction between MVs and COL1 (Hodroge et al., 2017). In particular, this interaction can be inhibited by masking the GFOGER sequence, which reveals the specific areas on the collagen fibers that bind to EVs (Krohn et al., 2016b; Hodroge et al., 2017). The collagen receptor discoidin domain receptor-1 (DDR-1) can regulate

collagen deposition and release of calcifying EVs by VSMCs through the TGF-β pathway. In calcification media, *DDR-1*$^{-/-}$ VSMCs increased the release of TGF-β1, which can stimulate P38 phosphorylation and inhibit the activation of SMPD3, thereby promoting EVs-mediated calcification and collagen matrix production (Krohn et al., 2016b).

The Signal Pathway Involved in Matrix Vesicles Regulating Vascular Calcification

During the vascular calcification process, the production and release of cellular MVs is the first step, while the uptake of MVs by recipient cells is also essential. The detailed molecular mechanisms regulating MVs secretion and inclusions in vascular calcification are quite complicated. For instance, uraemic EVs augment Ca- and phosphate-induced osteogenic transdifferentiation of VSMCs *via* activated AKT and ERK signaling and PiT-1 expression (Freise et al., 2021). The lysosomal sphingolipid/ceramide pathway may be crucial participants in the secretion of sEVs and phenotypic switch in arterial VSMCs (Bhat et al., 2020a). Warfarin is known to be an oral anticoagulant and an effective inducer of calcification, which could increase EVs release and VSMCs calcification *via* the PERK-ATF4 ER stress pathway (Furmanik et al., 2021). The autophagy pathway may be a key participant in the regulation of MVs-mediated vascular calcification progression (Dai et al., 2013). Through bioinformatic analysis using Ingenuity Pathway Analysis (IPA) revealed the up-regulation of key signaling pathways crucial to cardiovascular function in calcifying VIC-derived MVs in end-stage renal disease, including aldosterone, P2Y purinergic receptor signaling, and thrombin signaling pathways, Rho signaling, and metal binding (Cui et al., 2017). Cellular-derived MVs with characteristics of exosomes and low fetuin-A content from calcifying VSMCs of rats with CKD enhanced the calcification of recipient VSMCs by inducing cell signaling changes and phenotypic switch of recipient VSMCs (Chen et al., 2018). Several major cell signaling pathways were involved in this process: 1) mitogen-activated protein kinase (MAPK) signaling specifically, increased MEK1 and ERK signaling; 2) increased intracellular Ca from sarcoplasmic reticulum stress; 3) increased NADPH oxidase (NOX) and superoxide dismutase (SOD) activity; 4) activation and increased intracellular Ca, leading to reducing VSMCs calcification (Chen et al., 2018). EVs secreted from both patients with acute coronary syndrome and senescent ECs induce early senescence of recipient endothelial cells and cellular oxidative stress. MAPK, Akt, and p53 signaling pathways may be involved in this process (Blaser and Aikawa, 2018).

TOOLBOX: ISOLATION AND VALIDATION OF MATRIX VESICLES

Ultracentrifugation

UC is the most commonly used method for MVs purification at present. Differential centrifugation can be used to separate vesicles of similar sizes. UC is usually used in conjunction with sucrose density gradient centrifugation to separate low-abundance small vesicles (Hutcheson et al., 2014). Although this combined method can obtain highly purified MVs, it also has some disadvantages: the steps are complicated with an inconsistent recovery rate. Most importantly, repeated centrifugation is likely to disrupt vesicles and reduce their quality. Some soluble proteins may contaminate the sample by forming clumps with the vesicles, potentially impacting proteomic and RNA content analysis (Lobb et al., 2015).

Ultrafiltration

MVs can also be obtained by selective separation of samples with ultrafiltration membranes of different pore sizes. Compared to UC, UF is less time-consuming and does not require the use of special equipment (Cheruvanky et al., 2007). The combination of UF and size exclusion chromatography (UF/SEC) is superior to the traditional UC method in terms of production time, standardization, scalability, and vesicle yield. Compared with traditional UC, using UF/SEC, approximately 400 times more small extracellular vesicles (sEVs) per ml of media were recovered, and upscaling this process further increases sEVs yield by about 3-fold (Cardoso et al., 2021).

Magnetic Bead Sorting

CD63, CD31, CD9, 70 kDa heat shock proteins (HSP70), and tumor susceptibility gene 101 (TSG101) are the well-known marker genes of MVs. After the MVs are incubated with magnetic beads coated with anti-label antibodies, they can be adsorbed and separated. Using a process of immunoprecipitation based on polymeric beads that were modified with an antibody for tissue nonspecific alkaline phosphatase (TNALP), MVs were isolated from an organotypic culture model (Iordachescu et al., 2018). The magnetic bead sorting method has the advantages of high specificity, simple operation and can maintain the complete shape of MVs (Kluszczynska et al., 2019). However, antigen-antibody binding requires sufficient time for action, so this method generally has the problem of time-consuming operation and low extraction efficiency (Lane et al., 2017), and it may also be affected by the pH value and salt concentration of the separation solution.

Polymer-Based Precipitation

Because of its simplicity and feasibility, polymer-based precipitation such as polyethylene glycol (PEG) precipitation has gained popularity. After incubating with PEG at 4°C, the MVs are precipitated and recovered by filtration or centrifugation. Although this method is effective in obtaining small EVs (sEVs), some of the non-sEV contaminants are also precipitated at the same time (Nakai et al., 2016). Therefore, this method is not commonly used due to the shortcomings of low vesicle recovery rate, low purity, and uneven particle size of isolated MVs (Lobb et al., 2015).

In recent years, various extraction kits have been used for the isolation of MVs. These kits are increasingly popular because of their simple operation, high extraction efficiency, and the ability to extract urine, blood, cell supernatant, and other samples

separately. Researchers have developed other methods, including HPLC (high-performance liquid chromatography)-based protocols (Zeringer et al., 2015), affinity-capture methods (Iordachescu et al., 2018), microfluidic-based isolation of vesicles methods (Wang et al., 2013), acoustic-based purification methods (Lee et al., 2015), etc. Each of these separation methods has its unique advantages, but their disadvantages also limit their wide use.

THE IDENTIFICATION METHODS OF MATRIX VESICLES

Nanoparticle Tracking Analysis

NTA is one of the most commonly used methods to count the number of MV particles. NTA can analyze the size of small vesicles particles in batches and obtain a particle size distribution curve (Hoshino et al., 2020). It is easy to operate and can protect the structure and function of MVs from damage. However, the concentration of the sample particles greatly influences the results. Therefore, to obtain stable and reliable results, the sample needs to be diluted to an appropriate concentration.

Protein Marker Detection

Enzyme-linked immunosorbent assay (ELISA), flow cytometry and western blot can be used to detect MVs protein markers. Commonly used markers include CD31, CD9, CD63, annexins, integrin receptors, TSG101 and HSP70 (Shapiro et al., 2015).

Quantitative Real Time-Polymerase Chain Reaction Analysis

qRT-PCR is the most sensitive and reliable method to detect gene expression. MVs contain a large number of microRNAs and these microRNAs play an important role in the formation of mineral nucleation sites and the osteogenic differentiation of VSMCs. qRT-PCR is an indispensable method for studying these microRNAs (Sohn et al., 2015). At the same time, a bioanalyzer and droplet digital PCR(ddPCR) can be used to detect the RNA quality and quantity of MVs load.

Electron Microscopy

Transmission electron microscopy (TEM) is a standard morphological detection method for MVs. The particle size of MVs can be observed by TEM, and the MVs are spherical and cup holder-like structures (Greening et al., 2015). Now some laboratories are also beginning to use atomic force microscopes to look at the shape of vesicles. Density-dependent scanning electron microscopy (SEM) can image calcifying EVs *in-situ*, and assess their size, density, and biophysical accumulation in calcified tissues, hydrogels, or matrices (Blaser and Aikawa, 2018). With the help of super-resolution microscopy, it is possible to obtain *in situ* imaging of vesicles using confocal light-based approaches (Blaser and Aikawa, 2018).

Immunogold Labeling

Immunogold labeling is a kind of immunolabeling technology that uses colloidal gold as a tracer to participate in the antigen-antibody response. Exosomes were incubated with primary antibody and the secondary antibody conjugated to gold particles and then observed under an electron microscope after washing and counter staining (Hannafon et al., 2016). It has the advantages of simple and quick operation, high sensitivity, and stable markers.

DISCUSSION

Vascular calcification is a complex, active and highly regulated biological process. As important transporters for material transport and intercellular communication, MVs are closely related to vascular calcification. MVs can participate in vascular calcification by promoting the phenotypic transformation of VSMCs, regulating mineral deposits, mediating microRNAs transport, regulating cell signaling pathways (**Figure 3**).

MVs are endogenous nanovesicles secreted by living cells. Therefore, they are more suitable as therapeutic drug carriers due to their advantages of small particle size, low toxicity, non-immunogenicity, good permeability, and high targeting. Recent studies have shown that VSMCs-derived MVs have shown positive results in many disease models, such as reducing the size of myocardial infarction and improving the inflammation caused after myocardial infarction, resolving pulmonary hypertension, ameliorating renal fibrosis, and restoring neurovascular functions and plasticity (Blaser and Aikawa, 2018). In addition to using MVs as delivery vehicles, the contents of calcifying EVs themselves have also been proven to be an essential source of drug targets (Blaser and Aikawa, 2018). Therefore, MVs may be a new treatment for vascular calcification.

Additionally, researchers have successfully used exosomes to carry small molecules, nucleic acids, and proteins to treat various diseases in recent years. It may be possible to use exogenous engineered EVs as a viable therapeutic strategy for vascular calcification, whereby inhibitors of vascular calcification could be efficiently conveyed into atherosclerotic plaques or vascular microcalcification areas. However, the use of EVs as a nano-drug delivery system is still in its infancy in treating diseases, and researchers are still facing many problems and challenges, such as the low rate of drug encapsulation in EVs (Gaurav et al., 2021). So far, there is not a feasible method to treat vascular calcification. Some potential medications that address vascular calcification have been studied only in preclinical setups or lack extensive clinical research. Potential medications and treatment methods for addressing vascular calcification are listed in **Table 2**. The role of MVs in the occurrence and development of vascular calcification has not been clearly studied. We have not fully understood, under pathophysiological conditions, how the effective or key molecules in MVs change. This may be due to the disrupted

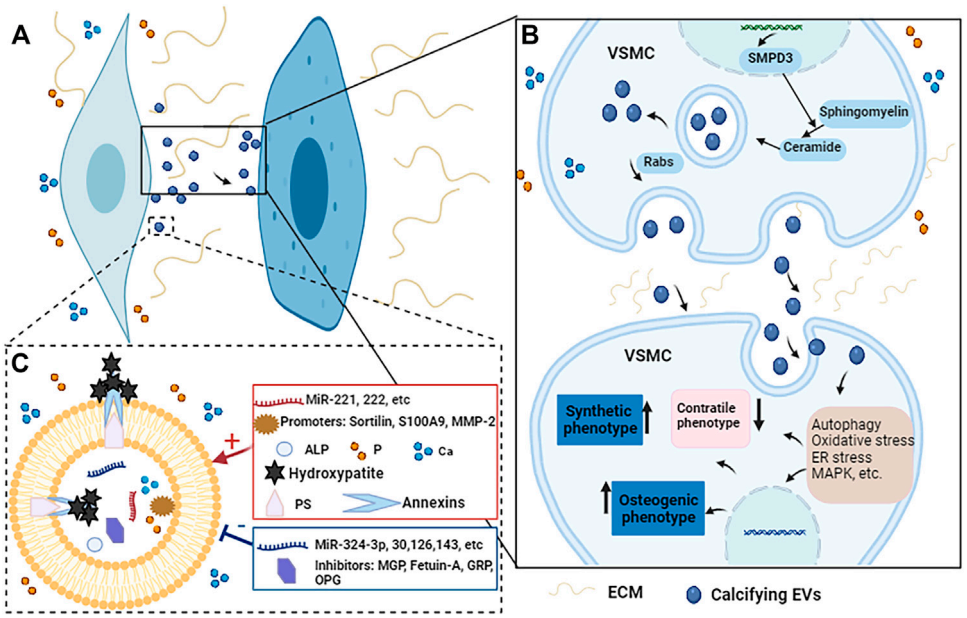

FIGURE 3 | The potential regulatory mechanisms of calcifying EVs regulate the phenotypic switch and osteogenic differentiation of VSMCs during vascular calcification. **(A)** When VSMCs are exposed to elevated Ca and P conditions, the calcifying EVs it releases act on the recipient VSMCs to change their phenotype and biological function. **(B)** Under pro-calcific milieu, SMPD3 can enhance the secretion of exosomes, which are secreted in a Rabs-dependent manner. Calcifying EVs can regulate the phenotypic transformation and osteogenic differentiation of recipient VSMCs through multiple signaling pathways such as autophagy, oxidative stress, ER stress, and MAPK, etc. **(C)** Moreover, the composition of calcifying EVs determines its potential to load hydroxyapatite. When EVs are exposed to high Ca and P conditions, the balance between calcification promoters and inhibitors in EVs is broken, increasing the content of promoters such as Ca, P, microRNAs, and annexins. At the same time, the concentration of some inhibitors such as MGP, fetuin-A, and some microRNAs is reduced. Therefore, the mineral concentration gradient between the intra- and extra-vesicular spaces drives the influx of P and Ca into EVs *via* suitable transporters to form mineral nucleation sites. The annexins and PS complexes provide hydroxyapatite nucleation sites, leading to calcifying EVs and microcalcification.

TABLE 2 | Potential medications and treatment methods to treat vascular calcification.

Potential medications and treatment methods	References
Piperlongumine	Shi et al. (2020)
Sevelamer	Drueke and Floege (2020)
Sodium thiosulfate	Omarjee et al. (2020)
SNF472, the hexasodium salt of phytate	Perello et al. (2020)
Denosumab and bisphosphonates	Florea et al. (2020); Goody et al. (2020)
Inositol phosphates derivatized with ethylene glycol oligomers	Schantl et al. (2020)
Mitoquinone	Cui et al. (2020)
Biguanide (Metformin), dipeptidyl Peptidase-4 inhibitors, sulfonylureas, sodium glucose cotransporter-2 inhibitors, thiazolidinediones, insulin, alpha glucosidase inhibitors	Ghosh et al. (2020)
ATP-based therapy	Villa-Bellosta (2019)
Teniposide	Liu et al. (2018)
Estrogen, growth hormone-releasing hormone and its agonist	Shen et al. (2018)
Fibulin-3	Luong et al. (2018)
Phosphate binders, statins, vitamin K	Florea et al. (2020)
Zinc sulfate	Voelkl et al. (2018b)
Locking with ^{18}F-NaF and loading with vitamin K	Florea et al. (2020)
Intravascular lithotripsy	Brinton et al. (2019)

balance between the promoters and inhibitors, the content of mirRNA-30, 125b, 126, 143, 145, fetuin-A, MGP, and GRP that inhibit calcification in MVs is reduced; in contrast, mirRNA-221, 222, annexins, MMP-2 are increased. How do the effective molecules interact with each other? For example, PS exposed on the outside of MVs membrane can bind to GRP and interact with annexins to form complexes that determine the formation of nucleation sites. How are the effective molecules packaged into the MVs? MVs are small in size, easy to penetrate biofilm, and lipid bilayer membrane structure can protect the small

RNAs and proteins in EVs from degradation by extracellular ribonuclease and proteases. MVs can enrich signal molecules and make them have a higher local concentration. How are MVs generated and released? SMPD3 is a key protein regulating MVs production. The small Rab GTPases such as Rab11, Rab27, Rab35 regulate MVs secretion by different ways mediating the transport of MVBs toward the plasma membrane. How are the targeted transport of MVs regulated, and how do target cells recruit and activate MVs? This may be because in pathological environments, MVs can induce receptor-mediated signal transduction *via* surface-binding ligands; deliver specific functional proteins and miRNAs to target cells through cells surface receptors. In order to find out the specific treatment methods of vascular calcification based on MVs for vascular calcification in future studies, we can focus on mineralization-related proteins and miRNAs in MVs, and we could use MVs as carriers to develop safer and more effective nanomedicines.

AUTHOR CONTRIBUTIONS

TL, HY, and XL designed the scope of the review. TL and HY wrote the manuscript. DZ, TF, MM, and JL performed the document searching and prepared the figures. XL and JL guided the planning and critically edited the manuscript. All authors read and approved the final manuscript.

FUNDING

This study was supported by the National Natural Science Foundation of China (11932014 and 31971239).

REFERENCES

Aday, S., Zoldan, J., Besnier, M., Carreto, L., Saif, J., Fernandes, R., et al. (2017). Synthetic Microparticles Conjugated with VEGF165 Improve the Survival of Endothelial Progenitor Cells via microRNA-17 Inhibition. *Nat. Commun.* 8 (1), 747. doi:10.1038/s41467-017-00746-7

Alique, M., Ruíz-Torres, M. P., Bodega, G., Noci, M. V., Troyano, N., Bohórquez, L., et al. (2017). Microvesicles from the Plasma of Elderly Subjects and from Senescent Endothelial Cells Promote Vascular Calcification. *Aging* 9 (3), 778–789. doi:10.18632/aging.101191

Bakhshian Nik, A., Hutcheson, J. D., and Aikawa, E. (2017). Extracellular Vesicles as Mediators of Cardiovascular Calcification. *Front. Cardiovasc. Med.* 4, 78. doi:10.3389/fcvm.2017.00078

Bhat, O. M., Yuan, X., Cain, C., Salloum, F. N., and Li, P. L. (2020a). Medial Calcification in the Arterial wall of Smooth Muscle Cell-specific Smpd1 Transgenic Mice: A Ceramide-mediated Vasculopathy. *J. Cel Mol Med* 24 (1), 539–553. doi:10.1111/jcmm.14761

Bhat, O. M., Yuan, X., Camus, S., Salloum, F. N., and Li, P.-L. (2020b). Abnormal Lysosomal Positioning and Small Extracellular Vesicle Secretion in Arterial Stiffening and Calcification of Mice Lacking Mucolipin 1 Gene. *Ijms* 21 (5), 1713. doi:10.3390/ijms21051713

Bjørklund, G., Svanberg, E., Dadar, M., Card, D. J., Chirumbolo, S., Harrington, D. J., et al. (2020). The Role of Matrix Gla Protein (MGP) in Vascular Calcification. *Cmc* 27 (10), 1647–1660. doi:10.2174/0929867325666180716104159

Blaser, M. C., and Aikawa, E. (2018). Roles and Regulation of Extracellular Vesicles in Cardiovascular Mineral Metabolism. *Front. Cardiovasc. Med.* 5, 187. doi:10.3389/fcvm.2018.00187

Bobryshev, Y., Orekhov, A., Sobenin, I., and Chistiakov, D. (2014). Role of Bone-type Tissue-Nonspecific Alkaline Phosphatase and PHOSPO1 in Vascular Calcification. *Cpd* 20 (37), 5821–5828. doi:10.2174/1381612820666140212193011

Bottini, M., Mebarek, S., Anderson, K. L., Strzelecka-Kiliszek, A., Bozycki, L., Simão, A. M. S., et al. (2018). Matrix Vesicles from Chondrocytes and Osteoblasts: Their Biogenesis, Properties, Functions and Biomimetic Models. *Biochim. Biophys. Acta (Bba) - Gen. Subjects* 1862 (3), 532–546. doi:10.1016/j.bbagen.2017.11.005

Boulanger, C. M., Loyer, X., Rautou, P.-E., and Amabile, N. (2017). Extracellular Vesicles in Coronary Artery Disease. *Nat. Rev. Cardiol.* 14 (5), 259–272. doi:10.1038/nrcardio.2017.7

Brinton, T. J., Ali, Z. A., Hill, J. M., Meredith, I. T., Maehara, A., Illindala, U., et al. (2019). Feasibility of Shockwave Coronary Intravascular Lithotripsy for the Treatment of Calcified Coronary Stenoses. *Circulation* 139 (6), 834–836. doi:10.1161/CIRCULATIONAHA.118.036531

Cardoso, R. M. S., Rodrigues, S. C., Gomes, C. F., Duarte, F. V., Romao, M., Leal, E. C., et al. (2021). Development of an Optimized and Scalable Method for Isolation of Umbilical Cord Blood-Derived Small Extracellular Vesicles for Future Clinical Use. *Stem Cell Transl Med* 10 (6), 910–921. doi:10.1002/sctm.20-0376

Chaturvedi, P., Chen, N. X., O'Neill, K., McClintick, J. N., Moe, S. M., and Janga, S. C. (2015). Differential miRNA Expression in Cells and Matrix Vesicles in Vascular Smooth Muscle Cells from Rats with Kidney Disease. *PLoS One* 10 (6), e0131589. doi:10.1371/journal.pone.0131589

Chen, N. X., and Moe, S. M. (2015). Pathophysiology of Vascular Calcification. *Curr. Osteoporos. Rep.* 13 (6), 372–380. doi:10.1007/s11914-015-0293-9

Chen, N. X., O'Neill, K., Chen, X., Kiattisunthorn, K., Gattone, V. H., and Moe, S. M. (2013). Transglutaminase 2 Accelerates Vascular Calcification in Chronic Kidney Disease. *Am. J. Nephrol.* 37 (3), 191–198. doi:10.1159/000347031

Chen, N. X., O'Neill, K. D., and Moe, S. M. (2018). Matrix Vesicles Induce Calcification of Recipient Vascular Smooth Muscle Cells through Multiple Signaling Pathways. *Kidney Int.* 93 (2), 343–354. doi:10.1016/j.kint.2017.07.019

Chen, N. X., O'Neill, K. D., Dominguez, J. M., Moe, S. M., and Moe, S. M. (2021). Regulation of Reactive Oxygen Species in the Pathogenesis of Matrix Vesicles Induced Calcification of Recipient Vascular Smooth Muscle Cells. *Vasc. Med.* 26, 585–594. doi:10.1177/1358863X211024721

Chen, Q., Bei, J.-J., Liu, C., Feng, S.-B., Zhao, W.-B., Zhou, Z., et al. (2016). HMGB1 Induces Secretion of Matrix Vesicles by Macrophages to Enhance Ectopic Mineralization. *PLoS One* 11 (5), e0156686. doi:10.1371/journal.pone.0156686

Chen, Q., Wang, Z.-Y., Chen, L.-Y., and Hu, H.-Y. (2017). Roles of High Mobility Group Box 1 in Cardiovascular Calcification. *Cell Physiol Biochem* 42 (2), 427–440. doi:10.1159/000477591

Chen, Y., Wang, L., Zheng, M., Zhu, C., Wang, G., Xia, Y., et al. (2022). Engineered Extracellular Vesicles for Concurrent Anti-PDL1 Immunotherapy and Chemotherapy. *Bioactive Mater.* 9, 251–265. doi:10.1016/j.bioactmat.2021.07.012

Cheruvanky, A., Zhou, H., Pisitkun, T., Kopp, J. B., Knepper, M. A., Yuen, P. S. T., et al. (2007). Rapid Isolation of Urinary Exosomal Biomarkers Using a Nanomembrane Ultrafiltration Concentrator. *Am. J. Physiology-Renal Physiol.* 292 (5), F1657–F1661. doi:10.1152/ajprenal.00434.2006

Cozzolino, M., Ciceri, P., Galassi, A., Mangano, M., Carugo, S., Capelli, I., et al. (2019). The Key Role of Phosphate on Vascular Calcification. *Toxins* 11 (4), 213. doi:10.3390/toxins11040213

Cui, L., Houston, D. A., Farquharson, C., and MacRae, V. E. (2016). Characterisation of Matrix Vesicles in Skeletal and Soft Tissue Mineralisation. *Bone* 87, 147–158. doi:10.1016/j.bone.2016.04.007

Cui, L., Rashdan, N. A., Zhu, D., Milne, E. M., Ajuh, P., Milne, G., et al. (2017). End Stage Renal Disease-Induced Hypercalcemia May Promote Aortic Valve Calcification via Annexin VI Enrichment of Valve Interstitial Cell Derived-Matrix Vesicles. *J. Cel Physiol* 232 (11), 2985–2995. doi:10.1002/jcp.25935

Cui, L., Zhou, Q., Zheng, X., Sun, B., and Zhao, S. (2020). Mitoquinone Attenuates Vascular Calcification by Suppressing Oxidative Stress and Reducing Apoptosis of Vascular Smooth Muscle Cells via the Keap1/Nrf2 Pathway. *Free Radic. Biol. Med.* 161, 23–31. doi:10.1016/j.freeradbiomed.2020.09.028

Dai, X.-Y., Zhao, M.-M., Cai, Y., Guan, Q.-C., Zhao, Y., Guan, Y., et al. (2013). Phosphate-induced Autophagy Counteracts Vascular Calcification by Reducing Matrix Vesicle Release. *Kidney Int.* 83 (6), 1042–1051. doi:10.1038/ki.2012.482

de Abreu, R. C., Fernandes, H., da Costa Martins, P. A., Sahoo, S., Emanueli, C., and Ferreira, L. (2020). Native and Bioengineered Extracellular Vesicles for Cardiovascular Therapeutics. *Nat. Rev. Cardiol.* 17 (11), 685–697. doi:10.1038/s41569-020-0389-5

Demer, L. L., and Tintut, Y. (2014). Inflammatory, Metabolic, and Genetic Mechanisms of Vascular Calcification. *Atvb* 34 (4), 715–723. doi:10.1161/ATVBAHA.113.302070

Drüeke, T. B., and Floege, J. (2020). Cardiovascular Complications of Chronic Kidney Disease: Pioneering Studies. *Kidney Int.* 98 (3), 522–526. doi:10.1016/j.kint.2020.07.001

Florea, A., Morgenroth, A., Bucerius, J., Schurgers, L. J., and Mottaghy, F. M. (2020). Locking and Loading the Bullet against Micro-calcification. *Eur. J. Prev. Cardiol.* 28, 1370–1375. doi:10.1177/2047487320911138

Freise, C., Querfeld, U., Ludwig, A., Hamm, B., Schnorr, J., and Taupitz, M. (2021). Uraemic Extracellular Vesicles Augment Osteogenic Transdifferentiation of Vascular Smooth Muscle Cells via Enhanced AKT Signalling and PiT-1 Expression. *J. Cel Mol Med* 25 (12), 5602–5614. doi:10.1111/jcmm.16572

Furmanik, M., Chatrou, M., van Gorp, R., Akbulut, A., Willems, B., Schmidt, H., et al. (2020). Reactive Oxygen-Forming Nox5 Links Vascular Smooth Muscle Cell Phenotypic Switching and Extracellular Vesicle-Mediated Vascular Calcification. *Circ. Res.* 127 (7), 911–927. doi:10.1161/CIRCRESAHA.119.316159

Furmanik, M., van Gorp, R., Whitehead, M., Ahmad, S., Bordoloi, J., Kapustin, A., et al. (2021). Endoplasmic Reticulum Stress Mediates Vascular Smooth Muscle Cell Calcification via Increased Release of Grp78 (Glucose-Regulated Protein, 78 kDa)-Loaded Extracellular Vesicles. *Atvb* 41 (2), 898–914. doi:10.1161/ATVBAHA.120.315506

Gaurav, I., Thakur, A., Iyaswamy, A., Wang, X., Chen, X., and Yang, Z. (2021). Factors Affecting Extracellular Vesicles Based Drug Delivery Systems. *Molecules* 26 (6), 1544. doi:10.3390/molecules26061544

Gebraad, A., Kornilov, R., Kaur, S., Miettinen, S., Haimi, S., Peltoniemi, H., et al. (2018). Monocyte-derived Extracellular Vesicles Stimulate Cytokine Secretion and Gene Expression of Matrix Metalloproteinases by Mesenchymal Stem/stromal Cells. *FEBS J.* 285 (12), 2337–2359. doi:10.1111/febs.14485

Genge, B. R., Wu, L. N. Y., and Wuthier, R. E. (2007). *In Vitro* Modeling of Matrix Vesicle Nucleation. *J. Biol. Chem.* 282 (36), 26035–26045. doi:10.1074/jbc.M701057200

Ghislat, G., and Knecht, E. (2012). New Ca2+-dependent Regulators of Autophagosome Maturation. *Communicative Integr. Biol.* 5 (4), 308–311. doi:10.4161/cib.20076

Ghosh, S., Luo, D., He, W., Chen, J., Su, X., and Huang, H. (2020). Diabetes and Calcification: The Potential Role of Anti-diabetic Drugs on Vascular Calcification Regression. *Pharmacol. Res.* 158, 104861. doi:10.1016/j.phrs.2020.104861

Goettsch, C., Hutcheson, J. D., and Aikawa, E. (2013). MicroRNA in Cardiovascular Calcification. *Circ. Res.* 112 (7), 1073–1084. doi:10.1161/CIRCRESAHA.113.300937

Goettsch, C., Hutcheson, J. D., Aikawa, M., Iwata, H., Pham, T., Nykjaer, A., et al. (2016). Sortilin Mediates Vascular Calcification via its Recruitment into Extracellular Vesicles. *J. Clin. Invest.* 126 (4), 1323–1336. doi:10.1172/JCI80851

Goettsch, C., Iwata, H., Hutcheson, J. D., O'Donnell, C. J., Chapurlat, R., Cook, N. R., et al. (2017). Serum Sortilin Associates with Aortic Calcification and Cardiovascular Risk in Men. *Atvb* 37 (5), 1005–1011. doi:10.1161/ATVBAHA.116.308932

Goody, P. R., Hosen, M. R., Christmann, D., Niepmann, S. T., Zietzer, A., Adam, M., et al. (2020). Aortic Valve Stenosis. *Atvb* 40 (4), 885–900. doi:10.1161/ATVBAHA.119.313067

Greening, D. W., Xu, R., Ji, H., Tauro, B. J., and Simpson, R. J. (2015). A Protocol for Exosome Isolation and Characterization: Evaluation of Ultracentrifugation, Density-Gradient Separation, and Immunoaffinity Capture Methods. *Methods Mol. Biol.* 1295, 179–209. doi:10.1007/978-1-4939-2550-6_15

Guo, Y., Bao, S., Guo, W., Diao, Z., Wang, L., Han, X., et al. (2019). Bone Marrow Mesenchymal Stem Cell-Derived Exosomes Alleviate High Phosphorus-Induced Vascular Smooth Muscle Cells Calcification by Modifying microRNA Profiles. *Funct. Integr. Genomics* 19 (4), 633–643. doi:10.1007/s10142-019-00669-0

Gurunathan, S., Kang, M.-H., Jeyaraj, M., Qasim, M., and Kim, J.-H. (2019). Review of the Isolation, Characterization, Biological Function, and Multifarious Therapeutic Approaches of Exosomes. *Cells* 8 (4), 307. doi:10.3390/cells8040307

Hannafon, B. N., Trigoso, Y. D., Calloway, C. L., Zhao, Y. D., Lum, D. H., Welm, A. L., et al. (2016). Plasma Exosome microRNAs Are Indicative of Breast Cancer. *Breast Cancer Res.* 18 (1), 90. doi:10.1186/s13058-016-0753-x

Hénaut, L., Sanchez-Nino, M. D., Aldamiz-Echevarría Castillo, G., Sanz, A. B., and Ortiz, A. (2016). Targeting Local Vascular and Systemic Consequences of Inflammation on Vascular and Cardiac Valve Calcification. *Expert Opin. Ther. Targets* 20 (1), 89–105. doi:10.1517/14728222.2015.1081685

Herrmann, J., Babic, M., Tölle, M., van der Giet, M., and Schuchardt, M. (2020). Research Models for Studying Vascular Calcification. *Ijms* 21 (6), 2204. doi:10.3390/ijms21062204

Hjortnaes, J., Shapero, K., Goettsch, C., Hutcheson, J. D., Keegan, J., Kluin, J., et al. (2015). Valvular Interstitial Cells Suppress Calcification of Valvular Endothelial Cells. *Atherosclerosis* 242 (1), 251–260. doi:10.1016/j.atherosclerosis.2015.07.008

Hodroge, A., Trécherel, E., Cornu, M., Darwiche, W., Mansour, A., Ait-Mohand, K., et al. (2017). Oligogalacturonic Acid Inhibits Vascular Calcification by Two Mechanisms. *Atvb* 37 (7), 1391–1401. doi:10.1161/ATVBAHA.117.309513

Hoshino, A., Kim, H. S., Bojmar, L., Gyan, K. E., Cioffi, M., Hernandez, J., et al. (2020). Extracellular Vesicle and Particle Biomarkers Define Multiple Human Cancers. *Cell* 182 (4), 1044–1061. doi:10.1016/j.cell.2020.07.009

Houben, E., Neradova, A., Schurgers, L. J., and Vervloet, M. (2016). The Influence of Phosphate, Calcium and Magnesium on Matrix Gla-Protein and Vascular Calcification: a Systematic Review. *G Ital. Nefrol* 33 (6), 1.

Hutcheson, J. D., Goettsch, C., Pham, T., Iwashita, M., Aikawa, M., Singh, S. A., et al. (2014). Enrichment of Calcifying Extracellular Vesicles Using Density-Based Ultracentrifugation Protocol. *J. Extracellular Vesicles* 3, 25129. doi:10.3402/jev.v3.25129

Icer, M. A., and Yıldıran, H. (2021). Effects of Fetuin-A with Diverse Functions and Multiple Mechanisms on Human Health. *Clin. Biochem.* 88, 1–10. doi:10.1016/j.clinbiochem.2020.11.004

Iordachescu, A., Hulley, P., and Grover, L. M. (2018). A Novel Method for the Collection of Nanoscopic Vesicles from an Organotypic Culture Model. *RSC Adv.* 8 (14), 7622–7632. doi:10.1039/c7ra12511a

Itel, F., Skovhus Thomsen, J., and Städler, B. (2018). Matrix Vesicles-Containing Microreactors as Support for Bonelike Osteoblasts to Enhance Biomineralization. *ACS Appl. Mater. Inter.* 10 (36), 30180–30190. doi:10.1021/acsami.8b10886

Itoh, S., Mizuno, K., Aikawa, M., and Aikawa, E. (2018). Dimerization of Sortilin Regulates its Trafficking to Extracellular Vesicles. *J. Biol. Chem.* 293 (12), 4532–4544. doi:10.1074/jbc.RA117.000732

Jain, M., Dev, R., Doddapattar, P., Kon, S., Dhanesha, N., and Chauhan, A. K. (2021). Integrin α9 Regulates Smooth Muscle Cell Phenotype Switching and Vascular Remodeling. *JCI Insight* 6 (10), 1. doi:10.1172/jci.insight.147134

Jing, L., Li, L., Ren, X., Sun, Z., Bao, Z., Yuan, G., et al. (2020). Role of Sortilin and Matrix Vesicles in Nε-Carboxymethyl-Lysine-Induced Diabetic Atherosclerotic Calcification. *Dmso* 13, 4141–4151. doi:10.2147/DMSO.S273029

Jing, L., Li, L., Sun, Z., Bao, Z., Shao, C., Yan, J., et al. (2019). Role of Matrix Vesicles in Bone-Vascular Cross-Talk. *J. Cardiovasc. Pharmacol.* 74 (5), 372–378. doi:10.1097/FJC.0000000000000720

Johnson, K. A., Polewski, M., and Terkeltaub, R. A. (2008). Transglutaminase 2 Is central to Induction of the Arterial Calcification Program by Smooth Muscle Cells. *Circ. Res.* 102 (5), 529–537. doi:10.1161/CIRCRESAHA.107.154260

Kapustin, A. N., Chatrou, M. L. L., Drozdov, I., Zheng, Y., Davidson, S. M., Soong, D., et al. (2015). Vascular Smooth Muscle Cell Calcification Is Mediated by Regulated Exosome Secretion. *Circ. Res.* 116 (8), 1312–1323. doi:10.1161/CIRCRESAHA.116.305012

Kapustin, A. N., Davies, J. D., Reynolds, J. L., McNair, R., Jones, G. T., Sidibe, A., et al. (2011). Calcium Regulates Key Components of Vascular Smooth Muscle Cell-Derived Matrix Vesicles to Enhance Mineralization. *Circ. Res.* 109 (1), e1–12. doi:10.1161/CIRCRESAHA.110.238808

Kapustin, A. N., and Shanahan, C. M. (2012). Calcium Regulation of Vascular Smooth Muscle Cell-Derived Matrix Vesicles. *Trends Cardiovasc. Med.* 22 (5), 133–137. doi:10.1016/j.tcm.2012.07.009

Kapustin, A. N., and Shanahan, C. M. (2016). Emerging Roles for Vascular Smooth Muscle Cell Exosomes in Calcification and Coagulation. *J. Physiol.* 594 (11), 2905–2914. doi:10.1113/JP271340

Kawakami, R., Katsuki, S., Travers, R., Romero, D. C., Becker-Greene, D., Passos, L. S. A., et al. (2020). S100A9-RAGE Axis Accelerates Formation of Macrophage-Mediated Extracellular Vesicle Microcalcification in Diabetes Mellitus. *Atvb* 40 (8), 1838–1853. doi:10.1161/ATVBAHA.118.314087

Khan, S. R., Canales, B. K., and Dominguez-Gutierrez, P. R. (2021). Randall's Plaque and Calcium Oxalate Stone Formation: Role for Immunity and Inflammation. *Nat. Rev. Nephrol.* 17 (6), 417–433. doi:10.1038/s41581-020-00392-1

Khavandgar, Z., Roman, H., Li, J., Lee, S., Vali, H., Brinckmann, J., et al. (2014). Elastin Haploinsufficiency Impedes the Progression of Arterial Calcification in MGP-Deficient Mice. *J. Bone Miner Res.* 29 (2), 327–337. doi:10.1002/jbmr.2039

Kiffer-Moreira, T., Yadav, M. C., Zhu, D., Narisawa, S., Sheen, C., Stec, B., et al. (2013). Pharmacological Inhibition of PHOSPHO1 Suppresses Vascular Smooth Muscle Cell Calcification. *J. Bone Miner Res.* 28 (1), 81–91. doi:10.1002/jbmr.1733

Kluszczynska, K., Czernek, L., Cypryk, W., Peczek, L., and Duchler, M. (2019). Methods for the Determination of the Purity of Exosomes. *Curr. Pharm. Des.* 25 (42), 4464–4485. doi:10.2174/1381612825666191206162712

Krohn, J. B., Hutcheson, J. D., Martínez-Martínez, E., and Aikawa, E. (2016a). Extracellular Vesicles in Cardiovascular Calcification: Expanding Current Paradigms. *J. Physiol.* 594 (11), 2895–2903. doi:10.1113/JP271338

Krohn, J. B., Hutcheson, J. D., Martínez-Martínez, E., Irvin, W. S., Bouten, C. V. C., Bertazzo, S., et al. (2016b). Discoidin Domain Receptor-1 Regulates Calcific Extracellular Vesicle Release in Vascular Smooth Muscle Cell Fibrocalcific Response via Transforming Growth Factor-β Signaling. *Atvb* 36 (3), 525–533. doi:10.1161/ATVBAHA.115.307009

Kubo, H. (2018). Extracellular Vesicles in Lung Disease. *Chest* 153 (1), 210–216. doi:10.1016/j.chest.2017.06.026

Kunitomi, Y., Hara, E. S., Okada, M., Nagaoka, N., Kuboki, T., Nakano, T., et al. (2019). Biomimetic Mineralization Using Matrix Vesicle Nanofragments. *J. Biomed. Mater. Res.* 107 (5), 1021–1030. doi:10.1002/jbm.a.36618

Lane, R. E., Korbie, D., Trau, M., and Hill, M. M. (2017). Purification Protocols for Extracellular Vesicles. *Methods Mol. Biol.* 1660, 111–130. doi:10.1007/978-1-4939-7253-1_10

Lee, K., Kim, H., and Jeong, D. (2014). Microtubule Stabilization Attenuates Vascular Calcification through the Inhibition of Osteogenic Signaling and Matrix Vesicle Release. *Biochem. Biophysical Res. Commun.* 451 (3), 436–441. doi:10.1016/j.bbrc.2014.08.007

Lee, K., Shao, H., Weissleder, R., and Lee, H. (2015). Acoustic Purification of Extracellular Microvesicles. *ACS Nano* 9 (3), 2321–2327. doi:10.1021/nn506538f

Li, Y., Sun, Z., Zhang, L., Yan, J., Shao, C., Jing, L., et al. (2020). Role of Macrophages in the Progression and Regression of Vascular Calcification. *Front. Pharmacol.* 11, 661. doi:10.3389/fphar.2020.00661

Lin, X., Zhu, T., Xu, F., Zhong, J.-Y., Li, F., Shan, S.-K., et al. (2020). Plasma Exosomes Derived from Patients with End-Stage Renal Disease and Renal Transplant Recipients Have Different Effects on Vascular Calcification. *Front. Cel Dev. Biol.* 8, 618228. doi:10.3389/fcell.2020.618228

Lin, Z., Rodriguez, N. E., Zhao, J., Ramey, A. N., Hyzy, S. L., Boyan, B. D., et al. (2016). Selective Enrichment of microRNAs in Extracellular Matrix Vesicles Produced by Growth Plate Chondrocytes. *Bone* 88, 47–55. doi:10.1016/j.bone.2016.03.018

Liu, L., Zeng, P., Yang, X., Duan, Y., Zhang, W., Ma, C., et al. (2018). Inhibition of Vascular Calcification. *Arterioscler Thromb. Vasc. Biol.* 38 (10), 2382–2395. doi:10.1161/ATVBAHA.118.311546

Lobb, R. J., Becker, M., Wen Wen, S., Wong, C. S. F., Wiegmans, A. P., Leimgruber, A., et al. (2015). Optimized Exosome Isolation Protocol for Cell Culture Supernatant and Human Plasma. *J. Extracellular Vesicles* 4, 27031. doi:10.3402/jev.v4.27031

Luong, T. T. D., Schelski, N., Boehme, B., Makridakis, M., Vlahou, A., Lang, F., et al. (2018). Fibulin-3 Attenuates Phosphate-Induced Vascular Smooth Muscle Cell Calcification by Inhibition of Oxidative Stress. *Cel Physiol Biochem* 46 (4), 1305–1316. doi:10.1159/000489144

Mathivanan, S., Ji, H., and Simpson, R. J. (2010). Exosomes: Extracellular Organelles Important in Intercellular Communication. *J. Proteomics* 73 (10), 1907–1920. doi:10.1016/j.jprot.2010.06.006

McCormick, M. M., Rahimi, F., Bobryshev, Y. V., Gaus, K., Zreiqat, H., Cai, H., et al. (2005). S100A8 and S100A9 in Human Arterial Wall. *J. Biol. Chem.* 280 (50), 41521–41529. doi:10.1074/jbc.M509442200

Melki, I., Tessandier, N., Zufferey, A., and Boilard, E. (2017). Platelet Microvesicles in Health and Disease. *Platelets* 28 (3), 214–221. doi:10.1080/09537104.2016.1265924

Montañez-Barragán, A., Gómez-Barrera, I., Sanchez-Niño, M. D., Ucero, A. C., González-Espinoza, L., and Ortiz, A. (2014). Osteoprotegerin and Kidney Disease. *J. Nephrol.* 27 (6), 607–617. doi:10.1007/s40620-014-0092-x

Nabhan, J. F., Hu, R., Oh, R. S., Cohen, S. N., and Lu, Q. (2012). Formation and Release of Arrestin Domain-Containing Protein 1-mediated Microvesicles (ARMMs) at Plasma Membrane by Recruitment of TSG101 Protein. *Proc. Natl. Acad. Sci.* 109 (11), 4146–4151. doi:10.1073/pnas.1200448109

Nakahara, T., Dweck, M. R., Narula, N., Pisapia, D., Narula, J., and Strauss, H. W. (2017). Coronary Artery Calcification. *JACC: Cardiovasc. Imaging* 10 (5), 582–593. doi:10.1016/j.jcmg.2017.03.005

Nakai, W., Yoshida, T., Diez, D., Miyatake, Y., Nishibu, T., Imawaka, N., et al. (2016). A Novel Affinity-Based Method for the Isolation of Highly Purified Extracellular Vesicles. *Sci. Rep.* 6, 33935. doi:10.1038/srep33935

New, S. E. P., Goettsch, C., Aikawa, M., Marchini, J. F., Shibasaki, M., Yabusaki, K., et al. (2013). Macrophage-Derived Matrix Vesicles. *Circ. Res.* 113 (1), 72–77. doi:10.1161/CIRCRESAHA.113.301036

Nguyen, N. T., Nguyen, T. T., Da Ly, D., Xia, J.-B., Qi, X.-F., Lee, I.-K., et al. (2020). Oxidative Stress by Ca2+ Overload Is Critical for Phosphate-Induced Vascular Calcification. *Am. J. Physiology-Heart Circulatory Physiol.* 319 (6), H1302–H1312. doi:10.1152/ajpheart.00305.2020

Nitta, K., and Ogawa, T. (2015). Vascular Calcification in End-Stage Renal Disease Patients. *Contrib. Nephrol.* 185, 156–167. doi:10.1159/000380980

Omarjee, L., Nitschke, Y., Verschuere, S., Bourrat, E., Vignon, M. D., Navasiolava, N., et al. (2020). Severe Early-onset Manifestations of Pseudoxanthoma Elasticum Resulting from the Cumulative Effects of Several Deleterious Mutations in ENPP1 , ABCC6 and HBB : Transient Improvement in Ectopic Calcification with Sodium Thiosulfate. *Br. J. Dermatol.* 183 (2), 367–372. doi:10.1111/bjd.18632

Pan, W., Liang, J., Tang, H., Fang, X., Wang, F., Ding, Y., et al. (2020). Differentially Expressed microRNA Profiles in Exosomes from Vascular Smooth Muscle Cells Associated with Coronary Artery Calcification. *Int. J. Biochem. Cel Biol.* 118, 105645. doi:10.1016/j.biocel.2019.105645

Perelló, J., Ferrer, M. D., Pérez, M., Kaesler, N., Brandenburg, V. M., Behets, G. J., et al. (2020). Mechanism of Action of SNF472, a Novel Calcification Inhibitor to Treat Vascular Calcification and Calciphylaxis. *Br. J. Pharmacol.* 177 (19), 4400–4415. doi:10.1111/bph.15163

Pescatore, L. A., Gamarra, L. F., and Liberman, M. (2019). Multifaceted Mechanisms of Vascular Calcification in Aging. *Atvb* 39 (7), 1307–1316. doi:10.1161/ATVBAHA.118.311576

Phadwal, K., Feng, D., Zhu, D., and MacRae, V. E. (2020). Autophagy as a Novel Therapeutic Target in Vascular Calcification. *Pharmacol. Ther.* 206, 107430. doi:10.1016/j.pharmthera.2019.107430

Proudfoot, D. (2019). Calcium Signaling and Tissue Calcification. *Cold Spring Harb Perspect. Biol.* 11 (10), a035303. doi:10.1101/cshperspect.a035303

Qi, Y., Dai, F., Gu, J., and Yao, W. (2019). Biomarkers in VSMC Phenotypic Modulation and Vascular Remodeling. *Pharmazie* 74 (12), 711–714. doi:10.1691/ph.2019.9743

Reynolds, J. L., Joannides, A. J., Skepper, J. N., McNair, R., Schurgers, L. J., Proudfoot, D., et al. (2004). Human Vascular Smooth Muscle Cells Undergo Vesicle-Mediated Calcification in Response to Changes in Extracellular Calcium and Phosphate Concentrations: a Potential Mechanism for Accelerated Vascular Calcification in ESRD. *J. Am. Soc. Nephrol.* 15 (11), 2857–2867. doi:10.1097/01.ASN.0000141960.01035.28

Schantl, A. E., Verhulst, A., Neven, E., Behets, G. J., D'Haese, P. C., Maillard, M., et al. (2020). Inhibition of Vascular Calcification by Inositol Phosphates Derivatized with Ethylene Glycol Oligomers. *Nat. Commun.* 11 (1), 721. doi:10.1038/s41467-019-14091-4

Shapiro, I. M., Landis, W. J., and Risbud, M. V. (2015). Matrix Vesicles: Are They Anchored Exosomes? *Bone* 79, 29–36. doi:10.1016/j.bone.2015.05.013

Shekar, C., and Budoff, M. (2018). Calcification of the Heart: Mechanisms and Therapeutic Avenues. *Expert Rev. Cardiovasc. Ther.* 16 (7), 527–536. doi:10.1080/14779072.2018.1484282

Shen, J., Zhang, N., Lin, Y.-N., Xiang, P., Liu, X.-b., Shan, P.-f., et al. (2018). Regulation of Vascular Calcification by Growth Hormone-Releasing Hormone and its Agonists. *Circ. Res.* 122 (10), 1395–1408. doi:10.1161/CIRCRESAHA.117.312418

Shi, W., Lu, J., Li, J., Qiu, M., Lu, Y., Gu, J., et al. (2020). Piperlongumine Attenuates High Calcium/Phosphate-Induced Arterial Calcification by Preserving P53/PTEN Signaling. *Front. Cardiovasc. Med.* 7, 625215. doi:10.3389/fcvm.2020.625215

Sohn, W., Kim, J., Kang, S. H., Yang, S. R., Cho, J.-Y., Cho, H. C., et al. (2015). Serum Exosomal microRNAs as Novel Biomarkers for Hepatocellular Carcinoma. *Exp. Mol. Med.* 47, e184. doi:10.1038/emm.2015.68

Ståhl, A.-l., Johansson, K., Mossberg, M., Kahn, R., and Karpman, D. (2019). Exosomes and Microvesicles in normal Physiology, Pathophysiology, and Renal Diseases. *Pediatr. Nephrol.* 34 (1), 11–30. doi:10.1007/s00467-017-3816-z

Sun, Z., Wang, Z., Li, L., Yan, J., Shao, C., Bao, Z., et al. (2019). RAGE/galectin-3 Yields Intraplaque Calcification Transformation via Sortilin. *Acta Diabetol.* 56 (4), 457–472. doi:10.1007/s00592-018-1273-1

Todorova, D., Simoncini, S., Lacroix, R., Sabatier, F., and Dignat-George, F. (2017). Extracellular Vesicles in Angiogenesis. *Circ. Res.* 120 (10), 1658–1673. doi:10.1161/CIRCRESAHA.117.309681

Tyson, K. L., Reynolds, J. L., McNair, R., Zhang, Q., Weissberg, P. L., and Shanahan, C. M. (2003). Osteo/chondrocytic Transcription Factors and Their Target Genes Exhibit Distinct Patterns of Expression in Human Arterial Calcification. *Atvb* 23 (3), 489–494. doi:10.1161/01.ATV.0000059406.92165.31

Veschi, E. A., Bolean, M., Strzelecka-Kiliszek, A., Bandorowicz-Pikula, J., Pikula, S., Granjon, T., et al. (2020). Localization of Annexin A6 in Matrix Vesicles during Physiological Mineralization. *Ijms* 21 (4), 1367. doi:10.3390/ijms21041367

Viegas, C. S. B., Costa, R. M., Santos, L., Videira, P. A., Silva, Z., Araújo, N., et al. (2017). Gla-rich Protein Function as an Anti-inflammatory Agent in Monocytes/macrophages: Implications for Calcification-Related Chronic Inflammatory Diseases. *PLoS One* 12 (5), e0177829. doi:10.1371/journal.pone.0177829

Viegas, C. S. B., Rafael, M. S., Enriquez, J. L., Teixeira, A., Vitorino, R., Luís, I. M., et al. (2015). Gla-rich Protein Acts as a Calcification Inhibitor in the Human Cardiovascular System. *Atvb* 35 (2), 399–408. doi:10.1161/ATVBAHA.114.304823

Viegas, C. S. B., Santos, L., Macedo, A. L., Matos, A. A., Silva, A. P., Neves, P. L., et al. (2018). Chronic Kidney Disease Circulating Calciprotein Particles and Extracellular Vesicles Promote Vascular Calcification. *Arterioscler Thromb. Vasc. Biol.* 38 (3), 575–587. doi:10.1161/ATVBAHA.117.310578

Viegas, C. S. B., and Simes, D. C. (2018). "Inflammation and Calcification in the Vascular Tree; Insights into Atherosclerosis," in *Immunity and Inflammation in Health and Disease*, 189–201. doi:10.1016/b978-0-12-805417-8.00015-9

Villa-Bellosta, R. (2019). ATP-based Therapy Prevents Vascular Calcification and Extends Longevity in a Mouse Model of Hutchinson-Gilford Progeria Syndrome. *Proc. Natl. Acad. Sci. USA* 116 (47), 23698–23704. doi:10.1073/pnas.1910972116

Voelkl, J., Luong, T. T. D., Tuffaha, R., Musculus, K., Auer, T., Lian, X., et al. (2018a). SGK1 Induces Vascular Smooth Muscle Cell Calcification through NF-Kb Signaling. *J. Clin. Invest.* 128 (7), 3024–3040. doi:10.1172/JCI96477

Voelkl, J., Tuffaha, R., Luong, T. T. D., Zickler, D., Masyout, J., Feger, M., et al. (2018b). Zinc Inhibits Phosphate-Induced Vascular Calcification through TNFAIP3-Mediated Suppression of NF-Kb. *Jasn* 29 (6), 1636–1648. doi:10.1681/ASN.2017050492

Wang, Z., Wu, H.-j., Fine, D., Schmulen, J., Hu, Y., Godin, B., et al. (2013). Ciliated Micropillars for the Microfluidic-Based Isolation of Nanoscale Lipid Vesicles. *Lab. Chip* 13 (15), 2879–2882. doi:10.1039/c3lc41343h

Wei, W., Guo, X., Gu, L., Jia, J., Yang, M., Yuan, W., et al. (2021). Bone Marrow Mesenchymal Stem Cell Exosomes Suppress Phosphate-Induced Aortic Calcification via SIRT6-HMGB1 Deacetylation. *Stem Cel Res Ther* 12 (1), 235. doi:10.1186/s13287-021-02307-8

Willems, B. A., Furmanik, M., Caron, M. M. J., Chatrou, M. L. L., Kusters, D. H. M., Welting, T. J. M., et al. (2018). Ucma/GRP Inhibits Phosphate-Induced Vascular Smooth Muscle Cell Calcification via SMAD-dependent BMP Signalling. *Sci. Rep.* 8 (1), 4961. doi:10.1038/s41598-018-23353-y

Xiao, H., Chen, J., Duan, L., and Li, S. (2021). Role of Emerging Vitamin K-dependent P-roteins: Growth A-rrest-specific P-rotein 6, Gla-rich P-rotein and P-eriostin (Review). *Int. J. Mol. Med.* 47 (3), 2. doi:10.3892/ijmm.2020.4835

Xiao, X., Yang, C., Qu, S.-L., Shao, Y.-D., Zhou, C.-Y., Chao, R., et al. (2020). S100 Proteins in Atherosclerosis. *Clinica Chim. Acta* 502, 293–304. doi:10.1016/j.cca.2019.11.019

Xu, F., Zhong, J. Y., Lin, X., Shan, S. K., Guo, B., Zheng, M. H., et al. (2020). Melatonin Alleviates Vascular Calcification and Ageing through Exosomal miR-204/miR-211 Cluster in a Paracrine Manner. *J. Pineal Res.* 68 (3), e12631. doi:10.1111/jpi.12631

Xu, J., Camfield, R., and Gorski, S. M. (2018). The Interplay between Exosomes and Autophagy - Partners in Crime. *J. Cel Sci.* 131 (15), jcs215210. doi:10.1242/jcs.215210

Zazzeroni, L., Faggioli, G., and Pasquinelli, G. (2018). Mechanisms of Arterial Calcification: The Role of Matrix Vesicles. *Eur. J. Vasc. Endovascular Surg.* 55 (3), 425–432. doi:10.1016/j.ejvs.2017.12.009

Zeringer, E., Barta, T., Li, M., and Vlassov, A. V. (2015). Strategies for Isolation of Exosomes. *Cold Spring Harb Protoc.* 2015 (4), pdb.top074476–323. doi:10.1101/pdb.top074476

Zhang, C., Zhang, K., Huang, F., Feng, W., Chen, J., Zhang, H., et al. (2018). Exosomes, the Message Transporters in Vascular Calcification. *J. Cel. Mol. Med.* 22 (9), 4024–4033. doi:10.1111/jcmm.13692

Zhang, J., Zhao, A., Sun, L., Chen, W., Zhang, H., Chen, Z., et al. (2017). Selective Surface Marker and miRNA Profiles of CD34+ Blast-Derived Microvesicles in Chronic Myelogenous Leukemia. *Oncol. Lett.* 14 (2), 1866–1874. doi:10.3892/ol.2017.6336

Conflict of Interest: The authors declare that the research was conducted in the absence of any commercial or financial relationships that could be construed as a potential conflict of interest.

Publisher's Note: All claims expressed in this article are solely those of the authors and do not necessarily represent those of their affiliated organizations, or those of the publisher, the editors and the reviewers. Any product that may be evaluated in this article, or claim that may be made by its manufacturer, is not guaranteed or endorsed by the publisher.

frontiers in Cell and Developmental Biology

REVIEW
published: 26 January 2022
doi: 10.3389/fcell.2022.813885

Role of Extracellular Vesicles as Potential Diagnostic and/or Therapeutic Biomarkers in Chronic Cardiovascular Diseases

Jose Luis Martin-Ventura[1,2*†], *Carmen Roncal*[2,3*†], *Josune Orbe*[2,3] *and Luis Miguel Blanco-Colio*[1,2]

[1]Vascular Research Laboratory, IIS-Fundación Jiménez-Díaz, Madrid, Spain, [2]CIBER de Enfermedades Cardiovasculares (CIBERCV), Madrid, Spain, [3]Laboratory of Atherothrombosis, Program of Cardiovascular Diseases, Cima Universidad de Navarra, Instituto de Investigación Sanitaria de Navarra, IdiSNA, Pamplona, Spain

OPEN ACCESS

Edited by:
Yang Shen,
Sichuan University, China

Reviewed by:
Marie-José Goumans,
Leiden University Medical Center, Netherlands
Juhui Qiu,
Chongqing University, China

***Correspondence:**
Jose Luis Martin-Ventura
jlmartin@fjd.es
Carmen Roncal
croncalm@unav.es

†ORCID:
Jose Luis Martin-Ventura
0000-0003-2090-8641
Carmen Roncal
0000-0003-0616-9600

Specialty section:
This article was submitted to Molecular and Cellular Pathology, a section of the journal Frontiers in Cell and Developmental Biology

Received: 12 November 2021
Accepted: 10 January 2022
Published: 26 January 2022

Citation:
Martin-Ventura JL, Roncal C, Orbe J and Blanco-Colio LM (2022) Role of Extracellular Vesicles as Potential Diagnostic and/or Therapeutic Biomarkers in Chronic Cardiovascular Diseases. Front. Cell Dev. Biol. 10:813885. doi: 10.3389/fcell.2022.813885

Cardiovascular diseases (CVDs) are the first cause of death worldwide. In recent years, there has been great interest in the analysis of extracellular vesicles (EVs), including exosomes and microparticles, as potential mediators of biological communication between circulating cells/plasma and cells of the vasculature. Besides their activity as biological effectors, EVs have been also investigated as circulating/systemic biomarkers in different acute and chronic CVDs. In this review, the role of EVs as potential diagnostic and prognostic biomarkers in chronic cardiovascular diseases, including atherosclerosis (mainly, peripheral arterial disease, PAD), aortic stenosis (AS) and aortic aneurysms (AAs), will be described. Mechanistically, we will analyze the implication of EVs in pathological processes associated to cardiovascular remodeling, with special emphasis in their role in vascular and valvular calcification. Specifically, we will focus on the participation of EVs in calcium accumulation in the pathological vascular wall and aortic valves, involving the phenotypic change of vascular smooth muscle cells (SMCs) or valvular interstitial cells (IC) to osteoblast-like cells. The knowledge of the implication of EVs in the pathogenic mechanisms of cardiovascular remodeling is still to be completely deciphered but there are promising results supporting their potential translational application to the diagnosis and therapy of different CVDs.

Keywords: extracelular vesicles, vascular smooth muscle cells, calcification, aneurysm, peripheral arterial disease

CARDIOVASCULAR DISEASES

CVDs, including heart, coronary, cerebrovascular, peripheral and aortic diseases, are the leading cause of morbidity and mortality in developed countries (Mannello and Medda, 2012). Atherosclerosis, considered the major precursor of CVDs, is a chronic pathology affecting large and medium size arteries that begins early in life, and progresses silently from its subclinical form to clinical symptoms according to the exposure to environmental risk factors (cholesterol, diabetes, hypertension, smoking, stress, sedentarism, microbioma, etc), and non-modifiable determinants such as age (Bray et al., 2021; Libby, 2021). Despite the therapeutic advances in controlling traditional risk factors, and the irruption of novel approaches including targeting inflammation, CVDs remain the primary cause of mortality worldwide, accounting for almost a third of annual deaths, 17.3

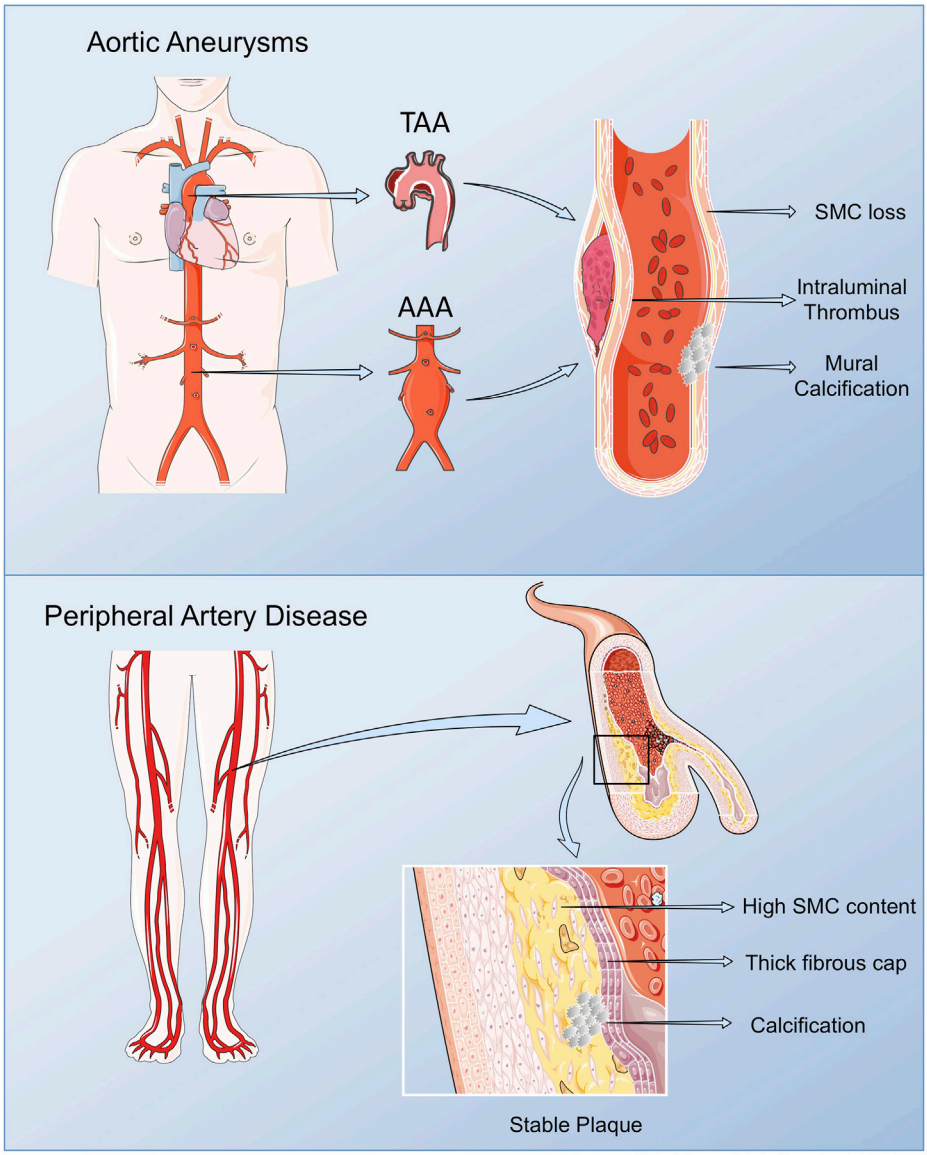

FIGURE 1 | Pathological vascular remodeling. Arterial remodeling in peripheral arteries and thoracic and abdominal aortas present some phenotypic particularities compared with vascular lesions in other vascular beds. Lower limb lesions are most frequently stable with low macrophage content, and a prevalence of vascular SMCs, resulting in plaques rich in collagen and elastic fibers, mostly calcified, with a non-significant lipid core. AAAs are characterized by the presence of an Intra Luminal Thrombus (ILT), rich in red blood cells (RBCs), neutrophils and platelets, and an aortic wall with low number of vascular SMCs in the remaining media, along with immune cell infiltrates, fibroblasts and neovessels in the adventitia. TAA display extensive remodeling of the ECM, vascular SMCs dysfunction and calcification, but ILT is not present. Figure created using Servier Medical Art images (https://smart.servier.com).

million per year, that are expected to grow to more than 23.6 million by 2030 due to lifestyle changes and aging (Roth et al., 2017). Arterial alterations can go unnoticed until symptoms develop, a sign of advanced disease, and thus are associated to a high risk of ischemic complications and death (Acosta et al., 2006; Roth et al., 2017; Timmis et al., 2020). In this context, extracellular vesicles (EVs) emerge as new players in the crosstalk between vascular and circulating cells, participating in cell to cell communication processes, and being biomarkers of cellular activation (Méndez-barbero et al., 2021).

Peripheral Arterial Disease

PAD includes a range of non-coronary arterial syndromes caused by alterations in the structure and function of arteries other than those supplying the heart or the brain, although in the current review, we will focus on lower extremity PAD referring to the chronic lower limb ischemia of atherosclerotic origin affecting the femoral, popliteal and saphenous arteries (Gerhard-Herman et al., 2017; Frank et al., 2019). PAD affects around 200 million people worldwide, and increases with age, presenting a prevalence of 10–25% in people older than 55 years, rising up to

40% on those older than 80. PAD is associated to a diminished quality of life affecting mobility, and in its more severe form, chronic limb threatening ischemia (CLTI), it might lead to limb amputation, and mortality in high rates (Fowkes et al., 2017). Taking in consideration that PAD is frequently accompanied by atherosclerosis in other vascular beds, it presents a superior risk of ischemic events and death compared with other CV pathologies (Fowkes et al., 2013; Jirak et al., 2018). As such, when associated with other comorbidities, specifically diabetes, the gold standard for PAD diagnosis, the ankle brachial index, losses sensitivity due to arterial calcification, contributing to its silent rates (Hajibandeh et al., 2017; Jirak et al., 2018). In consequence, and despite its bad prognosis, PAD still remains greatly underdiagnosed and undertreated (Norgren et al., 2007). The morphological analysis of femoral plaques revealed some differences when compared with those in coronary and cerebral arteries. In lower limb lesions, macrophage content is lower, while vascular SMCs are predominant, originating plaques rich in collagen and elastic fibers, mostly calcified, with a non-significant lipid core (Derksen et al., 2010; Kamenskiy et al., 2018). This phenotype stabilizes the plaque, slows its progression, and enables the activation of compensatory mechanisms, including collateral circulation, in surrounding tissues (Poredoš et al., 2021) (**Figure 1**).

Aortic Valve Stenosis

Degenerative AS is the most frequent form of acquired valvular heart disease in the developed countries, and the second most frequent cause for cardiac surgery, which prevalence will further increase with the aging of the population. The prevalence of AS in patients older than 75 years of age is 12.4%, and 3.4% have severe AS with an associated risk of death of 50% at 2 years (Iung and Vahanian, 2006; Nkomo et al., 2006; Kanwar et al., 2018). Normal aortic valves are composed of valvular endothelial cells (ECs), the ICs and extracellular matrix (ECM), while pathological aortic valves are characterized by endothelial dysfunction, lipoprotein accumulation, chronic inflammation, and calcium nodule deposits. Consequently, these pathological changes lead to the thickening and stiffness of the valve leaflets, restricting their opening and imposing an increased afterload on the left ventricle (O'Brien, 2006; Sritharen et al., 2017). Despite the associated clinical consequences, there is currently no effective therapy for AS other than aortic valve replacement (Aymond et al., 2021; Mantovani et al., 2021).

Aortic Aneurysms

AAs occurs when the progressive weakening of the aortic wall causes the aorta to enlarge and exceeds more than 3 cm. AAs are usually asymptomatic and are often detected as an incidental finding during the investigation of an unrelated problem or as a consequence of radiological screening. The only way to prevent aortic rupture or disection in patients with an AAs > 5–5.5 cm is surgery (Klink et al., 2011; Milewicz and Ramirez, 2019). AAs can be distinguished by their etiology into degenerative aneurysms and those associated with hereditary disorders or by their different location into abdominal aortic aneurysm (AAA) or thoracic aortic aneurysm (TAA) (Sakalihasan et al., 2005; Pinard et al., 2019). AAA is a major health problem, causing about 1–2% of male deaths in economically developed societies. TAA is a relatively common condition, found in up to 8% of men aged >65 years, and is responsible for considerable cardiovascular morbidity and mortality.

AAA share main CV risk factors with atherosclerosis, while the major risk factors for TAA are hypertension and an underlying genetic alteration or the presence of a bicuspid aortic valve (BAV). AAA is characterized by the presence of an Intra Luminal Thrombus (ILT), mainly composed by red blood cells (RBCs), neutrophils and platelets and an aortic wall with reduced number of vascular SMCs in the remaining media, along with immune cell infiltrates, fibroblasts and neovessels in the adventitia (Michel et al., 2011). Despite the origin of AAA still being poorly understood, proteolysis, oxidative stress, vascular SMCs phenotypic switch and apoptosis, immune-inflammatory responses and neoangiogenesis are mechanisms implicated in the formation and progression of AAA (Torres-Fonseca et al., 2019). Although AAA and TAA share some common mechanisms including proteolytic elastic tissue degeneration and vascular SMCs dysfunction, they present some striking differences: presence (AAA) or abscence (TAA) of ILT; secondary (AAA) versus primary (TAA) pathology of vascular SMCs; linkage (AAA) or not (TAA) to atheroma; monogenic (TAA) versus polygenic (AAA) determinants; age and gender issues (Michel et al., 2018; Martin-Blazquez et al., 2021) (**Figure 1**).

EXTRACELLULAR VESICLES

EVs are spherical lipid bilayers without nucleus, released to the extracellular space by most cell types, containing lipids, proteins, metabolites and nucleic acids from the cell of origin. The lipid bilayer protects EVs content from the activity of endogenous DNases, RNases or proteinases, and temperature or pH changes, and enables their separation from all body fluids and cell culture medium (Momen-Heravi et al., 2018) (**Figure 2**).

EVs are produced and released to the bloodstream in physiological and pathological conditions by all vascular and circulating cells, displaying a wide range of functions in the vasculature and in target tissues (Giró et al., 2021). The biological activities of EVs in recipient cells are displayed through different mechanisms (Russell et al., 2019). For instance, they can participate in receptor-ligand interactions promoting the activation of signaling pathways in host cells, release their content to the cytoplasm of recipient cells by fusion with the plasma membrane, or be internalized through endocytosis, phagocytosis or micropinocytosis. Finally, by carrying bioactive molecules in their surface, EVs can directly modify target proteins or ECMs components (van Niel et al., 2018). In this way, EVs regulate vascular homeostasis and participate in a myriad of pathological processes, including atherosclerosis initiation and progression, and aortic wall dilation (Méndez-barbero et al., 2021; Saenz-pipaon et al., 2021). Moreover, being their cargo particular to the cell type and the stimuli triggering their release, the analysis of their content might be useful to understand the pathophysiological

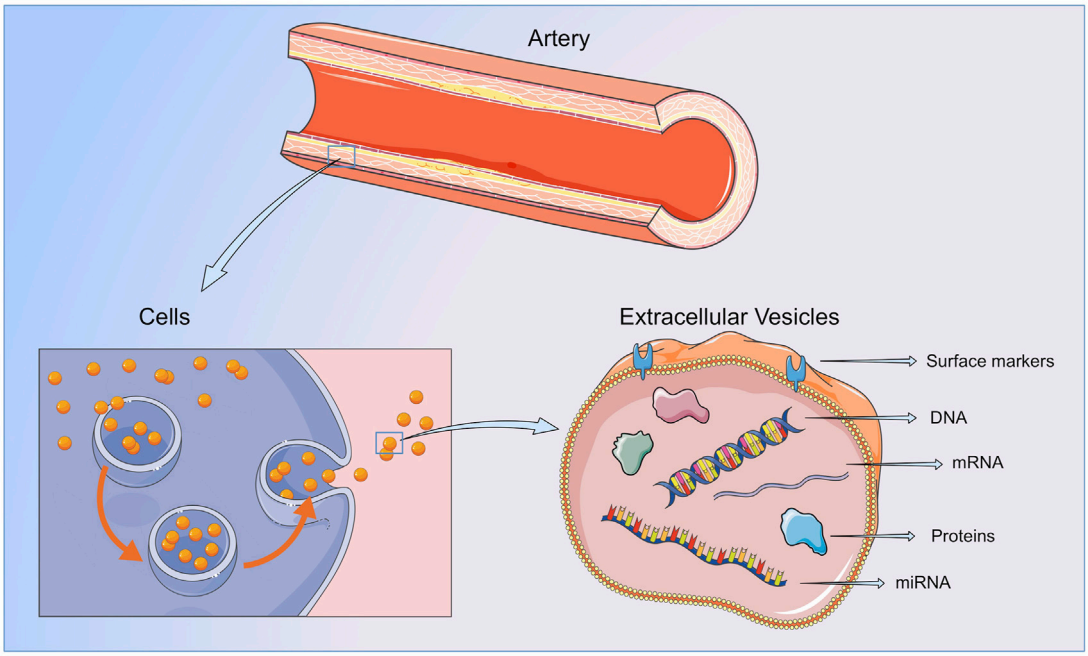

FIGURE 2 | Extracellular vesicles. EVs contain lipids, protein and nucleic acids from the cell or organ of origin and are released to the bloodstream by all cellular components of the vasculature and blood. By transferring their content to neighboring or distant cells or by direct interaction with the ECMs components, EVs are able to participate in all the steps of vessel remodeling. Figure created using Servier Medical Art images (https://smart.servier.com).

condition on which they have been originated (Shah et al., 2018; Théry et al., 2018). In addition, EVs can lead to the identification of novel diagnostic and prognostic biomarkers and therapeutic targets.

Traditionally, EVs have been classified according to their size and biogenesis in: exosomes, with diameters from 30 to 150 nm, generated by the inward budding of the endosomal membrane (Colombo et al., 2014); microvesicles, directly shed from the plasma membrane and polydisperse in size (100–1000 nm of diameter) (Connor et al., 2010; Boulanger et al., 2017; Taylor et al., 2020) and apoptotic bodies, generated in the late steps of programmed cell death with diameters of 1000–5,000 nm (Théry et al., 2018; van Niel et al., 2018). However, due to the significant overlap in size and composition between exosomes and microvesicles and following the latter recommendations (Théry et al., 2018), in this review we will use the umbrella term EVs to refer to exosomes and microvesicles (Théry et al., 2018; Russell et al., 2019).

EXTRACELLULAR VESICLES AND CARDIOVASCULAR DISEASES

EVs have attracted considerable interest in the CV field as reservoirs of molecules produced during arterial remodelling, and/or after acute or chronic ischemic events (Giró et al., 2021), and thus have been proposed as biomarkers in different CV conditions (**Table 1**). Likewise, increased levels of total EVs or specific EVs subpopulation, for instance those derived from platelet, ECs, erythrocytes or leukocytes, have been associated with the presence of CV risk factors (Amabile et al., 2014), including diabetes (Li et al., 2016), hypertension (Preston et al., 2003), hypercholesterolemia (Amabile et al., 2014) and smoking (Gordon et al., 2011), and with subclinical and clinical atherosclerosis (Suades et al., 2015; Saenz-Pipaon et al., 2020). In coronary pathologies, circulating EVs have been correlated with inflammatory and thrombophilic conditions. As such the number of endothelial and platelet derived EVs have been correlated with the circulating levels of IL-6 and CRP in patients with coronary heart disease (Cui et al., 2013); moreover *in vitro*, medium size vesicles from acute coronary syndrome patients displayed procoagulant activity, which was prevented when phosphatidylserine was blocked with lactadherin (Liu et al., 2016). EVs have been also postulated as markers of carotid plaque instability, reporting increased levels of platelet, endothelial, leukocyte and erythrocyte EVs in patients with myocardial infarction when compared with subjects with unstable and stable angina (Cui et al., 2013; Wekesa et al., 2014; Schiro et al., 2015; Liu et al., 2016; Suades et al., 2016; Vagida et al., 2016). Similar results were obtained when assessing the number of tissue factor and annexin V positive procoagulant EVs subpopulations (Cui et al., 2013; Wekesa et al., 2014). Coronary patients also displayed increased levels of endothelial EVs according to worse vascular function (Amabile et al., 2005; Koga et al., 2005; Werner et al., 2006), and an association between elevated endothelial and erythrocyte EVs and CV events has been also reported (Sinning et al., 2011; Fan et al., 2014; Giannopoulos et al., 2014). Furthermore, in stroke patients elevated levels of

TABLE 1 | Summary of studies showing a correlation between the levels of total or specific cell type EVs subpopulations, measured by flow cytometry, in circulation (plasma) and cardiovascular diseases.

Disease/patient group (*n* = number)	EVs type	Outcome	References
844 individuals of the Framingham Offspring cohort (mean age 66 + 9 years, 57% women) without cardiovascular disease	Endothelial (e)EVs subsets CD144+ $CD31^+CD41^-$	Association of eEVs with hypertension, triglycerides and metabolic syndrome and the Framingham risk score	Amabile et al. (2014)
Systemic review and meta-analysis of 48 studies involving 2,460 patients with type 2 DM and 1,880 non-diabetic controls	Specific surface markers	Total EVs, pEVs, mEVs and eEVs were higher in type 2 DM vs. controls	(Li et al., 2016)
Three groups: 1) untreated patients with severe uncontrolled hypertension, n = 24; 2) untreated patients with established mild hypertension, *n* = 19; and 3) normotensive volunteer subjects *n* = 16	eEVs: $CD31^+CD42^-$ Platelet (p)EVs: $CD41^+$	eEVs and pEVs were significantly increased in the severely hypertensive group	Preston et al. (2003)
Two groups: 1) High cardiovascular risk patients (*n* = 37); 2) age, gender, and treatment-matched controls (*n* = 37)	Total EVs (Annexin V+) pEVs TSP1+ PAC+ PAC + CD62P+ Tissue factor (TF)+ pEVs: CD142 + TSP1+ TF + monocyte (m)EVs: CD142 + $CD14^+$	Total EVs, pEVs, mEVs, and TF + EVs were significantly elevated in high risk patients vs. controls Levels of TF + mEVs and pEVs were associated to atherosclerotic burden	Suades et al. (2015)
Four groups: 40 patients with myocardial infarction (MI), 30 unstable angina (UA), 20 stable angina (SA), and 20 healthy individuals	pEVs: $CD41^+$ mEVs: $CD14^+$ Lymphocytes (l)EVs: $CD4^+$ eEVs: CD144+ TF + EVs: CD142+	eEVs and pEVs were significantly elevated in MI and UA vs SA and control No differences were observed in mEVs and lEVs among the groups TF + EVs were higher in MI and UA eEVs and pEVs levels correlated with IL-6 or CRP in coronary heart disease patients	Cui et al. (2013)
Patients with newly diagnosed acute coronary syndrome (ACS) were divided into 3 groups: 1) UA (*n* = 36), 2) NSTEMI (*n* = 22), and 3) STEMI (*n* = 42); and an additional group of *n* = 10 age and sex matched controls	Total EVs: Lactadherin+ pEVs: CD41a+ eEVs: $CD31^+$ mEVs: $CD14^+$ B-cells EVs: $CD19^+$ T cells EVs: $CD3^+$ Erythrocyte (ery)EVs: CD235a + TF + EVs: CD142+	Total EVs, pEVs and eEVs were higher in ACS groups vs controls Leu- and eryEVs were higher in the STEMI group vs UA and NSTEMI groups (both $p < 0.05$) *In vitro*, EVs form ACS patients displayed procoagulant activity	Liu et al. (2016)
CAD patients undergoing endarterectomy (*n* = 42), and age- and sex-matched controls (*n* = 73)	Ann V + EVs pEVs subsets $CD41^+$ Ann V + $CD41^+$ eEVs subsets $CD31^+CD41^-$ CD144+ CD146+ CD105+	Annexin V + EVs and pEVs subsets, were higher in cases vs. controls eEVs subsets were higher in patients with unstable vs. stable plaques eEVs and pEVs were significantly higher in patients with carotid stenosis vs. controls	Wekesa et al. (2014)
Patients undergoing carotid endarterectomy: *n* = 19 asymptomatic and *n* = 51 symptomatic patients (*n* = 51); and *n* = 20 healthy age-matched controls	eEVs: Ann V + $CD31^+CD42b-$ pEVs: Ann V + $CD31^+CD42b+$	No differences were observed between asymptomatic vs. symptomatic patients	Schiro et al. (2015)
STEMI patients (*n* = 40) treated by percutaneous coronary intervention (PCI); age, gender, risk factors and pharmacological treatments matched control group (*n* = 20); and patients recovering from STEMI (*n* = 20)	Total EVs (Ann V+) eEVs $CD31^+$ CD146+ CD62E+ pEVs: $CD61^+$ Leukocytes (leu)EVs: $CD45^+$ lEVs: CD45+/CD3+ mEVs: $CD14^+$	STEMI patients present increased levels of total EVs, LeuEVs subsets, eEVs subsets and PEVs	Suades et al. (2016)

(Continued on following page)

TABLE 1 | (*Continued*) Summary of studies showing a correlation between the levels of total or specific cell type EVs subpopulations, measured by flow cytometry, in circulation (plasma) and cardiovascular diseases.

Disease/patient group (*n* = number)	EVs type	Outcome	References
	neutrophil EVs: CD66b+ TF + EVs: CD142+		
17 healthy volunteers and 13 ACS.	Magnetic nanoparticles conjugated with anti-CD63/CD31 or anti-CD31 for eEVs, or with anti-CD63/CD41a or anti-CD41a antibodies for pEVs	ACs patients presented increased levels of EVs, mainly of platelet origin	Vagida et al. (2016)
44 end-stage renal failure patients (ESRF), and 32 healthy subjects	Ann V + EVs eEVs subsets $CD31^+$ CD144+ pEVs: $CD41^+$ eryEVs: CD235a+ Lymphocyte EVs: $CD3^+$ myeloid EVs: CD11b+ LeuEVs: $CD45^+$ Neutrophil EVs: CD66b+	Annexin V + EVs, eEVs, pEVs and eryEVs were increased in ESRF patients vs. controls Only eEVs correlated with arterial dysfunction	Amabile et al. (2005)
232 patients with DM and 102 controls	eEVs: CD144 + CD42b– In DM patients, eEVs were associated to a higher risk for CAD	eEVs levels were increased in DM vs. control	Koga et al. (2005)
CAD patients (*n* = 50)	eEVs: CD31 + Ann V+	Increased eEVs correlated with worse endothelial-dependent vasodilatation and independently predicted severe endothelial dysfunction	Werner et al. (2006)
CAD patients (*n* = 200)	eEVs: CD31 + Ann V+	eEVs were increased in patients with a first major adverse cardiovascular and cerebral events (MACCE) In the follow up eEVs were independently associated to higher risk of CV death, need for revascularization or MACCE.	Sinning et al. (2011)
Healthy controls (*n* = 80), chest paint patients: non-CAD (n = 94), SA (*n* = 111), and ACS (*n* = 145)	eEVs: CD146+	The levels of eEVs were increased in ACS > SA > non-CAD > controls eEVs levels were associated to higher risk of MACE in ACS group	Fan et al. (2014)
STEMI patients (*n* = 51) and age-matched controls (*n* = 50)	Ann V + EVs pEVs: $CD41^+$ eryEVs: CD235a+	eryEVs were increased in STEMI patients vs. controls No differences were found in pEvs eryEVs levels were independently associated to a higher risk of MACE during the follow-up	Giannopoulos et al. (2014)
Stroke patients: 1) mild stroke, *n* = 20; 2) moderate–severe stroke, *n* = 21; 3) age-matched controls, *n* = 23	eEVs subsets CD105 + CD41a-CD45– (E + eEVs) CD105 + CD144+ (C + eEVs) CD105 + PS + CD41a– (PS + eEVs) CD105 + $CD54^+CD45^-$ (I + eEVs)	PS + eEVs were increased in stroke patients vs. controls All eEVs subsets were elevated in moderate–severe stroke patients vs. controls Brain lesion volume was correlated E + eEVs, PS + eEVs and I+ eEVs levels	Simak et al. (2006)
Patients with acute stroke (*n* = 73), and patients with vascular risk factors but no stroke events (*n* = 275)	eEVs subsets CD31+/CD42b- CD31+/AV+	Levels of CD31+/AnnV+ and CD62E + eEVs subsets were greater in acute stroke patients vs. controls CD62E + eEVs were strongly associated with stroke severity and infarct volume CD62E+	Jung et al. (2009)
Patients with acute ischemic stroke (*n* = 68), and age- and sex-matched controls (*n* = 61)	eEVs subsets CD144 + CD41a– $CD31^+CD41a^-$ CD62E+ Ann V + CD62E+ pEVs: CD41a + CD144–	CD144+/CD41a–, $CD31^+CD41a^-$, CD62E+, and Annexin V + CD62E + eEVs, were significantly increased in acute ischemic stroke patients vs. controls CD144+/CD41a– eEVs were correlated with stroke severity	Li and Qin (2015)

(Continued on following page)

TABLE 1 | (*Continued*) Summary of studies showing a correlation between the levels of total or specific cell type EVs subpopulations, measured by flow cytometry, in circulation (plasma) and cardiovascular diseases.

Disease/patient group (*n* = number)	EVs type	Outcome	References
18 PAD patients and 12 asymptomatic controls	Total EVs: Lactadherin+ pEVs: CD41a+ eEVs subsets CD31$^+$ CD144 + LeuEVs: CD45$^+$ mEVs: CD14$^+$ B-cells EVs: CD19$^+$ T cells EVs: CD3$^+$ Neutrophil EVs: CD66b+	PAD patients presented increased levels of eEVs carrying the monomeric form of C-reactive protein (mCRP) Control subjects on statins presented a reduction in mCRP + eEVs eryEVs: CD235a+ Monomeric (m) or pentameric (p) CRP + EVs	Crawford et al. (2016)
PAD patients (*n* = 50) and controls (*n* = 50)	eEVs: CD144+ pEVs: CD42b+ LeuEVs: CD45$^+$ eryEVs: CD235+ Sonic Hedgedog (Shh)+EVs	PAD patients present increased levels of shh+ in all EVs subpopulations Shh + eEVs levels correlated with the number of collateral vessels in ischemic thighs of PAD patients (*n* = 18)	Giarretta et al. (2018)
PAD patients (*n* = 50) and controls (*n* = 50)	pEVs: CD41$^+$	Increased levels of pEVs in PAD patients vs controls	Zeiger et al. (2000)
PAD patients, *n* = 23 with severe disease (critical limb ischemia, CLI), 36 with moderate disease (intermittent claudication, IC), and *n* = 30 healthy controls	pEVs: CD61$^+$CD42b+	Gradual increased in pEVs levels according ro severity (CLI > IC > controls)	Tan et al. (2005)
Patients presenting stable angina (*n* = 10), peripheral arterial disease (*n* = 10), NSTEMI (*n* = 11) and STEMI myocardial infarction (*n* = 10), age- and sex matched older controls *n* = 10 and young healthy individuals (*n* = 10)	pEVs subsets Ann V + CD61$^+$CD62P+ Ann V + CD61$^+$CD63$^+$ eEVs: CD62E EryEVs: CD235a T- cells EVs CD4 + CD8$^+$ mEVs: CD14$^+$ B cells EVs: CD20$^+$ Neutrophil EVs: CD66e+	96% of the detected EVs were from platelet origin CD62P + pEVs increased in patients with NSTEMI and STEMI vs. older controls CD63+pEVs- were increased in patients with PAD, NSTEMI, and STEMI vs. older controls	van der Zee et al. (2006)
PAD patients (*n* = 45)	AnnexinV eEVs: CD62E+ pEVs: CD41/61+ LeuEVs: CD11b+ eryEVs: CD235a+ More than 85% of pEVs and eryEVs were Ann V+, while the percentage was lower for eEVs (70%) and LeuEVs (40%) The number pEVs were inversely correlated with procoagulant activity of plasma	In plasma of PAD patients pEVs were the most abundant subpopulation, followed by eryEVs, eEVs and LeuEVs	Saenz-Pipaon et al. (2020)
14 PAD patients and 15 normal controls PAD patients were treated with cilostazol (2 weeks) or cilostazol with dipyridamole (14 weeks)	pEVs: CD42$^+$	PAD patients presented increased levels of pEVs Cilostazol, and further, cilostazol with dipyridamole decreased pEVs levels in PAD patients	Nomura et al. (2004)
PAD patients (*n* = 19) randomly assigned to Atorvastatin or placebo treatment for 8 weeks	Total EVs: lactadherin pEVs CD42a + CD142+ CD42a + CD62P+ CD42a + CD61$^+$	Atorvastatin treatment reduced the number of CD142+, CD62P+ and CD61$^+$ pEVs vs placebo treated PAD patients	Mobarrez et al. (2011)
PAD patients (*n* = 19) randomly assigned to Atorvastatin or placebo treatment for 8 weeks	Total EVs eEVs		Mobarrez et al. (2012)

(Continued on following page)

TABLE 1 | (*Continued*) Summary of studies showing a correlation between the levels of total or specific cell type EVs subpopulations, measured by flow cytometry, in circulation (plasma) and cardiovascular diseases.

Disease/patient group (*n* = number)	EVs type	Outcome	References
	Lactdherin + CD144+ Lactadherin + CD144 + CD142+	Both CD144 + eEVs and CD144 + CD142+ eEVs were increased in patients on atorvastatin vs. placebo	
22 patients with severe aortic stenosis (AS) and 18 controls	eEVs: CD62E+ pEVs $CD31^+$ $CD61^+$ CD62P+ LeuEVs: CD11b+	pEVs, LeuEVs and eEVs were increased in AVS patients vs. control pEVs levels were correlated with shear stress and eEVs with the number of blood monocytes	Diehl et al. (2008)
Patients with severe AS. *n* = 28 with low coronary calcification (CAC) score, and *n* = 27 with high CAC score	eEVs CD144+ CD62E+ $CD31^+CD41^-$ pEVs: $CD41^+$ EVs trombin generation activity	The levels of pEVs and CD62E + eEVs were increased in high CAC score patients vs. low CAC score group, and correlated to the calcium score EVs thrombin generation activity was higher in patients with high CAC score	Horn et al. (2016)
56 severe AS patients undergoing transcatheter aortic valve implantation (TAVI)	eEVs CD144+ CD62E+ $CD31^+CD41^-$ pEVs: $CD41^+$	All eEVs subpopulations decreased 3 months after TAVI, along with an increase in the endothelial function	Horn et al. (2015)
92 severe AS patients undergoing TAVI	eEVs CD31 + Annexin+ CD31 + Annexin– $CD31^+CD42b$– CD62E+ pEVs: $CD31^+CD42b$+	The levels of CD62E + eEVs decreased gradually from pre-TAVI to post-TAVI (1 week, 1, 3 and 6 months) determination In contrast, circulating PEVs increased gradually after TAVI	Jung et al. (2017)
Patients with severe AS selected for percutaneous replacement of the aortic valve (*n* = 9)	eEVS: CD31 + Ann V+ pEVs: CD41 + Ann V+ LeuEVs: CD45 + Ann V+	No differences were observed between pre- and post-operative (5 days) levels of eEVs, pEVs or LeuEVs	Marchini et al. (2016)
135 patients undergoing surgical aortic valve replacement	small (s)EVs were quantified by nanoparticle tracking analysis (NTA)	sEVs decreased 24 h post-surgery, and recovered to pre-operative levels 7 days and 3 months post-procedure No association between sEVs and echocardiographic parameters before or after surgery (7 days and 3 months) were observed sEVs levels were correlated to prosthesis patients mismatch parameters at month 3 post-surgery	Weber et al. (2020)
AAA patients (blood samples and mural thrombi, *n* = 20), and sex and age-matched healthy individuals (blood samples, *n* = 20)	Annexin V + EVs pEVs: CD41 neutrophil EVs CD15 mEVs: CD14 eEVs: CD106 eryEVs: CD235	Circulating total EVs were significantly increased in AAA patients vs. controls Locally, luminal thrombus layers released larger quantities of annexin V-positive EV, mainly of platelet and neutrophil origin, compared to the intermediate and abluminal layers	Touat et al. (2006)
Controls (*n* = 66) and thoracic AA (TAA) patients associated to bicuspid aortic valves (BAV) (*n* = 15), or other origins (degenerative, *n* = 23)	Ann V + EVs pEVs: Ann V + $CD41^+$	The levels of EVs and pEVs were higher in TAA groups vs. control	Touat et al. (2008)

AAA: abdominal aortic aneurysm; ACS: acute coronary syndrome; AS: aortic stenosis; TAA: Thoracic aortic aneurysm; TAVI: transcatheter aortic valve implantation; CAD: coronary artery disease; CAC: coronary calcification score; DM: diabetes mellitus; ESRF: end-stage renal failure; CLI: critical limb ischemia; IC: Intermittent claudication; MI: myocardial infarction; PAD: peripheral arterial disease; SA: stable angina; UA: unstable angina; Ann V: Annexin V; EVs: Extracellular vesicles; eEVs: endothelial EVs; eryEVs: erythrocyte EVs; LeuEVs: leukocyte EVs; lEVs: Lymphocyte EVs; mEVs: monocyte EVs; pEVs: platelet EVs; (N)STMI: (non) ST Segment Elevation Myocardial Infarction; TF: Tissue factor; TSP-1: Thrombospondin-1; T; PAC: activated αIIbβ3-integrin.

specific subpopulations of endothelial derived EVs were associated to worse outcome (Simak et al., 2006; Jung et al., 2009; Li and Qin, 2015). In PAD, circulating EVs are mainly considered platelet activation markers (Zeiger et al., 2000; Saenz-Pipaon et al., 2020), while in AAA, EVs were enriched in proteins involved in the main pathological mechanisms leading to AAA development and progression, including oxidative stress, inflammation and thrombosis (Martinez-Pinna et al., 2014). Besides their role as biomarkers, EVs display biological activities and induce cellular responses *in vitro* and *in vivo* also during vessel remodelling, modulating endothelial (dys) function, leukocyte recruitment, foam cell formation, VSMCs proliferation and migration, apoptosis and necrotic core formation, plaque rupture and thrombosis. This topic has been extensively addressed in recent reviews (Zarà et al., 2019; Giró et al., 2021; Patel et al., 2021).

Extracellular Vesicles: Potential Biomarkers and Biological Effectors in Peripheral Arterial Disease

EVs have been investigated as biomarkers and biological effectors in PAD, displaying different effects according to their cargo and origin. It has been proposed that the elevated levels of endothelial EVs co-expressing the monomeric form of C-reactive protein (CRP) might potentially contribute to inflammation in PAD (Crawford et al., 2016), while endothelial cell derived EVs rich in the pro-angiogenic Sonic hedgehog protein correlated with the number of collateral vessels in ischemic thighs of PAD patients, suggesting their possible role in neovascularization (Giarretta et al., 2018). Among the different EVs lineages, platelet EVs, seemed to be most abundant in plasma of PAD patients (Saenz-Pipaon et al., 2020), and their elevated numbers were correlated with PAD diagnosis and prognosis (Zeiger et al., 2000; Tan et al., 2005; van der Zee et al., 2006). It should be considered, however, that within total platelet EVs, only those co-exposing either P-selectin or CD63 might reflect the degree of platelet activation *in vitro* (van der Zee et al., 2006). Based on those data, it has been suggested the potential benefit of modifying total EVs numbers or subpopulations by pharmacological treatments (Rosińska et al., 2017). As such, cilostazol induced a reduction in the total number of platelet EVs in PAD patients (Nomura et al., 2004), while atorvastatin modified specific platelet EVs subpopulations, reducing those positive for P-selectin, tissue factor and glycoprotein-IIIa (Mobarrez et al., 2011). Interestingly, atorvastatin displayed the opposite effect on endothelial EVs inducing their increase in circulation (Mobarrez et al., 2012).

EVs also encapsulate nucleic acids, mainly mRNA and non-coding RNAs, from the cells or organs of origin, that can be released to the circulation and display biological responses in neighboring or distant cells. As such, small EVs from PAD patients enriched in miR-21, miR-92a, miR-126, miR-143, miR-181b, and miR-221, increased vascular SMCs migration *in vitro* and inhibited that of ECs when compared with EVs from control patients (Sorrentino et al., 2020). Further, these authors also described that small EVs induced M1 polarization marker expression in macrophages *in vitro*, regardless of the pathophysiological condition from which EVs were isolated, control or PAD (Sorrentino et al., 2020). Moreover, the study of the transcriptional content of EVs might lead to the identification of new diagnosis and prognosis biomarkers, and therapeutic targets in PAD. In this regard, we found an upregulation of the S100A9 transcript after RNA-Seq analysis of plasma EVs in PAD patients (Saenz-Pipaon et al., 2020). Interestingly, as previously described (Engelberger et al., 2015; Dann et al., 2018), the protein encoded by S100A9, in circulation forming the heterocomplex S100A8/A9 or calprotectin, was elevated in PAD patients compared with controls and associated with a higher risk of mortality or amputation in the follow-up (Saenz-Pipaon et al., 2020), suggesting the potential of studying EVs content to identify novel biomarkers in chronic vascular diseases.

Regarding the biological activity of EVs, several authors have investigated their function in experimental models of hind limb ischemia using as source blood, tissues or cell culture conditioned medium. As such, in a rat model of femoral ischemia, platelet EVs from atherosclerotic patients increased the adhesion capacity of circulating angiogenic cells to the ischemic muscles and increased neovascularization, which was prevented when the coculture of EVs and circulating angiogenic cells was pretreated with a RANTES neutralizing antibody (Ohtsuka et al., 2013). In mouse, the proangiogenic effect of bone marrow–mononuclear cells was increased when administered together with EVs isolated from ischemic muscles in a mechanisms dependent on gp91 (Leroyer et al., 2009), while T lymphocyte-derived EVs enriched in Sonic hedgehog protein improved muscle recovery in a mechanism dependent on nitric oxide production (Benameur et al., 2010). Moreover, EVs from ETS variant transcription factor 2 transfected fibroblasts, increased neovascularization (Van Pham et al., 2017). In addition, recent findings indicate that the beneficial effects of stem cells in skeletal muscle repair might be partially mediated by EVs. As such, several authors reported improved muscle recovery by the intramuscular delivery of EVs generated by stem cells of different types, including mesenchymal, adipocyte, $CD34^+$ or urine-derived (Hu et al., 2015; Gangadaran et al., 2017; Mathiyalagan et al., 2017; Ju et al., 2018; Lopatina et al., 2018; Zhu et al., 2018; Figliolini et al., 2020; Zhang et al., 2021). Overall, EVs seem to participate in all steps of vascular and muscle remodelling in PAD.

Extracellular Vesicles: Possible Diagnostic and Prognostic Biomarkers in Aortic Stenosis

The possible utilization of EVs as diagnostic and prognostic biomarkers in AS, although still scarley studied, has been also addressed by several authors. Diehl et al. reported increased levels of leukocyte, platelet and endothelial derived EVs in patients with severe AS compared to controls (Diehl et al., 2008). In addition, they found a positive correlation between platelet and endothelial EVs, and shear stress and blood leukocyte numbers, respectively, in AS patients (Diehl et al., 2008). Other authors described that subjects with severe AS and high coronary calcification score

presented elevated levels of circulating endothelial and platelet derived EVs, and augmented EVs-associated thrombin activity, when compared with AS subjects with low coronary calcification score (Horn et al., 2016), suggesting the involvement of EVs in endothelial dysfunction, inflammation and valvular calcification.

Regarding the possible role of EVs as biomarkers for outcome assessment after valvular replacement, Marchini et al. found no differences in the concentration of total EVs, or in the levels of endothelial, platelet or leukocyte EVs early after surgery (5 days) compared to pre-procedure levels (Marchini et al., 2016). However, other authors reported a gradual decrease in endothelial EVs at longer time periods post-valvular replacement (1, 3 and 6 months) (Horn et al., 2015; Jung et al., 2017), accompanied by an improvement in the endothelial function (Horn et al., 2015) and an increase in platelet EVs (Jung et al., 2017). When it comes to small EVs or exosomes, their numbers acutely decrease after surgical valve replacement (24 h), going back to pre-operative levels 7 days and 3 months post-procedure, suggesting no alteration of small EVs release in response to valvular replacement (Weber et al., 2020). However, in a subgroup of patients, these authors described a positive correlation between increased levels of small EVs and patient-prosthesis mismatch parameters, and suggested the possible prognostic value of small EVs to estimate emerging patient-prosthesis mismatch and adverse outcomes in patients undergoing surgical aortic valve replacement (Weber et al., 2020). Locally, the *ex vivo* release of Annexin V + EVs to the conditioned medium was similar in ortic valves from patients suffering calcified AS of different origins, and no correlation between the released EVs and calcium content was observed (Kochtebane et al., 2013). Even if the summarized data points towards a role of EVs as biological effectors and biomarkers in AS, larger studies are needed to clarify their involment in the processes leading to AS initiation and progression.

Biological Role of Extracellular Vesicles in Aortic Aneurysms

As mentioned above, blood-borne EVs are mainly derived from activated platelets (Burnier et al., 2009), although leukocytes, red blood cells and ECs can also participate (Nomura, 2017). In this respect, platelet-derived EVs are increased in plasma of AAA patients (Touat et al., 2006) and TAA (Touat et al., 2008). Following a proteomic approach, we described increased ficolin-3 levels in EVs isolated from the plasma of patients with AAA (Martinez-Pinna et al., 2014). We also showed that ficolin-3 levels were increased in EVs of platelets from healthy subjects incubated with ADP, as well as in EVs isolated from AAA thrombus-conditioned media (Fernandez-García et al., 2017). The number of particles was higher in activated platelets and pathological tissue compared with healthy aorta. In addition, by flow cytometry, we observed that staining for platelets, and also leukocytes, was increased in EVs obtained from thrombus, compared with those from healthy aorta. Finally, ficolin-3 levels in plasma were associated to both AAA presence and evolution, suggesting its potential role as a diagnostic and prognostic biomarker (Fernandez-García et al., 2017). In addition, the contribution of neutrophils (Folkesson et al., 2015) and macrophages (Wang et al., 2019) to the release of EVs in human AAA was previously demonstrated. Moreover, in a latter study, the authors demonstrated that inhibiting small EVs biogenesis decreased experimental AAA associated to a reduction in MMP-2 expression (Wang et al., 2019), describing a pathogenic role of macrophage-derived small EVs production in AAA. Regarding TAA, where inflammatory cells are not present, vascular SMCs were tested to contribute to EVs release. In this study (Jia et al., 2017), mechanical stretch induced EVs production by vascular SMCs, which depended on endoplasmic reticulum (ER) stress. This process led to EC dysfunction and contributed to TAA formation, while an ER stress inhibitor blocked EV production *in vitro* and TAA formation and rupture. In addition, Han et al. demonstrated an upregulation of miR-106a in small EVs from plasma and tissue-conditioned media of AAA patients (Han et al., 2020). Interestingly, the authors demonstrated a pathogenic role of miR-106, by favoring vascular SMCs apoptosis and ECM degradation. However, the cell type involved in miR-106 upregulation was not identified. Moreover, treatment with EVs from mesenchymal stromal cells decreased AAA development and macrophage activation in mice by inducing miR-147 (Spinosa et al., 2018). All these data suggest a potential contribution of EVs with a positive or negative effect on AAs mechanisms and progression that depends on the cells of origin and the stimuli triggering EVs release.

ROLE OF EXTRACELLULAR VESICLES IN PATHOLOGICAL MECHANISMS INVOLVED IN VASCULAR REMODELING

Extracellular Vesicles and Phenotype Switch of Resident Vascular and Valvular Cells

Cardiovascular remodeling is a main driver of CVD, where vascular SMCs and valvular ICs play a central role. Most vascular SMCs in the vessel wall display a contractile phenotype, which allows them to maintain vascular tone. However, under pathological vascular remodeling, it is well established that vascular SMCs loses their contractile phenotype to one resembling other cell types. Novel technologies including vascular SMCs lineage tracing, single cell (sc)RNAseq of mouse and human atherosclerotic vessels, and human genomics, demonstrate a multipotential fate of dedifferentiated vascular SMCs to cell types including foam cells, osteochondrocytes or myofibroblasts, among others (Wirka et al., 2019; Pan et al., 2020; Hu Z. et al., 2021). Moreover, numerous studies have demonstrated the ability of valvular ICs to undergo osteogenic trans-differentiation (Rajamannan et al., 2005; Osman et al., 2006; Chen et al., 2009; Monzack and Masters, 2011). Similarly, vascular SMCs phenotypic switch, as shown by loss of contractility markers and increases in matrix metalloproteinases, preceded aortic aneurysm in mice. Very recently, it has been demonstrated that aneurysm

formation was driven by extensive reprogramming of contractile medial vascular SMCs to mesenchymal stem cell (MSC)- derived cell types including adipocytes, chondrocytes, osteoblasts, as well as macrophages that increased over time (Chen et al., 2020). The progressive accumulation of these cells provoked the loss of elastin fibers, intramural calcifications, massive lipid uptake and extensive inflammation. All this data supports the importance of vascular SMCs and valvular ICs phenotypic switch in pathological cardiovascular remodeling, although the exact impact of each phenotype is still under debate.

Regarding the potential contribution of EVs to vascular SMCs phenotypic switch, the incubation of human vascular SMCs with platelet EVs decreased the expression of contractile proteins, while inducing a synthetic proinflammatory phenotype resulting in increased IL-6 secretion and vascular SMCs migration and proliferation, through mechanisms involving CD40 and P-selectin interactions (Vajen et al., 2017). Under uremic conditions, EC-derived EVs stimulated vascular SMCs proliferation via TGF-beta (Ryu et al., 2019). Treatment with endothelial EVs reduced the proliferation and migration of vascular SMCs as well as lipid accumulation in vascular SMCs, while this beneficial effect was abolished or even reversed when treated with LPS-derived endothelial cell EVs (Xiang et al., 2021). ECs stimulated with oxysterol 7-ketocholesterol induced NLRP3 inflammasome activation and increased secretion of EVs that contain IL-1β. These EC-EVs rich in IL-1β promoted synthetic phenotype transition of co-cultured vascular SMCs, whereas EVs from unstimulated ECs had the opposite effects (Yuan et al., 2020). These last two recent results suggest a potential protective effect of EC-derived EVs on vascular SMCs, which seem to be impaired when produced under proinflammatory conditions, mimicking the pathological vascular wall.

The Role of Extracellular Vesicles in Vascular Calcification

Calcification has been associated to several CVDs, including atherosclerosis, aortic valve stenosis and aortic aneurysm. Calcium arterial coronary (CAC) score is a marker of CV events (Detrano et al., 2008). Initially, aortic valve calcification was also associated with cardiovascular events, although the association was attenuated after CAC was taken into account (Owens et al., 2012). More recently, it has been demonstrated that aortic valve calcification is independently associated with all-cause and CV deaths in patients with low coronary atherosclerosis burden (Han et al., 2021). Similarly, calcification in either the thoracic or the abdominal territory, has also been suggested as a potential contributor to aneurysm progression and mortality (Buijs et al., 2013; Chowdhury et al., 2018). The association of calcification with CV events depends on the arterial territory affected (Allison et al., 2012), but this association also differs between microcalcifications (<50 μm) or macrocalcifications (O'Neill et al., 2015). Macrocalcification in carotid atherosclerotic lesions correlated with a transcriptional profile typical for stable plaques, with altered vascular SMCs phenotype and ECM composition, and repressed inflammation (Karlöf et al., 2019). In contrast, microcalcifications that are present in high-risk atheroma, predicts adverse cardiovascular events, and is associated with increased morbidity and mortality (McEvoy et al., 2010). More recently, a prospective observational study has demonstrated that 18F-FDG and 18F-NaF PET/CT performed in the superficial femoral artery before and 6 weeks after angioplasty identified patients who would develop restenosis within 12 months (Chowdhury et al., 2020). Finally, in the prospective SoFIA3 study, aneurysms with higher 18F-fluoride uptake had 2.5 times more rapid aneurysm expansion, and experienced three times more AAA repair or rupture, compared with patients with less aneurysmal microcalcification (Forsythe et al., 2018). The deleterious effect of microcalcification on AAA expansion was further demonstrated in the experimental model of AngII (angiotensin II)-induced AAA in mice (Li et al., 2020). In this study, vascular SMCs–specific ablation of Runx2 (runt-related transcription factor 2) abrogated microcalcification and inhibited AngII-induced AAA formation. Similarly, conditional depletion of Runx2 in valvular ICs and sinus wall cells of LDLr−/−ApoB100 mice (a model of calcified aortic valve disease) improved aortic valve function by decreasing aortic valve calcification (Dharmarajan et al., 2021). All these data highlights the importance of vascular SMCs and valvular ICs-induced calcification in cardiovascular remodeling.

Previous studies identified vascular SMCs or valvular ICs expressing markers of osteochondrocytes, along with decreased expression of endogenous inhibitors of calcification, in pathological arteries and aortic valve lesions (Boström et al., 1993; O'Brien et al., 1995; Mohler et al., 2001; Rajamannan et al., 2003; Tyson et al., 2003; Dubis et al., 2016). There are several potential inducers of vascular SMCs or valvular ICs to an osteocondrogenic phenotype in atherosclerotic plaques, valves and aneurysms, including apoptosis, oxidative stress, mitochondrial dysfunction and probably, inflammation (through paracrine factors secreted by inflammatory cells) (Dweck et al., 2012; Durham et al., 2018; P ; Petsophonsakul et al., 2019). These modified vascular SMCs and valvular ICs favor vascular calcification through the release of calcifying EVs, a subpopulation traditionally known as matrix vesicles (MVs) (Shanahan et al., 2011). Later studies demonstrated that MVs are exosomes and show that factors that can increase exosome release can promote vascular calcification in response to environmental calcium stress (Kapustin et al., 2015). Interestingly, this study demonstrated that the inhibition of exosome release by a sphingomyelin phosphodiesterase 3 inhibitor blocks calcification. In addition, macrophages could also release calcifying EVs in atherosclerotic plaques and aortic valves (New et al., 2013; Passos et al., 2020).

Calcification, initially thought to be a passive process of calcium/phosphate precipitation in the ECMs, is nowadays described as an active-cell mediated process, which begins by aggregation of calcifying extracellular vesicles and the formation of microcalcifications, ultimate leading to large areas of calcification (Hutcheson et al., 2016). There are several events involved in vascular calcification, with a key role of EVs cargo as mediators of this process (**Figure 3**). The EVs cargo can be modified under a prolonged mineral imbalance and/or an

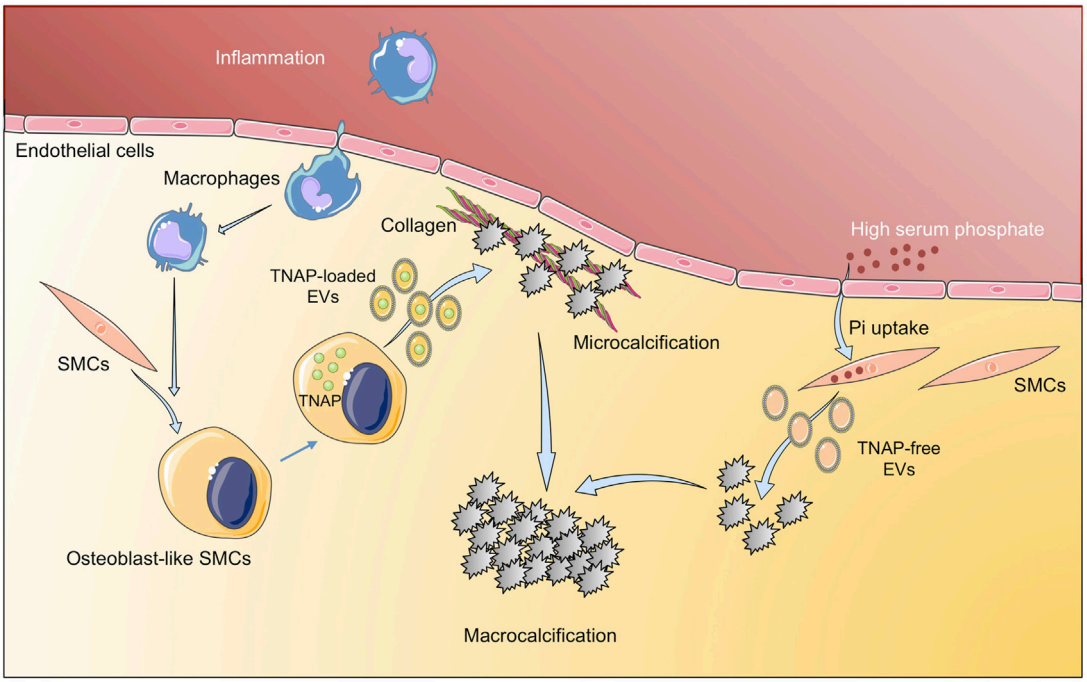

FIGURE 3 | Implication of extracellular vesicles in vascular calcification. Inflammatory environment induces osteogenic differentiation of SMC to osteoblast-like SMCs that release TNAP-loaded EV that aggregate into microcalcifications. In addition, high serum phosphate induces tissue calcification through EV with low TNAP. Figure created using Servier Medical Art images (https://smart.servier.com).

inflammatory environment, which results in a reduction of calcification inhibitors inside EVs and their enrichment in protein–lipid complexes consisting of phosphatidylserine (PS) and Annexin A6 (Kapustin et al., 2011). Tissue nonspecific alkaline phosphatase (TNAP), a key enzyme during calcification through the hydrolysis of extracellular pyrophosphate into phosphate, has been also found in vascular SMCs- derived calcifying EVs (Chen et al., 2008). Interestingly, phosphate-induced calcification increased the expression and activity of TNAP in cultured vascular SMCs with a osteocondrogenic phenotype (Villa-Bellosta, 2018), and the overexpression of TNAP is sufficient to induce medial calcification in aortic rings *ex vivo* (Villa-Bellosta et al., 2011). During the calcification process, TNAP along with annexins, mediates the interaction of EVs released by vascular SMCs and valvular ICs with the ECMs (predominantly type I collagen), initiating the mineralization process (Côté et al., 2012; Mathieu et al., 2014). Thus, some studies have tried to interfere with the mediators/molecular pathways involved in the production and release of calcifying EVs, and/or with those participating in the switch of vascular SMCs to the chondrogenic phenotype. In this respect, one of the most studied mediators is discoidin domain receptor-1 (DDR-1), a collagen-binding tyrosine kinase receptor that regulates vascular calcification and atherosclerosis (Ahmad et al., 2009). Interestingly, DDR-1 (−/−) vascular SMCs exhibited a 4-fold increase in EV release with elevated TNAP activity (Krohn et al., 2016). Very recently, it has been demonstrated that DDR-1 regulates the transdifferentiation of vascular SMCs to osteochondrocytic cells by sensing matrix stiffening during disease progression and transmitting contractile forces through the actin cytoskeleton (Ngai et al., 2020). Another study highlighting the importance of EVs cargo described a novel mechanism involving sortilin, a member of the vacuolar protein sorting 10 protein family of sorting receptors, that has been related to calcification and CVDs (Goettsch et al., 2018). Interestingly, sortilin induced calcification by favoring the loading of activated TNAP into EVs, which was independent of vascular SMCs osteochondrogenic reprogramming and did not affect bone mineralization (Goettsch et al., 2016). Moreover, loss- and gain-of-function studies, did not reveal a sortilin-dependent change in the number and size of EVs from calcifying vascular SMCs, further supporting that sortilin-induced calcification is dependent on the modulation of EVs cargo rather than on EVs number or subpopulation. More recently, Annexin A1, a protein associated with calcium binding and intracellular endosomal transport, has been identified as a main component in EVs present in atherosclerotic plaques and has been involved in EV tethering, leading to aggregation and ectopic calcification (Rogers et al., 2020a). Similar to EVs derived from calcifying vascular SMCs, the pro-calcified valvular ICs derived EVs showed up-regulation of several annexins. An *in vitro* study demonstrated EVs secretion with elevated calcium and Annexin A6 from rat VICs cultured with high calcium and phosphate and suggested a role in calcified aortic valve disease evidenced by co-localization of Annexin A6 with EVs in the aortic valve (Cui et al., 2017). In addition to TNAP and annexins as mediators of cardiovascular

calcification associated to their presence in EVs, other pathways have been studied. Two recent studies have analyzed the contribution of the Nox-5 subunit of NADPH oxidase in vascular calcification involving both, vascular SMCs phenotypic switch and EVs production. In a former study, it was demonstrated that switching from contractile to synthetic phenotype was required for vascular SMCs calcification, and that Ca^{2+}-dependent Nox5 expression increased oxidative stress, leading to elevated vascular SMCs-EVs release and subsequent calcification (Furmanik et al., 2020). More recently, the same group described that Nox5 was also the underlying mechanism by which nicotine induced vascular SMCs calcification and EV secretion, further supporting the role of smoking in pathological vascular remodeling and calcification (Petsophonsakul et al., 2021).

In spite of all this progress on the knowledge of mechanisms involved in cardiovascular calcification, there are currently no approved drugs to prevent or treat calcification (Aikawa and Blaser, 2021). Regarding potential therapeutic strategies based on natural compounds, oligogalacturonic acid (present in smooth pectin regions of the apple cell wall matrix) reduced vascular calcification by inhibition of osteogenic phenotype of vascular SMCs, and also by preventing EVs binding to type I collagen (Hodroge et al., 2017). A recent study tested the role of retinoids on vascular calcification, showing that acyclic retinoid inhibited cardiovascular cell calcification by attenuating TNAP activity and Runx2 expression without adverse effects on bone mineralization (Rogers et al., 2020b). However, these studies need to be performed *in vivo* to test its potential application. In this respect, a selective and orally bioavailable TNAP inhibitor attenuated the development of calcification in mice *in vivo*, without the deleterious effects on bone associated with other proposed treatment strategies (Ziegler et al., 2017; Tani et al., 2020); however, whether these strategies involved EVs and whether they could be applied in models of pathological cardiovascular remodeling deserve further studies.

CONCLUSION

Circulating EVs have been postulated as potential biomarkers in CVDs, as their absolute numbers, or the number of specific subpopulations have been associated to the incidence and prognosis of CVDs. In order to find novel biomarkers, different approaches on EVs have been used, from analysis of vascular SMCs-derived EVs under mineralization conditions (Kapustin et al., 2011), to AAA-tissue-derived EVs (Fernandez-García et al., 2017; Han et al., 2020) or plasma EVs from atherosclerotic patients (Madrigal-Matute et al., 2014; Saenz-Pipaon et al., 2020), among others. However, while many of these biomarkers demonstrate prognostic associations with CVD clinical outcomes, future research will be required to clarify their mechanistic roles and their potential clinical utility. Furthermore, current advances in -Omic approaches, mainly focused on improving sensitivity, will be crucial to dissect the molecular content of EVs in different pathological conditions, leading to the identification of differentially expressed RNAs, protein or metabolites, that will help to delineate the molecular profiles of different CVDs, and to identify novel diagnosis and prognosis biomarkers, as well as therapeutic targets.

In addition, EVs-based therapeutics have been proposed for several pathologies, including CVDs (Herrmann et al., 2021). Recently, the coating of stents with EVs resulted in accelerated re-endothelization and reduced instent re-stenosis compared to drug-eluting or bare-metal stents in mice (Hu S. et al., 2021). Similarly, the administration of EVs secreted by immortalized cardiosphere-derived cells, engineered to express high levels of b-catenin, modulated the immune response and improved cardiac function in an experimental model of cardiomyophaty in mice (Lin et al., 2021). We can thus envision the possibility to engineer EVs to modify their cargo and prevent vascular calcification and pathological remodeling. In this respect, Ldlr mRNA was encapsulated into EVs and then injected in atherosclerotic LDLR null mice, decreasing both hepatic steatosis and atherosclerotic lesions (Li et al., 2021). The translation of these experimental studies to humans is awaiting, and several clinical trials are in progress (Sahoo et al., 2021). At present we are only aware of one study performed with peripheral blood mononuclear cells obtained from patients with anthracycline-induced cardiomyopathy, reprogrammed into induced pluripotent stem cells and differentiated into cardiomyocytes. These cardiomyocytes were treated with EVs from mesenchymal stromal cells resulting in preserved mitochondrial function, augmentation of ATP production, mitigation of ROS production, and suppression of apoptosis (O'Brien et al., 2021), being all these processes involved in vascular calcification and pathological remodeling. In this study, large but not small EVs, had a therapeutic activity, while other studies in different pathologies have suggested the opposite view (Tieu et al., 2021), thus highlighting the need for a better standardization and characterization of the effect of different EVs subpopulations for translational therapeutic purposes.

AUTHOR CONTRIBUTIONS

JLM-V and CR wrote and edited the manuscript. LMB-C created the figures. LMB-C and JO critically reviewed and edited the manuscript. All authors read, and approved the submitted version.

FUNDING

This study was funded by the Spanish Ministry of Economy and Competitiveness (PID2019-106814RB-I00), Comunidad Autónoma de Madrid (Complemento II-CM, S2017/BMD-3673), Instituto de Salud Carlos III (ISCiii-FEDER) (IPT17/0019, PI18/01195, PI19/00065 PI19/00128, and RD21/0006/0008) co-funded by European Regional Development Fund "A way to make Europe (ISCiii-FEDER), Spanish Biomedical Research Centre in Cardiovascular Disease (CB16/11/00371 and CB16/11/00333), The Foundation for Applied Medical Research, Universidad de Navarra (Spain) and La Caixa" Banking Foundation (HR17-00247).

REFERENCES

Acosta, S., Ögren, M., Bengtsson, H., Bergqvist, D., Lindblad, B., and Zdanowski, Z. (2006). Increasing Incidence of Ruptured Abdominal Aortic Aneurysm: A Population-Based Study. *J. Vasc. Surg.* 44, 237–243. doi:10.1016/j.jvs.2006.04.037

Ahmad, P. J., Trcka, D., Xue, S., Franco, C., Speer, M. Y., Giachelli, C. M., et al. (2009). Discoidin Domain Receptor-1 Deficiency Attenuates Atherosclerotic Calcification and Smooth Muscle Cell-Mediated Mineralization. *Am. J. Pathol.* 175, 2686–2696. doi:10.2353/ajpath.2009.080734

Aikawa, E., and Blaser, M. C. (2021). 2020 Jeffrey M. Hoeg Award Lecture. *Atvb* 41, 117–127. doi:10.1161/ATVBAHA.120.314704

Allison, M. A., Hsi, S., Wassel, C. L., Morgan, C., Ix, J. H., Wright, C. M., et al. (2012). Calcified Atherosclerosis in Different Vascular Beds and the Risk of Mortality. *Arterioscler Thromb. Vasc. Biol.* 32, 140–146. doi:10.1161/ATVBAHA.111.235234

Amabile, N., Cheng, S., Renard, J. M., Larson, M. G., Ghorbani, A., McCabe, E., et al. (2014). Association of Circulating Endothelial Microparticles with Cardiometabolic Risk Factors in the Framingham Heart Study. *Eur. Heart J.* 35, 2972–2979. doi:10.1093/eurheartj/ehu153

Amabile, N., Guérin, A. P., Leroyer, A., Mallat, Z., Nguyen, C., Boddaert, J., et al. (2005). Circulating Endothelial Microparticles Are Associated with Vascular Dysfunction in Patients with End-Stage Renal Failure. *Jasn* 16, 3381–3388. doi:10.1681/ASN.2005050535

Aymond, J. D., Benn, F., Williams, C. M., Bernard, M. L., Hiltbold, A. E., Khatib, S., et al. (2021). Epidemiology, Evaluation, and Management of Conduction Disturbances after Transcatheter Aortic Valve Replacement. *Prog. Cardiovasc. Dis.* 66, 37–45. doi:10.1016/j.pcad.2021.06.004

Benameur, T., Soleti, R., Porro, C., Andriantsitohaina, R., and Martínez, M. C. (2010). Microparticles Carrying Sonic Hedgehog Favor Neovascularization through the Activation of Nitric Oxide Pathway in Mice. *PLoS One* 5, e12688–10. doi:10.1371/journal.pone.0012688

Boström, K., Watson, K. E., Horn, S., Wortham, C., Herman, I. M., and Demer, L. L. (1993). Bone Morphogenetic Protein Expression in Human Atherosclerotic Lesions. *J. Clin. Invest.* 91, 1800–1809. doi:10.1172/JCI116391

Boulanger, C. M., Loyer, X., Rautou, P.-E., and Amabile, N. (2017). Extracellular Vesicles in Coronary Artery Disease. *Nat. Rev. Cardiol.* 14, 259–272. doi:10.1038/nrcardio.2017.7

Bray, F., Laversanne, M., Cao, B., Varghese, C., Mikkelsen, B., Weiderpass, E., et al. (2021). Comparing Cancer and Cardiovascular Disease Trends in 20 Middle- or High-Income Countries 2000-19: A Pointer to National Trajectories towards Achieving Sustainable Development Goal Target 3.4. *Cancer Treat. Rev.* 100, 102290. doi:10.1016/j.ctrv.2021.102290

Buijs, R. V. C., Willems, T. P., Tio, R. A., Boersma, H. H., Tielliu, I. F. J., Slart, R. H. J. A., et al. (2013). Calcification as a Risk Factor for Rupture of Abdominal Aortic Aneurysm. *Eur. J. Vasc. Endovascular Surg.* 46, 542–548. doi:10.1016/j.ejvs.2013.09.006

Burnier, L., Fontana, P., Kwak, B. R., and Angelillo-Scherrer, A. (2009). Cell-derived Microparticles in Haemostasis and Vascular Medicine. *Thromb. Haemost.* 101, 439–451. doi:10.1160/th08-08-0521

Chen, J.-H., Yip, C. Y. Y., Sone, E. D., and Simmons, C. A. (2009). Identification and Characterization of Aortic Valve Mesenchymal Progenitor Cells with Robust Osteogenic Calcification Potential. *Am. J. Pathol.* 174, 1109–1119. doi:10.2353/ajpath.2009.080750

Chen, N. X., O'Neill, K. D., Chen, X., and Moe, S. M. (2008). Annexin-mediated Matrix Vesicle Calcification in Vascular Smooth Muscle Cells. *J. Bone Mineral Res.* 23, 1798–1805. doi:10.1359/jbmr.080604

Chen, P.-Y., Qin, L., Li, G., Malagon-Lopez, J., Wang, Z., Bergaya, S., et al. (2020). Smooth Muscle Cell Reprogramming in Aortic Aneurysms. *Cell Stem Cell* 26, 542–557. doi:10.1016/j.stem.2020.02.013

Chowdhury, M. M., Tarkin, J. M., Albaghdadi, M. S., Evans, N. R., Le, E. P. V., Berrett, T. B., et al. (2020). Vascular Positron Emission Tomography and Restenosis in Symptomatic Peripheral Arterial Disease. *JACC: Cardiovasc. ImagingImaging* 13, 1008–1017. doi:10.1016/j.jcmg.2019.03.031

Chowdhury, M. M., Zieliński, L. P., Sun, J. J., Lambracos, S., Boyle, J. R., Harrison, S. C., et al. (2018). Editor's Choice - Calcification of Thoracic and Abdominal Aneurysms Is Associated with Mortality and Morbidity. *Eur. J. Vasc. Endovascular Surg.* 55, 101–108. doi:10.1016/j.ejvs.2017.11.007

Colombo, M., Raposo, G., and Théry, C. (2014). Biogenesis, Secretion, and Intercellular Interactions of Exosomes and Other Extracellular Vesicles. *Annu. Rev. Cel Dev. Biol.* 30, 255–289. doi:10.1146/annurev-cellbio-101512-122326

Côté, N., El Husseini, D., Pépin, A., Guauque-Olarte, S., Ducharme, V., Bouchard-Cannon, P., et al. (2012). ATP Acts as a Survival Signal and Prevents the Mineralization of Aortic Valve. *J. Mol. Cell Cardiol.* 52, 1191–1202. doi:10.1016/j.yjmcc.2012.02.003

Crawford, J. R., Trial, J., Nambi, V., Hoogeveen, R. C., Taffet, G. E., and Entman, M. L. (2016). Plasma Levels of Endothelial Microparticles Bearing Monomeric C-Reactive Protein Are Increased in Peripheral Artery Disease. *J. Cardiovasc. Trans. Res.* 9, 184–193. doi:10.1007/s12265-016-9678-0

Cui, L., Rashdan, N. A., Zhu, D., Milne, E. M., Ajuh, P., Milne, G., et al. (2017). End Stage Renal Disease-Induced Hypercalcemia May Promote Aortic Valve Calcification via Annexin VI Enrichment of Valve Interstitial Cell Derived-Matrix Vesicles. *J. Cel. Physiol.* 232, 2985–2995. doi:10.1002/jcp.25935

Cui, Y., Zheng, L., Jiang, M., Jia, R., Zhang, X., Quan, Q., et al. (2013). Circulating Microparticles in Patients with Coronary Heart Disease and its Correlation with Interleukin-6 and C-Reactive Protein. *Mol. Biol. Rep.* 40, 6437–6442. doi:10.1007/s11033-013-2758-1

Dann, R., Hadi, T., Montenont, E., Boytard, L., Alebrahim, D., Feinstein, J., et al. (2018). Platelet-Derived MRP-14 Induces Monocyte Activation in Patients with Symptomatic Peripheral Artery Disease. *J. Am. Coll. Cardiol.* 71, 53–65. doi:10.1016/j.jacc.2017.10.072

Derksen, W. J. M., De Vries, J.-P. P. M., Vink, A., Velema, E., Vos, J.-A., De Kleijn, D., et al. (2010). Histologic Atherosclerotic Plaque Characteristics Are Associated with Restenosis Rates after Endarterectomy of the Common and Superficial Femoral Arteries. *J. Vasc. Surg.* 52, 592–599. doi:10.1016/J.JVS.2010.03.063

Detrano, R., Guerci, A. D., Carr, J. J., Bild, D. E., Burke, G., Folsom, A. R., et al. (2008). Coronary Calcium as a Predictor of Coronary Events in Four Racial or Ethnic Groups. *N. Engl. J. Med.* 358, 1336–1345. doi:10.1056/nejmoa072100

Dharmarajan, S., Speer, M. Y., Pierce, K., Lally, J., Leaf, E. M., Lin, M.-E., et al. (2021). Role of Runx2 in Calcific Aortic Valve Disease in Mouse Models. *Front. Cardiovasc. Med.* 8. doi:10.3389/fcvm.2021.687210

Dubis, J., Litwin, M., Michalowska, D., Zuk, N., Szczepanska-Buda, A., Grendziak, R., et al. (2016). Elevated Expression of Runt-Related Transcription Factors in Human Abdominal Aortic Aneurysm. *J. Biol. Regul. Homeost Agents* 30, 497–504.

Durham, A. L., Speer, M. Y., Scatena, M., Giachelli, C. M., and Shanahan, C. M. (2018). Role of Smooth Muscle Cells in Vascular Calcification: Implications in Atherosclerosis and Arterial Stiffness. *Cardiovasc. Res.* 114, 590–600. doi:10.1093/cvr/cvy010

Dweck, M. R., Boon, N. A., and Newby, D. E. (2012). Calcific Aortic Stenosis. *J. Am. Coll. Cardiol.* 60, 1854–1863. doi:10.1016/j.jacc.2012.02.093

Engelberger, R. P., Limacher, A., Kucher, N., Baumann, F., Silbernagel, G., Benghozi, R., et al. (2015). Biological Variation of Established and Novel Biomarkers for Atherosclerosis: Results from a Prospective, Parallel-Group Cohort Study. *Clinica Chim. Acta* 447, 16–22. doi:10.1016/j.cca.2015.05.003

Exner, T., Ma, D. D. F., Joseph, J. E., and Connor, D. E. (2010). The Majority of Circulating Platelet-Derived Microparticles Fail to Bind Annexin V, Lack Phospholipid-dependent Procoagulant Activity and Demonstrate Greater Expression of Glycoprotein Ib. *Thromb. Haemost.* 103, 1044–1052. doi:10.1160/TH09-09-0644

Fan, Y., Wang, L., Li, Y., Yin, Z., Xu, Z., and Wang, C. (2014). Quantification of Endothelial Microparticles on Modified Cytometric Bead Assay and Prognosis in Chest Pain Patients. *Circ. J.* 78, 206–214. doi:10.1253/circj.cj-13-0488

Fernandez-García, C.-E., Burillo, E., Lindholt, J. S., Martinez-Lopez, D., Pilely, K., Mazzeo, C., et al. (2017). Association of Ficolin-3 with Abdominal Aortic Aneurysm Presence and Progression. *J. Thromb. Haemost.* 15, 575–585. doi:10.1111/jth.13608

Figliolini, F., Ranghino, A., Grange, C., Cedrino, M., Tapparo, M., Cavallari, C., et al. (2020). Extracellular Vesicles from Adipose Stem Cells Prevent Muscle Damage and Inflammation in a Mouse Model of Hind Limb Ischemia. *Atvb* 40, 239–254. doi:10.1161/atvbaha.119.313506

Folkesson, M., Li, C., Frebelius, S., Swedenborg, J., Wågsäter, D., Williams, K. J., et al. (2015). Proteolytically Active ADAM10 and ADAM17 Carried on Membrane Microvesicles in Human Abdominal Aortic Aneurysms. *Thromb. Haemost.* 114, 1165–1174. doi:10.1160/TH14-10-0899

Forsythe, R. O., Dweck, M. R., McBride, O. M. B., Vesey, A. T., Semple, S. I., Shah, A. S. V., et al. (2018). 18F-Sodium Fluoride Uptake in Abdominal Aortic Aneurysms. *J. Am. Coll. Cardiol.* 71, 513–523. doi:10.1016/j.jacc.2017.11.053

Fowkes, F. G. R., Aboyans, V., Fowkes, F. J. I., McDermott, M. M., Sampson, U. K. A., and Criqui, M. H. (2017). Peripheral Artery Disease: Epidemiology and Global Perspectives. *Nat. Rev. Cardiol.* 14, 156–170. doi:10.1038/nrcardio.2016.179

Fowkes, F. G. R., Rudan, D., Rudan, I., Aboyans, V., Denenberg, J. O., McDermott, M. M., et al. (2013). Comparison of Global Estimates of Prevalence and Risk Factors for Peripheral Artery Disease in 2000 and 2010: a Systematic Review and Analysis. *The Lancet* 382, 1329–1340. doi:10.1016/S0140-6736(13)61249-0

Frank, U., Nikol, S., and Belch, J. (2019). 5 Conservative Treatment for PAD - Risk Factor Management. *Vasa* 48, 1–12. doi:10.1024/0301-1526/a000835

Furmanik, M., Chatrou, M., Van Gorp, R., Akbulut, A., Willems, B., Schmidt, H., et al. (2020). Reactive Oxygen-Forming Nox5 Links Vascular Smooth Muscle Cell Phenotypic Switching and Extracellular Vesicle-Mediated Vascular Calcification. *Circ. Res.* 127, 911–927. doi:10.1161/CIRCRESAHA.119.316159

Gangadaran, P., Rajendran, R. L., Lee, H. W., Kalimuthu, S., Hong, C. M., Jeong, S. Y., et al. (2017). Extracellular Vesicles from Mesenchymal Stem Cells Activates VEGF Receptors and Accelerates Recovery of Hindlimb Ischemia. *J. Controlled Release* 264, 112–126. doi:10.1016/j.jconrel.2017.08.022

Gerhard-Herman, M. D., Gornik, H. L., Barrett, C., Barshes, N. R., Corriere, M. A., Drachman, D. E., et al. (2017). 2016 AHA/ACC Guideline on the Management of Patients with Lower Extremity Peripheral Artery Disease: A Report of the American College of Cardiology/American Heart Association Task Force on Clinical Practice Guidelines. *Circulation* 135, e726–e779. doi:10.1161/CIR.0000000000000471

Giannopoulos, G., Oudatzis, G., Paterakis, G., Synetos, A., Tampaki, E., Bouras, G., et al. (2014). Red Blood Cell and Platelet Microparticles in Myocardial Infarction Patients Treated with Primary Angioplasty. *Int. J. Cardiol.* 176, 145–150. doi:10.1016/j.ijcard.2014.07.022

Giarretta, I., Gatto, I., Marcantoni, M., Lupi, G., Tonello, D., Gaetani, E., et al. (2018). Microparticles Carrying Sonic Hedgehog Are Increased in Humans with Peripheral Artery Disease. *Ijms* 19, 3954. doi:10.3390/ijms19123954

Giró, O., Jiménez, A., Pané, A., Badimon, L., Ortega, E., and Chiva-Blanch, G. (2021). Extracellular Vesicles in Atherothrombosis and Cardiovascular Disease: Friends and Foes. *Atherosclerosis* 330, 61–75. doi:10.1016/j.atherosclerosis.2021.07.002

Goettsch, C., Hutcheson, J. D., Aikawa, M., Iwata, H., Pham, T., Nykjaer, A., et al. (2016). Sortilin Mediates Vascular Calcification via its Recruitment into Extracellular Vesicles. *J. Clin. Invest.* 126, 1323–1336. doi:10.1172/JCI80851

Goettsch, C., Kjolby, M., and Aikawa, E. (2018). Sortilin and its Multiple Roles in Cardiovascular and Metabolic Diseases. *Atvb* 38, 19–25. doi:10.1161/ATVBAHA.117.310292

Gordon, C., Gudi, K., Krause, A., Sackrowitz, R., Harvey, B.-G., Strulovici-Barel, Y., et al. (2011). Circulating Endothelial Microparticles as a Measure of Early Lung Destruction in Cigarette Smokers. *Am. J. Respir. Crit. Care Med.* 184, 224–232. doi:10.1164/rccm.201012-2061OC

Hajibandeh, S., Hajibandeh, S., Shah, S., Child, E., Antoniou, G. A., and Torella, F. (2017). Prognostic Significance of Ankle Brachial Pressure index: A Systematic Review and Meta-Analysis. *Vascular* 25, 208–224. doi:10.1177/1708538116658392

Han, D., Cordoso, R., Whelton, S., Rozanski, A., Budoff, M. J., Miedema, M. D., et al. (2021). Prognostic Significance of Aortic Valve Calcium in Relation to Coronary Artery Calcification for Long-Term, Cause-specific Mortality: Results from the CAC Consortium. *Eur. Heart J. Cardiovasc. Imaging* 22, 1257–1263. doi:10.1093/ehjci/jeaa336

Han, Z. L., Wang, H. Q., Zhang, T. S., He, Y. X., and Zhou, H. (2020). Up-regulation of Exosomal miR-106a May Play a Significant Role in Abdominal Aortic Aneurysm by Inducing Vascular Smooth Muscle Cell Apoptosis and Targeting TIMP-2, an Inhibitor of Metallopeptidases that Suppresses Extracellular Matrix Degradation. *Eur. Rev. Med. Pharmacol. Sci.* 24, 8087–8095. doi:10.26355/eurrev_202008_22493

Herrmann, I. K., Wood, M. J. A., and Fuhrmann, G. (2021). Extracellular Vesicles as a Next-Generation Drug Delivery Platform. *Nat. Nanotechnol.* 16, 748–759. doi:10.1038/s41565-021-00931-2

Hodroge, A., Trécherel, E., Cornu, M., Darwiche, W., Mansour, A., Ait-Mohand, K., et al. (2017). Oligogalacturonic Acid Inhibits Vascular Calcification by Two Mechanisms. *Atvb* 37, 1391–1401. doi:10.1161/ATVBAHA.117.309513

Horn, P., Erkilet, G., Veulemans, V., Kröpil, P., Schurgers, L., Zeus, T., et al. (2016). Microparticle-induced Coagulation Relates to Coronary Artery Atherosclerosis in Severe Aortic Valve Stenosis. *PLoS One* 11, e0151499. doi:10.1371/journal.pone.0151499

Horn, P., Stern, D., Veulemans, V., Heiss, C., Zeus, T., Merx, M. W., et al. (2015). Improved Endothelial Function and Decreased Levels of Endothelium-Derived Microparticles after Transcatheter Aortic Valve Implantation. *EuroIntervention* 10, 1456–1463. doi:10.4244/EIJY14M10_02

Hu, G.-w., Li, Q., Niu, X., Hu, B., Liu, J., Zhou, S.-m., et al. (2015). Exosomes Secreted by Human-Induced Pluripotent Stem Cell-Derived Mesenchymal Stem Cells Attenuate Limb Ischemia by Promoting Angiogenesis in Mice. *Stem Cel Res. Ther.* 6. doi:10.1186/SCRT546

Hu, S., Li, Z., Shen, D., Zhu, D., Huang, K., Su, T., et al. (2021a). Exosome-eluting Stents for Vascular Healing after Ischaemic Injury. *Nat. Biomed. Eng.* 5, 1174–1188. doi:10.1038/s41551-021-00705-0

Hu, Z., Liu, W., Hua, X., Chen, X., Chang, Y., Hu, Y., et al. (2021b). Single-Cell Transcriptomic Atlas of Different Human Cardiac Arteries Identifies Cell Types Associated with Vascular Physiology. *Atvb* 41, 1408–1427. doi:10.1161/ATVBAHA.120.315373

Hutcheson, J. D., Goettsch, C., Bertazzo, S., Maldonado, N., Ruiz, J. L., Goh, W., et al. (2016). Genesis and Growth of Extracellular-Vesicle-Derived Microcalcification in Atherosclerotic Plaques. *Nat. Mater* 15, 335–343. doi:10.1038/nmat4519

Iung, B., and Vahanian, A. (2006). Valvular Heart Diseases in Elderly People. *The Lancet* 368, 969–971. doi:10.1016/S0140-6736(06)69216-7

Jia, L.-X., Zhang, W.-M., Li, T.-T., Liu, Y., Piao, C.-M., Ma, Y.-C., et al. (2017). ER Stress Dependent Microparticles Derived from Smooth Muscle Cells Promote Endothelial Dysfunction during Thoracic Aortic Aneurysm and Dissection. *Clin. Sci.* 131, 1287–1299. doi:10.1042/CS20170252

Jirak, P., Mirna, M., Wernly, B., Paar, V., Thieme, M., Betge, S., et al. (2018). Analysis of Novel Cardiovascular Biomarkers in Patients with Peripheral Artery Disease. *Minerva Med.* 109, 443–450. doi:10.23736/S0026-4806.18.05628-8

Ju, C., Shen, Y., Ma, G., Liu, Y., Cai, J., Kim, I.-m., et al. (2018). Transplantation of Cardiac Mesenchymal Stem Cell-Derived Exosomes Promotes Repair in Ischemic Myocardium. *J. Cardiovasc. Trans. Res.* 11, 420–428. doi:10.1007/s12265-018-9822-0

Jung, C., Lichtenauer, M., Figulla, H.-R., Wernly, B., Goebel, B., Foerster, M., et al. (2017). Microparticles in Patients Undergoing Transcatheter Aortic Valve Implantation (TAVI). *Heart Vessels* 32, 458–466. doi:10.1007/s00380-016-0885-z

Jung, K.-H., Chu, K., Lee, S.-T., Park, H.-K., Bahn, J.-J., Kim, D.-H., et al. (2009). Circulating Endothelial Microparticles as a Marker of Cerebrovascular Disease. *Ann. Neurol.* 66, 191–199. doi:10.1002/ana.21681

Kamenskiy, A., Poulson, W., Sim, S., Reilly, A., Luo, J., and Mactaggart, J. (2018). Prevalence of Calcification in Human Femoropopliteal Arteries and its Association with Demographics, Risk Factors, and Arterial Stiffness. *Atvb* 38, e48–e57. doi:10.1161/ATVBAHA.117.310490

Kanwar, A., Thaden, J. J., and Nkomo, V. T. (2018). Management of Patients with Aortic Valve Stenosis. *Mayo Clinic Proc.* 93, 488–508. doi:10.1016/j.mayocp.2018.01.020

Kapustin, A. N., Chatrou, M. L. L., Drozdov, I., Zheng, Y., Davidson, S. M., Soong, D., et al. (2015). Vascular Smooth Muscle Cell Calcification Is Mediated by Regulated Exosome Secretion. *Circ. Res.* 116, 1312–1323. doi:10.1161/CIRCRESAHA.116.305012

Kapustin, A. N., Davies, J. D., Reynolds, J. L., McNair, R., Jones, G. T., Sidibe, A., et al. (2011). Calcium Regulates Key Components of Vascular Smooth Muscle Cell-Derived Matrix Vesicles to Enhance Mineralization. *Circ. Res.* 109. doi:10.1161/CIRCRESAHA.110.238808

Karlöf, E., Seime, T., Dias, N., Lengquist, M., Witasp, A., Almqvist, H., et al. (2019). Correlation of Computed Tomography with Carotid Plaque Transcriptomes Associates Calcification with Lesion-Stabilization. *Atherosclerosis* 288, 175–185. doi:10.1016/j.atherosclerosis.2019.05.005

Klink, A., Hyafil, F., Rudd, J., Faries, P., Fuster, V., Mallat, Z., et al. (2011). Diagnostic and Therapeutic Strategies for Small Abdominal Aortic Aneurysms. *Nat. Rev. Cardiol.* 8, 338–347. doi:10.1038/nrcardio.2011.1

Kochtebane, N., Passefort, S., Choqueux, C., Ainoun, F., Achour, L., Michel, J. B., et al. (2013). Release of Leukotriene B4, Transforming Growth Factor-Beta1 and Microparticles in Relation to Aortic Valve Calcification. *J. Heart Valve Dis.* 22, 782–788. Available at: https://pubmed.ncbi.nlm.nih.gov/24597398/ (Accessed January 3, 2022).

Koga, H., Sugiyama, S., Kugiyama, K., Watanabe, K., Fukushima, H., Tanaka, T., et al. (2005). Elevated Levels of VE-Cadherin-Positive Endothelial Microparticles in Patients with Type 2 Diabetes Mellitus and Coronary Artery Disease. *J. Am. Coll. Cardiol.* 45, 1622–1630. doi:10.1016/j.jacc.2005.02.047

Krohn, J. B., Hutcheson, J. D., Martínez-Martínez, E., Irvin, W. S., Bouten, C. V. C., Bertazzo, S., et al. (2016). Discoidin Domain Receptor-1 Regulates Calcific Extracellular Vesicle Release in Vascular Smooth Muscle Cell Fibrocalcific Response via Transforming Growth Factor-β Signaling. *Atvb* 36, 525–533. doi:10.1161/ATVBAHA.115.307009

Leroyer, A. S., Ebrahimian, T. G., Cochain, C., Re´calde, A., Blanc-Brude, O., Mees, B., et al. (2009). Microparticles from Ischemic Muscle Promotes Postnatal Vasculogenesis. *Circulation* 119, 2808–2817. doi:10.1161/CIRCULATIONAHA.108.816710

Li, P., and Qin, C. (2015). Elevated Circulating VE-Cadherin+CD144+Endothelial Microparticles in Ischemic Cerebrovascular Disease. *Thromb. Res.* 135, 375–381. doi:10.1016/j.thromres.2014.12.006

Li, S., Wei, J., Zhang, C., Li, X., Meng, W., Mo, X., et al. (2016). Cell-Derived Microparticles in Patients with Type 2 Diabetes Mellitus: A Systematic Review and Meta-Analysis. *Cell. Physiol. Biochem.* 39, 2439–2450. doi:10.1159/000452512

Li, Z., Zhao, P., Zhang, Y., Wang, J., Wang, C., Liu, Y., et al. (2021). Exosome-based Ldlr Gene Therapy for Familial Hypercholesterolemia in a Mouse Model. *Theranostics* 11, 2953–2965. doi:10.7150/THNO.49874

Li, Z., Zhao, Z., Cai, Z., Sun, Y., Li, L., Yao, F., et al. (2020). Runx2 (Runt-Related Transcription Factor 2)-Mediated Microcalcification Is a Novel Pathological Characteristic and Potential Mediator of Abdominal Aortic Aneurysm. *Atvb* 40, 1352–1369. doi:10.1161/ATVBAHA.119.314113

Libby, P. (2021). The Changing Landscape of Atherosclerosis. *Nature* 592, 524–533. doi:10.1038/s41586-021-03392-8

Lin, Y.-N., Mesquita, T., Sanchez, L., Chen, Y.-H., Liu, W., Li, C., et al. (2021). Extracellular Vesicles from Immortalized Cardiosphere-Derived Cells Attenuate Arrhythmogenic Cardiomyopathy in Desmoglein-2 Mutant Mice. *Eur. Heart J.* 42, 3558–3571. doi:10.1093/eurheartj/ehab419

Liu, Y., He, Z., Zhang, Y., Dong, Z., Bi, Y., Kou, J., et al. (2016). Dissimilarity of Increased Phosphatidylserine-Positive Microparticles and Associated Coagulation Activation in Acute Coronary Syndromes. *Coron. Artery Dis.* 27, 365–375. doi:10.1097/MCA.0000000000000368

Lopatina, T., Favaro, E., Grange, C., Cedrino, M., Ranghino, A., Occhipinti, S., et al. (2018). PDGF Enhances the Protective Effect of Adipose Stem Cell-Derived Extracellular Vesicles in a Model of Acute Hindlimb Ischemia. *Sci. Rep.* 8. doi:10.1038/S41598-018-36143-3

Madrigal-Matute, J., Lindholt, J. S., Fernandez-Garcia, C. E., Benito-Martin, A., Burillo, E., Zalba, G., et al. (2014). Galectin-3, a Biomarker Linking Oxidative Stress and Inflammation with the Clinical Outcomes of Patients with Atherothrombosis. *Jaha* 3. doi:10.1161/JAHA.114.000785

Mannello, F., and Medda, V. (2012). Nuclear Localization of Matrix Metalloproteinases. *Prog. Histochem. Cytochem.* 47, 27–58. doi:10.1016/j.proghi.2011.12.002

Mantovani, F., Fanti, D., Tafciu, E., Fezzi, S., Setti, M., Rossi, A., et al. (2021). When Aortic Stenosis Is Not Alone: Epidemiology, Pathophysiology, Diagnosis and Management in Mixed and Combined Valvular Disease. *Front. Cardiovasc. Med.* 8, 744497. doi:10.3389/fcvm.2021.744497

Marchini, J. F., Miyakawa, A. A., Tarasoutchi, F., Krieger, J. E., Lemos, P., and Croce, K. (2016). Endothelial, Platelet, and Macrophage Microparticle Levels Do Not Change Acutely Following Transcatheter Aortic Valve Replacement. *J. Negat. Results Biomed.* 15. doi:10.1186/s12952-016-0051-2

Martin-Blazquez, A., Heredero, A., Aldamiz-Echevarria, G., Martin-Lorenzo, M., and Alvarez-Llamas, G. (2021). Non-syndromic Thoracic Aortic Aneurysm: Cellular and Molecular Insights. *J. Pathol.* 254, 229–238. doi:10.1002/path.5683

Martinez-Pinna, R., de Peredo, A. G., Monsarrat, B., Burlet-Schiltz, O., and Martin-Ventura, J. L. (2014). Label-free Quantitative Proteomic Analysis of Human Plasma-Derived Microvesicles to Find Protein Signatures of Abdominal Aortic Aneurysms. *Prot. Clin. Appl.* 8, 620–625. doi:10.1002/prca.201400010

Mathieu, P., Boulanger, M.-C., and Bouchareb, R. (2014). Molecular Biology of Calcific Aortic Valve Disease: Towards New Pharmacological Therapies. *Expert Rev. Cardiovasc. Ther.* 12, 851–862. doi:10.1586/14779072.2014.923756

Mathiyalagan, P., Liang, Y., Kim, D., Misener, S., Thorne, T., Kamide, C. E., et al. (2017). Angiogenic Mechanisms of Human CD34 + Stem Cell Exosomes in the Repair of Ischemic Hindlimb. *Circ. Res.* 120, 1466–1476. doi:10.1161/circresaha.116.310557

McEvoy, J. W., Blaha, M. J., DeFilippis, A. P., Budoff, M. J., Nasir, K., Blumenthal, R. S., et al. (2010). Coronary Artery Calcium Progression: An Important Clinical Measurement? *J. Am. Coll. Cardiol.* 56, 1613–1622. doi:10.1016/j.jacc.2010.06.038

Méndez-Barbero, N., Gutiérrez-Muñoz, C., and Blanco-Colio, L. (2021). Cellular Crosstalk between Endothelial and Smooth Muscle Cells in Vascular wall Remodeling. *Ijms* 22, 7284. doi:10.3390/ijms22147284

Michel, J.-B., Jondeau, G., and Milewicz, D. M. (2018). From Genetics to Response to Injury: Vascular Smooth Muscle Cells in Aneurysms and Dissections of the Ascending Aorta. *Cardiovasc. Res.* 114, 578–589. doi:10.1093/cvr/cvy006

Michel, J.-B., Martin-Ventura, J.-L., Egido, J., Sakalihasan, N., Treska, V., Lindholt, J., et al. (2011). Novel Aspects of the Pathogenesis of Aneurysms of the Abdominal Aorta in Humans. *Cardiovasc. Res.* 90, 18–27. doi:10.1093/cvr/cvq337

Milewicz, D. M., and Ramirez, F. (2019). Therapies for Thoracic Aortic Aneurysms and Acute Aortic Dissections. *Atvb* 39, 126–136. doi:10.1161/ATVBAHA.118.310956

Mobarrez, F., Egberg, N., Antovic, J., Bröijersen, A., Jörneskog, G., and Wallén, H. (2012). Release of Endothelial Microparticles *In Vivo* during Atorvastatin Treatment; A Randomized Double-Blind Placebo-Controlled Study. *Thromb. Res.* 129, 95–97. doi:10.1016/j.thromres.2011.09.027

Mobarrez, F., He, S., Bröijersen, A., Wiklund, B., Antovic, A., Antovic, J., et al. (2011). Atorvastatin Reduces Thrombin Generation and Expression of Tissue Factor, P-Selectin and GPIIIa on Platelet-Derived Microparticles in Patients with Peripheral Arterial Occlusive Disease. *Thromb. Haemost.* 106, 344–352. doi:10.1160/TH10-12-0810

Mohler, E. R., Gannon, F., Reynolds, C., Zimmerman, R., Keane, M. G., and Kaplan, F. S. (2001). Bone Formation and Inflammation in Cardiac Valves. *Circulation* 103, 1522–1528. doi:10.1161/01.CIR.103.11.1522

Momen-Heravi, F., Getting, S. J., and Moschos, S. A. (2018). Extracellular Vesicles and Their Nucleic Acids for Biomarker Discovery. *Pharmacol. Ther.* 192, 170–187. doi:10.1016/j.pharmthera.2018.08.002

Monzack, E. L., and Masters, K. S. (2011). Can Valvular Interstitial Cells Become True Osteoblasts? A Side-By-Side Comparison. *J. Heart Valve Dis.* 20, 449–463. Available at: https://pubmed.ncbi.nlm.nih.gov/21863660/(Accessed January 4, 2022).

New, S. E. P., Goettsch, C., Aikawa, M., Marchini, J. F., Shibasaki, M., Yabusaki, K., et al. (2013). Macrophage-Derived Matrix Vesicles. *Circ. Res.* 113, 72–77. doi:10.1161/CIRCRESAHA.113.301036

Ngai, D., Lino, M., Rothenberg, K. E., Simmons, C. A., Fernandez-Gonzalez, R., Bendeck, M. P., et al. (2020). DDR1 (Discoidin Domain Receptor-1)-RhoA (Ras Homolog Family Member A) Axis Senses Matrix Stiffness to Promote Vascular Calcification. *Atvb* 40, 1763–1776. doi:10.1161/ATVBAHA.120.314697

Nkomo, V. T., Gardin, J. M., Skelton, T. N., Gottdiener, J. S., Scott, C. G., and Enriquez-Sarano, M. (2006). Burden of Valvular Heart Diseases: a Population-Based Study. *The Lancet* 368, 1005–1011. doi:10.1016/S0140-6736(06)69208-8

Nomura, S. (2017). Extracellular Vesicles and Blood Diseases. *Int. J. Hematol.* 105, 392–405. doi:10.1007/s12185-017-2180-x

Nomura, S., Inami, N., Iwasaka, T., and Liu, Y. (2004). Platelet Activation Markers, Microparticles and Soluble Adhesion Molecules Are Elevated in Patients with Arteriosclerosis Obliterans: Therapeutic Effects by Cilostazol and Potentiation by Dipyridamole. *Platelets* 15, 167–172. doi:10.1080/09537100410001682779

Norgren, L., Hiatt, W. R., Dormandy, J. A., Nehler, M. R., Harris, K. A., Fowkes, F. G. R., et al. (2007). Inter-Society Consensus for the Management of Peripheral Arterial Disease (TASC II). *J. Vasc. Surg.* 45, S5–S67. doi:10.1016/j.jvs.2006.12.037

O'Brien, C. G., Ozen, M. O., Ikeda, G., Vaskova, E., Jung, J. H., Bayardo, N., et al. (2021). Mitochondria-Rich Extracellular Vesicles Rescue Patient-specific Cardiomyocytes from Doxorubicin Injury. *JACC: CardioOncology* 3, 428–440. doi:10.1016/j.jaccao.2021.05.006

O'Brien, K. D., Kuusisto, J., Reichenbach, D. D., Ferguson, M., Giachelli, C., Alpers, C. E., et al. (1995). Osteopontin Is Expressed in Human Aortic Valvular Lesions. *Circulation* 92, 2163–2168. doi:10.1161/01.CIR.92.8.2163

O'Brien, K. D. (2006). Pathogenesis of Calcific Aortic Valve Disease. *Atvb* 26, 1721–1728. doi:10.1161/01.ATV.0000227513.13697.ac

Ohtsuka, M., Sasaki, K.-i., Ueno, T., Seki, R., Nakayoshi, T., Koiwaya, H., et al. (2013). Platelet-derived Microparticles Augment the Adhesion and Neovascularization Capacities of Circulating Angiogenic Cells Obtained from Atherosclerotic Patients. *Atherosclerosis* 227, 275–282. doi:10.1016/j.atherosclerosis.2013.01.040

O'Neill, W. C., Han, K. H., Schneider, T. M., and Hennigar, R. A. (2015). Prevalence of Nonatheromatous Lesions in Peripheral Arterial Disease. *Atvb* 35, 439–447. doi:10.1161/ATVBAHA.114.304764

Osman, L., Yacoub, M. H., Latif, N., Amrani, M., and Chester, A. H. (2006). Role of Human Valve Interstitial Cells in Valve Calcification and Their Response to Atorvastatin. *Circulation* 114. doi:10.1161/CIRCULATIONAHA.105.001115

Owens, D. S., Budoff, M. J., Katz, R., Takasu, J., Shavelle, D. M., Carr, J. J., et al. (2012). Aortic Valve Calcium Independently Predicts Coronary and Cardiovascular Events in a Primary Prevention Population. *JACC: Cardiovasc. Imaging* 5, 619–625. doi:10.1016/j.jcmg.2011.12.023

Pan, H., Xue, C., Auerbach, B. J., Fan, J., Bashore, A. C., Cui, J., et al. (2020). Single-Cell Genomics Reveals a Novel Cell State during Smooth Muscle Cell Phenotypic Switching and Potential Therapeutic Targets for Atherosclerosis in Mouse and Human. *Circulation* 142, 2060–2075. doi:10.1161/CIRCULATIONAHA.120.048378

Passos, L. S. A., Lupieri, A., Becker-Greene, D., and Aikawa, E. (2020). Innate and Adaptive Immunity in Cardiovascular Calcification. *Atherosclerosis* 306, 59–67. doi:10.1016/j.atherosclerosis.2020.02.016

Patel, N., Chin, D. D., and Chung, E. J. (2021). Exosomes in Atherosclerosis, a Double-Edged Sword: Their Role in Disease Pathogenesis and Their Potential as Novel Therapeutics. *AAPS J.* 23. doi:10.1208/s12248-021-00621-w

Petsophonsakul, P., Burgmaier, M., Willems, B., Heeneman, S., Stadler, N., Gremse, F., et al. (2021). Nicotine Promotes Vascular Calcification via Intracellular Ca2+-Mediated, Nox5-Induced Oxidative Stress, and Extracellular Vesicle Release in Vascular Smooth Muscle Cells. *Cardiovasc. Res*. doi:10.1093/cvr/cvab244

Petsophonsakul., P., Furmanik, M., Forsythe, R., Dweck, M., Schurink, G. W., Natour, E., et al. (2019). Role of Vascular Smooth Muscle Cell Phenotypic Switching and Calcification in Aortic Aneurysm Formation. *Atvb* 39, 1351–1368. doi:10.1161/ATVBAHA.119.312787

Pinard, A., Jones, G. T., and Milewicz, D. M. (2019). Genetics of Thoracic and Abdominal Aortic Diseases. *Circ. Res.* 124, 588–606. doi:10.1161/CIRCRESAHA.118.312436

Poredoš, P., Cevc, M., and Blinc, A. (2021). Characteristics of Atherosclerosis in Femoropopliteal Artery and its Clinical Relevance. *Atherosclerosis* 335, 31–40. doi:10.1016/j.atherosclerosis.2021.09.012

Preston, R. A., Jy, W., Jimenez, J. J., Mauro, L. M., Horstman, L. L., Valle, M., et al. (2003). Effects of Severe Hypertension on Endothelial and Platelet Microparticles. *Hypertension* 41, 211–217. doi:10.1161/01.HYP.0000049760.15764.2D

Rajamannan, N. M., Nealis, T. B., Subramaniam, M., Pandya, S., Stock, S. R., Ignatiev, C. I., et al. (2005). Calcified Rheumatic Valve Neoangiogenesis Is Associated with Vascular Endothelial Growth Factor Expression and Osteoblast-like Bone Formation. *Circulation* 111, 3296–3301. doi:10.1161/CIRCULATIONAHA.104.473165

Rajamannan, N. M., Subramaniam, M., Rickard, D., Stock, S. R., Donovan, J., Springett, M., et al. (2003). Human Aortic Valve Calcification Is Associated with an Osteoblast Phenotype. *Circulation* 107, 2181–2184. doi:10.1161/01.CIR.0000070591.21548.69

Rogers, M. A., Buffolo, F., Schlotter, F., Atkins, S. K., Lee, L. H., Halu, A., et al. (2020a). Annexin A1-dependent Tethering Promotes Extracellular Vesicle Aggregation Revealed with Single-Extracellular Vesicle Analysis. *Sci. Adv.* 6. doi:10.1126/sciadv.abb1244

Rogers, M. A., Chen, J., Nallamshetty, S., Pham, T., Goto, S., Muehlschlegel, J. D., et al. (2020b). Retinoids Repress Human Cardiovascular Cell Calcification with Evidence for Distinct Selective Retinoid Modulator Effects. *Atvb* 40, 656–669. doi:10.1161/ATVBAHA.119.313366

Rosińska, J., Łukasik, M., and Kozubski, W. (2017). The Impact of Vascular Disease Treatment on Platelet-Derived Microvesicles. *Cardiovasc. Drugs Ther.* 31, 627–644. doi:10.1007/s10557-017-6757-7

Roth, G. A., Johnson, C., Abajobir, A., Abd-Allah, F., Abera, S. F., Abyu, G., et al. (2017). Global, Regional, and National Burden of Cardiovascular Diseases for 10 Causes, 1990 to 2015. *J. Am. Coll. Cardiol.* 70, 1–25. doi:10.1016/j.jacc.2017.04.052

Russell, A. E., Sneider, A., Witwer, K. W., Bergese, P., Bhattacharyya, S. N., Cocks, A., et al. (2019). Biological Membranes in EV Biogenesis, Stability, Uptake, and Cargo Transfer: an ISEV Position Paper Arising from the ISEV Membranes and EVs Workshop. *J. Extracellular Vesicles* 8, 1684862. doi:10.1080/20013078.2019.1684862

Ryu, J.-H., Jeon, E.-Y., and Kim, S.-J. (2019). Indoxyl Sulfate-Induced Extracellular Vesicles Released from Endothelial Cells Stimulate Vascular Smooth Muscle Cell Proliferation by Inducing Transforming Growth Factor-Beta Production. *J. Vasc. Res.* 56, 129–138. doi:10.1159/000496796

Saenz-Pipaon, G., San Martín, P., Planell, N., Maillo, A., Ravassa, S., Vilas-Zornoza, A., et al. (2020). Functional and Transcriptomic Analysis of Extracellular Vesicles Identifies Calprotectin as a New Prognostic Marker in Peripheral Arterial Disease (PAD). *J. Extracellular Vesicles* 9, 1729646. doi:10.1080/20013078.2020.1729646

Saenz-Pipaon, G., Martinez-Aguilar, E., Orbe, J., González Miqueo, A., Fernandez-Alonso, L., Paramo, J. A., et al. (2021). The Role of Circulating Biomarkers in Peripheral Arterial Disease. *Ijms* 22, 3601. doi:10.3390/ijms22073601

Sahoo, S., Adamiak, M., Mathiyalagan, P., Kenneweg, F., Kafert-Kasting, S., and Thum, T. (2021). Therapeutic and Diagnostic Translation of Extracellular Vesicles in Cardiovascular Diseases. *Circulation* 143, 1426–1449. doi:10.1161/CIRCULATIONAHA.120.049254

Sakalihasan, N., Limet, R., and Defawe, O. (2005). Abdominal Aortic Aneurysm. *The Lancet* 365, 1577–1589. doi:10.1016/S0140-6736(05)66459-8

Schiro, A., Wilkinson, F. L., Weston, R., Smyth, J. V., Serracino-Inglott, F., and Alexander, M. Y. (2015). Elevated Levels of Endothelial-Derived Microparticles and Serum CXCL9 and SCGF-β Are Associated with Unstable Asymptomatic Carotid Plaques. *Sci. Rep.* 5. doi:10.1038/srep16658

Shah, R., Patel, T., and Freedman, J. E. (2018). Circulating Extracellular Vesicles in Human Disease. *N. Engl. J. Med.* 379, 2179–2181. doi:10.1056/NEJMc1813170

Shanahan, C. M., Crouthamel, M. H., Kapustin, A., and Giachelli, C. M. (2011). Arterial Calcification in Chronic Kidney Disease: Key Roles for Calcium and Phosphate. *Circ. Res.* 109, 697–711. doi:10.1161/CIRCRESAHA.110.234914

Simak, J., Gelderman, M. P., Yu, H., Wright, V., and Baird, A. E. (2006). Circulating Endothelial Microparticles in Acute Ischemic Stroke: A Link to Severity, Lesion Volume and Outcome. *J. Thromb. Haemost.* 4, 1296–1302. doi:10.1111/j.1538-7836.2006.01911.x

Sinning, J.-M., Losch, J., Walenta, K., Böhm, M., Nickenig, G., and Werner, N. (2011). Circulating CD31+/Annexin V+ Microparticles Correlate with Cardiovascular Outcomes. *Eur. Heart J.* 32, 2034–2041. doi:10.1093/eurheartj/ehq478

Sorrentino, T. A., Duong, P., Bouchareychas, L., Chen, M., Chung, A., Schaller, M. S., et al. (2020). Circulating Exosomes from Patients with Peripheral Artery Disease Influence Vascular Cell Migration and Contain Distinct microRNA Cargo. *JVS: Vasc. Sci.* 1, 28–41. doi:10.1016/j.jvssci.2020.02.001

Sossong, V., Helbing, T., Beyersdorf, F., Olschewski, M., Bode, C., Diehl, P., et al. (2008). Increased Levels of Circulating Microparticles in Patients with Severe Aortic Valve Stenosis. *Thromb. Haemost.* 99, 711–719. doi:10.1160/TH07-05-0334

Spinosa, M., Lu, G., Su, G., Bontha, S. V., Gehrau, R., Salmon, M. D., et al. (2018). Human Mesenchymal Stromal Cell-derived Extracellular Vesicles Attenuate Aortic Aneurysm Formation and Macrophage Activation via microRNA-147. *FASEB j.* 32, 6038–6050. doi:10.1096/fj.201701138RR

Sritharen, Y., Enriquez-Sarano, M., Schaff, H. V., Casaclang-Verzosa, G., and Miller, J. D. (2017). Pathophysiology of Aortic Valve Stenosis: Is it Both Fibrocalcific and Sex Specific? *Physiology* 32, 182–196. doi:10.1152/physiol.00025.2016

Suades, R., Padró, T., Alonso, R., Mata, P., and Badimon, L. (2015). High Levels of TSP1+/CD142+ Platelet-Derived Microparticles Characterise Young Patients with High Cardiovascular Risk and Subclinical Atherosclerosis. *Thromb. Haemost.* 114, 1310–1321. doi:10.1160/TH15-04-0325

Suades, R., Padró, T., Crespo, J., Ramaiola, I., Martin-Yuste, V., Sabaté, M., et al. (2016). Circulating Microparticle Signature in Coronary and Peripheral Blood of ST Elevation Myocardial Infarction Patients in Relation to Pain-To-PCI Elapsed Time. *Int. J. Cardiol.* 202, 378–387. doi:10.1016/j.ijcard.2015.09.011

Tan, K. T., Tayebjee, M. H., Lynd, C., Blann, A. D., and Lip, G. Y. H. (2005). Platelet Microparticles and Soluble P Selectin in Peripheral Artery Disease: Relationship to Extent of Disease and Platelet Activation Markers. *Ann. Med.* 37, 61–66. doi:10.1080/07853890410018943

Tani, T., Fujiwara, M., Orimo, H., Shimizu, A., Narisawa, S., Pinkerton, A. B., et al. (2020). Inhibition of Tissue-nonspecific Alkaline Phosphatase Protects against Medial Arterial Calcification and Improves Survival Probability in the CKD-MBD Mouse Model. *J. Pathol.* 250, 30–41. doi:10.1002/path.5346

Taylor, J., Azimi, I., Monteith, G., and Bebawy, M. (2020). Ca2+mediates Extracellular Vesicle Biogenesis through Alternate Pathways in Malignancy. *J. Extracellular Vesicles* 9, 1734326. doi:10.1080/20013078.2020.1734326

Théry, C., Witwer, K. W., Aikawa, E., Alcaraz, M. J., Anderson, J. D., Andriantsitohaina, R., et al. (2018). Minimal Information for Studies of Extracellular Vesicles 2018 (MISEV2018): a Position Statement of the International Society for Extracellular Vesicles and Update of the MISEV2014 Guidelines. *J. Extracell. Vesicles* 7, 1535750. doi:10.1080/20013078.2018.1535750

Tieu, A., Hu, K., Gnyra, C., Montroy, J., Fergusson, D. A., Allan, D. S., et al. (2021). Mesenchymal Stromal Cell Extracellular Vesicles as Therapy for Acute and Chronic Respiratory Diseases: A Meta-analysis. *J. Extracellular Vesicles* 10. doi:10.1002/jev2.12141

Timmis, A., Townsend, N., Gale, C. P., Timmis, A., Townsend, N., Gale, C. P., et al. (2020). European Society of Cardiology: Cardiovascular Disease Statistics 2019 (Executive Summary). *Eur. Heart J. Qual. Care Clin. Outcomes* 6, 7–9. doi:10.1093/ehjqcco/qcz065

Torres-Fonseca, M., Galan, M., Martinez-Lopez, D., Cañes, L., Roldan-Montero, R., Alonso, J., et al. (2019). Pathophysiology of Abdominal Aortic Aneurysm: Biomarkers and Novel Therapeutic Targets. *Clínica e Investigación en Arteriosclerosis (English Edition)* 31, 166–177. doi:10.1016/j.arteri.2018.10.00210.1016/j.artere.2018.10.003

Touat, Z., Lepage, L., Ollivier, V., Nataf, P., Hvass, U., Labreuche, J., et al. (2008). Dilation-dependent Activation of Platelets and Prothrombin in Human Thoracic Ascending Aortic Aneurysm. *Atvb* 28, 940–946. doi:10.1161/ATVBAHA.107.158576

Touat, Z., Ollivier, V., Dai, J., Huisse, M.-G., Bezeaud, A., Sebbag, U., et al. (2006). Renewal of Mural Thrombus Releases Plasma Markers and Is Involved in Aortic Abdominal Aneurysm Evolution. *Am. J. Pathol.* 168, 1022–1030. doi:10.2353/ajpath.2006.050868

Tyson, K. L., Reynolds, J. L., McNair, R., Zhang, Q., Weissberg, P. L., and Shanahan, C. M. (2003). Osteo/chondrocytic Transcription Factors and Their Target Genes Exhibit Distinct Patterns of Expression in Human Arterial Calcification. *Atvb* 23, 489–494. doi:10.1161/01.ATV.0000059406.92165.31

Vagida, M. S., Arakelyan, A., Lebedeva, A. M., Grivel, J. C., Shpektor, A. V., Vasilieva, E. Y., et al. (2016). Analysis of Extracellular Vesicles Using Magnetic Nanoparticles in Blood of Patients with Acute Coronary Syndrome. *Biochem. Mosc.* 81, 382–391. doi:10.1134/S0006297916040088

Vajen, T., Benedikter, B. J., Heinzmann, A. C. A., Vasina, E. M., Henskens, Y., Parsons, M., et al. (2017). Platelet Extracellular Vesicles Induce a Pro-inflammatory Smooth Muscle Cell Phenotype. *J. Extracellular Vesicles* 6, 1322454. doi:10.1080/20013078.2017.1322454

van der Zee, P. M., Biro´, E., Ko, Y., de Winter, R. J., Hack, C. E., Sturk, A., et al. (2006). P-selectin- and CD63-Exposing Platelet Microparticles Reflect Platelet Activation in Peripheral Arterial Disease and Myocardial Infarction. *Clin. Chem.* 52, 657–664. doi:10.1373/clinchem.2005.057414

van Niel, G., D'Angelo, G., and Raposo, G. (2018). Shedding Light on the Cell Biology of Extracellular Vesicles. *Nat. Rev. Mol. Cel Biol.* 19, 213–228. doi:10.1038/nrm.2017.125

Van Pham, P., Vu, N. B., Dao, T. T.-T., Le, H. T.-N., Phi, L. T., Huynh, O. T., et al. (2017). Extracellular Vesicles of ETV2 Transfected Fibroblasts Stimulate Endothelial Cells and Improve Neovascularization in a Murine Model of Hindlimb Ischemia. *Cytotechnology* 69, 801–814. doi:10.1007/s10616-017-0095-2

Villa-Bellosta, R. (2018). Synthesis of Extracellular Pyrophosphate Increases in Vascular Smooth Muscle Cells during Phosphate-Induced Calcification. *Atvb* 38, 2137–2147. doi:10.1161/ATVBAHA.118.311444

Villa-Bellosta, R., Wang, X., Millán, J. L., Dubyak, G. R., and O'Neill, W. C. (2011). Extracellular Pyrophosphate Metabolism and Calcification in Vascular Smooth Muscle. *Am. J. Physiology-Heart Circulatory Physiol.* 301, H61–H68. doi:10.1152/ajpheart.01020.2010

Wang, Y., Jia, L., Xie, Y., Cai, Z., Liu, Z., Shen, J., et al. (2019). Involvement of Macrophage-Derived Exosomes in Abdominal Aortic Aneurysms Development. *Atherosclerosis* 289, 64–72. doi:10.1016/j.atherosclerosis.2019.08.016

Weber, A., Liu, S. S., Cardone, L., Rellecke, P., Sixt, S. U., Lichtenberg, A., et al. (2020). The Course of Circulating Small Extracellular Vesicles in Patients Undergoing Surgical Aortic Valve Replacement. *Biomed. Res. Int.* 2020, 1–12. doi:10.1155/2020/6381396

Wekesa, A. L., Cross, K. S., O'Donovan, O., Dowdall, J. F., O'Brien, O., Doyle, M., et al. (2014). Predicting Carotid Artery Disease and Plaque Instability from Cell-Derived Microparticles. *Eur. J. Vasc. Endovascular Surg.* 48, 489–495. doi:10.1016/j.ejvs.2014.08.007

Werner, N., Wassmann, S., Ahlers, P., Kosiol, S., and Nickenig, G. (2006). Circulating CD31+/Annexin V+Apoptotic Microparticles Correlate with Coronary Endothelial Function in Patients with Coronary Artery Disease. *Atvb* 26, 112–116. doi:10.1161/01.ATV.0000191634.13057.15

Wirka, R. C., Wagh, D., Paik, D. T., Pjanic, M., Nguyen, T., Miller, C. L., et al. (2019). Atheroprotective Roles of Smooth Muscle Cell Phenotypic Modulation and the TCF21 Disease Gene as Revealed by Single-Cell Analysis. *Nat. Med.* 25, 1280–1289. doi:10.1038/s41591-019-0512-5

Xiang, D., Li, Y., Cao, Y., Huang, Y., Zhou, L., Lin, X., et al. (2021). Different Effects of Endothelial Extracellular Vesicles and LPS-Induced Endothelial Extracellular Vesicles on Vascular Smooth Muscle Cells: Role of Curcumin and its Derivatives. *Front. Cardiovasc. Med.* 8. doi:10.3389/fcvm.2021.649352

Yuan, X., Bhat, O. M., Samidurai, A., Das, A., Zhang, Y., and Li, P.-L. (2020). Reversal of Endothelial Extracellular Vesicle-Induced Smooth Muscle Phenotype Transition by Hypercholesterolemia Stimulation: Role of NLRP3 Inflammasome Activation. *Front. Cel Dev. Biol.* 8. doi:10.3389/fcell.2020.597423

Zarà, M., Guidetti, G. F., Camera, M., Canobbio, I., Amadio, P., Torti, M., et al. (2019). Biology and Role of Extracellular Vesicles (Evs) in the Pathogenesis of Thrombosis. *Ijms* 20, 2840. doi:10.3390/ijms20112840

Zeiger, F., Stephan, S., Hoheisel, G., Pfeiffer, D., Ruehlmann, C., and Koksch, M. (2000). P-selectin Expression, Platelet Aggregates, and Platelet-Derived Microparticle Formation Are Increased in Peripheral Arterial Disease. *Blood Coagul. Fibrinolysis* 11, 723–728. doi:10.1097/00001721-200012000-00005

Zhang, X., Jiang, Y., Huang, Q., Wu, Z., Pu, H., Xu, Z., et al. (2021). Exosomes Derived from Adipose-Derived Stem Cells Overexpressing Glyoxalase-1 Protect Endothelial Cells and Enhance Angiogenesis in Type 2 Diabetic Mice with Limb Ischemia. *Stem Cel Res. Ther.* 12. doi:10.1186/s13287-021-02475-7

Zhu, Q., Li, Q., Niu, X., Zhang, G., Ling, X., Zhang, J., et al. (2018). Extracellular Vesicles Secreted by Human Urine-Derived Stem Cells Promote Ischemia Repair in a Mouse Model of Hind-Limb Ischemia. *Cel. Physiol. Biochem.* 47, 1181–1192. doi:10.1159/000490214

Ziegler, S. G., Ferreira, C. R., Macfarlane, E. G., Riddle, R. C., Tomlinson, R. E., Chew, E. Y., et al. (2017). Ectopic Calcification in Pseudoxanthoma Elasticum Responds to Inhibition of Tissue-Nonspecific Alkaline Phosphatase. *Sci. Transl. Med.* 9. doi:10.1126/scitranslmed.aal1669

Conflict of Interest: The authors declare that the research was conducted in the absence of any commercial or financial relationships that could be construed as a potential conflict of interest.

Publisher's Note: All claims expressed in this article are solely those of the authors and do not necessarily represent those of their affiliated organizations, or those of the publisher, the editors and the reviewers. Any product that may be evaluated in this article, or claim that may be made by its manufacturer, is not guaranteed or endorsed by the publisher.

frontiers in Cell and Developmental Biology

ORIGINAL RESEARCH
published: 09 March 2022
doi: 10.3389/fcell.2022.823450

Extracellular Vesicles From LPS-Treated Macrophages Aggravate Smooth Muscle Cell Calcification by Propagating Inflammation and Oxidative Stress

Linda Yaker[1], Abdellah Tebani[2,3], Céline Lesueur[2], Chloé Dias[4], Vincent Jung[5], Soumeya Bekri[2,3], Ida Chiara Guerrera[5], Saïd Kamel[1,6], Jérôme Ausseil[4,7†] and Agnès Boullier[1,6†]*

[1]MP3CV-UR7517, CURS-University of Picardie Jules Verne, Amiens, France, [2]INSERM U1245, CHU Rouen, Normandie University, UNIROUEN, Rouen, France, [3]Department of Metabolic Biochemistry, Rouen University Hospital, Rouen, France, [4]Infinity, INSERM UMR1291, CNRS UMR5051, University of Toulouse III, Toulouse, France, [5]INSERM US24/CNRS UAR3633, Proteomic Platform Necker, University of Paris—Federative Research Structure Necker, Paris, France, [6]Laboratory of Biochemistry, CHU Amiens-Picardie, Amiens, France, [7]Service de Biochimie, Institut Fédératif de Biologie, CHU Toulouse, Toulouse, France

OPEN ACCESS

Edited by:
Youhua Tan,
Hong Kong Polytechnic University, Hong Kong SAR, China

Reviewed by:
Yvonne Döring,
Universitätsspital Bern Departement Herz und Gefässe Universitätsklinik für Angiologie, Switzerland
Ulrike Resch,
Medical University of Vienna, Austria

***Correspondence:**
Agnès Boullier
Boullier.agnes@chu-amiens.fr

†These authors have contributed equally to this work and share last authorship

Specialty section:
This article was submitted to Molecular and Cellular Pathology, a section of the journal Frontiers in Cell and Developmental Biology

Received: *27 November 2021*
Accepted: *09 February 2022*
Published: *09 March 2022*

Citation:
Yaker L, Tebani A, Lesueur C, Dias C, Jung V, Bekri S, Guerrera IC, Kamel S, Ausseil J and Boullier A (2022) Extracellular Vesicles From LPS-Treated Macrophages Aggravate Smooth Muscle Cell Calcification by Propagating Inflammation and Oxidative Stress. Front. Cell Dev. Biol. 10:823450. doi: 10.3389/fcell.2022.823450

Background: Vascular calcification (VC) is a cardiovascular complication associated with a high mortality rate among patients with diseases such as atherosclerosis and chronic kidney disease. During VC, vascular smooth muscle cells (VSMCs) undergo an osteogenic switch and secrete a heterogeneous population of extracellular vesicles (EVs). Recent studies have shown involvement of EVs in the inflammation and oxidative stress observed in VC. We aimed to decipher the role and mechanism of action of macrophage-derived EVs in the propagation of inflammation and oxidative stress on VSMCs during VC.

Methods: The macrophage murine cell line RAW 264.7 treated with lipopolysaccharide (LPS-EK) was used as a cellular model for inflammatory and oxidative stress. EVs secreted by these macrophages were collected by ultracentrifugation and characterized by transmission electron microscopy, cryo-electron microscopy, nanoparticle tracking analysis, and the analysis of acetylcholinesterase activity, as well as that of CD9 and CD81 protein expression by western blotting. These EVs were added to a murine VSMC cell line (MOVAS-1) under calcifying conditions (4 mM Pi—7 or 14 days) and calcification assessed by the o-cresolphthalein calcium assay. EV protein content was analyzed in a proteomic study and EV cytokine content assessed using an MSD multiplex immunoassay.

Results: LPS-EK significantly decreased macrophage EV biogenesis. A 24-h treatment of VSMCs with these EVs induced both inflammatory and oxidative responses. LPS-EK-treated macrophage-derived EVs were enriched for pro-inflammatory cytokines and CAD, PAI-1, and Saa3 proteins, three molecules involved in inflammation, oxidative stress, and VC. Under calcifying conditions, these EVs significantly increase the calcification of VSMCs by increasing osteogenic markers and decreasing contractile marker expression.

Conclusion: Our results show that EVs derived from LPS-EK–treated-macrophages are able to induce pro-inflammatory and pro-oxidative responses in surrounding cells, such as VSMCs, thus aggravating the VC process.

Keywords: extracellular vesicles, vascular calcifcation, inflammation, oxidative stress, macrophages

1 INTRODUCTION

Vascular calcification (VC) is a cardiovascular complication found among patients with diseases such as diabetes, atherosclerosis, and chronic kidney disease (CKD) (Lee et al., 2020). VC is an active process (Demer and Tintut, 2008; Voelkl et al., 2019), characterized by an imbalance of calcium/phosphate homeostasis and hydroxyapatite mineral deposition, both in the intimal and medial layers of the artery (Demer and Tintut, 2008; Drüeke and Massy, 2011; Lee et al., 2020). Vascular smooth muscle cells (VSMCs), which represent the most abundant cell type in vessels, play a pivotal role in the initiation and development of VC (Jaminon et al., 2019). VSMCs undergo a phenotypic switch, with modification of osteogenic, contractile, and synthetic marker expression (Durham et al., 2018). Other cell types may be involved in the induction of the VC process, such as macrophages (Li Y. et al., 2020) and endothelial cells. Indeed, macrophages play an important role in the progression of VC by secreting inflammatory factors and inducing oxidative stress (Hénaut et al., 2019). As a consequence, macrophage-induced inflammation can reduce the production of VC inhibitors, such as fetuin-A (Moe and Chen, 2005), a protein that can bind excess mineral and increase their plasma solubility (Komaba and Fukagawa, 2009). Furthermore, an increase in reactive oxygen species (ROS) production is involved in VSMC osteochondrogenic trans-differentiation during the VC process (Tóth et al., 2020; Hu et al., 2021). Recent studies have highlighted the role of extracellular vesicles (EVs) in VC (Hodroge et al., 2017; Mansour et al., 2020; Yaker et al., 2020; Qin et al., 2021). These membrane-bound vesicles, secreted by prokaryotic and eukaryotic cells (Woith et al., 2019), can be of various origins, depending on their mode of biogenesis. For example, exosomes (50–150 nm) originate from endosomes and microvesicles (50–500 nm) generated by budding of the plasma membrane and apoptotic bodies (van Niel et al., 2018). Several studies have showed macrophage-derived EVs to promote VC (New et al., 2013; Chen et al., 2016; Kawakami et al., 2020). Analysis of their content identified a subset of molecules involved in inflammation and oxidative stress, such as pro-inflammatory cytokines (Fitzgerald et al., 2018; Aiello et al., 2020) and oxidant machinery proteins (Bodega et al., 2019). New *et al.* showed that macrophages can release calcifying EVs enriched for S100A9, a calcium-binding protein involved in mineralization (New et al., 2013). Furthermore, Kawakami *et al.* recently showed that calcifying EVs released by macrophages contribute to the formation of microcalcification (Kawakami et al., 2020). In addition, Chen *et al.* demonstrated that the cytokine HMGB1 can induce the secretion of macrophage-derived EVs involved in ectopic mineralization (Chen et al., 2016). Here, we aimed to investigate the role of macrophage-derived EVs in the propagation of inflammation and oxidative stress during the VC process.

2 MATERIALS AND METHODS

2.1 Cell Culture, Molecular, and Biochemical Reagents

Fetal bovine serum (FBS) and glutamine were purchased from Eurobio® (Les Ulis, France). Lipopolysaccharide from *Escherichia coli K12* (LPS-EK) was obtained from InvivoGen® (San Diego, California, United States) and inorganic phosphate (Pi) from Merck® (Darmstadt, Germany). Exosome-free FBS, TRIzol™ Reagent, RNase/DNase-free water, High-Capacity RNA-to-cDNA™ kits, BCA™ Protein Assay kits, and dihydroethidium (DHE) were purchased from Thermo Fisher Scientific® (Waltham, Massachusetts, United States). Takyon™ was obtained from Eurogentec® (Liège, Belgium). 2′, 7′-dichlorofluorescein diacetate (DCFH-DA) was purchased from Molecular Probes® (Eugene, Oregon, United States). All other molecular and biochemical reagents were obtained from Sigma-Aldrich® (Saint-Louis, Missouri, United States).

2.2 Culture and Treatment of Cells

2.2.1 Murine Macrophage Culture

Murine macrophages (RAW 264.7 ATCC® TIB-71™, Manassas, Virginia, United States) were maintained in DMEM 6546 medium supplemented with 10% FBS, 4 mM glutamine, 100 UI/ml penicillin, and 100 µg/ml streptomycin at 37°C in a 5% CO_2 humidified atmosphere. We first assessed RAW cell viability in the presence of 0.1 and 1 µg/ml LPS-EK, concentrations that are generally used to activated RAW macrophages (Pi et al., 2014). A 24-h treatment with LPS-EK induced 25% cell cytotoxicity (data not shown). RAW cells are known to be particularly sensitive to LPS, which could explain the cell growth inhibition observed in our experiment (Raschke et al., 1978). We then tested the treatment of RAW cells for only 6 h with LPS-EK and detected no cell cytotoxicity (**Supplementary Figure S1**). We thus used these experimental conditions for all further experiments.

2.2.1 Murine Aortic Vascular Smooth Muscle Cell Culture

Murine aortic VSMCs (MOVAS-1 ATCC® CRL-2797™, Manassas, Virginia, United States) were maintained in DMEM 6546 medium supplemented with 10% FBS, 4 mM glutamine, 100 UI/ml penicillin, 100 µg/ml streptomycin, and 200 µg/ml geneticin® (G418) at 37°C in a 5% CO_2 humidified atmosphere. To induce VSMC calcification, cells were treated in DMEM 6546 containing 1% FBS with 4 mM Pi for 14 days. The

media was changed twice a week. For each experiment, VSMCs were treated with macrophage-derived EVs isolated from the same volume of cell-culture medium.

2.3 Extracellular Vesicle Preparation and Characterization

2.3.1 Isolation of Extracellular Vesicles

Macrophages were seeded in 10-cm petri plates at a density of 30,000 cells/cm^2 and cultured in DMEM 6546 medium supplemented with 10% FBS. After 48 h, cells were washed with PBS then treated with various concentrations of LPS-EK in DMEM 6546 medium supplemented with 10% exosome-free FBS for 6 h. Cell debris was removed from cell-culture supernatants by centrifugation at 800 × g for 5 min at 4°C.

EVs were isolated from cell-culture supernatants of untreated (EV-CT) or LPS-EK treated (EV-LPS) macrophages by sequential centrifugation, as described previously by Chen et al. (2008). Briefly, supernatants were first ultracentrifuged at 100,000 × g for 50 min at 4°C. The pellet was then resuspended in cold Dulbecco's phosphate buffered saline (D-PBS) and centrifuged at 100,000 × g for another 50 min at 4°C. The final pellet was resuspended in D-PBS or RIPA buffer and the protein concentration determined using the BCA™ Protein Assay kit. EV samples were stored at −80°C for future analysis.

2.3.2 Characterization of Extracellular Vesicles

2.3.2.1 Transmission Electron Microscopy

EVs were isolated as described previously and resuspended in 50 µL Tris base buffer (100 mM, pH 7.4). EV samples were prepared for TEM using the conventional negative staining procedure. Briefly, 10 µL EV samples were absorbed for 2 min on formvar-carbon-coated copper grids preliminarily ionized using the PELCO easiGlow™ Glow Discharge Cleaning System (Ted Pella Inc., Redding, California, United States). Preparations were then blotted and negatively stained with 1% uranyl acetate for 1 min. Grids were examined using an 80 kV JEM-1400 electron microscope (JEOL Inc., Peabody, Massachusetts, United States) and images acquired with a digital camera (Gatan Orius, Gatan Inc., Pleasanton, California, United States).

2.3.2.2 Cryo-Electron Microscopy

To analyze the morphology of EVs by cryo-EM, 3 µL of EV sample was first deposited onto a glow-discharged 200-mesh lacey carbon grid. Prior to freezing, the grid was loaded into the thermostatic chamber of a Leica EM-GP automatic plunge Freezer, set to 20°C and 95% humidity. Excess solution was blotted from the grid for 1–2 s with a Whatman n°1 filter paper and the grid immediately flash frozen in liquid ethane cooled to −185°C. Specimens were then transferred into a Gatan 626 cryo-holder. Cryo EM was carried out using a Jeol 2,100 microscope equipped with a LaB6 cathode operating at 200 kV under low-dose conditions. Images were acquired using SerialEM software (Mastronarde, 2005), with the defocus ranging from 600 to 1,000 nm, using a Gatan US4000 CCD camera. This device was placed at the end of a GIF quantum energy filter (Gatan Inc. Berwyn, Pennsylvania, United States) operating in zero-energy-loss mode, with a slit width of 25 eV. Images were recorded at a magnification corresponding to a calibrated pixel size of 0.87 Å.

2.3.2.3 Nanoparticle Tracking Analysis (NTA)

EVs were resuspended in 50 µL D-PBS. Particle-size distribution and concentration were analyzed using a NanoSight LM10-HS instrument (Malvern Instruments Ltd., Malvern, United Kingdom) according to the manufacturer's instructions. Briefly, EV samples were diluted 100-fold in D-PBS and the diluted preparation injected into the chamber. Samples were analyzed at room temperature for 60 s. Three replicates were performed for each sample. Data were acquired and analyzed using NTA 2.2 Build 127 software (Malvern Instruments Ltd., Malvern, United Kingdom).

2.3.2.4 Specific Extracellular Vesicle Markers

EVs were characterized by analyzing tetraspanin (CD81, CD9) and β-actin protein expression by western blotting as recommended by the International Society for Extracellular Vesicles (ISEV) (Théry et al., 2018).

2.3.2.5 Measurement of Acetylcholinesterase Activity

Acetylcholinesterase activity was measured using a colorimetric assay as previously described by Ellman et al. (1961). Briefly, 200 µL D-PBS containing 1 mM acetylcholine and 0.1 mM 5, 5′-Dithiobis 2-nitrobenzoic acid (DNTB) was added to 100 µL EV sample. After a 15 min incubation at room temperature, the absorbance was read at 450 nm using an Envision microplate reader. Data are expressed as the percentage difference in absorbance compared to the control (assay diluent D-PBS).

2.4 Biochemical Assays

2.4.1 Cell Viability Assay

Cell viability was assessed using the WST-1 assay. Cells were seeded in 96-well plates at a density of 7,500 cells/well. After 48 h, cells were treated with LPS-EK or macrophage-derived EVs for 6 or 24 h, respectively. Ten percent dimethyl sulfoxide (DMSO) was used as a positive control for viability loss. The medium was then changed and the cells incubated in 100 µL DMEM 6546 medium containing 10 µL WST-1 reagent for 1 h at 37°C. Absorbance was measured at 450 nm using an Envision microplate reader (Perkin Elmer®, Waltham, Massachusetts, United States).

2.4.2 Calcification Assay

VSMC calcification was assessed by measuring the intracellular calcium concentration using the o-cresolphthalein assay as previously described (Ray Sarkar and Chauhan, 1967). The total cell protein concentration was assessed by the method of Peterson (Peterson, 1977) and used to normalize the intracellular calcium concentration.

2.4.3 Measurement of Oxidative Stress (ROS, O2•⁻, and NO Production)

The three fluorescent probes DCFH-DA, DHE, and DAF were used to measure ROS, O2•⁻, and NO production, respectively. Macrophages were seeded in white 96-well plates at a density of

7,500 cells/well. After 48 h, cells were washed twice with D-PBS and incubated at 37°C with 10 μM DCFH-DA for 30 min and then 10 μM DHE or 0.1 μM DAF for 1 h. Next, cells were washed twice with D-PBS and treated with LPS-EK or macrophage-derived EVs. Hydrogen peroxide (H_2O_2) at 50 and 500 μM was used as a positive control of ROS production. For certain experiments, the antioxidants N-acetyl-L-cysteine (NAC, 10 mM) and α-tocopherol (vitamin E, 10 μg/ml) were added to each well 1 h prior to treatment. For NO production, the iNOS substrate L-arginine was added to each well at 50 μM. All solutions were prepared in Krebs-Ringer-phosphate buffer (KRP). Fluorescence was measured using an Envision microplate reader (λ_{Ex} 492 nm, λ_{Em} 535 nm for DCFH-DA and DAF; λ_{Ex} 492 nm, λ_{Em} 615 nm for DHE).

2.4.4 Western Blot Analysis

After treatment, cells were washed twice with cold D-PBS and lysed with RIPA buffer, sonicated, and centrifuged (16,000 × g, 5 min, 4°C). Supernatants were collected in a new tube and the protein concentration determined using the BCA™ Protein Assay kit according to the manufacturer's instructions. Proteins were precipitated with methanol/chloroform (1/0.25; v/v) and centrifuged for 5 min at 16,000 × g at room temperature. The pellet was then resuspended in 4X Laemmli buffer and heated to 99°C for 5 min. Fifty μg of each protein sample was separated on a 12% SDS-PAGE gel and transferred onto a nitrocellulose membrane. After blocking, membranes were incubated overnight at 4°C with primary antibodies: rabbit anti-CD9 polyclonal antibody (1/1,000, GeneTex® GTX55564), goat anti-CD81 polyclonal antibody (1/1,000, Santa Cruz Biotechnology, Inc.® sc-31234), mouse monoclonal anti-β-actin antibody (1/5,000, Sigma-Aldrich® A1978, clone AC-15), rabbit anti-SMPD3 (1/10,000, Sigma-Aldrich® SAB2102245), or rabbit anti-p62/SQSTM1 (1/1,000, Sigma-Aldrich® P0067). After several washes, membranes were incubated with goat anti-rabbit IgG-HRP (1/5,000, Santa Cruz Biotechnology, Inc.® sc-2004), goat anti-mouse IgG-HRP (1/5,000, Santa Cruz Biotechnology, Inc.®, sc-2005), or rabbit anti-goat IgG (H + L)-HRP (1/5,000, Southern Biotech®, 6,160-05) for 1 h at room temperature. Then, proteins were visualized using ECL™ Western Blot Detection Reagents and a ChemiDoc™ MP Imaging System (Bio-Rad®, Hercules, California, United States). β-actin protein levels were quantified to normalize protein levels.

2.5 RNA Extraction and Quantitative Real-Time PCR

After treatment, cells were washed twice with D-PBS. RNA extraction was then performed using a mixture of TRIzol™ and chloroform (1/0.2; v/v). After a 15-min centrifugation (12,000 × g, 4°C), RNA was collected and precipitated with isopropanol. The RNA pellet was then washed twice with 70% ethanol and resuspended in 40 μL RNase/DNase-free water. The RNA concentration was determined using a NanoVue™ Plus device (Thermo Fisher Scientific®, Waltham, Massachusetts, United States). cDNA was synthesized using a High-Capacity RNA-to-cDNA™ kit according to the manufacturer's instructions. Quantitative real-time PCR was carried out using Takyon™ and specific primers (**Supplementary Table S1**). A CFX96 Touch Real-Time PCR Detection System (Bio-Rad®, Hercules, California, United States) was used with the following steps: 95°C for 15 s, followed by 40 cycles of 95°C for 15 s, 60°C for 1 min and 72°C for 30 s. β-actin was used as a housekeeping gene to normalize gene expression.

2.6 MSD Multiplex Immunoassay

Proinflammatory cytokine protein levels were measured in macrophages and EVs derived from macrophages using a proinflammatory panel® multiplex kit (V-PLEX® K15048D, Meso Scale Diagnostics®, Rockville, Maryland, United States) according to the manufacturer's instructions. Briefly, 50 μL/well of sample or calibrators was added to a 96-well plate pre-coated with capture antibodies. After a 2-h incubation with shaking at room temperature and three washes (D-PBS with 0.05% Tween 20), 25 μL 1X detection antibody solution was added to each well. After another 2-h incubation under the same conditions and three washes, 150 μL 2X Read Buffer T was added to each well. The plate was then analyzed using the MSD instrument (Meso Scale Diagnostics®, Rockville, Maryland, United States).

2.7 Mass Spectrometry Proteomic Analysis

2.7.1 Proteomic Digestion for Mass Spectrometry

An S-TrapTM microspin column digestion was performed on 10 μg of macrophage-derived EVs according to the manufacturer's instructions (Protifi, Hutington, United States). Briefly, samples were reduced with 20 mM tris (2-carboxyethyl) phosphine and then alkylated with 50 mM chloroacetamide for 15 min at room temperature. Aqueous phosphoric acid was then added to a final concentration of 1.2%, followed by the addition of S-Trap binding buffer (90% aqueous methanol, 100 mM tetraethylammonium bromide, pH 7.1). The mixtures were then loaded onto S-Trap columns. Two extra washing steps were performed to eliminate SDS. Samples were then digested with 1 μg trypsin (Promega, Madison, Wisconsin, United States) at 47°C for 1 h. After elution, peptides were vacuum dried and resuspended in 45 μL 2% acetonitrile/0.1% formic acid mixture in HPLC-grade water prior to MS analysis. A volume of 1 μL of the peptide suspension was injected into a nanoelute high-performance liquid chromatography (HPLC) system coupled to a timsTOF Pro mass spectrometer (Bruker Daltonics, Germany). HPLC separation was performed using a mixture of 0.1% formic acid in water, 2% acetonitrile (Solvent A), and 0.1% formic acid in acetonitrile (Solvent B) at 250 nL/min using a packed emitter column (C18, 25 cm × 75 μm 1.6 μm) (Ion Optics, Australia) with a gradient elution (2–11% solvent B ove r19 min, 11–16% over 7 min, 16–25% over 4 min, 25–80% over 3 min, and, finally, 80% for 7 min to wash the column). Mass-spectrometric data were acquired using the parallel accumulation serial fragmentation (PASEF) acquisition method. The measurements were carried out over an m/z range from 100 to 1700 Th, with ion mobility from 0.8 to 1.3 V s/cm^2 (1/k0). The total cycle time was set to 1.2 s and the number of PASEF MS/MS scans was set to 10. A total of 2,762 proteins was identified in at least 60% of all samples.

The mass spectrometry proteomics data have been deposited in the ProteomeXchange Consortium via the PRIDE (Perez-Riverol et al., 2019) partner repository with the dataset identifier PXD029441 and 10.6019/PXD029441.

2.7.2 Data Analysis

The data were analyzed using MaxQuant version 1.6.14.0 (Max-Planck, Munich, Germany) and searched using the Andromeda search engine against the UniProtKB/Swiss-Prot *Mus musculus* database (release 02-04-2020, 17040 entries). Mass deviations of 3 and 20 ppm were used to search parent mass and fragment ions, respectively. The minimum peptide length was set to seven amino acids and strict specificity for trypsin cleavage was required, allowing up to two missed cleavage sites. Carbamidomethylation (Cys) was set as a fixed modification, whereas oxidation (Met) and N-term acetylation were set as variable modifications. The false discovery rate (FDR) for both proteins and peptides was set to 1%. Scores were calculated in MaxQuant as previously described (Cox and Mann, 2008). The reverse and common contaminant hits were removed from the MaxQuant output. Proteins were quantified according to the MaxQuant label-free algorithm using LFQ intensities; protein quantification was obtained using at least two peptides per protein. Matches between runs were allowed. Statistical and bioinformatic analysis, including heatmaps, profile plots, and clustering, were performed using Perseus software (version 1.6.14.0) freely available at www.perseus-framework.org (Tyanova et al., 2016). For statistical comparisons, we set up five groups, each containing up to five biological replicates. We then filtered the data to keep only proteins with at least four valid values in at least one group. Next, the data were imputed to fill missing data points by creating a Gaussian distribution of random numbers with a standard deviation of 33% relative to the standard deviation of the measured values and a 1.8 standard deviation downshift of the mean to simulate the distribution of low-signal values. We performed an ANOVA test, FDR <0.05, S0 = 0.5. Hierarchical clustering of proteins that survived the test was performed using Perseus on log-transformed LFQ intensities after z-score normalization of the data using Euclidean distances.

2.8 Statistical Analysis

Statistical analyses were performed using GraphPad Prism (version 7.0, San Diego, California, United States). Wilcoxon-Mann-Whitney and Kruskal–Wallis tests were performed with a significance threshold of 0.05. Data are expressed as the mean ± standard error of mean (SEM) from at least three independent experiments.

Principal Component Analysis has been performed on log transformed and scaled values from targeted MSD multiplex immunoassay using the R package pcaMethods.

3 RESULTS

3.1 Effects of LPS-EK on Macrophages

3.1.1 Lipopolysaccharide From *Escherichia coli K12* Induces Inflammation in Macrophages

In setting up our cellular model of inflammation, we first verified the effect of LPS-EK on inflammation in RAW macrophages by measuring the mRNA levels of various pro-inflammatory cytokines (IL-6, IL-1β, TNF-α, and MIP-2), as well as that of the NLRP3 inflammasome marker, before and after treatment. The mRNA levels of these markers were all significantly higher after LPS-EK treatment than those of unstimulated macrophages (CT) (*$p < 0.05$ *vs.* CT, **Figure 1**). We also analyzed the levels of 10 proinflammatory cytokines in LPS-EK-treated or untreated macrophages using an MSD multiplex kit. Macrophages treated with LPS-EK showed significantly higher levels of these proinflammatory cytokines than untreated control cells (*$p < 0.05$ *vs.* CT, **Supplementary Figure S2**). These results show that LPS-EK induces an inflammatory response in our cellular model.

3.1.2 Lipopolysaccharide From *Escherichia coli K12* Induces Oxidative Stress in Macrophages

As oxidative stress is also involved in the calcification process, we next determined the effect of LPS on reactive oxygen species (ROS) production using the fluorescent probe DCFH-DA. ROS production by cells treated with LPS-EK was significantly higher than that of untreated cells (*$p < 0.05$ *vs.* CT) (**Figure 2A**). In addition, mRNA levels of two components of the antioxidant system, Keap1 and Nrf2, were lower after LPS-EK treatment, which could partially explain the increase in oxidative stress (*$p < 0.05$ *vs.* CT, **Figures 2E,F**). Among the various ROS, superoxide anions ($O_2^{\bullet-}$) play an important role in oxidative stress. We therefore investigated the effect of LPS-EK on $O_2^{\bullet-}$ production using the fluorescent probe DHE. Surprisingly, $O_2^{\bullet-}$ production was significantly lower in LPS-EK treated cells than in untreated cells (*$p < 0.05$ *vs.* CT, **Figure 2B**). We investigated this seeming discrepancy by measuring the mRNA levels for both Nox-2, the enzyme that synthesizes $O_2^{\bullet-}$, and superoxide dismutase (SOD-2), which is responsible for $O_2^{\bullet-}$ degradation. We observed significantly higher Nox-2 and lower SOD-2 mRNA levels in LPS-EK stimulated macrophages than in untreated macrophages (*$p < 0.05$ *vs.* CT, **Figures 2C,D**). Our results thus show that LPS-EK decreases superoxide anion production by decreasing Nox-2 expression and increasing SOD-2 expression. Superoxide anions can rapidly react with nitric oxide (NO) to form peroxynitrite ($ONOO^-$). Thus, we next investigated the effect of LPS-EK on NO production using the fluorescent probe DAF. NO production was significantly lower after LPS-EK treatment than in untreated cells ($p < 0.05$ *vs.* CT, **Figure 2G**), despite significantly higher levels of iNOS (*$p < 0.05$ *vs.* CT, **Figure 2H**). These results suggest that both decreases in NO and $O_2^{\bullet-}$ production may be partially explained by the formation of peroxynitrite.

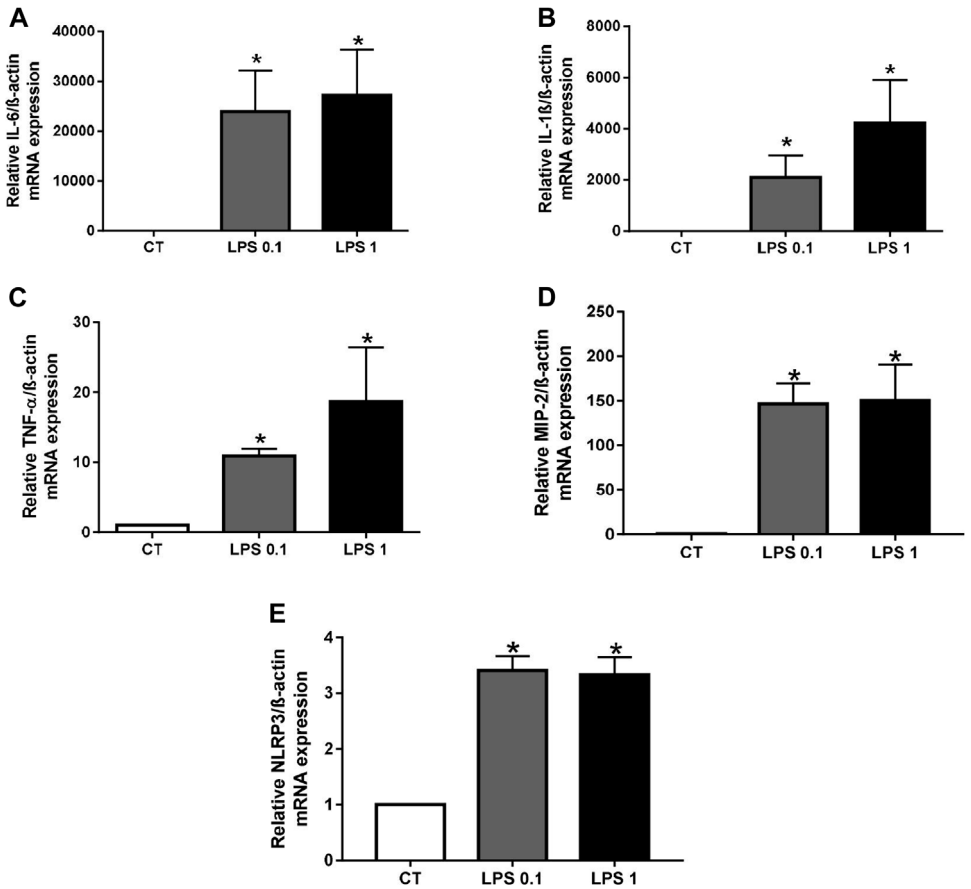

FIGURE 1 | Lipopolysaccharide-EK (LPS-EK) induces inflammation in macrophages. RAW cells were incubated with LPS-EK for 6 h. Gene expression of **(A)** IL-6, **(B)** IL-1β, **(C)** TNF-α, **(D)** MIP-2, and **(E)** NLRP3 was quantified by quantitative real-time PCR and normalized to that of the housekeeping gene ß-actin. Data are expressed as the mean ± SEM of four independent experiments performed in triplicate ($n = 4$). *$p < 0.05$ *vs*. CT, Mann-Whitney test. LPS 0.1: 0.1 μg/ml LPS-EK, LPS 1: 1 μg/ml LPS-EK.

3.1.3 Lipopolysaccharide From *Escherichia coli K12* Decreases Extracellular Vesicle Biogenesis in Macrophages

The aim of this study was to determine whether EVs can propagate inflammation and oxidative stress to recipient cells. Thus, we first studied EV biogenesis in RAW cells after LPS-EK treatment by analyzing the mRNA levels of various EV biogenesis markers (phospho-1, TNAP, and SMPD3) in LPS-EK-treated macrophages. The mRNA levels of these markers were all significantly lower in LPS-EK-treated cells than in unstimulated macrophages (*$p < 0.05$ *vs*. CT, **Figures 3A–C**), suggesting a decrease in EV biogenesis. SMPD3 protein levels were also significantly lower after 1 μg/ml LPS-EK treatment than in untreated macrophages (*$p < 0.05$ *vs*. CT, **Figure 3D**).

3.1.4 Lipopolysaccharide From *Escherichia coli K12* Decreases Autophagy in Macrophages

Recent studies have highlighted novel functions of autophagy in the biogenesis and secretion of EVs (Yang et al., 2021). Indeed, it has been shown that not only exosome biogenesis and autophagy share molecular machinery but also that substantial crosstalk exists between these two processes. We therefore analyzed the effect of LPS-EK on autophagy markers, such as ULK1, Beclin-1, Atg5, LC3a, and LC3b. The mRNA levels of all these markers were significantly lower after LPS-EK treatment than in unstimulated macrophages (*$p < 0.05$ *vs*. CT, **Figures 4A–E**), suggesting a decrease in the autophagy process. p62, also known as sequestome-1 (SQSTM), is an autophagy cargo receptor (Lamark et al., 2009) that can be used as a sensor of autophagic flux. Indeed, p62 accumulates when autophagy is inhibited and decreased levels of p62 can be observed when autophagy is induced. After LPS-EK treatment, p62 mRNA levels were higher than in unstimulated macrophages (*$p < 0.05$ *vs*. CT, **Figure 4F**), confirming inhibition of the autophagic flux. p62 protein levels were not modified after LPS-EK treatment relative to untreated cells (**Figure 4G**). Overall, our results show that LPS-EK not only induces inflammation and oxidative stress

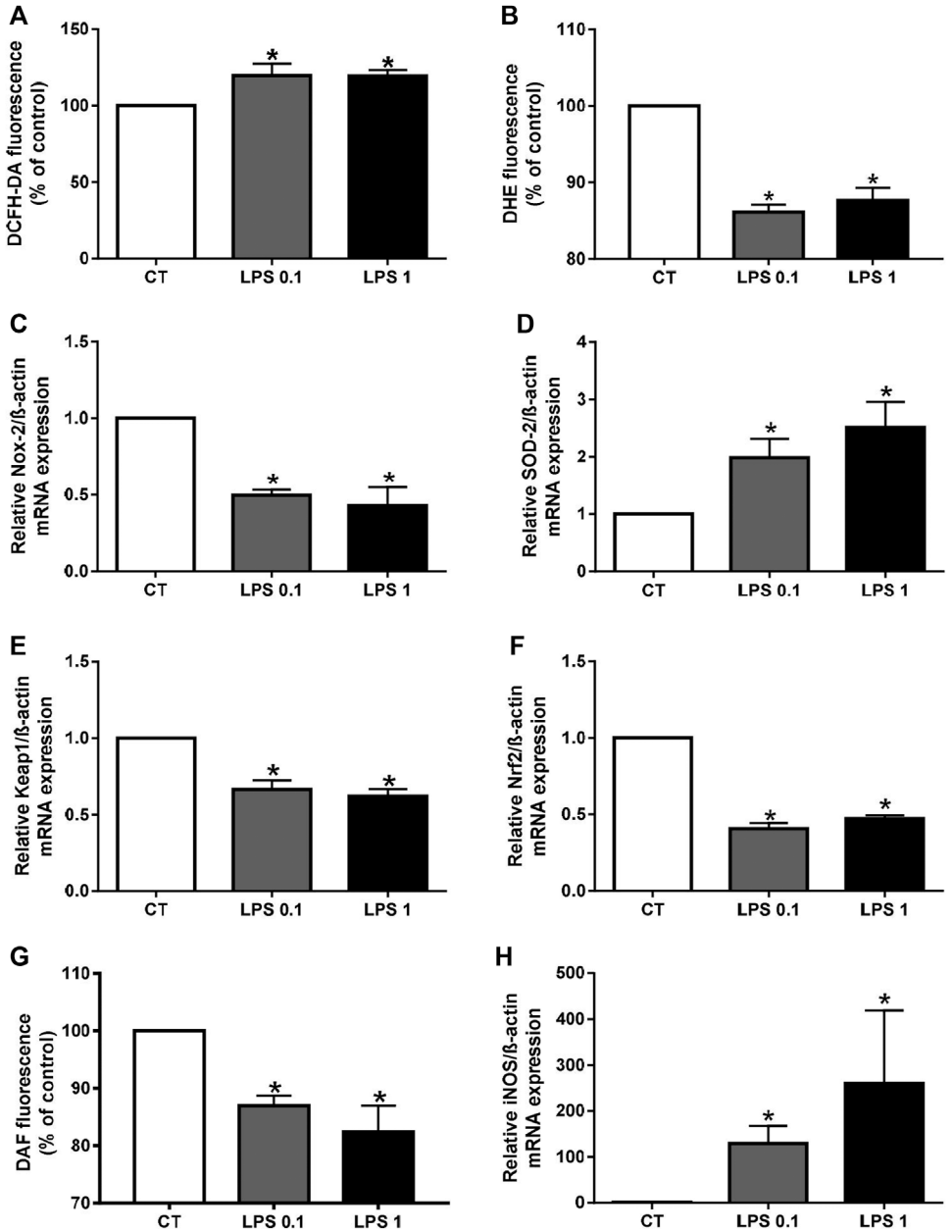

FIGURE 2 | Lipopolysaccharide-EK (LPS-EK) induces oxidative stress in macrophages. ROS **(A)**, $O2^{\bullet-}$ **(B)**, and NO **(G)** production in RAW cells was measured using the fluorescent probes DCF, DHE, and DAF, respectively. Gene expression of **(C)** Nox-2, **(D)** SOD-2, **(E)** Keap1, **(F)** Nrf2, and **(H)** iNOS was quantified by quantitative real-time PCR and normalized to that of the housekeeping gene ß-actin. Data are expressed as the mean ± SEM of four independent experiments performed in triplicate ($n = 4$). *$p < 0.05$ *vs*. CT, Mann-Whitney test. LPS 0.1: 0.1 µg/ml LPS-EK, LPS 1: 1 µg/ml LPS-EK.

in RAW cells but also decreases autophagy and EV biogenesis.

3.2 Effects of EV-LPS on Smooth Muscle Cells

3.2.1 Characterization of Macrophage-Derived EVs

We characterized macrophage-derived EVs by their morphology, size, and concentration (**Figure 5**) using transmission electron microscopy (TEM) (**Figure 5A**), cryo-electron microscopy (cryo-EM) (**Figure 5B**), and nanoparticle-tracking analyses (NTA) (**Figure 5C**). The particle size for exosomes is between 50 and 150 nm and between 50 and 500 nm for microvesicles (van Niel et al., 2018). The average particle size detected by NTA was 139 nm for EVs isolated from untreated macrophages (EV-CT) and 130 nm for EVs isolated from LPS-EK-treated macrophages (EV-LPS) (**Figure 5C**). Thus, our EV samples were likely enriched for both exosomes and microvesicles. Furthermore,

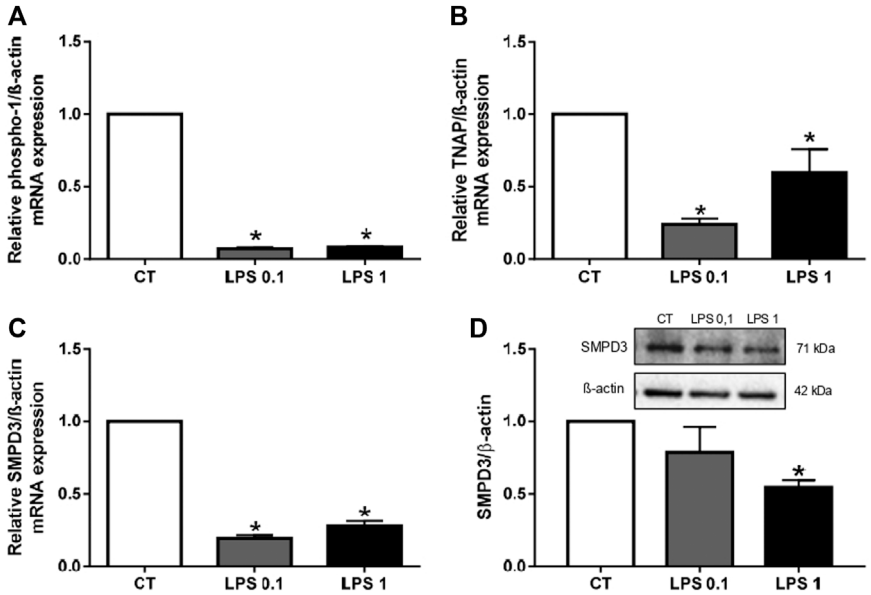

FIGURE 3 | Lipopolysaccharide-EK (LPS-EK) decreases EV biogenesis in macrophages. RAW cells were incubated with LPS-EK for 6 h. Gene expression of EV of the biogenesis markers **(A)** phospho-1, **(B)** TNAP, and **(C)** SMPD3 was then quantified by RT-qPCR and normalized to that of the housekeeping gene ß-actin. **(D)** SMPD3 protein expression was studied by western blotting and normalized to that of the housekeeping gene ß-actin. Data are expressed as the mean ± SEM of four independent experiments performed in triplicate (n = 4). *p < 0.05 *vs*. CT, Mann-Whitney test. LPS 0.1: 0.1 µg/ml LPS-EK, LPS 1: 1 µg/ml LPS-EK.

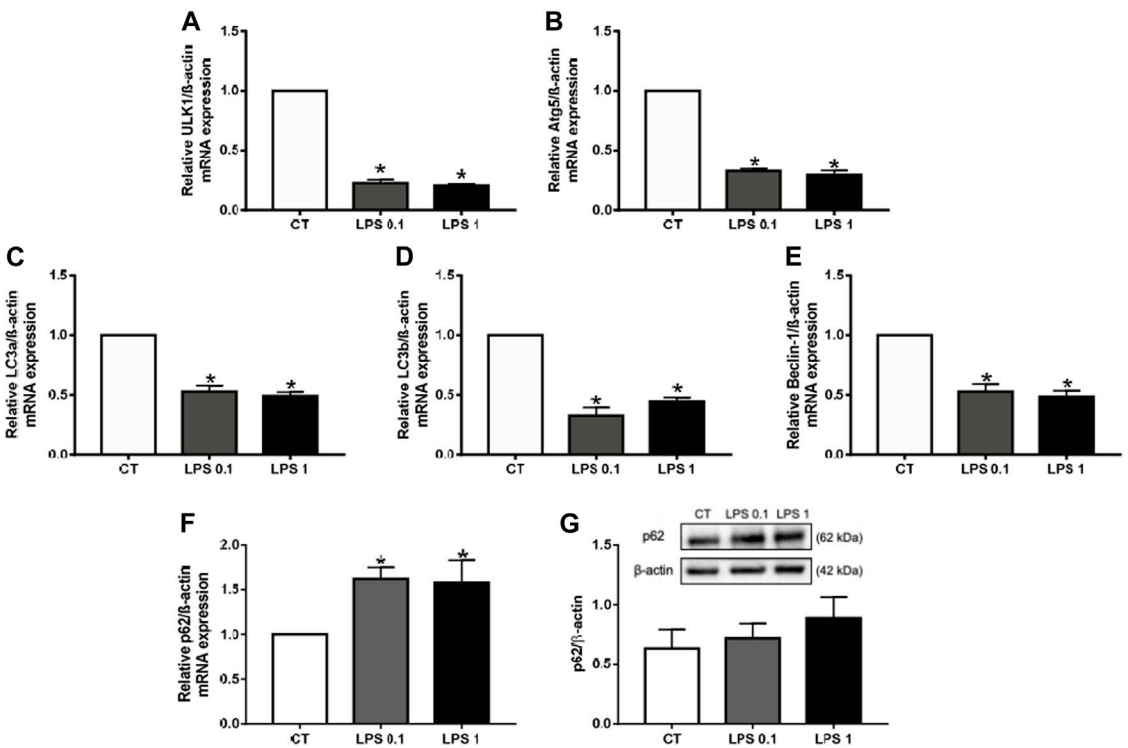

FIGURE 4 | Lipopolysaccharide-EK (LPS-EK) decreases autophagy in macrophages. RAW cells were incubated with LPS-EK for 6 h. Gene expression of the autophagy markers **(A)** ULK1, **(B)** Atg5, **(C)** LC3a, **(D)** LC3b, **(E)** Beclin-1, and **(F)** p62 was then quantified by RT-qPCR and normalized to that of the housekeeping gene ß-actin. **(G)** p62 protein expression was studied by western blotting and normalized to that of the housekeeping gene ß-actin. Data are expressed as the mean ± SEM of four independent experiments performed in triplicate (n = 4). *p < 0.05 *vs*. CT, Mann-Whitney test. LPS 0.1: 0.1 µg/ml LPS-EK, LPS 1: 1 µg/ml LPS-EK.

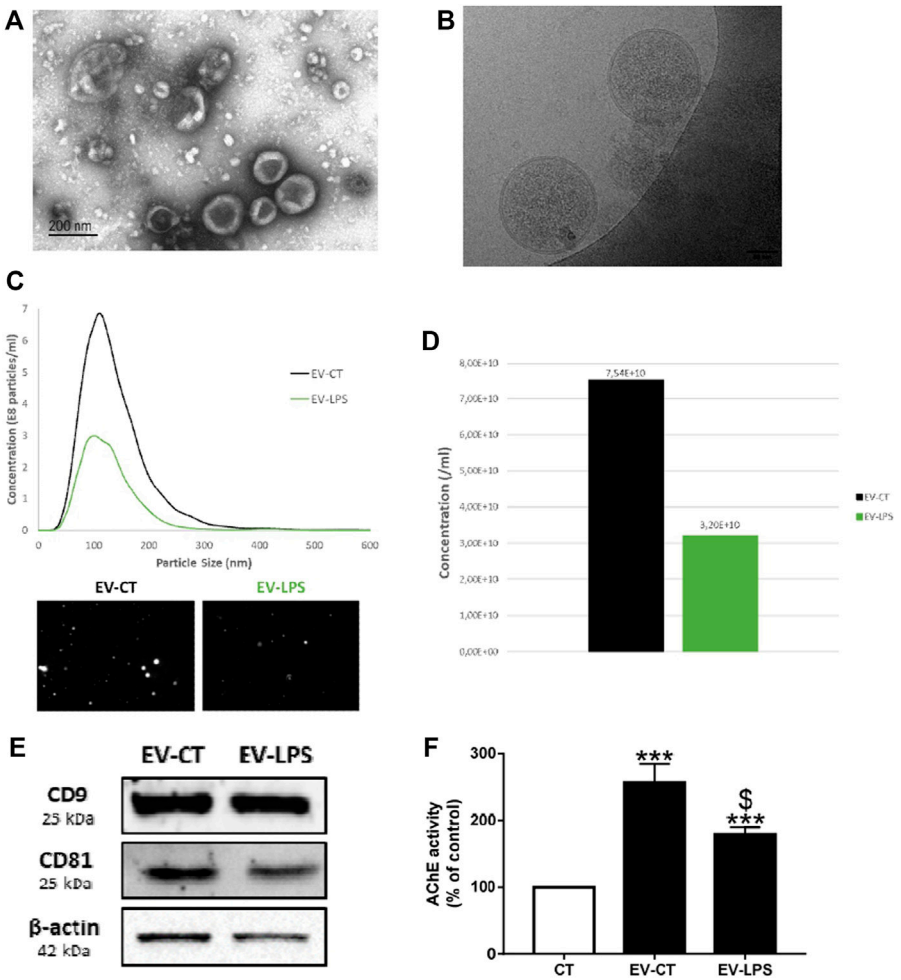

FIGURE 5 | Characterization of macrophage-derived EVs. EVs were isolated from the culture media of RAW cells incubated with (EV-LPS) or without (EV-CT) 1 μg/ml lipopolysaccharide-EK (LPS-EK) for 6 h. Evaluation of EV morphology by **(A)** transmission electron microscopy (TEM) and **(B)** cryo-electron microscopy (cryo-EM). **(C)** Particle-size distribution and **(D)** the total concentration of macrophage-derived EVs were measured by nanoparticle-tracking analysis (NTA). **(E)** CD9, CD81, and β-actin protein expression were assessed by western blotting. **(F)** Quantification of the enzymatic activity of acetylcholinesterase (AChE) in macrophage-derived EVs. Control AChE activity in the assay diluent 1X-D-PBS (CT) was defined as 100%. Data are expressed as the mean ± SEM of seven independent experiments performed in triplicate ($n = 7$). ***$p < 0.001$ *vs*. CT; \$$p < 0.05$ *vs*. EV-CT, Mann-Whitney test.

we verified EV membrane integrity by cryo-EM (**Figure 5B**). Indeed, we could observe a discernible lipid bilayer and internal vesicular structures (**Figure 5B**). The diameter of EVs can vary, as well as the content. The International Society for Extracellular Vesicles (ISEV) has published recommendations for EV characterization (Théry et al., 2018). Indeed, two categories of markers must be analyzed in sample preparations to confirm the presence of EVs: transmembrane proteins, such as tetraspanins, and cytosolic proteins recovered in EVs (Théry et al., 2018). Thus, we performed western blotting to determine the presence of EV-specific tetraspanin (CD9, CD81) and β-actin and detected all of these EV markers in our EV samples (**Figure 5E**). Acetylcholinesterase (AChE) is expressed in macrophages (Fujii et al., 2017) and can also be found in macrophage-derived EVs. According to the ISEV, AChE activity can also be used to characterize EVs (**Figure 5F**). Overall, these results confirm the presence of EVs in both preparations. LPS-EK treatment of macrophages resulted in a lower number of EVs than in control untreated cells (**Figure 5D**). Indeed, we detected 7.54×10^{10} particles in the EV-CT sample, whereas the EV-LPS preparation contained 3.20×10^{10} particles. Furthermore, we observed significantly less AChE in the EV-LPS preparation than in the EV-CT preparation. Both results could be explained by the lower amount of secreted EVs due to decreased EV biogenesis after LPS-EK treatment (\$$p < 0.05$ *vs*. EV-CT, **Figure 5F**). Importantly, the EVs were isolated from the same volume of cell-culture media.

3.2.2 Effect of Macrophage-Derived EVs on MOVAS Cell Viability

We next studied the effects of macrophage-derived EVs on the smooth muscle cell line MOVAS-1. Cell viability was first assessed after 24 h of treatment with macrophage-derived EVs. EVs secreted

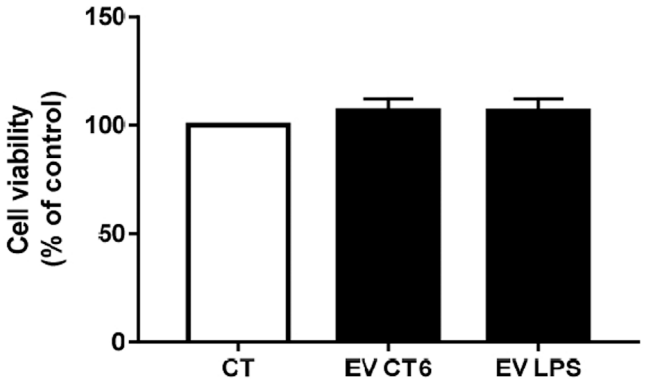

FIGURE 6 | Effect of macrophage-derived EVs on smooth muscle cell viability. MOVAS-1 cells were incubated for 24 h with EVs secreted by either treated (1 µg/ml LPS-EK; EV-LPS) or untreated macrophages (EV-CT) or without (CT). Cell viability was measured using the WST-1 assay. The viability of cells incubated without EVs (CT) was defined as 100%. Data are expressed as the mean ± SEM of four independent experiments performed in triplicate ($n = 4$). $p < 0.05$ is considered significant, Wilcoxon- Mann-Whitney test.

by macrophages did not affect smooth muscle cell viability relative to untreated cells (CT), regardless of the treatment (**Figure 6**).

3.2.3 EV-LPS Induce Inflammation in Smooth Muscle Cells

Our objective was to study the propagation of inflammation from macrophages to smooth muscle cells. Thus, we measured the mRNA levels of proinflammatory cytokines (IL-6, IL-1ß, and TNF-α) in MOVAS cells treated with macrophage-derived EVs. We observed significantly higher proinflammatory cytokine mRNA levels after 24 h of treatment of smooth muscle cells with EV-LPS than in untreated cells (CT) (*$p < 0.05$ *vs.* CT, **Figure 7**). There was no effect of EVs derived from control cells (EV-CT) on cytokine levels. A comparison of the effects of the two populations of EVs showed only the increase in IL-6 mRNA levels to be significant ($ $p < 0.05$ *vs.* EV-CT, **Figure 7A**). These results show that EV-LPS are able to induce inflammation mainly *via* an increase in IL-6 expression.

3.2.4 EV-LPS Induces Oxidative Stress in Smooth Muscle Cells

We investigated the effect of macrophage-derived EVs on oxidative stress in smooth muscle cells by measuring intracellular ROS production. Both EV preparations (EV-CT and EV-LPS) significantly increased ROS production over that of untreated smooth muscle cells (*$p < 0.05$ *vs.* CT, **Figure 8**). This result suggests that the effect of macrophage-derived EVs on oxidative stress in smooth muscle cells is independent of macrophage treatment. We next measured mRNA levels of antioxidant enzymes (SOD-1, SOD-2) and nuclear receptors (Nrf2, and Keap1) involved in the antioxidant response. Surprisingly, the mRNA levels of all markers were significantly higher in cells incubated with EV-LPS than in untreated cells (CT) (*$p < 0.05$ *vs.* CT, **Figure 9**). Only SOD-2 mRNA levels were higher in MOVAS cells treated with EV-LPS than those treated with EV-CT ($$p < 0.05$ *vs.* EV-CT, **Figure 9B**). Overall, these results suggest that EV-LPS can affect the oxidative stress response of smooth muscle cells.

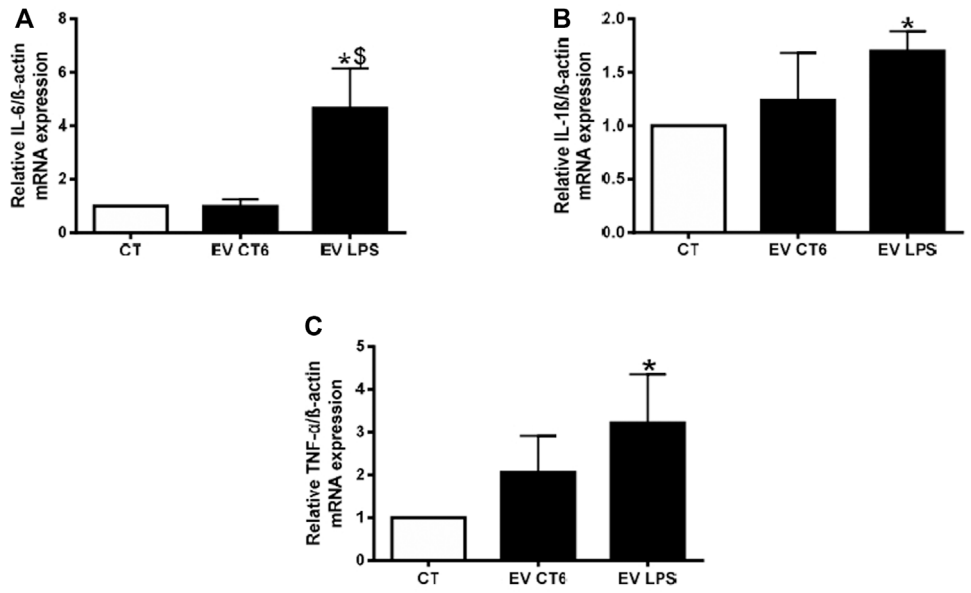

FIGURE 7 | EV-LPS increases cytokine gene expression in smooth muscle cells. MOVAS-1 cells were incubated with RAW cell-derived EVs for 24 h. Gene expression of **(A)** IL-6, **(B)** IL-1ß, and **(C)** TNF-α was then quantified by quantitative real-time PCR and normalized to that of the housekeeping gene ß-actin. Data are expressed as the mean ± SEM of four independent experiments performed in triplicate ($n = 4$). *$p < 0.05$ *vs.* CT, $$p < 0.05$ *vs.* EV-CT, Mann-Whitney test. EV-CT: EV-derived from untreated macrophages, EV-LPS: EV-derived from LPS-EK-treated macrophages.

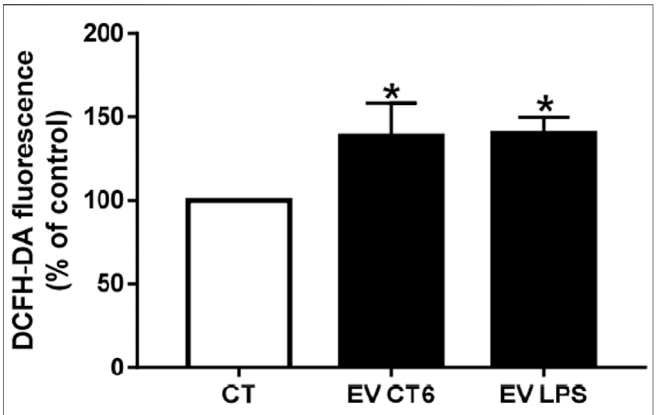

FIGURE 8 | Macrophage-derived EVs induce ROS production in smooth muscle cells. MOVAS-1 cells were incubated with 10 μM DCFH-DA in D-PBS at 37°C for 30 min and then treated with macrophage-derived EVs for 24 h. ROS production was determined by measuring fluorescence (λEx 492 nm, λEm 535 nm). ROS production by untreated control cells (CT) was defined as 100%. Data are expressed as the mean ± SEM of four independent experiments performed in triplicate ($n = 4$). *$p < 0.05$ *vs*. CT, Mann-Whitney test. EV-CT: EV-derived from untreated macrophages, EV-LPS: EV-derived from LPS-EK-treated macrophages.

3.2.5 Analysis of the Content of EV-LPS

Inflammation is known to play an important role in vascular calcification. We thus first analyzed the inflammatory content of EVs by measuring the expression of 10 proinflammatory cytokines in EV-LPS and EV-CT using an MSD multiplex kit. Proinflammatory cytokine levels were, indeed, significantly higher in EV-LPS than EV-CT6 (*$p < 0.05$ *vs.* CT, **Supplementary Figure S3**). We further analyzed the data using an unsupervised analysis approach to visualize any samples that clustered based on their inflammatory profile. The principal component analysis score plot showed a clear separation between the inflammatory profiles of EV-CT6 and EV-LPS (**Figure 10**). These results show that there is a specific inflammatory profile that distinguishes between these two conditions. We then analyzed the EV protein content by mass spectrometry and detected several EV-specific proteins in our samples, confirming the presence of EVs in our preparations (**Supplementary Table S2**). Furthermore, the level of three proteins in EV LPS were higher than in EV CT6: cis-aconitate decarboxylase (CAD), encoded by the *immunoresponsive gene 1* (*Irg1*); plasminogen activator inhibitor-1 (PAI-1), encoded by the *Serpine1* gene; and serum amyloid A-3 protein (Saa3), encoded by the *Saa3* gene ($p < 0.01$ *vs.* EV CT6, **Figure 11**).

3.2.6 EV-LPS Increase Pi-Induced Calcification by Inducing the Osteogenic Switch of Smooth Muscle Cells

Oxidative stress and inflammation are two processes known to play an important role in vascular calcification. Our results show that EV-derived macrophages can induce both oxidative stress and inflammation. Thus, we next determined the effect of these EVs on Pi-induced calcification in smooth muscle cells. MOVAS cells were simultaneously treated with 4 mM Pi and macrophage-derived EVs for 14 days (**Figure 12A**) or macrophage-derived

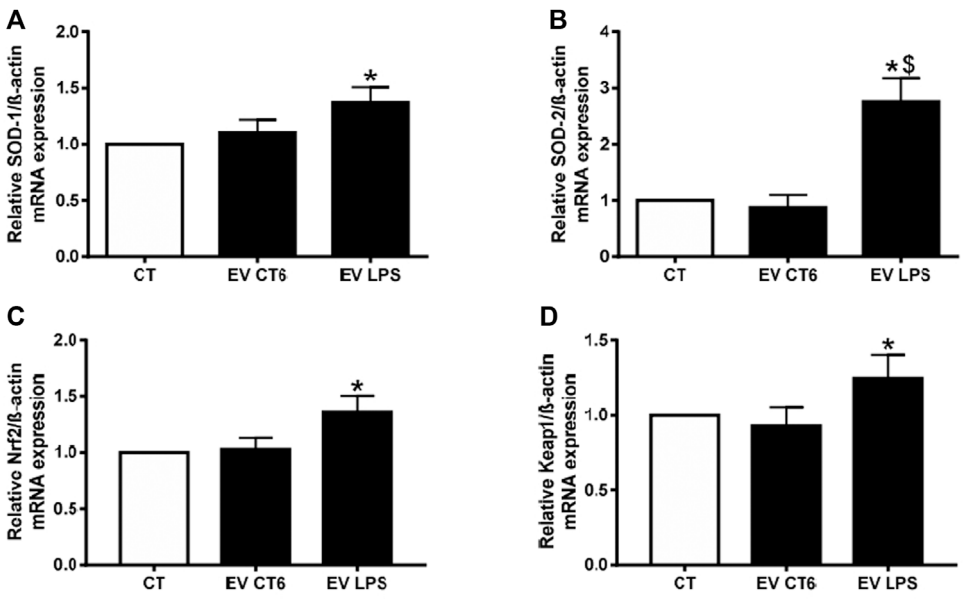

FIGURE 9 | EV-LPS increase antioxidant marker gene expression in smooth muscle cells. MOVAS-1 cells were incubated with EVs-derived RAW cells for 24 h. Gene expression of **(A)** SOD-1, **(B)** SOD-2, **(C)** Nrf2, and **(D)** Keap1 was then quantified by quantitative real-time PCR and normalized to that of the housekeeping gene ß-actin. Data are expressed as the mean ± SEM of four independent experiments performed in triplicate ($n = 4$). *$p < 0.05$ *vs*. CT, $$p < 0.05$ *vs*. EV-CT, Mann-Whitney test. EV-CT: EV-derived from untreated macrophages, EV-LPS: EV-derived from LPS-EK-treated macrophages.

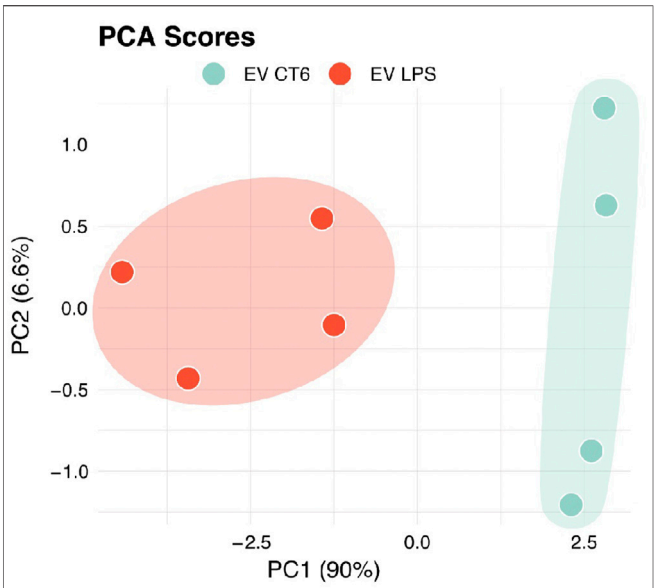

FIGURE 10 | Principal component analysis score plot of EV-CT6 and EV-LPS. EVs were isolated from the culture media of RAW cells incubated with (EV-LPS) or without (EV-CT6) LPS-EK. Proinflammatory cytokine protein levels (IL-1ß, IL-2, IL-4, IL-5, IL-6, IL-10, IL-12p70, TNF-α, IFN-γ, and KC-GRO) were measured in EVs derived from the macrophages using an MSD multiplex immunoassay. PCA analysis score plot is performed using four independent experiments (n = 4).

EVs for the last 7 days only (**Figure 12B**) of the induction of calcification. The intracellular calcium concentration in the smooth muscle cells was significantly higher after 14 days of treatment with Pi and EV-LPS than in cells treated with Pi and EV-CT ($ $p < 0.05$ *vs.* EV-CT, **Figure 12A**). Moreover, the intracellular calcium concentration was significantly higher after 7 days of treatment of Pi-treated smooth muscle cells with EV-LPS than Pi treatment alone (*$p < 0.05$ *vs.* 4 mM Pi, **Figure 12B**). These results suggest that EV-LPS can significantly induce calcification in MOVAS-1 cells. We can rule out that this effect was due to the presence of LPS-EK in EVs, as LPS-EK alone, with or without 4 mM Pi, had no effect on calcification (data not shown). We next measured the mRNA level of matrix gla protein (MGP), an inhibitor of vascular calcification. The level of MGP mRNA was significantly lower after 7 days of treatment of smooth muscle cells with 4 mM Pi and EV-LPS than in cells treated with Pi alone (*$p < 0.05$ *vs.* 4 mM Pi, **Figure 13**). The observed increase in calcification may therefore be partially due to a decrease in the level of calcification inhibitors, such as MGP.

Smooth muscle cells can adopt a contractile, synthetic, or osteochondrogenic phenotype, depending on their environment (Durham et al., 2018). During vascular calcification, smooth muscle cells undergo an osteogenic switch to become osteoblast-like cells (Durham et al., 2018). We investigated whether this phenotypic change occurred in our experiments by measuring the mRNA levels of several osteogenic markers, such as osterix (Osx) and osteocalcin (OCN), as well as alpha-smooth muscle actin

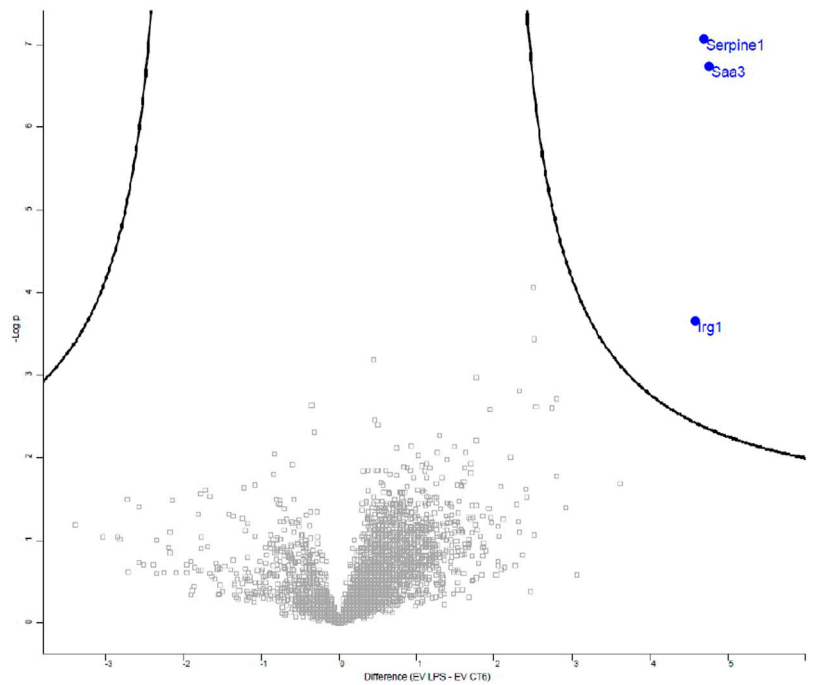

FIGURE 11 | Volcano plot representing the effects of lipopolysaccharide-EK (LPS-EK) on the protein content of macrophage-derived extracellular vesicles (EVs). EVs were isolated from the culture media of RAW cells incubated with (EV-LPS) or without (EV-CT6) lipopolysaccharide-EK (LPS-EK). High-performance liquid chromatography (HPLC) coupled to mass spectrometry analysis was performed. An unpaired Student's t test was conducted and a p-value < 0.01 and a false discovery rate (FDR) < 5% were used. Five independent experiments were performed.

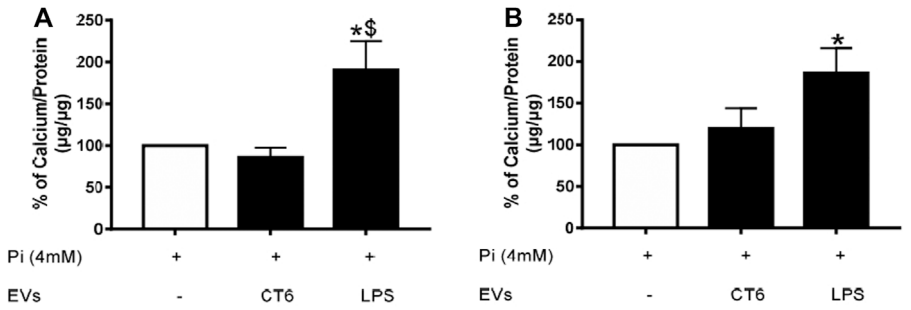

FIGURE 12 | EV-LPS enhance Pi-induced calcification in smooth muscle cells. Calcification in MOVAS-1 cells was induced by incubation with 4 mM Pi with or without RAW cell-derived EVs for **(A)** 14 days or **(B)** during the last 7 days of a 14-day calcification induction. Calcification was then measured using the OCP method. Data are expressed as the mean ± SEM of four independent experiments performed in triplicate ($n = 4$). *$p < 0.05$ *vs.* 4 mM Pi, $$p < 0.05$ *vs.* EV-CT, Mann-Whitney test. EV-CT: EVs derived from untreated macrophages, EV-LPS: EVs derived from LPS-EK-treated macrophages.

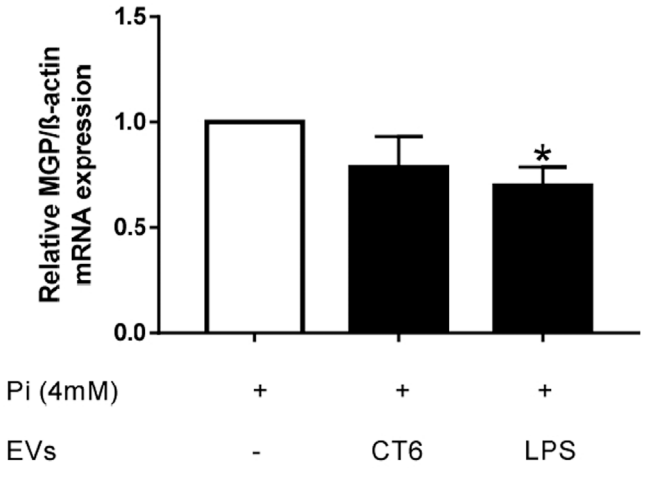

FIGURE 13 | EV-LPS decrease MGP gene expression in smooth muscle cells. MOVAS-1 cells were incubated for 7 days with 4 mM Pi with or without EVs secreted by RAW cells. Gene expression of MGP was then quantified by quantitative real-time PCR and normalized to that of the housekeeping gene ß-actin. Data are expressed as the mean ± SEM of seven independent experiments performed in triplicate ($n = 7$). *$p < 0.05$ *vs.* 4 mM Pi, Mann-Whitney test. EV-CT: EVs derived from untreated macrophages, EV-LPS: EVs derived from LPS-EK-treated macrophages.

(α-SMA), a marker of the contractile phenotype. Osx and OCN mRNA levels were significantly higher in Pi-treated smooth muscle cells incubated with EV-LPS than Pi-treated smooth muscle cells, suggesting an osteogenic switch of the MOVAS-1 cells (*$p < 0.05$ *vs.* 4 mM Pi, **$p < 0.01$ *vs.* 4 mM Pi, **Figures 14A,B**). We also observed higher Osx and Ocn mRNA levels after treatment of Pi-treated smooth muscle cells with EV-CT, but without reaching significance. This result can be explained by the higher amount of EVs in the EV-CT preparation. At the same time, α-SMA mRNA levels were significantly lower than in Pi-treated smooth muscle cells (**$p <$ 0.01 *vs.* 4 mM Pi, **Figure 14C**). Overall, these results show that EV-LPS induce an osteogenic switch of smooth muscle cells, which could, in turn, promote calcification.

4 DISCUSSION

Vascular calcification (VC) is a complex process involving various molecular and cellular mechanisms, such as the VSMC osteogenic switch, loss of VC inhibitors, cell death, and dysregulation of Ca^{2+}/Pi homeostasis, as well as matrix degradation and modification (Lee et al., 2020). Macrophages are among the main sources of inflammation and oxidative stress (Castaneda et al., 2017) and associated with arterial calcification (Agharazii et al., 2015). Indeed, Aikawa *et al.* showed co-localization of calcification and macrophages in atherosclerotic plaques of apolipoprotein E-deficient mice by image analysis, suggesting a prominent role of these cells and inflammation in calcification (Aikawa et al., 2007). In addition, a number of studies have shown macrophage-derived EVs to be mediators of VC (New et al., 2013; Chen et al., 2016; Li Y. et al., 2020; Kawakami et al., 2020). In this context, we hypothesized that macrophage-derived EVs secreted under pro-inflammatory and pro-oxidative conditions may increase VSMC calcification by propagating inflammation and oxidative stress. We tested our hypothesis by treating a murine VSMC cell line with EVs derived from LPS treated-murine macrophages. We then analyzed the effect of macrophage-derived EVs on the calcium content and levels of inflammatory, oxidative stress, and osteogenic markers in VSMCs. Moreover, we analyzed the protein content of EVs secreted by such activated macrophages.

We show that LPS-EK induces an inflammatory response in macrophages, as demonstrated by the significant increase in mRNA levels of pro-inflammatory cytokines (IL-6, IL-1ß, and TNF-α). These results are in accordance with those in the literature, as activation of TLR4 by LPS triggers activation of the MyD88-dependent pathway, inducing pro-inflammatory cytokine gene transcription. NLRP3, an activator protein of the inflammasome has also been shown to be significantly upregulated after LPS treatment (He et al., 2016). Our results show that LPS-EK induces pro-inflammatory M1 polarization of RAW cells, in accordance with the results of a study of Li *et al.* performed in the U937 monocyte cell line (Li et al., 2017). LPS-EK also induced oxidative stress, as shown by the significant increase in ROS production, as previously reported. In parallel,

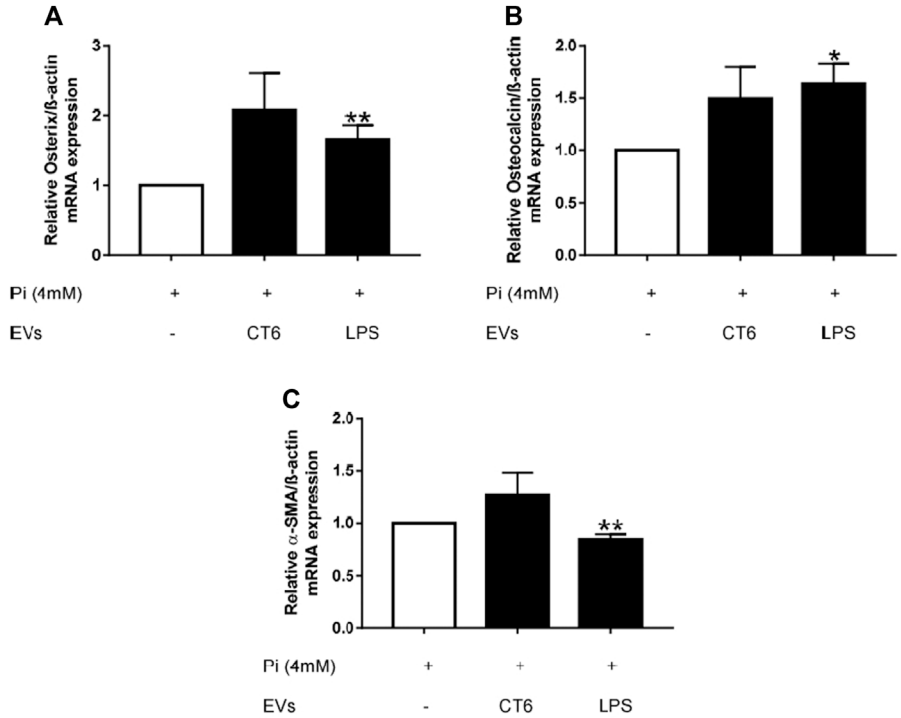

FIGURE 14 | EV-LPS increase osteogenic marker gene expression and decrease contractile marker gene expression in smooth muscle cells. MOVAS-1 cells were incubated with 4 mM Pi, with or without RAW cell-derived EVs, for 7 days. Gene expression of **(A)** osterix, **(B)** osteocalcin, and **(C)** α-SMA was then quantified by quantitative real-time PCR and normalized to that of the housekeeping gene ß-actin. Data are expressed as the mean ± SEM of at least four independent experiments performed in triplicate ($n = 4$). *$p < 0.05$ *vs*. 4 mM Pi, **$p < 0.01$ *vs*. 4 mM Pi, Mann Whitney test. EV-CT: EVs derived from untreated macrophages, EV-LPS: EVs derived from LPS-EK-treated macrophages.

we showed a significant decrease in the expression of genes involved in the antioxidant system, such as Nrf2/Keap. Nrf2 is a transcriptional factor that induces the expression of antioxidant genes. Under basal conditions, Keap1 forms a complex with Nrf2 to induce its degradation by the proteasome. Under conditions of oxidative stress, modifications of the cysteine residues of Keap1 inhibit its interaction with Nrf2, allowing its nuclear translocation and protection of cells against oxidative stress. The observed decrease in Keap1 mRNA levels could be explained by the induction of protective mechanism activated by the cells to counteract ROS production. Surprisingly, despite an increase in ROS production, we showed a significant decrease in $O_2^{\bullet-}$ production, which can be explained by both a decrease in Nox-2 levels and an increase in its degradation by SOD-2. This discrepancy can be partially explained by the fact that $O_2^{\bullet-}$ can rapidly react with NO to form peroxynitrite ($ONOO^-$), which mediates oxidative responses. Indeed, under LPS treatment, we observed a decrease in NO production, despite an increase in iNOS, an enzyme that produces NO.

As already shown (Liu et al., 2017; Bell et al., 2019), LPS-EK inhibited EV biogenesis by decreasing the expression of several markers of EV biogenesis, such as sphingomyelin phosphodiesterase 3 (SMPD3), phospho-1, and tissue nonspecific phosphatase alkaline phosphatase (TNAP). These results were confirmed by NTA analysis, which showed a reduced number of secreted EVs after LPS treatment. A similar result was reported by Bell *et al.* in AC16 human cardiomyocytes (Bell et al., 2019). In our cellular model, LPS-EK significantly decreased the expression of autophagic markers (Atg5, beclin1, ULK). Autophagy has already been shown to play an important role in EV biogenesis (Yang et al., 2021). This was confirmed by a significant increase in p62 expression after LPS treatment, as it has been shown that p62 protein accumulates upon inhibition of autophagy (Lamark et al., 2009). Interestingly, Liu et al. recently demonstrated a link between autophagy and macrophage polarization, showing that inhibition of autophagy induces the polarization of macrophages towards a pro-inflammatory M1 phenotype (Liu et al., 2015), a phenotype that we observed in our cells after treatment with LPS-EK. Moreover, Zhao *et al.* have shown that autophagy contributes to redox homeostasis, not only by clearing oxidized cellular components, but also by promoting antioxidant defenses *via* the p62/Keap1/Nrf2 pathway (Zhao et al., 2019). Therefore, a deficiency in autophagy, as observed in our cellular model, would decrease antioxidant defenses, which could also explain the observed increase in oxidative stress.

We investigated whether EVs secreted by LPS-treated cells play a role in VC by incubating VSMCs with EV-LPS. We show that EV-LPS induces inflammation and oxidative stress in VSMCs, with a significant increase in the expression of pro-inflammatory cytokines (IL6, IL1β, TNFα). Assessment of the inflammatory profile of the secreted EVs showed that EV-LPS are

in fact enriched in these proinflammatory cytokines, consistent with the M1 polarization of RAW cells observed after treatment with LPS-EK. Cytokines are key players in cell-cell communication and play important roles in several biological processes, such as cell differentiation and inflammation. Various secretory pathways are responsible for their release, such as the classical ER/Golgi route and the unconventional pathway, also known as unconventional protein secretion (UPS). Recently, cytokines have been shown to be capable of reaching the extracellular milieu *via* a novel secretory pathway through EVs. Fitzgerald et al. thus showed that cytokine encapsulation into EVs is a general biological phenomenon observed *in vitro* and *in vivo* (Fitzgerald et al., 2018). Interestingly the profile of such encapsulated cytokines changes in response to various stimuli, suggesting that cytokine association with EVs is not specific to any particular cytokine, as all cytokines can be encapsulated. Tokarz et al. showed, for example, that the association of specific cytokines with EVs is strongly influenced by disease duration and treatment in diabetes (Tokarz et al., 2015). Such an association between cytokines and EVs appears to result from a specific physiological need, depending on whether the cytokines act near the Ev-secreting cells or at a distance. Indeed, Fitzgerald et al. (2018) showed that tissue explants, in which cells are in proximity with each other, secrete more soluble cytokine than cells in suspension, in which cytokines are more highly associated with EVs to allow their interaction with recipient cells at a distance. It is therefore possible that pro-inflammatory cytokines from M1 macrophages are carried by EVs secreted by these cells to induce a pro-inflammatory microenvironment for recipient cells, such as VSMCs. Moreover, several studies have shown that inflammatory cytokines have biological effects in VSMCs (Nilsson, 1993). For example, Barillari *et al.* showed that IL-1β, TNF-α, and IFN-γ released by activated immune cells enhance the expression of α5β1 integrin, a fibronectin receptor, leading to an increase in VSMC proliferation and migration, two mechanisms required for the formation of atherosclerotic lesions (Barillari et al., 2001). Our results also show that EV-LPS induce oxidative stress, as demonstrated by increased ROS production and decreased expression of antioxidant enzyme genes. However, EVs from non-treated cells (EV-CT) were also able to induce oxidative stress. Nevertheless, it is worthwhile noting that we treated cells with equivalent volumes of EV preparations. As LPS-treated cells secreted fewer EVs than control cells, it is likely that using the same volumes to treat VSMCs resulted in treating them with a lower number of EV-LPS than EV-CT, thus underestimating the effects of EV-LPS on VSMCs. These results confirm our hypothesis that EVs secreted under pro-inflammatory and pro-oxidative conditions are able to propagate inflammation and oxidative stress to surrounding cells, such as VSMCs. Finally, EV-LPS enhanced Pi-induced calcification of VSMCs by inducing the VSMC osteogenic switch and decreasing expression of the calcification inhibitor, MGP. These effects were intrinsic to EVs, as LPS alone had no effect on calcification. Moreover, in a similar manner, the study of Li *et al.* showed that the conditioned medium of LPS-treated macrophages induces an osteogenic switch of valve interstitial cells by increasing OPN, BMP-2, and ALP expression (Li et al., 2017). Furthermore, the aforementioned study showed that the increase in IL-6, IL-1β, and TNF-α in the conditioned medium was associated with an increase in the production of MMPs, which contribute to extracellular matrix degradation, remodeling, and valve calcification (Li et al., 2017).

Proteomic analysis highlighted the upregulation of three proteins in EV-LPS relative to EV-CT: cis-aconitate decarboxylase (CAD), plasminogen activator inhibitor-1 (PAI-1), and serum amyloid A-3 protein (Saa3). CAD, a mitochondrial enzyme encoded by immunoresponsive gene 1 (Irg1) and involved in itaconate production, is known to be upregulated in macrophages under pro-inflammatory conditions (Basler et al., 2006; Németh et al., 2016; Tallam et al., 2016; Song et al., 2020). Itaconate has been shown to be an immunoregulatory and anti-oxidant molecule (Lampropoulou et al., 2016; Mills et al., 2018; Li R. et al., 2020; Song et al., 2020). Itaconate has also been shown to promote IL-1β production and inflammatory apoptosis when administered at high doses to bone marrow-derived dendritic cells (Muri et al., 2020). In addition, the production of ROS can be mediated by Irg1 induction (Tan et al., 2016). In our study, EV-LPS were enriched in CAD. It is thus possible that this enzyme may induce the production of itaconate in VSMCs when transferred to the recipient cells via EVs, leading to inflammation and oxidative stress. PAI-1 is known to inhibit the action of plasminogen activators, such as tPA and uPA. First, several studies have already shown the upregulation of PAI-1 expression in LPS-treated cells (Wang et al., 2014; Ren et al., 2015) and an immunoregulatory role for PAI-1 through the TLR4 signaling pathway (Gupta et al., 2016). PAI-1 levels also increase under oxidative conditions (Vulin and Stanley, 2004). The higher amount of PAI-1 found in EV-LPS could be explained by macrophage activation. Numerous studies have shown PAI-1 to be associated with atherosclerotic lesions. Indeed, PAI-1 levels are high in atherosclerotic coronary arteries (Schneiderman et al., 1992; Lupu et al., 1993; Raghunath et al., 1995; Padró et al., 1997). PAI-1 expression was also found to be higher in CKD patients than healthy individuals (Ouyang et al., 2013). Furthermore, a number of studies have shown that PAI-1 is linked to VC. The upregulation of PAI-1 was, indeed, shown to be proportional to the calcium content in 65 calcified aortic valves (Kochtebane et al., 2014). Another study showed PAI-1 to positively correlate with vascular media thickness and calcification (Ouyang et al., 2013). PAI-1 transported by EV-LPS could thus participate in the aggravation of the VC process, as observed under our experimental conditions. Finally, Saa3, a member of apolipoproteins associated with high-density lipoprotein (HDL) in plasma, was only overexpressed in EV-LPS. As for CAD and PAI-1, Saa3 was upregulated after LPS treatment (Meek et al., 1992; Reigstad et al., 2009). Several studies have shown Saa proteins to have cytokine-like activity and to be able to activate several receptors, such as TLRs, and transcription factors, such as NF-κB (Ye and Sun, 2015). In addition, a number of studies have highlighted the role of Saa proteins in calcification (Tanaka et al., 2011; Ebert et al., 2015; Zhang et al., 2017). Saa proteins induce the production of pro-inflammatory cytokines and the osteogenic differentiation of mesenchymal stem cells *via* the TLR4 receptor (Ebert et al., 2015). Zhang *et al.* also showed that Saa proteins can

induce the VSMC osteogenic switch through the p38 MAPK signaling pathway (Zhang et al., 2017). Furthermore, Saa proteins can increase calcium entry in human coronary artery smooth muscle cells (Tanaka et al., 2011). Thus, it is possible that Saa3 transported by EVs increases Pi entry into VSMCs and enhances the VSMC osteogenic switch.

In conclusion, we show a direct contribution of macrophages in the microcalcification process *via* EV secretion, an alternative pathway, in addition to the VSMC osteogenic switch. Indeed, EV-LPS, enriched for molecules involved in inflammation, oxidative stress, and VC mechanisms, were able to create an inflammatory microenvironment for surrounding cells, such as VSMCs, which in turn underwent an osteogenic switch, leading to increasing calcification. As atherosclerotic plaques containing microcalcifications are more susceptible to rupture and cardiovascular accidents, this study suggests that EVs could be used as non-invasive biomarkers to better stratify patients with a high risk of CV. Moreover, such EVs could therefore also be a therapeutic target to limit VC in patients.

DATA AVAILABILITY STATEMENT

The data presented in the study are deposited in the PRIDE repository, accession number PXD029441(http://www.proteomexchange.org).

AUTHOR CONTRIBUTIONS

AB and JA designed the experiments and performed the relevant literature research and data analysis. LY contributed to experimentation and analysis of the results. CD and LY contributed to the structural analysis of EVs by NTA. VJ and IG performed the proteomic analysis. LY and CL contributed to the analysis of EV content by V-Plex. AT and SB provided important input to the data analysis on the V-Plex assay. LY, AB, and JA contributed to the writing of the manuscript. AB, SK, SB, AT, IG, and JA reviewed and edited the paper. All authors contributed to the article and approved the submitted version.

FUNDING

LY was financially supported by the French Research Ministry. This work was financially supported by the Université de Picardie Jules Verne.

ACKNOWLEDGMENTS

This work benefited from the assistance of Stephanie Balor and Vanessa Soldan from the Multiscale Electron Imaging platform (METi) of the Centre de Biologie Intégrative (CBI), Toulouse, France.

SUPPLEMENTARY MATERIAL

The Supplementary Material for this article can be found online at: https://www.frontiersin.org/articles/10.3389/fcell.2022.823450/full#supplementary-material

REFERENCES

Agharazii, M., St-Louis, R., Gautier-Bastien, A., Ung, R.-V., Mokas, S., Larivière, R., et al. (2015). Inflammatory Cytokines and Reactive Oxygen Species as Mediators of Chronic Kidney Disease-Related Vascular Calcification. *Am. J. Hypertens.* 28, 746–755. doi:10.1093/ajh/hpu225

Aiello, A., Giannessi, F., Percario, Z. A., and Affabris, E. (2020). An Emerging Interplay between Extracellular Vesicles and Cytokines. *Cytokine Growth Factor. Rev.* 51, 49–60. doi:10.1016/j.cytogfr.2019.12.003

Aikawa, E., Nahrendorf, M., Figueiredo, J.-L., Swirski, F. K., Shtatland, T., Kohler, R. H., et al. (2007). Osteogenesis Associates with Inflammation in Early-Stage Atherosclerosis Evaluated by Molecular Imaging *In Vivo*. *Circulation* 116, 2841–2850. doi:10.1161/CIRCULATIONAHA.107.732867

Barillari, G., Albonici, L., Incerpi, S., Bogetto, L., Pistritto, G., Volpi, A., et al. (2001). Inflammatory Cytokines Stimulate Vascular Smooth Muscle Cells Locomotion and Growth by Enhancing α5β1 Integrin Expression and Function. *Atherosclerosis* 154, 377–385. doi:10.1016/s0021-9150(00)00506-2

Basler, T., Jeckstadt, S., Valentin-Weigand, P., and Goethe, R. (2006). Mycobacterium Paratuberculosis, Mycobacterium Smegmatis, and Lipopolysaccharide Induce Different Transcriptional and post-transcriptional Regulation of the IRG1 Gene in Murine Macrophages. *J. Leukoc. Biol.* 79, 628–638. doi:10.1189/jlb.0905520

Bell, C. R., Jones, L. B., Crenshaw, B. J., Kumar, S., Rowe, G. C., Sims, B., et al. (2019). The Role of Lipopolysaccharide-Induced Extracellular Vesicles in Cardiac Cell Death. *Biology* 8, 69. doi:10.3390/biology8040069

Bodega, G., Alique, M., Puebla, L., Carracedo, J., and Ramírez, R. M. (2019). Microvesicles: ROS Scavengers and ROS Producers. *J. Extracellular Vesicles* 8, 1626654. doi:10.1080/20013078.2019.1626654

Castaneda, O. A., Lee, S.-C., Ho, C.-T., and Huang, T.-C. (2017). Macrophages in Oxidative Stress and Models to Evaluate the Antioxidant Function of Dietary Natural Compounds. *J. Food Drug Anal.* 25, 111–118. doi:10.1016/j.jfda.2016.11.006

Chen, N. X., O'Neill, K. D., Chen, X., and Moe, S. M. (2008). Annexin-mediated Matrix Vesicle Calcification in Vascular Smooth Muscle Cells. *J. Bone Mineral Res.* 23, 1798–1805. doi:10.1359/jbmr.080604

Chen, Q., Bei, J.-J., Liu, C., Feng, S.-B., Zhao, W.-B., Zhou, Z., et al. (2016). HMGB1 Induces Secretion of Matrix Vesicles by Macrophages to Enhance Ectopic Mineralization. *PLoS ONE* 11, e0156686. doi:10.1371/journal.pone.0156686

Cox, J., and Mann, M. (2008). MaxQuant Enables High Peptide Identification Rates, Individualized p.p.b.-range Mass Accuracies and Proteome-wide Protein Quantification. *Nat. Biotechnol.* 26, 1367–1372. doi:10.1038/nbt.1511

Demer, L. L., and Tintut, Y. (2008). Vascular Calcification. *Circulation* 117, 2938–2948. doi:10.1161/CIRCULATIONAHA.107.743161

Drüeke, T. B., and Massy, Z. A. (2011). Medial or Intimal Calcification in CKD-Does it Matter? *Nat. Rev. Nephrol.* 7, 250–251. doi:10.1038/nrneph.2011.41

Durham, A. L., Speer, M. Y., Scatena, M., Giachelli, C. M., and Shanahan, C. M. (2018). Role of Smooth Muscle Cells in Vascular Calcification: Implications in Atherosclerosis and Arterial Stiffness. *Cardiovasc. Res.* 114, 590–600. doi:10.1093/cvr/cvy010

Ebert, R., Benisch, P., Krug, M., Zeck, S., Meißner-Weigl, J., Steinert, A., et al. (2015). Acute Phase Serum Amyloid A Induces Proinflammatory Cytokines and Mineralization via Toll-like Receptor 4 in Mesenchymal Stem Cells. *Stem Cel Res.* 15, 231–239. doi:10.1016/j.scr.2015.06.008

Ellman, G. L., Courtney, K. D., Andres, V., and Featherstone, R. M. (1961). A New and Rapid Colorimetric Determination of Acetylcholinesterase Activity. *Biochem. Pharmacol.* 7, 88–95. doi:10.1016/0006-2952(61)90145-9

Fitzgerald, W., Freeman, M. L., Lederman, M. M., Vasilieva, E., Romero, R., and Margolis, L. (2018). A System of Cytokines Encapsulated in ExtraCellular Vesicles. *Sci. Rep.* 8, 8973. doi:10.1038/s41598-018-27190-x

Fujii, T., Mashimo, M., Moriwaki, Y., Misawa, H., Ono, S., Horiguchi, K., et al. (2017). Physiological Functions of the Cholinergic System in Immune Cells. *J. Pharmacol. Sci.* 134, 1–21. doi:10.1016/j.jphs.2017.05.002

Gupta, K. K., Xu, Z., Castellino, F. J., and Ploplis, V. A. (2016). Plasminogen Activator Inhibitor-1 Stimulates Macrophage Activation through Toll-like Receptor-4. *Biochem. Biophysical Res. Commun.* 477, 503–508. doi:10.1016/j.bbrc.2016.06.065

He, Y., Hara, H., and Núñez, G. (2016). Mechanism and Regulation of NLRP3 Inflammasome Activation. *Trends Biochem. Sci.* 41, 1012–1021. doi:10.1016/j.tibs.2016.09.002

Hénaut, L., Candellier, A., Boudot, C., Grissi, M., Mentaverri, R., Choukroun, G., et al. (2019). New Insights into the Roles of Monocytes/Macrophages in Cardiovascular Calcification Associated with Chronic Kidney Disease. *Toxins* 11, 529. doi:10.3390/toxins11090529

Hodroge, A., Trécherel, E., Cornu, M., Darwiche, W., Mansour, A., Ait-Mohand, K., et al. (2017). Oligogalacturonic Acid Inhibits Vascular Calcification by Two Mechanisms. *Atvb* 37, 1391–1401. doi:10.1161/atvbaha.117.309513

Hu, C.-T., Shao, Y.-D., Liu, Y.-Z., Xiao, X., Cheng, Z.-B., Qu, S.-L., et al. (2021). Oxidative Stress in Vascular Calcification. *Clinica Chim. Acta* 519, 101–110. doi:10.1016/j.cca.2021.04.012

Jaminon, A., Reesink, K., Kroon, A., and Schurgers, L. (2019). The Role of Vascular Smooth Muscle Cells in Arterial Remodeling: Focus on Calcification-Related Processes. *Ijms* 20, 5694. doi:10.3390/ijms20225694

Kawakami, R., Katsuki, S., Travers, R., Romero, D. C., Becker-Greene, D., Passos, L. S. A., et al. (2020). S100A9-RAGE Axis Accelerates Formation of Macrophage-Mediated Extracellular Vesicle Microcalcification in Diabetes Mellitus. *Atvb* 40, 1838–1853. doi:10.1161/ATVBAHA.118.314087

Kochtebane, N., Alzahrani, A. M. M., and Bartegi, A. (2014). Expression of uPA, tPA, and PAI-1 in Calcified Aortic Valves. *Biochem. Res. Int.* 2014, 1. doi:10.1155/2014/658643

Komaba, H., and Fukagawa, M. (2009). Fetuin-mineral Complex: a New Potential Biomarker for Vascular Calcification? *Kidney Int.* 75, 874–876. doi:10.1038/ki.2009.52

Lamark, T., Kirkin, V., Dikic, I., and Johansen, T. (2009). NBR1 and P62 as Cargo Receptors for Selective Autophagy of Ubiquitinated Targets. *Cell Cycle* 8, 1986–1990. doi:10.4161/cc.8.13.8892

Lampropoulou, V., Sergushichev, A., Bambouskova, M., Nair, S., Vincent, E. E., Loginicheva, E., et al. (2016). Itaconate Links Inhibition of Succinate Dehydrogenase with Macrophage Metabolic Remodeling and Regulation of Inflammation. *Cel Metab.* 24, 158–166. doi:10.1016/j.cmet.2016.06.004

Lee, S. J., Lee, I.-K., and Jeon, J.-H. (2020). Vascular Calcification-New Insights into its Mechanism. *Ijms* 21, 2685. doi:10.3390/ijms21082685

Li, G., Qiao, W., Zhang, W., Li, F., Shi, J., and Dong, N. (2017). The Shift of Macrophages toward M1 Phenotype Promotes Aortic Valvular Calcification. *J. Thorac. Cardiovasc. Surg.* 153, 1318–1327. doi:10.1016/j.jtcvs.2017.01.052

Li, R., Zhang, P., Wang, Y., and Tao, K. (2020a). Itaconate: A Metabolite Regulates Inflammation Response and Oxidative Stress. *Oxidative Med. Cell Longevity* 2020, 1. doi:10.1155/2020/5404780

Li, Y., Sun, Z., Zhang, L., Yan, J., Shao, C., Jing, L., et al. (2020b). Role of Macrophages in the Progression and Regression of Vascular Calcification. *Front. Pharmacol.* 11. doi:10.3389/fphar.2020.00661

Liu, F., Li, X., Yue, H., Ji, J., You, M., Ding, L., et al. (2017). TLR-induced SMPD3 Defects Enhance Inflammatory Response of B Cell and Macrophage in the Pathogenesis of SLE. *Scand. J. Immunol.* 86, 377–388. doi:10.1111/sji.12611

Liu, K., Zhao, E., Ilyas, G., Lalazar, G., Lin, Y., Haseeb, M., et al. (2015). Impaired Macrophage Autophagy Increases the Immune Response in Obese Mice by Promoting Proinflammatory Macrophage Polarization. *Autophagy* 11, 271–284. doi:10.1080/15548627.2015.1009787

Lupu, F., Bergonzelli, G. E., Heim, D. A., Cousin, E., Genton, C. Y., Bachmann, F., et al. (1993). Localization and Production of Plasminogen Activator Inhibitor-1 in Human Healthy and Atherosclerotic Arteries. *Arterioscler Thromb.* 13, 1090–1100. doi:10.1161/01.atv.13.7.1090

Mansour, A., Darwiche, W., Yaker, L., Da Nascimento, S., Gomila, C., Rossi, C., et al. (2020). GFOGER Peptide Modifies the Protein Content of Extracellular Vesicles and Inhibits Vascular Calcification. *Front. Cel Dev. Biol.* 8, 589761. doi:10.3389/fcell.2020.589761

Mastronarde, D. N. (2005). Automated Electron Microscope Tomography Using Robust Prediction of Specimen Movements. *J. Struct. Biol.* 152, 36–51. doi:10.1016/j.jsb.2005.07.007

Meek, R. L., Eriksen, N., and Benditt, E. P. (1992). Murine Serum Amyloid A3 Is a High Density Apolipoprotein and Is Secreted by Macrophages. *Proc. Natl. Acad. Sci.* 89, 7949–7952. doi:10.1073/pnas.89.17.7949

Mills, E. L., Ryan, D. G., Prag, H. A., Dikovskaya, D., Menon, D., Zaslona, Z., et al. (2018). Itaconate Is an Anti-inflammatory Metabolite that Activates Nrf2 via Alkylation of KEAP1. *Nature* 556, 113–117. doi:10.1038/nature25986

Moe, S. M., and Chen, N. X. (2005). Inflammation and Vascular Calcification. *Blood Purif.* 23, 64–71. doi:10.1159/000082013

Muri, J., Wolleb, H., Broz, P., Carreira, E. M., and Kopf, M. (2020). Electrophilic Nrf2 Activators and Itaconate Inhibit Inflammation at Low Dose and Promote IL-1β Production and Inflammatory Apoptosis at High Dose. *Redox Biol.* 36, 101647. doi:10.1016/j.redox.2020.101647

Németh, B., Doczi, J., Csete, D., Kacso, G., Ravasz, D., Adams, D., et al. (2016). Abolition of Mitochondrial Substrate-level Phosphorylation by Itaconic Acid Produced by LPS-induced Irg1 Expression in Cells of Murine Macrophage Lineage. *FASEB j.* 30, 286–300. doi:10.1096/fj.15-279398

New, S. E. P., Goettsch, C., Aikawa, M., Marchini, J. F., Shibasaki, M., Yabusaki, K., et al. (2013). Macrophage-Derived Matrix Vesicles. *Circ. Res.* 113, 72–77. doi:10.1161/CIRCRESAHA.113.301036

Nilsson, J. (1993). Cytokines and Smooth Muscle Cells in Atherosclerosis. *Cardiovasc. Res.* 27, 1184–1190. doi:10.1093/cvr/27.7.1184

Ouyang, L., Peng, Y., Wu, G., Xu, X., and He, Z. (2013). Efffect of Plasminogen Activator Inhibitor-1 and Endothelin-1 on the Atherosclerosis in the Maintenance Hemodialysis Patients. *Zhong Nan Da Xue Xue Bao Yi Xue Ban* 38, 458–467. doi:10.3969/j.issn.1672-7347.2013.05.004

Padró, T., Steins, M., Li, C.-X., Mesters, R. M., Hammel, D., Scheld, H. H., et al. (1997). Comparative Analysis of Plasminogen Activator Inhibitor-1 Expression in Different Types of Atherosclerotic Lesions in Coronary Arteries from Human Heart Explants. *Cardiovasc. Res.* 36, 28–36. doi:10.1016/S0008-6363(97)00144-2

Perez-Riverol, Y., Csordas, A., Bai, J., Bernal-Llinares, M., Hewapathirana, S., Kundu, D. J., et al. (2019). The PRIDE Database and Related Tools and Resources in 2019: Improving Support for Quantification Data. *Nucleic Acids Res.* 47 (D1), D442–D450. doi:10.1093/nar/gky1106

Peterson, G. L. (1977). A simplification of the protein assay method of Lowry et al. which is more generally applicable. *Anal. Biochem.* 83, 346–356. doi:10.1016/0003-2697(77)90043-4

Pi, J., Li, T., Liu, J., Su, X., Wang, R., Yang, F., et al. (2014). Detection of Lipopolysaccharide Induced Inflammatory Responses in RAW264.7 Macrophages Using Atomic Force Microscope. *Micron* 65, 1–9. doi:10.1016/j.micron.2014.03.012

Qin, Z., Liao, R., Xiong, Y., Jiang, L., Li, J., Wang, L., et al. (2021). A Narrative Review of Exosomes in Vascular Calcification. *Ann. Transl. Med.* 9, 579. doi:10.21037/atm-20-7355

Raghunath, P. N., Tomaszewski, J. E., Brady, S. T., Caron, R. J., Okada, S. S., and Barnathan, E. S. (1995). Plasminogen Activator System in Human Coronary Atherosclerosis. *Atvb* 15, 1432–1443. doi:10.1161/01.atv.15.9.1432

Raschke, W. C., Baird, S., Ralph, P., and Nakoinz, I. (1978). Functional Macrophage Cell Lines Transformed by Abelson Leukemia Virus. *Cell* 15, 261–267. doi:10.1016/0092-8674(78)90101-0

Ray Sarkar, B. C., and Chauhan, U. P. S. (1967). A New Method for Determining Micro Quantities of Calcium in Biological Materials. *Anal. Biochem.* 20, 155–166. doi:10.1016/0003-2697(67)90273-4

Reigstad, C. S., Lundén, G. Ö., Felin, J., and Bäckhed, F. (2009). Regulation of Serum Amyloid A3 (SAA3) in Mouse Colonic Epithelium and Adipose Tissue by the Intestinal Microbiota. *PLOS ONE* 4, e5842. doi:10.1371/journal.pone.0005842

Ren, W., Wang, Z., Hua, F., and Zhu, L. (2015). Plasminogen Activator Inhibitor-1 Regulates LPS-Induced TLR4/MD-2 Pathway Activation and Inflammation in Alveolar Macrophages. *Inflammation* 38, 384–393. doi:10.1007/s10753-014-0042-8

Schneiderman, J., Sawdey, M. S., Keeton, M. R., Bordin, G. M., Bernstein, E. F., Dilley, R. B., et al. (1992). Increased Type 1 Plasminogen Activator Inhibitor Gene Expression in Atherosclerotic Human Arteries. *Proc. Natl. Acad. Sci.* 89, 6998–7002. doi:10.1073/pnas.89.15.6998

Song, H., Xu, T., Feng, X., Lai, Y., Yang, Y., Zheng, H., et al. (2020). Itaconate Prevents Abdominal Aortic Aneurysm Formation through Inhibiting Inflammation via Activation of Nrf2. *EBioMedicine* 57, 102832. doi:10.1016/j.ebiom.2020.102832

Tallam, A., Perumal, T. M., Antony, P. M., Jäger, C., Fritz, J. V., Vallar, L., et al. (2016). Gene Regulatory Network Inference of Immunoresponsive Gene 1 (IRG1) Identifies Interferon Regulatory Factor 1 (IRF1) as its Transcriptional Regulator in Mammalian Macrophages. *PLOS ONE* 11, e0149050. doi:10.1371/journal.pone.0149050

Tan, H.-Y., Wang, N., Li, S., Hong, M., Wang, X., and Feng, Y. (2016). The Reactive Oxygen Species in Macrophage Polarization: Reflecting its Dual Role in Progression and Treatment of Human Diseases. *Oxidative Med. Cell Longevity* 2016, 1. doi:10.1155/2016/2795090

Tanaka, T., Ikeda, K., Yamamoto, Y., Iida, H., Kikuchi, H., Morita, T., et al. (2011). Effects of Serum Amyloid a and Lysophosphatidylcholine on Intracellular Calcium Concentration in Human Coronary Artery Smooth Muscle Cells. *Int. Heart J.* 52, 185–193. doi:10.1536/ihj.52.185

Théry, C., Witwer, K. W., Aikawa, E., Alcaraz, M. J., Anderson, J. D., Andriantsitohaina, R., et al. (2018). Minimal Information for Studies of Extracellular Vesicles 2018 (MISEV2018): a Position Statement of the International Society for Extracellular Vesicles and Update of the MISEV2014 Guidelines. *J. Extracell. Vesicles* 7, 1535750. doi:10.1080/20013078.2018.1535750

Tokarz, A., Szuścik, I., Kuśnierz-Cabala, B., Kapusta, M., Konkolewska, M., Żurakowski, A., et al. (2015). Extracellular Vesicles Participate in the Transport of Cytokines and Angiogenic Factors in Diabetic Patients with Ocular Complications. *Folia Med. Cracov* 55, 35–48.

Tóth, A., Balogh, E., and Jeney, V. (2020). Regulation of Vascular Calcification by Reactive Oxygen Species. *Antioxidants* 9, 963. doi:10.3390/antiox9100963

Tyanova, S., Temu, T., Sinitcyn, P., Carlson, A., Hein, M. Y., Geiger, T., et al. (2016). The Perseus Computational Platform for Comprehensive Analysis of (Prote)omics Data. *Nat. Methods* 13, 731–740. doi:10.1038/nmeth.3901

van Niel, G., D'Angelo, G., and Raposo, G. (2018). Shedding Light on the Cell Biology of Extracellular Vesicles. *Nat. Rev. Mol. Cel Biol.* 19, 213–228. doi:10.1038/nrm.2017.125

Voelkl, J., Lang, F., Eckardt, K.-U., Amann, K., Kuro-O, M., Pasch, A., et al. (2019). Signaling Pathways Involved in Vascular Smooth Muscle Cell Calcification during Hyperphosphatemia. *Cell. Mol. Life Sci.* 76, 2077–2091. doi:10.1007/s00018-019-03054-z

Vulin, A. I., and Stanley, F. M. (2004). Oxidative Stress Activates the Plasminogen Activator Inhibitor Type 1 (PAI-1) Promoter through an AP-1 Response Element and Cooperates with Insulin for Additive Effects on PAI-1 Transcription. *J. Biol. Chem.* 279, 25172–25178. doi:10.1074/jbc.M403184200

Wang, Z.-H., Ren, W.-Y., Zhu, L., and Hu, L.-J. (2014). Plasminogen Activator Inhibitor-1 Regulates LPS Induced Inflammation in Rat Macrophages through Autophagy Activation. *Scientific World J.* 2014, 1. doi:10.1155/2014/189168

Woith, E., Fuhrmann, G., and Melzig, M. F. (2019). Extracellular Vesicles-Connecting Kingdoms. *Ijms* 20, 5695. doi:10.3390/ijms20225695

Yaker, L., Kamel, S., Ausseil, J., and Boullier, A. (2020). Effects of Chronic Kidney Disease and Uremic Toxins on Extracellular Vesicle Biology. *Toxins* 12, 811. doi:10.3390/toxins12120811

Yang, X., Song, X., Li, Z., Liu, N., Yan, Y., and Liu, B. (202110562). Crosstalk between Extracellular Vesicles and Autophagy in Cardiovascular Pathophysiology. *Pharmacol. Res.* 172, 105628. doi:10.1016/j.phrs.2021.105628

Ye, R. D., and Sun, L. (2015). Emerging Functions of Serum Amyloid A in Inflammation. *J. Leukoc. Biol.* 98, 923–929. doi:10.1189/jlb.3VMR0315-080R

Zhang, X., Chen, J., and Wang, S. (2017). Serum Amyloid A Induces a Vascular Smooth Muscle Cell Phenotype Switch through the P38 MAPK Signaling Pathway. *Biomed. Res. Int.* 2017, 1. doi:10.1155/2017/4941379

Zhao, L., Li, H., Wang, Y., Zheng, A., Cao, L., and Liu, J. (2019). Autophagy Deficiency Leads to Impaired Antioxidant Defense via P62-Foxo1/3 Axis. *Oxidative Med. Cell Longevity* 2019, 1–15. doi:10.1155/2019/2526314

Conflict of Interest: The authors declare that the research was conducted in the absence of any commercial or financial relationships that could be construed as a potential conflict of interest.

Publisher's Note: All claims expressed in this article are solely those of the authors and do not necessarily represent those of their affiliated organizations, or those of the publisher, the editors, and the reviewers. Any product that may be evaluated in this article, or claim that may be made by its manufacturer, is not guaranteed or endorsed by the publisher.

frontiers in Cell and Developmental Biology

REVIEW
published: 31 March 2022
doi: 10.3389/fcell.2022.860005

Cellular Chitchatting: Exploring the Role of Exosomes as Cardiovascular Risk Factors

Giulia Germena[1,2]*, *Laura Cecilia Zelarayán*[2,3] *and Rabea Hinkel*[1,2,4]*

[1]Laboratory Animal Science Unit, Leibniz-Institut für Primatenforschung, Deutsches Primatenzentrum GmbH, Göttingen, Germany, [2]DZHK (German Center for Cardiovascular Research), Partner Site Göttingen, Göttingen, Germany, [3]Institute of Pharmacology and Toxicology, University Medical Center Göttingen, Göttingen, Germany, [4]Institute for Animal Hygiene, Animal Welfare and Farm Animal Behaviour (ITTN), Stiftung Tierärztliche Hochschule Hannover, University of Veterinary Medicine, Hannover, Germany

Exosomes are small bi-lipid membranous vesicles (30–150 nm) containing different biological material such as proteins, lipids and nucleic acid. These small vesicles, inducing a cell to cell signaling pathway, are able to mediate multidirectional crosstalk to maintain homeostasis or modulate disease processes. With their various contents, exosomes sort and transfer specific information from their origin to a recipient cell, from a tissue or organ in the close proximity or at distance, generating an intra-inter tissue or organ communication. In the last decade exosomes have been identified in multiple organs and fluids under different pathological conditions. In particular, while the content and the abundance of exosome is now a diagnostic marker for cardiovascular diseases, their role in context-specific physiological and pathophysiological conditions in the cardiovascular system remains largely unknown. We summarize here the current knowledge on the role of exosomes as mediators of cardiovascular diseases in several pathophysiological conditions such as atherosclerosis and diabetes. In addition, we describe evidence of intercellular connection among multiple cell type (cardiac, vasculature, immune cells) as well as the challenge of their *in vivo* analysis.

Keywords: exosomes, diabetes, exercice, atherosclerosis, cardiovascular disease

OPEN ACCESS

Edited by:
Xiaoheng Liu,
Sichuan University, China

Reviewed by:
Jafar Rezaie,
Urmia University of Medical Sciences, Iran
Marc Poirot,
Institut National de la Santé et de la Recherche Médicale, France

***Correspondence:**
Giulia Germena
ggermena@dpz.eu
Rabea Hinkel
rhinkel@dpz.eu

Specialty section:
This article was submitted to Molecular and Cellular Pathology, a section of the journal Frontiers in Cell and Developmental Biology

Received: *22 January 2022*
Accepted: *16 March 2022*
Published: *31 March 2022*

Citation:
Germena G, Zelarayán LC and Hinkel R (2022) Cellular Chitchatting: Exploring the Role of Exosomes as Cardiovascular Risk Factors. Front. Cell Dev. Biol. 10:860005. doi: 10.3389/fcell.2022.860005

INTRODUCTION

Extracellular vesicles (EVs), with their size range of 30–2000 nm in diameter, are a heterogeneous group of secreted bilayer lipid particles originated from the endocytic pathway (Raposo and Stoorvogel, 2013).

In response to stimulation, EVs are secreted in the extracellular milieu by several cell types. They can transport a variety of substances including proteins, mRNAs, miRNAs, DNA and lipids, that can act as autocrine or paracrine factors but can also be shuttled to other cell types. EVs are classified as exosomes (Exos), microvesicles (MVs) and apoptotic bodies on the basis of their biogenesis and size. EVs are extensively described elsewhere (Gurung et al., 2021) and for the purpose of this review, only a general description is provided.

Within the extracellular vesicles groups, exosomes are 30–300 nm heterogeneous vesicles generated by the endocytic pathway in a three-step process including: 1-intracellular invagination of endosomes generating intraluminal vesicles (ILVs), 2-formation of multivesicular bodies (MVBs) and 3-released by fusion with the plasma membrane (Kowal et al., 2014).

MVBs (or late endosomes) are formed by the maturation of early endosomes and their formation involves the activation of the endosomal sorting complex required for transport (ESCRT) machinery, that drives membrane budding by recognizing and sequestering ubiquitinated proteins. Even though ESCRT proteins appear to be essential for MVEs generation, a second ESCRT-independent pathway has been suggested *via* a tetraspanin-dependent mechanism in which CD81, CD9 and CD63 are key players (Stuffers et al., 2009) (Van-Niel et al., 2011). Tetraspanins are integral membrane proteins in exosomes. Through their interaction with other transmembrane and cytosolic proteins as well as lipids, tetraspanins participate in protein loading into exosomes (Villarroya-Beltri et al., 2014).

Once generated, MVBs could undergoes different fates. While some MVBs can fuse with lysosomes to be degraded overlapping with the autophagy pathway, the presence of specific receptors, such as EGFR, direct the MVBs through the recycling endosome allowing the recycle of the receptor back to the plasma membrane. Another fates for the MVBs is the release into the extracellular compartment *via* the secretory pathway (Baixauli et al., 2014) (Fader and Colombo, 2009) (Hassanpour et al., 2020).

Both pathways are regulated by small GTPases of the Rab family. For example, while Rab7 has been involved in the degradation pathway, Rab27 and Rab11 regulate the MVBs fusion to the plasma membrane (Ostrowski et al., 2010).

In contrast to the above described, particles with a size ranging between 100 and 1000 nm are categorized as microvesicles. While exosomes are generated by inward budding, microvesicles are formed by outward budding of cytoplasmic protrusions followed by extracellular membrane scission. In addition, the biosynthesis of MVs is dependent on the interaction between phospholipids and protein of the cytoskeleton (Clancy et al., 2021).

The larger subtype of EVs, with a size up to 5 μm are the apoptotic bodies. The formation of these particles is associated with programmed cell death and the process is characterized by plasma membrane blebbing (more information regarding this process are available in (Raposo and Stoorvogel, 2013).

The size variety of EVs, the heterogeneity and the lack of well identified markers, as well as of standard isolation protocols generated some confusion and debate in the exosome research field. In order to shed some light, in 2014, the International Society for Extracellular Vesicles provided biochemical, biophysical and functional guidelines that should be applied in EVs biology (Lotvall et al., 2014). With the same objective, in the last years, multiple consortiums (EV-TRACK Consortium–2017) and databases (Vesiclepedia–Exocarta) were generated. Given the increasing popularity of exosomes, extensive efforts have been done to improve their isolation methods. Ultracentrifugation, filtration and immunoaffinity isolation are only some examples of the possible isolation methods available for EVs isolation. Although no EV isolation method yet exists that can be considered as a gold standard, since residual proteins and/or lipoproteins remains problematic, differential centrifugation has long been regarded as the gold standard technique (Sluijter et al., 2018).

As above mentioned, exosomes are defined by their size and their specific endosome associated protein contents. However, isolation methods based on ultracentrifugation separation rely on a pure size dependent isolation, without taking in account the intracellular origin of the vesicles. In 2016, the group of Kowal (Kowal et al., 2016) demonstrated that the presence of specific tetraspanins (CD9, CD63 and CD81) characterizes endosome-derived vesicles (exosome) and a couple of years later, in 2019, Jeppesen et al. performed a deep re-assessment of exosome composition generating the background for a clearer understanding of small EVs heterogeneity (Jeppesen et al., 2019). Nevertheless, before these milestone studies, only few reports studying the role of EVs in multiple pathology clearly demonstrated the tetraspanins positivity of the ultracentrifuge derived small vesicles EVs. Since current isolation protocols result in an enrichment of vesicles population rather than their complete purification, it is more accurate to refer to purified vesicle as EVs (Sluijter et al., 2018). For these reasons, in this review we will use the general nomenclature small EVs even if differentially state in the original paper.

In recent years, the identification of the cargo of small EVs has been under investigation.

Two main classes of proteins can be distinguished: 1- proteins that constitute small EVs and are independent from the cells of origin; 2- proteins that are dependent on the cell type and on the cellular pathophysiological condition (He C. et al., 2018).

Typical proteins found in small EVs (most frequently identified on Exocarta) are tetraspanins, proteins involved in membrane transport and fusion (annexins and Rab-GTPases), components of the ESCRT machinery (Alix and TSG101) and proteins facilitating protein folding (Hsp70 and Hsp90). In addition to these constitutively proteins, small EVs transport biomolecules that specifically characterize the pathophysiological status of the producing cells were found (Chen et al., 2016) (Shepherd et al., 2021) (Rezaie et al., 2021).

The specific exosome content could be used as markers for multiple pathologies but in the last year small EVs have been shown to play a role in the development of atherosclerosis and diabetic cardiovascular pathology.

In this review we will provide insight into small EVs as mediators of cardiovascular diseases and we will describe their fundamental role as intercellular connection among multiple cell type (cardiac, vasculature, immune cells).

THE INTRACARDIAC "WHISPER GAME"

Tight balance of intra-intercellular communication is necessary to maintain heart integrity [for more information please refer to review (Martins-Marques et al., 2021)].

Many pathological stimuli are affecting cell types other than cardiomyocyte, which ultimately induces a phenotypic response in cardiomyocyte (Tirziu et al., 2010). For example, fibroblasts play a key role in regulating multiple functions and activity of the cellular component of the heart compartment. In fact, cardiac fibroblasts modulate cardiomyocyte hypertrophy, contractility and electrical behavior (LaFramboise et al., 2007).

In this context, the evaluation of the miRNA content of small EVs derived from cardiac fibroblast revealed high abundance of

many miRNA passenger strands, which normally undergo intracellular degradation, in particular miRNA21–3p (miRNA-21*). This miRNA induces cardiomyocyte hypertrophy by targeting multiple pro-hypertrophic gene expression (Bang et al., 2014).

Fibroblast activation with Angiotensin II (AngII) or TGFβ induces the release of small EVs that, once internalized into endothelial cells or cardiomyocytes, are able to strongly modulate cell behavior (Ranjan et al., 2021).

For example, endothelial cells treated with small EVs derived from TGFβ activated fibroblast displayed impaired functions, characterized by decreased tube formation and cell migration (effects mediated by miRNA200a-3p) (Ranjan et al., 2021). This effect could be part of a signaling cascade where endothelial cells, under stress conditions such as high glucose, activate fibroblast through TGF-β1 enriched small EVs (Zhang et al., 2021) and this activation leads to the release of small EVs loaded with miRNA200a-3p that impairs endothelial functions.

As aforementioned, fibroblasts do not exclusively communicate with endothelial cells but are also able to modulate cardiomyocyte functions.

AngII, a well know hypertrophic stimulus, enhances fibroblast small EVs release through the activation of the AngII receptor types I and II. Treatment of cardiomyocytes with these small EVs upregulates RAS *via* MAPKs and Akt inducing hypertrophy (Lyu et al., 2015).

A similar effect has been shown with small EVs derived from fibroblast treated with TGFβ. These small EVs are able to induce a heart failure phenotype in cardiomyocyte indicating that exosome signaling from fibroblast contributes to disease progression in heart failure (Basma et al., 2019). This communication between fibroblast and cardiomyocyte is not unidirectional. It has been shown that cardiomyocyte derived small EVs are able to induce fibroblast proliferation and differentiation into myofibroblast by transferring miRNA208a (Yang et al., 2018). Moreover, circulating exosomes induced by cardiac pressure overload contain functional angiotensin II type 1 receptors (AT1R). Exogenously administered AT1R-enriched exosomes target cardiomyocytes, skeletal myocytes, and mesenteric resistance vessels and are sufficient to confer blood pressure responsiveness to angiotensin II infusion in AT1R knockout mice (Pironti et al., 2015).

For the purpose of illustration, we can compare these multiple interactions to a symphonic orchestra. As in an orchestra, all the elements need to be properly connected and working in synchro to create a perfect harmony; that, in our case, is a functional heart. When external factors influence one single component, all the others are also affected. In the next chapter we will analyze how small EVs connect different cellular type in multiple cardiovascular diseases.

TRICK AND TREAT: SMALL EVS IN DIABETES

Diabetes is a complex disorder characterized by a persistent elevated blood glucose level from insulin deficiency or resistance that leads to the development of life-threatening complications. On the basis of the pathophysiology, it is possible to classify diabetes in different subtypes (Wagner et al., 2021). For the purpose of our review, we will mainly focus on Type 1 and Type 2 diabetes.

Type I Diabetes

Type 1 diabetes mellitus (T1DM) is an autoimmune disorder characterized by beta-cell dysfunction leading to insulin deficiency. In the last years, small EVs have been associated to T1DM, in particular in the onset and progression of the disease. Interestingly, it has been shown that small EVs derived from pancreatic islets (human and rat) and mouse insulinoma present disease-specific content such as the island antigens glutamate decarboxylase (GAD65) and islet-associated protein (IA-2) (Sheng et al., 2011), (Cianciaruso et al., 2017). These proteins are able to activate antigen presentation by dendritic cells leading to T-cell activation and the initiation of the autoimmune response (Cianciaruso et al., 2017). If administered *in vivo*, these small EVs are able to induce insulitis in non-obese diabetes resistant mouse models indicating their autoimmunity potential to trigger islets inflammation. Together with auto antigens like GAD65, small EVs derived from pancreatic islets contain distinctive miRNA, such as miRNA29b. This specific miRNA modulates innate and antigen specific immune response by stimulating IFNα, IL-10 and IL-6 secretion (Salama et al., 2014). Other miRNAs playing a role in promoting immune cells recruitment and exacerbating beta cell apoptosis are miRNA142–3p/5p and miRNA155. These miRNAs promote the expression, exclusively in beta cells, of specific chemokine genes such as *Ccl2*, *Ccl7* and *Cxcl10*. Intriguingly, the sources of these microRNAs are T-lymphocyte small EVs (Guay et al., 2019). These observations pointed out the importance of small EVs transfer as a communication mode between immune and insulin-secreting cells. While the aforementioned studies were performed *in vitro* or in murine model, the analysis of small EVs derived from diabetic patients confirmed the presence of deregulated miRNA involved in T1DM progression. These results demonstrate the feasibility of using small EVs derived miRNA signature as clinical applicable biomarkers of T1DM (Guay et al., 2019). Currently, positivity for multiple autoantibodies is the only available biomarker for T1DM (Verge et al., 1996) (Bingley et al., 2003). Recently, the level of miRNA21–5p contained in serum derived small EVs has been proposed as a promising future T1DM biomarker (Lakhter et al., 2018). Unfortunately, due to its key role in regulating vital pathways, miRNA21 has been found frequently deregulated in multiple pathological conditions, from cancer to cardiovascular diseases (Jenike and Halushka, 2021). In this view, miRNA21 could be seen as a potential therapeutic target instead of a biomarker. In this regard, current therapeutic strategies are mainly focusing on attenuating symptoms *via* damping the inflammation and supporting beta cell functions. Treatments with stem cells used to regenerate beta cells have already been proposed, however, next generation therapeutic tools focus now on the potentiality of small EVs delivery (Babaei and Rezaie, 2021). In this context, the comparison of the regenerative effects of mesenchymal stem cells

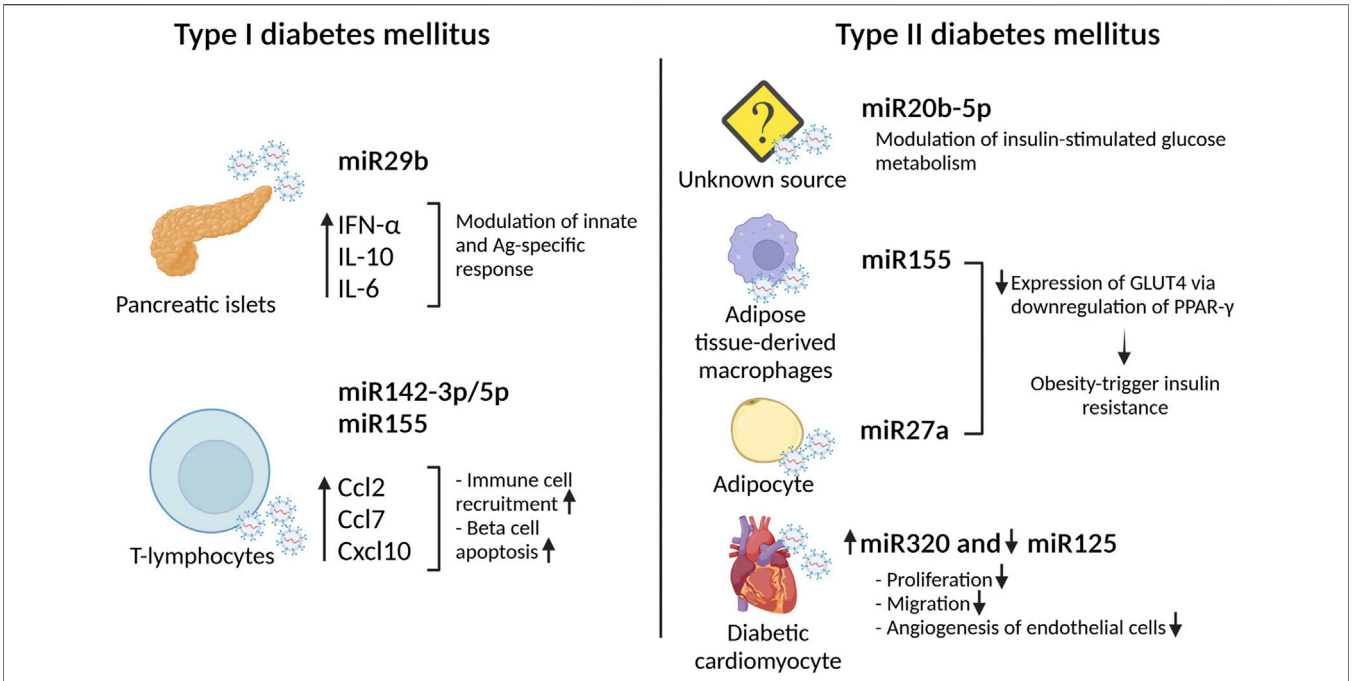

FIGURE 1 | Small EVs miRNA effect in type I and type II diabetes mellitus. Effects of different small EVs loaded with specific miRNA in the development of diabetes.

(MSCs) derived small EVs and MSCs themselves has been tested in a T1DM rat model (Sabry et al., 2020). Serum glucose and plasma insulin level were used as read out for the therapeutic effects and pancreatic tissue regeneration was evaluated *via* histology and expression of specific beta cells genes. In both cases, MSCs derived small EVs showed superior results than MSCs themselves. In a murine streptozocin (STZ)-induced T1DM model, the infusion of exosomes derived from adipose tissue-derived MSCs leads to an increase of pancreatic islet and an increase in regulatory T-cell population. In particular, an amelioration of autoimmune reaction is sufficient to induce an increase in islet and the maintenance of blood glucose level (Nojehdehi et al., 2018). Taken together, small EVs could be a potent tool to modulate immune response and thus improve islet functionality and transplantation (Wen et al., 2016) (**Figure 1**)

Type 2 Diabetes

Type 2 diabetes (T2DM) is a metabolic disease, occurring mainly in individual over age 45, characterized by insulin resistance largely associated with adiposity and/or by impaired insulin secretion (Jeong et al., 2010). It has been shown that diabetic patients present a greater number of circulating small EVs when compared to normal glucose healthy donor. These specific EVs are mainly generated in response to insulin resistance. Once released, these insulin related EVs, are predominately up-taken by leukocyte and mediate the release of inflammatory cytokine inducing an inflammatory status (Freeman et al., 2018). Another factor playing a pivotal role in T2DM onset and progression is obesity. Also in this case, small EVs may play a role. Indeed, enrichment of specific miRNA has been observed in plasma EVs isolated from obese mice. In addition, administration of these specific EVs in lean mice was able to induce glucose intolerance and insulin resistance, indicating the strict bound between obesity induced release of small EVs and T2DM onset (Castano et al., 2018). From a molecular point of view, *via* binding to the insulin receptor, insulin induces a signaling cascade that involves Akt phosphorylation on position S473 and in turn GLUT4 transporter translocation from the cytosol to the plasma membrane allowing glucose uptake in skeletal muscle cells. Small EVs circulating in T2DM patient's blood present high levels of miRNA20b-5p that modulate insulin-stimulated glucose metabolism by regulating Akt signaling pathway (Katayama et al., 2019). While the origins of the aforementioned EVs are yet unknown, it has been demonstrated that EVs containing miRNA155 or miRNA27a, originated from adipose tissue-derived macrophages and adipocytes respectively, are able to decrease the expression of GLUT4 *via* downregulation of PPARγ playing thus a role in the development of obesity-triggered insulin resistance (Ying et al., 2017) (Yu et al., 2018) **Figure 1**.

Multiple pathological conditions characterizing diabetes such as high levels of systemic inflammatory cytokines and chronic hyperglycemia are consider risk factors for cardiac damage. In particular, the deleterious effect of persistent high glucose levels leads to cardiac dysfunction known as diabetic cardiomyopathy (DCM). In this context, diabetic hearts display defective angiogenesis. Co-culture experiments of cardiac endothelial cells with diabetic cardiomyocyte provided evidence that the cardiomyocytes modulate specific endothelial functions such as proliferation inhibition (Wang et al., 2014). Further analysis demonstrated that small EVs derived from diabetic cardiomyocyte inhibit proliferation, migration and angiogenesis capabilities of endothelial cells (Wang et al.,

2014). In particular, these EVs presented high levels of miRNA320 and low levels of miRNA125 in comparison to EVs derived from non-diabetic cardiomyocytes *in vivo*. Downregulation of miRNA320 targets including IGF-1, Hsp20 and Ets2 inhibited endothelial migration and tube formation indicating that EVs derived from cardiomyocytes exert an anti-angiogenic function upon T2DM (Wang et al., 2009). Interestingly, one of the miRNA320 targets, Hsp20 has been involved in the development of DCM. Cardiac specific Hsp20 overexpression induces the release of EVs able to attenuate cardiac disfunctions. Of importance, these EVs present higher levels of p-Akt, Survivin, and SOD1, molecules able to promote endothelial cell proliferation and to protect against cardiac adverse remodeling (Wang et al., 2016). Microvascular rarefaction guided by endothelial dysfunction is one of the major signs of DCM, thus, the maintenance of functional/vital endothelial compartment also leads to cardiomyocyte survival and efficient cardiac functions (Kibel et al., 2017) (**Figure 1**).

Relevance of Exercise for EVs in T2DM

One interesting preventive/therapeutic approach for T2DM is the implementation of a regular physical activity. In fact, multiple studies show that diabetic cardiovascular complications benefit from exercise. Endurance exercise induces the release, *via* small EVs, of factors named "exerkines" able to potentially counteract diabetic effects and thus representing a potential therapeutic approach to the treatment of obesity and associated disorders (Safdar and Tarnopolsky, 2018). In particular, physical activity is associated with a significant increase of small EVs circulating in the blood of healthy individuals subjected to an exercise protocol (Fruhbeis et al., 2015). The content of these EVs, including plasma based circulating miRNA, has been involved in angiogenesis, inflammation, cardiac contractility and hypoxia/ischemia adaptation (Baggish et al., 2011). One of the first studies analyzing the effect of EVs in a diabetic context demonstrated that in response to exercise, the release in the heart tissue and serum of small EVs containing specific miRNA (miRNA29b and miRNA455) is able to downregulate MMP9 expression in the heart, thus mitigating cardiac fibrosis. These results lead to the hypothesis that exercise mediated release of small EVs loaded with MMP9 silencing miRNA could represent a potential therapeutic strategy to treat diabetic patients presenting cardiovascular dysfunctions (Chaturvedi et al., 2015). A more recent study demonstrates that, in mice, high intensity interval training induces an increase of circulating EVs released by the muscles, with high expression of miRNA133a and miRNA133b. These miRNAs, targeting the insulin downstream transcription factor FoxO1, are able to induce metabolic effects in the liver such as a reduction in gluconeogenesis. Overall, the iv injection in sedentary mice with these EVs improves glucose tolerance and insulin sensitivity, indicating an improvement of the metabolic homeostasis (Castano et al., 2020). Not only these "exercised" small EVs are able to ameliorate a metabolic impairment, but it has also been shown that small EVs isolated from the plasma of exercised humans or rats, exert a protective effect in an *in vivo* model of myocardial ischemia/reperfusion injury. In particular, these effects were attributed to miRNA342–5p and its antiapoptotic effects in cardiomyocytes. The study of the origin of the exosomal miRNA342–5p highlighted the importance of aortic endothelial cells. In particular, *in vitro* studies determined that fluid shear stress induces miRNA342–5p expression and its subsequent release from endothelial cells. These data indicate that the increase blood flow/shear stress triggered by exercise could potentially confer salutary cardioprotective effects by inducing the generation of exerkines (Hou et al., 2019). Another of the beneficial effects of exercise is the promotion of angiogenesis (Laufs et al., 2004). In this view, it has been shown that exercise could induce the release from the liver of small EVs loaded with miRNA122–5p that promote an increase of capillary density in skeletal muscles (Lou et al., 2021). On the basis of what we describe here, multiple organs benefit from exercise and these effects are modulated by small EVs release (**Figure 2**). For a comprehensive analysis of the role of endurance exercise and small EVs in the treatment of metabolic disorder we suggest the following exhaustive reviews (Safdar et al., 2016) (Safdar and Tarnopolsky, 2018).

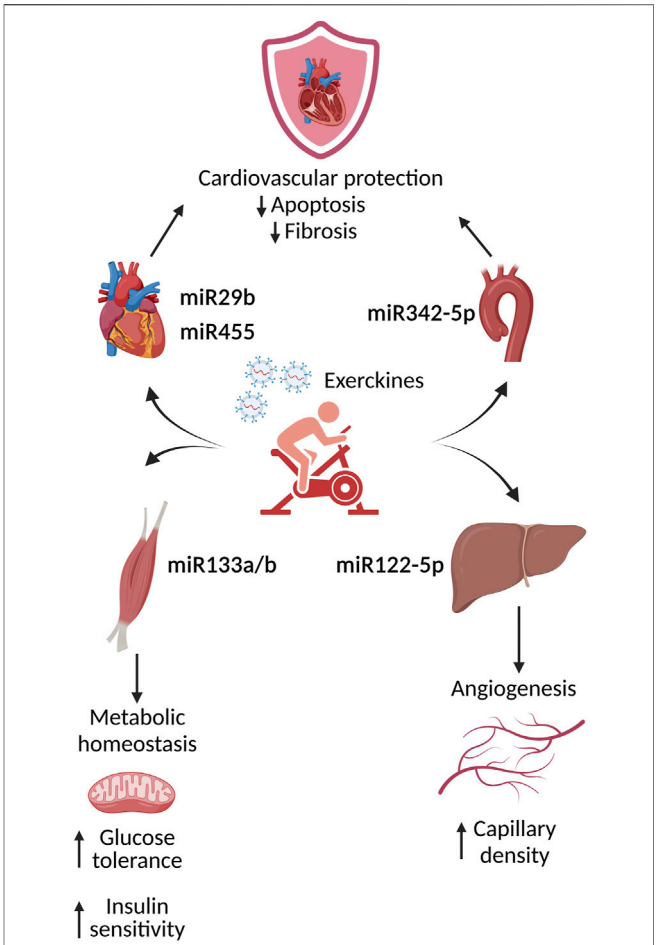

FIGURE 2 | Physiological effects of the induced exerkines upon exercise. During exercise, multiple organs release exosome containing factors, such as miRNA, called exerkines. These molecules are able to activate intra-intercellular pathways leading to an amelioration and protection of the cardiovascular compartment.

SMALL EVS IN ATHEROSCLEROSIS: THE BLUEPRINT OF THE WALL

Atherosclerosis is a complex multifactorial degenerative disease involving metabolism, the cardiovascular and the immune systems. Endothelial and immune cells activation due to the exposure to cardiovascular risk factor such as obesity, smoking and hypertension, and the subsequent foam cells accumulation, are events required for the formation of the atherosclerotic plaque (Mudau et al., 2012). Exchange of information between these cellular types is a fundamental driver of the pathology (Roy et al., 2021). In support of this, in the last years, small EVs have been shown to be involved in multiple steps of pathological progression of atherogenesis.

Endothelial cell inflammation is the initial step driving the cascade of events leading to the atherosclerotic plaques. After endothelial cells activation, cells from the immune compartment, especially monocytes, are recruited and adhere to the arterial lumen where they form the plaque (for a comprehensive analysis regarding the role of macrophages in atherogenesis please refer to (Farahi et al., 2021). Small EVs released by monocytes stressed by oxidized lipoprotein (oxLDL) are able to induce pro adhesion molecules, the NO pathway and to exacerbate vascular inflammation (Madrigal-Matute et al., 2015), (Mastronardi et al., 2011), (Tang et al., 2016).

The tight interconnection between endothelial cells and macrophages has been investigated. While small EVs derived from oxLDL-treated endothelial cells promote M2 macrophage polarization, (Huang et al., 2018), small EVs released from macrophages negatively regulate endothelial cell migration stimulating the trafficking of internalized β1 integrin to the lysosomal compartment resulting in proteolytic degradation (Lee et al., 2014). A peculiarity of small EVs derived from atherogenic macrophages is the capability of the transfer of specific miRNA, e.g., miRNA146a, and thus inducing an atherogenic phenotype. In particular, the treatment of naïve macrophages with small EVs derived from atherogenic macrophages is able to inhibit their migration at the same extend as the donor macrophages (Nguyen et al., 2018). A follow up study on exosomal miRNA146a secreted by oxLDL-treated macrophages demonstrated the role of this specific miRNA in promoting ROS and NETs release *via* targeting SOD2. In particular, miRNA146a induces oxidative stress promoting NETs formation and leading to atherosclerosis progression (Zhang et al., 2019). Furthermore, it has been shown that small EVs produced by polarized (IL4) bone marrow-derived macrophages contain anti-inflammatory miRNAs (miRNA99a/146b/378a) able to suppress inflammation and foster M2 polarization in recipient macrophages. Repeated infusions of these particular small EVs into ApoE$^{-/-}$mice [the most widely used preclinical model of atherosclerosis (Jawien, 2012)] fed a Western diet lead to a reduction in necrotic lesion areas. This collectively stabilizes atheroma indicating that small EVs produced by cultured macrophages have an anti-inflammatory effect. Furthermore, polarized macrophages produce exosomes with an enhanced capacity to resolve inflammation *via* anti-inflammatory miRNA cargo, including in atherosclerotic lesions (Bouchareychas et al., 2020) (**Figure 3**).

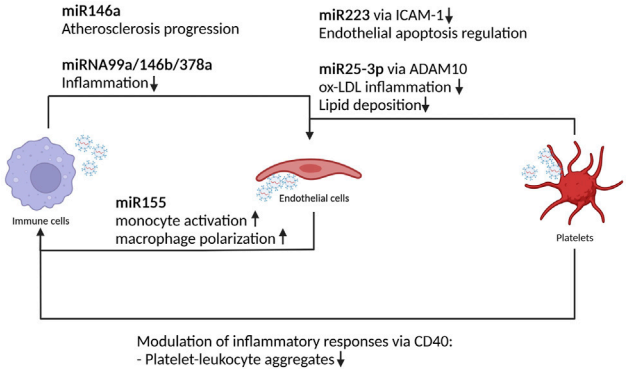

FIGURE 3 | Platelets, immune and endothelial cells derived EVs miRNA effect in atherosclerosis. Schematic representation of the crosstalk between immune cells, EC and platelets driving atherosclerosis pathogenesis. The exchange of miRNA modulates inflammatory response and endothelial activation status leading to atherosclerosis onset and progression.

As aforementioned, small EVs derived from cells of the immune compartment are able to modulate the activation status of endothelial cells. Is this true also in the other direction? It has been shown that small EVs released from TNFα stimulated endothelial cells are loaded with a cocktail of inflammatory markers, chemokines, and cytokines (such as ICAM-1, CCL-2, IL-6, IL-8, CXCL-10, CCL-5, and TNF-α) which, when transferred to monocyte are able to induce reprogramming toward a pro- or anti-inflammatory phenotypes (Hosseinkhani et al., 2018). Another study demonstrated that macrophage treatment with small EVs derived from ox-LDL stimulated endothelial cells are able to modulate monocyte/macrophage phenotype. In particular, these small EVs are rich of miRNA155. This particular miRNA stimulates monocyte activation and promotes macrophage polarization towards proinflammatory M1 macrophages. The authors were able to reverse this phenotype taking advantage of the properties of the Kruppel like factor 2 (KLF2) (He S. et al., 2018). KLF2 is a shear stress induced transcriptional factor with protecting effects against atherosclerosis. In particular, KLF2 modulates the expression of different miRNA cluster (such as the miRNA143/145). *In vivo*, small EVs from KLF2-expressing endothelial cells reduced atherosclerotic lesion formation in the aorta of ApoE $^{-/-}$ mice (Hergenreider et al., 2012). They also suppressed monocyte activation by enhancing immunomodulatory responses and diminishing proinflammatory responses by decreasing proinflammatory M1 macrophages and increasing anti-inflammatory M2 macrophages (He S. et al., 2018).

In an already complex cellular network leading to plaque formation, the role of a new player has been recently pinpointed, namely the platelets (Hundelshausen and Lievens, 2011). Platelet-derived small EVs modulate multiple endothelial and monocyte functions (Barry et al., 1998). In particular, small EVs from thrombin activated platelet modulate inflammatory

immune responses *via* cluster of differentiation 40 (CD40) ligands (Kaneider et al., 2003). Platelet CD40 mediates the formation of platelet-leukocyte aggregates and, in absence of CD40, leukocytes are less prone to adhere to thrombi. In an $ApoE^{-/-}$ mouse model, plaques of mice receiving CD40-deficient platelets are less advanced and contain less immune cell infiltration (Gerdes et al., 2016). Thrombin activated platelet are enriched with miRNA223 that inhibits ICAM-1 expression during inflammation and regulates endothelial apoptosis (Li et al., 2017). Another miRNA involved in atherosclerosis and highly expressed in platelet small EVs is miRNAR25–3p that, when acting on the ADAM10 metalloprotease, inhibits ox-LDL inflammation and lipid deposition (Yao et al., 2019). **Figure 3**.

Through an organ culture approach, the *in vitro* analysis of the inflammatory process occurring in human atherosclerosis demonstrated that the monocyte-platelet interaction is driving the composition of specific small EVs. In particular, the platelet's activation status plays a pivotal role in the small EVs pro inflammatory content. Inhibition of platelets activation leads to a milder inflammatory phenotype, suggesting a synergistic role of monocyte/platelet aggregates in releasing functional EVs (Oggero et al., 2021).

SUMMARY/CONCLUSION

Taken together, we can conclude that the EVs mediated signaling adds a higher complexity to an already complex mechanism of direct cell-to-cell interaction, such as monocyte-endothelial cell. The discovery of small EVs is allowing to understand new types of cellular communication and at the same time could become a powerful tool for the development of new therapeutic approaches. Besides the therapeutic use of EVs in cardiovascular disease as a scavenger for e.g., miRNAs, they might also be suitable for novel biomarkers allowing for a precise and early disease diagnosis, as well as prognostic marker for the progression of the cardiovascular disease.

AUTHOR CONTRIBUTIONS

All authors listed have made a substantial, direct, and intellectual contribution to the work and approved it for publication.

FUNDING

This research was funded by Deutsche Sonderforschungsbereich (CRC) 1002 and the DZHK (German Center for Cardiovascular Research) to RH and LZ. In addition, RH received funding by the European Research Council (ERC.StG 758087). LZ received further funding by European Research Council, EURISE2020 and CRYSTAL3.

ACKNOWLEDGMENTS

We acknowledge Gabriela M. Lobo Vallejo for English language editing and Izzatullo Sobitov for the design of the figures using BioRender.com.

REFERENCES

Babaei, M., and Rezaie, J. (2021). Application of Stem Cell-Derived Exosomes in Ischemic Diseases: Opportunity and Limitations. *J. Transl Med.* 19 (1), 196. doi:10.1186/s12967-021-02863-w

Baggish, A. L., Hale, A., Weiner, R. B., Lewis, G. D., Systrom, D., Wang, F., et al. (2011). Dynamic Regulation of Circulating microRNA during Acute Exhaustive Exercise and Sustained Aerobic Exercise Training. *J. Physiol.* 589 (Pt 16), 3983–3994. doi:10.1113/jphysiol.2011.213363

Baixauli, F., Lã³pez-OtÃn, C., and Mittelbrunn, M. (2014). Exosomes and Autophagy: Coordinated Mechanisms for the Maintenance of Cellular Fitness. *Front. Immunol.* 5, 403. doi:10.3389/fimmu.2014.00403

Bang, C., Batkai, S., Dangwal, S., Gupta, S. K., Foinquinos, A., Holzmann, A., et al. (2014). Cardiac Fibroblast-Derived microRNA Passenger Strand-Enriched Exosomes Mediate Cardiomyocyte Hypertrophy. *J. Clin. Invest.* 124 (5), 2136–2146. doi:10.1172/JCI70577

Barry, O. P., Praticò, D., Savani, R. C., and FitzGerald, G. A. (1998). Modulation of Monocyte-Endothelial Cell Interactions by Platelet Microparticles. *J. Clin. Invest.* 102 (1), 136–144. doi:10.1172/JCI2592

Basma, H., Johanson, A. N., Dhar, K., Anderson, D., Qiu, F., Rennard, S., et al. (2019). TGF-β Induces a Heart Failure Phenotype via Fibroblasts Exosome Signaling. *Heliyon* 5 (10), e02633. doi:10.1016/j.heliyon.2019.e02633

Bingley, P. J., Bonifacio, E., and Mueller, P. W. (2003). Diabetes Antibody Standardization Program: First Assay Proficiency Evaluation. *Diabetes* 52 (5), 1128–1136. doi:10.2337/diabetes.52.5.1128

Bouchareychas, L., Duong, P., Covarrubias, S., Alsop, E., Phu, T. A., Chung, A., et al. (2020). Macrophage Exosomes Resolve Atherosclerosis by Regulating Hematopoiesis and Inflammation via MicroRNA Cargo. *Cel Rep.* 32 (2), 107881. doi:10.1016/j.celrep.2020.107881

Castaño, C., Kalko, S., Novials, A., and Párrizas, M. (2018). Obesity-associated Exosomal miRNAs Modulate Glucose and Lipid Metabolism in Mice. *Proc. Natl. Acad. Sci. U.S.A.* 115 (48), 12158–12163. doi:10.1073/pnas.1808855115

Castaño, C., Mirasierra, M., Vallejo, M., Novials, A., and Párrizas, M. (2020). Delivery of Muscle-Derived Exosomal miRNAs Induced by HIIT Improves Insulin Sensitivity through Down-Regulation of Hepatic FoxO1 in Mice. *Proc. Natl. Acad. Sci. U.S.A.* 117 (48), 30335–30343. doi:10.1073/pnas.2016112117

Chaturvedi, P., Kalani, A., Medina, I., Familtseva, A., and Tyagi, S. C. (2015). Cardiosome Mediated Regulation of MMP9 in Diabetic Heart: Role of Mir29b and Mir455 in Exercise. *J. Cel. Mol. Med.* 19 (9), 2153–2161. doi:10.1111/jcmm.12589

Chen, Q., Takada, R., Noda, C., Kobayashi, S., and Takada, S. (2016). Different Populations of Wnt-Containing Vesicles Are Individually Released from Polarized Epithelial Cells. *Sci. Rep.* 6, 35562. doi:10.1038/srep35562

Cianciaruso, C., Phelps, E. A., Pasquier, M., Hamelin, R., Demurtas, D., Alibashe Ahmed, M., et al. (2017). Primary Human and Rat β-Cells Release the Intracellular Autoantigens GAD65, IA-2, and Proinsulin in Exosomes Together with Cytokine-Induced Enhancers of Immunity. *Diabetes* 66 (2), 460–473. doi:10.2337/db16-0671

Clancy, J. W., Schmidtmann, M., and D'Souza-Schorey, C. (2021). The Ins and Outs of Microvesicles. *FASEB BioAdvances* 3 (6), 399–406. doi:10.1096/fba.2020-00127

Fader, C. M., and Colombo, M. I. (2009). Autophagy and Multivesicular Bodies: Two Closely Related Partners. *Cell Death Differ* 16 (1), 70–78. doi:10.1038/cdd.2008.168

Farahi, L., Sinha, S. K., and Lusis, A. J. (2021). Roles of Macrophages in Atherogenesis. *Front. Pharmacol.* 12, 785220. doi:10.3389/fphar.2021.785220

Freeman, D. W., Noren Hooten, N., Eitan, E., Green, J., Mode, N. A., Bodogai, M., et al. (2018). Altered Extracellular Vesicle Concentration, Cargo, and Function in Diabetes. *Diabetes* 67 (11), 2377–2388. doi:10.2337/db17-1308

Frühbeis, C., Helmig, S., Tug, S., Simon, P., and Krämer-Albers, E.-M. (2015). Physical Exercise Induces Rapid Release of Small Extracellular Vesicles into the Circulation. *J. Extracellular Vesicles* 4, 28239. doi:10.3402/jev.v4.28239

Gerdes, N., Seijkens, T., Lievens, D., Kuijpers, M. J. E., Winkels, H., Projahn, D., et al. (2016). Platelet CD40 Exacerbates Atherosclerosis by Transcellular Activation of Endothelial Cells and Leukocytes. *Atvb* 36 (3), 482–490. doi:10.1161/ATVBAHA.115.307074

Guay, C., Kruit, J. K., Rome, S., Menoud, V., Mulder, N. L., Jurdzinski, A., et al. (2019). Lymphocyte-Derived Exosomal MicroRNAs Promote Pancreatic β Cell Death and May Contribute to Type 1 Diabetes Development. *Cel Metab.* 29 (2), 348–361. doi:10.1016/j.cmet.2018.09.011

Gurung, S., Perocheau, D., Touramanidou, L., and Baruteau, J. (2021). The Exosome Journey: from Biogenesis to Uptake and Intracellular Signalling. *Cell Commun Signal* 19 (1), 47. doi:10.1186/s12964-021-00730-1

Hassanpour, M., Rezabakhsh, A., Rezaie, J., Nouri, M., and Rahbarghazi, R. (2020). Exosomal Cargos Modulate Autophagy in Recipient Cells via Different Signaling Pathways. *Cell Biosci* 10, 92. doi:10.1186/s13578-020-00455-7

He, C., Zheng, S., Luo, Y., and Wang, B. (2018). Exosome Theranostics: Biology and Translational Medicine. *Theranostics* 8 (1), 237–255. doi:10.7150/thno.21945

He, S., Wu, C., Xiao, J., Li, D., Sun, Z., and Li, M. (2018). Endothelial Extracellular Vesicles Modulate the Macrophage Phenotype: Potential Implications in Atherosclerosis. *Scand. J. Immunol.* 87 (4), e12648. doi:10.1111/sji.12648

Hergenreider, E., Heydt, S., Tréguer, K., Boettger, T., Horrevoets, A. J. G., Zeiher, A. M., et al. (2012). Atheroprotective Communication between Endothelial Cells and Smooth Muscle Cells through miRNAs. *Nat. Cel Biol* 14 (3), 249–256. doi:10.1038/ncb2441

Hosseinkhani, B., Kuypers, S., van den Akker, N. M. S., Molin, D. G. M., and Michiels, L. (2018). Extracellular Vesicles Work as a Functional Inflammatory Mediator between Vascular Endothelial Cells and Immune Cells. *Front. Immunol.* 9, 1789. doi:10.3389/fimmu.2018.01789

Hou, Z., Qin, X., Hu, Y., Zhang, X., Li, G., Wu, J., et al. (2019). Longterm Exercise-Derived Exosomal miR-342-5p. *Circ. Res.* 124 (9), 1386–1400. doi:10.1161/CIRCRESAHA.118.314635

Huang, C., Han, J., Wu, Y., Li, S., Wang, Q., Lin, W., et al. (2018). Exosomal MALAT1 Derived from Oxidized Low-Density Lipoprotein-Treated Endothelial Cells Promotes M2 Macrophage Polarization. *Mol. Med. Rep.* 18 (1), 509–515. doi:10.3892/mmr.2018.8982

Hundelshausen, P. v., and Lievens, D. (2011). Platelets in Atherosclerosis. *Thromb. Haemost.* 106 (5), 827–838. doi:10.1160/TH11-08-0592

Jawien, J. (2012). The Role of an Experimental Model of Atherosclerosis: apoE-Knockout Mice in Developing New Drugs against Atherogenesis. *Cpb* 13 (13), 2435–2439. doi:10.2174/138920101208062435

Jenike, A. E., and Halushka, M. K. (2021). miR-21: a Non-specific Biomarker of All Maladies. *Biomark Res.* 9 (1), 18. doi:10.1186/s40364-021-00272-1

Jeong, S. U., Kang, D. G., Lee, D. H., Lee, K. W., Lim, D.-M., Kim, B. J., et al. (2010). Clinical Characteristics of Type 2 Diabetes Patients According to Family History of Diabetes. *Korean Diabetes J.* 34 (4), 222–228. doi:10.4093/kdj.2010.34.4.222

Jeppesen, D. K., Fenix, A. M., Franklin, J. L., Higginbotham, J. N., Zhang, Q., Zimmerman, L. J., et al. (2019). Reassessment of Exosome Composition. *Cell* 177 (2), 428–445. doi:10.1016/j.cell.2019.02.029

Kaneider, N. C., Kaser, A., Tilg, H., Ricevuti, G., and Wiedermann, C. J. (2003). CD40 Ligand-dependent Maturation of Human Monocyte-Derived Dendritic Cells by Activated Platelets. *Int. J. Immunopathol Pharmacol.* 16 (3), 225–231. doi:10.1177/039463200301600307

Katayama, M., Wiklander, O. P. B., Fritz, T., Caidahl, K., El-Andaloussi, S., Zierath, J. R., et al. (2019). Circulating Exosomal miR-20b-5p Is Elevated in Type 2 Diabetes and Could Impair Insulin Action in Human Skeletal Muscle. *Diabetes* 68 (3), 515–526. doi:10.2337/db18-0470

Kibel, A., Selthofer-Relatic, K., Drenjancevic, I., Bacun, T., Bosnjak, I., Kibel, D., et al. (2017). Coronary Microvascular Dysfunction in Diabetes Mellitus. *J. Int. Med. Res.* 45 (6), 1901–1929. doi:10.1177/0300060516675504

Kowal, J., Arras, G., Colombo, M., Jouve, M., Morath, J. P., Primdal-Bengtson, B., et al. (2016). Proteomic Comparison Defines Novel Markers to Characterize Heterogeneous Populations of Extracellular Vesicle Subtypes. *Proc. Natl. Acad. Sci. U.S.A.* 113 (8), E968–E977. doi:10.1073/pnas.1521230113

Kowal, J., Tkach, M., and Théry, C. (2014). Biogenesis and Secretion of Exosomes. *Curr. Opin. Cel Biol.* 29, 116–125. doi:10.1016/j.ceb.2014.05.004

LaFramboise, W. A., Scalise, D., Stoodley, P., Graner, S. R., Guthrie, R. D., Magovern, J. A., et al. (2007). Cardiac Fibroblasts Influence Cardiomyocyte Phenotype *In Vitro*. *Am. J. Physiology-Cell Physiol.* 292 (5), C1799–C1808. doi:10.1152/ajpcell.00166.2006

Lakhter, A. J., Pratt, R. E., Moore, R. E., Doucette, K. K., Maier, B. F., DiMeglio, L. A., et al. (2018). Beta Cell Extracellular Vesicle miR-21-5p Cargo Is Increased in Response to Inflammatory Cytokines and Serves as a Biomarker of Type 1 Diabetes. *Diabetologia* 61 (5), 1124–1134. doi:10.1007/s00125-018-4559-5

Laufs, U., Werner, N., Link, A., Endres, M., Wassmann, S., Jürgens, K., et al. (2004). Physical Training Increases Endothelial Progenitor Cells, Inhibits Neointima Formation, and Enhances Angiogenesis. *Circulation* 109 (2), 220–226. doi:10.1161/01.CIR.0000109141.48980.37

Lee, H. D., Kim, Y. H., and Kim, D.-S. (2014). Exosomes Derived from Human Macrophages Suppress Endothelial Cell Migration by Controlling Integrin Trafficking. *Eur. J. Immunol.* 44 (4), 1156–1169. doi:10.1002/eji.201343660

Li, J., Tan, M., Xiang, Q., Zhou, Z., and Yan, H. (2017). Thrombin-activated Platelet-Derived Exosomes Regulate Endothelial Cell Expression of ICAM-1 via microRNA-223 during the Thrombosis-Inflammation Response. *Thromb. Res.* 154, 96–105. doi:10.1016/j.thromres.2017.04.016

Lötvall, J., Hill, A. F., Hochberg, F., Buzás, E. I., Di Vizio, D., Gardiner, C., et al. (2014). Minimal Experimental Requirements for Definition of Extracellular Vesicles and Their Functions: a Position Statement from the International Society for Extracellular Vesicles. *J. Extracellular Vesicles* 3, 26913. doi:10.3402/jev.v3.26913

Lou, J., Wu, J., Feng, M., Dang, X., Wu, G., Yang, H., et al. (2021). Exercise Promotes Angiogenesis by Enhancing Endothelial Cell Fatty Acid Utilization via Liver-Derived Extracellular Vesicle miR-122-5p. *J. Sport Health Sci.* doi:10.1016/j.jshs.2021.09.009

Lyu, L., Wang, H., Li, B., Qin, Q., Qi, L., Nagarkatti, M., et al. (2015). A Critical Role of Cardiac Fibroblast-Derived Exosomes in Activating Renin Angiotensin System in Cardiomyocytes. *J. Mol. Cell Cardiol.* 89 (Pt B), 268–279. doi:10.1016/j.yjmcc.2015.10.022

Madrigal-Matute, J., Fernandez-Garcia, C.-E., Blanco-Colio, L. M., Burillo, E., Fortuño, A., Martinez-Pinna, R., et al. (2015). Thioredoxin-1/peroxiredoxin-1 as Sensors of Oxidative Stress Mediated by NADPH Oxidase Activity in Atherosclerosis. *Free Radic. Biol. Med.* 86, 352–361. doi:10.1016/j.freeradbiomed.2015.06.001

Martins-Marques, T., Hausenloy, D. J., Sluijter, J. P. G., Leybaert, L., and Girao, H. (2021). Intercellular Communication in the Heart: Therapeutic Opportunities for Cardiac Ischemia. *Trends Mol. Med.* 27 (3), 248–262. doi:10.1016/j.molmed.2020.10.002

Mastronardi, M. L., Mostefai, H. A., Soleti, R., Agouni, A., Martínez, M. C., and Andriantsitohaina, R. (2011). Microparticles from Apoptotic Monocytes Enhance Nitrosative Stress in Human Endothelial Cells. *Fundam. Clin. Pharmacol.* 25 (6), 653–660. doi:10.1111/j.1472-8206.2010.00898.x

Mudau, M., Genis, A., Lochner, A., and Strijdom, H. (2012). Endothelial Dysfunction : the Early Predictor of Atherosclerosis. *Cardiovasc. J. Africa* 23 (4), 222–231. doi:10.5830/CVJA-2011-068

Nguyen, M.-A., Karunakaran, D., Geoffrion, M., Cheng, H. S., Tandoc, K., Perisic Matic, L., et al. (2018). Extracellular Vesicles Secreted by Atherogenic Macrophages Transfer MicroRNA to Inhibit Cell Migration. *Atvb* 38 (1), 49–63. doi:10.1161/ATVBAHA.117.309795

Nojehdehi, S., Soudi, S., Hesampour, A., Rasouli, S., Soleimani, M., and Hashemi, S. M. (2018). Immunomodulatory Effects of Mesenchymal Stem Cell-Derived Exosomes on Experimental Type-1 Autoimmune Diabetes. *J. Cel Biochem* 119 (11), 9433–9443. doi:10.1002/jcb.27260

Oggero, S., Gaetano, M., Marcone, S., Fitzsimons, S., Pinto, A. L., Ikramova, D., et al. (2021). Extracellular Vesicles from Monocyte/platelet Aggregates Modulate Human Atherosclerotic Plaque Reactivity. *J. Extracellular Vesicles* 10 (6), 12084. doi:10.1002/jev2.12084

Ostrowski, M., Carmo, N. B., Krumeich, S., Fanget, I., Raposo, G., Savina, A., et al. (2010). Rab27a and Rab27b Control Different Steps of the Exosome Secretion Pathway. *Nat. Cel Biol* 12 (1), 19–30. doi:10.1038/ncb2000

Pironti, G., Strachan, R. T., Abraham, D., Mon-Wei Yu, S., Chen, M., Chen, W., et al. (2015). Circulating Exosomes Induced by Cardiac Pressure Overload Contain Functional Angiotensin II Type 1 Receptors. *Circulation* 131 (24), 2120–2130. doi:10.1161/CIRCULATIONAHA.115.015687

Ranjan, P., Kumari, R., Goswami, S. K., Li, J., Pal, H., Suleiman, Z., et al. (2021). Myofibroblast-Derived Exosome Induce Cardiac Endothelial Cell Dysfunction. *Front. Cardiovasc. Med.* 8, 676267. doi:10.3389/fcvm.2021.676267

Raposo, G., and Stoorvogel, W. (2013). Extracellular Vesicles: Exosomes, Microvesicles, and Friends. *J. Cel Biol* 200 (4), 373–383. doi:10.1083/jcb.201211138

Rezaie, J., Aslan, C., Ahmadi, M., Zolbanin, N. M., Kashanchi, F., and Jafari, R. (2021). The Versatile Role of Exosomes in Human Retroviral Infections: from Immunopathogenesis to Clinical Application. *Cel Biosci* 11 (1), 19. doi:10.1186/s13578-021-00537-0

Roy, A., Saqib, U., and Baig, M. S. (2021). NOS1-mediated Macrophage and Endothelial Cell Interaction in the Progression of Atherosclerosis. *Cell Biol Int* 45 (6), 1191–1201. doi:10.1002/cbin.11558

Sabry, D., Marzouk, S., Zakaria, R., Ibrahim, H. A., and Samir, M. (2020). The Effect of Exosomes Derived from Mesenchymal Stem Cells in the Treatment of Induced Type 1 Diabetes Mellitus in Rats. *Biotechnol. Lett.* 42 (8), 1597–1610. doi:10.1007/s10529-020-02908-y

Safdar, A., Saleem, A., and Tarnopolsky, M. A. (2016). The Potential of Endurance Exercise-Derived Exosomes to Treat Metabolic Diseases. *Nat. Rev. Endocrinol.* 12 (9), 504–517. doi:10.1038/nrendo.2016.76

Safdar, A., and Tarnopolsky, M. A. (2018). Exosomes as Mediators of the Systemic Adaptations to Endurance Exercise. *Cold Spring Harb Perspect. Med.* 8 (3), a029827. doi:10.1101/cshperspect.a029827

Salama, A., Fichou, N., Allard, M., Dubreil, L., De Beaurepaire, L., Viel, A., et al. (2014). MicroRNA-29b Modulates Innate and Antigen-specific Immune Responses in Mouse Models of Autoimmunity. *PLoS One* 9 (9), e106153. doi:10.1371/journal.pone.0106153

Sheng, H., Hassanali, S., Nugent, C., Wen, L., Hamilton-Williams, E., Dias, P., et al. (2011). Insulinoma-released Exosomes or Microparticles Are Immunostimulatory and Can Activate Autoreactive T Cells Spontaneously Developed in Nonobese Diabetic Mice. *J.I.* 187 (4), 1591–1600. doi:10.4049/jimmunol.1100231

Shepherd, M. C., Radnaa, E., Tantengco, O. A., Kechichian, T., Urrabaz-Garza, R., Kammala, A. K., et al. (2021). Extracellular Vesicles from Maternal Uterine Cells Exposed to Risk Factors Cause Fetal Inflammatory Response. *Cel Commun Signal* 19 (1), 100. doi:10.1186/s12964-021-00782-3

Sluijter, J. P. G., Davidson, S. M., Boulanger, C. M., Buzás, E. I., de Kleijn, D. P. V., Engel, F. B., et al. (2018). Extracellular Vesicles in Diagnostics and Therapy of the Ischaemic Heart: Position Paper from the Working Group on Cellular Biology of the Heart of the European Society of Cardiology. *Cardiovasc. Res.* 114 (1), 19–34. doi:10.1093/cvr/cvx211

Stuffers, S., Sem Wegner, C., Stenmark, H., and Brech, A. (2009). Multivesicular Endosome Biogenesis in the Absence of ESCRTs. *Traffic* 10 (7), 925–937. doi:10.1111/j.1600-0854.2009.00920.x

Tang, N., Sun, B., Gupta, A., Rempel, H., and Pulliam, L. (2016). Monocyte Exosomes Induce Adhesion Molecules and Cytokines via Activation of NF-κB in Endothelial Cells. *FASEB j.* 30 (9), 3097–3106. doi:10.1096/fj.201600368RR

Tirziu, D., Giordano, F. J., and Simons, M. (2010). Cell Communications in the Heart. *Circulation* 122 (9), 928–937. doi:10.1161/CIRCULATIONAHA.108.847731

Van-Niel, G., Charrin, S., Simoes, S., Romao, M., Rochin, L., Saftig, P., et al. (2011). The Tetraspanin CD63 Regulates ESCRT-independent and -dependent Endosomal Sorting during Melanogenesis. *Develop. Cel* 21 (4), 708–721. doi:10.1016/j.devcel.2011.08.019

Verge, C. F., Gianani, R., Kawasaki, E., Yu, L., Pietropaolo, M., Chase, H. P., et al. (1996). Prediction of Type I Diabetes in First-Degree Relatives Using a Combination of Insulin, GAD, and ICA512bdc/IA-2 Autoantibodies. *Diabetes* 45 (7), 926–933. doi:10.2337/diab.45.7.926

Villarroya-Beltri, C., Baixauli, F., Gutiérrez-Vázquez, C., Sánchez-Madrid, F., and Mittelbrunn, M. (2014). Sorting it Out: Regulation of Exosome Loading. *Semin. Cancer Biol.* 28, 3–13. doi:10.1016/j.semcancer.2014.04.009

Wagner, R., Heni, M., Tabák, A. G., Machann, J., Schick, F., Randrianarisoa, E., et al. (2021). Pathophysiology-based Subphenotyping of Individuals at Elevated Risk for Type 2 Diabetes. *Nat. Med.* 27 (1), 49–57. doi:10.1038/s41591-020-1116-9

Wang, X., Gu, H., Huang, W., Peng, J., Li, Y., Yang, L., et al. (2016). Hsp20-Mediated Activation of Exosome Biogenesis in Cardiomyocytes Improves Cardiac Function and Angiogenesis in Diabetic Mice. *Diabetes* 65 (10), 3111–3128. doi:10.2337/db15-1563

Wang, X., Huang, W., Liu, G., Cai, W., Millard, R. W., Wang, Y., et al. (2014). Cardiomyocytes Mediate Anti-angiogenesis in Type 2 Diabetic Rats through the Exosomal Transfer of miR-320 into Endothelial Cells. *J. Mol. Cell Cardiol.* 74, 139–150. doi:10.1016/j.yjmcc.2014.05.001

Wang, X., Qian, R., Zhang, W., Chen, S., Jin, H., and Hu, R. (2009). MicroRNA-320 Expression in Myocardial Microvascular Endothelial Cells and its Relationship with Insulin-like Growth Factor-1 in Type 2 Diabetic Rats. *Clin. Exp. Pharmacol. Physiol.* 36 (2), 181–188. doi:10.1111/j.1440-1681.2008.05057.x

Wen, D., Peng, Y., Liu, D., Weizmann, Y., and Mahato, R. I. (2016). Mesenchymal Stem Cell and Derived Exosome as Small RNA Carrier and Immunomodulator to Improve Islet Transplantation. *J. Controlled Release* 238, 166–175. doi:10.1016/j.jconrel.2016.07.044

Yang, J., Yu, X., Xue, F., Li, Y., Liu, W., and Zhang, S. (2018). Exosomes Derived from Cardiomyocytes Promote Cardiac Fibrosis via Myocyte-Fibroblast Cross-Talk. *Am. J. Transl Res.* 10 (12), 4350–4366.

Yao, Y., Sun, W., Sun, Q., Jing, B., Liu, S., Liu, X., et al. (2019). Platelet-Derived Exosomal MicroRNA-25-3p Inhibits Coronary Vascular Endothelial Cell Inflammation through Adam10 via the NF-Kb Signaling Pathway in ApoE−/− Mice. *Front. Immunol.* 10, 2205. doi:10.3389/fimmu.2019.02205

Ying, W., Riopel, M., Bandyopadhyay, G., Dong, Y., Birmingham, A., Seo, J. B., et al. (2017). Adipose Tissue Macrophage-Derived Exosomal miRNAs Can Modulate *In Vivo* and *In Vitro* Insulin Sensitivity. *Cell* 171(2), 372–384. doi:10.1016/j.cell.2017.08.035

Yu, Y., Du, H., Wei, S., Feng, L., Li, J., Yao, F., et al. (2018). Adipocyte-Derived Exosomal MiR-27a Induces Insulin Resistance in Skeletal Muscle through Repression of PPARγ. *Theranostics* 8 (8), 2171–2188. doi:10.7150/thno.22565

Zhang, Y.-G., Song, Y., Guo, X.-L., Miao, R.-Y., Fu, Y.-Q., Miao, C.-F., et al. (2019). Exosomes Derived from oxLDL-Stimulated Macrophages Induce Neutrophil Extracellular Traps to Drive Atherosclerosis. *Cell Cycle* 18 (20), 2672–2682. doi:10.1080/15384101.2019.1654797

Zhang, Y., Zhu, Z., Wang, T., Dong, Y., Fan, Y., and Sun, D. (2021). TGF-β1-containing Exosomes from Cardiac Microvascular Endothelial Cells Mediate Cardiac Fibroblast Activation under High Glucose Conditions. *Biochem. Cel Biol.* 99 (6), 693–699. doi:10.1139/bcb-2020-0624

Conflict of Interest: The authors declare that the research was conducted in the absence of any commercial or financial relationships that could be construed as a potential conflict of interest.

Publisher's Note: All claims expressed in this article are solely those of the authors and do not necessarily represent those of their affiliated organizations, or those of the publisher, the editors and the reviewers. Any product that may be evaluated in this article, or claim that may be made by its manufacturer, is not guaranteed or endorsed by the publisher.

frontiers | Frontiers in Cell and Developmental Biology

REVIEW
published: 04 April 2022
doi: 10.3389/fcell.2022.804247

Emerging Roles of Extracellular Vesicle-Delivered Circular RNAs in Atherosclerosis

Cheng Wen†, *Bowei Li*†, *Lei Nie*†, *Ling Mao* * *and Yuanpeng Xia* *

Department of Neurology, Union Hospital, Tongji Medical College, Huazhong University of Science and Technology, Wuhan, China

Atherosclerosis (AS) is universally defined as chronic vascular inflammation induced by dyslipidaemia, obesity, hypertension, diabetes and other risk factors. Extracellular vesicles as information transmitters regulate intracellular interactions and their important cargo circular RNAs are involved in the pathological process of AS. In this review, we summarize the current data to elucidate the emerging roles of extracellular vesicle-derived circular RNAs (EV-circRNAs) in AS and the mechanism by which EV-circRNAs affect the development of AS. Additionally, we discuss their vital role in the progression from risk factors to AS and highlight their great potential for use as diagnostic biomarkers of and novel therapeutic strategies for AS.

Keywords: atherosclerosis, extracellular vesicle, circular RNA (circRNA), Biomarker (BM), therapy

OPEN ACCESS

Edited by:
Youhua Tan,
Hong Kong Polytechnic University,
Hong Kong SAR, China

Reviewed by:
Xiangyang Zhu,
Mayo Clinic, United States
Yang Shen,
Sichuan University, China

***Correspondence:**
Ling Mao
maoling13096@163.com
Yuanpeng Xia
xiayuanpeng@hust.edu.cn

†*These authors have contributed equally to this work and share first authorship*

Specialty section:
This article was submitted to Molecular and Cellular Pathology, a section of the journal Frontiers in Cell and Developmental Biology

Received: *29 October 2021*
Accepted: *09 March 2022*
Published: *04 April 2022*

Citation:
Wen C, Li B, Nie L, Mao L and Xia Y (2022) Emerging Roles of Extracellular Vesicle-Delivered Circular RNAs in Atherosclerosis. Front. Cell Dev. Biol. 10:804247. doi: 10.3389/fcell.2022.804247

INTRODUCTION

Atherosclerosis (AS) is a major cause of vascular death and results in ischaemic cardio-cerebrovascular disease and peripheral arterial disease worldwide (Herrington et al., 2016). Multiple risk factors, including but not limited to dyslipidaemia, diabetes, obesity and hypertension, were identified in early studies. Emerging evidence indicates that chronic infection plays a critical role in the pathological progression of AS (Pothineni et al., 2017). The continual influence of blood lipids and glucose, high vascular pressure and infectious agents leads to endothelial cells (ECs) dysfunction, chemotactic movement of monocytes towards vascular vessel walls, foam cell formation and phenotypic changes in smooth muscle cells (SMCs), eventually causing AS initiation and progression.

Circular RNAs (circRNAs) are a novel type of noncoding RNAs produced by back-splicing, which is a noncanonical splicing event. CircRNAs have a covalently closed single-stranded structure that is resistant to degradation by exonucleases (Kristensen et al., 2019). Initially, circRNAs were regarded as "evolutionary junk" originating from aberrant splicing events (Cocquerelle et al., 1993). However, in the past few years, the development of high-throughput sequencing techniques and circRNA-specific bioinformatics algorithms has contributed to the discovery of vast quantities of circRNAs. Studies have identified circRNAs expressed in cell-type- and tissue-specific patterns (Salzman et al., 2013; Szabo et al., 2015). CircRNA expression profiles associated with features of human tissues and signs of multiple diseases have been identified, and significant differences in these profiles indicate that circRNAs are involved in the pathological process of various disease (**Figure 1** and **Table 1**), such as cardiovascular disease (Yu et al., 2020a), neurodegenerative disease (Li et al., 2020) and cancer (Fu et al., 2018). Qidong Cao et al. (2020) revealed a strong link between circRNAs and AS by summarizing the molecular mechanism by which circRNAs function in ECs, macrophages and vascular SMCs (VSMCs) in AS (**Figure 2** and **Table 2**).

Extracellular vehicles (EVs), membrane-enclosed nanoscale particles derived from donor cells, carry proteins, RNAs and lipids to recipient cells and serve as intracellular communication mediators (Kim et al., 20172017). According to their size and biogenesis, EVs are classified into three types: exosomes,

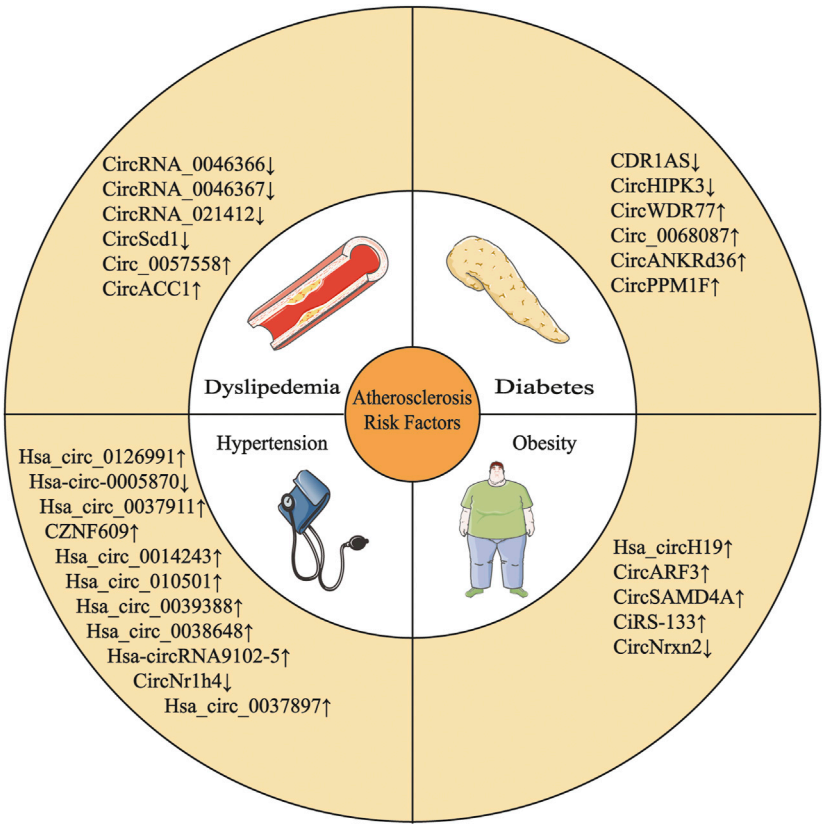

FIGURE 1 | Multiple circRNAs are involved in the development of AS risk factors. ↑: upregulation; ↓: downregulation.

microvesicles and apoptotic bodies. Yang Li and his colleague first showed abundant and stable circRNAs in exosomes, and more than 1,000 circRNAs were found in human serum exosomes (Li et al., 2015). Some EV-circRNAs are even richer than their linear counterparts (Lasda and Parker, 2016). EVs are recognized and endocytosed by specific cells via specific interactions between surface membrane proteins, enabling the EV-circRNAs characteristic of tissue-specific regulation (Pegtel and Gould, 2019). Many studies have recently reported that EV-circRNAs are released into the microenvironment and participate in the metastasis, invasion and migration of tumour cells (Seimiya et al., 2020). Additionally, these circRNAs are closely related to AS, as indicated by their influence on EC function, VSMCs and macrophages as mediators of cell-to-cell communication.

In this review, we summarize the research progress of EV-circRNAs in AS and discuss their biological functions and significance in the pathogenesis of AS in the presence of risk or induction factors. In addition, we discuss the potential clinical applications of EV-circRNAs as biomarkers and treatment strategies in AS.

RELEASE OF EV

EVs have been a research hotpot for a few years and some researchers have comprehensively reviewed the release mechanism of EVs. At present, it is generally believed that the formation of exosomes initiates early endosome formation by cell invagination. Then, under the regulation of the endosomal transport complex and some related proteins, early endosomes bud into the lumen of multivesicular bodies (MVBs). MVBs fuse with the cell membrane and secrete intracavitary vesicles called exosomes through the regulation of RAB enzymes in the GTPase family. Microvesicles, in contrast, are formed directly by budding and shedding of the plasma membrane (van Niel et al., 2018; Thietart and Rautou, 2020).

Stress conditions induce the release of EVs. *In vitro* tests have validated that shear stress, high glucose and the concentration of oxidatively modified low-density lipoprotein (oxLDL), TNFα and calcium can increase the exosome level. Thus, proatherogenic stimulation is strongly associated with the release of EVs (Giró et al., 2021).

EV-CIRCRNAS ARE INVOLVED IN AS RISK FACTORS

CircRNAs are Involved in AS Risk Factors

Dyslipidaemia

In recent years, circRNAs have been reported to participate in lipid metabolism. It has been found that in HepG2 cells treated

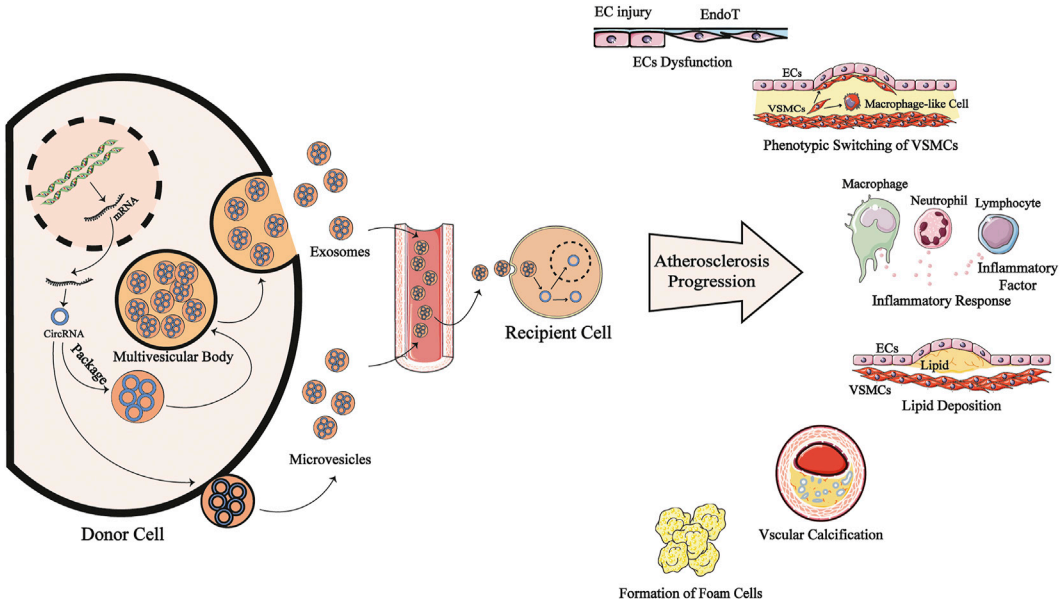

FIGURE 2 | EV-transmitted circRNAs are involved in the progression of AS. CircRNAs are produced by back-splicing from mRNA and put into extracellular vesicles mainly exosomes and microvesicles, becoming EV-circRNAs. This process may be interfered by risk factors of antheroslerosis. After entering systemic circulation, theses EV-circRNAs are transported to recipient cells and regulating cells function in cytoplasm or nucleus. They may modulate the dysfunction of endothelial cells, phenotype switching of VSMCs, inflammatory response, lipid deposition, vascular calcification and the formation of form cells to participate in antherosclerosis pathogenesis. CircRNA: circular RNA; mRNA: messenger RNA; ECs: endotherlial cells; VSMCs: vascular smooth muscle cells; EndoT; Endothelial mesenchymal transition.

with a high-fat diet (HFD), circRNA_0046366 promotes the accumulation of PPARα protein, which is translocated into the nucleus where it facilitates the transcriptional activation of lipid metabolism-associated genes (Guo et al., 2017a; Guo et al., 2018). Abnormalities in circRNA_021412/miR-1972/LPIN1 signalling lead to hepatic steatosis via the imbalance between catalytic separation and adipogenesis (Guo et al., 2017b). CircScd1 impedes lipid droplet formation and triglyceride (TG) content via the JAK2/STAT5 pathway in a HFD-fed mouse model (Li et al., 2019a). Overexpression of circ_0057558 positively correlates with TGs and modulates lipid metabolism in prostate cancer and facilitates lipogenesis and TG secretion in nonalcoholic fatty liver disease (Xia et al., 2018; Chen et al., 2021). CircACC1 was demonstrated to facilitate the stability and activity of AMPK, the central regulatory protein in energy metabolism (Li et al., 2019b). Most of these studies on circRNAs in lipid metabolism were focused on hepatic steatosis and cancer metabolic reprogramming, and few studies were focused on the influence of the reverse cholesterol transition, an important pathological process in the development of AS.

Diabetes Mellitus

CDR1AS was the first circRNA found to be associated with diabetes mellitus (DM), and it is the most compelling. The study showed that CDR1AS increased insulin content and secretion through the CDR1AS/miR-7/Myrip/Pax6 axis; in contrast, a subsequent study showed that a reduction in miR-7 decreased insulin secretion, while the overall insulin content was unaffected, and it diminished β cell proliferation without stimulating apoptosis in islets of db/db mice (Xu et al., 2015; Stoll et al., 2018). Silencing circHIPK3 led to negative regulation of the proliferation and insulin secretion capacity and survival in β cells (Stoll et al., 2018). Interestingly, circHIPK3 was downregulated in primary human aortic endothelial cells (HAECs), and accelerated HAECs apoptosis (Cao et al., 2018). Both EC injury and VSMC proliferation participate in AS, and some circRNAs probably play an important role in the pathological progression of AS induced by hyperglycaemia. CircWDR77 was reported to be the most significantly upregulated transcript in VSMCs under high-glucose conditions compared to its level in control VSMCs (Chen et al., 2017). Hsa_circ_0068087 and circANKRd36 were found to be correlated with chronic inflammation and vascular EC dysfunction in DM (Fang et al., 2018a; Cheng et al., 2019). In recent years, researchers have collected peripheral blood or islet samples from DM patients and healthy controls and performed comprehensive comparisons with microarrays. Large amounts of circRNAs have been found to be remarkably differentially expressed in human α and β cells and blood cells (Kaur et al., 2018; Stoll et al., 2018; Yang et al., 2020a; Luo et al., 2021). Among these circRNAs, circPPM1F was upregulated in mononuclear cells in the peripheral blood of children with T1DM, and it promoted M1 macrophage activation and facilitated injury to pancreatic islets in diabetic mice by competitively interacting with HUR, inhibiting the expression of PPM1F (Zhang et al., 2020a).

Obesity

Substantial efforts have been devoted to analysing the mechanism by which circRNAs influence the development of obesity, such as

TABLE 1 | CircRNAs are involved in the development of AS risk factors.

Risk factor	CircRNA	Dysregulation	Function	Cell/Model	Ref
Dyslipedemia	CircRNA_0046367	Down	Prevent hepatoxicity of lipid peroxidation against hepatic steatosis	HepG2 cells	Guo et al. (2017a)
	CircRNA_0046366	Down	Facilitate the transcriptional activation of lipid metabolism-associated genes	HepG2 cells	Guo et al. (2018)
	CircRNA_021412	Down	Disturb the balance between catalytic separation and adipogenesis	HepG2 cells	Guo et al. (2017b)
	CircScd1	Down	Impede lipid droplet formation and triglyceride content	AML-12 cells	Li et al. (2019a)
	Circ_0057558	Up	Facillitate lipogenesis and TG secretion	Huh-7 and HepG2 cells	Chen et al. (2021)
	CircACC1	Up	Facilitate the stability and activity of AMPK	HCT116 and LO2 cells	Li et al. (2019b)
	CDR1AS	Down	Increase insulin content and secretion	MIN6 cells	Xu et al. (2015)
Diabetes	CircHIPK3	Down	Impair the proliferation and capacity of insulin secretion and survival	Human islets cells	Cao et al. (2018)
	CircWDR77	Up	Promote high glucose induced proliferation and migration	Human VSMCs	Chen et al. (2017)
	Circ_0068087	Up	Promote chronic inflammation and vascular EC dysfunction in HG condition	HUVECs	Cheng et al. (2019)
	CircANKRd36	Up	Promote inflammation and cell apoptosis in the pancreatic tissues	T2DM rat model	Fang et al. (2018a)
	CircPPM1F	Up	promote activation and facilitate injury in pancreatic islets	PBMCs	Zhang et al. (2020a)
	Hsa_circH19	Up	Alleviate adipogenic differentiation	Human ADSCs	Zhu et al. (2020a)
Obesity	CircARF3	Up	Alleviate mitophagy-mediated inflammation and adipose inflammation	preadipocyte	Zhang et al. (2019a)
	CircSAMD4A	Up	Promote the differentiation of preadipocytes and obesity	preadipocyte	Liu et al. (2020)
	CircNrxn2	Down	Alleviate e WAT browning	preadipocyte	Zhang et al. (2019b)
	CiRS-133	Up	Promote WAT browning	preadipocyte	Zhang et al. (2019c)
	Has_circ_0126991	Up	Unknown	—	Liu et al. (2019a)
Hypertension	Has_circ_0005870	Down	Unknown	—	Wu et al. (2017)
	Has_circ_0037911	Up	Chang the concentration of Scr	—	Bao et al. (2018)
	CircZNF609	Up	Inhibit endothelial cell migration, tube formation, and apoptosis	HUVECs	Liu et al. (2017)
	Has_circ_0014243	Up	Unknown	—	Zheng et al. (2019)
	Hsa_circ_0105015	Up	Inflammatory pathways	HUVECs	He et al. (2021)
	Hsa_circ_0039388	Up	Enhance viability and invasive properties	HASMCs	Yin et al. (2020)
	Hsa_circ_0038648	Up	Enhance viability and invasive properties	HASMCs	Yin et al. (2020)
	Has-circRNA9102-5	Up	Unknown	—	Zheng et al. (2020)
	CircNr1h4	Down	Involved in hypertensive kidney injury	Mouse kidney collecting duct cells	Lu et al. (2020)
	Hsa_circ_0037897	Up	Unknown	—	Tao et al. (2021)

TG, total cholesterol; AMPK, AMP-activated protein kinase; EC, endothelial cell; HG, high glucose; WAT, white adipose tissue; Scr, serum creatinine; VSMCs, vascular smooth muscle cells; T2DM, type 2 diabetes mellitus; PBMCs, peripheral blood mononuclear cells; ADSCs, adipose-derived stem cells; HUVECs, human vein endothelial cells; HASMCs, human aortic endothelial cells.

the role of circRNAs in fat formation. Hsa_circH19 overexpression was found to protect against obesity, and interestingly, it was also upregulated in metabolic syndrome (MetS) and related to lipid-related parameters. The deletion of circH19 activated the transcription of lipogenic genes, leading to the differentiation of human adipose-derived stem cells (ADSCs) and buffering lipid flux (Zhu et al., 2020a). Excess adiposity induces the recruitment of immune cells, mainly macrophages, to fat depots, which release proinflammatory cytokines/chemokines that activate chronic and low-grade inflammation (Reilly and Saltiel, 2017). CircARF3 block the effects of miR-103, which result in the activation of TRAF3 expression, suppress the nuclear factor κB (NF-κB) pathway, exacerbate mitophagy and inhibit NLRP3 inflammasome activation, ultimately alleviating mitophagy-mediated inflammation in mouse adipose tissue (Zhang et al., 2019a). A new strategy was provided in this study to prevent adipose inflammation in obesity disorder. Obesity is partially attributed to genetic factors, and Cheng et al. illustrated that circRNAs contribute to lipogenesis and the development of chronic metabolic disease in the offspring of mothers with obesity, and they hypothesized that circRNAs may be involved in epigenetic regulation (Chen et al., 2020a). Studies have shown that circRNAs are closely related to adipogenesis and that their expression is dynamically regulated during adipogenesis (Sun et al., 2020). For example, circSAMD4A expression was significantly higher among differentially expressed circRNAs, and the circSAMD4A/miR-138-5p/EZH2 axis was proven to modulate the differentiation of preadipocytes in a mouse

TABLE 2 | EV-circRNAs and their partners related to atherosclerosis.

CircRNA	Source	Recipient cell	Downstream pathways	Biological functions	Ref
CircIARS	Plasma	HMVECs	miR-122/RhoA	Reduce the permeability of the endothelial monolayer	Li et al. (2018)
Circ_0003204	Plasma	HUAECs	miR-370-3p/TGFβR2/Phosph-Smad3	Inhibit the proliferation, migration and tubular formation	Drew et al. (1981)
cPWWP2A	pericytes	HRVECs	miR-579–Angiopoietin1/ Occludin/SIRT1	Affect the proliferation and migration of ECs and the formation of tubular structures	Wang et al. (2019a)
CircHIPK3	CMs	CMVECs	miR-29a/IGF-1	Inhibit the apoptosis of CMVECs and the production of ROS	Wen et al. (2021)
circRNA-0006896	Serum	HUVECs	miR-1264-DNMT1	Enhance proliferation and migration in HUVECs	Peng et al. (2021)
CircRNA-0077930	HUVECs	VSMCs	miR-622/Kras	Induce the VSMCs senescence	Chen et al. (2015)
CircDLGAP4	Plasma	Mouse brain ECs and MCs	miR-143/HECTD1	Inhibit EndoMT	Yang et al. (2018)
			miR-143/ERBB3/p-NFκB/ MMP-2	Promote growth and fibrosis of MCs	Aimes and Quigley, (1995)

HMVECs, human microvascular endothelial cells; HRVECs, human retinal vascular endothelial cells; HUAECs, human atrial endothelial cells; CMs, cardiomyocytes; CMVECs, cardiac microvascular endothelial cells; HUVECs, human umbilical vein endothelial cells; MCs, mesangial cells; ROS, reactive oxygen species; EndoMT, endothelial-mesenchymal transition.

model (Liu et al., 2020). In addition to participating in regulating adipogenesis, circRNAs have been shown to influence the browning of white adipose tissue (WAT), which was found to be a novel method of obesity prevention because it promoted energy metabolism. Both ciRS-133 and circNrxn2 have been implicated in WAT browning. CiRS-133 in plasma exosomes obtained from gastric cancer patients stimulated WAT browning by activating PRDM16, and circNrxn2 had the same effect by increasing the expression levels of fibroblast growth factor 10 (FGF10) in mice fed a HFD (Zhang et al., 2019b; Zhang et al., 2019c).

Hypertension

Hypertension is a systemic disease, and its complex pathogenesis makes it difficult to elucidate the precise molecular mechanisms involved. Numerous studies have demonstrated that circRNAs are potential biomarkers and important modulators in hypertension (Liu et al., 2017; Wu et al., 2017; Bao et al., 2018; Liu et al., 2019a; Zheng et al., 2019; Lu et al., 2020; Yin et al., 2020; Zheng et al., 2020; He et al., 2021; Tao et al., 2021). CircRNA array analysis of blood samples obtained from patients with essential hypertension and healthy individuals showed that the expression of circRNAs was significantly different between these groups. These researchers found that high expression of circRNAs was accompanied by low expression of relevant miRNAs, and they hypothesized that circRNAs may participate in the development of hypertension by acting as miRNA sponges. The upregulation of hsa-circRNA9102-5 expression was accompanied by the downregulation of hsa-miR-150-5p expression (Zheng et al., 2020), which was proven to promote angiogenesis and EC migration *in vitro* and *in vivo* in vascular ECs (Li et al., 2013). In addition, hsa-circ-0105015 expression was upregulated and hsa-miR-637 expression was downregulated in HAECs and human vein ECs (HUVECs) treated with TNF-α, suggesting that these circRNAs may be associated with vascular inflammation and endothelial dysfunction in hypertension (Yao et al., 2021).

EV-CircRNAs are Involved in Risk Factors for AS Formation and Development

EVs can act as biological vectors carrying nucleic acids, proteins and lipids through their interaction with recipient cells involved in the pathogenesis of human disease. Exosomes are effective mediators between key cells involved in diabetes and AS. It was reported that obesity changed the miRNA profile of circulating exosomes, inducing glucose intolerance and dyslipidaemia in lean mice (Castaño et al., 2018). EVs containing miR-221–3P from perivascular adipose tissue (PVAT) mediate vascular remodelling by inducing phenotypic switching of vascular cells and inducing inflammatory responses in PVAT (Zhu et al., 2019a). Visceral fat–derived exosomes, irrespective of obesity, stimulated foam cell formation from macrophages through the interference of mediated cholesterol efflux induced by ABCA1 and ABCG1 and the inhibition of M1 phenotype switching during atherogenesis (Xie et al., 2018). Under high-glucose conditions, cardiomyocytes of rats with type 2 DM (T2DM) released 'harmful' exosomes that impaired endothelial function. Cystatin C was proven to be a potentially useful marker in the early stage of AS in T2DM patients without obvious thickening of arterial wall, (Kaneko et al., 2018). A significant relation between EV-cystatin C and MetS was observed in patients with clinically manifested vascular disease (Kranendonk et al., 2014). High glucose levels induce an increase in S100A9, which was proven to accelerate the secretion and calcification-induction potential of EVs derived from primary macrophages (Xie et al., 2018). Small extracellular vesicles (sEVs), described as EVs originating from the endosomal compartment, are increased in patients with MetS (Hafiane and Daskalopoulou, 2018; Simon et al., 2018); in these patients, circulating sEVs may contribute to metabolic endotoxaemia, leading to endothelial dysfunction by delivering LPS and inducing TLR4-dependent ROS production (Ali et al., 2021). The hallmark of AS is low-grade vascular inflammation, and hyperglycaemia induces the activation of monocytes and ECs and the production of cytokines and adhesion molecules, such as intracellular adhesion molecule type-I (ICAM-1) (Altannavch

et al., 2004). High glucose levels led to elevated concentrations of exosomes produced by ECs and monocytes. *In vivo*, these exosomes increased ICAM-1 expression in Mono-Mac-6 cell, monocyte and HUVEC models, suggesting that exosomes may be involved in the potential mechanism underlying inflammatory cell activation in DMT2 and in diabetic complications in cardiovascular system (Sáez et al., 2019).

Hypertension may impair the function of vascular components by changing the components of EVs. The level of miR-17, a negative regulator of ICAM1, was decreased in macrophage-derived exosomes obtained from rats with hypertension, and these exosomes elevated the expression levels of ICAM1 and PAI-1 in HCAECs. The study suggested that EC-related inflammation under hypertensive conditions is caused, at least in part, by macrophage-derived exosomes. The angiotensin-converting enzyme (ACE) content was increased and the miR-155-5p content was reduced in adventitial fibroblast-derived EVs obtained from spontaneously hypertensive rats (SHRs) but not in normotensive Wistar–Kyoto rats (WKRs). These SHR-derived EVs promoted the proliferation of both WKR-VSMCs and SHR-VSMCs and led to deterioration in vascular remodelling after intravenous injection of SHR-EVs in WKRs and SHRs (Ren et al., 2020).

EV-CIRCRNAS IN THE PROGRESSION OF AS

A crucial process in AS development is foam cell formation and accumulation within the lipid-rich subendothelial space of the affected artery (Bäck et al., 2019). Initially, the aforementioned proatherogenic factors lead to EC injury or even dysfunction (Zhu et al., 2018). Lipids in the blood enter the arterial wall, and monocytes are attracted to the area and then differentiate into macrophages. Activated macrophages phagocytose accumulating lipids and secrete chemokines and inflammatory cytokines (Tabas and Lichtman, 2017). With the development of chronic inflammation, VSMCs induce phenotypic changes, phagocytose lipids, and migrate to the subintima of arteries. Due to lipid metabolic pathway dysregulation, lipid-dense macrophages and VSMCs, called foam cells, eventually undergo apoptosis, leading to necrotic core formation. In the late stage of AS, extracellular matrix (ECM) proteins are degraded by inflammatory cytokines and matrix metalloproteinases (MMPs), resulting in plaque rupture, and leading to myocardial infarction (MI) or stroke (Doyle and Caplice, 2007). Increasing evidence has implicated EV-circRNAs in the pathogenesis of AS, and a comprehensive understanding of the functional mechanism of their roles will lay a solid foundation for the development of EV circRNA-based diagnostic and therapeutic interventions in AS.

EC Dysfunction

EC Injury

According to the injury response theory, AS is considered to be the result of chronic inflammation in the arterial wall that damages ECs. The initiating factor of AS is EC function disruption. Furthermore, EC damage causes leukocyte adhesion, vasoconstriction, platelet activation, oxidative stress and inflammation, thrombosis, and blood coagulation and ultimately leads to cardiovascular disease (Behrendt and Ganz, 2002).

Increasing evidence shows that noncoding RNAs carried in exosomes are involved in regulating the occurrence of EC dysfunction. CircIARS is elevated in plasma exosomes and tumour tissues from patients with pancreatic cancer, and it reverses the inhibition of the target gene RhoA by accelerating the adsorption of miR-122 onto human microvascular ECs, which reduces the permeability of the endothelial monolayer (Li et al., 2018). An atherosclerotic cell model generated by stimulants such as oxLDL, proinflammatory cytokines, advanced glycation end products and reactive oxygen species (ROS) verified that circRNAs were associated with the regulation of EC functions. CIRC_0003204 expression was downregulated in HAECs treated with oxLDL to inhibit the proliferation, migration and tubular formation of atherosclerotic ECs through the miR-370–33p/TGFβR2/p-Smad3 axis. CIRC_0003204 expression was found to be remarkably increased in plasma exosomes in patients with cerebral AS, suggesting that it may be transported from exosomes to vascular ECs, where it plays a role (Drew et al., 1981). The circRNA cPWWP2A regulates diabetic retinal microangiopathy by participating in the crosstalk between pericytes and ECs. cPWWP2A mainly exists in the cytoplasm of pericytes in the retina. Hyperglycemia increases the expression of cPWWP2A in these pericytes but does not affect ECs. It was confirmed that cPWWP2A was transported between pericytes and ECs by exosomes, affecting the proliferation and migration of ECs and the formation of tubular structures (Liu et al., 2019b). Exosomal circHIPK3 derived from cardiomyocytes preconditioned through hypoxia exposure was transferred to cardiac microvascular ECs (CMVECs) under oxidative stress conditions. CirHIPK3 inhibited the apoptosis of CMVECs and the production of ROS, providing new insights into the mechanism of microvascular dysfunction induced by hypoxia (Wang et al., 2019a). The Serum exosomal circRNAs expression profile of patients with stable plaque atherosclerosis (SA) and unstable/vulnerable plaque atherosclerosis (UA) was explored by circRNA array, and circRNA-0006896, upregulated both in SA plaque and HUVECs, significantly enhances proliferation and migration in HUVECs treated with serum exosomes of SA patients (Wen et al., 2021). Additionally, circ-USP36 was found to be elevated in serum samples of atherosclerotic patients and to promote the apoptosis and inflammation of HUVSMCs and HUVECs activated by ox-LDL (Peng et al., 2021). CircRNA ZNF609 was significantly upregulated in peripheral blood leukocytes in patients with coronary artery disease. It was verified through *in vitro* experiments that circRNA ZNF609 plays a protective role by inhibiting the release of proinflammatory factors and the apoptosis of HUVECs subjected to oxidative and hypoxic stress (Liu et al., 2017; Liang et al., 2020). Evidence suggests that microvesicles produced by ageing ECs in culture promote the calcification of VSMCs (Alique et al., 2017). In subsequent research, circRNA-0077930 in hyperglycaemia-stimulated vascular EC exosomes

was found to induce the senescence of VSMCs and was closely related to cardiovascular disease in diabetic complications (Wang et al., 2020a).

An increasing number of studies have concentrated on the effect of circular RNAs on EC function. The mechanism by which exosomal-derived circRNAs affect ECs has not been fully explained. CircRNAs, which can affect the function of ECs and other cells, may be involved in the crosstalk and progression of AS *via* exosomal cargo transport.

Endothelial-Mesenchymal Transition

Endothelial-mesenchymal transition (EndoMT) is characterized by phenotypic changes in normal ECs manifesting by the acquisition of mesenchymal cell morphology and properties similar to those of fibroblasts and SMCs, including the promotion of proliferation, migration, expression of various leukocyte adhesion molecules, and secretion of ECM proteins such as fibronectin and collagen. EndoMT promotes the progression of AS (Chen et al., 2015), and endothelial lineage tracking showed that EndoMT is an important mechanism for the accumulation of activated fibroblasts and SMC-like cells in atherosclerotic plaques (Evrard et al., 2016). EndoMT is involved in the regulation of inflammation in the pathological process of AS. Inflammatory factors relieve FGFR1 inhibition of the TGFβ signalling pathway [TGF-β plays a central role in promoting the progression of EndoMT (Medici et al., 2010; van Meeteren and ten Dijke, 2012)] by inhibiting the expression of FGFR1, promoting the interstitial movement of ECs and promoting the expansion of plaques (Chen et al., 2015). In addition, EndoMT also affects the phenotype of unstable plaques. EndoMT-derived fibroblasts can affect the stability of atherosclerotic lesions by changing the balance of collagen and MMPs and by promoting the transition of stable plaques into collagen-deficient and easily ruptured plaques with thinner fibre caps (Evrard et al., 2016).

An increasing number of miRNAs have been confirmed to participate in EndoMT, and circRNAs have also been confirmed to function as sponging miRNAs to regulate EndoMT (Hulshoff et al., 2019). In rat coronary EndoMT induced by TGF-β1, 102 circRNAs were differentially expressed, 66 circRNAs were upregulated and 36 circRNAs were downregulated (Herrington et al., 2016). CircDLGAP4 acted as a miR-143 sponge to inhibit the expression of HECTD1, tight junction proteins and mesenchymal markers and to inhibit EndoMT (Bai et al., 2018). Li Yang et al. studied HVMECs *in vitro* and confirmed that circHECW2 inhibited its effect by sponging MIR30D and that MIR30D targeted ATG5 to inhibit the EndoMT of cells (Yang et al., 2018). Moreover, circHECTD1 inhibited the interstitial movement of mouse lung microvascular ECs induced by SiO2 by regulating the expression of its host gene, hectd1 (Fang et al., 2018b). Multiple exosomal circRNAs were reported to induce epithelial-mesenchymal transition (EMT) to promote the malignant phenotype and the metastasis and invasion of cancer cells (Chen et al., 2018a; Wang et al., 2020b; Zhu et al., 2020b; Wang et al., 2021a). EndoMT, a specialized form of EMT, has similar morphological and molecular characteristics to EMT and was shown to be modulated by exosomal circRNAs in recent studies. After being found in acute ischaemic stroke, circ_DLGAP4 was studied in exosomes. Exo-circ_DLGAP4 was increased in the serum of diabetic kidney patients and T2DM patients as well as in the culture medium of high glucose-treated mesangial cells (MCs). Circ_DLGAP4 promoted the growth and fibrosis of MCs by combining with miR-143 and then inhibiting the protein expression of ERBB3/p-NF-κB/MMP-2 (Bai et al., 2020a). Notably, activated NF-κB participates in inflammation-induced EndoMT because it is an important transcription factor of the FGF2 gene, a direct mediator of EndoMT (Bai et al., 2020a). Furthermore, some studies reported that increased expression of MMP-2 affected cell migration by degrading specific ECM components and exhibiting a mesenchymal phenotype (Aimes and Quigley, 1995; Giannelli et al., 1997; Song et al., 1999). According to these results, circ_DLGAP4 in plasma exosomes may play a protective role in pathophysiological progression by inhibiting EndoMT.

Although few studies have investigated how exosomal circRNAs modulate EndoMT in AS, multiple reports have indicated that exosomes are associated with cell-to-cell communication in EndoMT, especially in communication between ECs and macrophages. YING YANG et al. found that foam cells derived from M1 macrophages upregulated CCl-4 to induce EndoMT and accelerate the progression of AS by increasing endothelial permeability and monocyte adhesion, disrupting endothelial function (Yang et al., 2017). Alexandra et al. proved that ECs can acquire mesenchymal characteristics and an incomplete EndoMT phenotype through interaction with macrophages. Macrophages promote the expression of endothelial colony-stimulating factor, and conditioned medium from cells undergoing EndoMT reduces the proliferation and the expression of antigen-presenting cell markers and TNF-α in macrophages treated with ox-LDL (Helmke et al., 2019). Endothelial cells and macrophages play important roles in AS. Cells undergoing EndoMT interact with macrophages, but the molecular mechanism of this interaction remains to be studied. Evidence showing that exosomes and circular RNA participate in information transmission between ECs and macrophages may provide new ideas for potential therapy.

Phenotypic Switching of VSMCs

In the process of AS phenotypic switching, VSMCs decrease the expression of a range of 'SMC markers' (including smooth muscle cell myosin heavy chain, SM22α/tagln, and smooth muscle cell actin) and increase the capacity for cell proliferation, migration and secretion of various extracellular matrix proteins and cytokines (Alexander and Owens, 2012; Bennett et al., 2016). This process has been considered of great importance to AS. EVs function as messengers among atherosclerotic-associated cells. Macrophage- and EC-derived EVs regulate phenotypic switching of VSMCs, which has been proven *in vitro*. Macrophage foam cell-derived EVs enhance VSMC migration and adhesion capacity, but the effective cargo is unknown for these changes (Niu et al., 2016). Noncoding RNAs have been found to be involved in this progression, with miR221, miR-222, miR-21-

3p, microRNA-19b-3p, and LINC01005 mediating phenotypic modulation by activating synthetic genes or promoting VSMC proliferation and migration to accelerate AS development (Leung et al., 2013; Zhu et al., 2019a; Wang et al., 2019b; Zhang et al., 2020b; Wang et al., 2022a). microRNA-92a from EC-derived EVs has a similar functional mechanism to macrophage-derived EVs (Wang et al., 2022b). Interestingly, in obese mice fed a HFD, VSMCs can take up EVs derived from perivascular adipose tissue and their packaged miRNAs tested *in vivo* and *in vitro*, and miR-221-3p as a highly enriched miRNAs leads to vascular dysfunction by restraining the expression of contractile genes, provoking early-stage vascular remodelling under the obesity-associated inflammation conditions (Li et al., 2019c). These data further elucidate the mechanism of how obesity develops into vascular dysfunction in AS.

EV-circRNAs were first found to regulate VSMC function. Under high-glucose conditions, circRNA-0077930 is transported by HUVEC exosomes to induce the senescence of VSMCs in diabetic vascular complications (Wang et al., 2020a). However, other pathological changes in VSMCs have not been intensively studied. While multiple circRNAs have been reported to regulate VSMC phenotypic switching (Kong et al., 2019; Peng et al., 2020a; Sun et al., 2021; He et al., 2022), whether EV-circRNAs are involved in crosstalk among the three types of cells has not been sufficiently studied and few definite conclusions can be reached.

Inflammatory Response

Inflammation Induced by Infection

Increasing evidence has indicated that infection is closely related to AS and that pathogens influence the progression of AS in a direct or indirect way. A large number of infectious agents were detected in AS plaques but not within normal blood vessels, including *Porphyromonas gingivalis* (Velsko et al., 2014), *Treponema denticola* (Chukkapalli et al., 2014), Hepatitis C virus (HCV) (Boddi et al., 2010), *Chlamydia pneumoniae* and *Helicobacter pylori* (HP) (Kaplan et al., 2006) and cytomegalovirus (Cao et al., 2017), which indicated a direct role for pathogens in local plaque development. Pathogen infection at nonvascular sites, such as C. pneumoniae located in the lung, HCV located in the liver and HP located in the gastric area, also accelerates AS indirectly by activating the immune system and inducing chronic low-grade inflammation. These pathogens ultimately promote AS by activating EC inflammatory responses, increasing macrophage-derived foam cell formation, promoting SMC proliferation and migration and inhibiting apoptosis.

In 1976, circular RNAs were first discovered in Sendai virus and plant viroids by electron microscopy (Kolakofsky, 1976; Sanger et al., 1976). Several circRNAs from virus or host cells were reported to be important in the biological behaviours of pathogens in infected cells. In 2018, Yue Zhang and his colleagues found that 1,365 circRNAs were differentially expressed between 3 HARRT-naive patients with early HIV-1 infection and 3 healthy controls, including 912 upregulated circRNAs and 453 downregulated circRNAs. These circRNAs were then found to be involved in the immune, inflammatory, and defence responses to viral infection, playing important roles in the pathogenesis and disease progression of HIV infection (Zhang et al., 2018a). CircPSDD3 regulated RNA amplification in a pro-viral manner during a post translational step by binding factor eIF4A3 and inhibiting the nonsense-mediated decay (NMD) pathway to enhance HCV RNA imbalances in infected liver cells. CircGATAD2A regulates H1N1 replication in VPS34-dependent autophagy in the A549 cell line (Yu et al., 2019). Jingui Deng et al. reported that human cytomegalovirus (HCMV) influenced host circRNA transcription and suggested multiple functions of circSP100 with multiple important HCMV-encoded proteins through circSP100-binding sites (Deng et al., 2021). In addition to interacting with viral proteins, circRNAs participate in P. gingivalis-induced periodontal inflammation. The circRNA CDR1as was downregulated in human periodontal ligament stem cells (PDLSCs) in the context of inflammation induced by P. gingivalis-derived lipopolysaccharide. CDR1as enhanced PDLSC proliferation through the CDR1as/miR-7/ERK pathway upon both overexpression and knockdown of CDR1as (Wang et al., 2019c). CircRasGEF1B, which has a human homologue with similar properties, upregulates the expression of ICAM-1, inducing LPS stimulation. This effect was proven to depend on the activation of NF-κB through the TLR/LPS pathway (Ng et al., 2016). This finding indicates that circRNAs may regulate the phenotypic transformation of monocytes in the innate response. According to these studies, increasing the abundance of infectious agents regulated by circRNAs may increase pathogen abundance in blood circulation, enhance systemic inflammation, promote pathogen invasion into blood vessel walls and activate ECs to induce serious atherosclerotic changes. CircRNAs seem to play irreplaceable roles in infection-associated AS.

Bacteria release membrane vesicles (BMVs), which have a structure similar to that of EVs and a distinct composition and content, play a pivotal role in the survival and replication of bacteria in infectious hosts by affecting virulence, horizontal gene transfer, export of cellular metabolites, phage infection and cell-to-cell communication (Mashburn and Whiteley, 2005; Toyofuku et al., 2019). Outer membrane vesicles (OMVs) primarily originate from Gram-negative bacteria. *P. gingivalis* participate in the pathological process of cardiovascular diseases such as AS and thromboembolism. A study indicated that OMV exposure led to increased runt-related transcription factor 2 (Runx2) expression and subsequently affected ERK signalling to promote VSMC calcification. However, the contributing OMV component is unknown (Yang et al., 2016). Bacteria also modulate the formation and components of EVs in infected host cells involved in infection-induced AS. Epidemiological and clinical studies showed a close correlation between infection with CagA-positive HP and a high incidence of AS and plaque instability compared to the effect of infection with CagA-negative HP (Pietroiusti et al., 2002; Zhang et al., 2008). In a recent study, serum-derived EVs carried CagA into the blood circulation in patients infected with CagA-positive HP (Shimoda et al., 2016). Further research revealed that CagA was packaged into exosomes derived from infected gastric epithelial cells and was taken up in aortic plaques, where it promoted AS by inducing macrophage foam cell formation (Yang et al., 2019). CagA-

containing exosomes enter ECs and impair their function. Researchers used exosomes obtained from conditioned medium obtained from human gastric epithelial cell culture with $CagA^+$ HP or serum exosomes derived from patients or mice with HP infection and proved that these exosomes significantly decreased EC functions, reducing EC migration, tube formation, and proliferation *in vitro* (Xia et al., 2020).

Viruses that infect cells may increase and/or alter exosomal content under pathological or stress conditions (de Jong et al., 2012), and this alteration may be the mechanism underlying the systemic response caused by local infection. In HIV-infected individuals, monocytes are activated into an IFNα phenotype, and the levels of circulating LPS are elevated. Exosomes from activated monocytes enter ECs and cause injury via the TLR4 and NF-κB pathways, which may contribute to vascular disease in people with HIV infection and other diseases associated with chronic immune activation (Tang et al., 2016). D.R.A. Reis et al. (2020) hypothesized that human papilloma virus (HPV) infection can enhance systemic inflammation and modulate the release of nucleic acids carried by EVs directly targeting blood vessels, which may be the reason for the high risk of cardiovascular diseases in infected patients and may promote atheroma formation, and they discussed possible experimental approaches on the basis of extensive literature.

Proinflammatory Mechanism

EVs derived from steatotic hepatocytes accelerate endothelial inflammation and promote atherogenesis by suppressing KLF4 and activating NF-κB (Jiang et al., 2020). Exosomes derived from mature dendritic cells play a role similar to those of steatotic hepatocytes by triggering the NF-κB pathway (Gao et al., 2016). Large circulating EVs in MetS participate in enhanced SMC proliferation, migration, a proinflammatory profile, and activation of the ERK5/p38 pathway, leading to vascular inflammation and remodelling in AS. During inflammation, exosomes secreted by macrophage-transported microRNAs accelerate the development of AS (Nguyen et al., 2018; Fitzsimons et al., 2020). In addition, exosomes from platelets, vessel cells (He et al., 2018; Bai et al., 2020b), inflammatory adipocytes (Wadey et al., 2019) and dendritic cells increased the level of inflammatory factors and recruited inflammatory cells and promoted their adhesion to the vessel wall, leading to a chronic inflammatory response process in AS. Multiple circRNAs (circ_0004104 (Zhang et al., 2021a), circular ANRIL (Song et al., 2017), circTM7SF3 (Wang and Bai, 2021), circUSP36 (Miao et al., 2021) and so on) were upregulated in AS and demonstrated to induce vascular EC injury and oxidative stress and inflammation. Circ_GRN and Circ_CHFR were also upregulated in atherosclerotic serum and expedited the inflammation of human vascular muscle cells (Zhuang et al., 2020; Li et al., 2021a). The aforementioned diseases are closely linked to systemic inflammation and the induction of oxidative stress in cells indicating a possible mechanism by which these diseases change the contents of EVs transported during the pathogenesis of AS.

Orally administered *Lactobacillus* strains reportedly reduced inflammatory cytokine production in mice. The anti-inflammatory activity was partially mediated by circulating exosomes decreasing the production of TNF-α and IL-6 in macrophages (Aoki-Yoshida et al., 2017). Gingival mesenchymal stem cell-derived exosomes play important roles in periodontitis-related AS. They reduced the expression of inflammatory factors and the amount released, promoted the polarization of proinflammatory macrophages into an anti-inflammatory phenotype, and inhibited lipid accumulation in a high-lipid microenvironment (Zhang et al., 2021b). Exosomes secreted by naive bone marrow-derived macrophages (BMDM-EXOs) transmit anti-inflammatory microRNAs to recipient macrophages, which foster M2 polarization by targeting NF-κB and TNF-α signalling (Bouchareychas et al., 2020). T helper (Th17) cells were shown to promote AS in their role as a novel subset of lymphocytes (Bouchareychas et al., 2020). ECs that activated CD137 signalling by an anti-CD137 antibody increased the expression of pAkt and NF-κB and induced an increase in IL6 in exosomes secreted by ECs. Furthermore, exosomes derived from CD137-modified ECs enhanced Th17 cell responses to promote plaque inflammation and stimulate EC dysfunction in AS (Xu et al., 2020a).

Lipid Deposition

During AS, lipids gradually accumulate in the subendothelial space of impaired arteries, resulting in several lipid modification processes followed by macrophage and smooth muscle cell uptake in the arterial wall (Maguire et al., 2019). Exosomes, as transporters of proteins related to the modulation of this process, were reported to be secreted. CD36-containing exosomes derived from adipocytes mediated lipid uptake and HepG2 cell damage. Specifically, the study showed that exosomes derived from CD36-knockdown adipocytes were related to decreased lipid accumulation and apoptosis rate of HepG2 cells (Yan et al., 2021). However, brown adipose tissue-derived exosomes were proven to play a protective role in alleviating lipid accumulation in mice fed a HFD (Zhou et al., 2020).

circRNA_0046367 is an endogenous modulator of miR-34a that underlies hepatic steatosis. Its normalized expression promotes steatosis resolution by restoring the activity of peroxisome proliferator-activated receptor α (PPARα) and transcriptionally activating lipid metabolism-associated genes (Guo et al., 2017a). Overexpressed cirHIPK3 reduced the accumulation of lipids in HUVECs by activating autophagy, and both the reduction in lipids and activated autophagy led to attenuated AS. The stable knockdown of hsa_circH19 in human ADSCs upregulated the expression of lipogenesis-related genes and increased the number of lipid droplets formed (Zhu et al., 2020a). It was reported that circ_0075932 was highly expressed in adipose tissue but was found to be expressed at relatively low levels in most tissues. In obese patients and burned skin, hsa_circ_0075932 was significantly upregulated and was transmitted by exosomes from adipocytes to dermal keratinocytes to promote cell apoptosis and inflammation (Zhang et al., 2019d). However, the author did not explore the effect of this circRNA on lipid accumulation in the pathological progression in obese individuals.

EVs and circRNAs play various roles in the process of lipid metabolism and can provide therapeutic suggestions for interfering with lipid deposition and the progression of atherosclerosis.

Formation of Foam Cells

Adipose tissue (AT) secretes hundreds of bioactive compounds, especially proinflammatory cytokines, and is recognized as an active endocrine organ. Exosomes isolated from visceral AT in HFD-induced obese mice significantly facilitated the generation of macrophage foam cells by downregulating ABCA1 and ABCG1 expression (Xie et al., 2018). In an early study, heat shock protein 27 (HSP27) was shown to be atheroprotective in a mouse model of AS but only in female mice. Macrophages secrete HSP27 via exosomes after stimulation with oestrogen (Rayner et al., 2009), and HSP27 reduces foam cell formation and atherogenesis by binding scavenger receptor-A on the surface of macrophages and reducing the uptake of acetylated LDL (ac-LDL) and inflammatory cytokine release (Rayner et al., 2008). Platelet-derived exosomes rapidly decreased the CD36 level in macrophages through enhanced ubiquitination and subsequent proteasome degradation, which reduced lipid load and interfered with the formation of foam cells (Srikanthan et al., 2014). Downregulation of CD36 attenuated lipid loading onto macrophages and the formation of foam cells. In other studies, exosomes derived from dendritic cells (Lin et al., 2021), adipocytes (Xie et al., 2018), HP-infected gastric epithelial cells (Yang et al., 2019) have been implicated in regulating macrophage foam cell formation to modulate AS process. In another study, EVs secreted by macrophage-derived foam cells activated the ERK and Akt pathways and promoted migration and adhesion in VSMCs (Niu et al., 2016), which may be involved in crosstalk of the AS microenvironment.

According to the Gene Expression Omnibus database, in human THP-1 macrophages treated with ox-LDL (an *in vitro* AS model), 29 circRNAs were differentially expressed, as determined through linear models using the microarray data method. The study also predicted a circRNA/lncRNA-miRNA-mRNA network in ox-LDL-induced foam cells and indicated that the circRNAs were closely linked to foam cell formation (Wang et al., 2019d). In a recent study, the upregulation of circDENND1B significantly attenuated foam cell formation induced by ox-LDL by promoting cholesterol efflux (Xu et al., 2021a). In patients with a high coronary atherosclerotic burden, plasma levels of hsa_circ_0001445 are low. Furthermore, an *in vitro* test confirmed that hsa_circ_0001445 expression in human coronary SMCs and EVs is reduced under atherogenic lipoprotein conditions. (Vilades et al., 2020). Upregulation of circ-0029589 in ox-LDL-stimulated VSMCs promote the expression of insulin-like growth factor 2 and stromal interaction molecule and VSMC proliferation, migration and apoptosis (Liang et al., 2021). However, in ox-LDL-stimulated macrophages, circ-0029589 attenuated an increase in methylation levels, which contributed to the mechanism by which stromal interaction molecule 1 induced macrophage apoptosis during AS progression (Yu et al., 2020b; Guo et al., 2020; Huang et al., 2020). Further study of circ-0029589 expression levels in exosomes in the plasma or plaque microenvironment will reveal the crosstalk and functional mechanisms involved in the combined action of SMCs and macrophages.

Vascular Classification

Vascular classification is a significant hallmark of AS. EV is associated with the initiation and progression of vascular calcification. Under pathological stimulation, macrophages and SMCs secrete EVs, which accumulate between collagen fibres and act as nucleation sites for ectopic mineralization of vascular walls, causing the formation of microcalcifications and macrocalcifications (Buffolo et al., 2022). It was reported that SMC-derived EVs initiate microcalcification in atherosclerotic plaques. Under hyperglycaemic conditions, S100A9 is upregulated and promotes macrophage release of calcific EVs, contributing to the formation of microcalcification within plaques (Kawakami et al., 2020).

Thousands of circRNAs have been detected in calcified human aortic valves, suggesting that they might be associated with vascular calcification (Chen et al., 2018b). Through analysing RNA sequencing and *in vitro* experimental data, circSamd4a has been found to be decreased in the VSMCs of rats and to have anti-calcification functions (Ryu et al., 2020). Melatonin contributes to ameliorating AS by counteracting the pyroptosis of ECs, inhibiting mitophagy activation and the NLRP3 inflammasome and regulating macrophage polarization to stabilize rupture-prone vulnerable plaques (Zhang et al., 2018b; Ma et al., 20182018; Ding et al., 2019). Furthermore, melatonin has been shown to reduce the level of circRIC3, contributing to ameliorate aortic valve calcification (Wang et al., 2020c). The circRNA TGFBR2 promotes aortic valve calcification via regulating osteoblast differentiation (Yu et al., 2021). Conversely, circSmoc1-2 has protective functions in vascular calcification by decreasing calcium deposition in VSMCs (Ryu et al., 2022). The association among EVs, circRNAs and vascular calcification should be taken into account because direct evidence of EV-circRNAs regulating vascular calcification is limited.

EV-CIRCRNAS AS NOVEL BIOMARKERS OF AS

Advantages of EV-CircRNAs as Biomarkers of AS

The clinical diagnosis of AS depends mainly on examination of images showing changes caused by arteriostenosis or plaque formation. Existing serum biomarkers, such as inflammatory cytokines (Hansson et al., 2006) and cholesterol and lipoprotein (Hoefer et al., 2015), lack specificity, and it is difficult to show different stages of AS, especially the early stage of AS.

Many circRNAs are abundantly expressed, some in a tissue- and developmental stage-specific manner, and numerous studies have shown significantly different expression levels between patients and healthy controls in many human diseases, such as aAS, Alzheimer's disease, and malignant tumours. Hence, circRNAs have potential roles in noninvasive diagnosis and

assessment in different disease stages (Jeck et al., 2013; Salzman et al., 2013; Hanan et al., 2017). Because of the novel characteristics and stability conferred by the covalently closed continuous loop structure and endonuclease resistance, circRNAs show intra- and extracellular stability and a long half-life (Jeck et al., 2013). CircRNAs are generally distributed in plasma (Zheng et al., 2017), urine (Chen et al., 2018a; Kölling et al., 2019), saliva (Bahn et al., 2015; Jafari Ghods, 2018) and cerebrospinal fluid (Li et al., 2020) secreted by tissue cells directly or packaged on EVs. Sumeng Wang et al. summarized the expression patterns of circRNAs in bodily fluids in multiple cancers and characterized their clinical application in liquid biopsy (Wang et al., 2021b). Li et al. first showed the existence of extensive circRNAs in exosomes, and the ratio of circRNA levels to linear RNA levels in exosomes was nearly 6-fold higher than the proportion in cells (Li et al., 2015). CircRNAs contained in EVs, especially in exosomes, are regarded as potential biomarkers and novel therapeutic targets in multiple cancers and immune and renal diseases (Jiang et al., 2020). These study results indicate that the expression pattern of EV-circRNAs may be significant in AS clinical diagnosis.

Potential EV-CircRNAs as Biomarkers in AS

Serum levels of circR-284 were significantly elevated, while those of miR-221 were lower in acutely symptomatic patients than in asymptomatic patients. The ratio of serum circR-284: miR221 showed favourable sensitivity and specificity for use in detecting plaque rupture and stroke (Bazan et al., 2017). In addition, in coronary artery disease (CAD) patients, the expression levels of 795 circRNAs were found to be substantially different from those of controls (fold change [FC]>1.5), with 624 circRNAs upregulated and 171 circRNAs downregulated at a significant level ($p < 0.05$). Among these circRNAs, the area under the curve (AUC) of hsa_circ_0004104 and hsa_circ_0001879 combined with CAD risk factors and conventional markers (smoking and total cholesterol [TC] and serum creatinine levels) was 0.832 (95% CI, 0.788–0.876; $p < 0.001$), the sensitivity was 0.668 and the specificity was 0.890, demonstrating that these circRNAs can potentially advance the diagnosis and prognosis of CAD (Wang et al., 2019e). Hsa_circ_0001445 is stable in plasma samples, and its lower plasma levels in patients are accompanied by a higher coronary atherosclerotic burden, which leads to the identification of coronary AS in patients suspected of having stable CAD (Vilades et al., 2020). Circ-DLGAP4 downregulation in peripheral blood mononuclear cells (PBMCs) of acute ischaemic stroke (AIS) patients showed promise for predicting the risk and severity of AIS. The study suggested that PBMC circ-DLGAP4 was negatively associated with inflammation levels in AIS (Zhu et al., 2019b). Studying patients with large-artery AS (LAA)-type AIS, Wangtao Zhang et al. identified 182 upregulated and 176 downregulated circRNAs and identified hsa_circRNA_0001599, with sensitivity and specificity values of 64.41 and 89.93%, as a putative circRNA biomarker for diagnosis (Li et al., 2021b).

Since they are enveloped by bilayer lipid membranes, circRNAs can be stably transferred through bodily fluid over long distances. The detection of tissue-specific markers on EV membranes helps to distinguish the sources of circRNAs, which are produced by multiple tissue cells. This possibility suggests that circRNAs enriched in EVs may contain information to help with diagnosis and prognosis. Compared to non-AS patients, the circ_0003204 level in EVs obtained from cerebral AS patients was markedly higher, which indicated a higher risk of life-ending events, and HAECs exposed to ox-LDL exhibited a similar tendency. Significantly, the AUC of the combination of circ_0003204 in plasma EVs and LDL cholesterol (LDL-C) levels used for predicting cerebral AS was 0.875, demonstrating its potential diagnostic value in cerebral AS (Zhang et al., 2020c). Circ_DLGAP4, which is involved in AIS, was recently found to be increased in exosomes isolated from patients with diabetic kidney disease, who have a high risk of developing cardiovascular disease (Bai et al., 2020a). Numerous studies have been concerned with the involvement of EVs in atherogenesis and atheroprotection (Peng et al., 2020b). CircRNAs, as important cargoes enriched in EVs, have great diagnostic and prognostic potential in AS, but relevant research has been limited to date.

THERAPEUTIC POTENTIAL OF EV-CIRCRNAS IN AS

EV-CircRNAs Provide a Novel Therapeutic Target for AS

Numerous studies have found that exosomal circRNAs play a major part in crosstalk in the tumour microenvironment. Exosomal transfer of circRNA influences proliferation, apoptosis, migration (Wu et al., 2020), the malignant phenotype (Fang et al., 2020), the EMT (Xu et al., 2021b) and chemoresistance (Xu et al., 2021c) of tumour cells to promote or inhibit tumour invasion and metastasis. Furthermore, exosomal circRNA obtained from tumour cells enhanced circRNA expression in surrounding normal cells and stimulated EMT progression (Fang et al., 2020). CircFNDC3B and circFNDC3B-enriched exosomes inhibited the angiogenic properties of colorectal cancer (Zeng et al., 2020). Many transmitted circRNAs have been proven to play a tumour-promoting role in cancer and may act as novel therapeutic targets for the therapy in malignant tumours. For example, CircEhmt1 was upregulated in pericytes induced by hypoxic conditions and was transferred from pericytes to endotheliocytes via exosomes, which may be a protective mechanism against high glucose-induced injury conferred by circEhmt1 overexpression (Ye et al., 2021). EV-circRNAs can participate in proatherogenic or antiatherogenic processes by acting on ECs injury, lipid accumulation, vesicular inflammation, and the phenotypic transition of SMCs. Thus, interfering with these functions of circRNAs may be a novel therapeutic target for AS.

EV-CircRNAs From Modified Cells for Use in Novel Therapeutic Strategies for AS

According to their long half-life, low immunogenicity and capacity to cross biological barriers, EVs, especially exosomes, have been novel hotspots in therapeutic research because of their

great potential as "natural nanoparticles" that can deliver therapeutic substances (Jiang and Gao, 2017). Exosomes derived from circAkap7-modified adipose-derived mesenchymal stem cells show therapeutic effects on cerebral ischaemic injury, as proven in a mouse model of transient middle cerebral artery occlusion (tMCAO). The study showed that Exo-circAkap7 treatment reduced the infarct volume and tMCAO-induced sensorimotor dysfunctions by attenuating cerebral apoptosis. Further study revealed that the protective mechanism conferred by Exo-circAkap7 involves the promotion of ATG12-mediated autophagy and NRF-mediated oxidative stress and inflammatory responses to oxygen- and glucose-deprivation/reoxygenation induction in primary astrocytes cocultured with exo-circAkap7 *in vitro* (Xu et al., 2020b). Early studies have indicated that endothelial progenitor cells (EPCs) play significant roles in atherogenesis by mobilizing EPCs in bone marrow and mediating the regeneration of ECs to repair injured sites (Condon et al., 2004; Hunting et al., 2005). Rongfeng Shi also found that exosomes derived from mmu_circ_0000250-modified ADSCs restored the function of vascular EPCs under high-glucose conditions by activating autophagy, an outcome validated by evidence of a reverse effect induced by treatment with the autophagy inhibitor chloroquine (CQ). In EPCs, mmu_circ_0000250 elevated the expression of the SIRT1 upstream modulator of autophagy via miR-128 absorption (Shi et al., 2020). Ischaemic stroke is the primary cause of permanent disability and mortality in numerous types of AS. We developed a technology that successfully delivered stroke patient-implicated circSMCH1 to the brain through engineered EVs, and the administration of circSMCH1 significantly improved functional recovery after stroke by enhancing neuroplasticity and inhibiting glial reactivity and peripheral immune cell infiltration (Yang et al., 2020b). Exosomes derived from ischaemic-preconditioned astrocyte-conditioned medium (IPAS-CM) exerted neuroprotection. CircSHOC2 in IPAS-EXOs ameliorated neuronal apoptosis and suppressed neuronal injury by regulating autophagy through modulating the miR-7670–3p/SIRT1 axis (Chen et al., 2020b). These studies provide new insight into therapeutic strategies for stroke treatment. Modified EV-circRNAs can significantly influence the physiological and pathological pathways in AS, providing a novel therapeutic strategy for AS.

With the characteristics of high specificity and low immunogenicity, EVs show good prospects for use in the precise treatment of AS lesions and other applications. The combination of exosomes and circRNAs is a very promising treatment strategy in the near future.

CONCLUSION AND FUTURE PERSPECTIVES

Over the past few decades, our understanding of the classical risk factors for atherosclerotic progression has improved rapidly. The molecular mechanism by which these factors lead to AS development has been largely clarified. In recent years, circRNAs in EVs have become a new hot topic in human disease research. EVs were found to be important immune transporters in metabolic diseases and AS. Under the pathological conditions of high glucose, abnormal lipid levels and/or high inflammatory cytokine levels, EVs, the crucial mediators of intracellular communication, serve as cellular function modulators or products of cellular function modulation.

CircRNAs, as the main cargoes in EVs, have been proven to be significant in AS progression. The following interaction between proatherogenic factors and EV-circRNAs has been established: circRNAs modulate proatherogenic factors, and antiatherogenic factors change the level or variety of circRNAs in EVs. Because of their stability, specificity, significant differences in expression and multiple functions, EV-circRNAs show great potential as reliable biomarkers and contributors to therapeutic strategies in different stages of AS.

Considering the studies explored in this review, proatherogenic factors can change circRNA levels in AS-associated cells by modulating the packaging of circRNAs in EVs during AS pathogenesis. Taken together, the cells involved in the progression of AS such as ECs, macrophages, and SMCs have the potential to become donor cells based on different stimuli, while EV-cirRNAs are involved in the regulation of the interaction between cells, resulting in the destruction of the endothelial cell barrier, macrophage and smooth muscle cell foaming, and smooth muscle cell phenotype transformation, etc., are involved in the progression of atherosclerosis. The mechanism by which donor cells release EV-cirRNA needs to be further explored.

On the basis of this phenomenon, the development of EV-circRNAs to modulate various signalling pathways in anti-AS processes may be a promising approach. However, direct research on the effects of EV-circRNAs on AS development is still insufficient to clarify the exact molecular mechanism involved in the effects of EV-circRNAs and proatherogenic factors on AS. Additional investigation of the predictive roles and functions of EV-circRNAs in AS will lead to a better understanding of the pathophysiological and physiological processes of AS and will hopefully lead to intense research in this area.

AUTHOR CONTRIBUTIONS

CW, BL and LN wrote the manuscript. YX and LM designed the studies and approved the manuscript.

FUNDING

This work was supported by the National Natural Science Foundation of China (No. 81771249 to YX, No. 81974182 and No. 82171325 to LM).

ACKNOWLEDGMENTS

We thank our teachers for the valuable discussion.

REFERENCES

Aimes, R. T., and Quigley, J. P. (1995). Matrix Metalloproteinase-2 Is an Interstitial Collagenase. *J. Biol. Chem.* 270, 5872–5876. doi:10.1074/jbc.270.11.5872

Alexander, M. R., and Owens, G. K. (2012). Epigenetic Control of Smooth Muscle Cell Differentiation and Phenotypic Switching in Vascular Development and Disease. *Annu. Rev. Physiol.* 74, 13–40. doi:10.1146/annurev-physiol-012110-142315

Ali, S., Malloci, M., Safiedeen, Z., Soleti, R., Vergori, L., Vidal-Gómez, X., et al. (2021). LPS-enriched Small Extracellular Vesicles from Metabolic Syndrome Patients Trigger Endothelial Dysfunction by Activation of TLR4. *Metabolism* 118, 154727. doi:10.1016/j.metabol.2021.154727

Alique, M., Ruíz-Torres, M. P., Bodega, G., Noci, M. V., Troyano, N., Bohórquez, L., et al. (2017). Microvesicles from the Plasma of Elderly Subjects and from Senescent Endothelial Cells Promote Vascular Calcification. *Aging* 9, 778–789. doi:10.18632/aging.101191

Altannavch, T. S., Roubalová, K., Kucera, P., and Andel, M. (2004). Effect of High Glucose Concentrations on Expression of ELAM-1, VCAM-1 and ICAM-1 in HUVEC with and without Cytokine Activation. *Physiol. Res.* 53, 77–82.

Aoki-Yoshida, A., Saito, S., Tsuruta, T., Ohsumi, A., Tsunoda, H., and Sonoyama, K. (2017). Exosomes Isolated from Sera of Mice Fed Lactobacillus Strains Affect Inflammatory Cytokine Production in Macrophages *In Vitro*. *Biochem. Biophysical Res. Commun.* 489, 248–254. doi:10.1016/j.bbrc.2017.05.152

Bäck, M., Yurdagul, A., Jr., Tabas, I., Öörni, K., and Kovanen, P. T. (2019). Inflammation and its Resolution in Atherosclerosis: Mediators and Therapeutic Opportunities. *Nat. Rev. Cardiol.* 16, 389–406. doi:10.1038/s41569-019-0169-2

Bahn, J. H., Zhang, Q., Li, F., Chan, T.-M., Lin, X., Kim, Y., et al. (2015). The Landscape of microRNA, Piwi-Interacting RNA, and Circular RNA in Human Saliva. *Clin. Chem.* 61, 221–230. doi:10.1373/clinchem.2014.230433

Bai, S., Xiong, X., Tang, B., Ji, T., Li, X., Qu, X., et al. (2020). Exosomal circ_DLGAP4 Promotes Diabetic Kidney Disease Progression by Sponging miR-143 and Targeting ERBB3/NF-Kb/mmp-2 axis. *Cell Death Dis* 11, 1008. doi:10.1038/s41419-020-03169-3

Bai, S., Yin, Q., Dong, T., Dai, F., Qin, Y., Ye, L., et al. (2020). Endothelial Progenitor Cell-Derived Exosomes Ameliorate Endothelial Dysfunction in a Mouse Model of Diabetes. *Biomed. Pharmacother.* 131, 110756. doi:10.1016/j.biopha.2020.110756

Bai, Y., Zhang, Y., Han, B., Yang, L., Chen, X., Huang, R., et al. (2018). Circular RNA DLGAP4 Ameliorates Ischemic Stroke Outcomes by Targeting miR-143 to Regulate Endothelial-Mesenchymal Transition Associated with Blood-Brain Barrier Integrity. *J. Neurosci.* 38, 32–50. doi:10.1523/JNEUROSCI.1348-17.2017

Bao, X., Zheng, S., Mao, S., Gu, T., Liu, S., Sun, J., et al. (2018). A Potential Risk Factor of Essential Hypertension in Case-Control Study: Circular RNA Hsa_circ_0037911. *Biochem. Biophysical Res. Commun.* 498, 789–794. doi:10.1016/j.bbrc.2018.03.059

Bazan, H. A., Hatfield, S. A., Brug, A., Brooks, A. J., Lightell, D. J., and Woods, T. C. (2017). Carotid Plaque Rupture Is Accompanied by an Increase in the Ratio of Serum circR-284 to miR-221 Levels. *Circ. Cardiovasc. Genet.* 10, e001720. doi:10.1161/CIRCGENETICS.117.001720

Behrendt, D., and Ganz, P. (2002). Endothelial Function. From Vascular Biology to Clinical Applications. *Am. J. Cardiol.* 90, 40L–48L. doi:10.1016/s0002-9149(02)02963-6

Bennett, M. R., Sinha, S., and Owens, G. K. (2016). Vascular Smooth Muscle Cells in Atherosclerosis. *Circ. Res.* 118, 692–702. doi:10.1161/CIRCRESAHA.115.306361

Boddi, M., Abbate, R., Chellini, B., Giusti, B., Giannini, C., Pratesi, G., et al. (2010). Hepatitis C Virus RNA Localization in Human Carotid Plaques. *J. Clin. Virol.* 47, 72–75. doi:10.1016/j.jcv.2009.10.005

Bouchareychas, L., Duong, P., Covarrubias, S., Alsop, E., Phu, T. A., Chung, A., et al. (2020). Macrophage Exosomes Resolve Atherosclerosis by Regulating Hematopoiesis and Inflammation via MicroRNA Cargo. *Cel Rep.* 32, 107881. doi:10.1016/j.celrep.2020.107881

Buffolo, F., Monticone, S., Camussi, G., and Aikawa, E. (2022). Role of Extracellular Vesicles in the Pathogenesis of Vascular Damage. *Hypertension* 1, 1. doi:10.1161/HYPERTENSIONAHA.121.17957

Cao, J., Mao, Y., Dong, B., Guan, W., Shi, J., and Wang, S. (2017). Detection of Specific Chlamydia Pneumoniae and Cytomegalovirus Antigens in Human Carotid Atherosclerotic Plaque in a Chinese Population. *Oncotarget* 8, 55435–55442. doi:10.18632/oncotarget.19314

Cao, Q., Guo, Z., Du, S., Ling, H., and Song, C. (2020). Circular RNAs in the Pathogenesis of Atherosclerosis. *Life Sci.* 255, 117837. doi:10.1016/j.lfs.2020.117837

Cao, Y., Yuan, G., Zhang, Y., and Lu, R. (2018). High Glucose-Induced circHIPK3 Downregulation Mediates Endothelial Cell Injury. *Biochem. Biophysical Res. Commun.* 507, 362–368. doi:10.1016/j.bbrc.2018.11.041

Castaño, C., Kalko, S., Novials, A., and Párrizas, M. (2018). Obesity-associated Exosomal miRNAs Modulate Glucose and Lipid Metabolism in Mice. *Proc. Natl. Acad. Sci. U.S.A.* 115, 12158–12163. doi:10.1073/pnas.1808855115

Chen, J., Cui, L., Yuan, J., Zhang, Y., and Sang, H. (2017). Circular RNA WDR77 Target FGF-2 to Regulate Vascular Smooth Muscle Cells Proliferation and Migration by Sponging miR-124. *Biochem. Biophysical Res. Commun.* 494, 126–132. doi:10.1016/j.bbrc.2017.10.068

Chen, J., Wang, J., Jiang, Y., Gu, W., Ni, B., Sun, H., et al. (2018). Identification of Circular RNAs in Human Aortic Valves. *Gene* 642, 135–144. doi:10.1016/j.gene.2017.10.016

Chen, P.-Y., Qin, L., Baeyens, N., Li, G., Afolabi, T., Budatha, M., et al. (2015). Endothelial-to-mesenchymal Transition Drives Atherosclerosis Progression. *J. Clin. Invest.* 125, 4514–4528. doi:10.1172/JCI82719

Chen, Q., Liu, M., Luo, Y., Yu, H., Zhang, J., Li, D., et al. (2020). Maternal Obesity Alters circRNA Expression and the Potential Role of mmu_circRNA_0000660 via Sponging miR_693 in Offspring Liver at Weaning Age. *Gene* 731, 144354. doi:10.1016/j.gene.2020.144354

Chen, W., Wang, H., Zhu, Z., Feng, J., and Chen, L. (2020). Exosome-Shuttled circSHOC2 from IPASs Regulates Neuronal Autophagy and Ameliorates Ischemic Brain Injury via the miR-7670-3p/SIRT1 Axis. *Mol. Ther. - Nucleic Acids* 22, 657–672. doi:10.1016/j.omtn.2020.09.027

Chen, X., Tan, Q. Q., Tan, X. R., Li, S. J., and Zhang, X. X. (2021). Circ_0057558 Promotes Nonalcoholic Fatty Liver Disease by Regulating ROCK1/AMPK Signaling through Targeting miR-206. *Cel Death Dis* 12, 809. doi:10.1038/s41419-021-04090-z

Chen, X., Chen, R.-X., Wei, W.-S., Li, Y.-H., Feng, Z.-H., Tan, L., et al. (2018). PRMT5 Circular RNA Promotes Metastasis of Urothelial Carcinoma of the Bladder through Sponging miR-30c to Induce Epithelial-Mesenchymal Transition. *Clin. Cancer Res.* 24, 6319–6330. doi:10.1158/1078-0432.CCR-18-1270

Cheng, J., Liu, Q., Hu, N., Zheng, F., Zhang, X., Ni, Y., et al. (2019). Downregulation of Hsa_circ_0068087 Ameliorates TLR4/NF-Kb/nlrp3 Inflammasome-Mediated Inflammation and Endothelial Cell Dysfunction in High Glucose Conditioned by Sponging miR-197. *Gene* 709, 1–7. doi:10.1016/j.gene.2019.05.012

Chukkapalli, S. S., Rivera, M. F., Velsko, I. M., Lee, J.-Y., Chen, H., Zheng, D., et al. (2014). Invasion of Oral and Aortic Tissues by Oral Spirochete Treponema Denticola in ApoE −/− Mice Causally Links Periodontal Disease and Atherosclerosis. *Infect. Immun.* 82, 1959–1967. doi:10.1128/IAI.01511-14

Cocquerelle, C., Mascrez, B., Hétuin, D., and Bailleul, B. (1993). Mis-splicing Yields Circular RNA Molecules. *FASEB J.* 7, 155–160. doi:10.1096/fasebj.7.1.7678559

Condon, E. T., Wang, J. H., and Redmond, H. P. (2004). Surgical Injury Induces the Mobilization of Endothelial Progenitor Cells. *Surgery* 135, 657–661. doi:10.1016/j.surg.2003.10.012

de Jong, O. G., Verhaar, M. C., Chen, Y., Vader, P., Gremmels, H., Posthuma, G., et al. (2012). Cellular Stress Conditions Are Reflected in the Protein and RNA Content of Endothelial Cell-Derived Exosomes. *J. Extracellular Vesicles* 1, 18396. doi:10.3402/jev.v1i0.18396

Deng, J., Huang, Y., Wang, Q., Li, J., Ma, Y., Qi, Y., et al. (2021). Human Cytomegalovirus Influences Host circRNA Transcriptions during Productive Infection. *Virol. Sin* 36, 241–253. doi:10.1007/s12250-020-00275-6

Ding, S., Lin, N., Sheng, X., Zhao, Y., Su, Y., Xu, L., et al. (2019). Melatonin Stabilizes Rupture-prone Vulnerable Plaques via Regulating Macrophage Polarization in a Nuclear Circadian Receptor RORα-dependent Manner. *J. Pineal Res.* 67, e12581. doi:10.1111/jpi.12581

Doyle, B., and Caplice, N. (2007). Plaque Neovascularization and Antiangiogenic Therapy for Atherosclerosis. *J. Am. Coll. Cardiol.* 49, 2073–2080. doi:10.1016/j.jacc.2007.01.089

Drew, H. R., Wing, R. M., Takano, T., Broka, C., Tanaka, S., Itakura, K., et al. (1981). Structure of a B-DNA Dodecamer: Conformation and Dynamics. *Proc. Natl. Acad. Sci. U.S.A.* 78, 2179–2183. doi:10.1073/pnas.78.4.2179

Evrard, S. M., Lecce, L., Michelis, K. C., Nomura-Kitabayashi, A., Pandey, G., Purushothaman, K.-R., et al. (2016). Endothelial to Mesenchymal Transition Is Common in Atherosclerotic Lesions and Is Associated with Plaque Instability. *Nat. Commun.* 7, 11853. doi:10.1038/ncomms11853

Fang, K., Chen, X., Qiu, F., Xu, J., Xiong, H., and Zhang, Z. (2020). Serum-Derived Exosomes-Mediated Circular RNA ARHGAP10 Modulates the Progression of Non-small-cell Lung Cancer through the miR-638/FAM83F Axis. *Cancer Biother. Radiopharm.* 1, 1. doi:10.1089/cbr.2019.3534

Fang, S., Guo, H., Cheng, Y., Zhou, Z., Zhang, W., Han, B., et al. (2018). circHECTD1 Promotes the Silica-Induced Pulmonary Endothelial-Mesenchymal Transition via HECTD1. *Cel Death Dis* 9, 396. doi:10.1038/s41419-018-0432-1

Fang, Y., Wang, X., Li, W., Han, J., Jin, J., Su, F., et al. (2018). Screening of Circular RNAs and Validation of circANKRD36 Associated with Inflammation in Patients with Type 2 Diabetes Mellitus. *Int. J. Mol. Med.* 42, 1865–1874. doi:10.3892/ijmm.2018.3783

Fitzsimons, S., Oggero, S., Bruen, R., McCarthy, C., Strowitzki, M. J., Mahon, N. G., et al. (2020). microRNA-155 Is Decreased during Atherosclerosis Regression and Is Increased in Urinary Extracellular Vesicles during Atherosclerosis Progression. *Front. Immunol.* 11, 576516. doi:10.3389/fimmu.2020.576516

Fu, B., Zhang, A., Li, M., Pan, L., Tang, W., An, M., et al. (2018). Circular RNA Profile of Breast Cancer Brain Metastasis: Identification of Potential Biomarkers and Therapeutic Targets. *Epigenomics* 10, 1619–1630. doi:10.2217/epi-2018-0090

Gao, W., Liu, H., Yuan, J., Wu, C., Huang, D., Ma, Y., et al. (2016). Exosomes Derived from Mature Dendritic Cells Increase Endothelial Inflammation and Atherosclerosis via Membrane TNF -α Mediated NF -κB Pathway. *J. Cel. Mol. Med.* 20, 2318–2327. doi:10.1111/jcmm.12923

Giannelli, G., Falk-Marzillier, J., Schiraldi, O., Stetler-Stevenson, W. G., and Quaranta, V. (1997). Induction of Cell Migration by Matrix Metalloprotease-2 Cleavage of Laminin-5. *Science* 277, 225–228. doi:10.1126/science.277.5323.225

Giró, O., Jiménez, A., Pané, A., Badimon, L., Ortega, E., and Chiva-Blanch, G. (2021). Extracellular Vesicles in Atherothrombosis and Cardiovascular Disease: Friends and Foes. *Atherosclerosis* 330, 61–75. doi:10.1016/j.atherosclerosis.2021.07.002

Guo, M., Yan, R., Ji, Q., Yao, H., Sun, M., Duan, L., et al. (2020). IFN Regulatory Factor-1 Induced Macrophage Pyroptosis by Modulating m6A Modification of Circ_0029589 in Patients with Acute Coronary Syndrome. *Int. Immunopharmacology* 86, 106800. doi:10.1016/j.intimp.2020.106800

Guo, X.-Y., Chen, J.-N., Sun, F., Wang, Y.-Q., Pan, Q., and Fan, J.-G. (2017). circRNA_0046367 Prevents Hepatoxicity of Lipid Peroxidation: An Inhibitory Role against Hepatic Steatosis. *Oxidative Med. Cell Longevity* 2017, 1–16. doi:10.1155/2017/3960197

Guo, X.-Y., He, C.-X., Wang, Y.-Q., Sun, C., Li, G.-M., Su, Q., et al. (2017). Circular RNA Profiling and Bioinformatic Modeling Identify its Regulatory Role in Hepatic Steatosis. *Biomed. Res. Int.* 2017, 1–13. doi:10.1155/2017/5936171

Guo, X.-Y., Sun, F., Chen, J.-N., Wang, Y.-Q., Pan, Q., and Fan, J.-G. (2018). circRNA_0046366 Inhibits Hepatocellular Steatosis by Normalization of PPAR Signaling. *Wjg* 24, 323–337. doi:10.3748/wjg.v24.i3.323

Hafiane, A., and Daskalopoulou, S. S. (2018). Extracellular Vesicles Characteristics and Emerging Roles in Atherosclerotic Cardiovascular Disease. *Metabolism* 85, 213–222. doi:10.1016/j.metabol.2018.04.008

Hanan, M., Soreq, H., and Kadener, S. (2017). CircRNAs in the Brain. *RNA Biol.* 14, 1028–1034. doi:10.1080/15476286.2016.1255398

Hansson, G. K., Robertson, A.-K. L., and Söderberg-Nauclér, C. (2006). Inflammation and Atherosclerosis. *Annu. Rev. Pathol. Mech. Dis.* 1, 297–329. doi:10.1146/annurev.pathol.1.110304.100100

He, S., Wu, C., Xiao, J., Li, D., Sun, Z., and Li, M. (2018). Endothelial Extracellular Vesicles Modulate the Macrophage Phenotype: Potential Implications in Atherosclerosis. *Scand. J. Immunol.* 87, e12648. doi:10.1111/sji.12648

He, X., Bao, X., Tao, Z., Sun, J., Zheng, S., Zhong, F., et al. (2021). The Microarray Identification Circular RNA Hsa_circ_0105015 Up-regulated Involving Inflammation Pathway in Essential Hypertension. *J. Clin. Lab. Anal.* 35, e23603. doi:10.1002/jcla.23603

He, X., Li, X., Han, Y., Chen, G., Xu, T., Cai, D., et al. (2022). CircRNA Chordc1 Protects Mice from Abdominal Aortic Aneurysm by Contributing to the Phenotype and Growth of Vascular Smooth Muscle Cells. *Mol. Ther. - Nucleic Acids* 27, 81–98. doi:10.1016/j.omtn.2021.11.005

Helmke, A., Casper, J., Nordlohne, J., David, S., Haller, H., Zeisberg, E. M., et al. (2019). Endothelial-to-mesenchymal Transition Shapes the Atherosclerotic Plaque and Modulates Macrophage Function. *FASEB j.* 33, 2278–2289. doi:10.1096/fj.201801238R

Herrington, W., Lacey, B., Sherliker, P., Armitage, J., and Lewington, S. (2016). Epidemiology of Atherosclerosis and the Potential to Reduce the Global Burden of Atherothrombotic Disease. *Circ. Res.* 118, 535–546. doi:10.1161/CIRCRESAHA.115.307611

Hoefer, I. E., Steffens, S., Ala-Korpela, M., Bäck, M., Badimon, L., Bochaton-Piallat, M.-L., et al. (2015). Novel Methodologies for Biomarker Discovery in Atherosclerosis. *Eur. Heart J.* 36, 2635–2642. doi:10.1093/eurheartj/ehv236

Huang, Z., Li, P., Wu, L., Zhang, D., Du, B., Liang, C., et al. (2020). Hsa_circ_0029589 Knockdown Inhibits the Proliferation, Migration and Invasion of Vascular Smooth Muscle Cells via Regulating miR-214-3p and STIM1. *Life Sci.* 259, 118251. doi:10.1016/j.lfs.2020.118251

Hulshoff, M. S., Del Monte-Nieto, G., Kovacic, J., and Krenning, G. (2019). Non-coding RNA in Endothelial-To-Mesenchymal Transition. *Cardiovasc. Res.* 115, 1716–1731. doi:10.1093/cvr/cvz211

Hunting, C. B., Noort, W. A., and Zwaginga, J. J. (2005). Circulating Endothelial (Progenitor) Cells Reflect the State of the Endothelium: Vascular Injury, Repair and Neovascularization. *Vox Sang* 88, 1–9. doi:10.1111/j.1423-0410.2005.00589.x

Jafari Ghods, F. (2018). Circular RNA in Saliva. *Adv. Exp. Med. Biol.* 1087, 131–139. doi:10.1007/978-981-13-1426-1_11

Jeck, W. R., Sorrentino, J. A., Wang, K., Slevin, M. K., Burd, C. E., Liu, J., et al. (2013). Circular RNAs Are Abundant, Conserved, and Associated with ALU Repeats. *RNA* 19, 141–157. doi:10.1261/rna.035667.112

Jiang, F., Chen, Q., Wang, W., Ling, Y., Yan, Y., and Xia, P. (2020). Hepatocyte-derived Extracellular Vesicles Promote Endothelial Inflammation and Atherogenesis via microRNA-1. *J. Hepatol.* 72, 156–166. doi:10.1016/j.jhep.2019.09.014

Jiang, X.-C., and Gao, J.-Q. (2017). Exosomes as Novel Bio-Carriers for Gene and Drug Delivery. *Int. J. Pharmaceutics* 521, 167–175. doi:10.1016/j.ijpharm.2017.02.038

Kaneko, R., Sawada, S., Tokita, A., Honkura, R., Tamura, N., Kodama, S., et al. (2018). Serum Cystatin C Level Is Associated with Carotid Arterial wall Elasticity in Subjects with Type 2 Diabetes Mellitus: A Potential Marker of Early-Stage Atherosclerosis. *Diabetes Res. Clin. Pract.* 139, 43–51. doi:10.1016/j.diabres.2018.02.003

Kaplan, M., Yavuz, S. S., Cinar, B., Koksal, V., Kut, M. S., Yapici, F., et al. (2006). Detection of Chlamydia Pneumoniae and *Helicobacter pylori* in Atherosclerotic Plaques of Carotid Artery by Polymerase Chain Reaction. *Int. J. Infect. Dis.* 10, 116–123. doi:10.1016/j.ijid.2004.10.008

Kaur, S., Mirza, A., and Pociot, F. (2018). Cell Type-Selective Expression of Circular RNAs in Human Pancreatic Islets. *ncRNA* 4, 38. doi:10.3390/ncrna4040038

Kawakami, R., Katsuki, S., Travers, R., Romero, D. C., Becker-Greene, D., Passos, L. S. A., et al. (2020). S100A9-RAGE Axis Accelerates Formation of Macrophage-Mediated Extracellular Vesicle Microcalcification in Diabetes Mellitus. *Atvb* 40, 1838–1853. doi:10.1161/ATVBAHA.118.314087

Kim, K. M., Abdelmohsen, K., Mustapic, M., Kapogiannis, D., and Gorospe, M. (20172017). RNA in Extracellular Vesicles. *WIREs RNA* 8, e1413. doi:10.1002/wrna.1413

Kolakofsky, D. (1976). Isolation and Characterization of Sendai Virus DI-RNAs. *Cell* 8, 547–555. doi:10.1016/0092-8674(76)90223-3

Kölling, M., Haddad, G., Wegmann, U., Kistler, A., Bosakova, A., Seeger, H., et al. (2019). Circular RNAs in Urine of Kidney Transplant Patients with Acute T Cell-Mediated Allograft Rejection. *Clin. Chem.* 65, 1287–1294. doi:10.1373/clinchem.2019.305854

Kong, P., Yu, Y., Wang, L., Dou, Y.-Q., Zhang, X.-H., Cui, Y., et al. (2019). circ-Sirt1 Controls NF-Kb Activation via Sequence-specific Interaction and Enhancement of SIRT1 Expression by Binding to miR-132/212 in Vascular Smooth Muscle Cells. *Nucleic Acids Res.* 47, 3580–3593. doi:10.1093/nar/gkz141

Kranendonk, M. E., de Kleijn, D. P., Kalkhoven, E., Kanhai, D. A., Uiterwaal, C. S., van der Graaf, Y., et al. (2014). Extracellular Vesicle Markers in Relation to

Obesity and Metabolic Complications in Patients with Manifest Cardiovascular Disease. *Cardiovasc. Diabetol.* 13, 37. doi:10.1186/1475-2840-13-37

Kristensen, L. S., Andersen, M. S., Stagsted, L. V. W., Ebbesen, K. K., Hansen, T. B., and Kjems, J. (2019). The Biogenesis, Biology and Characterization of Circular RNAs. *Nat. Rev. Genet.* 20, 675–691. doi:10.1038/s41576-019-0158-7

Lasda, E., and Parker, R. (2016). Circular RNAs Co-precipitate with Extracellular Vesicles: A Possible Mechanism for circRNA Clearance. *PLoS One* 11, e0148407. doi:10.1371/journal.pone.0148407

Leung, A., Trac, C., Jin, W., Lanting, L., Akbany, A., Sætrom, P., et al. (2013). Novel Long Noncoding RNAs Are Regulated by Angiotensin II in Vascular Smooth Muscle Cells. *Circ. Res.* 113, 266–278. doi:10.1161/CIRCRESAHA.112.300849

Li, J., Li, Z., Jiang, P., Peng, M., Zhang, X., Chen, K., et al. (2018). Circular RNA IARS (Circ-IARS) Secreted by Pancreatic Cancer Cells and Located within Exosomes Regulates Endothelial Monolayer Permeability to Promote Tumor Metastasis. *J. Exp. Clin. Cancer Res.* 37, 177. doi:10.1186/s13046-018-0822-3

Li, J., Zhang, Y., Liu, Y., Dai, X., Li, W., Cai, X., et al. (2013). Microvesicle-mediated Transfer of microRNA-150 from Monocytes to Endothelial Cells Promotes Angiogenesis. *J. Biol. Chem.* 288, 23586–23596. doi:10.1074/jbc.M113.489302

Li, P., Shan, K., Liu, Y., Zhang, Y., Xu, L., and Xu, L. (2019). CircScd1 Promotes Fatty Liver Disease via the Janus Kinase 2/Signal Transducer and Activator of Transcription 5 Pathway. *Dig. Dis. Sci.* 64, 113–122. doi:10.1007/s10620-018-5290-2

Li, Q., Wang, Y., Wu, S., Zhou, Z., Ding, X., Shi, R., et al. (2019). CircACC1 Regulates Assembly and Activation of AMPK Complex under Metabolic Stress. *Cel Metab.* 30, 157–173. e157. doi:10.1016/j.cmet.2019.05.009

Li, S., Hu, W., Deng, F., Chen, S., Zhu, P., Wang, M., et al. (2021). Identification of Circular RNA Hsa_circ_0001599 as a Novel Biomarker for Large-Artery Atherosclerotic Stroke. *DNA Cel Biol.* 40, 457–468. doi:10.1089/dna.2020.5662

Li, X., Ballantyne, L. L., Yu, Y., and Funk, C. D. (2019). Perivascular Adipose Tissue-Derived Extracellular Vesicle miR-221-3p Mediates Vascular Remodeling. *FASEB j.* 33, 12704–12722. doi:10.1096/fj.201901548R

Li, X., Li, L., Dong, X., Ding, J., Ma, H., and Han, W. (2021). Circ_GRN Promotes the Proliferation, Migration, and Inflammation of Vascular Smooth Muscle Cells in Atherosclerosis through miR-214-3p/FOXO1 Axis. *J. Cardiovasc. Pharmacol.* 77, 470–479. doi:10.1097/FJC.0000000000000982

Li, Y., Fan, H., Sun, J., Ni, M., Zhang, L., Chen, C., et al. (2020). Circular RNA Expression Profile of Alzheimer's Disease and its Clinical Significance as Biomarkers for the Disease Risk and Progression. *Int. J. Biochem. Cel Biol.* 123, 105747. doi:10.1016/j.biocel.2020.105747

Li, Y., Zheng, Q., Bao, C., Li, S., Guo, W., Zhao, J., et al. (2015). Circular RNA Is Enriched and Stable in Exosomes: a Promising Biomarker for Cancer Diagnosis. *Cell Res* 25, 981–984. doi:10.1038/cr.2015.82

Liang, B., Li, M., Deng, Q., Wang, C., Rong, J., He, S., et al. (2020). CircRNA ZNF609 in Peripheral Blood Leukocytes Acts as a Protective Factor and a Potential Biomarker for Coronary Artery Disease. *Ann. Transl Med.* 8, 741. doi:10.21037/atm-19-4728

Liang, G., Chen, S., Xin, S., and Dong, L. (2021). Overexpression of Hsa_circ_0001445 Reverses oxLDL-induced I-nhibition of HUVEC P-roliferation via SRSF1. *Mol. Med. Rep.* 24, 507. doi:10.3892/mmr.2021.12146

Lin, B., Xie, W., Zeng, C., Wu, X., Chen, A., Li, H., et al. (2021). Transfer of Exosomal microRNA-203-3p from Dendritic Cells to Bone Marrow-Derived Macrophages Reduces Development of Atherosclerosis by Downregulating Ctss in Mice. *aging* 13, 15638–15658. doi:10.18632/aging.103842

Liu, C., Ge, H.-M., Liu, B.-H., Dong, R., Shan, K., Chen, X., et al. (2019). Targeting Pericyte-Endothelial Cell Crosstalk by Circular RNA-cPWWP2A Inhibition Aggravates Diabetes-Induced Microvascular Dysfunction. *Proc. Natl. Acad. Sci. U.S.A.* 116, 7455–7464. doi:10.1073/pnas.1814874116

Liu, C., Yao, M.-D., Li, C.-P., Shan, K., Yang, H., Wang, J.-J., et al. (2017). Silencing of Circular RNA-Znf609 Ameliorates Vascular Endothelial Dysfunction. *Theranostics* 7, 2863–2877. doi:10.7150/thno.19353

Liu, L., Gu, T., Bao, X., Zheng, S., Zhao, J., and Zhang, L. (2019). Microarray Profiling of Circular RNA Identifies Hsa_circ_0126991 as a Potential Risk Factor for Essential Hypertension. *Cytogenet. Genome Res.* 157, 203–212. doi:10.1159/000500063

Liu, Y., Liu, H., Li, Y., Mao, R., Yang, H., Zhang, Y., et al. (2020). Circular RNA SAMD4A Controls Adipogenesis in Obesity through the miR-138-5p/EZH2 axis. *Theranostics* 10, 4705–4719. doi:10.7150/thno.42417

Lu, C., Chen, B., Chen, C., Li, H., Wang, D., Tan, Y., et al. (2020). CircNr1h4 Regulates the Pathological Process of Renal Injury in Salt-sensitive Hypertensive Mice by Targeting miR-155-5p. *J. Cel Mol Med* 24, 1700–1712. doi:10.1111/jcmm.14863

Luo, S., Deng, M., Xie, Z., Li, X., Huang, G., and Zhou, Z. (2021). Circulating Circular RNAs Profiles Associated with Type 1 Diabetes. *Diabetes Metab. Res. Rev.* 37, e3394. doi:10.1002/dmrr.3394

Ma, S., Chen, J., Feng, J., Zhang, R., Fan, M., Han, D., et al. (20182018). Melatonin Ameliorates the Progression of Atherosclerosis via Mitophagy Activation and NLRP3 Inflammasome Inhibition. *Oxidative Med. Cell Longevity* 2018, 1–12. doi:10.1155/2018/9286458

Maguire, E. M., Pearce, S. W. A., and Xiao, Q. (2019). Foam Cell Formation: A New Target for Fighting Atherosclerosis and Cardiovascular Disease. *Vasc. Pharmacol.* 112, 54–71. doi:10.1016/j.vph.2018.08.002

Mashburn, L. M., and Whiteley, M. (2005). Membrane Vesicles Traffic Signals and Facilitate Group Activities in a Prokaryote. *Nature* 437, 422–425. doi:10.1038/nature03925

Medici, D., Shore, E. M., Lounev, V. Y., Kaplan, F. S., Kalluri, R., and Olsen, B. R. (2010). Conversion of Vascular Endothelial Cells into Multipotent Stem-like Cells. *Nat. Med.* 16, 1400–1406. doi:10.1038/nm.2252

Miao, J., Wang, B., Shao, R., and Wang, Y. (2021). CircUSP36 Knockdown Alleviates Oxidized Low-density L-ipoprotein-induced C-ell I-njury and I-nflammatory R-esponses in H-uman U-mbilical V-ein E-ndothelial C-ells via the miR-20a-5p/ROCK2 axis. *Int. J. Mol. Med.* 47, 40. doi:10.3892/ijmm.2021.4873

Ng, W. L., Marinov, G. K., Liau, E. S., Lam, Y. L., Lim, Y.-Y., and Ea, C.-K. (2016). Inducible RasGEF1B Circular RNA Is a Positive Regulator of ICAM-1 in the TLR4/LPS Pathway. *RNA Biol.* 13, 861–871. doi:10.1080/15476286.2016.1207036

Nguyen, M.-A., Karunakaran, D., Geoffrion, M., Cheng, H. S., Tandoc, K., Perisic Matic, L., et al. (2018). Extracellular Vesicles Secreted by Atherogenic Macrophages Transfer MicroRNA to Inhibit Cell Migration. *Atvb* 38, 49–63. doi:10.1161/ATVBAHA.117.309795

Niu, C., Wang, X., Zhao, M., Cai, T., Liu, P., Li, J., et al. (2016). Macrophage Foam Cell-Derived Extracellular Vesicles Promote Vascular Smooth Muscle Cell Migration and Adhesion. *Jaha* 5, e004099. doi:10.1161/JAHA.116.004099

Pegtel, D. M., and Gould, S. J. (2019). Exosomes. *Annu. Rev. Biochem.* 88, 487–514. doi:10.1146/annurev-biochem-013118-111902

Peng, K., Jiang, P., Du, Y., Zeng, D., Zhao, J., Li, M., et al. (2021). Oxidized Low-density Lipoprotein Accelerates the Injury of Endothelial Cells via circ-USP36/miR -98-5p/VCAM1 axis. *IUBMB Life* 73, 177–187. doi:10.1002/iub.2419

Peng, M., Liu, X., and Xu, G. (2020). Extracellular Vesicles as Messengers in Atherosclerosis. *J. Cardiovasc. Trans. Res.* 13, 121–130. doi:10.1007/s12265-019-09923-z

Peng, W., Li, T., Pi, S., Huang, L., and Liu, Y. (2020). Suppression of Circular RNA circDHCR24 Alleviates Aortic Smooth Muscle Cell Proliferation and Migration by Targeting miR-149-5p/MMP9 axis. *Biochem. Biophysical Res. Commun.* 529, 753–759. doi:10.1016/j.bbrc.2020.06.067

Pietroiusti, A., Diomedi, M., Silvestrini, M., Cupini, L. M., Luzzi, I., Gomez-Miguel, M. J., et al. (2002). Cytotoxin-Associated Gene-A-Positive *Helicobacter pylori* Strains Are Associated with Atherosclerotic Stroke. *Circulation* 106, 580–584. doi:10.1161/01.cir.0000023894.10871.2f

Pothineni, N. V. K., Subramany, S., Kuriakose, K., Shirazi, L. F., Romeo, F., Shah, P. K., et al. (2017). Infections, Atherosclerosis, and Coronary Heart Disease. *Eur. Heart J.* 38, 3195–3201. doi:10.1093/eurheartj/ehx362

Rayner, K., Chen, Y.-X., McNulty, M., Simard, T., Zhao, X., Wells, D. J., et al. (2008). Extracellular Release of the Atheroprotective Heat Shock Protein 27 Is Mediated by Estrogen and Competitively Inhibits acLDL Binding to Scavenger Receptor-A. *Circ. Res.* 103, 133–141. doi:10.1161/CIRCRESAHA.108.172155

Rayner, K., Sun, J., Chen, Y.-X., McNulty, M., Simard, T., Zhao, X., et al. (2009). Heat Shock Protein 27 Protects against Atherogenesis via an Estrogen-dependent Mechanism. *Atvb* 29, 1751–1756. doi:10.1161/ATVBAHA.109.193656

Reilly, S. M., and Saltiel, A. R. (2017). Adapting to Obesity with Adipose Tissue Inflammation. *Nat. Rev. Endocrinol.* 13, 633–643. doi:10.1038/nrendo.2017.90

Reis, D. R. A., Medeiros-Fonseca, B., Costa, J. M., de Oliveira Neto, C. P., Gil da Costa, R. M., Oliveira, P. A., et al. (2020). HPV Infection as a Risk Factor for

Atherosclerosis: A Connecting Hypothesis. *Med. Hypotheses* 144, 109979. doi:10.1016/j.mehy.2020.109979

Ren, X. S., Tong, Y., Qiu, Y., Ye, C., Wu, N., Xiong, X. Q., et al. (2020). MiR155-5p in Adventitial Fibroblasts-derived Extracellular Vesicles Inhibits Vascular Smooth Muscle Cell Proliferation via Suppressing Angiotensin-converting Enzyme Expression. *J. Extracellular Vesicles* 9, 1698795. doi:10.1080/20013078.2019.1698795

Ryu, J., Choe, N., Kwon, D.-H., Shin, S., Lim, Y.-H., Yoon, G., et al. (2022). Circular RNA circSmoc1-2 Regulates Vascular Calcification by Acting as a miR-874-3p Sponge in Vascular Smooth Muscle Cells. *Mol. Ther. - Nucleic Acids* 27, 645–655. doi:10.1016/j.omtn.2021.12.031

Ryu, J., Kwon, D.-H., Choe, N., Shin, S., Jeong, G., Lim, Y.-H., et al. (2020). Characterization of Circular RNAs in Vascular Smooth Muscle Cells with Vascular Calcification. *Mol. Ther. - Nucleic Acids* 19, 31–41. doi:10.1016/j.omtn.2019.11.001

Sáez, T., de Vos, P., Kuipers, J., Sobrevia, L., and Faas, M. M. (2019). Exosomes Derived from Monocytes and from Endothelial Cells Mediate Monocyte and Endothelial Cell Activation under High D-Glucose Conditions. *Immunobiology* 224, 325–333. doi:10.1016/j.imbio.2019.02.004

Salzman, J., Chen, R. E., Olsen, M. N., Wang, P. L., and Brown, P. O. (2013). Cell-type Specific Features of Circular RNA Expression. *Plos Genet.* 9, e1003777. doi:10.1371/journal.pgen.1003777

Sanger, H. L., Klotz, G., Riesner, D., Gross, H. J., and Kleinschmidt, A. K. (1976). Viroids Are Single-Stranded Covalently Closed Circular RNA Molecules Existing as Highly Base-Paired Rod-like Structures. *Proc. Natl. Acad. Sci. U.S.A.* 73, 3852–3856. doi:10.1073/pnas.73.11.3852

Seimiya, T., Otsuka, M., Iwata, T., Shibata, C., Tanaka, E., Suzuki, T., et al. (2020). Emerging Roles of Exosomal Circular RNAs in Cancer. *Front. Cel Dev. Biol.* 8, 568366. doi:10.3389/fcell.2020.568366

Shi, R., Jin, Y., Hu, W., Lian, W., Cao, C., Han, S., et al. (2020). Exosomes Derived from Mmu_circ_0000250-Modified Adipose-Derived Mesenchymal Stem Cells Promote Wound Healing in Diabetic Mice by Inducing miR-128-3p/SIRT1-Mediated Autophagy. *Am. J. Physiology-Cell Physiol.* 318, C848–C856. doi:10.1152/ajpcell.00041.2020

Shimoda, A., Ueda, K., Nishiumi, S., Murata-Kamiya, N., Mukai, S.-a., Sawada, S.-i., et al. (2016). Exosomes as Nanocarriers for Systemic Delivery of the *Helicobacter pylori* Virulence Factor CagA. *Sci. Rep.* 6, 18346. doi:10.1038/srep18346

Simon, C., Greening, D. W., Bolumar, D., Balaguer, N., Salamonsen, L. A., and Vilella, F. (2018). Extracellular Vesicles in Human Reproduction in Health and Disease. *Endocr. Rev.* 39, 292–332. doi:10.1210/er.2017-00229

Song, C.-L., Wang, J.-P., Xue, X., Liu, N., Zhang, X.-H., Zhao, Z., et al. (2017). Effect of Circular ANRIL on the Inflammatory Response of Vascular Endothelial Cells in a Rat Model of Coronary Atherosclerosis. *Cell Physiol Biochem* 42, 1202–1212. doi:10.1159/000478918

Song, W., Majka, S. M., and McGuire, P. G. (1999). Hepatocyte Growth Factor Expression in the Developing Myocardium: Evidence for a Role in the Regulation of the Mesenchymal Cell Phenotype and Urokinase Expression. *Dev. Dyn.* 214, 92–100. doi:10.1002/(sici)1097-0177(199901)214:1<92::aid-dvdy9>3.0.co;2-x

Srikanthan, S., Li, W., Silverstein, R. L., and McIntyre, T. M. (2014). Exosome Poly-Ubiquitin Inhibits Platelet Activation, Downregulates CD36 and Inhibits Pro-atherothrombotic Cellular Functions. *J. Thromb. Haemost.* 12, 1906–1917. doi:10.1111/jth.12712

Stoll, L., Sobel, J., Rodriguez-Trejo, A., Guay, C., Lee, K., Venø, M. T., et al. (2018). Circular RNAs as Novel Regulators of β-cell Functions in normal and Disease Conditions. *Mol. Metab.* 9, 69–83. doi:10.1016/j.molmet.2018.01.010

Sun, C., Li, J., Li, Y., Li, L., and Huang, G. (2021). Circular RNA circUBR4 Regulates Ox-LDL-Induced Proliferation and Migration of Vascular Smooth Muscle Cells through miR-185-5p/FRS2 axis. *Mol. Cel Biochem* 476, 3899–3910. doi:10.1007/s11010-021-04207-0

Sun, W., Sun, X., Chu, W., Yu, S., Dong, F., and Xu, G. (2020). CircRNA Expression Profiles in Human Visceral Preadipocytes and Adipocytes. *Mol. Med. Rep.* 21, 815–821. doi:10.3892/mmr.2019.10886

Szabo, L., Morey, R., Palpant, N. J., Wang, P. L., Afari, N., Jiang, C., et al. (2015). Statistically Based Splicing Detection Reveals Neural Enrichment and Tissue-specific Induction of Circular RNA during Human Fetal Development. *Genome Biol.* 16, 126. doi:10.1186/s13059-015-0690-5

Tabas, I., and Lichtman, A. H. (2017). Monocyte-Macrophages and T Cells in Atherosclerosis. *Immunity* 47, 621–634. doi:10.1016/j.immuni.2017.09.008

Tang, N., Sun, B., Gupta, A., Rempel, H., and Pulliam, L. (2016). Monocyte Exosomes Induce Adhesion Molecules and Cytokines via Activation of NF-κB in Endothelial Cells. *FASEB j.* 30, 3097–3106. doi:10.1096/fj.201600368RR

Tao, Z., Zheng, S., He, X., Sun, J., He, C., and Zhang, L. (2021). Hsa_circ_0037897 May Be a Risk Factor for Essential Hypertension via Hsa-miR-145-5p. *Clin. Exp. Hypertens.* 43, 281–286. doi:10.1080/10641963.2020.1860081

Thietart, S., and Rautou, P.-E. (2020). Extracellular Vesicles as Biomarkers in Liver Diseases: A Clinician's point of View. *J. Hepatol.* 73, 1507–1525. doi:10.1016/j.jhep.2020.07.014

Toyofuku, M., Nomura, N., and Eberl, L. (2019). Types and Origins of Bacterial Membrane Vesicles. *Nat. Rev. Microbiol.* 17, 13–24. doi:10.1038/s41579-018-0112-2

van Meeteren, L. A., and ten Dijke, P. (2012). Regulation of Endothelial Cell Plasticity by TGF-β. *Cell Tissue Res* 347, 177–186. doi:10.1007/s00441-011-1222-6

van Niel, G., D'Angelo, G., and Raposo, G. (2018). Shedding Light on the Cell Biology of Extracellular Vesicles. *Nat. Rev. Mol. Cel Biol* 19, 213–228. doi:10.1038/nrm.2017.125

Velsko, I. M., Chukkapalli, S. S., Rivera, M. F., Lee, J.-Y., Chen, H., Zheng, D., et al. (2014). Active Invasion of Oral and Aortic Tissues by Porphyromonas Gingivalis in Mice Causally Links Periodontitis and Atherosclerosis. *PLoS One* 9, e97811. doi:10.1371/journal.pone.0097811

Vilades, D., Martínez-Camblor, P., Ferrero-Gregori, A., Bär, C., Lu, D., Xiao, K., et al. (2020). Plasma Circular RNA Hsa_circ_0001445 and Coronary Artery Disease: Performance as a Biomarker. *FASEB j.* 34, 4403–4414. doi:10.1096/fj.201902507R

Wadey, R. M., Connolly, K. D., Mathew, D., Walters, G., Rees, D. A., and James, P. E. (2019). Inflammatory Adipocyte-Derived Extracellular Vesicles Promote Leukocyte Attachment to Vascular Endothelial Cells. *Atherosclerosis* 283, 19–27. doi:10.1016/j.atherosclerosis.2019.01.013

Wang, C., Wu, H., Xing, Y., Ye, Y., He, F., Yin, Q., et al. (2022). Endothelial-derived Extracellular microRNA-92a Promotes Arterial Stiffness by Regulating Phenotype Changes of Vascular Smooth Muscle Cells. *Sci. Rep.* 12, 344. doi:10.1038/s41598-021-04341-1

Wang, F., Chen, X., Han, Y., Xi, S., and Wu, G. (2019). circRNA CDR1as Regulated the Proliferation of Human Periodontal Ligament Stem Cells under a Lipopolysaccharide-Induced Inflammatory Condition. *Mediators Inflamm.* 2019, 1–9. doi:10.1155/2019/1625381

Wang, H., Wei, M., Kang, Y., Xing, J., and Zhao, Y. (2020). Circular RNA circ_PVT1 Induces Epithelial-Mesenchymal Transition to Promote Metastasis of Cervical Cancer. *aging* 12, 20139–20151. doi:10.18632/aging.103679

Wang, L., Shen, C., Wang, Y., Zou, T., Zhu, H., Lu, X., et al. (2019). Identification of Circular RNA Hsa_circ_0001879 and Hsa_circ_0004104 as Novel Biomarkers for Coronary Artery Disease. *Atherosclerosis* 286, 88–96. doi:10.1016/j.atherosclerosis.2019.05.006

Wang, L., Zheng, Z., Feng, X., Zang, X., Ding, W., Wu, F., et al. (2019). circRNA/lncRNA-miRNA-mRNA Network in Oxidized, Low-Density, Lipoprotein-Induced Foam Cells. *DNA Cel Biol.* 38, 1499–1511. doi:10.1089/dna.2019.4865

Wang, Q., Dong, Y., and Wang, H. (2022). microRNA-19b-3p-containing Extracellular Vesicles Derived from Macrophages Promote the Development of Atherosclerosis by Targeting JAZF1. *J. Cell. Mol. Medi* 26, 48–59. doi:10.1111/jcmm.16938

Wang, S., Zhang, K., Tan, S., Xin, J., Yuan, Q., Xu, H., et al. (2021). Circular RNAs in Body Fluids as Cancer Biomarkers: the New Frontier of Liquid Biopsies. *Mol. Cancer* 20, 13. doi:10.1186/s12943-020-01298-z

Wang, S., Zhan, J., Lin, X., Wang, Y., Wang, Y., and Liu, Y. (2020). CircRNA -0077930 from Hyperglycaemia-stimulated Vascular Endothelial Cell Exosomes Regulates Senescence in Vascular Smooth Muscle Cells. *Cell Biochem Funct* 38, 1056–1068. doi:10.1002/cbf.3543

Wang, X., and Bai, M. (2021). CircTM7SF3 Contributes to Oxidized Low-Density Lipoprotein-Induced Apoptosis, Inflammation and Oxidative Stress through Targeting miR-206/ASPH axis in Atherosclerosis Cell Model *In Vitro*. *BMC Cardiovasc. Disord.* 21, 51. doi:10.1186/s12872-020-01800-x

Wang, Y., Han, D., Zhou, T., Zhang, J., Liu, C., Cao, F., et al. (2020). Melatonin Ameliorates Aortic Valve Calcification via the Regulation of Circular RNA

CircRIC3/miR-204-5p/DPP4 Signaling in Valvular Interstitial Cells. *J. Pineal Res.* 69, e12666. doi:10.1111/jpi.12666

Wang, Y., Wang, H., Zheng, R., Wu, P., Sun, Z., Chen, J., et al. (2021). Circular RNA ITCH Suppresses Metastasis of Gastric Cancer via Regulating miR-199a-5p/Klotho axis. *Cell Cycle* 20, 522–536. doi:10.1080/15384101.2021.1878327

Wang, Y., Zhao, R., Liu, W., Wang, Z., Rong, J., Long, X., et al. (2019). Exosomal circHIPK3 Released from Hypoxia-Pretreated Cardiomyocytes Regulates Oxidative Damage in Cardiac Microvascular Endothelial Cells via the miR-29a/IGF-1 Pathway. *Oxidative Med. Cell Longevity* 2019, 1–28. doi:10.1155/2019/7954657

Wang, Z., Zhu, H., Shi, H., Zhao, H., Gao, R., Weng, X., et al. (2019). Exosomes Derived from M1 Macrophages Aggravate Neointimal Hyperplasia Following Carotid Artery Injuries in Mice through miR-222/CDKN1B/CDKN1C Pathway. *Cel Death Dis* 10, 422. doi:10.1038/s41419-019-1667-1

Wen, Y., Chun, Y., Lian, Z., Yong, Z., Lan, Y., Huan, L., et al. (2021). circRNA-0006896-miR1264-DNMT1 axis P-lays an I-mportant R-ole in C-arotid P-laque D-estabilization by R-egulating the B-ehavior of E-ndothelial C-ells in A-therosclerosis. *Mol. Med. Rep.* 23, 311. doi:10.3892/mmr.2021.11950

Wu, G., Zhou, W., Pan, X., Sun, Z., Sun, Y., Xu, H., et al. (2020). Circular RNA Profiling Reveals Exosomal Circ_0006156 as a Novel Biomarker in Papillary Thyroid Cancer. *Mol. Ther. - Nucleic Acids* 19, 1134–1144. doi:10.1016/j.omtn.2019.12.025

Wu, N., Jin, L., and Cai, J. (2017). Profiling and Bioinformatics Analyses Reveal Differential Circular RNA Expression in Hypertensive Patients. *Clin. Exp. Hypertens.* 39, 454–459. doi:10.1080/10641963.2016.1273944

Xia, Q., Ding, T., Zhang, G., Li, Z., Zeng, L., Zhu, Y., et al. (2018). Circular RNA Expression Profiling Identifies Prostate Cancer- Specific circRNAs in Prostate Cancer. *Cel Physiol Biochem* 50, 1903–1915. doi:10.1159/000494870

Xia, X., Zhang, L., Chi, J., Li, H., Liu, X., Hu, T., et al. (2020). *Helicobacter pylori* Infection Impairs Endothelial Function through an Exosome-Mediated Mechanism. *Jaha* 9, e014120. doi:10.1161/JAHA.119.014120

Xie, Z., Wang, X., Liu, X., Du, H., Sun, C., Shao, X., et al. (2018). Adipose-Derived Exosomes Exert Proatherogenic Effects by Regulating Macrophage Foam Cell Formation and Polarization. *Jaha* 7, e007442. doi:10.1161/JAHA.117.007442

Xu, F., Shen, L., Chen, H., Wang, R., Zang, T., Qian, J., et al. (2021). circDENND1B Participates in the Antiatherosclerotic Effect of IL-1β Monoclonal Antibody in Mouse by Promoting Cholesterol Efflux via miR-17-5p/Abca1 Axis. *Front. Cel Dev. Biol.* 9, 652032. doi:10.3389/fcell.2021.652032

Xu, H., Guo, S., Li, W., and Yu, P. (2015). The Circular RNA Cdr1as, via miR-7 and its Targets, Regulates Insulin Transcription and Secretion in Islet Cells. *Sci. Rep.* 5, 12453. doi:10.1038/srep12453

Xu, L., Geng, T., Zang, G., Bo, L., Liang, Y., Zhou, H., et al. (2020). Exosome Derived from CD137-modified Endothelial Cells Regulates the Th17 Responses in Atherosclerosis. *J. Cel Mol Med* 24, 4659–4667. doi:10.1111/jcmm.15130

Xu, L., Ji, H., Jiang, Y., Cai, L., Lai, X., Wu, F., et al. (2020). Exosomes Derived from CircAkap7-Modified Adipose-Derived Mesenchymal Stem Cells Protect against Cerebral Ischemic Injury. *Front. Cel Dev. Biol.* 8, 569977. doi:10.3389/fcell.2020.569977

Xu, L., Liao, W.-L., Lu, Q.-J., Zhang, P., Zhu, J., and Jiang, G.-N. (2021). Hypoxic Tumor-Derived Exosomal Circular RNA SETDB1 Promotes Invasive Growth and EMT via the miR-7/Sp1 axis in Lung Adenocarcinoma. *Mol. Ther. - Nucleic Acids* 23, 1078–1092. doi:10.1016/j.omtn.2021.01.019

Xu, Y., Qiu, A., Peng, F., Tan, X., Wang, J., and Gong, X. (2021). Exosomal Transfer of Circular RNA FBXW7 Ameliorates the Chemoresistance to Oxaliplatin in Colorectal Cancer by Sponging miR-18b-5p. *neo* 68, 108–118. doi:10.4149/neo_2020_200417N414

Yan, C., Tian, X., Li, J., Liu, D., Ye, D., Xie, Z., et al. (2021). A High-Fat Diet Attenuates AMPK α1 in Adipocytes to Induce Exosome Shedding and Nonalcoholic Fatty Liver Development *In Vivo*. *Diabetes* 70, 577–588. doi:10.2337/db20-0146

Yang, F., Chen, Y., Xue, Z., Lv, Y., Shen, L., Li, K., et al. (2020). High-Throughput Sequencing and Exploration of the lncRNA-circRNA-miRNA-mRNA Network in Type 2 Diabetes Mellitus. *Biomed. Res. Int.* 2020, 1–13. doi:10.1155/2020/8162524

Yang, L., Han, B., Zhang, Y., Bai, Y., Chao, J., Hu, G., et al. (2018). Engagement of Circular RNA HECW2 in the Nonautophagic Role of ATG5 Implicated in the Endothelial-Mesenchymal Transition. *Autophagy* 14, 404–418. doi:10.1080/15548627.2017.1414755

Yang, L., Han, B., Zhang, Z., Wang, S., Bai, Y., Zhang, Y., et al. (2020). Extracellular Vesicle-Mediated Delivery of Circular RNA SCMH1 Promotes Functional Recovery in Rodent and Nonhuman Primate Ischemic Stroke Models. *Circulation* 142, 556–574. doi:10.1161/CIRCULATIONAHA.120.045765

Yang, S., Xia, Y.-p., Luo, X.-y., Chen, S.-l., Li, B.-w., Ye, Z.-m., et al. (2019). Exosomal CagA Derived from Helicobacter Pylori-Infected Gastric Epithelial Cells Induces Macrophage Foam Cell Formation and Promotes Atherosclerosis. *J. Mol. Cell Cardiol.* 135, 40–51. doi:10.1016/j.yjmcc.2019.07.011

Yang, W. W., Guo, B., Jia, W. Y., and Jia, Y. (2016). Porphyromonas Gingivalis-Derived Outer Membrane Vesicles Promote Calcification of Vascular Smooth Muscle Cells through ERK1/2-RUNX2. *FEBS Open Bio* 6, 1310–1319. doi:10.1002/2211-5463.12151

Yang, Y., Luo, N.-S., Ying, R., Xie, Y., Chen, J.-Y., Wang, X.-Q., et al. (2017). Macrophage-derived Foam Cells Impair Endothelial Barrier Function by Inducing Endothelial-Mesenchymal Transition via CCL-4. *Int. J. Mol. Med.* 40, 558–568. doi:10.3892/ijmm.2017.3034

Yao, J., Wu, D., Zhang, C., Yan, T., Zhao, Y., Shen, H., et al. (2021). Macrophage IRX3 Promotes Diet-Induced Obesity and Metabolic Inflammation. *Nat. Immunol.* 22, 1268–1279. doi:10.1038/s41590-021-01023-y

Ye, L., Guo, H., Wang, Y., Peng, Y., Zhang, Y., Li, S., et al. (2021). Exosomal circEhmt1 Released from Hypoxia-Pretreated Pericytes Regulates High Glucose-Induced Microvascular Dysfunction via the NFIA/NLRP3 Pathway. *Oxidative Med. Cell Longevity* 2021, 1–13. doi:10.1155/2021/8833098

Yin, L., Yao, J., Deng, G., Wang, X., Cai, W., and Shen, J. (2020). Identification of Candidate lncRNAs and circRNAs Regulating WNT3/β-Catenin Signaling in Essential Hypertension. *Aging* 12, 8261–8288. doi:10.18632/aging.103137

Yu, C., Wu, D., Zhao, C., and Wu, C. (2021). CircRNA TGFBR2/MiR-25-3p/TWIST1 axis Regulates Osteoblast Differentiation of Human Aortic Valve Interstitial Cells. *J. Bone Miner Metab.* 39, 360–371. doi:10.1007/s00774-020-01164-4

Yu, F., Tie, Y., Zhang, Y., Wang, Z., Yu, L., Zhong, L., et al. (2020). Circular RNA Expression Profiles and Bioinformatic Analysis in Coronary Heart Disease. *Epigenomics* 12, 439–454. doi:10.2217/epi-2019-0369

Yu, H., Zhao, L., Zhao, Y., Fei, J., and Zhang, W. (2020). Circular RNA Circ_0029589 Regulates Proliferation, Migration, Invasion, and Apoptosis in Ox-LDL-Stimulated VSMCs by Regulating miR-424-5p/IGF2 axis. *Vasc. Pharmacol.* 135, 106782. doi:10.1016/j.vph.2020.106782

Yu, T., Ding, Y., Zhang, Y., Liu, Y., Li, Y., Lei, J., et al. (2019). Circular RNA GATAD2A Promotes H1N1 Replication through Inhibiting Autophagy. *Vet. Microbiol.* 231, 238–245. doi:10.1016/j.vetmic.2019.03.012

Zeng, W., Liu, Y., Li, W. T., Li, Y., and Zhu, J. F. (2020). CircFNDC3B Sequestrates miR-937-5p to Derepress TIMP3 and Inhibit Colorectal Cancer Progression. *Mol. Oncol.* 14, 2960–2984. doi:10.1002/1878-0261.12796

Zhang, C., Wang, L., and Shen, Y. (2021). Circ_0004104 Knockdown Alleviates Oxidized Low-Density Lipoprotein-Induced Dysfunction in Vascular Endothelial Cells through Targeting miR-328-3p/TRIM14 axis in Atherosclerosis. *BMC Cardiovasc. Disord.* 21, 207. doi:10.1186/s12872-021-02012-7

Zhang, C., Han, X., Yang, L., Fu, J., Sun, C., Huang, S., et al. (2020). Circular RNA circPPM1F Modulates M1 Macrophage Activation and Pancreatic Islet Inflammation in Type 1 Diabetes Mellitus. *Theranostics* 10, 10908–10924. doi:10.7150/thno.48264

Zhang, H., Zhu, L., Bai, M., Liu, Y., Zhan, Y., Deng, T., et al. (2019). Exosomal circRNA Derived from Gastric Tumor Promotes white Adipose browning by Targeting the miR-133/PRDM16 Pathway. *Int. J. Cancer* 144, 2501–2515. doi:10.1002/ijc.31977

Zhang, S., Guo, Y., Ma, Y., and Teng, Y. (2008). Cytotoxin-associated Gene-A-Seropositive Virulent Strains of *Helicobacter pylori* and Atherosclerotic Diseases: a Systematic Review. *Chin. Med. J.* 121, 946–951. doi:10.1097/00029330-200805020-00015

Zhang, S., Song, G., Yuan, J., Qiao, S., Xu, S., Si, Z., et al. (2020). RETRACTED ARTICLE: Circular RNA Circ_0003204 Inhibits Proliferation, Migration and Tube Formation of Endothelial Cell in Atherosclerosis via miR-370-3p/TGFβR2/phosph-SMAD3 axis. *J. Biomed. Sci.* 27, 11. doi:10.1186/s12929-019-0595-9

Zhang, T., Zhang, Z., Xia, T., Liu, C., and Sun, C. (2019). circNrxn2 Promoted WAT Browning via Sponging miR-103 to Relieve its Inhibition of FGF10 in HFD Mice. *Mol. Ther. - Nucleic Acids* 17, 551–562. doi:10.1016/j.omtn.2019.06.019

Zhang, X., Chen, L., Xiao, B., Liu, H., and Su, Y. (2019). Circ_0075932 in Adipocyte-Derived Exosomes Induces Inflammation and Apoptosis in Human Dermal Keratinocytes by Directly Binding with PUM2 and Promoting PUM2-Mediated Activation of AuroraA/NF-Kb Pathway. *Biochem. Biophysical Res. Commun.* 511, 551–558. doi:10.1016/j.bbrc.2019.02.082

Zhang, Y., Liu, X., Bai, X., Lin, Y., Li, Z., Fu, J., et al. (2018). Melatonin Prevents Endothelial Cell Pyroptosis via Regulation of Long Noncoding RNA MEG3/miR-223/NLRP3 axis. *J. Pineal Res.* 64, e12449. doi:10.1111/jpi.12449

Zhang, Y., Wang, Z., Shi, B., Li, Y., Wang, R., Sun, J., et al. (2021). Effect of Gingival Mesenchymal Stem Cell-Derived Exosomes on Inflammatory Macrophages in a High-Lipid Microenvironment. *Int. Immunopharmacology* 94, 107455. doi:10.1016/j.intimp.2021.107455

Zhang, Y., Zhang, H., An, M., Zhao, B., Ding, H., Zhang, Z., et al. (2018). Crosstalk in Competing Endogenous RNA Networks Reveals New Circular RNAs Involved in the Pathogenesis of Early HIV Infection. *J. Transl Med.* 16, 332. doi:10.1186/s12967-018-1706-1

Zhang, Z., Yi, D., Zhou, J., Zheng, Y., Gao, Z., Hu, X., et al. (2020). Exosomal LINC01005 Derived from Oxidized Low-density Lipoprotein-treated Endothelial Cells Regulates Vascular Smooth Muscle Cell Phenotypic Switch. *Biofactors* 46, 743–753. doi:10.1002/biof.1665

Zhang, Z., Zhang, T., Feng, R., Huang, H., Xia, T., and Sun, C. (2019). circARF3 Alleviates Mitophagy-Mediated Inflammation by Targeting miR-103/TRAF3 in Mouse Adipose Tissue. *Mol. Ther. - Nucleic Acids* 14, 192–203. doi:10.1016/j.omtn.2018.11.014

Zheng, J., Li, Z., Wang, T., Zhao, Y., and Wang, Y. (2017). Microarray Expression Profile of Circular RNAs in Plasma from Primary Biliary Cholangitis Patients. *Cel Physiol Biochem* 44, 1271–1281. doi:10.1159/000485487

Zheng, S., Gu, T., Bao, X., Sun, J., Zhao, J., Zhang, T., et al. (2019). Circular RNA Hsa_circ_0014243 May Serve as a Diagnostic Biomarker for Essential Hypertension. *Exp. Ther. Med.* 17, 1728–1736. doi:10.3892/etm.2018.7107

Zheng, S., He, X., Sun, J., Li, Q., Zhang, T., and Zhang, L. (2020). The Up-regulated hsa-circRNA9102-5 May Be a Risk Factor for Essential Hypertension. *J. Clin. Lab. Anal.* 34, e23339. doi:10.1002/jcla.23339

Zhou, X., Li, Z., Qi, M., Zhao, P., Duan, Y., Yang, G., et al. (2020). Brown Adipose Tissue-Derived Exosomes Mitigate the Metabolic Syndrome in High Fat Diet Mice. *Theranostics* 10, 8197–8210. doi:10.7150/thno.43968

Zhu, C., Su, Y., Liu, L., Wang, S., Liu, Y., and Wu, J. (2020). Circular RNA Hsa_circ_0004277 Stimulates Malignant Phenotype of Hepatocellular Carcinoma and Epithelial-Mesenchymal Transition of Peripheral Cells. *Front. Cel Dev. Biol.* 8, 585565. doi:10.3389/fcell.2020.585565

Zhu, J., Liu, B., Wang, Z., Wang, D., Ni, H., Zhang, L., et al. (2019). Exosomes from Nicotine-Stimulated Macrophages Accelerate Atherosclerosis through miR-21-3p/PTEN-Mediated VSMC Migration and Proliferation. *Theranostics* 9, 6901–6919. doi:10.7150/thno.37357

Zhu, X., Ding, J., Wang, B., Wang, J., and Xu, M. (2019). Circular RNA DLGAP4 Is Down-Regulated and Negatively Correlates with Severity, Inflammatory Cytokine Expression and Pro-inflammatory Gene miR-143 Expression in Acute Ischemic Stroke Patients. *Int. J. Clin. Exp. Pathol.* 12, 941–948.

Zhu, Y., Gui, W., Lin, X., and Li, H. (2020). Knock-down of Circular RNA H19 Induces Human Adipose-Derived Stem Cells Adipogenic Differentiation via a Mechanism Involving the Polypyrimidine Tract-Binding Protein 1. *Exp. Cel Res.* 387, 111753. doi:10.1016/j.yexcr.2019.111753

Zhu, Y., Xian, X., Wang, Z., Bi, Y., Chen, Q., Han, X., et al. (2018). Research Progress on the Relationship between Atherosclerosis and Inflammation. *Biomolecules* 8, 80. doi:10.3390/biom8030080

Zhuang, J. B., Li, T., Hu, X. M., Ning, M., Gao, W. Q., Lang, Y. H., et al. (2020). Circ_CHFR Expedites Cell Growth, Migration and Inflammation in Ox-LDL-Treated Human Vascular Smooth Muscle Cells via the miR-214-3p/Wnt3/β-Catenin Pathway. *Eur. Rev. Med. Pharmacol. Sci.* 24, 3282–3292. doi:10.26355/eurrev_202003_20696

Conflict of Interest: The authors declare that the research was conducted in the absence of any commercial or financial relationships that could be construed as a potential conflict of interest.

Publisher's Note: All claims expressed in this article are solely those of the authors and do not necessarily represent those of their affiliated organizations, or those of the publisher, the editors and the reviewers. Any product that may be evaluated in this article, or claim that may be made by its manufacturer, is not guaranteed or endorsed by the publisher.

frontiers in Cell and Developmental Biology

ORIGINAL RESEARCH
published: 18 March 2022
doi: 10.3389/fcell.2022.817180

Therapeutic Potential of Stem Cell-Derived Extracellular Vesicles on Atherosclerosis-Induced Vascular Dysfunction and Its Key Molecular Players

*Ioana Karla Comarița[1†], Alexandra Vîlcu[1†], Alina Constantin[1], Anastasia Procopciuc[1], Florentina Safciuc[1], Nicoleta Alexandru[1], Emanuel Dragan[1], Miruna Nemecz[1], Alexandru Filippi[3], Leona Chițoiu[2], Mihaela Gherghiceanu[2,3] and Adriana Georgescu[1]**

[1]Institute of Cellular Biology and Pathology 'Nicolae Simionescu' of Romanian Academy, Bucharest, Romania, [2]'Victor Babeș' National Institute of Pathology, Bucharest, Romania, [3]'Carol Davila' University of Medicine and Pharmacy, Bucharest, Romania

OPEN ACCESS

Edited by:
Xiaoheng Liu,
Sichuan University, China

Reviewed by:
Ewa Stepien,
Jagiellonian University, Poland
Panpan Wang,
Jinan University, China

***Correspondence:**
Adriana Georgescu
adriana.georgescu@icbp.ro

[†]These authors have contributed equally to this work

Specialty section:
This article was submitted to Molecular and Cellular Pathology, a section of the journal Frontiers in Cell and Developmental Biology

Received: *17 November 2021*
Accepted: *10 February 2022*
Published: *18 March 2022*

Citation:
Comarița IK, Vîlcu A, Constantin A, Procopciuc A, Safciuc F, Alexandru N, Dragan E, Nemecz M, Filippi A, Chițoiu L, Gherghiceanu M and Georgescu A (2022) Therapeutic Potential of Stem Cell-Derived Extracellular Vesicles on Atherosclerosis-Induced Vascular Dysfunction and Its Key Molecular Players. Front. Cell Dev. Biol. 10:817180. doi: 10.3389/fcell.2022.817180

Atherosclerosis is a progressive, chronic inflammatory disease of the large arteries caused by the constant accumulation of cholesterol, followed by endothelial dysfunction and vascular inflammation. We hypothesized that delivery of extracellular vesicles (EVs), recognized for their potential as therapeutic targets and tools, could restore vascular function in atherosclerosis. We explored by comparison the potential beneficial effects of EVs from subcutaneous adipose tissue stem cells (EVs (ADSCs)) or bone marrow mesenchymal stem cells (EVs (MSCs)) on the consequences of atherogenic diet on vascular health. Also, the influences of siRNA-targeting Smad2/3 (Smad2/3siRNA) on endothelial dysfunction and its key molecular players were analyzed. For this study, an animal model of atherosclerosis (HH) was transplanted with EVs (ADSCs) or EVs (MSCs) transfected or not with Smad2/3siRNA. For controls, healthy or HH animals were used. The results indicated that by comparison with the HH group, the treatment with EVs(ADSCs) or EVs(MSCs) alone or in combination with Smad2/3siRNA of HH animals induced a significant decrease in the main plasma parameters and a noticeable improvement in the structure and function of the thoracic aorta and carotid artery along with a decrease in the selected molecular and cellular targets mediating their changes in atherosclerosis: **1)** a decrease in expression of structural and inflammatory markers COL1A1, α-SMA, Cx43, VCAM-1, and MMP-2; **2)** a slight infiltration of total/M1 macrophages and T-cells; **3)** a reduced level of cytosolic ROS production; **4)** a significant diminution in plasma concentrations of TGF-β1 and Ang II proteins; **5)** significant structural and functional improvements (thinning of the arterial wall, increase of the inner diameter, enhanced distensibility, diminished VTI and Vel, and augmented contractile and relaxation responses); **6)** a reduced protein expression profile of Smad2/3, ATF-2, and NF-kBp50/p65 and a significant decrease in the expression levels of miR-21, miR-29a, miR-192, miR-200b, miR-210, and miR-146a. We can conclude that **1)** stem cell-derived EV therapies, especially the EVs (ADSCs) led to regression of structural and functional changes in the vascular wall and of key orchestrator expression in the atherosclerosis-induced endothelial

dysfunction; **2)** transfection of EVs with Smad2/3siRNA amplified the ability of EVs(ADSCs) or EVs(MSCs) to regress the inflammation-mediated atherosclerotic process.

Keywords: vascular dysfunction, inflammation, atherosclerosis, cardiovascular diseases, extracellular vesicles, siRNA Smad2/3

INTRODUCTION

Atherosclerosis is a chronic, fibroproliferative inflammatory disease that affects the structure and function of large and medium arteries. To this day, it is considered the main cause of cardiovascular disease (CVD), with a very high mortality and morbidity rate in developed countries.

Atherogenesis is a slow, multistage process involving successive events and is characterized by the accumulation of lipids, especially cholesterol crystals in the vascular intima, macrophage infiltration, smooth muscle cell (SMC) proliferation with changing phenotype, accumulation of connective tissue components that by fibroblasts and calcification determine stiffening of the arteries, obstruction of blood flow, and formation of thrombus (Manduteanu & Simionescu, 2012).

Atherosclerosis is a progressive, complex vascular disease with an autoimmune component, which is not only a degenerative consequence, inevitable aging, but also an inflammatory condition, which can be transformed into an acute clinical event, by rupture of the atheroma plaque, clot formation, and by installing thrombosis (Amaya-Amaya, Montoya-Sanchez, & Rojas-Villarraga, 2014). In the context of atherosclerotic disease, there is a tight link between immunological and metabolic processes, especially the interaction between lipids (mainly cholesterol), the way in which activates the cells of the immune system and the associated inflammatory response. The evolution of atherosclerotic disease is induced by the innate and adaptive immune system responses that are regulated by a diversity of cytokines (Ait-Oufella, Taleb, Mallat, & Tedgui, 2011; Buckley & Ramji, 2015). Transforming growth factor beta 1 (TGF-β1) is a pleiotropic cytokine that can be either pro-atherogenic or antiatherogenic depending on the neighboring conditions (McLaren, Michael, Ashlin, & Ramji, 2011; Ramji & Davies, 2015). The TGF-β1 intervenes in the canonical signaling pathway that mediates the formation of the complex with Smad2 and Smad3 proteins. Any disturbance in the expression of TGF-β1 causes the initiation of important vascular effects that influence the way the atherosclerotic lesion evolves such as fibrosis induction, extracellular matrix (ECM) remodeling and change of vascular smooth-muscle cells (VSMCs) into a pathological phenotype, lipid accumulation followed by stimulating the expression of biglycan, promotion of cell apoptosis, and increase of gene expression of molecules with pro-atherogenic properties (e.g., plasminogen activator inhibitor type 1 (PAI-1) and monocyte chemoattractant protein-1 (MCP-1)). Moreover, it is well acknowledged that target genes activated and regulated by the TGF-β1/Smad2/3 signaling pathway, considered a hallmark of many vascular diseases, encode for type I and III collagen, connective tissue growth factor (CTGF), and ECM, which are key events in the development of vascular intimal hyperplasia (Kalinina et al., 2004; Schiffer, von Gersdorff, Bitzer, Susztak, & Bottinger, 2000).

Numerous animal studies with diet-induced atherosclerosis have been able to provide essential information on understanding the mechanisms underlying this pathology (Georgescu et al., 2016). Many studies have shown that when endothelial cells are activated, they secrete a number of nanovesicles that would help initiate and aggravate the atherogenic process. The term nanovesicles, also known as extracellular vesicles (EVs), bring together two separate classes of small particles of the order of nm called exosomes (40–100 nm) and microparticles (MPs) or microvesicles (MVs) (100–1,500 nm) that are released by cells physiologically, and in pathological conditions this release is amplified (Alexandru et al., 2021; Simionescu, Zonda, Petrovici, & Georgescu, 2021). These vesicles are rich in lipids, proteins, and microRNAs (miRNAs) and have the ability to regulate posttranscriptional gene expression in target cells (Constantin, Filippi, Alexandru, Nemecz, & Georgescu, 2020). The data claim that after their release into the circulation, they would fuse with the target cells using receptor–ligand structures, transferring inflammatory cellular components that originate from the source cells to the recipient cells (Georgescu & Simionescu, 2021). In this way, they become nanocarriers that could also carry a separate class of endogenous miRNAs, affecting gene and protein expression, aggravating the evolution of the pathology as a whole; thus, they can be seen as biomarkers for endothelial dysfunction when their circulating levels are increased (Georgescu et al., 2009; Georgescu et al., 2012).

In this consensus, the ability of vesicles to become messengers of healthy biological information was also observed when released by clinically healthy cells (Alexandru et al., 2017; Alexandru et al., 2020). Also, more and more treatments are being developed on the use of miRNA-based therapeutic strategies in an attempt to modulate and ameliorate their effect. It is known that this complex regulatory network is involved in numerous intracellular signaling pathways disrupting the function of gene and/or several genes that could aggravate and contribute to complications, especially when these miRNAs are overexpressed. Therefore, new approaches to inhibit altered miRNAs could improve and mitigate these changes by restoring normal function. Therapeutic strategies based on targeting short nucleic acids on transcription factors could modulate the transduction of signals in the intracellular network both transcriptionally and posttranscriptionally, inhibiting the expression of target genes involved in inflammation, fibrosis, and vascular remodeling due to atherosclerosis. The most widely used systems today are nonviral lipid and polymer-based siRNA delivery systems

called lipoplexes, polyplexes, or liposomes, with dimensions ranging from 100–200 nm, which when administered systemically showed that they have been extensively taken up by the vasculature of the heart. All of these features should be considered for their implementation in clinical trials/application.

According to these data, the use of EVs that are lipid bilayer-delimited particles could serve as exogenous siRNA embedding systems and can be used as RNA interference-based therapy for silencing the genes involved in downstream signaling of pro-inflammatory and pro-angiogenic stimuli (Dorsett & Tuschl, 2004; Kowalski et al., 2011; Youn & Park, 2015). Also, the potential of using a targeted therapy based on Smad2/3 siRNA to block Smad2/3, pivotal downstream effectors in development of atheroma function, could protect against atherosclerosis development.

However, there are not enough data on new approaches by which these noncellular therapeutic agents could detect the first signs of the disease and also the effective way in which they could regress the changes already installed. Currently, the implementation and development of emerging technologies that allow the identification of biomarkers could represent a new stage in the early diagnosis of atherosclerotic CVD. These would be an essential step in how patients can be monitored depending on the prognosis of the disease, the risk of developing complications, and their use for therapeutic purposes.

Based on all these data, we set out to investigate the effects of EVs-based nanotherapeutics on atherosclerosis-induced vascular dysfunction and its key molecular players. Since Smad2/3-mediated TGF-β1/AngII signaling is known to have a decisive role in vascular inflammation and atherogenesis, we decided to block SMAD 2/3 as well. For this purpose, an animal model of atherosclerosis, hypertensive–hyperlipidemic (HH) hamster, was transplanted with EVs (ADSCs) or EVs (MSCs) transfected or not with Smad2/3 siRNA. Generally speaking, EV or the RNA interference technologies are widely applied in the development of experimental therapeutic for many diseases. We analyzed by comparing the effects of EVs (ADSCs) or EVs (MSCs) transfected or not with Smad2/3 siRNA on consequences of atherogenic diet on vascular health.

MATERIALS AND METHODS

Experimental Murine Models With Diet-Induced Atherosclerotic Cardiovascular Disease Transplanted With Extracellular Vesicles (Adipose Tissue Stem Cells) or Extracellular Vesicles (Mesenchymal Stem Cells) Transfected or Not With Smad2/3 siRNA

A total of 77 male golden Syrian hamsters, 3 months of age, 117.8 ± 2.81 g body weight, were divided into seven experimental groups: normal healthy animals fed with standard food containing basal 1%NaCl for 4 months (*C group*); simultaneously, hypertensive–hyperlipidemic animals generated by combining two feeding conditions (the standard chow enriched with 3% cholesterol and 15% butter for hyperlipemia and 8% NaCl gavage for hypertension) administered daily for 4 months (*HH group*); HH animals transplanted with 100 μg/ml EVs (ADSCs) or EVs (MSCs) obtained from healthy hamsters, transfected or not with 100 nM Smad2/3 siRNA, by using retro-orbital sinus injections (in a volume of 300 μL phosphate-buffered saline (PBS)) once a month for 4 months, starting with the second week of the atherogenic diet (*HH-EVs (ADSCs), HH-EVs (MSCs)*, *HH-EVs (ADSCs)+ Smad2/3 siRNA*, and *HH-EVs (MSCs)+ Smad2/3 siRNA* groups); HH animals treated with Smad2/3 siRNA (100 nM in a volume of 300 μL PBS) via subcutaneous injections administrated once a month for 4 months, starting with the second week of the atherogenic diet (*HH-Smad2/3 siRNA group*) (**Figure 1**).

All experimental groups of hamsters thus obtained were kept in the same housing conditions at 25°C with a 12/12 h light/dark cycle. At the end of the 4 months (16 weeks) of the diet, hamsters were weighed to assess body weight and anesthetized with 2% isoflurane for blood collection. Subsequently, they were sacrificed under anesthesia (a mixture of 80 mg ketamine, 10 mg xylazine, and 2 mg acepromazine/kg body weight in a sterile isotonic saline (0.9% saline)), perfused with PBS containing 1 mM $CaCl_2$ for tissues blood removal, in order to collect the organs of interest (thoracic aorta and carotid arteries for biochemical, structural, and functional assays). All the protocols for animal use were approved by the Ethics Committee from the Institute of Cellular Biology and Pathology "Nicolae Simionescu" according to Decision No.11/08.08.2017 and National Sanitary Veterinary and Food Safety Authority (Bucharest, Romania) in compliance with Project Authorization No. 575/13.11.2020. Also, all the experiments on animals were conducted in accordance with the Guide of the Care and Use of Laboratory Animals published by the US National Institutes of Health (NIH publication no. 85–23, revised 1996) and were conducted in accordance with national, European, and international legislation on the use of experimental animals in biomedical research.

Isolation and Characterization of Adipose Tissue Stem Cells and BM-Mesenchymal Stem Cells

In order to obtain ADSCs and BM-MSCs, two main tissue sources were used: subcutaneous adipose tissue and hematogenous bone marrow tissue from the tibia and femoral marrow compartments, harvested from 50 hamsters of healthy origin. The cells obtained in the primary culture were kept in an incubator with 5% CO_2 and maintained at 37°C until they reached confluence in DMEM/F-12 (Dulbecco's modified Eagle medium/nutrient mixture F-12) (Gibco) containing 10% fetal bovine serum (FBS) (Gibco) for ADSC and DMEM, high glucose, GlutaMAX™ Supplement, and pyruvate (Gibco) with 10% FBS for BM-MSC, and both media being supplemented with 1% antibiotics (mix of penicillin, neomycin, and streptomycin). The percentage of cell viability was evaluated by trypan blue exclusion assay. When culture reached about 90% confluence (within 2–3 days), cells were treated with 0.25% trypsin and subcultured at a split ratio of 1:3. The cells at passage three were used for the specific

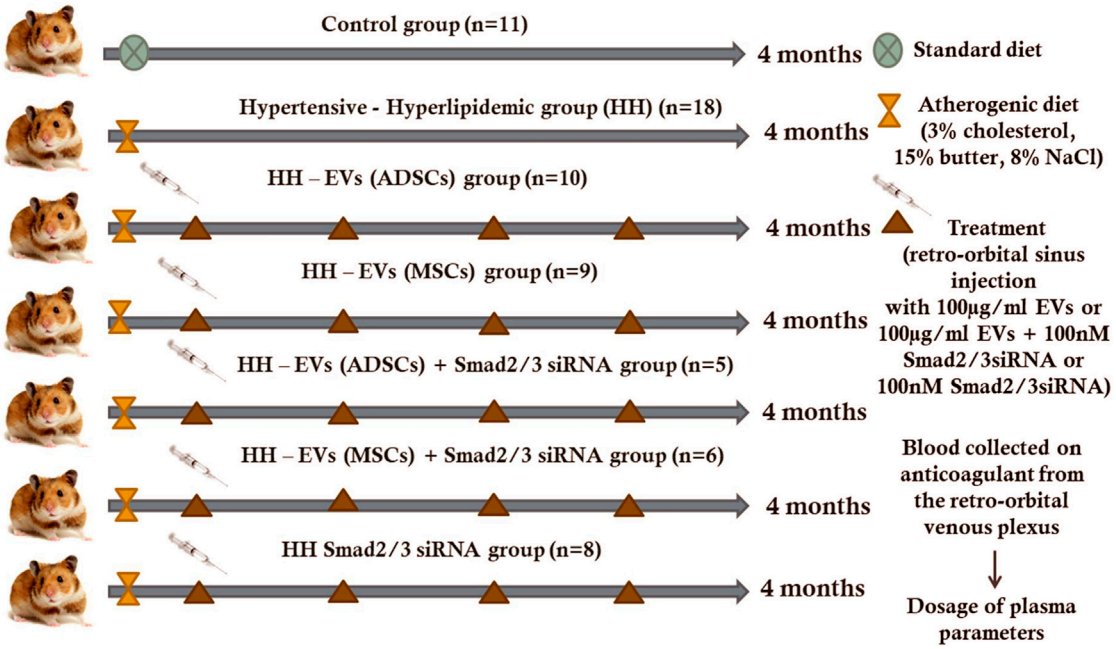

FIGURE 1 | *Schematic representation of experimental animal models obtained for a period of 4 months.* Golden Syrian hamsters (67 males and 3 months old) were divided into seven experimental groups: **(1)** control *(C group)*; **(2)** simultaneously hypertensive–hyperlipidemic *(HH group)*; **(3,4)** HH hamsters with retro-orbital sinus injection containing 100 µg/ml EVs from both ADSCs and BM-MSCs ***(HH-EVs (ADSCs) group and HH-EVs (MSCs) group)***; **(5,6)** HH hamsters with retro-orbital sinus injection containing 100 µg/ml EVs (from ADSCs or BM-MSCs) transfected with 100 nM Smad2/3 siRNA *(HH-EVs (ADSCs)+Smad2/3 siRNA group and HH-EVs (MSCs)+ Smad2/3 siRNA group)*; **(7)** HH hamsters with subcutaneous injection containing 100 nM Smad2/3 siRNA *(HH-Smad2/3 siRNA group)*. The HH group was obtained by combining the atherogenic and high-salt diet.

characterization. The presence of stem cell markers, namely CD73, CD90, CD29, CD44, CD117 (antibodies from R&D Systems), and CD105 (antibody from BioLegend) and the absence of markers of hematopoietic cells, namely CD45 (antibody from BioLegend), CD14, and CD31 (antibodies from R&D Systems) were analyzed by flow cytometry.

Obtaining and Characterization of Extracellular Vesicles (Adipose Tissue Stem Cells) and Extracellular Vesicles (Mesenchymal Stem Cells)

The MSCs (ADSCs or BM-MSCs) at passage five were kept in a serum-free medium for 48 h in order to release EVs (ADSCs) or EVs (MSCs). Repeated centrifugations and ultracentrifugations were performed on the cell-conditioned medium for EV isolation. Centrifugation at 2,500 *g* for 10 min was used to remove cellular debris and 16.000 x g for 5 min to remove apoptotic bodies. After that, the supernatant was subjected to ultracentrifugation at 100.000 x g for 20 h at 4°C to obtain EVs (microvesicles (MVs or MPs) and exosomes) in the pellet. Then, the EVs obtained in the pellet were washed with sterile PBS at 100.000 x g for 2 h and 30 min at 4°C. Finally, the pellet containing EVs was resuspended in 500 µL sterile PBS and maintained at −80°C until further analysis. To highlight the presence of both exosomes (50–100 nm) and microvesicles (100–1,000 nm), the particle size was assessed using a Malvern Zetasizer Nano ZS. The characterization of EVs isolated from the culture medium from both ADSCs and BM-MSCs was performed by flow cytometry following the presence of the markers $CD63^+$ (for exosomes) (Thermo Fisher) and Annexin V^+ (for microvesicles) (SantaCruz Biotechnology, Inc.). To evaluate the accuracy and repeatability of EV size, a comparative method, namely transmission electron microscopy (TEM, FEI Talos F200C) was employed according to the protocol described by Sorop et al., (2020). In brief, negative staining for TEM was performed on carbon-coated copper grids (100 mesh; Agar Scientific). A volume of 5 µL of sample containing EVs was incubated for 2 min on grids at room temperature (RT) and stained with 2% uranyl acetate. Image acquisition was performed at RT using a 200 kV Talos F200C TEM (Thermo Fisher Scientific).

Transfection of Extracellular Vesicles With Smad2/3 siRNA

Lipofectamine™ RNAiMAX transfection reagent (Thermo Fisher Scientific) was used to transfect EVs with a siRNA-targeting Smad2/3 (100 nM final concentration) (Santa Cruz Biotechnology, Inc.) according to the manufacturer's protocol. In brief, two different mixtures were made, one consisting of 3 µL Smad2/3 siRNA and 50 µL OPTI-MEM (Gibco by Life Technologies) and the other of 3 µL Lipofectamine and 50 µL OPTI-MEM, which were later homogenized. A volume of 100 µg/ml EVs (ADSCs) or EVs (MSCs) was added to the resulting mix, incubated for 72 h at 37°C in 5% CO_2 atmosphere, and ultracentrifuged at 100.000xg for 2 h at 4°C. The resulting

pellet containing 100 μg/ml transfected EVs was resuspended in 300 μL PBS. The efficiency of EV transfection was verified with siRNA-FITC, used as a positive control, by flow cytometry.

Analysis of the Main Plasma Parameters of Experimental Models

The plasma samples were obtained from all experimental animal groups by collecting about 1 ml venous blood from the retro-orbital plexus in vacutainers containing EDTA (EDTA-treated tubes) and centrifuging at 2,500 x g for 10 min at 4°C. This procedure was performed monthly for 4 months of follow-up under light anesthesia with 2% isoflurane (inhalation vapor: Isoflutek 1000 mg/g) with pre-weighing of animals under fasting conditions.

The plasma levels of total cholesterol, HDL-cholesterol, LDL-cholesterol, triglycerides, and glucose were determined by a colorimetric method using commercially available kits from DIALAB GmbH, Vienna, Austria. The samples were made in duplicate and measured at a wavelength between 500–600 nm (Tecan Infinite M200 PRO).

Echocardiographic Evaluation of the Arterial Wall Structure

For this analysis, the high-resolution ultrasonic imaging system for small animals (Vevo2100) was used. Prior to the procedure, the hamster fur on the chest was removed using an electric hair clipper so as not to interfere with the signal from the device. The animals were anesthetized throughout this diagnostic procedure with 2% isoflurane and placed on a heated platform to keep their body temperature constant. Vital signs (heart rate and pulse) were constantly monitored. Transthoracic echocardiography consisted of parasternal sections on the long axis to determine the thickness of the vascular wall and the inner diameter recorded in the B mode (two-dimensional). The B mode is a major method that helps to assess the anatomical and functional characteristics of the heart and blood vessels. With the help of the M mode, flat sections were obtained, and the diameter in systole and diastole could be measured. For large blood vessels such as the thoracic aorta, VTI (velocity time integral) and VEL (blood velocity) were measured, and the records being obtained in the pulsed wave (PW) Doppler mode that analyzes the hemodynamic characteristics of blood flow. The images were stored in the ultrasound system hard-drive and transferred to an external memory hard-drive for offline analysis. The processing of the images obtained from all experimental animal groups was performed with the help of VevoLab300 software. Echocardiographic evaluation was performed at the end of 4 months of experimental diet/treatment, and the results were compared with the C group.

Myographic Analysis of Functional Responses of Isolated Blood Vessels

Vascular dysfunction was analyzed by a myograph technique (device that investigates vascular reactivity) used to explore the ability of blood vessels (thoracic aorta and carotid artery) to contract or relax. The blood vessels that were taken for myographic analysis were not previously washed with PBS with $CaCl_2$ to avoid endothelial damage. The isolated arterial segments were mounted on the Multi Myograph System-model 620 M in combination with the Automatic Buffer Filler System-625FS (Danish Myo Technology, DMT). For these experiments, ACh (acetylcholine) was used to induce vessel relaxation and NA (noradrenaline), to induce vessel contraction. In order to record the physiological activity of smooth muscle cells (SMCs), the blood vessels (~200 μm diameter) were cleaned off lipids, cut under a microscope to a length of 3 mm, mounted on the wire-myograph chamber, and immersed in HEPES sodium salt buffer, pH = 7.45 at 37°C. The optimal operating diameter was determined and calibrated, and the standard start procedure was applied to verify the integrity of the mounted blood vessels and the presence of the intact endothelium, by stimulation with 3×10^{-7} M NA. Throughout the experiment, O_2 was constantly bubbled into the myograph's organ chamber to maintain the function of the blood vessels. Subsequently, the responses of blood vessels in the presence of curves of increasing concentrations of NA or ACh were recorded in real time. The concentration curve used was as follows: 10^{-8} M, 3×10^{-8} M, 10^{-7} M, 3×10^{-7} M, 10^{-6} M, 3×10^{-6} M, 10^{-5} M, 3×10^{-5} M, and 10^{-4} M for both NA and ACh. The forces developed by the blood vessels in the presence of the vasoconstrictor or vasodilator agonists were recorded at an interval of 2 min. Finally, the wire tension (mN/mm) developed by the blood vessels in the presence of the vasoconstrictor NA and the relaxation in the presence of the vasodilator ACh, calculated as a percentage (%) of the maximum precontraction at NA, were evaluated. Data acquisition was performed using a PowerLab 4/26 hardware (ADInstruments) and images recorded with LabChart 7 (multichannel chart recorder) software.

Analysis of the Plasma Ang II and TGF-β1 Levels

After 4 months of the hyperlipemic–hypertensive diet, the blood collected on anticoagulant from the retro-orbital venous plexus was centrifuged at 2,500 x g for 10 min at 4°C to obtain plasma. Subsequently, plasma angiotensin II (Ang II) and transforming growth factor beta 1 (TGF-β1) levels were determined using the commercial Angiotensin II EIA Kit (Sigma-Aldrich) and Human/Mouse TGF-beta 1 Uncoated ELISA Kit (Invitrogen) according to the manufacturer's protocol. The samples were read on the spectrophotometer (Tecan Infinite M200 PRO) at a wavelength suggested by the manufacturer (450 nm).

Immunofluorescence Staining and Image Analysis for Detection of Inflammatory Markers

After perfusion by ventricular puncture, the interest organs including thoracic aorta and carotid arteries were excised, immersed in 2% paraformaldehyde (PFA) cryoprotection solution in 0.1 M phosphate buffer, and left at 4°C overnight.

Subsequently, the samples were washed with phosphate buffer, subjected to consecutive baths of glycerol of different concentrations (5% for 15 min, 10% for 1 h, 20% overnight, and 50% for 1 h, at 4°C), and kept in the freezer (−20°C) until their processing. To perform the histological sections, the samples were washed (successive washes with 3% sucrose solution in phosphate buffer, 6x for 15 min) and immersed for 30 min in OCT (Tissue-Tek, Sakura). After 30 min, the samples were removed from the OCT, immersed for 30–45 s in liquid nitrogen, and placed in the cryotome (Leica CM1850), where they were mounted on the cutting support. The tissue block was mounted on the mold, and cryosections (5 µm thickness) cut using a microtome blade (MX35 Ultra, Thermo Scientific) were attached to glass slides (Superfrost Plus from Thermo Scientific treated with poly-L-lysine for a better adhesion of the sections on the support), incubated for 30 min at 37°C, and stored at 4°C until use. For immunostaining, the following essential steps were completed: defrosting sections at room temperature (RT), fixing with cold methanol (−20°C), incubation with $NaBH_4$ for 1 h at 4°C to reduce tissue autofluorescence, permeabilization with 0.2% Triton X-100 in PBS containing 0.05% Tween 20 (AppliChem) for 30 min at RT, encircling sections on the slide with a lipid pen (Invitrogen), and blocking nonspecific sites with 10% goat serum (Invitrogen). The sections were incubated overnight at 4°C with the following primary antibodies (diluted in PBS with 1% BSA (bovine serum albumin)) used for: COL1A (1:250, Santa Cruz Biotechnology), α-SMA (1:200, Cell Signaling Technology), Cx43 (1:200, Thermo Fisher Scientific), MMP-2 (1:200, Santa Cruz Biotechnology), VCAM-1 (1:200, Santa Cruz Biotechnology), $CD3e^+$ (1:200, Thermo Fisher Scientific), $CD68^+$ (1:200, Santa Cruz Biotechnology), and MHC-II^+ (1:250, Thermo Fisher Scientific). Then, the sections were washed three times with PBS, incubated with the secondary antibody labeled with Alexa Fluor 568 goat anti-rabbit IgG (H + L) 1:1,000 or Alexa Fluor 647 donkey anti-mouse IgG (H + L) 1: 500 or Alexa Fluor 488 goat anti-rabbit IgG (H + L) 1: 500, and washed three times with PBS. Subsequently, DAPI solution (5 mg/ml in 10 mM PBS) was added for 5 min to label the nuclei, and sections were washed three times with PBS. Finally, a liquid mountant (ProLong, Invitrogen) was applied directly to fluorescently labeled tissue samples on microscope slides.

In separate experiments, the ROS (reactive oxygen species) expression level was analyzed by adding 6 µM DHE (fluorochrome dihydroethidium, Sigma-Aldrich) on tissue sections for 30 min at RT. The images were captured and analyzed under an inverted fluorescent microscope (Axio Vert. A1 Fl, Carl Zeiss, software Axio Vision Rel 483SE64-SP1), under ×20 magnification. Image analysis was performed with the help of the ImageJ program.

Protein Expression Evaluation by Western Blot Analysis

Protein Extraction

For the protein extraction, RIPA buffer (Thermo Scientific) containing 100 mM PMSF, a cocktail of phosphatase B inhibitors and protease inhibitors, was added to the tissue (thoracic aorta and carotid artery). The samples were minced into very small pieces using scissors and homogenized at 5,000 rpm x five rounds for 2 min each, using the Minilys Personal High Power Tissue Homogenizer (Bertin Technologies) and glass beads with 1 mm diameter. After processing, the tubes were left in the refrigerator overnight, centrifuged the next day at 15600 rpm, for 5 min, at 4°C, and then the supernatant containing the protein lysate was transferred to new tubes and stored at -20°C until the protein concentration was dosed. To determine the protein concentration, BCA Protein Assay Kit (ThermoScientific) was used. The samples were read in duplicate at an absorbance of 562 nm at a detection range of 20–2000 µg/ml and reported on a standard curve of BSA.

Gel Electrophoresis and Immnunoblotting

The samples (100 µg/lane for the thoracic aorta and 50 µg/lane for the carotid artery) were separated by SDS-PAGE gels and subsequently electrophoretically transferred to a nitrocellulose membrane. A wide range molecular weight marker (6.5÷200 kDa) (Sigma) was loaded into one lane as a standard. Prior to antibody labeling, the nitrocellulose membrane was immersed in a nonspecific site blocking solution (TBS solution with 3% BSA (Applichem) or TBS solution with 5% Blotto, nonfat dry milk (Santa Cruz Biotechnology)), then incubated with primary monoclonal antibodies: β-actin–used as a loading control (1:200, SantaCruz Biotechnology), ATF2 (1:500, Thermo Fisher Scientific), SMAD2/3 (1:1,000, Thermo Fisher Scientific), pSMAD2/3 (1:1,000, Thermo Fisher Scientific), and NF-kB p50/NF-kB p65 (1:200, SantaCruz Biotechnology), which recognize the protein of interest. Incubation with primary antibodies was performed overnight at 4°C. Washing extensively was followed to remove unbound antibodies, and incubation with secondary antibodies coupled with horseradish peroxidase (HRP), anti-mouse antibodies (1:2000, Thermo Fisher Scientific), or anti-rabbit antibodies (1:5,000, Thermo Fisher Scientific), which specifically recognize primary antibodies. Incubation with secondary antibodies was performed for 1 h at RT. Detection of intensity of bands was made in the presence of ECL (enhanced chemiluminescent substrate for HRP detection), and the TotalLab program was used to quantify the information. The investigated protein bands were reported to the band corresponding to β-actin, a housekeeping reference protein.

Ribonucleic Acid Extraction and Quantification of miRNAs by Real-Time Quantitative Polymerase Chain Reaction Analysis

Total RNA was extracted from cryopreserved tissue (thoracic aorta and carotid artery) using miReasy Micro Kit (QIAGEN). In brief, the tissue was weighed (~10 mg) and crushed very well using fine scissors. Over the tissue fragments, 1.4 mm zirconium oxide beads (Precellys) and 700 µL lysis buffer (QIAzol Lysis Reagent) were added. The samples were grounded at 1800rpm, 6x for 1 min on ice, placed for 10 min at −20°C, left for 10 min at RT, centrifuged at 10,000 x g for 5 min at 4°C, and the supernatant was

processed according to the manufacturer's protocol. Finally, RNA was eluted in 16 μL RNase-free water. The RNA purity and concentration were evaluated by spectrophotometry using NanoDrop 2000c (Thermo Fisher) and kept at −80°C until examinations. The reverse-transcription of RNA was performed using TaqMan MicroRNA Reverse Trascription Kit (Applied Biosystems) in combination with TaqMan-Gene Expression Master Mix according to the instructions of the manufacturer on a Veriti real-time PCR system (Applied Biosystems). The study of miRNA expression was carried out on six miRNAs: hsa-miR-21(ID:0,000,397), hsa-miR-192 (ID: 000,491), hsa-miR-200b (ID:002,251), hsa-miR-29a (ID: 002,112), hsa-miR-210 (ID:000,512), and hsa-miR-146a (ID: 000,468). Each reaction was performed in triplicate. The miRNA expression level was normalized to U6 small nucleolar RNA snRU6 (ID:00,197) and quantified using the $2^{-\Delta\Delta Ct}$ calculation method. The VIIA7 software v1.2 (Applied Biosystems) with the automatic quantification cycle (Cq) setting was used to analyze the data according to the protocol described by Alexandru et al., (2017); Alexandru et al., (2019); Alexandru et al., (2020).

RESULTS

Characterization of Adipose Tissue Stem Cells and BM-Mesenchymal Stem Cells Revealed the Presence of Stem Cell-Specific Markers

The analysis of cells at passage three by flow cytometry was able to validate the phenotype of the two MSC types, some isolated from subcutaneous adipose tissue called ADSCs and others from bone marrow aspirate called BM-MSCs. As expected, the results showed that both cell types displayed specific markers for stem cells, namely CD73, CD90, CD105, CD29, CD44, and CD117 but were negative for specific markers of hematopoietic cells, namely CD45, CD14, and CD31 (the results are not shown, but some of them are found in the article published by Constantin et al., 2017).

Characterization of Extracellular Vesicles From the Secretome of Adipose Tissue Stem Cells or BM-Mesenchymal Stem Cells Disclosed the Existence of Both Microvesicles and Exosomes

EVs were isolated from the secretome of healthy hamster adipose tissue-derived stem cells (ADSCs) or of bone marrow-derived stem cells (BM-MSCs) and kept for 48 h in media without serum. The EVs thus obtained (EVs (ADSCs) and EVs (MSCs)) were analyzed by Zetasizer Nano ZS ZEN3600 to establish their size (**Figure 2**). The distribution curves of the EV dimensions are bimodal, both in the case of EVs (ADSCs) and EVs (MSCs), and the values of particle dimensions (Z) being between 50 and 100 nm for exosomes (~30%) and between 100 and 1,000 nm for microvesicles (~70%) (**Figure 2**).

Flow cytometry analysis confirmed the presence in the purified EV fraction (EVs(ADSCs) and EVs (MSCs)) of both exosomes ($CD63^+$, $CD9^+$, and $CD81^+$) and microvesicles (AnnexinV+) (**Figures 3A–C**).

Subsequently, EVs were examined by TEM to confirm their size and characterize them from a structural point of view (**Figure 4**). Analysis by TEM showed that these EV fractions obtained from both ADSCs and BM-MSCs contain heterogenous particles of larger or smaller dimensions in a range of values specific to exosomes and microvesicles. These particles have a typical cup-shaped structure with a membrane and cytoplasm. Analyzing by comparison between EVs (ADSCs) and EVs(MSCs), it was observed that EVs(ADSCs) are larger than EVs(MSCs), meaning that in the fraction of EVs the percentage of microvesicles is higher than that of the exosomes (**Figure 4**).

The seven investigated experimental animal groups (*C*, *HH*, *HH-EVs(ADSCs)*, *HH-EVs(MSCs)*, *HH-EVs(ADSCs)+Smad2/3siRNA*, *HH-EVs(MSCs)+Smad2/3siRNA*, and *HH-Smad2/3siRNA*) were evaluated for body weight and plasma parameters (glucose, total cholesterol, HDL-cholesterol, LDL-cholesterol, and triglycerides) at the beginning of the experimental period and the end of each month over the 4-month experimental period, while they were on an atherogenic diet (food enriched with 15% butter and 3% cholesterol) and received daily gavage with 8% NaCl.

The weighing of the hamsters revealed a slight insignificant decrease at two, three, and four months of diet in the case of hamster in the HH group, while in the control hamsters, the weight was constant throughout the experimental period. The treated groups showed a slight weight gain, especially in the HH-Smad2/siRNA and HH-EVs (MSCs) groups (**Table 1**).

Regarding the biochemical parameters, compared to the control group, the hamsters from the HH group showed a significant increase in plasma concentrations of total cholesterol (5.01 times), LDL-cholesterol (8.62 times), and triglycerides (11.48 times) throughout the experimental period. For HDL-cholesterol, the values for HH group remained constant in the first 2 months of the diet, while in the third and fourth month they began to grow, registering a statistically significant increase in the fourth month of the diet (2.01 times) (**Table 1**). In addition, blood glucose values did not differ significantly between the seven experimental groups, and the values being relatively constant during the 4 months of diet and treatment (**Table 1**).

Concerning the effects of the treatments, both EVs and EVs transfected with Smad2/3siRNA treatment led to a significant reduction in the levels of total cholesterol (2.62 times for EVs (ADSCs) and 2.13 times for EVs (MSCs)), triglycerides (5.05 times for EVs (ADSCs) and 6.11 times for EVs (MSCs)), and LDL-cholesterol (2.06 times for EVs (ADSCs) and 2.09 times for EVs (MSCs)). The combined administration of EVs and Smad2/3 siRNA had a beneficial effect on plasma parameters significantly decreasing their levels compared with those in the HH group. The values were comparable to those obtained in the case of single therapy with EVs (ADSCs) or EVs (MSCs) (**Table 1**). Treatments based on EVs (ADSCs) and EVs (MSCs) alone or in combination with Smad2/3siRNA and administration of Smad2/3siRNA alone had a beneficial effect

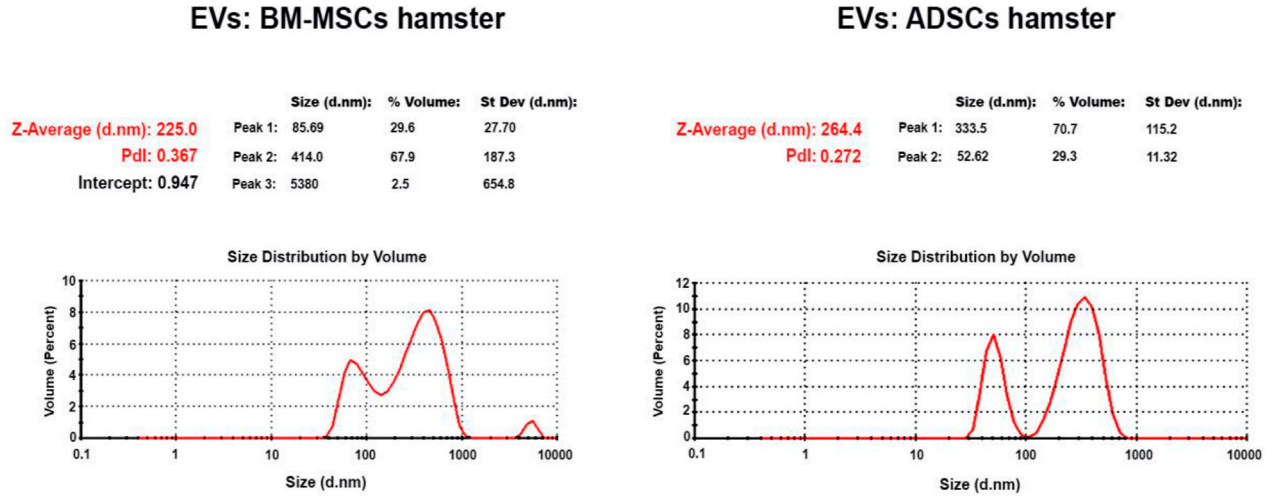

FIGURE 2 | Particle size distribution of EVs secreted in the culture medium by ADSCs and BM-MSCs showed two different populations represented by the two peaks; the first peak at the small size range (~50–100 nm) specific to exosomes and the second at the high-size range (~100–1000 nm) specific to microvesicles (*Y*-axis represents the number of EVs, and the *X*-axis represents the size of EVs).

on plasma parameters reducing the levels compared with those in the HH group. HH-Smad2/3siRNA is the only experimental group that recorded a significant increase in triglyceride levels compared to both the control and the other treated groups (**Table 1**).

It was also observed that following the administration of the atherogenic diet, the liver was affected, having a yellow and greasy appearance, which indicates the presence of hepatic steatosis, and the plasma had a milky, dense consistency due to the accumulation of a large amount of lipids in the bloodstream. A visible improvement of the appearance of the liver and blood was noticed in the groups of treated animals. It is important to mention that the significant change in the lipid profile, a risk factor correlated with the development of atherosclerosis, proves that hamsters in the HH group are dyslipidemic. Our previous results have shown that this group of hamsters (HH) also presented significant increases in systolic and diastolic blood pressure and heart rate (Georgescu et al., 2012), which suggest that the HH group is also hypertensive. These cumulative results prove that the HH group is hypertensive–hyperlipidemic, which means that the experimental model, the hypertensive–hyperlipemic hamster, was successfully obtained.

Echocardiographic Evaluation Revealed the Vascular Structural and Blood Flow Changes Induced by the Atherogenic Diet; the Stem Cell-Derived Extracellular Vesicle-Based Treatment Produced a Noticeable Improvement in Them

To determine whether the atherogenic diet affects vascular integrity, we investigated the structure and function of the thoracic aorta and carotid artery by echocardiography. First, we followed the thickness of the vascular wall and the inner diameter of the thoracic aorta using B-mode recordings. Thickening of the vascular wall was observed in group HH compared to control group (**Figures 5A, B1**). In all groups that received treatment (HH-EVs(ADSCs), HH-EVs(MSCs), HH-EVs(ADSCs)+ Smad2/3siRNA, and HH-EVs(MSCs)+ Smad2/3siRNA), a significant decrease in the thickness of the vascular wall was observed compared to that of the HH group, meaning that this treatment improves the functionality of the blood vessels (**Figures 5A, B1**). Regarding the inner diameter, no significant changes were observed between all investigated experimental groups (**Figures 5A, B2**). Through the recordings in M-mode, we followed the diameter in systole and diastole. The difference between the diameter in systole and that in diastole provides information on the elasticity of the blood vessel. The HH group recorded significantly lower values than the control group, while in the two treated groups an improvement was observed in terms of blood vessel distensibility (**Figures 5C,D**). The groups that received treatment based on EVs (ADSCs) or EVs (ADSCs) transfected with Smad2/3siRNA had a better result in restoring the elasticity/distensibility of the arterial wall (**Figures 5C,D**). Quite the opposite, the treatment based on EVs from MSCs did not bring any noticeable enhancements (**Figures 5C,D**). Through the recordings in the pulsed Doppler-mode, we followed two characteristic parameters for the hemodynamics of the blood flow–velocity time integral (VTI), which represents the length of the ejection tract measured in mm, and velocity (Vel) (blood flow rate measured in mm/s) at the thoracic aorta. The analysis of the images showed that the HH group registered significantly increased values (***$p < 0.005$) for both Vel and VTI correlated with the structural changes in the arterial wall and the increase in blood pressure triggered after daily administration of gavage with 8% NaCl, for 16 experimental weeks compared to the control group (**Figures 5E, F1,F2**). The groups of treated animals (HH-EVs(ADSCs), HH-EVs(MSCs),

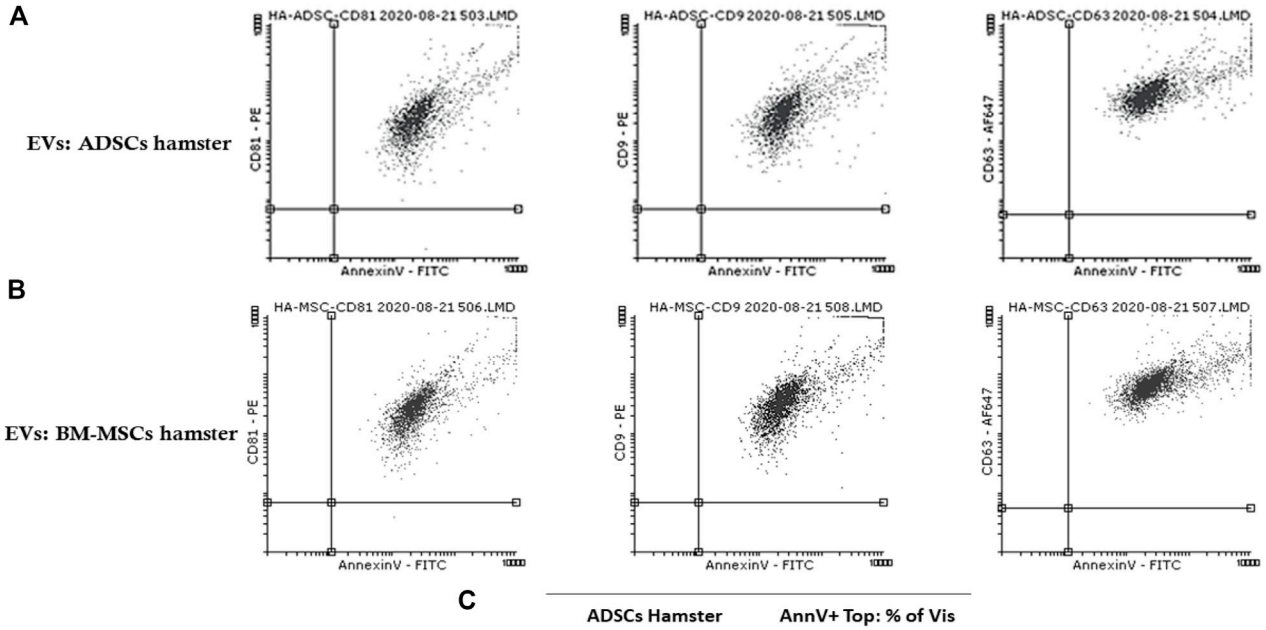

C

ADSCs Hamster	AnnV+ Top: % of Vis
AFL-ADSCs	4.3
CD81⁺/AnnexinV⁺	99.1
CD9⁺/AnnexinV⁺	100.0
CD63⁺/AnnexinV⁺	99.2
BM-MSCs Hamster	
CD81⁺/AnnexinV⁺	99.8
CD9⁺/AnnexinV⁺	100
CD63⁺/AnnexinV⁺	100

FIGURE 3 | Detection and characterization by flow cytometry of EVs isolated from the culture medium from ADSCs/BM-MSCs of healthy hamsters highlight the presence of both exosomes ($CD63^+$, $CD9^+$, and $CD81^+$) and microvesicles ($AnnexinV^+$). **(A)** Representative dot plots double-stained with purified EVs from ADSC fraction with $CD81^+$ (labeled with PE)/Annexin V^+ (labeled with FITC), $CD9^+$ (labeled with PE)/Annexin V^+ (labeled with FITC), and $CD63^+$ (labeled with AF647)/Annexin V^+ (labeled with FITC); **(B)** representative dot plots double-stained with purified EVs from the BM-MSC fraction with $CD81^+$ (labeled with PE)/Annexin V^+ (labeled with FITC), $CD9^+$ (labeled with PE)/Annexin V^+ (labeled with FITC), and $CD63^+$ (labeled with AF647)/Annexin V^+ (labeled with FITC) **(C)** Percentage of EV specific markers for both exosomes and microvesicles.

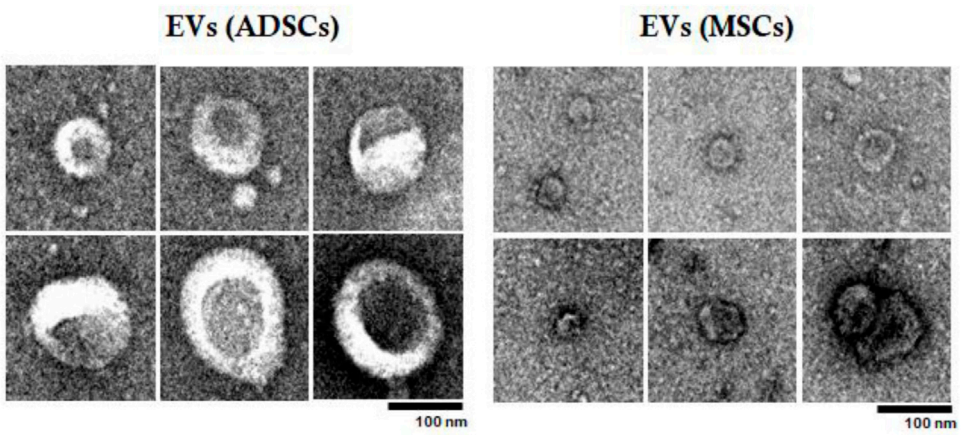

FIGURE 4 | Examination of EVs (ADSCs) and EVs (MSCs) by transmission electron microscopy (TEM). EVs were collected from the secretome of healthy hamster adipose tissue-derived stem cells (ADSCs) or of bone marrow-derived stem cells (BM-MSCs). The effect of atherogenic diet and treatment on main plasma parameters were investigated.

TABLE 1 | Clinical characteristics and biochemical parameters of the seven experimental animal groups, control (C); simultaneously hypertensive–hyperlipidemic (HH); HH-EVs(ADSCs), HH-EVs(MSCs), HH-EVs(ADSCs)+Smad2/3siRNA, HH-EVs(MSCs)+Smad2/3siRNA, and HH-Smad2/3 siRNA, after 16 weeks of standard diet or atherogenic diet, and at 14 weeks post-treatment with EVs (ADSCs) or EVs (MSCs) transfected or not with Smad2/3siRNA during the diet-induced atherosclerotic process. Data are means ± SD of duplicate determinations. The statistical significance, noticeably different, was represented as $^{***}p < 0.005$, $^{**}p < 0.01$, $^{*}p < 0.05$ values versus control group and $^{###}p < 0.005$, $^{##}p < 0.01$, $^{#}p < 0.05$ values versus HH group. Two-way ANOVA and Bonferroni post-test were applied.

After 16 weeks of standard diet/ atherogenic diet	Control (n = 11)	HH (n = 18)	HH-EVs (ADSCs) (n = 10)	HH-EVs (MSCs) (n = 9)	HH-EVs (ADSCs) + Smad2/3 siRNA (n = 5)	HH-EVs (MSCs) + Smad2/3 siRNA (n = 6)	HH-Smad2/3 siRNA (n = 8)
Initial body weight (g)	117.8 ± 2.81	125.9 ± 3.90	122.5 ± 3.93	132.78 ± 5.51	132.17 ± 7.3	147.33 ± 6.82	128.11 ± 5.62
Final body weight (g)	116 ± 3.39	99.38 ± 2.76	110.9 ± 5.97	121.55 ± 6.07	105.33 ± 4.74	110.33 ± 8.36	120.5 ± 3.65
Glycemia (mg/dl)	116.02 ± 22.69	137.76 ± 48.25	137.97 ± 19.16	152.5 ± 21.81	108.81 ± 29.49	125.2 ± 16.1	133.96 ± 9.42
Cholesterol (mg/dl)	128.04 ± 14.47	641.66 ± 26.13 ($^{***}p < 0.005$)	244.45 ± 60.6 ($^{###}p < 0.005$)	300.83 ± 60.77 ($^{*}p < 0.05$) ($^{###}p < 0.005$)	208.22 ± 37.7 ($^{###}p < 0.005$)	267.1 ± 64.12 ($^{###}p < 0.005$)	201.7 ± 36.47$^{###}$ $p < 0.005$)
Triglycerides (mg/dl)	93.42 ± 4.17	1,073 ± 6.87 ($^{***}p < 0.005$)	212.26 ± 3.42 ($^{###}p < 0.005$)	175.43 ± 5.62 ($^{###}p < 0.005$)	202.82 ± 4.89 ($^{###}p < 0.005$)	217.31 ± 6.87 ($^{###}p < 0.005$)	652.22 ± 55.75 ($^{***}p < 0.005$) ($^{###}p < 0.005$)
HDL cholesterol (mg/dl)	54.44 ± 6.47	109.73 ± 49.59 ($^{**}p < 0.01$)	89.71 ± 29.72 ($^{*}p < 0.05$)	82.67 ± 25.27	97.41 ± 3.97	90.24 ± 25.77	91.43 ± 23.52
LDL cholesterol (mg/dl)	73.67 ± 4.69	635.43 ± 8.8 ($^{***}p < 0.005$)	307.09 ± 7.23 ($^{***}p < 0.005$) ($^{##}p < 0.01$)	303.18 ± 8.4 ($^{***}p < 0.005$) ($^{##}p < 0.01$)	280.26 ± 2.3 ($^{**}p < 0.01$) ($^{##}p < 0.01$)	364.18 ± 5.24 ($^{***}p < 0.005$) ($^{##}p < 0.01$)	284.94 ± 43.91 ($^{***}p < 0.005$) ($^{##}p < 0.01$)

HH-EVs(ADSCs)+Smad2/3siRNA, and HH-EVs(MSCs)+Smad2/3siRNA) showed significantly lower values for VTI than HH, especially those transfected with Smad2/3siRNA (**Figures 5E, F1**). The measurements that characterize velocity showed that there is no difference between the treated groups, only a slight decrease compared to the HH group, without statistical significance (**Figures 5E, F2**). The VTI and Vel are two important parameters that give not only an image of the global systolic function but also of the structural and functional changes at the level of the isolated thoracic aorta from all investigated groups. The increase of these parameters suggests the presence of structural alterations and the debut of vascular dysfunction in animals in the HH group. Another investigated blood vessel was the carotid artery. Echocardiographic recordings in the B-mode showed significantly increased values of vascular wall thickness in the HH group ($^{***}p < 0.005$) compared to that in the healthy animals, accompanied by a slight decrease in inner diameter (**Figures 5G, H1,H2**). As for the animals that received EV-based treatment (HH-EVs(ADSCs), HH-EVs(MSCs), HH-EVs(ADSCs)+Smad2/3siRNA, and HH-EVs(MSCs)+Smad2/3siRNA), they had significantly reduced values in the thickness of the vascular wall compared to that of the HH group ($###p < 0.005$), showing that the treatment improves the vascular structure in smaller vessels as well (**Figures 5G, H1**). No visible and statistical difference in the thickness of the vascular wall was observed between the groups of treated animals (**Figures 5G, H1**). In terms of inner diameter, no statistically significant differences were found between the investigated experimental animal groups: C; HH; HH-EVs(ADSCs), HH-EVs(MSCs), HH-EVs(ADSCs)+Smad2/3siRNA, and HH-EVs(MSCs)+Smad2/3siRNA (**Figures 5G, H2**). This was because the carotid artery is a small blood vessel, and we could not follow the other structural and functional changes by echocardiography.

Vascular Myography Showed Altered Functional Responses of Blood Vessels After 4 months of Atherogenic Diet; Favorable Effects of Treatment With Extracellular Vesicles (Adipose Tissue Stem Cells) or Extracellular Vesicles (Mesenchymal Stem Cells) Transfected or Not With Smad2/3 siRNA

To explore whether the atherogenic diet or treatment administration has the desired effects, namely to induce pathophysiological changes specific to the atherosclerosis process or recover them, changes in vascular tone were analyzed (**Figures 6**, **7**). Using the myograph technique, the ability to contract and relax of the thoracic aorta and carotid artery, in all experimental animal groups, was investigated. It is known that the regulation of vascular tone is controlled by the contractile/relaxing capacity of SMCs, and any change in response can be correlated with the vascular endothelium damage. The experimental results revealed that in both arteries (thoracic aorta and carotid artery), the maximum values recorded at 10^{-4} M NA-induced contraction and 10^{-5}M/10^{-6} M ACh-induced relaxation were significantly reduced in the HH group compared with those of the control group (**Figures 6**, **7**), indicating the onset/debut of vascular endothelial dysfunction as a result of atherogenic diet. Isometric force

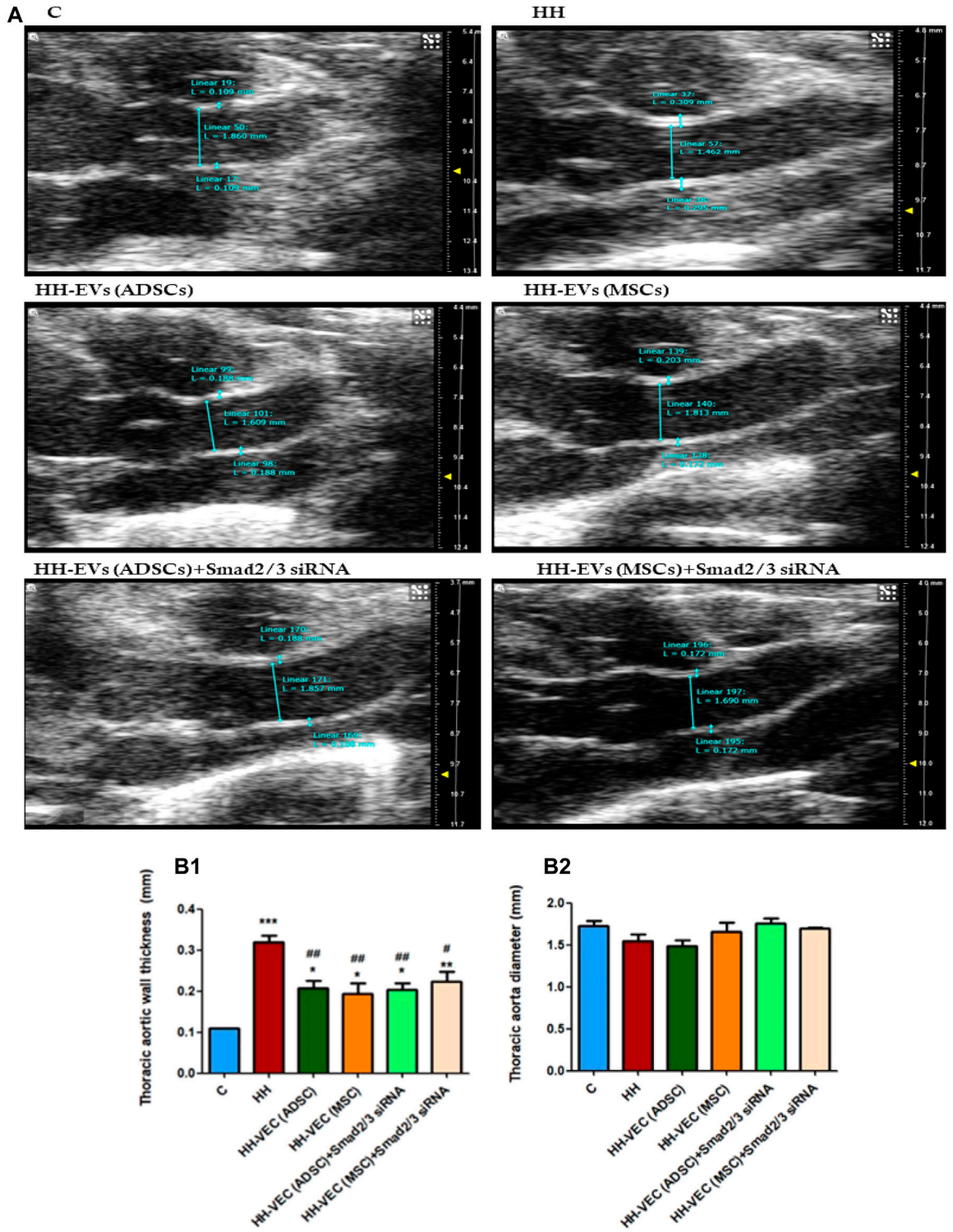

FIGURE 5 | Changes in the blood flow and structure of the thoracic aorta and carotid artery were isolated from the investigated experimental groups (C, HH, HH-EVs(ADSCs), HH-EVs(MSCs), HH-EVs(ADSCs)+Smad2/3siRNA, and HH-EVs(MSCs)+Smad2/3siRNA) as a measure of vascular rigidity. **(A)** Representative B-mode recordings, which highlight the wall thickness and the inner diameter of the thoracic aorta; **(B)** graphical representation of wall thickness (mm) **(B.1)** and inner diameter (mm) **(B.2)** in the case of the thoracic aorta; **(C)** representative records obtained in M-mode, which highlight the diameter in systole and diastole of the thoracic aorta; **(D)** graphical representation of thoracic aortic distensibility (mm); **(E)** representative recordings obtained in pulsed Doppler-mode, which highlight the velocity time integral (VTI) and velocity (Vel) of the thoracic aorta; **(F)** graphical representation of velocity (mm/s) **(F.1)** and velocity time integral (mm) **(F.2)** at the level of the thoracic aorta; **(G)** representative B-mode recordings, which highlight the wall thickness and the inner diameter of the carotid artery; **(H)** graphical representation of wall thickness (mm) **(H.1)** and inner diameter (mm) **(H.2)** in the case of the carotid artery. Data are shown as the mean ± SD of each experimental group after 4 months of diet and treatment. The statistical significance, noticeably different, is represented as $^{***}p < 0.005$, $^{**}p < 0.01$, $^{*}p < 0.05$ versus control group and $^{\#\#\#}p < 0.005$, $^{\#\#}p < 0.01$, $^{\#}p < 0.05$ versus HH group. The values were calculated by two-way ANOVA and Bonferroni post-test.

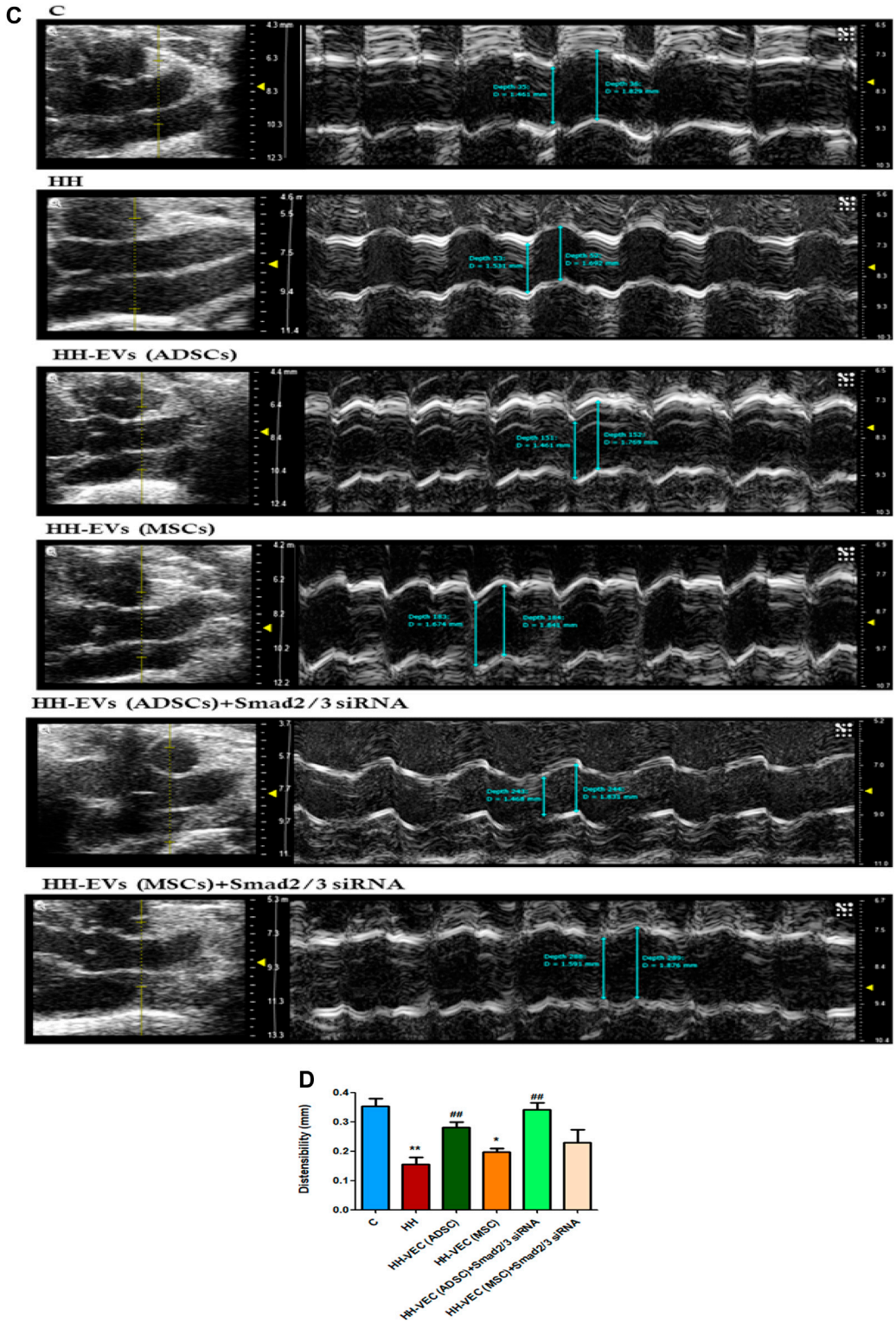

FIGURE 5 | (Continued).

measurements using the wire myograph technique on the thoracic aorta and carotid artery showed that the contractile response was 1.58 times and 1.06 times, respectively, lower in the HH group than that of the C group (**Figure 7A**). As for the endothelium-dependent responses to ACh, these were 2.10 times reduced in the thoracic aorta and 2.18 times reduced in the carotid

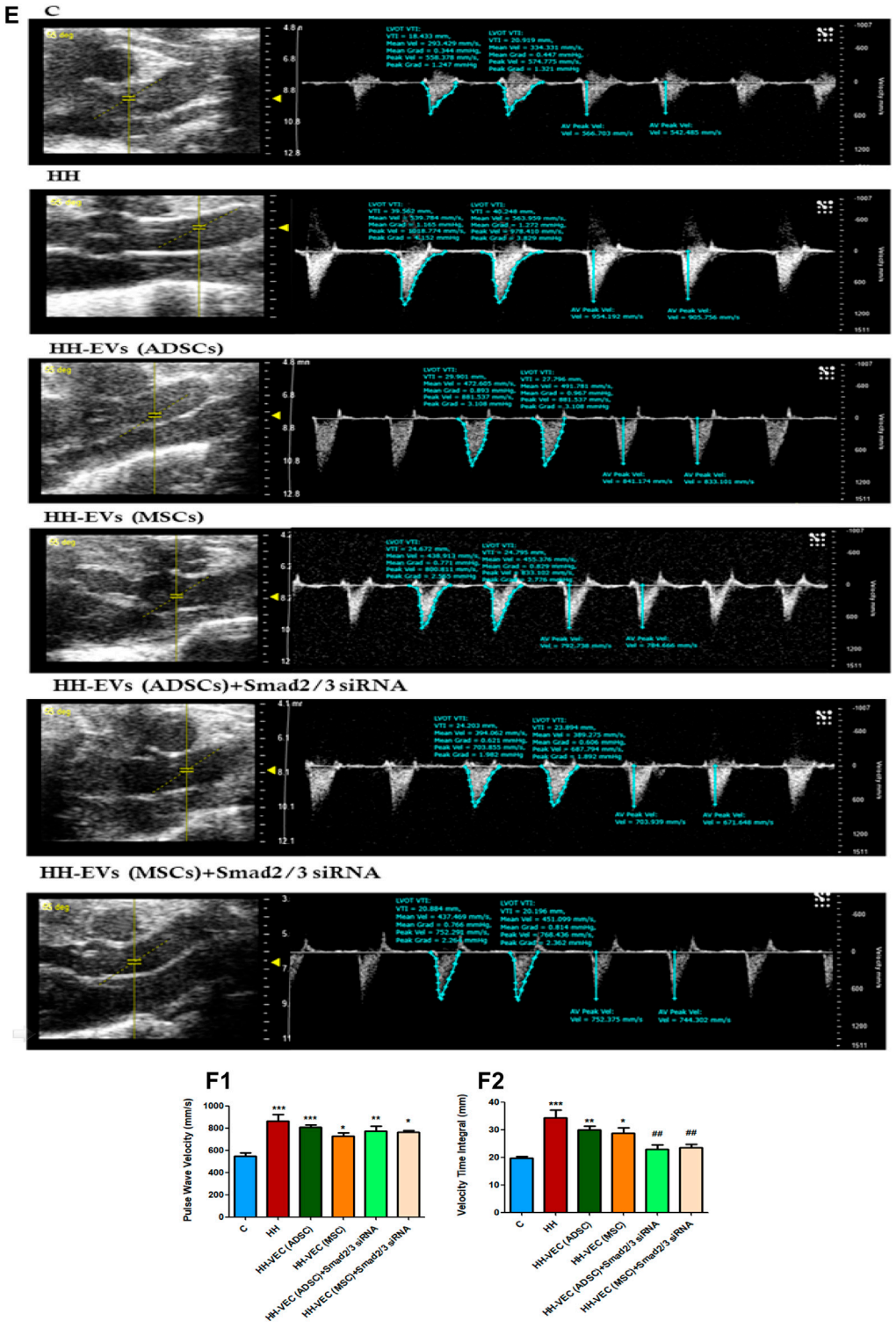

FIGURE 5 | (Continued).

artery when comparing the HH group with those of the C group (**Figure 7B**). Treatment with EVs (ADSCs) alone or in combination with Smad2/3 siRNA re-established the contractile function of the thoracic aorta at values close to normal (**Figure 7A**). The other types of treatment with EVs (MSCs) alone or in combination with Smad2/3 siRNA and Smad2/3siRNA alone significantly increased NA

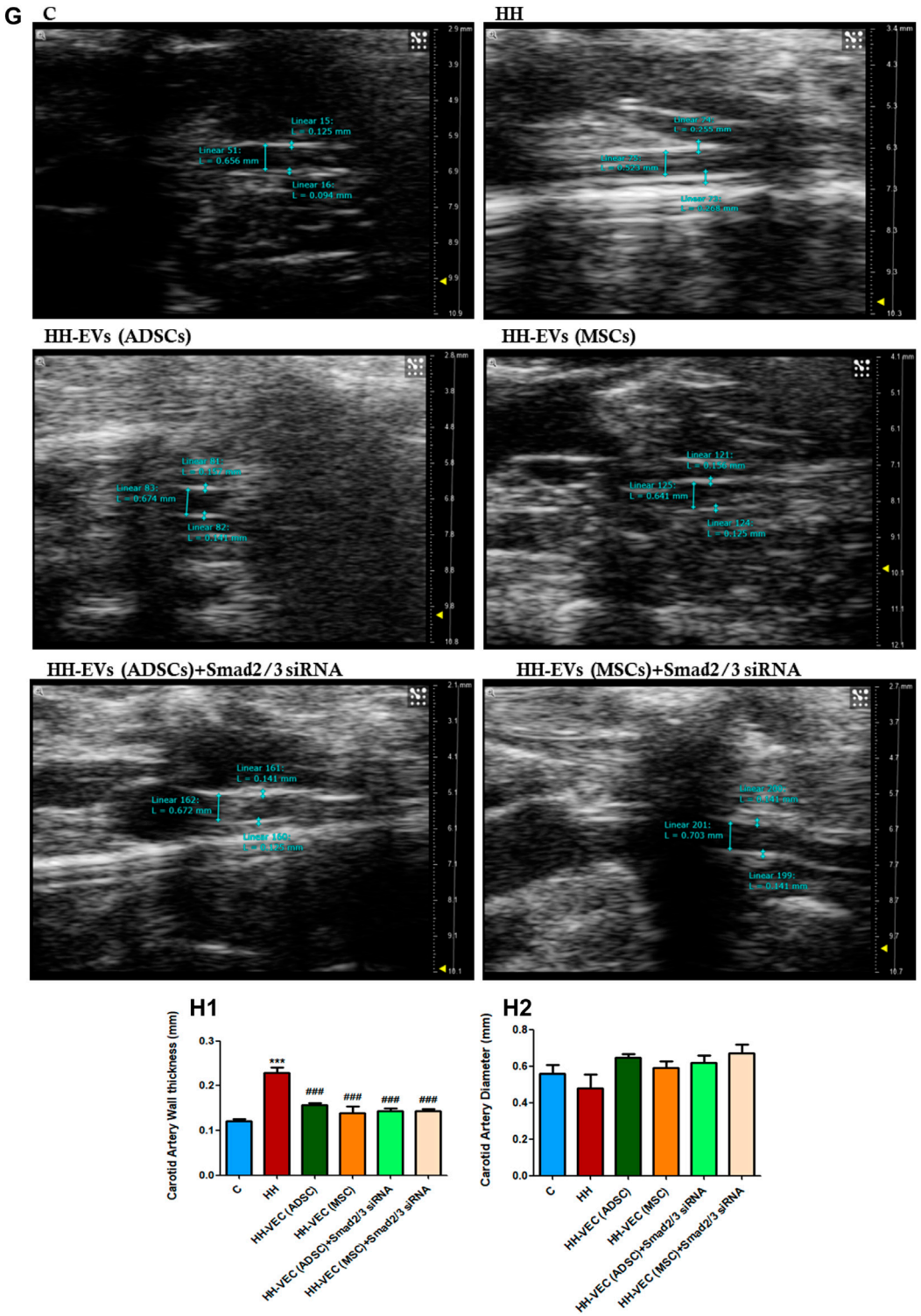

FIGURE 5 | (Continued).

contractile response of the thoracic aorta compared to that of the HH group but not as good as the one reported for EVs(ADSCs) (**Figure 7A**). In the case of the carotid artery, no difference in tension developed to the NA vasoconstrictor agent could be distinguished between all groups of treated animals and the values being relatively close to those of the control group, meaning that all types of treatments had a similar contribution to improving contractile function (**Figure 7A**). Likewise, the treatment with the

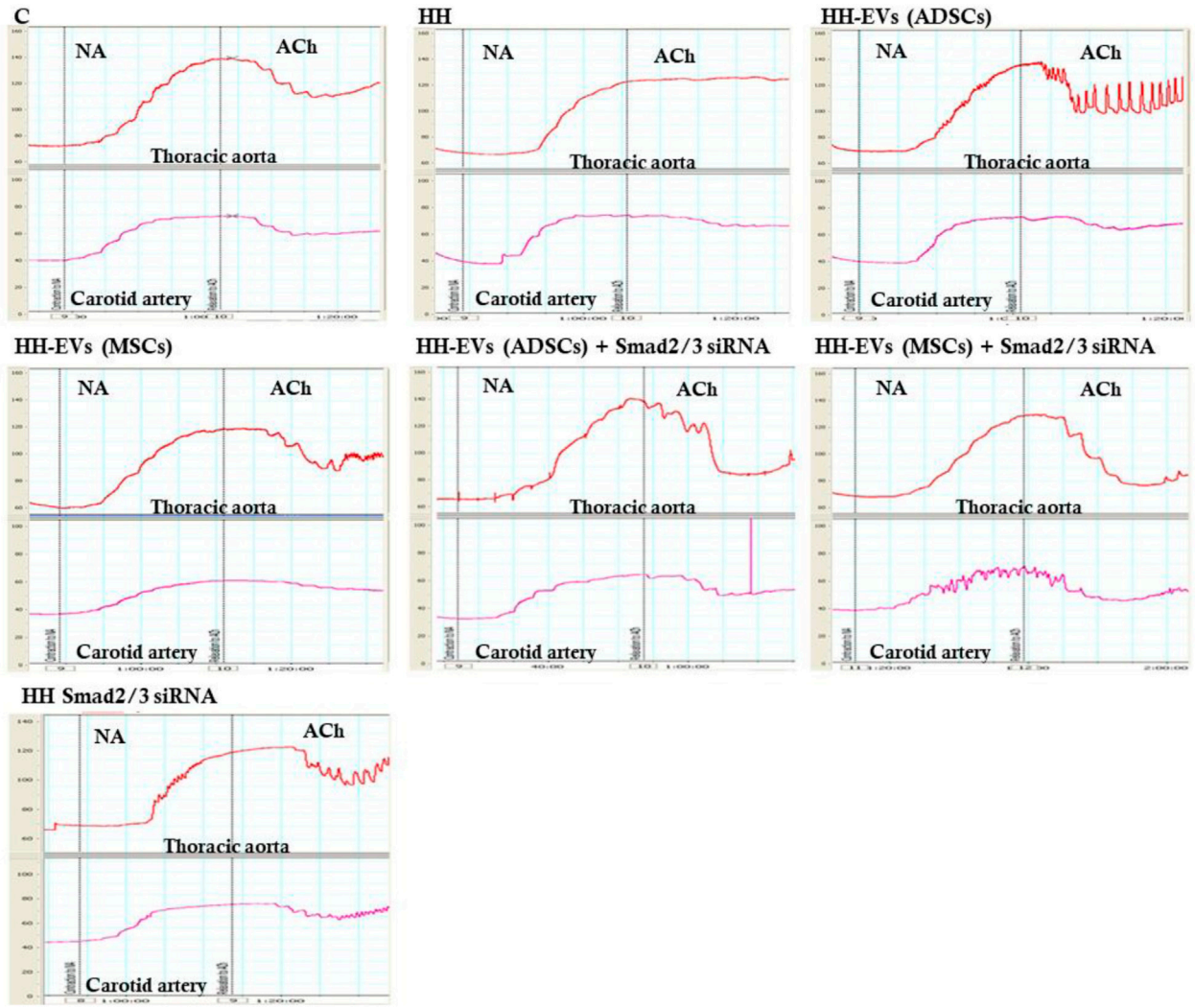

FIGURE 6 | Representative images with myograph recordings at selected time points: for the contraction function to NA (10^{-8} M ÷ 10^{-4} M) and relaxation to ACh (10^{-8} M ÷ 10^{-4} M) in the thoracic aorta (red) and carotid artery (purple) in all investigated experimental groups: C, HH, HH-EVs(ADSCs), HH-EVs(MSCs), HH-EVs(ADSCs)+Smad2/3siRNA, HH-EVs(MSCs)+Smad2/3siRNA, and HH-Smad2/3siRNA. Images were recorded with LabChart 7 software.

stem cell-derived EVs alone or in combination with Smad2/3 siRNA was favorable in terms of restoring the ability of both blood vessels investigated to relax, helping to improve the functionality initially affected (**Figure 7B**). The best ACh relaxation response was observed at the HH-EVs(MSCs)+Smad2/3siRNA group which registered a value above that of the control group (**Figure 7B**). The arteries from HH-EVs(MSCs) and HH-EVs(ADSCs)+Smad2/3 siRNA animal groups relaxed to very similar values between them, close to those in the control group (**Figure 7B**). Also, the reported response to ACh of arteries from HH-EVs(ADSCs) and HH- Smad2/3siRNA groups was significantly higher than that from the HH group, but the values were lower than those in the control group (**Figure 7B**). **Figure 6** shows the representative recordings obtained with the help of LabChart 7 software for NA contraction and ACh relaxation responses for each individual experimental group. Contraction to NA (10^{-8} M-10^{-4} M) was measured as the tension developed in the vascular wall (mN/mm), and endothelium-dependent relaxation to ACh (10^{-8} M-10^{-4} M) was calculated as a percentage of the maximum NA pre-contraction. All these data indicate that treatment administered to the HH group not only ameliorates vascular dysfunction but also improves the functionality of the blood vessel. These results reinforce the fact that stem cell-derived EV -based treatment improves vascular wall integrity in terms of structuring the functionality.

In order to analyze the effects that the administered atherogenic diet has on the morphogenic cytokine profile *in vivo*, we measured the plasma levels of TGF-β1 and AngII obtained by collecting blood from the retro-orbital venous plexus from all groups of experimental animals using the ELISA technique (**Figure 8**). These two molecules cause the activation of the transcription factors Smad 2/3, NF-kB, and ATF-2, which increase the expression of the inflammatory markers that we analyzed later and whose expression also proved to be elevated. The

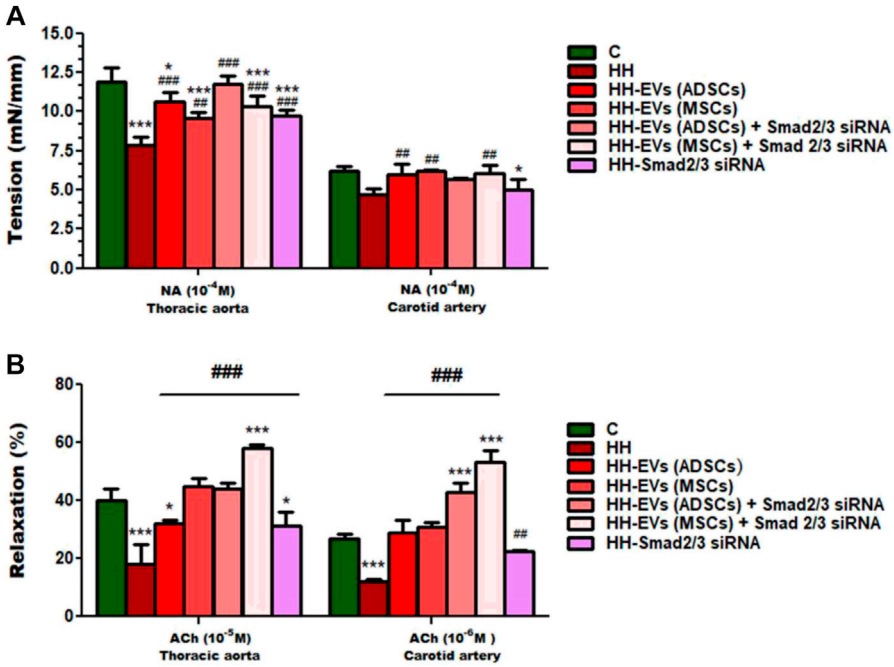

FIGURE 7 | Measures of vascular reactivity of the thoracic aorta (left) and carotid artery (right) explanted from all hamster groups (C, HH, HH-EVs(ADSCs), HH-EVs(MSCs), HH-EVs(ADSCs)+Smad2/3siRNA, HH-EVs(MSCs)+Smad2/3siRNA, and HH-Smad2/3siRNA) by using the myograph technique, in terms of **(A)** contraction to NA and **(B)** relaxation to ACh. Maximal contractile force developed by the thoracic aorta and carotid artery was measured to be 10^{-4} M NA, and maximal relaxation values were recorded to be 10^{-5} M ACh for the thoracic aorta and 10^{-6} M ACh for the carotid artery. Data are mean ± SD of four independent experiments for each investigated treated group and five independent experiments for control and HH groups. The statistical significance, noticeably different, was represented as $^{***}p < 0.005$ and $^{*}p < 0.05$ versus control group and $^{###}p < 0.005$ and $^{##}p < 0.01$ versus HH group. The values were calculated by two-way ANOVA and Bonferroni post-test. Enhanced plasma TGF-β1 and AngII levels in atherosclerosis are reduced after the administration of EVs (ADSCs) or EVs (MSCs) transfected or not with Smad2/3 siRNA.

results showed that the plasma levels of both TGF-β1 and AngII were statistically significantly increased in the HH group compared to those of the control group ($^{***}p < 0.005$) (**Figure 8**). Enhanced plasma TGF-β1 and AngII levels correlate with identified structural and functional changes in the thoracic aorta and carotid artery isolated from hamsters in the HH group, which mimic human atherosclerosis.

For groups of hamsters who received treatment, the plasma TGF-β1 and AngII levels were much lower overall, with the exception of the HH-EVs(MSCs) group in which AngII levels were not reduced (**Figure 8**). Treatment based on EVs from ADSCs or MSCs had a slightly better effect on reducing TGF-β1 levels than treatment based on EVs transfected with Smad2/3 siRNA, but without statistical significance (**Figure 8**). The biggest reduction in TGF-β1 levels was observed in the Smad2/3siRNA group ($^{###}p < 0.005$) (**Figure 8**). As for plasma, the AngII levels were significantly reduced for the hamsters in HH-EVs (ADSCs), HH-EVs (ADSCs) + Smad2/3 siRNA, HH-EVs (MSCs) + Smad2/3 siRNA, and HH- Smad2/3 siRNA groups compared to those of the HH hamster group (**Figure 8**). Again, as in the case of TGF-β1, Smad2/3 siRNA-only treatment greatly reduced plasma AngII levels (**Figure 8**).

It is important to note that stem cell-derived EV-based treatment regressed the HH-caused alterations in TGF-β1 and AngII pro-inflammatory molecule expressions with a key role in the atherosclerosis-induced vascular dysfunction.

Extracellular Vesicles (Adipose Tissue Stem Cells) and Extracellular Vesicles (Mesenchymal Stem Cells) Transfected or Not With Smad2/3 siRNA Reduced the Expression of Inflammatory Markers in the Wall of the Thoracic Aorta and Carotid Artery Affected by Experimental Hypertension-Hyperlipidemia

To investigate consequences of atherogenic diet and stem cell-derived EV-based treatment on the vascular wall health, the protein expression of some specific inflammatory markers was analyzed by immunofluorescence performed on sections of the thoracic aorta and carotid artery isolated from all animal experimental groups (**Figure 9**; **Table 2**). The examined pro-inflammatory markers as part of the atherosclerotic process were collagen type I (COL1A1) that intervenes in the fibrotic process, connexin 43 (CX43) which forms the myo-endothelial gap junctions, α-SMA which plays an important role in the SMC contraction, VCAM-1 with role in cell adhesion, and MMP-2 with involvement in ECM degradation and vascular remodeling. Also, the total macrophages ($CD68^{+}$), M1 pro-inflammatory macrophages

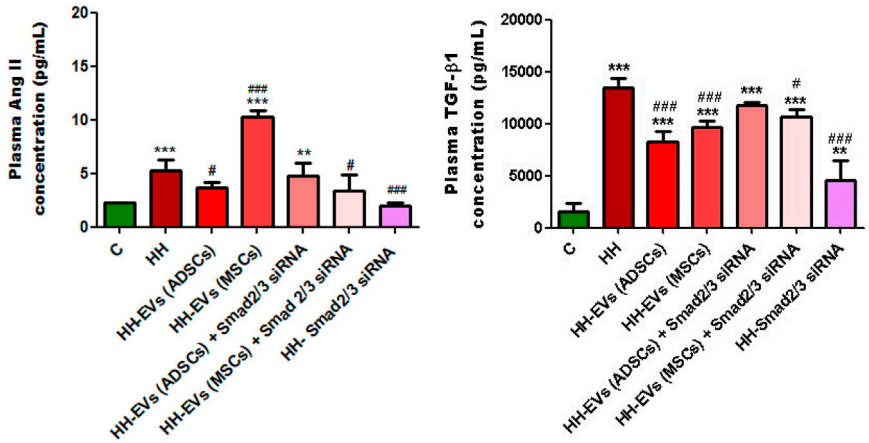

FIGURE 8 | Analysis of plasma TGF-β1 and AngII levels by the enzyme-linked immunosorbent assay (ELISA) method, for all experimental groups: C, HH, HH-EVs(ADSCs), HH-EVs(MSCs), HH-EVs(ADSCs)+Smad2/3siRNA, HH-EVs(MSCs)+Smad2/3siRNA, and HH-Smad2/3siRNA. The measurements were performed in triplicate, and the results were depicted as mean ± SD. The statistical significance, noticeably different, was represented as $^{***}p < 0.005$, $^{**}p < 0.01$ versus control group and $^{###}p < 0.005$, $^{#}p < 0.05$ versus HH group. The values were calculated by two-way ANOVA and Bonferroni post-test.

(MHC-II$^+$), and the immune cell infiltrate represented by T lymphocytes (CD3e$^+$) that support the inflammatory process characteristic of atherosclerosis were followed (**Figure 9**). Our results showed that all these investigated inflammatory markers had a significantly increased level of protein expression at the HH group compared to that of the C group, meaning that these pro-inflammatory *markers are* abundantly released in the thoracic aorta and carotid artery after 4 months of atherogenic diet (**Figure 9**; **Table 2**). The presence of inflammatory markers in the vascular wall may lead to structural and architectural changes recorded by the echocardiography and myograph technique.

Regarding the effect of the treatment administered concomitantly with the atherogenic diet, it was observed that in the case of the inflammatory marker COL1A1 in the thoracic and carotid artery, the treatment with EVs (ADSCs) or EVs (MSCs) generated a strong reduction of its expression, and the calculated values being even lower than those observed in the case of the control group (**Figure 9**; **Table 2**). For the other types of treatment applied, the protein expression for COL1A1 had a decreasing trend compared to the values observed in the case of atherogenic diet in both vessels investigated and statistically significant differences being registered in the carotid artery in the case of Smad2/3 siRNA treatment ($^{###}p < 0.005$) (**Figure 9**; **Table 2**).

In terms of protein expression for Cx43 and α-SMA, analysis of fluorescence images and their quantification showed that they are significantly higher in the HH group than in the control group in both the thoracic aorta and the carotid artery ($^{***}p < 0.005$) (**Figure 9**; **Table 2**). These results demonstrate that in the structure of the vascular wall, there are changes closely associated with the state of inflammation characteristic of the atherogenic process. Applied treatment based on EVs and Smad2/3 siRNA reduced Cx43 and α-SMA expressions, the best effect being obtained in the case of the HH-EVs(ADSCs)+Smad2/3siRNA and HH-Smad2/3siRNA groups for α-SMA ($^{###}p < 0.005$) and in the case of the HH-EVs(ADSC) and HH-Smad2/3siRNA groups for Cx43, in the thoracic aorta ($p < 0.005$) (**Figure 9**; **Table 2**). However, regardless of the group, therapy with EVs transfected or not with Smad2/3 siRNA and the administration of Smad2/3 siRNA as such managed to positively modulate the architecture of the investigated arteries (**Figure 9**; **Table 2**). Interestingly, some values were lower than those of the control.

The marker for endothelial activation represented by VCAM-1 had registered values with a fulminant growth trend in the HH group ($^{***}p < 0.005$) compared to those of the control group (**Figure 9**; **Table 2**). A considerable improvement observed by lowering VCAM-1 expression levels in both arteries was seen in all groups after treatment administration for 4 months. It should be noted that the treatment made the expression of the protein lower than that measured in control animals (**Figure 9**; **Table 2**).

Quantification of MMP-2 expression revealed the same tendency as previously observed in VCAM-1 with an extremely high level in the HH group and with values close to or even lower than those in healthy animals (**Figure 9**; **Table 2**). Last, we investigated the inflammatory infiltrate with immune cells (total macrophages, pro-inflammatory macrophages M1, and T lymphocytes) in the arterial wall of the thoracic aorta and carotid artery. The increased averaged values of fluorescence obtained in the HH group showed that the atherogenic diet and gavage significantly enlarged the percentage of infiltration of these cells into the arterial wall compared to that of control animals (**Figure 9**; **Table 2**). It could also be seen that after treatment and further administration of the diet, inflammation is reduced, being maintained around control values. The exception was the HH group treated with EVs (MSCs) in which values of fluorescence were equivalent to those from the untreated HH group, indicating that the administration of EVs (MSCs) did not have the desired effect, especially on total and M1 macrophage infiltration in the carotid artery (**Figure 9**; **Table 2**).

Analysis of the cytosolic ROS expression level generated in the thoracic aorta of all seven experimental groups revealed that all

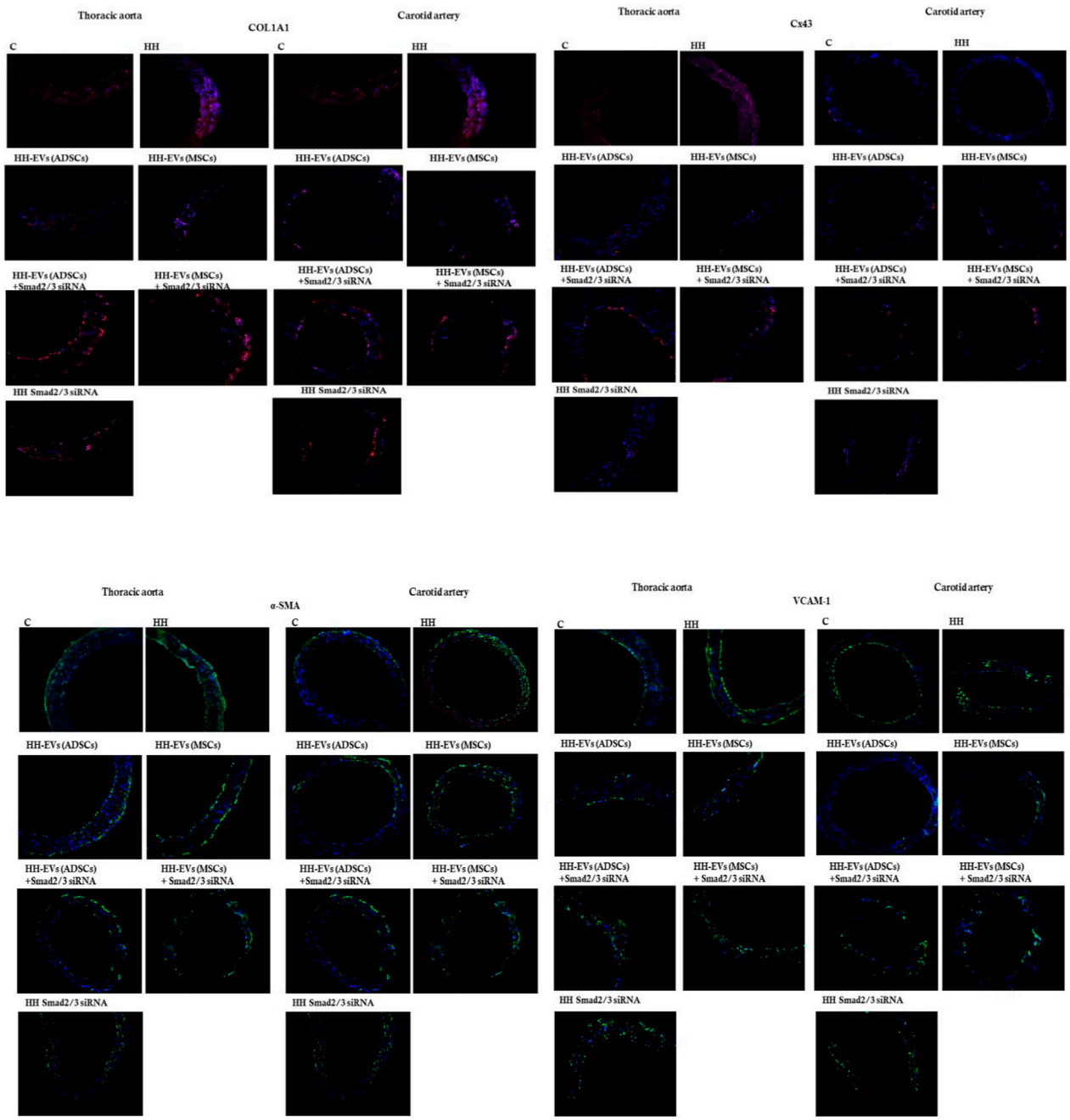

FIGURE 9 | Representative immunofluorescence images for the evaluation of inflammatory markers specific to vascular dysfunction after 4 months of the hyperlipemic–hypertensive diet and the stem cell-derived EV-based treatment or siRNA-based treatment. The thin cryosections from the thoracic aorta (on the left) and carotid artery (on the right) harvested from all experimental groups (C, HH, HH-EVs (ADSCs), HH-EVs (MSCs), HH-EVs(ADSCs)+Smad2/3siRNA, HH-EVs(MSCs)+Smad2/3siRNA, and HH-Smad2/3siRNA) were immuno-labeled for the following: **1)** structural proteins: collagen type I (COL1A1) alpha smooth muscle actin (α-SMA), and connexin 43 (Cx43); **2)** proteins involved in cell adhesion and vascular remodeling: matrix metalloproteinase-2 (MMP-2) and vascular cell adhesion molecule-1 (VCAM-1); **3)** immune cell infiltrate: T cells (CD3e+), total macrophages ($CD68^+$), and M1 macrophages (MHC-II+); and **4)** cytosolic ROS production (dihydroethidium (DHE) was oxidized by cytosolic ROS to fluorescent ethidium bromide that intercalates DNA yielding a bright red nuclear fluorescence). Nuclei were shown in blue fluorescence by DAPI dye staining. Each experiment point was performed in triplicate, from two different sets of experiments. A total of five different microscopic fields for each experimental point were analyzed. Total magnification: ×20. The images were quantified using the ImageJ program.

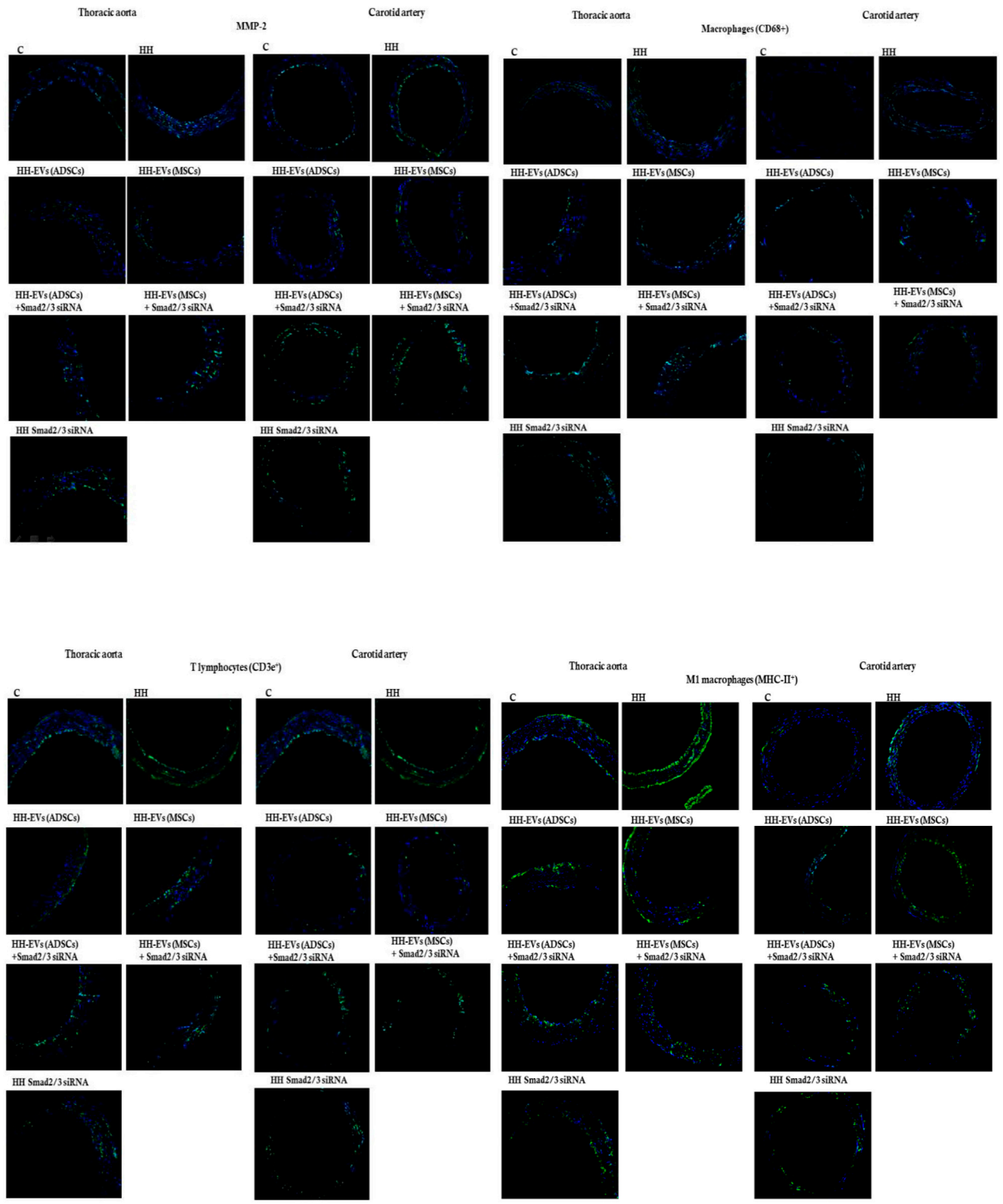

FIGURE 9 | (Continued).

treated groups had low statistical values compared to those of the HH group ($^{###}p < 0.005$), at which the fluorescence values were significantly increased compared to those measured in group C ($^{***}p < 0.005$) (**Figure 9**; **Table 2**). In the case of the carotid artery, the best reduction in ROS levels was observed at the HH-EVs (ADSCs) and HH Smad2/3 siRNA groups ($^{###}p < 0.005$), while

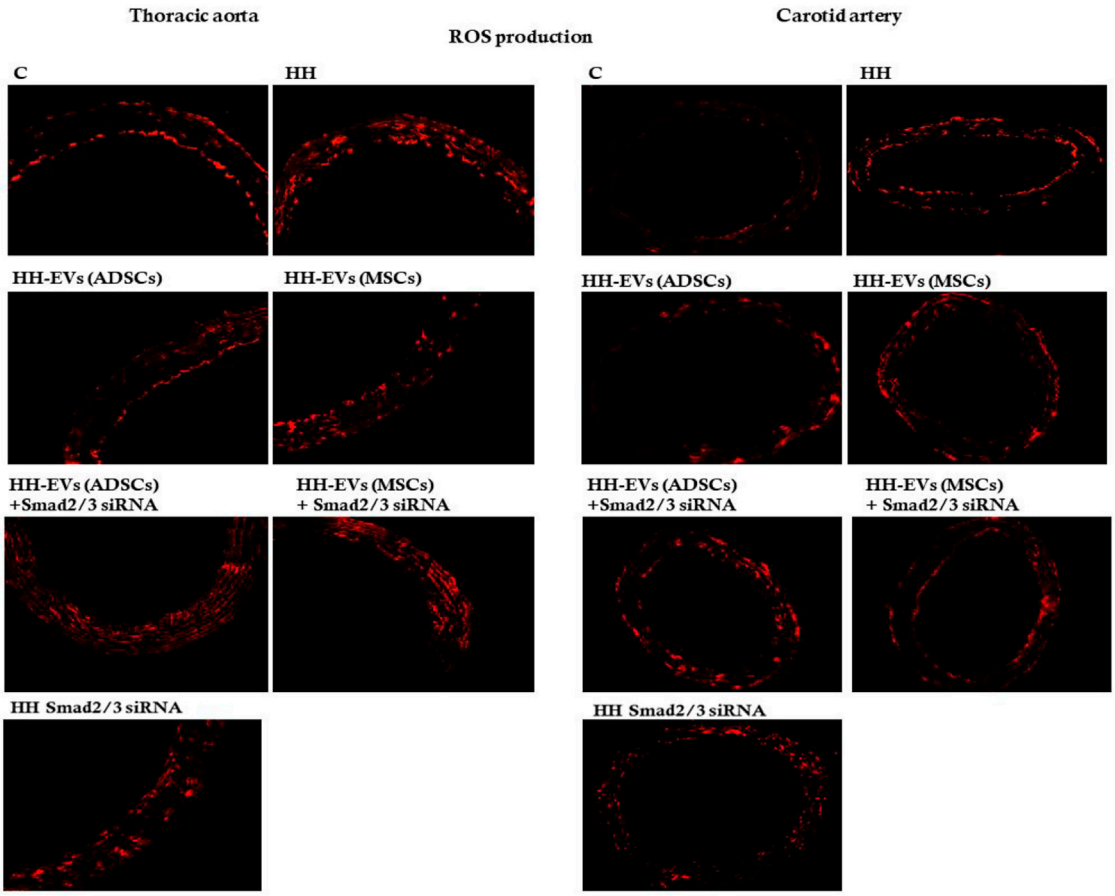

FIGURE 9 | (Continued).

the rest of the treated groups also having a significant decrease in the fluorescence level compared to the HH group (**Figure 9**; **Table 2**). These results showed that treatment administration greatly diminished ROS release in the vascular wall, thus contributing to the improvement of blood vessel function.

Extracellular Vesicles (Adipose Tissue Stem Cells) and Extracellular Vesicles (Mesenchymal Stem Cells) Transfected or Not With Smad2/3 siRNA Decreased the Expression Profile of the Key Molecules That Modulate the Inflammatory Response in the Vascular Wall

Because our results showed that the plasma levels of AngII and TGF-β1 were increased after atherogenic diet, we thought that the molecules involved in their signaling pathways could be responsible for the changes in structural, functional, and inflammatory markers of the vascular wall in the process of atherosclerosis. As a result, the expressions of transcription factors Smad2/3, ATF-2, and NF-kB p50/p65 (**Figures 10**, **11**) and miR21, miR192, miR200, and miR29 (**Figure 12**) in the thoracic aorta and carotid artery explanted from all experimental groups were evaluated.

The data showed that the protein expressions of pSmad2/3, Smad2/3, pATF-2, ATF-2, and NF-kB p50/p65 molecules were significantly increased in the thoracic aorta explanted from HH hamsters (***$p < 0.005$), while in the carotid artery from the HH group only expressions of SMAD2/3 and ATF2 molecules were significantly augmented (**$p < 0.01$) (**Figures 10**, **11**). These results compared to those in healthy animals claim that the diet accelerated changes at the cellular level with alterations in the regulation of the transcription of numerous genes. The SMAD2/3 transcription factor whose expression was found to be elevated in the HH group was targeted by EV-based treatment by transfecting them with SMAD2/3siRNA. Accordingly, HH animals that were injected with EVs from ADSCs or MSCs transfected or not with Smad2/3 siRNA had a reduced level of SMAD2/3 protein in both types of arteries investigated (**Figures 10**, **11**). No noticeable reduction on SMAD2/3 protein expression was detected following Smad2/3siRNA treatment only, meaning that the presence of EV as a transport system for siRNAs is essential for blocking SMAD2/3.

Regarding the other molecules investigated, the allogenic administration of EVs (ADSCs) or EVs (MSCs) transfected or

TABLE 2 | Quantification of the stained areas of inflammatory markers from the fluorescence images of the thoracic aorta and carotid artery sections collected from all investigated animal groups. Results were expressed as mean ± SD. The statistical significance, noticeably different, was represented as $^{***}p < 0.005$, $^{**}p < 0.01$, $^{*}p < 0.05$ values versus control group and $^{\#\#\#}p < 0.005$, $^{\#\#}p < 0.01$, $^{\#}p < 0.05$ values versus HH group. Two-way ANOVA and Bonferroni post-test were applied.

Stained areas	Control (n = 11)	HH (n = 18)	HH-EVs (ADSCs) (n = 10)	HH-EVs (MSCs) (n = 9)	HH-EVs (ADSCs) +Smad2/3 siRNA (n = 5)	HH-EVs (MSCs) +Smad2/3 siRNA (n = 6)	HH-Smad2/3 siRNA (n = 8)
Alpha smooth muscle actin (α-SMA)							
Thoracic aorta	160.63 ± 28.9	240.22 ± 19.08 ($^{***}p < 0.005$)	185.80 ± 25.93 ($^{\#\#\#}p < 0.005$)	170.17 ± 33.19 ($^{\#\#\#}p < 0.005$)	149.60 ± 30.13 ($^{\#\#\#}p < 0.005$)	153.79 ± 15.65 ($^{\#\#\#}p < 0.005$)	132.16 ± 16.62 ($^{*}p < 0.05$) ($^{\#\#\#}p < 0.005$)
Carotid artery	148.75 ± 36.38	236.99 ± 9.46 ($^{***}p < 0.005$)	202.35 ± 16.78 ($^{**}p < 0.01$)	180.69 ± 33.51 ($^{\#\#}p < 0.01$)	135.59 ± 24.51 ($^{\#\#\#}p < 0.005$)	172.04 ± 12.63 ($^{\#\#}p < 0.01$)	143.17 ± 15.94 ($^{\#\#\#}p < 0.005$)
Collagen type I (COL1A1)							
Thoracic aorta	129.25 ± 27.24	248.93 ± 38.96 ($^{***}p < 0.005$)	114.57 ± 31.04 ($^{\#\#\#}p < 0.005$)	81.51 ± 22.96 ($^{*}p < 0.05$) ($^{\#\#\#}p < 0.005$)	196.17 ± 46.82 ($^{**}p < 0.01$) ($^{\#}p < 0.05$)	225.15 ± 43.90 ($^{***}p < 0.005$)	181.11 ± 47.84 ($^{**}p < 0.01$) ($^{\#\#}p < 0.01$)
Carotid artery	217.32 ± 15.49	281.88 ± 12.53 ($^{*}p < 0.05$)	88.82 ± 23.87 ($^{**}p < 0.01$) ($^{\#\#\#}p < 0.005$)	97.98 ± 21.49 ($^{**}p < 0.01$) ($^{\#\#\#}p < 0.005$)	221.27 ± 48.36	207.76 ± 63.62 ($^{\#\#}p < 0.01$)	103.77 ± 38.19 ($^{*}p < 0.05$) ($^{\#\#\#}p < 0.005$)
Connexin 43 (Cx43)							
Thoracic aorta	138.09 ± 12.14	211.94 ± 19.87 ($^{***}p < 0.005$)	46.34 ± 19.01 ($^{***}p < 0.005$) ($^{\#\#\#}p < 0.005$)	118.01 ± 43.88 ($^{\#\#\#}p < 0.005$)	135.64 ± 17.53 ($^{\#\#\#}p < 0.005$)	102.72 ± 31.16 ($^{*}p < 0.05$) ($^{\#\#\#}p < 0.005$)	47.39 ± 16.05 ($^{***}p < 0.005$) ($^{\#\#\#}p < 0.005$)
Carotid artery	46.72 ± 80.4	118.60 ± 34.76 ($^{**}p < 0.01$)	47.29 ± 19.43	74.79 ± 45.70	98.14 ± 8.02	101.62 ± 18.87	40.69 ± 14.24 ($^{\#\#\#}p < 0.005$)
Vascular cell adhesion molecule-1 (VCAM-1)							
Thoracic aorta	271.15 ± 32.45	489.07 ± 35.31 ($^{***}p < 0.005$)	152.16 ± 31.72 ($^{***}p < 0.005$) ($^{\#\#\#}p < 0.005$)	183.43 ± 44.48 ($^{***}p < 0.005$) ($^{\#\#\#}p < 0.005$)	140.59 ± 23.09 ($^{***}p < 0.005$) ($^{\#\#\#}p < 0.005$)	173.22 ± 18.97 ($^{***}p < 0.005$) ($^{\#\#\#}p < 0.005$)	151.10 ± 15.83 ($^{***}p < 0.005$) ($^{\#\#\#}p < 0.005$)
Carotid artery	156.20 ± 26.03	232.08 ± 43.61 ($^{**}p < 0.01$)	119.19 ± 23.13 ($^{\#\#\#}p < 0.005$)	119.87 ± 21.03 ($^{\#\#\#}p < 0.005$)	145.41 ± 20.45 ($^{\#\#\#}p < 0.005$)	145.94 ± 18.14 ($^{\#\#\#}p < 0.005$)	132.1 ± 10.36 ($^{\#\#\#}p < 0.005$)
Matrix Metalloproteinase-2 (MMP-2)							
Thoracic aorta	222.97 ± 41.18	460.46 ± 65.94 ($^{***}p < 0.005$)	88.62 ± 20.53 ($^{***}p < 0.005$) ($^{\#\#\#}p < 0.005$)	93.50 ± 25.42 ($^{***}p < 0.005$) ($^{\#\#\#}p < 0.005$)	110.45 ± 16.56 ($^{***}p < 0.005$) ($^{\#\#\#}p < 0.005$)	109.79 ± 9.10 ($^{***}p < 0.005$) ($^{\#\#\#}p < 0.005$)	125.83 ± 27.36 ($^{***}p < 0.005$) ($^{\#\#\#}p < 0.005$)
Carotid artery	133.87 ± 15.33	324.68 ± 25.94 ($^{***}p < 0.005$)	109.00 ± 8.86 ($^{\#\#\#}p < 0.005$)	91.39 ± 17.20 ($^{*}p < 0.05$) ($^{\#\#\#}p < 0.005$)	171.31 ± 15.96 ($^{\#\#\#}p < 0.005$)	131.99 ± 20.24 ($^{\#\#\#}p < 0.005$)	102.99 ± 19.66 ($^{\#\#\#}p < 0.005$)
T cells (CD3e+)							
Thoracic aorta	132.10 ± 11.27	231.07 ± 55.07 ($^{***}p < 0.005$)	112.51 ± 38.95 ($^{\#\#\#}p < 0.005$)	105.15 ± 30.57 ($^{\#\#\#}p < 0.005$)	114.76 ± 22.53 ($^{\#\#\#}p < 0.005$)	98.80 ± 25.07 ($^{\#\#\#}p < 0.005$)	91.84 ± 19.61 ($^{*}p < 0.05$) ($^{\#\#\#}p < 0.005$)
Carotid artery	70.56 ± 11.33	153.98 ± 51.99 ($^{**}p < 0.01$)	81.18 ± 29.12 ($^{\#\#}p < 0.01$)	117.18 ± 24.66	86.03 ± 11.13 ($^{\#}p < 0.05$)	129.89 ± 28.07	96.08 ± 20.76 ($^{\#}p < 0.05$)
Macrophages (CD68⁺)							
Thoracic aorta	93.50 ± 17.05	246.48 ± 19.18 ($^{***}p < 0.005$)	100.53 ± 19.18 ($^{\#\#\#}p < 0.005$)	84.54 ± 25.62 ($^{\#\#\#}p < 0.005$)	64.45 ± 17.87 ($^{\#\#\#}p < 0.005$)	75.17 ± 16.55 ($^{\#\#\#}p < 0.005$)	86.13 ± 19.67 ($^{\#\#\#}p < 0.005$)
Carotid artery	55.30 ± 3.53	114.67 ± 8.43 ($^{**}p < 0.01$)	82.31 ± 21.11	129.36 ± 21.03 ($^{***}p < 0.005$)	39.46 ± 7.01 ($^{\#\#\#}p < 0.005$)	47.59 ± 22.57 ($^{\#\#\#}p < 0.005$)	84.97 ± 25.13
Macrophages M1 (MHC-II+)							
Thoracic aorta	246.28 ± 20.80	378.20 ± 51.64 ($^{***}p < 0.005$)	133.00 ± 24.88 ($^{***}p < 0.005$) ($^{\#\#\#}p < 0.005$)	206.41 ± 21.71 ($^{*}p < 0.05$) ($^{\#\#\#}p < 0.005$)	118.80 ± 15.13 ($^{***}p < 0.005$) ($^{\#\#\#}p < 0.005$)	124.06 ± 15.52 ($^{***}p < 0.005$) ($^{\#\#\#}p < 0.005$)	131.74 ± 21.32 ($^{***}p < 0.005$) ($^{\#\#\#}p < 0.005$)
Carotid artery	71.68 ± 2.63	152.35 ± 17.54 ($^{***}p < 0.005$)	128.43 ± 24.92 ($^{**}p < 0.01$)	189.88 ± 45.23 ($^{***}p < 0.005$) ($^{\#}p < 0.05$)	117.25 ± 13.83	119.33 ± 22.83 ($^{*}p < 0.05$)	104.71 ± 17.49 ($^{\#\#\#}p < 0.005$)
ROS (reactive oxygen species)							
Thoracic aorta	4.76 ± 0.67	7.88 ± 0.88 ($^{***}p < 0.005$)	4.69 ± 1.16 ($^{\#\#\#}p < 0.005$)	4.59 ± 0.80 ($^{\#\#\#}p < 0.005$)	5.61 ± 0.73 ($^{\#\#\#}p < 0.005$)	5.17 ± 0.83 ($^{\#\#\#}p < 0.005$)	5.49 ± 0.66 ($^{\#\#\#}p < 0.005$)
Carotid artery	4.28 ± 0.64	6.58 ± 0.85 ($^{***}p < 0.005$)	3.82 ± 1.16 ($^{\#\#\#}p < 0.005$)	4.79 ± 0.88 ($^{\#\#\#}p < 0.005$)	5.97 ± 0.55 ($^{**}p < 0.01$)	4.96 ± 1.42 ($^{\#\#}p < 0.01$)	3.85 ± 0.79 ($^{\#\#\#}p < 0.005$)

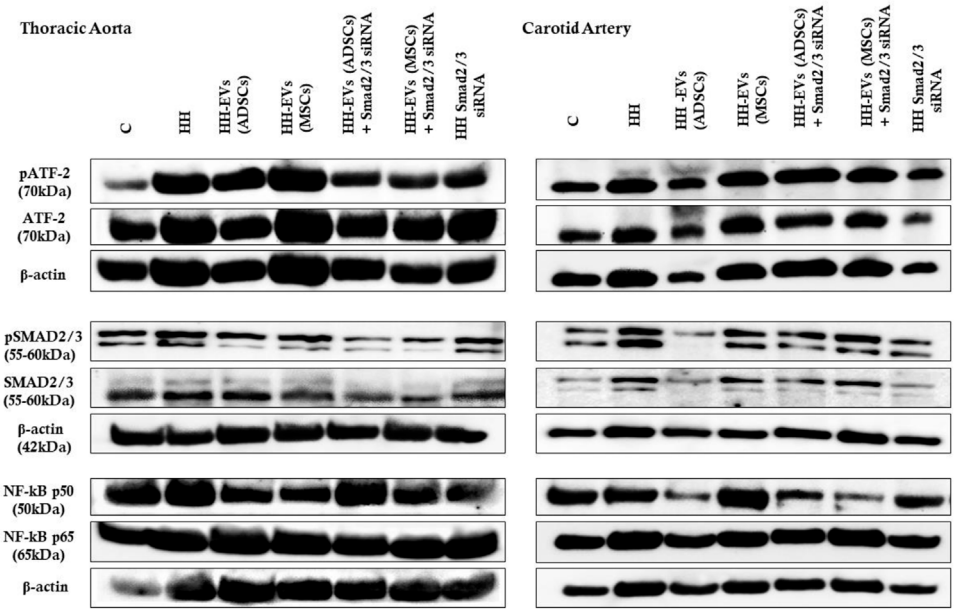

FIGURE 10 | Representative Western blotting images of the expression levels of pATF-2, ATF-2, pSMAD2/3, SMAD2/3, NF-kBp50, NF-kBp65, and β-actin in both thoracic aorta (left) and carotid artery (right) explanted from all seven experimental animal groups.

not with Smad2/3 siRNA and single administration of SMAD2/3siRNA significantly diminished ATF-2 protein expression in the thoracic aorta ($^{###}p < 0.005$, $^{##}p < 0.01$) and carotid artery ($^{***}p < 0.005$, $^{**}p < 0.01$, $^{##}p < 0.01$) (**Figures 10**, **11**).

Afterward, the expression of NF-kB transcription factor with the two subunits p50 and p65 was followed. For the NF-kB p50 subunit, at the level of the thoracic aorta, the administration of EVs (ADSCs), EVs (MSCs), or EVs(ADSCs) transfected with SMAD2/3siRNA significantly reduced its expression level ($^{###}p < 0.005$, $^{##}p < 0.01$), while the treatment with EVs(MSCs) transfected with SMAD2/3siRNA or SMAD2/3siRNA generated an insignificant reduction (**Figures 10**, **11**). For the carotid artery, the protein expression of the NF-kB p50 subunit was significantly diminished by EVs (ADSCs) transfected or not with SMAD2/3siRNA and EVs (MSCs) transfected with SMAD2/3siRNA ($^{##}p < 0.01$, $^{#}p < 0.05$) (**Figures 10**, **11**).

In parallel experiments, it was shown that the NF-kB p65 expression level was significantly reduced after 4 months of treatment with EVs (ADSCs) or EVs (MSCs) transfected or not with Smad2/3 siRNA or SMAD2/3siRNA in the thoracic aorta, and the values were close to those from the control animals ($^{###}p < 0.005$) (**Figures 10**, **11**). It is worth noting that treatment based on EVs from ADSCs and MSCs had the best results (**Figures 10**, **11**). In addition, NF-kB p65 expression in the carotid artery level was unchanged by all types of treatment administered (**Figures 10**, **11**).

In addition to Smad2/3, ATF-2, and NF-kB p50/p65 molecules, the alterations in the expressions of some miRs could also induce the increased levels of inflammatory markers generating events that contribute to the progression and aggravation of the atherosclerotic lesion. Thus, miRNA-21, miRNA-192, miRNA-200b, miRNA-29a, miRNA-210, and miRNA-146a were selected on the basis of their implication in atherosclerosis, endothelial activation, and inflammation. Each of the selected miRNAs was individually quantified from the thoracic aorta and carotid artery at the end of the experimental period, harvested from the seven experimental groups (**Figures 12A,B**). The expressions of these miRNAs were compared not only with the HH group but also with the group of healthy animals taken as the control group. The results showed that all selected miRNAs had significantly upregulated levels in the HH hamsters compared to those quantified at hamsters in the control group both in the thoracic aorta and carotid artery ($^{***}p < 0.005$, $^{**}p < 0.01$) (**Figures 12A,B**).

For the entire miRNA panel (miRNA-21, miRNA-192, miRNA-200b, miRNA-29a, miRNA-210, and miRNA-146a) examined in the thoracic aorta, all types of treatment investigated greatly reduced the expression with values in the range of those obtained in healthy animals ($^{###}p < 0.005$, $^{##}p < 0.01$, $^{#}p < 0.05$) (**Figures 12A**).

In the carotid artery, the effect of treatment on the investigated miRNA panel was approximately the same, except for the allogenic administration of EVs (MSCs) transfected with Smad2/3siRNA that had no positive therapeutic effects on miR21, miR-192, miR-210, and miR-146a levels (**Figures 12,B**), and Smad2/3siRNA alone failed to reduce the expression of the six miRNAs investigated but instead recorded similar values to those of HH animals (**Figures 12,B**).

It can be concluded that EV (ADSC)-based therapy has a better overall outcome which makes a significant contribution to the suppression of diet-induced changes in the inflammatory process.

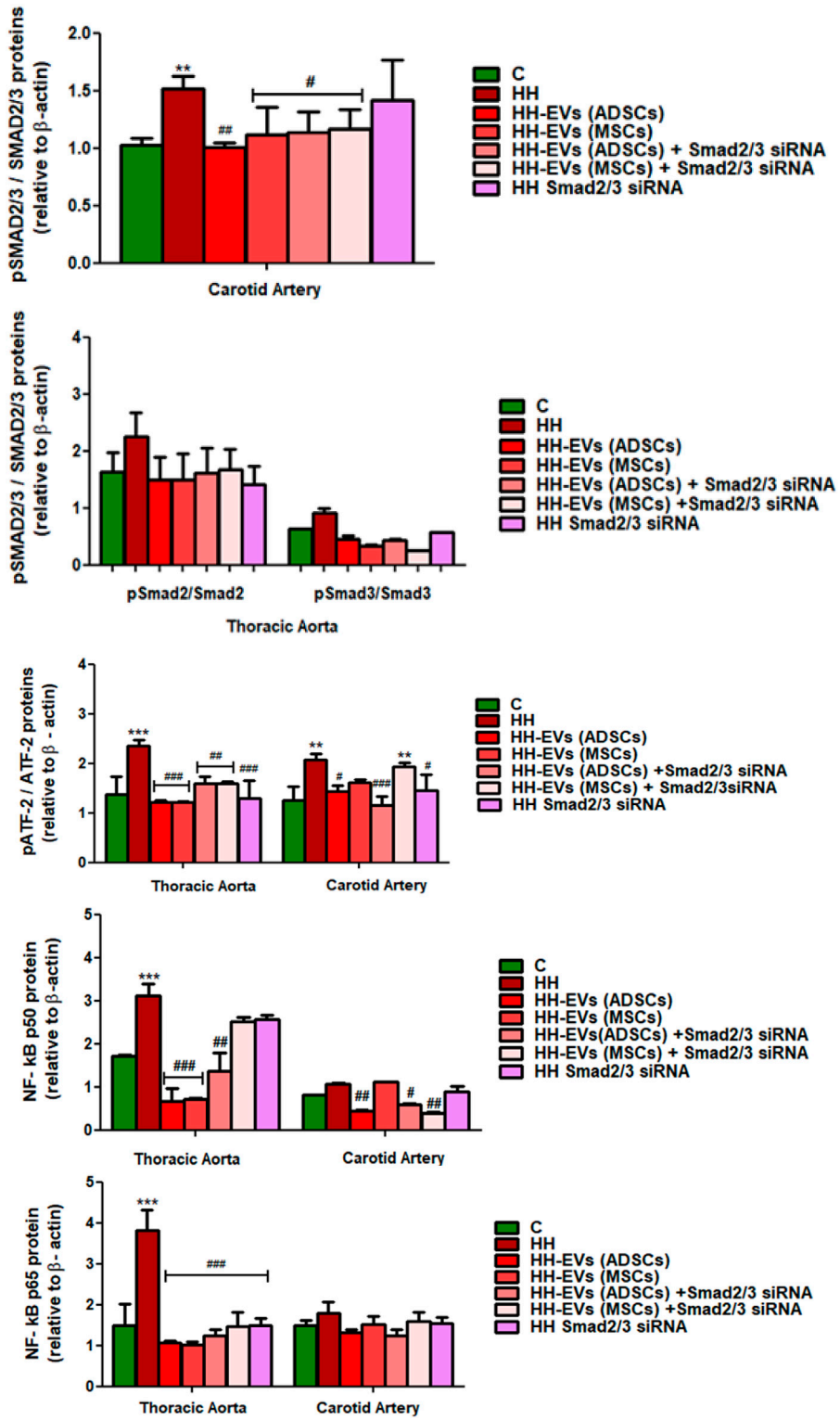

FIGURE 11 | Western Blot analysis for relative expression of specific pro-inflammatory molecules (proteins): pATF-2, ATF-2, pSMAD2/3, SMAD2/3, and NF-kBp50/p65. Histograms show a quantitative representation of the protein levels obtained from all investigated groups of four independent experiments after 4 months of diet and treatment. Each value represents the mean ± SD. The statistical significance, noticeably different, was represented as $^{***}p < 0.005$, $^{**}p < 0.01$ values versus control group and $^{###}p < 0.005$, $^{##}p < 0.01$, $^{#}p < 0.05$ values versus HH group. Statistical analysis was conducted using two-way ANOVA and Bonferroni post-test. The gray intensity of related proteins was analyzed by the TotalLab TL120 program. The housekeeping β-actin protein was used as an internal control for protein normalization and monitor for equal loading. Note that the β-actin expression fluctuated upon the treatment or under physiological and pathological conditions.

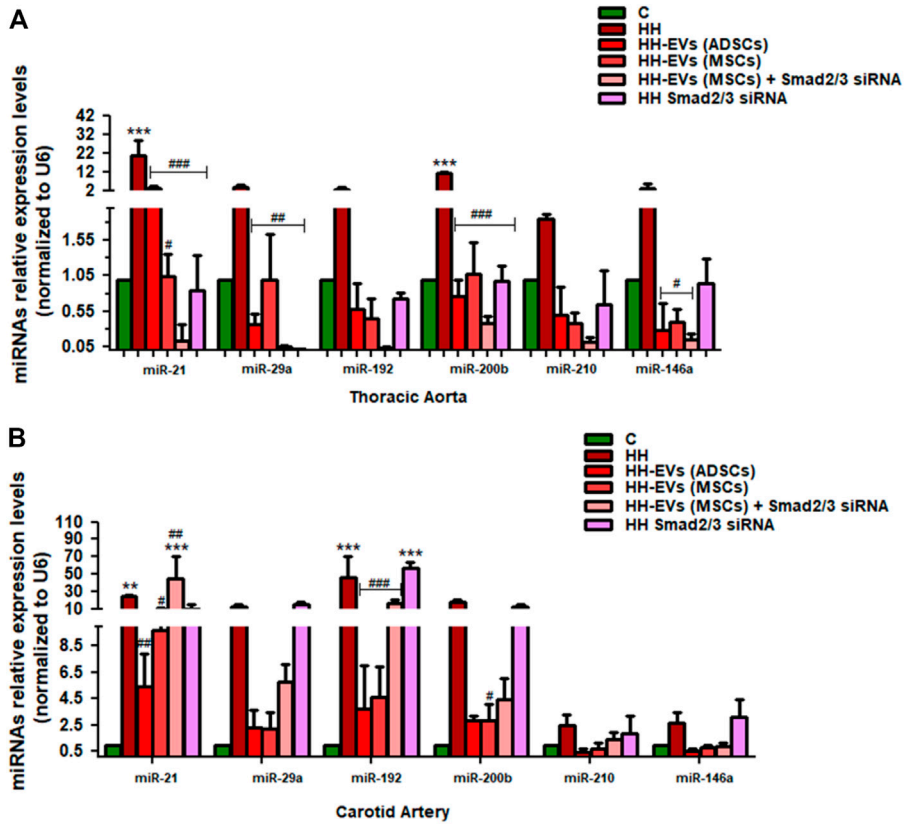

FIGURE 12 | Relative expression levels of six miRNAs (miRNA-21, miRNA-192, miRNA-200b, miRNA-29a, miRNA-210, and miRNA-146a) extracted from two types of tissue **(A)** thoracic aorta **(B)** and carotid artery, explanted from all groups of investigated animals. Total RNA was extracted and used for RT-qPCR. The expression of the miRNA panel was validated using three tissue samples from each artery and matched normal tissue samples. The miRNA expression was normalized using snRU6 as a reference gene. *p*-values of significant differences between the groups were calculated and represented as $^{***}p < 0.005$, $^{**}p < 0.01$, $^{*}p < 0.05$ for values vs. control group and $^{###}p < 0.005$, $^{##}p < 0.01$, $^{#}p < 0.05$ for values vs. HH group (two-way ANOVA Bonferroni post-test analysis). The mean fold change in expression of the target miRNA was calculated using ΔΔCt = ΔCt (a target sample) – ΔCt (a reference sample). For the control sample, ΔΔCt equals 0 and 2° equals 1; therefore, fold change in gene expression relative to control equals 1.

DISCUSSION

It is already known that atherosclerosis is an arterial chronic disease with a progressive evolution in which increased oxidized LDL levels, accumulation of immune cells, and reduced NO bioavailability contribute to the onset of inflammation and subsequently to endothelial damage, severe lesions, and thrombus formation.

In this context, we hypothesized that delivery of extracellular vesicles (EVs), recognized for their potential as therapeutic targets and tools, could restore impaired arterial function in atherosclerosis. Accordingly, we explored the potential beneficial effects of EVs from subcutaneous adipose tissue stem cells (EVs (ADSCs)) or bone marrow mesenchymal stem cells (EVs (MSCs)) transfected or not with Smad2/3 siRNA on vascular dysfunction and its key molecular players.

Thus, the golden Syrian hamster was used to obtain the experimental model of atherosclerosis, also called the hypertensive-hyperlipidemic (HH) hamster. There are a number of arguments that support the use of this animal model to study the complex process of atherosclerosis. It is known that the hamster has been used as an experimental model of induced atherosclerosis since the early 1980s because it has a number of advantages: a low rate of endogenous cholesterol synthesis, secretion of apolipoprotein B-100 by the liver, and complete assimilation of LDL-cholesterol by the receptor involved in the signaling pathway. It has also been shown that the morphology of foam cells formed or lesions in the thoracic aorta are similar to those present in humans (Dillard, Matthan, & Lichtenstein, 2010; Simionescu et al., 1996; Simionescu, Sima, Dobrian, Tirziu, & Simionescu, 1993).

The starting point in characterizing our animal model of atherosclerosis was the evaluation of the basic plasma parameters known to be drastically altered after the administration of the atherogenic diet. The first biochemical changes were observed as early as the second week of the atherogenic diet, so we decided that treatment should be begun at that time. Throughout the experiment, we wanted to investigate the effects of EV-based therapy under conditions of high-fat diet and saline for 4 months and whether it brings improvements in the regression of the atherosclerotic changes in the structure, function, and inflammatory markers of the arterial wall.

The obtained results showed that by comparison with the HH group examined for 4 months on the atherogenic diet enriched with sodium chloride, the administration of EVs(ADSCs) or EVs(MSCs), transfected or not with Smad2/3siRNA, or Smad2/3 siRNA alone of HH animals induced a significant reduction in the plasma levels of total cholesterol, LDL-cholesterol, and triglycerides. Also, the milky white plasma full of lipids, along with the presence of hepatic steatosis in the HH group, was no longer a surprise to us, but it was like a reconfirmation that the diet accelerates the development of atheroma plaque, with rapid progression of atherosclerosis in the arterial sector (Georgescu et al., 2012; Georgescu et al., 2016; Alexandru et al., 2020).

Our findings also validate numerous data being present in the literature that support the fact that this animal model is indicated in the study of vascular pathophysiological changes attributed to atherosclerosis. Thus, we have shown here the presence of the structural and functional changes at the vascular level in the HH group, which are the consequence of disrupting the integrity of vascular endothelium. Our subsequent echocardiographic recordings spread the light on the effect of treatment on the alterations already present in the HH group. The arterial wall thickness observed at the HH group may be associated with the migration of SMCs at the subendothelial level along with the formation of fibro-lipid plaque characteristic of the atherosclerotic process. The inner diameter of the thoracic aorta, although slightly reduced in the case of the HH group, did not significantly show different changes in the control and treated hamsters. Reduced vascular distensibility recorded at the HH group is the result of stiffening of the vascular wall, a process characteristic of atherosclerosis. Thickened vascular wall, reduction of the inner diameter, and stiffening of the wall detected at the HH group by echocardiography may be the consequences of changing the lipid profile, the deposition and accumulation of cholesterol (mainly LDL particles), and fatty substances in the arterial wall and possibly of the formation of atherosclerotic plaque (atheroma) (Pirillo, Bonacina, Norata, & Catapano, 2018; Milutinovic, Suput, & Zorc-Pleskovic, 2020). With the aim of better outlines the functionality of the blood vessel highlighted by echocardiography, we resorted to myographic experiments. Thus, we saw in real time the capacity of contraction and relaxation of the arterial wall for the two blood vessels investigated, namely the thoracic aorta and carotid artery. Following the analysis of the results, we were able to conclude that the animals which received a high-fat diet showed severely impaired functionality compared to control animals, which supports the results from echocardiography. All these results, which show that the wall structure of the thoracic aorta and carotid artery is affected in the case of the HH group, are characteristic of atherosclerotic cardiovascular disease.

Also, from our obtained data, we can appreciate that the administration of EV-based treatment to HH animals, in which the disease has already settled, had beneficial effects on the structure and function of the vascular wall. More specifically, the echocardiographic results of our study revealed that the allogenic administration of EVs (ADSCs) or EVs (MSCs) transfected or not with Smad2/3siRNA or Smad2/3siRNA alone significantly reduced the thickness of the vascular wall of the thoracic aorta/carotid artery, had no significant changes on inner diameter of the arterial wall (thoracic aorta/carotid artery), and significantly diminished values for VTI and velocity of the thoracic aorta compared to those of HH. Note that, EV-based treatment from ADSCs and the one transfected with Smad2/3 siRNA had a better result in restoring the elasticity/distensibility of the wall of the thoracic aorta. Moreover, our results showed a favorable trend in terms of restoring arterial functionality, with values that remained within the scope of those obtained at control. Specifically, the treatment was capable to improve vascular reactivity, respectively, the contractile and relaxing responses of thoracic aorta and carotid artery: the treatment with EVs (ADSCs) transfected or not with Smad2/3 siRNA re-established the contractile function of the investigated vessels to values close to normal, while the best response to relaxation was observed in the HH-EVs(MSCs) group transfected with Smad2/3 siRNA which registered a value above that in the control group in both investigated arteries. This fact proves that this pathology accompanied by vascular dysfunction can be remedied/regressed by treatments based on EVs transfected or not with Smad2/3siRNA. All these results regarding structural and functional changes of the vascular wall in atherosclerosis and their regression following treatment with EVs are supported by our previous work in which we only investigated the effect of microvesicles (Alexandru et al., 2020).

The next step in our study was to investigate specific inflammatory markers that could generate vascular dysfunction in our atherosclerosis model and that could be targets of proposed therapy. It is generally agreed that Ang II is a potent vasoconstrictor that activates TGF-β1, a cytokine involved in the regulation of various intracellular signaling cascades, especially of the SMAD-independent pathway. Any disturbance in the signaling pathway could lead to pathophysiological changes in vasculature with an impact on cardiovascular disease.

In this context, the influence of atherogenic diet or of EV-based treatment on plasma TGF-β1 and AngII levels was investigated. The analysis of these parameters at the HH group showed a marked increase in them, meaning that the inflammatory process is strong and sustained. Also, the results exhibited a correlation directly proportional between plasma TGF-β1 and AngII levels and identified structural and functional changes in the thoracic aorta and carotid artery from HH hamsters. For groups of hamsters who received treatment, the plasma TGF-β1 and AngII levels were much lower overall, with the exception of the HH-EVs (MSCs) group in which AngII levels were not reduced. As a result, we could conclude that therapy with EVs transfected or not with Smad2/3 siRNA reduced the inflammatory condition, thus helping to regress the atherosclerosis-associated dysfunction already installed. There are no published data to show the beneficial effect of stem cell-derived EVs on the plasma TGF-β1 and AngII levels in the atherosclerotic process.

In order to have a better overview of the consequences that the activation of key regulatory molecules has on the atherogenic

process, we focused on investigating specific structural and inflammatory markers by immunofluorescence. As far as we know from extensive studies, the increased expression of many proteins has been directly associated not only with changes that occur at the time of vascular endothelial damage/injury but also with the complications that follow. In this sense, a first important experimental observation of our study was about the histological structure of the vascular wall, which in the HH group showed disorganization in the architecture of the tunics in the two types of blood vessels examined (thoracic aorta and carotid artery). Also, COL1A expression in the thoracic aorta and carotid artery and Cx43 expression in the thoracic aorta almost increased double at animals with atherogenic diet (HH group). These increases were attributed to the growth of plasma TGF-β1 and AngII levels found by us at the HH group. Our results are consistent with other studies that have shown changes in the vascular wall composition, namely the increase of COL1A1 synthesis due to intensification of the inflammatory process and the activation of the cytokine TGF-β1 which supports the fibrotic process through its response to mechanical stress. Also, the expression of Cx43 was found to be induced in endothelial cells exposed to disturbed flow (Morel, 2014). In addition, our results revealed VCAM-1 and MMP-2 overexpression in endothelial cells, respectively, in SMCs, in the vascular wall of the thoracic aorta and carotid artery after the administration of the atherogenic diet for 4 months. VCAM-1, a protein expressed on the surface of activated endothelial cells, is considered an early manifestation of cholesterol-induced atherosclerosis. It recruits monocytes from the bloodstream, participating in their internalization in the vascular wall, thus generating the release of cytokines and chemokines at the site of injury, culminating in the development of vascular diseases such as atherosclerosis (Mu, Chen, Gong, Zheng, & Xing, 2015). Their expression is modulated not only by Ang II but also by oxidative stress, which we observed in the thoracic aorta and carotid artery from the HH group. Oxidative stress crowns and maintains the state of inflammation at the vascular level, and its elevated values can be associated not only with damage to the endothelium of the arteries and its activation but also with an increase in oxidized LDL in the vascular intima (Davignon & Ganz, 2004; Matsuzawa & Lerman, 2014; Pacurari, Kafoury, Tchounwou, & Ndebele, 2014; Kattoor, Pothineni, Palagiri, & Mehta, 2017; Pirillo et al., 2018). Also, it was demonstrated that the increase in vascular permeability, represented by high levels of VCAM-1, leads to the exacerbation of the levels of inflammatory cells, especially of the circulating monocytes those in the subendothelial space differentiating into macrophages (Wu, Li, Hou, & Chu, 2017; Groh, Keating, Joosten, Netea, & Riksen, 2018; Orekhov & Sobenin, 2019).

In our experiments, the selected markers, $CD68^+$, $CD3e^+$, and $MHC\text{-}II^+$ had marked increases that reconfirm that the high-fat diet administered to the HH group aggravated the inflammation, influencing all the other molecules investigated.

Following the interpretation of the results, the data obtained claim that the treatment drastically reduced the vascular inflammatory microenvironment. Thus, for groups of hamsters who received treatment consisting of EVs (ADSCs) or EVs(MSCs) transfected or not with Smad2/3siRNA or Smad2/3siRNA alone, the COL1A1, Cx43, VCAM-1 and MMP2 levels were significantly reduced compared to HH group. Likewise, the treatment reduced the expression of total macrophages ($CD68^+$), T cells ($CD3e^+$), M1 macrophages ($MHC\text{-}II^+$) in all treated groups, with the exception of the HH-EVs (MSCs) group in which M1 macrophage infiltration was not affected by treatment. In addition, the treatment administration considerably reduced long-term production of cytosolic ROS in the vascular beds (thoracic aorta/carotid artery) from all treated hamster groups, modulating the activity of the main orchestrators of inflammation-mediated atherosclerotic CVD progression. Noteworthy, the effect of stem cell-derived EV treatment on these molecules has not been shown in any other study. Until now EVs were mostly noticed as biomarkers or communication entities in different physiological ant pathological situations. Their potential as drug delivery systems has been recently noticed and disseminated in different medical applications: in cardiac regeneration (Gasecka et al., 2018), cancer treatment and also in nuclear medicine as radionuclide carriers. A recent opinion-paper on EVs as theranostic agents discussed the benefits of radiolabeled EVs in diagnostic and interventional medicine (Stępień and Rząca, 2021).

Furthermore, we were preoccupied with the examination of the mechanism responsible for generating biochemical, structural, and functional changes in the HH group. As plasma levels of Ang II and TGF-β1 were found to be elevated by the atherogenic diet, we questioned whether the SMAD2/3 signaling pathway is responsible for the exacerbated release of inflammatory markers in the vascular wall. Thus, the next step was to investigate other molecules involved, which in turn transduce signals to the nucleus and control the activity of genes with role in various cellular processes. Consequently, the analysis of protein expression revealed a marked increase in transcription factors Smad2/3, ATF-2, and NF-kBp50/p65 responsible for maintaining the inflammatory state in the arterial wall from the HH group. The increased expression of these molecules is mainly attributed to not only the fat-rich diet administered for 16 weeks but also the way in which the activation of key mediators of inflammation causes the cascade release of other molecules involved, thus maintaining the progression and aggravation of atherosclerotic injury/lesion. For example, NF-kB activation by oxidative stress and inflammation could suppress contractility in SMCs, and in this way it could generate the vascular dysfunction associated with atherosclerosis. As for the effect of therapy on these key molecules, our data exhibited that the allogenic administration of EVs (ADSCs) or EVs (MSCs) transfected or not with Smad2/3 siRNA and single administration of SMAD2/3siRNA reduced their protein expression in the vascular bed. There were some peculiarities that are worth mentioning, namely the treatment with EVs (MSCs) transfected with Smad2/3 siRNA generated an insignificant reduction on the NF-kB p50 expression level, while the NF-kB p65 expression level was unchanged in the carotid artery.

In our study, we were concerned to further examine the mechanism responsible for generating inflammatory markers

in the arterial wall with a role in the structural and functional changes observed in the thoracic aorta and carotid artery isolated from the HH group. Consequently, we decided to choose a panel of six miRNAs (hsa-miR-21, hsa-miR-192, hsa-miR-200b, hsa-miR-29a, hsa-miR-210, and hsa-miR-146a) whose expressions are known to be upregulated in the atherosclerotic lesion/fibroatheroma following the release of pro-inflammatory cytokines. Recent studies have shown that there are a multitude of miRNAs associated with the atherogenic process whose expression profiles differ significantly between atherosclerotic plaques and control arteries. In human atherosclerotic lesions, miR-21 expression was observed to be upregulated. This increase was correlated and promoted by the activation of TGF-β1 which determines the posttranscriptional processing of the primary transcript of miR-21 by the Drosha complex. The sheer stress exerted on the endothelial cells induced the overexpression of miR-21 and in VSMCs it determines the change of the phenotype into a synthetic, proliferative one, promoting neointimal growth (Weber, Baker, Moore, & Searles, 2010). Also, miR-146a plays a very important role in promoting the proliferation of VSMCs *in vitro* and vascular neointimal hyperplasia *in vivo* because it targets Krüppel-like factor (KLF4) by reducing its level (Sun et al., 2011). In addition to the action of the TGF-β1/Smad2/3 signaling pathway on the expression of miR-29a which is involved in a number of processes related to vascular abnormalities present in atherosclerosis such as proliferation and migration of VSMCs, epithelial–mesenchymal transition (EMT), and ECM remodeling and angiogenesis, recent studies have also shown a close link between increased miR-29a expression and oxidized LDL levels. These levels have been found increased in plasma in patients with atherosclerosis and are thought to be responsible for the worsening of the disease. Hence, this association shows a good predictive value and can be a possible biomarker for atherosclerosis (Huang et al., 2016). In patients with ischemia caused by heart failure, circulating levels for miR-192 were markedly increased being associated with acute myocardial infarction (Ali Sheikh et al., 2016). Likewise, miR-200b was found to be significantly elevated not only in stroke patients with enhanced plaque (Kim et al., 2015) but also to promote endothelial cell apoptosis under oxidative stress (Zhang, Cheng, Du, Zhang, & Zhang, 2021). The highest levels in miR-210 expression were also observed at the site of more stable carotid plaques and aberrant expression that leads to endothelial cell apoptosis both *in vitro* and *in vivo*, aggravating the progression of atherosclerosis (Li, Yang, Zhang, & Yang, 2017). In our animal model with diet-induced atherosclerosis, obtained data confirmed the previously mentioned literature on miR-21, miR-192, miR-200b, miR-29a, miR-210, and miR-146a expressions in both the thoracic aorta and carotid artery, providing a better understanding of how these molecules regulate atherosclerosis-prone genes. All of these miRs that we investigated in our study, whose gene expressions were found to be elevated at the HH group, are directly associated with main plasma parameters (cholesterol, LDL-cholesterol, and triglycerides) and inflammatory molecules (Ang II and TGF-β1) from the same experimental group. Also, the EV-based treatment brought a significant improvement on the molecules involved in the Ang II/TGF-β1/Smad2/3 signaling pathway, and the results obtained were correlated with the expression levels of miRNA-21, miRNA-192, miRNA-200b, miRNA-29a, miRNA-210, and miRNA-146a. This therapy had a direct impact on the downregulation of genes expressed primarily in endothelial cells, influencing their response to a variety of pathophysiological stimuli. Specifically, the treatment with EVs (ADSCs) or EVs (MSCs) transfected or not with Smad2/3 siRNA or SMAD2/3siRNA alone diminished the expression of miRNA-21, miRNA-192, miRNA-200b, miRNA-29a, miRNA-210, and miRNA-146a in the thoracic aorta and carotid artery with some small exceptions, namely the allogenic administration of EVs (MSCs) transfected with Smad2/3siRNA had no positive therapeutic effects on miR21, miR-192, miR-210, and miR-146a levels in the carotid artery. These positive effects of EVs (ADSCs) or EVs (MSCs) on the proteins and miRNAs found to be modified in the atherosclerotic vascular wall could be attributed to their biological cargo, especially to the miRNAs they contain. In other words, stem cell-derived EVs significantly decreased specific markers of atherosclerosis-induced vascular dysfunction, and these effects could be partly due to their content in miRNAs. These data may provide new alternatives for therapeutic strategies targeting CVD.

Study Limitations

There are some limitations of our study that we feel responsible for mentioning, are as follows: **1)** many factors can affect the quality and quantity of the EVs produced from the ADSCs/MSCs, such as cellular confluence, early versus later passage of cells, oxygen concentration, cytokines, and serum content of the medium. To avoid some of these problems, in our study, the MSCs (ADSCs or BM-MSCs) at passage five were kept in a serum-free medium for 48 h in order to release EVs (ADSCs) or EVs (MSCs)**; 2)** EVs, collected from the conditioned media of the ADSCs and MSCs, were stored at −80°C until use but not more than 2–3 weeks. However, experiments characterizing them by flow cytometry, electron microscopy, and zeta nanosizer also performed on these EVs showed that their number and structure were not affected by the freezing/thawing procedure; **3)** because the administration of EVs is systemic, there is a possibility that a fairly high percentage can reach the liver. However, our previous studies in which PKH26-labeled MVs administered systemically were quantified under IVIS spectrum equipment which showed that they reach several organs/tissues (liver, lung, kidney, brain, heart, thoracic aorta, and mesenteric resistance arteries), which explains their beneficial action in the vascular wall; **4)** there are some situations in which EV therapy alone has obviously better effects than therapy with EVs which contain siRNA against SMAD2/3. One explanation could be that the mechanisms involved in the complex process of atherosclerosis are multiple, and SMAD2/3 does not always play a key role in all the processes involved; **5)** regarding the clinical applications of EVs, the potential side effects of such therapy should always be considered. It is

important to mention that in our present study, we have not observed any possible side effects of systemic delivery of autologous EVs.

CONCLUSION

Based on all the results previously mentioned and on some limitations inherent in an experimental model, we can conclude that our study demonstrates that the diet enriched with butter, cholesterol, and gavage with NaCl administered for 4 months generated the animal model with atherosclerotic cardiovascular disease, with vascular dysfunction. Dietary- and gavage-induced changes were evident both in plasma biochemical parameters (altered lipid profile: elevated plasma concentrations of total cholesterol, triglycerides, and LDL-cholesterol) and in inflammatory molecules (increased levels of Ang II and TGF-β1) that were associated with amplified expression of cytosolic ROS production and Smad2/3 molecule. All these changes lead to the progression of alterations in structural and inflammatory molecules in the arterial wall associated with the onset of vascular dysfunction. We also observed that vascular function was affected by low levels of contractile responses to NA and diminished relaxation to ACh together with increased pulse wave velocity and velocity time integral, arterial wall thickness and reduced internal diameter, and distensibility, in both the thoracic aorta and carotid artery in the HH group. These pathophysiological changes observed in the animal model with diet-induced atherosclerosis reproduce quite faithfully the vascular lesions present in the patient with atherosclerotic cardiovascular disease.

In addition, the characterization of EVs, in terms of size and specific markers for exosomes and microparticles, was an extremely important step in our study, performed before obtaining the experimental animal model, to ensure that their isolation is effective. Then, we checked and optimized the transfection rate with Smad2/3 siRNA to use it further as a treatment for the regression of atherosclerotic disease. These steps formed the basis of the therapeutic strategy we implemented in this study. Although the groups of animals that received treatment also received a diet high in fat and saline, the EV therapy was able to regress the arterial changes already installed. Of all the analyzed data, the best results on therapy were seen in the groups in which the treatment was based on EVs not only from ADSCs mainly but also from MSCs. However, there were also situations in which the transfection of EVs with Smad2/3 siRNA had a better effect, amplifying the ability of ADSCs or MSCs to regress endothelial dysfunction or even the administration as such of Smad2/3 siRNA had a better effect.

At the beginning of the study, we aimed to establish the optimal source for the generation of EVs from ADSCs or MSCs with therapeutic potential. Our data strongly suggest that ADSCs seem to be the best option both in terms of obtaining them in culture and using them as an optimal source for EV release with potentially beneficial effects in restoring endothelial dysfunction. Another very important aspect when it comes to treatment is the fact that the therapeutic effect has been maintained throughout the 16 experimental weeks. Based on these observations, it is reasonable to state that EVs(ADSCs) and Smad2/3 siRNA-based therapy may be a feasible therapeutic option and a promising approach for patients with atherosclerotic cardiovascular disease/vascular pathologies.

DATA AVAILABILITY STATEMENT

The raw data supporting the conclusion of this article will be made available by the authors, without undue reservation.

ETHICS STATEMENT

The animal study was reviewed and approved by the Ethics Committee from the Institute of Cellular Biology and Pathology "Nicolae Simionescu" according to Decision no.11/08.08.2017 and National Sanitary Veterinary and Food Safety Authority (Bucharest, Romania) in compliance with Project Authorization no. 575/13.11.2020.

AUTHOR CONTRIBUTIONS

AG designed the research. IC, AC, AV, AP, NA, MN, FS, and AF performed the research. IC, AC, AF, and AG analyzed the data. AG and IC wrote the manuscript. AG reviewed the manuscript and obtained funding. All authors contributed to the article and approved the submitted version.

FUNDING

This work was supported by two grants from the Romanian National Authority for Scientific Research, CNCS–UEFISCDI, project no. PN-III-P1-1.2-PCCDI-2017–0527 (Contract No. 83PCCDI/2018) and project no. PN-III-P1-1.1-TE-2019-0811 within PNCDI III (Contract no. TE 97/2020) and by the Romanian Academy.

ACKNOWLEDGMENTS

The authors appreciate the dedicated work of scientific research assistant Marilena Isachi (biochemistry) and Marcela Toader and Carolina Ilie (animal care and feeding).

REFERENCES

Ait-Oufella, H., Taleb, S., Mallat, Z., and Tedgui, A. (2011). Recent Advances on the Role of Cytokines in Atherosclerosis. *Atvb* 31 (5), 969–979. doi:10.1161/ATVBAHA.110.207415

Alexandru, N., Andrei, E., Niculescu, L., Dragan, E., Ristoiu, V., and Georgescu, A. (2017). Microparticles of Healthy Origins Improve Endothelial Progenitor Cell Dysfunction via microRNA Transfer in an Atherosclerotic Hamster Model. *Acta Physiol.* 221 (4), 230–249. doi:10.1111/apha.12896

Alexandru, N., Andrei, E., Safciuc, F., Dragan, E., Balahura, A. M., Badila, E., et al. (2020). Intravenous Administration of Allogenic Cell-Derived Microvesicles of Healthy Origins Defends against Atherosclerotic Cardiovascular Disease Development by a Direct Action on Endothelial Progenitor Cells. *Cells* 9 (2), 423. doi:10.3390/cells9020423

Alexandru, N., Constantin, A., Nemecz, M., Comarița, I. K., Vîlcu, A., Procopciuc, A., et al. (2019). Hypertension Associated with Hyperlipidemia Induced Different MicroRNA Expression Profiles in Plasma, Platelets, and Platelet-Derived Microvesicles; Effects of Endothelial Progenitor Cell Therapy. *Front. Med.* 6, 280. doi:10.3389/fmed.2019.00280

Alexandru, N., Procopciuc, A., Vîlcu, A., Comarița, I. K., Bădilă, E., and Georgescu, A. (2021). Extracellular Vesicles-Incorporated microRNA Signature as Biomarker and Diagnosis of Prediabetes State and its Complications. *Rev. Endocr. Metab. Disord.* 1, 1. doi:10.1007/s11154-021-09664-y

Ali Sheikh, M. S., Salma, U., Zhang, B., Chen, J., Zhuang, J., and Ping, Z. (20162016). Diagnostic, Prognostic, and Therapeutic Value of Circulating miRNAs in Heart Failure Patients Associated with Oxidative Stress. *Oxidative Med. Cell Longevity* 2016, 1–13. doi:10.1155/2016/5893064

Amaya-Amaya, J., Montoya-Sánchez, L., and Rojas-Villarraga, A. (2014). Cardiovascular Involvement in Autoimmune Diseases. *Biomed. Res. Int.* 2014, 1–31. doi:10.1155/2014/367359

Buckley, M. L., and Ramji, D. P. (2015). The Influence of Dysfunctional Signaling and Lipid Homeostasis in Mediating the Inflammatory Responses during Atherosclerosis. *Biochim. Biophys. Acta (Bba) - Mol. Basis Dis.* 1852 (7), 1498–1510. doi:10.1016/j.bbadis.2015.04.011

Constantin, A., Dumitrescu, M., Mihai, M. C., Jianu, D., and Simionescu, M. (2017). CO2 Laser Increases the Regenerative Capacity of Human Adipose-Derived Stem Cells by a Mechanism Involving the Redox State and Enhanced Secretion of Pro-angiogenic Molecules. *Lasers Med. Sci.* 32 (1), 117–127. doi:10.1007/s10103-016-2093-6

Constantin, A., Filippi, A., Alexandru, N., Nemecz, M., and Georgescu, A. (2020). Extracellular Vesicles from Adipose Tissue Stem Cells in Diabetes and Associated Cardiovascular Disease; Pathobiological Impact and Therapeutic Potential. *Ijms* 21 (24), 9598. doi:10.3390/ijms21249598

Davignon, J., and Ganz, P. (2004). Role of Endothelial Dysfunction in Atherosclerosis. *Circulation* 109 (23 Suppl. 1), III27–32. doi:10.1161/01.CIR.0000131515.03336.f8

Dillard, A., Matthan, N. R., and Lichtenstein, A. H. (2010). Use of Hamster as a Model to Study Diet-Induced Atherosclerosis. *Nutr. Metab.* 7, 89. doi:10.1186/1743-7075-7-89

Dorsett, Y., and Tuschl, T. (2004). siRNAs: Applications in Functional Genomics and Potential as Therapeutics. *Nat. Rev. Drug Discov.* 3 (4), 318–329. doi:10.1038/nrd1345

Gąsecka, A., van der Pol, E., Nieuwland, R., and Stępień, E. (2018). Extracellular Vesicles in post-infarct Ventricular Remodelling. *Kardiol Pol.* 76 (1), 69–76. doi:10.5603/KP.a2017.0178

Georgescu, A., Alexandru, N., Andrei, E., Dragan, E., Cochior, D., and Dias, S. (2016). Effects of Transplanted Circulating Endothelial Progenitor Cells and Platelet Microparticles in Atherosclerosis Development. *Biol. Cel* 108 (8), 219–243. doi:10.1111/boc.201500104

Georgescu, A., Alexandru, N., Andrei, E., Titorencu, I., Dragan, E., Tarziu, C., et al. (2012). Circulating Microparticles and Endothelial Progenitor Cells in Atherosclerosis: Pharmacological Effects of Irbesartan. *J. Thromb. Haemost.* 10 (4), 680–691. doi:10.1111/j.1538-7836.2012.04650.x

Georgescu, A., Alexandru, N., Popov, D., Amuzescu, M., Andrei, E., Zamfir, C., et al. (2009). Chronic Venous Insufficiency Is Associated with Elevated Level of Circulating Microparticles. *J. Thromb. Haemost.* 7 (9), 1566–1575. doi:10.1111/j.1538-7836.2009.03525.x

Georgescu, A., and Simionescu, M. (2021). Extracellular Vesicles: Versatile Nanomediators, Potential Biomarkers and Therapeutic Agents in Atherosclerosis and COVID-19-Related Thrombosis. *Ijms* 22 (11), 5967. doi:10.3390/ijms22115967

Groh, L., Keating, S. T., Joosten, L. A. B., Netea, M. G., and Riksen, N. P. (2018). Monocyte and Macrophage Immunometabolism in Atherosclerosis. *Semin. Immunopathol* 40 (2), 203–214. doi:10.1007/s00281-017-0656-7

Huang, Y.-Q., Cai, A.-P., Chen, J.-Y., Huang, C., Li, J., and Feng, Y.-Q. (2016). The Relationship of Plasma miR-29a and Oxidized Low Density Lipoprotein with Atherosclerosis. *Cell Physiol Biochem* 40 (6), 1521–1528. doi:10.1159/000453202

Kalinina, N., Agrotis, A., Antropova, Y., Ilyinskaya, O., Smirnov, V., Tararak, E., et al. (2004). Smad Expression in Human Atherosclerotic Lesions. *Atvb* 24 (8), 1391–1396. doi:10.1161/01.ATV.0000133605.89421.79

Kattoor, A. J., Pothineni, N. V. K., Palagiri, D., and Mehta, J. L. (2017). Oxidative Stress in Atherosclerosis. *Curr. Atheroscler. Rep.* 19 (11), 42. doi:10.1007/s11883-017-0678-6

Kim, J.-M., Jung, K.-H., Chu, K., Lee, S.-T., Ban, J., Moon, J., et al. (2015). Atherosclerosis-Related Circulating MicroRNAs as a Predictor of Stroke Recurrence. *Transl. Stroke Res.* 6 (3), 191–197. doi:10.1007/s12975-015-0390-1

Kowalski, P. S., Leus, N. G. J., Scherphof, G. L., Ruiters, M. H. J., Kamps, J. A. A. M., and Molema, G. (2011). Targeted siRNA Delivery to Diseased Microvascular Endothelial Cells-Cellular and Molecular Concepts. *IUBMB Life* 63 (8), 648–658. doi:10.1002/iub.487

Li, Y., Yang, C., Zhang, L., and Yang, P. (2017). MicroRNA-210 Induces Endothelial Cell Apoptosis by Directly Targeting PDK1 in the Setting of Atherosclerosis. *Cell Mol Biol Lett* 22, 3. doi:10.1186/s11658-017-0033-5

Manduteanu, I., and Simionescu, M. (2012). Inflammation in Atherosclerosis: a Cause or a Result of Vascular Disorders? *J. Cel. Mol. Med.* 16 (9), 1978–1990. doi:10.1111/j.1582-4934.2012.01552.x

Matsuzawa, Y., and Lerman, A. (2014). Endothelial Dysfunction and Coronary Artery Disease. *Coron. Artery Dis.* 25 (8), 713–724. doi:10.1097/MCA.0000000000000178

McLaren, J. E., Michael, D. R., Ashlin, T. G., and Ramji, D. P. (2011). Cytokines, Macrophage Lipid Metabolism and Foam Cells: Implications for Cardiovascular Disease Therapy. *Prog. Lipid Res.* 50 (4), 331–347. doi:10.1016/j.plipres.2011.04.002

Milutinović, A., Šuput, D., and Zorc-Pleskovič, R. (2020). Pathogenesis of Atherosclerosis in the tunica Intima, media, and Adventitia of Coronary Arteries: An Updated Review. *Bosn J. Basic Med. Sci.* 20 (1), 21–30. doi:10.17305/bjbms.2019.4320

Morel, S. (2014). Multiple Roles of Connexins in Atherosclerosis- and Restenosis-Induced Vascular Remodelling. *J. Vasc. Res.* 51 (2), 149–161. doi:10.1159/000362122

Mu, W., Chen, M., Gong, Z., Zheng, F., and Xing, Q. (2015). Expression of Vascular Cell Adhesion Molecule-1 in the Aortic Tissues of Atherosclerotic Patients and the Associated Clinical Implications. *Exp. Ther. Med.* 10 (2), 423–428. doi:10.3892/etm.2015.2540

Orekhov, A. N., and Sobenin, I. A. (2019). Modified and Dysfunctional Lipoproteins in Atherosclerosis: Effectors or Biomarkers? *Cmc* 26 (9), 1512–1524. doi:10.2174/0929867325666180320121137

Pacurari, M., Kafoury, R., Tchounwou, P. B., and Ndebele, K. (2014). The Renin-Angiotensin-Aldosterone System in Vascular Inflammation and Remodeling. *Int. J. Inflamm.* 2014, 1–13. doi:10.1155/2014/689360

Pirillo, A., Bonacina, F., Norata, G. D., and Catapano, A. L. (2018). The Interplay of Lipids, Lipoproteins, and Immunity in Atherosclerosis. *Curr. Atheroscler. Rep.* 20 (3), 12. doi:10.1007/s11883-018-0715-0

Ramji, D. P., and Davies, T. S. (2015). Cytokines in Atherosclerosis: Key Players in All Stages of Disease and Promising Therapeutic Targets. *Cytokine Growth Factor. Rev.* 26 (6), 673–685. doi:10.1016/j.cytogfr.2015.04.003

Schiffer, M., von Gersdorff, G., Bitzer, M., Susztak, K., and Böttinger, E. P. (2000). Smad Proteins and Transforming Growth Factor-β Signaling. *Kidney Int.* 58, S45–S52. doi:10.1046/j.1523-1755.2000.07708.x

Simionescu, M., Popov, D., Sima, A., Hasu, M., Costache, G., Faitar, S., et al. (1996). Pathobiochemistry of Combined Diabetes and Atherosclerosis Studied on a

Novel Animal Model. The Hyperlipemic-Hyperglycemic Hamster. *Am. J. Pathol.* 148 (3), 997–1014.

Simionescu, N., Sima, A., Dobrian, A., Tirziu, D., and Simionescu, M. (1993). Pathobiochemical Changes of the Arterial wall at the Inception of Atherosclerosis. *Curr. Top. Pathol.* 87, 1–45. doi:10.1007/978-3-642-76849-1_1

Simionescu, N., Zonda, R., Petrovici, A. R., and Georgescu, A. (2021). The Multifaceted Role of Extracellular Vesicles in Glioblastoma: microRNA Nanocarriers for Disease Progression and Gene Therapy. *Pharmaceutics* 13 (7), 988. doi:10.3390/pharmaceutics13070988

Sorop, A., Iacob, R., Iacob, S., Constantinescu, D., Chitoiu, L., Fertig, T. E., et al. (2020). Plasma Small Extracellular Vesicles Derived miR-21-5p and miR-92a-3p as Potential Biomarkers for Hepatocellular Carcinoma Screening. *Front. Genet.* 11, 712. doi:10.3389/fgene.2020.00712

Stępień, E. Ł., and Rząca, C. (2021). Novel Biomarker and Drug Delivery Systems for Theranostics - Extracellular Vesicles. *Bio-Algorithms and Med-Systems* 17 (4), 301–309. doi:10.1515/bams-2021-0183

Sun, S. G., Zheng, B., Han, M., Fang, X. M., Li, H. X., Miao, S. B., et al. (2011). miR-146a and Krüppel-like Factor 4 Form a Feedback Loop to Participate in Vascular Smooth Muscle Cell Proliferation. *EMBO Rep.* 12 (1), 56–62. doi:10.1038/embor.2010.172

Weber, M., Baker, M. B., Moore, J. P., and Searles, C. D. (2010). MiR-21 Is Induced in Endothelial Cells by Shear Stress and Modulates Apoptosis and eNOS Activity. *Biochem. Biophysical Res. Commun.* 393 (4), 643–648. doi:10.1016/j.bbrc.2010.02.045

Wu, M.-Y., Li, C.-J., Hou, M.-F., and Chu, P.-Y. (2017). New Insights into the Role of Inflammation in the Pathogenesis of Atherosclerosis. *Ijms* 18 (10), 2034. doi:10.3390/ijms18102034

Youn, S. W., and Park, K. K. (2015). Small-Nucleic-Acid-Based Therapeutic Strategy Targeting the Transcription Factors Regulating the Vascular Inflammation, Remodeling and Fibrosis in Atherosclerosis. *Int. J. Mol. Sci.* 16 (5), 11804–11833. doi:10.3390/ijms160511804

Zhang, F., Cheng, N., Du, J., Zhang, H., and Zhang, C. (2021). MicroRNA-200b-3p Promotes Endothelial Cell Apoptosis by Targeting HDAC4 in Atherosclerosis. *BMC Cardiovasc. Disord.* 21 (1), 172. doi:10.1186/s12872-021-01980-0

Conflict of Interest: The authors declare that the research was conducted in the absence of any commercial or financial relationships that could be construed as a potential conflict of interest.

Publisher's Note: All claims expressed in this article are solely those of the authors and do not necessarily represent those of their affiliated organizations, or those of the publisher, the editors, and the reviewers. Any product that may be evaluated in this article, or claim that may be made by its manufacturer, is not guaranteed or endorsed by the publisher.

frontiers | Frontiers in Cell and Developmental Biology

REVIEW
published: 13 April 2022
doi: 10.3389/fcell.2022.823387

NLRP3-Mediated Inflammation in Atherosclerosis and Associated Therapeutics

*Na Lu[1], Weijia Cheng[1], Dongling Liu[1], Gang Liu[1], Can Cui[1,2], Chaoli Feng[1] and Xianwei Wang[1,2]**

[1]Henan Key Laboratory of Medical Tissue Regeneration, School of Basic Medical Sciences, Xinxiang Medical University, Xinxiang, China, [2]Department of Cardiology, The First Affiliated Hospital of Xinxiang Medical University, Xinxiang, China

The NLRP3 inflammasome is a crucial constituent of the body's innate immune system, and a multiprotein platform which is initiated by pattern recognition receptors (PRRs). Its activation leads to caspase-1 maturation and release of inflammatory cytokines, interleukin-1β (IL-1β) and IL-18, and subsequently causes pyroptosis. Recently, the excess activation of NLRP3 inflammasome has been confirmed to mediate inflammatory responses and to participate in genesis and development of atherosclerosis. Therefore, the progress on the discovery of specific inhibitors against the NLRP3 inflammasome and the upstream and downstream inflammatory factors has become potential targets for clinical treatment. Here we review the recently described mechanisms about the NLRP3 inflammasome activation, and discuss emphatically the pharmacological interventions using statins and natural medication for atherosclerosis associated with NLRP3 inflammasome.

Keywords: NLRP3 inflammasome, atherosclerosis, mechanism, therapeutics, inflammation

OPEN ACCESS

Edited by:
Yang Shen,
Sichuan University, China

Reviewed by:
Gauhar Rehman,
Abdul Wali Khan University Mardan, Pakistan
Xiaoyan Zhu,
The Affiliated Hospital of Qingdao University, China

****Correspondence:***
Xianwei Wang
wangxianwei1116@126.com

Specialty section:
This article was submitted to Molecular and Cellular Pathology, a section of the journal Frontiers in Cell and Developmental Biology

Received: *27 November 2021*
Accepted: *24 February 2022*
Published: *13 April 2022*

Citation:
Lu N, Cheng W, Liu D, Liu G, Cui C, Feng C and Wang X (2022) NLRP3-Mediated Inflammation in Atherosclerosis and Associated Therapeutics. Front. Cell Dev. Biol. 10:823387. doi: 10.3389/fcell.2022.823387

INTRODUCTION

Atherosclerosis (AS) is a long-term slow-developing inflammatory disease of the arteries and is the rationale of about 45% of all deaths in westernized society (Pahwa and Jialal, 2021). The pathophysiological process triggers the formation of lipid-rich atherosclerotic plaques at specific sites in medium- and large-sized arteries. The progressive slow-growth plaques lead to narrowing and hardening of arteries and rupture or erosion of existing plaques may result in acute arterial occlusion by subsequent thrombus formation (Nettersheim et al., 2020). These pathological events are one of the most critical risk factors in various cardiovascular diseases like ischemic heart disease, cerebrovascular disease, and peripheral artery disease (Montarello et al., 2020). Multiple studies have indicated that abnormal inflammation and lipid metabolism promote plaque formation in blood vessel wall of arteries. Inflammasomes are intracellular sensors that result in inflammaging in different pathological conditions, and several studies suggested thier functions in pathological process of AS. NLRP3, a well-known member in inflammasomes, is essential for AS and is enhanced in aortas derived from high-risk AS patients of diabetes, smokers, hypercholesterolemia, and hypertension. Moreover, impaired atherosclerosis progression and stabilization of atherosclerotic plaque were observed due to NLRP3 deficiency (Grebe et al., 2018).

NLRP3 inflammasome can be activated by different pathological changes including reactive oxygen species (ROS) overproduction, mtDNA damage, mitochondrial dysfunction, lysosomal rupture, and excessive endoplasmic reticulum (ER) stress etc. (Hoseini et al., 2018). Activated

NLRP3 inflammasome causes consequent inflammation by inducing caspase-1 and various inflammatory cytokines like IL-1β and IL-18, and subsequently induces pyroptosis (Liaqat et al., 2020). Since NLRP3 inflammasome involves the cross-talk between inflammation and lipid metabolism, intensively investigating its roles in AS and pharmacological interventions appears to be important for the prevention and treatment of AS.

This review summarizes the mechanisms of atherogenesis mediated by NLRP3 inflammasome, and further discusses the potential pharmacological interventions targeting NLRP3-mediated inflammation in AS.

NLRP3 INFLAMMASOME

In the case of various endogenous tissue-cell injuries or exogenous infections, intrinsic immune cells (macrophages, neutrophils, dendritic cells, etc.) in different tissues and organs recognize pathogen-associated molecular patterns (PAMPs) and damage-associated molecular patterns (DAMPs) such as lipopolysaccharide, microbial nucleic acid molecules, hemolysin, acid uric acid crystals, coxsackie virus through various pattern recognition receptors (PRRs), and activate downstream inflammatory signal transduction, promoting innate and adaptive immune responses (Broz and Dixit, 2016).

Several subgroups of PRRs have been identified, which contain toll-like receptors (TLRs), RIG-I-like receptor (RLRs), C type lectin receptors (CLRs), nucleotide-binding oligomerization domain (NOD)-like receptors (NLRs) and AIM2-like receptors (ALRs) (Jannuzzi et al., 2020). Among them, NLRs are evolutionarily-conserved sensors. After activation of NLRs, a multi-protein complex, namely inflammasome, is formed in the cytoplasm, which is composed of receptor protein, adaptor protein and effector protein precursors. NLRs inflammasome mainly includes NLRP3, NLRP1, NLRP6, NLRP7, and NLRP12 (Zheng et al., 2021). The NLRP3 inflammasome, that widely exists in human monocytes, macrophages, T cells, B cells and other immune cells, is constituted by the NLRP3 receptor protein, apoptosis associated speck-like protein (ASC) with a caspase recruitment domain, and pro-caspase-1. NLRP3 inflammasome activation is initiated by endogenous or exogenous DAMPs following with the forming NLRP3 molecular complex in the cell solutes, resulting in caspase-1 and IL-1β-dependent pyroptosis that participates in the sterile inflammatory process (Yin et al., 2018; Sharma and de Alba, 2021).

The NLRP3 receptor is composed of an N-terminal pyrin domain (PYD), a central nucleotide binding or oligomerization domain (NACHT) and a C-terminal leucine-rich repeats (LRRs) motif (Dolasia et al., 2018). ASC, as a bridging protein, is composed of an N-terminal PYD domain and a C-terminal caspase-1 recruitment domain (CARD), which is responsible for connecting upstream NLRP3 and downstream caspase-1 (de Alba, 2019). Pro-caspase-1 contains CARD and catalytic domains (Wang Y. et al., 2020).

The activation of NLRP3 inflammasome is initiated by sensing various intracellular or extracellular signals including ATP, nigericin, monosodium urate (MSU), fungi, viruses and bacteria that generate pore-forming toxins (Tourkochristou et al., 2019). When DAMPs are recognized, LRRs regulates NLRP3 ubiquitination and interacts with NLRP3 inducers, which results in NACHT domain oligomerization, exposing the PYD domain to recruit the adaptor protein ASC containing PYD. Pro-caspase-1 containing CARD is subsequently recruited to the CARD domain of ASC. Pro-caspase-1 clustering induces its auto-cleavage and the formation of activated caspase-1 that promotes the maturation and release of IL-1β and IL-18 (Kelley et al., 2019). Besides, caspase-1 also enhances the activation and release of Gasdermin D (GSDMD) to mediate inflammatory programmed cell death (Wang Z. et al., 2020). Abnormal activation of NLRP3 inflammasome is pathogenic and involved in many diseases, such as hypertension, diabetes and other inflammatory diseases (Weber et al., 2020) (**Figure 1**).

MECHANISMS OF NLRP3 INFLAMMASOME ACTIVATION IN ATHEROGENESIS

Under the normal physiological conditions, NLRP3 keeps an inactive state of self-inhibition regulated by Heat Shock Protein 90 (HPS90) (Liu D. et al., 2018). NLRP3 inflammasome activation requires double signals: signal one is a pre-stimulation signal that stimulates TLRs and TNF receptors on cell membrane through TLR4/MyD88, TRIP/nuclear factor κB (NF-κB) and other signaling pathways; the activated NF-κB initiates expression of NLRP3, pro-IL-1β and pro-IL-18 (Swanson et al., 2019). Signal two is activation signal; at this step, PAMPs and DAMPs stimulate the assembly of NLRP3, ASC and pro-caspase-1, and finally activate the inflammasome (Swanson et al., 2019). NLRP3 inflammasome can be activated by various kinds of PAMPs including microbial pore-forming toxins, viral RNA and bacterial surface proteins, as well as a large variety of DAMPs including calcium pyrophosphate dihydrate (CPPD), MSU, silica, asbestos, extracellular ATP, amyloid-β or glucose, saturated fatty acids, hyaluronan and ionophore nigericin (Chakrabarti et al., 2015; Gong T. et al., 2018). Moreover, lipopolysaccharide (LPS) can also mediate the noncanonical activation of NLRP3 which relys on caspase-11 (Shi et al., 2014). However, the specific activation mechanism is still controversial, and there are accepted NLRP3 activation hypotheses (**Figure 1**).

K^+ Efflux

K^+ efflux is a main factor to trigger NLRP3, which induces the upregulation of NLRP3 molecules and promotes the assembly of the inflammasome complex (Gritsenko et al., 2020). ATP is a P2X7 receptor (P2X7R) agonist and also an inflammasome activator. Activated P2X7R causes K^+ efflux by creating some channels correlated to hemi channel protein and pannexin-1 on the cell membrane. This biological occurrence leads to internalization of extracellular NLRP3 activators into cytoplasmic compartments from where the NLRP3 complex is generated, and IL-1β and IL-18 are released (Hoseini et al., 2018;

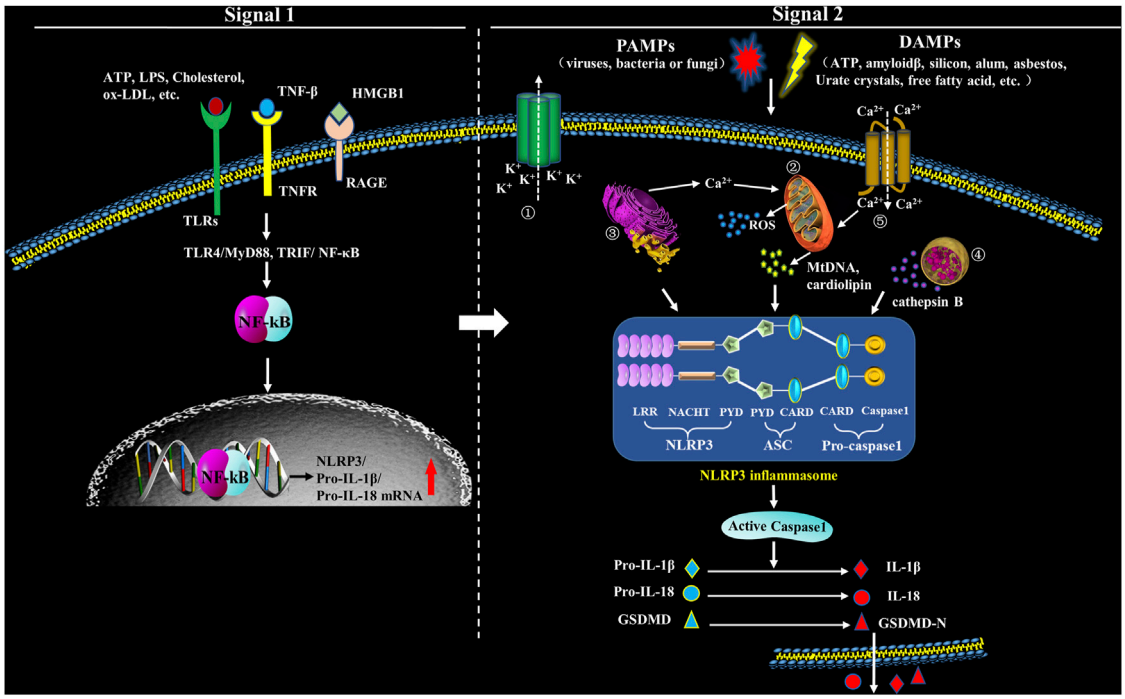

FIGURE 1 | Formation and structure of NLRP3 inflammasome. Upon exposure to PAMPs or DAMPs, TLRs will be phosphorylated, which will subsequently promote translocation of NF-κB into the nucleus and activate it, which has an action to promote the transcription of NLRP3, leading to expression of pro-IL-1β and pro-IL-18 that locate in the cytoplasm before maturation. Therefore, the signals in this step (Signal 1) are priming. The second step signals (Signal 2) are triggering and have an action to activate the inflammasome via promoting oligomerization of NLRP3, ASC and procaspase-1. The complex formation of NLRP3 inflammasome, then, catalyzes the conversion of pro-caspase-1 to caspase-1, which cleaves pro-IL-1β and pro-IL-18, and subsequently cuases extracellular secretion of IL-1β and IL-18. In the second step, five models have been introduced to explicate inflammasome activation: ① Multiple signal transduction pathways triggered by PAMPs/DAMPs all depending on K^+ efflux, which subsequently cause the interaction among different NLRP3-NEK (NIMA related kinase) and NLRP3 inflammasome activation. ② PAMPs and DAMPs trigger the production of reactive oxygen species (ROS), impair mitochondria, and cause autophagic dysfunction which resut in the assembly of NLRP3 inflammasome and activate the inflammasome complex. ③ Endoplasmic reticulum (ER) stress activates NLRP3 inflammasome through various factors, including UPR, ROS production, calcium homeostasis and/or lipid metabolism. ④ Uptake of crystalline or other ligands such as monosodium urate (MSU), amyloid-β and silica causes lysosomal rupture and leakage of lysosomal contents like cathepsin B, thus resulting in the activation of NLRP3 inflammasome. ⑤ Agonists of NLRP3 induce Ca^{2+} from extracellular milieu and from ER Ca^{2+} stores release to cytoplasm, resulting in cytosolic Ca^{2+} increase. The overload of mitochondrial Ca^{2+} would cause mitochondrial ROS production, mitochondrial DNA (mtDNA) damage and release of mitochondrial contents, which in turn triggers the activation of NLRP3 inflammasome.

Pelegrin, 2021). P2X7R also phosphorylates and activates double-stranded RNA-dependent protein kinase (PKR) which interacts with different inflammasome core proteins containing NLRP1, NLRP3, NLRC4 and AIM2 and mediates downstream inflammatory response (Peng et al., 2015). It is shown that P2X7R is critical in the development of AS by regulating PKR phosphorylation-induced NLRP3 inflammasome activation (Peng et al., 2015).

In the process of NLRP3 activation, K^+ efflux mainly plays a role in the upstream of ASC. However, NEK7 belongs to NIMA-related kinases family, is a downstream modulator in K^+ efflux signaling (Pelegrin, 2021). NEK7 controls the activation and oligomerization of NLRP3 by binding to LRR domain in NLRP3 complex (He et al., 2016). NEK7 depletion or anti-inflammatory medications could block the interplay between NEK7 and NLRP3, and thus inhibit NLRP3 inflammasome activation (Liu H. et al., 2020). NEK7 deficiency leads to attenuated caspase-1 maturation and IL-1β secretion (Swanson et al., 2019). Recent investigations also demonstrated that the activation of NEK7/NLRP3 inflammasome signaling is a fundamental step in atherogenesis (Cai et al., 2020) (**Figure 2**).

Mitochondrial Damage and Reactive Oxygen Species

Mitochondrial dysfunction and ROS generation are proposed common downstream events after PAMPs and DAMPs recognition (Gurung et al., 2015). Mitochondria are intracellular organelles that are responsible in numerous cellular processes including inflammation, calcium homeostasis, redox signaling and apoptosis. Under cellular stress, altered mitochondrial dynamics and mitochondrial cristae remodeling are revealed. Up-regulated mitochondrial ROS (mtROS) production and down-regulated mitochondrial membrane potential (MMP) as well as imbalanced calcium homeostasis are also observed. Subsequently, activation of mitochondrial permeability transition pore (mPTP) and release of mitochondrial DNA (mtDNA) occur. The above

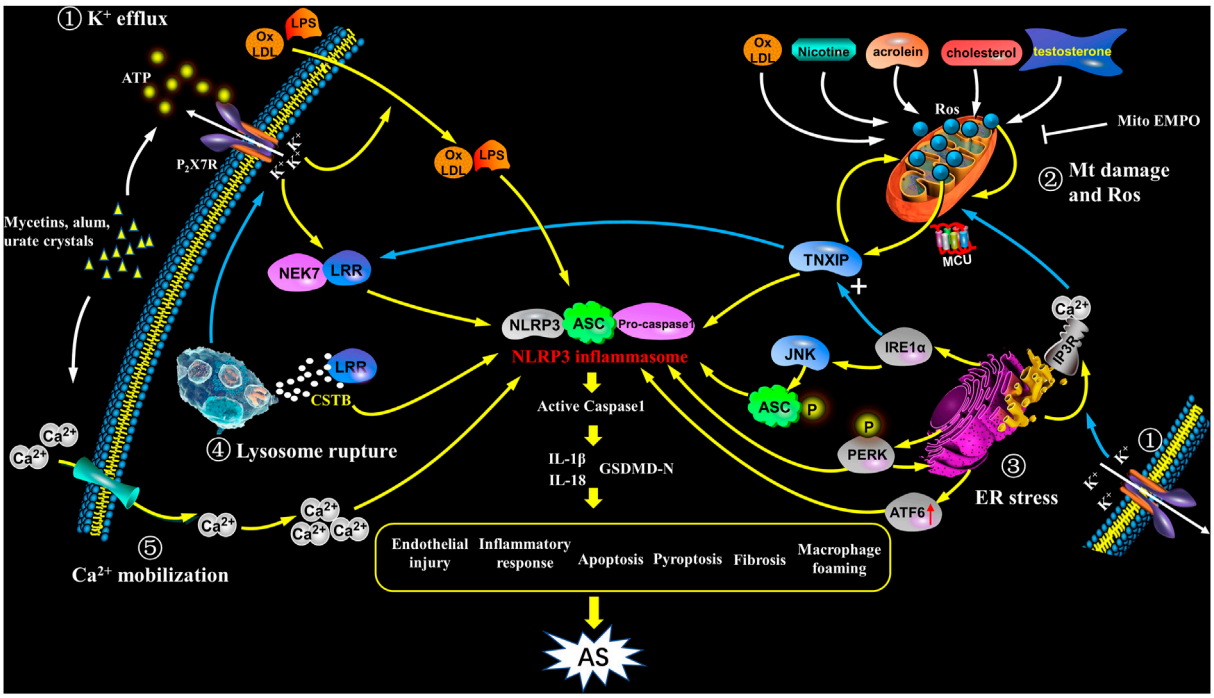

FIGURE 2 | Activation of NLRP3 inflammasome in atherosclerosis. NIRP3 inflammasome activation plays a key role in atherogenesis, but its specific mechanisms still remain unkown. The following points are summarized: ① K^+ efflux: The binding of bacterins, urate crystals, ATP, etc. to the P2X7 receptor leads to K^+ efflux, and its downstream signal NEK7 in complex with LRR domain induces an up-regulation and activation of NLRP3, as well as assembly of the inflammasome, which participates in atherogenesis; K^+ efflux causes extracellular NLRP3 agonists entering the cytoplasm and facilitates them recognizing and binding to the NLRP3 complex, as a result causing the release of IL-1β and IL-18; further, K^+ efflux promotes the release of Ca^{2+} in the ER. ② Mitochondrial damage and reactive oxygen species: ox-LDL, nicotine, acrolein, cholesterol crystals and testosterone etc. cause mitochondrial damage and dysfunction, and activate NLRP3 inflammasome to induce AS through mtROS/TXNIP/NLRP3 signaling. ③ ER stress: In the case of ER stress, after IRE1α is activated, it not only up-regulates the expression of TXNIP, but also acts on its downstream target JNK to phosphorylate ASC; at the same time, PERK phosphorylation promotes NLRP3 activation, and enhances caspase-1 and IL-1β secretion as well as ER Ca^{2+} flux; ATF6 expression is also up-regulated; the above signaling pathways have the potential to activate NLRP3 inflammasome which promotes the early progress of AS. In addition, ER acts as a Ca^{2+} reservoir, under ER stress, a large amount of Ca^{2+} flows out into mitochondria through the MCU complex, resulting in Ca^{2+} overload and mitochondrial instability, indirectly activates NLRP3 inflammation. ④ Lysosome rupture: Some particulate matters, such as β-amyloid, cholesterol crystals, and calcium crystals, are phagocytosed by cells and cause lysosomes rupture, releasing cathepsin B (CSTB), and then CSTB conjugates LRR domain, finally activates NLRP3. ⑤ Ca^{2+}mobilization: In cases of infection, inflammation, etc., the increase in extracellular calcium allows Ca^{2+} to enter the cell and acts as a second messenger to trigger the release of Ca^{2+} from the intracellular organelles. The high level of Ca^{2+} in cytoplasm triggers assembly of inflammasome and participates in the development of AS. In addition, Ca^{2+} influx and K^+ outflow are coordinated with each other during NLRP3 activation.

processes would lead to damage and inflammatory responses by activating NF-κB and NLRP3 inflammasomes. Additionally, mitochondrial dysfunction-induced mtROS production may strengthen NLRP3 activation, which in turn provokes the amplified mitochondrial damage (Li et al., 2021).

NLRP3 activators-mediated mitochondrial destabilization triggers mitochondrial content release. These contents act as downstream signals to activate NLRP3 inflammasome (Yu and Lee, 2016). This may attribute to recognition of NLRP3 to a broad range of stimuli with distinct chemical and structural characteristics.

ROS is one of the major signals for NLRP3 inflammasome activation because ROS production is sensitive to most of NLRP3 stimuli. There are several sources for ROS production, particularly mitochondrial damage and dysfunction (Abais et al., 2015). Pathogens, a kind of endogenous danger signals and exogenous irritants induce mtROS production directly or indirectly as NLRP3 activators. ATP, urea microcrystals and nigericin could decrease mitochondrial membrane potential (MMP), and facilitate the ROS generation and NLRP3-dependent IL-1β release (Wang et al., 2019). Mitochondrial permeability transition (MPTP) promotes mtROS generation and expression of NLRP3 and cleaved caspase-1 via membrane potential dissipation, which can be reversed by MPTP and mtROS inhibitors (Zhuang et al., 2015; Wu H.-Y. et al., 2018). NLRP3 inflammasome activation was strengthened in LPS and ATP stimulated macrophages through enhanced ROS release and cytoplasmic translocation of mtDNA. Moreover, translocation of mtDNA into the cytosol directly contributed to caspase-1 maturation and IL-1β and IL-18 secretion (Jo et al., 2016). It has also been observed that Nicotine facilitates atherogenesis through ROS/NLRP3-mediated pyroptosis of endothelial cells (Wu X. et al., 2018). Jiang et al. found that acrolein treatment induced ROS generation, NLRP3 inflammasome activation and

pyroptosis in human umbilical vein endothelial cells (HUVECs), which is proposed to be linked to cardiovascular diseases, such as AS (Jiang et al., 2018). Kotla et al. demonstrated that generation of ROS via BTK-p300-STAT1-PPARgamma pathway was critical in cholesterol crystals-induced NLRP3 activation and foam cell formation (Kotla et al., 2017). Alves et al. found that supraphysiological levels of testosterone induced vascular dysfunction and atherogenesis through promoting mtROS generation and NLRP3 inflammasome activation. It has been shown that the activation of NLRP3 inflammasome is the continuous step of mtROS generation induced by NLRP3 activators (Dai et al., 2017; Alves et al., 2020). Recent studies provided new evidence that NLRP3 inflammasome was activated due to the energy metabolism disorders in mitochondria and increased ROS in $ApoE^{-/-}$ mice and human artery endothelial cells (HAECs) treated with ox-LDL, which contributed to atherogenesis through causing endothelial dysfunction (Xie et al., 2020). These findings indicate that mtROS production and mitochondrial damage-caused NLRP3 inflammasome activation are critical factors in the development of AS.

Thioredoxin interacting protein (TXNIP) is a protein essential for the oxidative stress-mediated NLRP3 inflammasome activation. ROS increase activates TXNIP which in turn induces ROS production. ROS can also activate NLRP3 inflammasome through facilitating the binding of TXNIP and NLRP3 (Sun et al., 2016). In addition, TXNIP induces mtDNA oxidation and NIMA-related kinase 7(NEK7) activation by stimulating ROS production (Wang WW. et al., 2020). Treating bone marrow-derived macrophages (BMDMs) with nicotine *in vitro* causes mitochondrial damage and ROS production, which activates TXNIP/NLRP3 inflammasome signaling and promotes pyroptosis, as evidenced by caspase-1 maturation and increased production of IL-1β, IL-18 and GSDMD. Nicotine intake by $ApoE^{-/-}$ mice fed with a high-fat diet recapitulated those phenotypes (Mao et al., 2021). Dramatically reduced ROS generation is observed in TXNIP-deficient mice, and TXNIP deficiency inhibits NLRP3 inflammasome expression and IL-1β release (Zhou et al., 2010). Recent studies provided evidence that mitochondria-targeted antioxidant MitoTEMPO prevented mtROS overproduction, NLRP3 inflammasome overactivation and NLRP3 and TXNIP co-localization after simulated injury (Wen et al., 2018). Similarly, ROS inhibitors also prevent priming signal in the process of NLRP3 inflammasome activation (Zhong et al., 2018). Therefore, targeting the ROS/TXNIP/NLRP3-mediated pyroptotic pathway in macrophages may ameliorate AS.

Double-stranded RNA-dependent protein kinase (PKR) is another key molecule in ROS-mediated canonical NLRP3 inflammasome activation. It was demonstrated that inhibition of PKR blocked IL-1β production (Lin et al., 2021; Stunnenberg et al., 2021). PKR regulates the inflammasome assembly by activating NF-κB, MAP kinases ERK1/2, JNK and p38 (Stunnenberg et al., 2021). However, the function of ROS/PKR/NLRP3 pathway in atherogenesis has not been reported.

K^+ efflux, ER stress, lysosome rupture, and cathepsin B (SCTB) also cause ROS production (Kelley et al., 2019). Some studies showed that NADPH- and mitochondria-derived ROS production both participate in regulating NLRP3 inflammasome activation (Wang et al., 2017a; Chen H. et al., 2019), but some other studies indictaed that mtROS generation is not essential for the inflammasome activation (Kelley et al., 2019). Particularly, ROS are dispensable in NLRP3 activation following treating macrophages with linezolid (oxazolidinone class of antibiotics) or infecting macrophages with influenza and encephalomyocarditis viruses (Gurung et al., 2015). Thus, the specific role of ROS production in inflammasome activation remains to be investigated (Abais et al., 2015) (**Figure 2**).

Endoplasmic Reticulum Stress(ER Stress)

ER is a dynamic intracellular organelle whereases proteins are synthesized, modified and folded and is critical to cellular function of organelle networks. Misfolded and/or unfolded proteins are generated under the stress of altered calcium homeostasis, infection, and hypoxia. The aggregation and overload of these proteins disrupt the ER homeostasis and result in a stress condition of ER, which is termed ER stress (Chen H. et al., 2019). ER stress modulates the activation of NLRP3 inflammasome through various mediators such as unfolded protein response (UPR), lipid metabolism, calcium and ROS production. Several investigations showed that both ER stress and NLRP3 inflammasome activation promote AS progression (Chen X. et al., 2019).

Latest evidence indicated that ER played a key role in NLRP3 inflammasome activation. UPR is initiated to restore ER homeostasis followed by ER stress. Three ER transmembrane sensors including inositol-requiring enzyme 1α (IRE1α), activating transcription factor 6 (ATF6) and protein kinase RNA-like ER kinase (PERK) initiate UPR response under ER stress and take part in enhanced NLRP3 expression and activation (Zhou et al., 2020).

IRE1α is essential in NLRP3 inflammasome activation mediated by ER stress and serves as potential therapeutic target for inflammatory-associated disorders, such as and viral myocarditis (Bronner et al., 2015).

Following IRE1α activation in ER stress, miR17, a TXNIP-destabilizing micro-RNA, is degraded with subsequently upregulated expression of TXNIP (Talty et al., 2019). TXNIP traffic to mitochondria and is associated with thioredoxin-2, which facilitates the disassociation of ROS from mitochondria. The increased ROS production favors the leakage of mitochondrial contents such as mtDNA, cytochrome C and cardiolipin; and subsequently provokes NLRP3 inflammasome assembly. Also, the following production of proinflammatory cytokines IL-1β and IL-18 is involved in atherogenesis (Chen et al., 2018). The activated IRE1α has an action to upregulate TXNIP at both transcritional and protein levels through inhibiting miR17 expression in mouse embryo fibroblasts (MEFs), and to trigger NLRP3 inflammasome activation (Lerner et al., 2012). Knockdown of TXNIP inhibits NLRP3 inflammasome activation induced by ethanol, fructose and trimethylamine-N-oxide expose, or following ischemia/

reperfusion injury (Zhou et al., 2020). However, the specific effect/mechanism on NLRP3 inflammasome activation during AS is still not completely understood. Moreover, under excess ER stress, persistent IRE1α oligomerization activates its downstream target JNK. The JNK signaling is enhanced by E3 ligase carboxyl terminus of HSC70-interacting protein (CHIP)-mediated IRE1α ubiquitination (Zhu et al., 2014). Also, PERK/eIF-2α acts as an alternative signaling pathway in JNK activation. JNK activation is in upstream of ASC phosphorylation, which activates caspase-1 through NLRP3 inflammasome (Hara et al., 2013; Bronner et al., 2015), which promotes the formation of early AS (Babaev et al., 2016).

PERK, a transmembrane protein kinase, connects NLRP3 inflammasome through mitochondria-associated membranes (MAMs) (Han et al., 2018), and engages in NLRP3 inflammasome activation (Lebeaupin et al., 2015). PERK deficiency results in mitochondrial fragmentation and shorted ER–mitochondria communication that decrease ROS production depending on the level of ER stress and the activity of NLRP3 inflammasome (Diaz et al., 2021). Meanwhile, PERK inhibitor disrupts ER-derived Ca^{2+} release due to MAMs perturbation, thus blocking activation of the inflammasome (Zhou et al., 2020). Studies also showed that ox-LDL upregulated PERK phosphorylation, and expression level of inflammation-related molecules in endothelial cells (ECs) (Hang et al., 2020). Moreover, the downregulated NLRP3 at protein level was observed in the tunicamycin-treated AML12 cells in parallel with downregulation of PERK (Han et al., 2018). Treatment with puerarin significantly reversed NLRP3 inflammasome activation through inhibiting Amyloid β (Aβ) 1–40-induced phosphorylation of PERK and IRE1 in ARPE-19 cells (Wang et al., 2017b). Moreover, 2,3,5-trichloro-6-phenyl-[1,4]-benzoquinone (PCB29-pQ) induces the activation of p-PERK in ER stress response, which is responsible for downstream lipid accumulation and pro-inflammatory cytokines release in $ApoE^{-/-}$ mice, ultimately leading to AS (Yang et al., 2020). These above studies implied that PERK maybe involve genesis and development of AS by activating NLRP3 inflammasome.

ATF6 is an ER-resident type II transmembrane glycoprotein and constitutively expressed with an inactive form (Stengel et al., 2020). Silver nanoparticles of 15 nm (AgNP15)-induced ATF6 degradation causes NLRP3 activation and IL-1β secretion with subsequent pyroptosis (Simard et al., 2015). Recent research has found that endothelial Nox4 dysfunction upregulates ATF6 probably by its induction of ER stress, and found inhibition of ER stress or ATF6 is beneficial to alleviate AS caused by endothelial Nox4 dysfunction (Yu et al., 2021). However, the role of ATF6 in NLRP3-induced AS is still not determined.

ER, as a Ca^{2+} storage is also important in cytosolic Ca^{2+} homeostasis. Inositol-1,4,5-triphosphate receptor (IP_3R) regulates ER Ca^{2+} efflux, which serves an ER stress marker (Santulli et al., 2017). The ER Ca^{2+} efflux mediated by IP_3R is essential for cell physiological functions. The efflux of Ca^{2+} is reduced by IP3R in the state of mild ER stress, but increased in the state of severe ER stress (Yue et al., 2020). The overload of cytosolic Ca^{2+} leads to mitochondrial Ca^{2+} influx mediated by mitochondrial calcium uniporter (MCU) in the inner mitochondrial membrane (IMM) and voltage-dependent anion-selective channel (VDAC) in the outer mitochondrial membrane (OMM). This event results in mitochondrial Ca^{2+} overload and destabilization (Pathak and Trebak, 2018). As a consequence, mitochondrial molecules like mtDNA and cardiolipin release or externalization into the cytoplasmic (Khwaja et al., 2021). The binding of oxidized mtDNA, cardiolipin and NLRP3 facilitates the formation of NLPR3 complex with consequently proinflammatory cytokines production and pyroptosis (Liu Q. et al., 2018). In summary, ER stress activates NLRP3 inflammasome through multiple upstream signals, including the UPR, calcium and ROS generation. ER stress-mediated NLRP3 inflammasome activation may also be critical in AS development (Chen X. et al., 2019) (**Figure 2**).

Lysosome Rupture

Lysosome rupture is also involved in the activation of NLRP3 inflammasome (**Figure 1**). Lysosome rupture occurs in macrophages that uptake metabolic and exogenous substances like amyloid-β, cholesterol crystals, alum, silica, asbestos and calcium crystal. CSTB is released following lysosome rupture, which binds and activates NLRP3 by recognizing LRR domain (Bai et al., 2018). Liu et al. found that inhibiting CSTB suppressed the NLRP3 signal in tubular epithelial cells exposed to albumin (Liu et al., 2015). Angiotensin II-enhanced lysosomal membrane permeabilization induces CSTB release from lysosomes and the consequent NLRP3 inflammasome activation (Lian et al., 2018). CSTB deficiency causes dramatically inhibited activation of caspase-1, IL-1β and ASC speck in BMDMs (Bone marrow-derived macrophages) exposed to different kinds of stimuli for NLRP3 activation such as ATP, crystals and nigericin (Chevriaux et al., 2020). These studies support that CSTB release and distribution are essential for NLRP3 signal activation. The latest study suggested that lysosome rupture might be critical event in atherogensis through activating NLRP3 inflammasome (He et al., 2021). However, mechanisms of lysosomal disruption in NLRP3 inflammasome-mediated AS need to be further elucidated in the future (Hoseini et al., 2018) (**Figure 2**).

Calcium Mobilization

Mobilization of Ca^{2+} occurs by Ca^{2+} influx from extracellular fluid or Ca^{2+} influx from ER-Ca^{2+} stores and the biological event is critical for NLRP3 activation (Swanson et al., 2019). Ca^{2+} influx consequently occurs in mitochondria, and mitochondrial Ca^{2+} overload as well as accumulated cytoplasmic Ca^{2+} involve the activation of NLRP3 inflammasome (Lee G.-S. et al., 2012). Pretreatment with Ca^{2+}-chelating agent BAPTA-AM prior to stimulation with LPS and ATP or exposing to *mycobacterium* abscessus attenuated activation of NLRP3 inflammasome in macrophages (Lee H. M. et al., 2012). Also, ATP and cholesterol-dependent cytolysin-mediated Ca^{2+} influx

induced the atctivation of NLRP3 inflammasome in macrophages pre-treated with LPS (Feldmeyer et al., 2007; Chu et al., 2009).

Furthermore, K^+ efflux and Ca^{2+} flux are proposed as coordinated regulators in NLRP3 activation. K^+ efflux promotes ER Ca^{2+} efflux followed by plasma Ca^{2+} channels activation (Yaron et al., 2015). It has been observed that ATP primed P2X7 induces a weak Ca^{2+} influx and coordinating K^+ efflux with following $Ca2^+$ mobilization (Di et al., 2018). Additionally, NLRP3 activation induced by nigericin, alum, monosodium urate crystals is dependent on Ca^{2+} flux and K^+ efflux (Gong T. et al., 2018). However, several studies demonstrated that Ca^{2+} flux is the downstream effector of NLRP3 and caspase one activation after the stimulation by some stimuli. So this contradictory result suggests that Ca^{2+} flux might not be essential for NLRP3 activation (Katsnelson et al., 2015). Thus, whether Ca^{2+} flux is essential for NLRP3 activation is needed to be identified.

In addition, increased extracellular calcium has a role as a danger signal and amplifier of inflammation. Increased extracellular calcium at sites of infection, inflammation or cell activation activates the NLRP3 inflammasome via stimulation of G protein-coupled calcium sensing receptors (Hoseini et al., 2018). NLRP3 activation is mediated by signaling through the calcium-sensing receptor and GPRC6A via the phosphatidyl inositol/Ca^{2+} pathway (Alphonse et al., 2016). The resulting increase in the intracellular calcium concentration triggers inflammasome assembly and caspase-1 maturation. In conclusion, calcium mobilization may activate NLRP3 through multiple pathways and participate in the occurrence and development of AS.

In a word, assembly of inflammasome complexes is an innate immune response to various pathological signals and mediates IL-1β and IL-18 release, and subsequently pyroptosis. The most well-investigated inflammasome, NLRP3, senses intracellular events induced by different stimuli such as PAMPs or DAMPs. For instance, various signals including mtROS production, oxidized mtDNA release, and cardiolipin externalization are downstream effectors of mitochondrial dysfunction in NLRP3 inflammasome activation (Yu and Lee, 2016). The internalized small particles including alum, silica, and CPPD crystals are perpetrators of lysosomal rupture which mediates downstream K^+ efflux or cathepsins release and these events have been proved to be critical in NLRP3 inflammasome activation (Orlowski et al., 2015). Besides mitochondrial dysfunction and lysosomal membrane rupture, different types of ion fluxes such as K^+ efflux, Ca^{2+}mobilization, and Cl^-efflux, are also the key upstream events in the process of NLRP3 inflammasome activation (Gong T. et al., 2018). In addition, the Golgi apparatus is also proposed to involve NLRP3 inflammasome activation (Wang Y. et al., 2020). However, given the diversity of NLRP3 activators, precise mechanism of NLRP3 activation remains to be further investigated. Overall, different upstream cellular processes initiate NLRP3 inflammasome activation independently or by their interplay (Fusco et al., 2020), and its activation is also affected by multiple factors, such as Guanylact-binding Protein 5 (Gbp5), microRNA223 (miR-223) (Neudecker et al., 2017), calcium-sensitive receptors, double-standard RNA activated protein kinase (PKR) (Boriushkin et al., 2016), etc. Further, mitochondrial dysfunction, excessive ER stress and lysosome rupture are also the important events in atherogenesis involved in NLRP3 inflammasome activation (Hoseini et al., 2018) (**Figure 2**).

NLRP3 INFLAMMASOME ACTIVATION IS INVOLVED IN AS

In recent studies, AS has been suggested as a lipid-related inflammatory disease, and the activation of NLRP3 inflammasome serves as a bridge between lipid metabolism and inflammation since two major events in atherosclerotic plaques, crystalline cholesterol and ox-LDL are involved in NLRP3 inflammasome activation (Fusco et al., 2020).

Many studies have suggested the relevance of NLRP3 inflammasome and AS occurrence by analyzing aortic NLRP3 expression in the patients with AS (Paramel Varghese et al., 2016). The key components of NLRP3 inflammasome, such NLRP3, caspase-1 and ASC were highly expressed in the aortic and carotid plaques, as well as the subcutaneous adipose tissue in the patients with AS. The expression level of these components is related to disease severity of AS (Bando et al., 2015; Shi et al., 2015). Meanwhile, several studies revealed that smoking, hypertension and diet with rich in saturated fatty acids and glucose might coordinatingly contribute to NLRP3 activation in myeloid cells of the AS patients (Baldrighi et al., 2017). Besides, Varghese et al. analyzed the transcripts of NLRP3 inflammasome and release of IL-1β in atherosclerotic plaques in the individuals with or without myocardial infarction (Varghese et al., 2016). NLRP3, ASC, caspase-1, IL-1β and IL-18 at the transcriptional level were dramatically upregulated in atherosclerotic plaques. NLRP3 mRNA was also remarkably upregulated in the plaques of symptomatic patients. Further study suggested that the dysregulation of NLRP3 inflammasome and its genetic variants may contribute to atherogenesis (Paramel Varghese et al., 2016).

Components of NLRP3 complex have been reported to be constitutively expressed in both innate and adative immune cells like monocytes, macrophages, dendritic cells and T cells (Wang and Hauenstein, 2020). In innate immune cells derived from different AS animal models, upregulated NLRP3 expression was observed (Liaqat et al., 2020). The importantance of NLRP3 inflammasome and its effectors, as well as their mediated pyroptosis in the development of AS has been proved by different investigations.

Duewell first demonstrated that formation of crystalline cholesterol was an endogenous molecular event triggering NLRP3 inflammasome activation and resulting in IL-1β release, and subsequently leading to inflammation (Duewell et al., 2010). Several other studies also demonstrated NLRP3 inflammasome playing a critical role in atherogenesis.

Hendrikx et al. found that the activation caspase-1 and caspase-11 participated in the genesis and development of AS (Hendrikx et al., 2015). Wang et al. reported that homocysteine could activate NLRP3 inflammasome in a ROS-dependent pathway in macrophages, and the activation of inflammasome promoted inflammatory response and plaque formation in $ApoE^{-/-}$ mice (Wang R. et al., 2017). Wu et al. showed that atherosclerotic plaque size and inflammatory cytokine production were increased in nicotine-treated $ApoE^{-/-}$ mice fed with high-fat diet (Wu X. et al., 2018); They also showed that nicotine-ROS production was the upstream signals to NLRP3-ASC-pyroptosis pathway and pyroptosis might be cellular mechanism underlying the pro-atherosclerotic effect of nicotine (Wu X. et al., 2018). Latest investigation revealed that the NLRP3 inflammasome activation was prior to formation of significant plaque burden or early atherogenesis in mice fed with Western diet. After fed with Western diet for 8 weeks, $LDLR^{-/-}/NLRP3^{-/-}$ mice presented smaller atherosclerotic lesion as compared to $LDLR^{-/-}$ mice (Christ et al., 2018). Also, knockout of NLRP3 in $ApoE^{-/-}$ mice also resulted in a declined AS progression, suggesting

TABLE 1 | Mechanisms and target molecules of potential drugs acting on NLRP3 inflammasome in therapies of atherosclerosis (AS).

Anti-inflammatory Drug	Suppressed Inflammasome	Mechanism or Drug Targets	Ref
Atorvastatin	NLRP3, caspase-1, GSDMD, IL-1β, and IL-18	Regulates pyroptosis to against the development of atherosclerosis via TLR4/MyD88/NF-kB pathway	Kong et al., 2016b
		Protects atherosclerosis via inducing autophagy by NEXN-AS1/NEXN pathway	Wu et al. (2020b)
Simvastatin or Mevastatin	NLRP3	Suppresses functions of ox-LDL and TNF-α	Wang et al., 2017d
		Upregulates the reduced expression of Klf2 and Foxp1 in atherosusceptible vascular endothelium and alleviates vascular inflammation	Lv et al. (2017)
Rosuvastatin	NLRP3, IL-18, and IL-1β	Downregulates cathepsin-B and its downstream signals	Altaf et al. (2015)
Arglabin	NLRP3	Reduces inflammation and plasma lipids, and increases autophagy	Abderrazak et al. (2015)
		Induces the proinflammatory M1 macrophages into the anti-inflammatory M2 phenotype	
Andrographolide	NLRP3, caspase-1 and IL-1β	Inhibits NF-κB activation and ROS generation	Kumar et al., 2020
		Reduces the expression of active caspase-1	Cabrera et al., 2017
		Suppresses overexpression of microglial MIP-1α, P2X7R and its downstream signaling mediators including NLRP3, caspase-1 and mature IL-1β	Das et al., 2017
		Disrupts the assembly of NLRP3 inflammasome complex	Lin et al., 2018
		Triggers mitophagy	Wu et al. (2018c)
Tanshinone IIA	NLRP3, caspase-1, IL-1β, and IL-18	Protects atherosclerosis via decreasing the expression of scavenger receptors such as LOX-1 and CD36	Cai et al., 2016
		Inhibits NF-κB activation	Li et al., 2017 Wen et al. (2020)
Salidroside	caspase-1, IL-1β	Inhibits NLRP3-related pyroptosis by suppressing expression of IL-1β and GSDMD.	Zhao et al., 2021a Xing et al. (2020)
Curcumin	NLRP3, caspase-1, and IL-1β	Reduces the expression of NLRP3 and secretion of the cleaved caspase-1 and IL-1β in macrophages	Singh et al., 2021
		Inhibits the activation of NF-κB in macrophages by reducing TLR4 and MyD88 expression	Zhang et al., 2018
		Attenuates NLRP3 inflammasome activation and IL-1β release by reversing PMA-induced P2X7R activation	Momtazi-Borojeni et al., 2021
		Suppresses TLR4/MyD88/NF-κB and P2X7R pathways	Kong et al. (2016a)
Triptolide	NLRP3, IL-1β, and IL-18	Inhibits NLRP3 inflammasome by reducing the levels of TLR4	Pan et al., 2019
		Suppresses the activation of NLRP3 inflammasome and expression of inflammatory molecules such as MCP-1, IL-1β, IL-18 and VCAM-1	Wu et al., 2019
		Inhibits macrophage infiltration	Islam et al., 2020
		Blocks NLRP3/TGF1β/Smad pathway	Li et al., 2017
		Attenuates the activation of NLRP3 by regulating hsa-miR20b	Qian et al. (2019)
Clematichinenoside AR	NLRP3	Inhibits foam cell formation and cholesterol accumulation	Diao, (2021)
		Induces autophagy and reduces the secretion of NLRP3 inflammasome	
Hydroxysafflor yellow A	NLRP3	Regulates PI3K/Akt/mTOR, TNFR1/NF-κB, and TLR4/Rac1/Akt signaling pathways to inhibit NLRP3 inflammasome	Xue et al. (2021)
MCC950	NLRP3, caspase-1, and IL-1β	Reduces the transcription of ICAM-1 and VCAM-1 in the carotids	Wu et al., 2020a
		Regulates chloride efflux, chloride intracellular channels	van der Heijden et al., 2017
		Weakens caspase-1 and IL-1β secretion	Ma et al. (2021)
		Inhibits proliferation of macrophages and T cells	
Melatonin	NLRP3, IL-1β	Induces mitophagy	Zhao et al., 2021b
		Attenuates Sirt3/Foxo3a/Parkin signaling pathway	Ma et al. (2018)
Canakinumab	IL-1β	Neutralizes IL-1β antibody selectively	Gomez et al., 2018
		Impairs high-sensitive C-reactive protein, decreases plasma lipid	Ridker et al. (2020)

NLRP3 inflammasome activation involving atherogenesis (Grebe et al., 2018).

Overall, numerous experimental and epidemiological results confirmed the role of NLRP3 inflammasome in atherogenesis and other CVDs.

INHIBITION OF NLRP3 INFLAMMASOME REDUCES AS

A clinical trial named Canakinumab Anti-Inflammatory Thrombosis Outcomes Study "CANTOS" was performed to analyze effect of canakinumab (a monoclonal antibody selectively blocking IL-1β) in patients with a steady CAD (Ridker P. M. et al., 2017). The results of CANTOS first revealed a dramatic decrease in major adverse cardiovascular events after Canakinumab treatment. The study further determined the critical role of NLRP3 inflammasome-mediated inflammatory responses in the progression of AS (Ridker P. M. et al., 2017), thus inhibiting NLRP3 activation might be a novel strategy to prevent and treat AS (Ridker PM. et al., 2017). Currently, approaches in inhibiting NLRP3 inflammasome divide into two strategies, directly inhibiting NLRP3 and indirectly inhibiting upstream or downstream signaling events (Liu D. et al., 2020), but the related mechanisms and the exact targets are not fully clarified, thus future investigation on the molecular targeted drugs on NLRP3 are required (Parsamanesh et al., 2019).

Statins

Statins are a class of HMG-CoA (3-hy-droxy-3-methylglutaryl coenzyme A) reductase inhibitors and have cholesterol-lowering effect. Statins also show their beneficial effects on vascular inflammation. Recent clinical studies have demonstrated the efficacy of statins in improving endothelial function and stabilizing plaques. Statins has been considered to be a potential pharmaceutical approach in inhibiting AS genesis by impeding inflammatory processes (Bahrami et al., 2018) (**Table 1**).

Routine treatment with atorvastatin inhibits TLR4/MyD88/NF-kB pathway-mediated NLRP3 inflammasome activation and IL-1β generation in human monocytic cells (THP-1) (Kong et al., 2016b). Wu et al. showed that atorvastatin could inhibit pyroptosis by downregulating the components in inflammasome complex and decrease downstream effectors IL-1β, IL-18 and GSDMD (Wu L.-M. et al., 2020). Atorvastatin also inhibits the development of AS via NEXN-AS1-NEXN (a long non-coding RNA; lncRNA)-mediated pyroptosis (Wu L.-M. et al., 2020). Atorvastatin was also proved to enhance the stability of vulnerable plaques and decrease the degree of atherosclerosis in mice (Peng et al., 2018). Atorvastatin had been found to inhibit the activation of NLRP3 inflammasome, release of IL-1β and IL-18 and excess autophagy in the vulnerable atherosclerotic plaques (Peng et al., 2018). Moreover, atorvastatin was also observed to attenuate lipid deposition and inflammatory response, inhibit NLRP3 inflammasome activation and enhance autophagy in macrophages exposed to ox-LDL *in vitro* (Peng et al., 2018). All of above beneficial effects could be eliminated by an autophagy inhibitor 3-methyladenine (Peng et al., 2018). Thus, it is proposed that atorvastatin acts as an autophagy inducer in stabilizing vulnerable atherosclerotic plaques.

Wang et al. showed that simvastatin and mevastatin both markedly inhibited ox-LDL and TNF-α-stimulated NLRP3 inflammasome activation in ECs. They also demonstrated that statin suppressed NLRP3 inflammasome activation by blocking NF-κB to bind to the promoter regions of NLRP3 gene upon exposure to atherogenic inducers like ox-LDL and TNF-α in ECs (Wang S. et al., 2017). Lv et al. revealed a Klf2-Foxp1 transcriptional network in endothelium as a novel regulator of inflammasome activation for genesis of atherosclerosis. Simvastatin upregulated the reduced expression of Klf2 and Foxp1 in atherosusceptible vascular endothelium and alleviated vascular inflammation, indicating a novel atheroprotective mechanism for simvastatin (Lv et al., 2017).

Altaf et al. had investigated the effect of rosuvastatin on activity of NLRP3 inflammasome in monocytes from peripheral blood of the patients suffered from acute coronary syndromes. This finding indicated that application of high dose of rosuvastatin could downregulate NLRP3 and its downstream effectors, thus alleviate inflammatory response in atherogenesis (Altaf et al., 2015). In addition, Abderrazak et al. have proved that arglabin (a natural inhibitor of inflammasome NLRP3) reduces inflammation and plasma lipids, increases autophagy. It may potentially be involved in anti-atherogenic effects of ApoE$^{-/-}$ mice (Abderrazak et al., 2015). The above studies revealed the potential role of NLRP3 in pathogenesis and management of AS and acute coronary syndrome. Although great progress has been achieved in defining the role of NLRP3 inflammasomes in coronary AS, the key mechanisms of statins family in atherosclerotic development are not evidently identified. Additional work still needs to focus on regulation of statins in inflammatory response and clinical implications (Parsamanesh et al., 2019).

Natural Medication

Natural medicines, especially extracts from Chinese herbs have been demonstrated to regulate NLRP3 inflammasome activation in target cells such as ECs, SMCs, macrophages and nerve cells. And it is mainly manifested as an inhibitory effect, including inhibiting TLRs and NLRP3 expression, decreasing caspase-1 activity, and reducing the release of inflammatory factors, thereby regulating cell pyrolysis and slowing the development of AS (Nasonov and Popkova, 2018) (**Figure 3**; **Table 1**).

Andrographolide (Andro), the bitter diterpene lactone, is a bioactive component of Andrographis paniculata (Kumar et al., 2020). It inhibits LPS-stimulated NLRP3 inflammasome disassembly and IL-1β maturation through inhibiting NF-κB activation in fat-laden HepG2 cells, and reduces inflammation, thus fibrosis is also observed in AS after Andro treatment (Cabrera et al., 2017). Andro also inhibits the activation of NLRP3 inflammasome in macrophages by disruption of NLRP3 inflammasome complex formation; more importantly, Andro aslo has the action to trigger mitophagy in macrophages, which in turn inactivates NLRP3 inflammasome (Guo et al.,

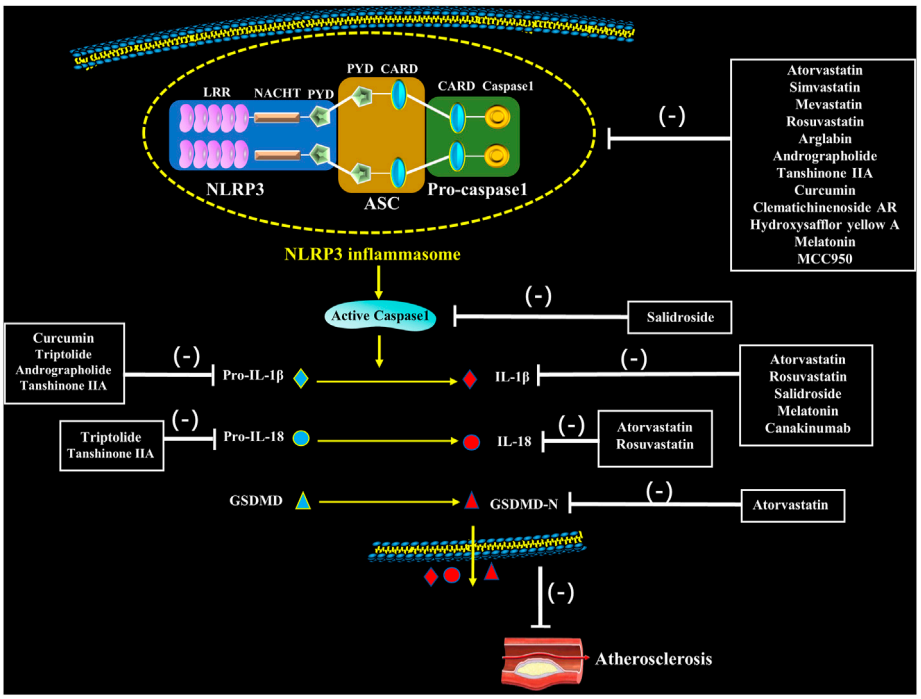

FIGURE 3 | Pharmacological interventions on atherosclerosis through potentially targeting to NLRP3 inflammasome. Statins, natural medication and novel medication directly or indirectly inhibit assembly and activation of NLRP3 inflammasome as well as secretion of IL-1β and IL-18, which inhibit the occurrence of atherosclerosis.

2014). Andro also down-regulates microglial macrophage inflammatory protein 1-alpha (MIP-1α), NLRP3 and P2X7, as well as its downstream signals caspase-1 and IL-1β (Das et al., 2017). Studies have shown that application of Andro ameliorates atherogenesis in ApoE$^{-/-}$ mice by inhibiting NLRP3, ROS production, and foam cell formation *in vivo* (Wu et al., 2018c; Lin et al., 2018), indicating a good prospect to use Andro preventing and treating AS. Andro is loaded to poly (propylene sulphide) (PEG-PPS) and poly (ethylene glycol) micelle which possess the capability of Andro release in ROS-abundant atherosclerotic plaques, and can synchronically attenuate inflammatory response and oxidative injury, suggesting a novel approach in AS prevention and treatment (Wu et al., 2018b).

0–2.5 μg/ml Tanshinone IIA (Tan IIA) exhibited its protective effect by suppressing the activation of NLRP3 and maturation of caspase-1, IL-1β, and IL-18 in BV-2 cells (Cai et al., 2016). Decreased expression levels of TLR4, MyD88, NF-κB, NLRP3, TNF-α and IL-4, and increased expression of IL-10, TGF-β, PTEN, PI3K as well as phosphorylation levels of AKT were verified in Tan IIA administrated rats (Li et al., 2017). Impaired NLRP3 inflammasome activation is revealed in Tan IIA treated ApoE$^{-/-}$ mice fed with high-fat diet. Tan IIA also blocks ox-LDL-stimulated activation of NLRP3 inflammasome *in vitro*, and exerts anti-atherogenesis effect through different signaling pathways. Theoretically, Tan IIA inhibits NLRP3 inflammasome activation by blocking ox-LDL-induced activation of NF-κB and expression of lectin-like oxidized LDL receptor-1 (LOX-1) and CD36, which subsequently mediate mitochondrial and lysosomal damage (Wen et al., 2020).

Salidroside (SAL), a phenylpropane glycoside, is the main effective ingredient of the plateau plant Rhodiola. Until now, several *in vivo* investigations showed the positive effect of SAL in AS treatment (Zhao C. C. et al., 2021). However, little is known of its mechanism in regulation of NIRP3 inflammasome. Xing and coworkers investigated the effect of SAL on pyroptosis and AS-related inflammation. Significantly smaller atherosclerotic plaque in aorta was determined in AS mice model administrated of SAL. Meanwhile, SAL also inhibited pyroptosis through suppressing expression of IL-1β and GSDMD. Furthermore, SAL also alleviated caspase-1 maturation and IL-1β release in HUVECs primed by LPS and ATP. These data reveal that SAL exerts its anti-inflammatory effect in AS via inhibiting NLRP3-mediated pyroptosis (Xing et al., 2020). Thus, SAL is a promising molecule for treating CVD.

Curcumin, a natural compound extracted from Curcuma longa L. rhizomes has potent action to attenuate oxidative stress, inflammatory response and atherosclerosis (Singh et al., 2021). Increasing evidence indicates that curcumin slows down the progression and development of AS via regulating various signaling molecules (Zhang et al., 2018; Momtazi-Borojeni et al., 2021), but its effect on NLRP3 is rarely reported. Few experiments have confirmed that curcumin has a function to inhibit NLRP3 inflammasome action and IL-1β secretion, thus to attenuate

inflammatory response (Gong Z. et al., 2018; Yin et al., 2018). Kong et al. reported that curcumin significantly reduced the expression of NLRP3 and secretion of the cleaved caspase-1 and IL-1β in phorbol 12-myristate 13-acetate (PMA)-induced macrophages; moreover, curcumin also markedly inhibited the activation of NF-κB in PMA-induced macrophages by reducing TLR4 expression and myeloid differentiation factor 88 (MyD88). Curcumin treatment results in an attenuated NLRP3 inflammasome activation and IL-1β release by reversing PMA-induced P2X7R activation. Also P2X7R knockdown declines NF-κB activation in PMA-induced macrophages. Thus, curcumin impairs development of AS through suppressing NLRP3 inflammasome activation, which is involved in the activity of TLR4, MyD88, NF-κB and P2X7R (Kong et al., 2016a). Additional studies are required to enhance our understanding in the mechanism of curcumin in AS development (Singh et al., 2021). Moreover, coupling curcumin to nanomicelles (Li et al., 2020; Helli et al., 2021), might be a valuable way to ameliorate its oral bioavailability and clinical efficacy (Pechanova et al., 2020).

Triptolide (TPL) is an active natural compound with anti-inflammatory activities in various cell types. Studies have proved that TPL has an action to inhibit activation of NLRP3 inflammasome (Pan et al., 2019; Wu et al., 2019). Concentrations of IL-1β and IL-18 in serum dramatically down-regulated and expressions of NLRP3 and TLR4 also reduced in rats treated with TPL (Islam et al., 2020). It may suppress the activation of NLRP3 inflammasome and expression of inflammatory molecules such as macrophage chemoattractant protein-1 (MCP-1), IL-1β, IL-18 and vascular cell adhesion molecule-1 (VCAM-1); Moreover, macrophage infiltration can also be inhibited by TPL (Li et al., 2017). NLRP3–TGF1β-Smad pathway is also blocked by TPL, indicating its potential approach for alleviating cardiac fibrosis via targeting NLRP3 inflammasome (Pan et al., 2019). Further, TPL also attenuated the activation of NLRP3 by regulating hsa-miR20b in both mice and THP-1 cells (Qian et al., 2019). It reveals that TPL can inhibit AS progression by inhibition of inflammaging and regulation of lipid metabolism, providing a new insight on use of TPL to treat AS in clinical (Luo and Yang, 2016).

Clematichinenoside AR (AR) is the one of the main effective fractions from a traditional Chinese herb Clematis chinensis with potential therapeutical properties on many diseases, including AS. A study showed that application of AR inhibited foam cell formation and cholesterol accumulation; AR initiated its biological function by inducing autophagy and reducing the secretion of NLRP3 inflammasome-mediated inflammatory cytokines; these events were impaired by the autophagy inhibitor bafilomycin A1 (Diao, 2021). AR was observed to inhibit foam cell formation and the following inflammatory reaction in RAW264.7 cells exposed to ox-LDL, thus confirming AR as a potential pharmacological intervention for AS treatment.

Hydroxysafflor yellow A (HSYA), a natural ingredient from Carthamus tinctorius has a promising therapeutic effect for prevention and treatment of AS. It has been studied that HSYA alleviates AS with suppression VSMC proliferation, endothelial dysfunction, foam cell formation, and platelet activation by regulating PI3K/Akt/TOR, NLRP3 inflammasome, TNFR1/NF-κB and TLR4/Rac1/Akt signaling pathways (Xue et al., 2021). Besides, HSYA contributes to decreased blood lipids and vascular inflammation as well as protected pancreatic beta cells, reducing the harm from risk factors of AS (Xue et al., 2021). Also the further clinical trials of HSYA remain to be performed for its clinical application. In a word, Chinese herb extracts with inhibitory activities on NLRP3 inflammasome might be a novel approach against atherosclerotic diseases.

Overall, in past few years, several natural compounds have been discovered as potential agents in AS treatment. However, more investigations should focus on their mechanisms alleviating AS.

Novel Medication

A few new targets and compounds for treatment of AS are verified through NLRP3 inflammasome pathway (**Figure 3**). MCC950 is a small molecular compound that specifically blocks NLRP3 inflammasome, correlating with chloride intracellular channels and chloride efflux (Wu D. et al., 2020). Van der Heijden's findings showed that blocking activation of NLRP3 inflammasome using MCC950 remarkably delayed the development of atherosclerotic lesions. In addition, application of MCC950 also reduced the transcription of intercellular adhesion molecule 1 (ICAM-1) and VCAM-1 in the carotids of mice (van der Heijden et al., 2017). Sharma et al. found MCC950 ameliorated diabetes-caused AS by reducing inflammation and improving vascular function in the $ApoE^{-/-}$ mice treated with streptozotocin; additionally, in a range of cell lines (THP-1 cells, BMDM, aortic SMCs from humans with diabetes and phorbol 12-myristate 13-acetate-stimulated human macrophages), MCC950 markedly weakened caspase-1 and IL-1β secretion under high glucose or LPS stimulation (Sharma et al., 2021). Recently, Ma et al. loaded MCC950 to platelet-derived extracellular vesicles (PEVs) for AS-targeted therapy. They found that application of MCC950-PEVs markedly reduced the formation of atherosclerotic plaques, lowered inflammatory response in the local tissues and inhibited proliferation of macrophages and T cells in plaques of $ApoE^{-/-}$ mice (Ma et al., 2021). In summary, specific inhibiting NLRP3 using MCC950 is probably a potential therapeutic strategy to inhibit atherosclerotic lesion development. In addition, sodium glucose cotransporter-2 (SGLT2) inhibitor dapagliflozin partially reversed the formation of AS in the diabetic $ApoE^{-/-}$ mice, inhibited macrophage infiltration, and strengthened plaque stability. These effects may be dependent on the inhibitory effect on IL-1β release through ROS/NLRP3/caspase-1 signaling (Leng et al., 2016). It is clear that dapagliflozin might be therapeutic agent for high-fat derived diabetic AS.

Recent study proves melatonin as a new target for therapeutic intervention for AS. The decreased AS plaque size and vulnerability were determined in atherosclerotic mouse model treated with melatonin. Reduced activation of NLRP3 inflammasome and maturation of IL-1 β were also

found in atherosclerotic lesions (Zhao Z. et al., 2021). Ma et al. showed that melatonin partially prevented atherosclerotic progression through inducing mitophagy and attenuating Sirt3/FOXO3a/Parkin-mediated NLRP3 inflammasome activation (Ma et al., 2018).

Blocking IL-1β is another therapeutic remedy for treating AS. Cancakinumab, a monoclonal antibody that selectively binds and blocks IL-1β may improve advanced plaque stability. Gomez et al. had verified the effect of canakincumab on the advanced AS in the SMC lineage-tracing ApoE$^{-/-}$ mice (Gomez et al., 2018). Surprisingly, they found that canakincumab treatment between 18 and 26 weeks induced a marked reduction of collagen content in SMCs and increased resident macrophages in fibrous plaques. Further, canakinumab treatment completely inhibited beneficial outward remodeling (Gomez et al., 2018). Canakinumab treatment may alleviate the recrudesce of cardiovascular diseases. A new clinical study also suggested that canakinumab dramatically impaired high-sensitive C-reactive protein, decreased plasma lipid and ameliorated AS (Wang Y. et al., 2020). In addition, a marked residual inflammatory risk from IL-6 and IL-18 has been verified during the treatment of atherothrombosis using canakinumab, indicating that new inhibitors to block IL-6 and IL-18 or other cytokines are needed to be developed in the future (Ridker et al., 2020).

The above NLRP3 inflammasome-molecules showed potentially clinical value. However, continuous investigations still need to determine the mechanisms of NLRP3 regulating AS and the applicability of NLRP3 inflammasome-targeting molecules in the clinical trials. In addition, Shen et al. found that PUFAs had an action to attenuate NLRP3 activation and IL-1β secretion in blood monocytes derived from LDLR$^{-/-}$ mice; furthermore, PUFA-enriched diets enhanced autophagy and ameliorated mitochondrial dysfunction in macrophages primed by LPS and palmitate (Shen et al., 2017). In conclusion, PUFA-enriched diets reduce AS and macrophage inflammation, partially by attenuating activation of NLRP3 inflammasome and activating autophagy of macrophages (Shen et al., 2017).

In short, drugs aimed at inhibiting the activity of NLRP3 inflammasome have been developed one after another. It not only confirmed the inflammatory theory of AS, but also made it clear that anti-inflammatory has become a new way to treat AS and other cardiovascular diseases.

SUMMARY

The NLRP3 inflammasome, an innate immune signaling complex, is always activated by a series of endogenous stimuli in the process of atherosclerotic plaque formation, such as ox-LDL and cholesterol crystals. Numerous studies have suggested that the activation of NLRP3 inflammasome contributes to inflamming of vasculature in genesis and progression of AS (Shao et al., 2015). With intensive studies on NLRP3 activation, intervention of NLRP3 as a remedy to prevent and treat AS has been greatly progressing. Therapeutic approaches in clinical trials via specifically inhibiting NLRP3 inflammasome for AS have been improved quickly, especially as a practice to protect tissue against inflammation and injury. Many advancing therapeutics only restrain the activation of NLRP3, but do not influence the action of other inflammasome units (Swanson et al., 2019). Thus, continuously developing the specific NLRP3 inhibitors may be promising the therapeutic remedies to solve atherogenesis.

AUTHOR CONTRIBUTIONS

NL and XW were in charge of searching the related literature and wrote the manuscript. WC and GL were responsible for drawing pictures. DL gave her valuable suggestions. CC and CF participated in typesetting. XW revised the manuscript.

FUNDING

This work was supported by the National Natural Science Foundation of China (Nos. 81873459 and U1804166), Henan Outstanding Young Scholars Fund (No: 212300410012), research grant of Xinxiang Medical University (No. 300/505410).

REFERENCES

Abais, J. M., Xia, M., Zhang, Y., Boini, K. M., and Li, P.-L. (2015). Redox Regulation of NLRP3 Inflammasomes: ROS as Trigger or Effector? *Antioxid. Redox Signaling* 22 (13), 1111–1129. doi:10.1089/ars.2014.5994

Abderrazak, A., Couchie, D., Mahmood, D. F. D., Elhage, R., Vindis, C., Laffargue, M., et al. (2015). Anti-Inflammatory and Antiatherogenic Effects of the NLRP3 Inflammasome Inhibitor Arglabin in ApoE 2 .Ki Mice Fed a High-Fat Diet. *Circulation* 131 (12), 1061–1070. doi:10.1161/CIRCULATIONAHA.114.013730

Alphonse, M. P., Duong, T. T., Shumitzu, C., Hoang, T. L., McCrindle, B. W., Franco, A., et al. (2016). Inositol-Triphosphate 3-Kinase C Mediates Inflammasome Activation and Treatment Response in Kawasaki Disease. *J.I.* 197 (9), 3481–3489. doi:10.4049/jimmunol.1600388

Altaf, A., Qu, P., Zhao, Y., Wang, H., Lou, D., and Niu, N. (2015). NLRP3 Inflammasome in Peripheral Blood Monocytes of Acute Coronary Syndrome Patients and its Relationship with Statins. *Coron. Artery Dis.* 26 (5), 409–421. doi:10.1097/MCA.0000000000000255

Alves, J. V., da Costa, R. M., Pereira, C. A., Fedoce, A. G., Silva, C. A. A., Carneiro, F. S., et al. (2020). Supraphysiological Levels of Testosterone Induce Vascular Dysfunction via Activation of the NLRP3 Inflammasome. *Front. Immunol.* 11, 1647. doi:10.3389/fimmu.2020.01647

Babaev, V. R., Yeung, M., Erbay, E., Ding, L., Zhang, Y., May, J. M., et al. (2016). Jnk1 Deficiency in Hematopoietic Cells Suppresses Macrophage Apoptosis and Increases Atherosclerosis in Low-Density Lipoprotein Receptor Null Mice. *Atvb* 36 (6), 1122–1131. doi:10.1161/ATVBAHA.116.307580

Bahrami, A., Parsamanesh, N., Atkin, S. L., Banach, M., and Sahebkar, A. (2018). Effect of Statins on Toll-like Receptors: a New Insight to Pleiotropic Effects. *Pharmacol. Res.* 135, 230–238. doi:10.1016/j.phrs.2018.08.014

Bai, H., Yang, B., Yu, W., Xiao, Y., Yu, D., and Zhang, Q. (2018). Cathepsin B Links Oxidative Stress to the Activation of NLRP3 Inflammasome. *Exp. Cel Res.* 362 (1), 180–187. doi:10.1016/j.yexcr.2017.11.015

Baldrighi, M., Mallat, Z., and Li, X. (2017). NLRP3 Inflammasome Pathways in Atherosclerosis. *Atherosclerosis* 267, 127–138. doi:10.1016/j.atherosclerosis.2017.10.027

Bando, S., Fukuda, D., Soeki, T., Nishimoto, S., Uematsu, E., Matsuura, T., et al. (2015). Expression of NLRP3 in Subcutaneous Adipose Tissue Is

Associated with Coronary Atherosclerosis. *Atherosclerosis* 242 (2), 407–414. doi:10.1016/j.atherosclerosis.2015.07.043

Boriushkin, E., Wang, J. J., Li, J., Bhatta, M., and Zhang, S. X. (2016). p58IPK Suppresses NLRP3 Inflammasome Activation and IL-1β Production via Inhibition of PKR in Macrophages. *Sci. Rep.* 6, 25013. doi:10.1038/srep25013

Bronner, D. N., Abuaita, B. H., Chen, X., Fitzgerald, K. A., Nuñez, G., He, Y., et al. (2015). Endoplasmic Reticulum Stress Activates the Inflammasome via NLRP3- and Caspase-2-Driven Mitochondrial Damage. *Immunity* 43 (3), 451–462. doi:10.1016/j.immuni.2015.08.008

Broz, P., and Dixit, V. M. (2016). Inflammasomes: Mechanism of Assembly, Regulation and Signalling. *Nat. Rev. Immunol.* 16 (7), 407–420. doi:10.1038/nri.2016.58

Cabrera, D., Wree, A., Povero, D., Solís, N., Hernandez, A., Pizarro, M., et al. (2017). Andrographolide Ameliorates Inflammation and Fibrogenesis and Attenuates Inflammasome Activation in Experimental Non-alcoholic Steatohepatitis. *Sci. Rep.* 7 (1), 3491. doi:10.1038/s41598-017-03675-z

Cai, H., Wang, P., Zhang, B., and Dong, X. (2020). Expression of the NEK7/NLRP3 Inflammasome Pathway in Patients with Diabetic Lower Extremity Arterial Disease. *BMJ Open Diab Res. Care* 8 (2), e001808. doi:10.1136/bmjdrc-2020-001808

Cai, L., Yi, X. B., Yuan, L. B., and Gong, G. (2016). [The Protective Effect of Tanshinone IIA on Oxygen-Glucose Deprivation and Reperfusion Injury of MicrogliaThrough the NLRP3 Inflammatory Signaling Pathway]. *Sichuan Da Xue Xue Bao Yi Xue Ban* 47 (5), 660–664.

Chakrabarti, A., Banerjee, S., Franchi, L., Loo, Y.-M., Gale, M., Jr., Núñez, G., et al. (2015). RNase L Activates the NLRP3 Inflammasome during Viral Infections. *Cell Host & Microbe* 17 (4), 466–477. doi:10.1016/j.chom.2015.02.010

Chen, D., Dixon, B. J., Doycheva, D. M., Li, B., Zhang, Y., Hu, Q., et al. (2018). IRE1α Inhibition Decreased TXNIP/NLRP3 Inflammasome Activation through miR-17-5p after Neonatal Hypoxic-Ischemic Brain Injury in Rats. *J. Neuroinflammation* 15 (1), 32. doi:10.1186/s12974-018-1077-9

Chen, H., Lin, H., Xie, S., Huang, B., Qian, Y., Chen, K., et al. (2019a). Myricetin Inhibits NLRP3 Inflammasome Activation via Reduction of ROS-dependent Ubiquitination of ASC and Promotion of ROS-independent NLRP3 Ubiquitination. *Toxicol. Appl. Pharmacol.* 365, 19–29. doi:10.1016/j.taap.2018.12.019

Chen, X., Guo, X., Ge, Q., Zhao, Y., Mu, H., and Zhang, J. (2019b). ER Stress Activates the NLRP3 Inflammasome: A Novel Mechanism of Atherosclerosis. *Oxidative Med. Cell Longevity* 2019, 1–18. doi:10.1155/2019/3462530

Chevriaux, A., Pilot, T., Derangère, V., Simonin, H., Martine, P., Chalmin, F., et al. (2020). Cathepsin B Is Required for NLRP3 Inflammasome Activation in Macrophages, through NLRP3 Interaction. *Front. Cel Dev. Biol.* 8, 167. doi:10.3389/fcell.2020.00167

Christ, A., Günther, P., Lauterbach, M. A. R., Duewell, P., Biswas, D., Pelka, K., et al. (2018). Western Diet Triggers NLRP3-dependent Innate Immune Reprogramming. *Cell* 172 (1-2), 162–175. e114. doi:10.1016/j.cell.2017.12.013

Chu, J., Thomas, L. M., Watkins, S. C., Franchi, L., Núñez, G., and Salter, R. D. (2009). Cholesterol-dependent Cytolysins Induce Rapid Release of Mature IL-1β from Murine Macrophages in a NLRP3 Inflammasome and Cathepsin B-dependent Manner. *J. Leukoc. Biol.* 86 (5), 1227–1238. doi:10.1189/jlb.0309164

Dai, J., Zhang, X., Wang, Y., Chen, H., and Chai, Y. (2017). ROS-activated NLRP3 Inflammasome Initiates Inflammation in Delayed Wound Healing in Diabetic Rats. *Int. J. Clin. Exp. Pathol.* 10 (9), 9902–9909.

Das, S., Mishra, K. P., Ganju, L., and Singh, S. B. (2017). Andrographolide - A Promising Therapeutic Agent, Negatively Regulates Glial Cell Derived Neurodegeneration of Prefrontal Cortex, hippocampus and Working Memory Impairment. *J. Neuroimmunology* 313, 161–175. doi:10.1016/j.jneuroim.2017.11.003

de Alba, E. (2019). Structure, Interactions and Self-Assembly of ASC-dependent Inflammasomes. *Arch. Biochem. Biophys.* 670, 15–31. doi:10.1016/j.abb.2019.05.023

Di, A., Xiong, S., Ye, Z., Malireddi, R. K. S., Kometani, S., Zhong, M., et al. (2018). The TWIK2 Potassium Efflux Channel in Macrophages Mediates NLRP3 Inflammasome-Induced Inflammation. *Immunity* 49 (1), 56–65. doi:10.1016/j.immuni.2018.04.032

Diao, Y. (2021). Clematichinenoside AR Alleviates Foam Cell Formation and the Inflammatory Response in Ox-LDL-Induced RAW264.7 Cells by Activating Autophagy. *Inflammation* 44 (2), 758–768. doi:10.1007/s10753-020-01375-x

Díaz, P., Sandoval-Bórquez, A., Bravo-Sagua, R., Quest, A. F. G., and Lavandero, S. (2021). Perspectives on Organelle Interaction, Protein Dysregulation, and Cancer Disease. *Front. Cel Dev. Biol.* 9, 613336. doi:10.3389/fcell.2021.613336

Dolasia, K., Bisht, M. K., Pradhan, G., Udgata, A., and Mukhopadhyay, S. (2018). TLRs/NLRs: Shaping the Landscape of Host Immunity. *Int. Rev. Immunol.* 37 (1), 3–19. doi:10.1080/08830185.2017.1397656

Duewell, P., Kono, H., Rayner, K. J., Sirois, C. M., Vladimer, G., Bauernfeind, F. G., et al. (2010). NLRP3 Inflammasomes Are Required for Atherogenesis and Activated by Cholesterol Crystals. *Nature* 464 (7293), 1357–1361. doi:10.1038/nature08938

Feldmeyer, L., Keller, M., Niklaus, G., Hohl, D., Werner, S., and Beer, H.-D. (2007). The Inflammasome Mediates UVB-Induced Activation and Secretion of Interleukin-1β by Keratinocytes. *Curr. Biol.* 17 (13), 1140–1145. doi:10.1016/j.cub.2007.05.074

Fusco, R., Siracusa, R., Genovese, T., Cuzzocrea, S., and Di Paola, R. (2020). Focus on the Role of NLRP3 Inflammasome in Diseases. *Ijms* 21 (12), 4223. doi:10.3390/ijms21124223

Gomez, D., Baylis, R. A., Durgin, B. G., Newman, A. A. C., Alencar, G. F., Mahan, S., et al. (2018). Interleukin-1β Has Atheroprotective Effects in Advanced Atherosclerotic Lesions of Mice. *Nat. Med.* 24 (9), 1418–1429. doi:10.1038/s41591-018-0124-5

Gong, T., Yang, Y., Jin, T., Jiang, W., and Zhou, R. (2018a). Orchestration of NLRP3 Inflammasome Activation by Ion Fluxes. *Trends Immunol.* 39 (5), 393–406. doi:10.1016/j.it.2018.01.009

Gong, Z., Zhao, S., Zhou, J., Yan, J., Wang, L., Du, X., et al. (2018b). Curcumin Alleviates DSS-Induced Colitis via Inhibiting NLRP3 Inflammsome Activation and IL-1β Production. *Mol. Immunol.* 104, 11–19. doi:10.1016/j.molimm.2018.09.004

Grebe, A., Hoss, F., and Latz, E. (2018). NLRP3 Inflammasome and the IL-1 Pathway in Atherosclerosis. *Circ. Res.* 122 (12), 1722–1740. doi:10.1161/CIRCRESAHA.118.311362

Gritsenko, A., Yu, S., Martin-Sanchez, F., Diaz-Del-Olmo, I., Nichols, E.-M., Davis, D. M., et al. (2020). Priming Is Dispensable for NLRP3 Inflammasome Activation in Human Monocytes *In Vitro*. *Front. Immunol.* 11, 565924. doi:10.3389/fimmu.2020.565924

Guo, W., Sun, Y., Liu, W., Wu, X., Guo, L., Cai, P., et al. (2014). Small Molecule-Driven Mitophagy-Mediated NLRP3 Inflammasome Inhibition Is Responsible for the Prevention of Colitis-Associated Cancer. *Autophagy* 10 (6), 972–985. doi:10.4161/auto.28374

Gurung, P., Lukens, J. R., and Kanneganti, T.-D. (2015). Mitochondria: Diversity in the Regulation of the NLRP3 Inflammasome. *Trends Mol. Med.* 21 (3), 193–201. doi:10.1016/j.molmed.2014.11.008

Han, C. Y., Rho, H. S., Kim, A., Kim, T. H., Jang, K., Jun, D. W., et al. (2018). FXR Inhibits Endoplasmic Reticulum Stress-Induced NLRP3 Inflammasome in Hepatocytes and Ameliorates Liver Injury. *Cel Rep.* 24 (11), 2985–2999. doi:10.1016/j.celrep.2018.07.068

Hang, L., Peng, Y., Xiang, R., Li, X., and Li, Z. (2020). Ox-LDL Causes Endothelial Cell Injury through ASK1/NLRP3-Mediated Inflammasome Activation via Endoplasmic Reticulum Stress. *Ddt* 14, 731–744. doi:10.2147/DDDT.S231916

Hara, H., Tsuchiya, K., Kawamura, I., Fang, R., Hernandez-Cuellar, E., Shen, Y., et al. (2013). Phosphorylation of the Adaptor ASC Acts as a Molecular Switch that Controls the Formation of Speck-like Aggregates and Inflammasome Activity. *Nat. Immunol.* 14 (12), 1247–1255. doi:10.1038/ni.2749

He, X., Fan, X., Bai, B., Lu, N., Zhang, S., and Zhang, L. (2021). Pyroptosis Is a Critical Immune-Inflammatory Response Involved in Atherosclerosis. *Pharmacol. Res.* 165, 105447. doi:10.1016/j.phrs.2021.105447

He, Y., Zeng, M. Y., Yang, D., Motro, B., and Núñez, G. (2016). NEK7 Is an Essential Mediator of NLRP3 Activation Downstream of Potassium Efflux. *Nature* 530 (7590), 354–357. doi:10.1038/nature16959

Helli, B., Gerami, H., Kavianpour, M., Heybar, H., Hosseini, S. K., and Haghighian, H. K. (2021). Curcumin Nanomicelle Improves Lipid Profile, Stress Oxidative Factors and Inflammatory Markers in Patients Undergoing Coronary Elective Angioplasty; A Randomized Clinical Trial. *Emiddt* 21, 2090–2098. doi:10.2174/1871530321666210104145231

Hendrikx, T., Jeurissen, M. L. J., van Gorp, P. J., Gijbels, M. J., Walenbergh, S. M. A., Houben, T., et al. (2015). Bone Marrow-specific Caspase-1/11 Deficiency Inhibits

Atherosclerosis Development inLdlr−/−mice. *FEBS J.* 282 (12), 2327–2338. doi:10.1111/febs.13279

Hoseini, Z., Sepahvand, F., Rashidi, B., Sahebkar, A., Masoudifar, A., and Mirzaei, H. (2018). NLRP3 Inflammasome: Its Regulation and Involvement in Atherosclerosis. *J. Cel Physiol* 233 (3), 2116–2132. doi:10.1002/jcp.25930

Islam, M. T., Bardaweel, S. K., Mubarak, M. S., Koch, W., Gaweł-Beben, K., Antosiewicz, B., et al. (2020). Immunomodulatory Effects of Diterpenes and Their Derivatives through NLRP3 Inflammasome Pathway: A Review. *Front. Immunol.* 11, 572136. doi:10.3389/fimmu.2020.572136

Jannuzzi, G. P., de Almeida, J. R. F., Paulo, L. N. M., de Almeida, S. R., and Ferreira, K. S. (2020). Intracellular PRRs Activation in Targeting the Immune Response against Fungal Infections. *Front. Cel. Infect. Microbiol.* 10, 591970. doi:10.3389/fcimb.2020.591970

Jiang, C., Jiang, L., Li, Q., Liu, X., Zhang, T., Dong, L., et al. (2018). Acrolein Induces NLRP3 Inflammasome-Mediated Pyroptosis and Suppresses Migration via ROS-dependent Autophagy in Vascular Endothelial Cells. *Toxicology* 410, 26–40. doi:10.1016/j.tox.2018.09.002

Jo, E.-K., Kim, J. K., Shin, D.-M., and Sasakawa, C. (2016). Molecular Mechanisms Regulating NLRP3 Inflammasome Activation. *Cell Mol Immunol* 13 (2), 148–159. doi:10.1038/cmi.2015.95

Katsnelson, M. A., Rucker, L. G., Russo, H. M., and Dubyak, G. R. (2015). K+ Efflux Agonists Induce NLRP3 Inflammasome Activation Independently of Ca2+ Signaling. *J.I.* 194 (8), 3937–3952. doi:10.4049/jimmunol.1402658

Kelley, N., Jeltema, D., Duan, Y., and He, Y. (2019). The NLRP3 Inflammasome: An Overview of Mechanisms of Activation and Regulation. *Ijms* 20 (13), 3328. doi:10.3390/ijms20133328

Khwaja, B., Thankam, F. G., and Agrawal, D. K. (2021). Mitochondrial DAMPs and Altered Mitochondrial Dynamics in OxLDL burden in Atherosclerosis. *Mol. Cel Biochem* 476 (4), 1915–1928. doi:10.1007/s11010-021-04061-0

Kong, F., Ye, B., Cao, J., Cai, X., Lin, L., Huang, S., et al. (2016a). Curcumin Represses NLRP3 Inflammasome Activation via TLR4/MyD88/NF-Kb and P2X7R Signaling in PMA-Induced Macrophages. *Front. Pharmacol.* 7, 369. doi:10.3389/fphar.2016.00369

Kong, F., Ye, B., Lin, L., Cai, X., Huang, W., and Huang, Z. (2016b). Atorvastatin Suppresses NLRP3 Inflammasome Activation via TLR4/MyD88/NF-Kb Signaling in PMA-Stimulated THP-1 Monocytes. *Biomed. Pharmacother.* 82, 167–172. doi:10.1016/j.biopha.2016.04.043

Kotla, S., Singh, N. K., and Rao, G. N. (2017). ROS via BTK-P300-STAT1-Ppary Signaling Activation Mediates Cholesterol Crystals-Induced CD36 Expression and Foam Cell Formation. *Redox Biol.* 11, 350–364. doi:10.1016/j.redox.2016.12.005

Kumar, G., Singh, D., Tali, J. A., Dheer, D., and Shankar, R. (2020). Andrographolide: Chemical Modification and its Effect on Biological Activities. *Bioorg. Chem.* 95, 103511. doi:10.1016/j.bioorg.2019.103511

Lebeaupin, C., Proics, E., de Bieville, C. H. D., Rousseau, D., Bonnafous, S., Patouraux, S., et al. (2015). ER Stress Induces NLRP3 Inflammasome Activation and Hepatocyte Death. *Cell Death Dis* 6, e1879. doi:10.1038/cddis.2015.248

Lee, G.-S., Subramanian, N., Kim, A. I., Aksentijevich, I., Goldbach-Mansky, R., Sacks, D. B., et al. (2012a). The Calcium-Sensing Receptor Regulates the NLRP3 Inflammasome through Ca2+ and cAMP. *Nature* 492 (7427), 123–127. doi:10.1038/nature11588

Lee, H. M., Yuk, J. M., Kim, K. H., Jang, J., Kang, G., Park, J. B., et al. (2012b). Mycobacterium Abscessus Activates the NLRP3 Inflammasome via Dectin-1-Syk and p62/SQSTM1. *Immunol. Cel Biol* 90 (6), 601–610. doi:10.1038/icb.2011.72

Leng, W., Ouyang, X., Lei, X., Wu, M., Chen, L., Wu, Q., et al. (2016). The SGLT-2 Inhibitor Dapagliflozin Has a Therapeutic Effect on Atherosclerosis in Diabetic ApoE−/−Mice. *Mediators Inflamm.* 2016, 1–13. doi:10.1155/2016/6305735

Lerner, A. G., Upton, J.-P., Praveen, P. V. K., Ghosh, R., Nakagawa, Y., Igbaria, A., et al. (2012). IRE1α Induces Thioredoxin-Interacting Protein to Activate the NLRP3 Inflammasome and Promote Programmed Cell Death under Irremediable ER Stress. *Cel Metab.* 16 (2), 250–264. doi:10.1016/j.cmet.2012.07.007

Li, D., Yang, S., Xing, Y., Pan, L., Zhao, R., Zhao, Y., et al. (2021). Novel Insights and Current Evidence for Mechanisms of Atherosclerosis: Mitochondrial Dynamics as a Potential Therapeutic Target. *Front. Cel Dev. Biol.* 9, 673839. doi:10.3389/fcell.2021.673839

Li, L., Zhang, X., Pi, C., Yang, H., Zheng, X., Zhao, L., et al. (2020). Review of Curcumin Physicochemical Targeting Delivery System. *Ijn* Vol. 15, 9799–9821. doi:10.2147/IJN.S276201

Li, R., Lu, K., Wang, Y., Chen, M., Zhang, F., Shen, H., et al. (2017). Triptolide Attenuates Pressure Overload-Induced Myocardial Remodeling in Mice via the Inhibition of NLRP3 Inflammasome Expression. *Biochem. Biophysical Res. Commun.* 485 (1), 69–75. doi:10.1016/j.bbrc.2017.02.021

Lian, D., Lai, J., Wu, Y., Wang, L., Chen, Y., Zhang, Y., et al. (2018). Cathepsin B-Mediated NLRP3 Inflammasome Formation and Activation in Angiotensin II -Induced Hypertensive Mice: Role of Macrophage Digestion Dysfunction. *Cell Physiol Biochem* 50 (4), 1585–1600. doi:10.1159/000494656

Liaqat, A., Asad, M., Shoukat, F., and Khan, A.-U. (2020). A Spotlight on the Underlying Activation Mechanisms of the NLRP3 Inflammasome and its Role in Atherosclerosis: A Review. *Inflammation* 43 (6), 2011–2020. doi:10.1007/s10753-020-01290-1

Lin, H.-C., Chen, Y.-J., Wei, Y.-H., Lin, H.-A., Chen, C.-C., Liu, T.-F., et al. (2021). Lactic Acid Fermentation Is Required for NLRP3 Inflammasome Activation. *Front. Immunol.* 12, 630380. doi:10.3389/fimmu.2021.630380

Lin, H.-C., Lii, C.-K., Chen, H.-C., Lin, A.-H., Yang, Y.-C., and Chen, H.-W. (2018). Andrographolide Inhibits Oxidized LDL-Induced Cholesterol Accumulation and Foam Cell Formation in Macrophages. *Am. J. Chin. Med.* 46 (1), 87–106. doi:10.1142/S0192415X18500052

Liu, D., Wen, Y., Tang, T.-T., Lv, L.-L., Tang, R.-N., Liu, H., et al. (2015). Megalin/Cubulin-Lysosome-mediated Albumin Reabsorption Is Involved in the Tubular Cell Activation of NLRP3 Inflammasome and Tubulointerstitial Inflammation. *J. Biol. Chem.* 290 (29), 18018–18028. doi:10.1074/jbc.M115.662064

Liu, D., Zeng, X., Li, X., Cui, C., Hou, R., Guo, Z., et al. (2020a). Advances in the Molecular Mechanisms of NLRP3 Inflammasome Activators and Inactivators. *Biochem. Pharmacol.* 175, 113863. doi:10.1016/j.bcp.2020.113863

Liu, D., Zeng, X., Li, X., Mehta, J. L., and Wang, X. (2018a). Role of NLRP3 Inflammasome in the Pathogenesis of Cardiovascular Diseases. *Basic Res. Cardiol.* 113 (1), 5. doi:10.1007/s00395-017-0663-9

Liu, H., Gu, C., Liu, M., Liu, G., and Wang, Y. (2020b). NEK7 Mediated Assembly and Activation of NLRP3 Inflammasome Downstream of Potassium Efflux in Ventilator-Induced Lung Injury. *Biochem. Pharmacol.* 177, 113998. doi:10.1016/j.bcp.2020.113998

Liu, Q., Zhang, D., Hu, D., Zhou, X., and Zhou, Y. (2018b). The Role of Mitochondria in NLRP3 Inflammasome Activation. *Mol. Immunol.* 103, 115–124. doi:10.1016/j.molimm.2018.09.010

Luo, L., and Yang, T. (2016). Triptolide Inhibits the Progression of Atherosclerosis in Apolipoprotein E−/− Mice. *Exp. Ther. Med.* 12 (4), 2307–2313. doi:10.3892/etm.2016.3619

Lv, Z.-H., Phuong, T. A., Jin, S.-J., Li, X.-X., and Xu, M. (2017). Protection by Simvastatin on Hyperglycemia-Induced Endothelial Dysfunction through Inhibiting NLRP3 Inflammasomes. *Oncotarget* 8 (53), 91291–91305. doi:10.18632/oncotarget.20443

Ma, Q., Fan, Q., Han, X., Dong, Z., Xu, J., Bai, J., et al. (2021). Platelet-derived Extracellular Vesicles to Target Plaque Inflammation for Effective Anti-atherosclerotic Therapy. *J. Controlled Release* 329, 445–453. doi:10.1016/j.jconrel.2020.11.064

Ma, S., Chen, J., Feng, J., Zhang, R., Fan, M., Han, D., et al. (2018). Melatonin Ameliorates the Progression of Atherosclerosis via Mitophagy Activation and NLRP3 Inflammasome Inhibition. *Oxidative Med. Cell Longevity* 2018, 1–12. doi:10.1155/2018/9286458

Mao, C., Li, D., Zhou, E., Zhang, J., Wang, C., and Xue, C. (2021). Nicotine Exacerbates Atherosclerosis through a Macrophage-Mediated Endothelial Injury Pathway. *Aging* 13 (5), 7627–7643. doi:10.18632/aging.202660

Momtazi-Borojeni, A. A., Zabihi, N. A., Bagheri, R. K., Majeed, M., Jamialahmadi, T., and Sahebkar, A. (2021). Intravenous Curcumin Mitigates Atherosclerosis Progression in Cholesterol-Fed Rabbits. *Adv. Exp. Med. Biol.* 1308, 45–54. doi:10.1007/978-3-030-64872-5_5

Montarello, N. J., Nguyen, M. T., Wong, D. T. L., Nicholls, S. J., and Psaltis, P. J. (2020). Inflammation in Coronary Atherosclerosis and its Therapeutic Implications. *Cardiovasc. Drugs Ther.* 36, 347–362. doi:10.1007/s10557-020-07106-6

Nasonov, E. L., Popkova, T. V., and Popkova, T. V. (2018). Atherosclerosis: Perspectives of Anti-inflammatory Therapy. *Ther. Arch.* 90 (5), 4–12. doi:10.26442/terarkh20189054-12

Nettersheim, F. S., De Vore, L., and Winkels, H. (2020). Vaccination in Atherosclerosis. *Cells* 9 (12), 2560. doi:10.3390/cells9122560

Neudecker, V., Haneklaus, M., Jensen, O., Khailova, L., Masterson, J. C., Tye, H., et al. (2017). Myeloid-derived miR-223 Regulates Intestinal Inflammation via Repression of the NLRP3 Inflammasome. *J. Exp. Med.* 214 (6), 1737–1752. doi:10.1084/jem.20160462

Orlowski, G. M., Colbert, J. D., Sharma, S., Bogyo, M., Robertson, S. A., and Rock, K. L. (2015). Multiple Cathepsins Promote Pro-IL-1β Synthesis and NLRP3-Mediated IL-1β Activation. *J.I.* 195 (4), 1685–1697. doi:10.4049/jimmunol.1500509

Pahwa, R., and Jialal, I. (2021). "Atherosclerosis," in *StatPearls* (Treasure Island (FL).

Pan, X.-C., Liu, Y., Cen, Y.-Y., Xiong, Y.-L., Li, J.-M., Ding, Y.-Y., et al. (2019). Dual Role of Triptolide in Interrupting the NLRP3 Inflammasome Pathway to Attenuate Cardiac Fibrosis. *Ijms* 20 (2), 360. doi:10.3390/ijms20020360

Paramel Varghese, G., Folkersen, L., Strawbridge, R. J., Halvorsen, B., Yndestad, A., Ranheim, T., et al. (2016). NLRP3 Inflammasome Expression and Activation in Human Atherosclerosis. *Jaha* 5 (5), e003031. doi:10.1161/JAHA.115.003031

Parsamanesh, N., Moossavi, M., Bahrami, A., Fereidouni, M., Barreto, G., and Sahebkar, A. (2019). NLRP3 Inflammasome as a Treatment Target in Atherosclerosis: A Focus on Statin Therapy. *Int. Immunopharmacology* 73, 146–155. doi:10.1016/j.intimp.2019.05.006

Pathak, T., and Trebak, M. (2018). Mitochondrial Ca2+ Signaling. *Pharmacol. Ther.* 192, 112–123. doi:10.1016/j.pharmthera.2018.07.001

Pechanova, O., Dayar, E., and Cebova, M. (2020). Therapeutic Potential of Polyphenols-Loaded Polymeric Nanoparticles in Cardiovascular System. *Molecules* 25 (15), 3322. doi:10.3390/molecules25153322

Pelegrin, P. (2021). P2X7 Receptor and the NLRP3 Inflammasome: Partners in Crime. *Biochem. Pharmacol.* 187, 114385. doi:10.1016/j.bcp.2020.114385

Peng, K., Liu, L., Wei, D., Lv, Y., Wang, G., Xiong, W., et al. (2015). P2X7R Is Involved in the Progression of Atherosclerosis by Promoting NLRP3 Inflammasome Activation. *Int. J. Mol. Med.* 35 (5), 1179–1188. doi:10.3892/ijmm.2015.2129

Peng, S., Xu, L.-W., Che, X.-Y., Xiao, Q.-Q., Pu, J., Shao, Q., et al. (2018). Atorvastatin Inhibits Inflammatory Response, Attenuates Lipid Deposition, and Improves the Stability of Vulnerable Atherosclerotic Plaques by Modulating Autophagy. *Front. Pharmacol.* 9, 438. doi:10.3389/fphar.2018.00438

Qian, K., Zhang, L., and Shi, K. (2019). Triptolide Prevents Osteoarthritis via Inhibiting Hsa-miR-20b. *Inflammopharmacol* 27 (1), 109–119. doi:10.1007/s10787-018-0509-6

Ridker, P. M., MacFadyen, J. G., Thuren, T., Everett, B. M., Libby, P., Glynn, R. J., et al. (2017b). Effect of Interleukin-1β Inhibition with Canakinumab on Incident Lung Cancer in Patients with Atherosclerosis: Exploratory Results from a Randomised, Double-Blind, Placebo-Controlled Trial. *Lancet* 390 (10105), 1833–1842. doi:10.1016/S0140-6736(17)32247-X

Ridker, P. M., Everett, B. M., Thuren, T., MacFadyen, J. G., Chang, W. H., Ballantyne, C., et al. (2017a). Antiinflammatory Therapy with Canakinumab for Atherosclerotic Disease. *N. Engl. J. Med.* 377 (12), 1119–1131. doi:10.1056/NEJMoa1707914

Ridker, P. M., MacFadyen, J. G., Thuren, T., and Libby, P. (2020). Residual Inflammatory Risk Associated with Interleukin-18 and Interleukin-6 after Successful Interleukin-1β Inhibition with Canakinumab: Further Rationale for the Development of Targeted Anti-cytokine Therapies for the Treatment of Atherothrombosis. *Eur. Heart J.* 41 (23), 2153–2163. doi:10.1093/eurheartj/ehz542

Santulli, G., Nakashima, R., Yuan, Q., and Marks, A. R. (2017). Intracellular Calcium Release Channels: an Update. *J. Physiol.* 595 (10), 3041–3051. doi:10.1113/JP272781

Shao, B.-Z., Xu, Z.-Q., Han, B.-Z., Su, D.-F., and Liu, C. (2015). NLRP3 Inflammasome and its Inhibitors: a Review. *Front. Pharmacol.* 6, 262. doi:10.3389/fphar.2015.00262

Sharma, A., Choi, J. S. Y., Stefanovic, N., Al-Sharea, A., Simpson, D. S., Mukhamedova, N., et al. (2021). Specific NLRP3 Inhibition Protects against Diabetes-Associated Atherosclerosis. *Diabetes* 70 (3), 772–787. doi:10.2337/db20-0357

Sharma, M., and de Alba, E. (2021). Structure, Activation and Regulation of NLRP3 and AIM2 Inflammasomes. *Ijms* 22 (2), 872. doi:10.3390/ijms22020872

Shen, L., Yang, Y., Ou, T., Key, C.-C. C., Tong, S. H., Sequeira, R. C., et al. (2017). Dietary PUFAs Attenuate NLRP3 Inflammasome Activation via Enhancing Macrophage Autophagy. *J. Lipid Res.* 58 (9), 1808–1821. doi:10.1194/jlr.M075879

Shi, J., Zhao, Y., Wang, Y., Gao, W., Ding, J., Li, P., et al. (2014). Inflammatory Caspases Are Innate Immune Receptors for Intracellular LPS. *Nature* 514 (7521), 187–192. doi:10.1038/nature13683

Shi, X., Xie, W.-L., Kong, W.-W., Chen, D., and Qu, P. (2015). Expression of the NLRP3 Inflammasome in Carotid Atherosclerosis. *J. Stroke Cerebrovasc. Dis.* 24 (11), 2455–2466. doi:10.1016/j.jstrokecerebrovasdis.2015.03.024

Simard, J.-C., Vallieres, F., de Liz, R., Lavastre, V., and Girard, D. (2015). Silver Nanoparticles Induce Degradation of the Endoplasmic Reticulum Stress Sensor Activating Transcription Factor-6 Leading to Activation of the NLRP-3 Inflammasome. *J. Biol. Chem.* 290 (9), 5926–5939. doi:10.1074/jbc.M114.610899

Singh, L., Sharma, S., Xu, S., Tewari, D., and Fang, J. (2021). Curcumin as a Natural Remedy for Atherosclerosis: A Pharmacological Review. *Molecules* 26 (13), 4036. doi:10.3390/molecules26134036

Stengel, S. T., Fazio, A., Lipinski, S., Jahn, M. T., Aden, K., Ito, G., et al. (2020). Activating Transcription Factor 6 Mediates Inflammatory Signals in Intestinal Epithelial Cells upon Endoplasmic Reticulum Stress. *Gastroenterology* 159 (4), 1357–1374. e1310. doi:10.1053/j.gastro.2020.06.088

Stunnenberg, M., Hamme, J. L., Trimp, M., Gringhuis, S. I., and Geijtenbeek, T. B. H. (2021). Abortive HIV-1 RNA Induces pro-IL-1β Maturation via Protein Kinase PKR and Inflammasome Activation in Humans. *Eur. J. Immunol.* 51, 2464–2477. doi:10.1002/eji.202149275

Sun, X., Jiao, X., Ma, Y., Liu, Y., Zhang, L., He, Y., et al. (2016). Trimethylamine N-Oxide Induces Inflammation and Endothelial Dysfunction in Human Umbilical Vein Endothelial Cells via Activating ROS-TXNIP-NLRP3 Inflammasome. *Biochem. Biophysical Res. Commun.* 481 (1-2), 63–70. doi:10.1016/j.bbrc.2016.11.017

Swanson, K. V., Deng, M., and Ting, J. P.-Y. (2019). The NLRP3 Inflammasome: Molecular Activation and Regulation to Therapeutics. *Nat. Rev. Immunol.* 19 (8), 477–489. doi:10.1038/s41577-019-0165-0

Talty, A., Deegan, S., Ljujic, M., Mnich, K., Naicker, S. D., Quandt, D., et al. (2019). Inhibition of IRE1α RNase Activity Reduces NLRP3 Inflammasome Assembly and Processing of pro-IL1β. *Cel Death Dis* 10 (9), 622. doi:10.1038/s41419-019-1847-z

Tourkochristou, E., Aggeletopoulou, I., Konstantakis, C., and Triantos, C. (2019). Role of NLRP3 Inflammasome in Inflammatory Bowel Diseases. *Wjg* 25 (33), 4796–4804. doi:10.3748/wjg.v25.i33.4796

van der Heijden, T., Kritikou, E., Venema, W., van Duijn, J., van Santbrink, P. J., Slütter, B., et al. (2017). NLRP3 Inflammasome Inhibition by MCC950 Reduces Atherosclerotic Lesion Development in Apolipoprotein E-Deficient Mice-Brief Report. *Atvb* 37 (8), 1457–1461. doi:10.1161/ATVBAHA.117.309575

Wang, K., Yao, Y., Zhu, X., Zhang, K., Zhou, F., and Zhu, L. (2017a). Amyloid β Induces NLRP3 Inflammasome Activation in Retinal Pigment Epithelial Cells via NADPH Oxidase- and Mitochondria-dependent ROS Production. *J. Biochem. Mol. Toxicol.* 31 (6), e21887. doi:10.1002/jbt.21887

Wang, K., Zhu, X., Zhang, K., Yao, Y., Zhuang, M., Tan, C., et al. (2017b). Puerarin Inhibits Amyloid β-induced NLRP3 Inflammasome Activation in Retinal Pigment Epithelial Cells via Suppressing ROS-dependent Oxidative and Endoplasmic Reticulum Stresses. *Exp. Cel Res.* 357 (2), 335–340. doi:10.1016/j.yexcr.2017.05.030

Wang, L., and Hauenstein, A. V. (2020). The NLRP3 Inflammasome: Mechanism of Action, Role in Disease and Therapies. *Mol. Aspects Med.* 76, 100889. doi:10.1016/j.mam.2020.100889

Wang, R., Wang, Y., Mu, N., Lou, X., Li, W., Chen, Y., et al. (2017c). Activation of NLRP3 Inflammasomes Contributes to Hyperhomocysteinemia-Aggravated Inflammation and Atherosclerosis in apoE-Deficient Mice. *Lab. Invest.* 97 (8), 922–934. doi:10.1038/labinvest.2017.30

Wang, S., Xie, X., Lei, T., Zhang, K., Lai, B., Zhang, Z., et al. (2017d). Statins Attenuate Activation of the NLRP3 Inflammasome by Oxidized LDL or TNFα in Vascular Endothelial Cells through a PXR-dependent Mechanism. *Mol. Pharmacol.* 92 (3), 256–264. doi:10.1124/mol.116.108100

Wang, W. W., Han, W. B., Wan, Y. G., Tu, Y., Liu, B. H., Liu, Y. L., et al. (2020a). [Molecular Regulative Mechanisms of NLRP3 Inflammasome Activation in

Diabetic Nephropathy and Interventional Effects of Chinese Herbal Medicine]. *Zhongguo Zhong Yao Za Zhi* 45 (1), 7–13. doi:10.19540/j.cnki.cjcmm.20190618.402

Wang, Y., Liu, X., Shi, H., Yu, Y., Yu, Y., Li, M., et al. (2020b). NLRP3 Inflammasome, an Immune-Inflammatory Target in Pathogenesis and Treatment of Cardiovascular Diseases. *Clin. Translational Med.* 10 (1), 91–106. doi:10.1002/ctm2.13

Wang, Y., Shi, P., Chen, Q., Huang, Z., Zou, D., Zhang, J., et al. (2019). Mitochondrial ROS Promote Macrophage Pyroptosis by Inducing GSDMD Oxidation. *J. Mol. Cel Biol* 11 (12), 1069–1082. doi:10.1093/jmcb/mjz020

Wang, Z., Zhang, S., Xiao, Y., Zhang, W., Wu, S., Qin, T., et al. (2020c). NLRP3 Inflammasome and Inflammatory Diseases. *Oxidative Med. Cell Longevity* 2020, 1–11. doi:10.1155/2020/4063562

Weber, A. N. R., Bittner, Z. A., Shankar, S., Liu, X., Chang, T.-H., Jin, T., et al. (2020). Recent Insights into the Regulatory Networks of NLRP3 Inflammasome Activation. *J. Cel Sci* 133 (23), jcs248344. doi:10.1242/jcs.248344

Wen, J., Chang, Y., Huo, S., Li, W., Huang, H., Gao, Y., et al. (2020). Tanshinone IIA Attenuates Atherosclerosis via Inhibiting NLRP3 Inflammasome Activation. *Aging* 13 (1), 910–932. doi:10.18632/aging.202202

Wen, Y., Liu, Y.-R., Tang, T.-T., Pan, M.-M., Xu, S.-C., Ma, K.-L., et al. (2018). mROS-TXNIP axis Activates NLRP3 Inflammasome to Mediate Renal Injury during Ischemic AKI. *Int. J. Biochem. Cel Biol.* 98, 43–53. doi:10.1016/j.biocel.2018.02.015

Wu, D., Chen, Y., Sun, Y., Gao, Q., Li, H., Yang, Z., et al. (2020a). Target of MCC950 in Inhibition of NLRP3 Inflammasome Activation: a Literature Review. *Inflammation* 43 (1), 17–23. doi:10.1007/s10753-019-01098-8

Wu, H.-Y., Huang, C.-H., Lin, Y.-H., Wang, C.-C., and Jan, T.-R. (2018a). Cannabidiol Induced Apoptosis in Human Monocytes through Mitochondrial Permeability Transition Pore-Mediated ROS Production. *Free Radic. Biol. Med.* 124, 311–318. doi:10.1016/j.freeradbiomed.2018.06.023

Wu, L.-M., Wu, S.-G., Chen, F., Wu, Q., Wu, C.-M., Kang, C.-M., et al. (2020b). Atorvastatin Inhibits Pyroptosis through the lncRNA NEXN-AS1/NEXN Pathway in Human Vascular Endothelial Cells. *Atherosclerosis* 293, 26–34. doi:10.1016/j.atherosclerosis.2019.11.033

Wu, T., Chen, X., Wang, Y., Xiao, H., Peng, Y., Lin, L., et al. (2018b). Aortic Plaque-Targeted Andrographolide Delivery with Oxidation-Sensitive Micelle Effectively Treats Atherosclerosis via Simultaneous ROS Capture and Anti-inflammation. *Nanomedicine: Nanotechnology, Biol. Med.* 14 (7), 2215–2226. doi:10.1016/j.nano.2018.06.010

Wu, T., Peng, Y., Yan, S., Li, N., Chen, Y., and Lan, T. (2018c). Andrographolide Ameliorates Atherosclerosis by Suppressing Pro-inflammation and ROS Generation-Mediated Foam Cell Formation. *Inflammation* 41 (5), 1681–1689. doi:10.1007/s10753-018-0812-9

Wu, W., Liu, B. H., Wan, Y. G., Sun, W., Liu, Y. L., Wang, W. W., et al. (2019). [Triptolide Inhibits NLRP3 Inflammasome Activation and Ameliorates Podocyte Epithelial-Mesenchymal Transition Induced by High Glucose]. *Zhongguo Zhong Yao Za Zhi* 44 (24), 5457–5464. doi:10.19540/j.cnki.cjcmm.20191114.401

Wu, X., Zhang, H., Qi, W., Zhang, Y., Li, J., Li, Z., et al. (2018d). Nicotine Promotes Atherosclerosis via ROS-NLRP3-Mediated Endothelial Cell Pyroptosis. *Cel Death Dis* 9 (2), 171. doi:10.1038/s41419-017-0257-3

Xie, T., Wang, C., Jin, Y., Meng, Q., Liu, Q., Wu, J., et al. (2020). CoenzymeQ10-Induced Activation of AMPK-YAP-OPA1 Pathway Alleviates Atherosclerosis by Improving Mitochondrial Function, Inhibiting Oxidative Stress and Promoting Energy Metabolism. *Front. Pharmacol.* 11, 1034. doi:10.3389/fphar.2020.01034

Xing, S.-S., Yang, J., Li, W.-j., Li, J., Chen, L., Yang, Y.-t., et al. (2020). Salidroside Decreases Atherosclerosis Plaque Formation via Inhibiting Endothelial Cell Pyroptosis. *Inflammation* 43 (2), 433–440. doi:10.1007/s10753-019-01106-x

Xue, X., Deng, Y., Wang, J., Zhou, M., Liao, L., Wang, C., et al. (2021). Hydroxysafflor Yellow A, a Natural Compound from Carthamus tinctorius L with Good Effect of Alleviating Atherosclerosis. *Phytomedicine* 91, 153694. doi:10.1016/j.phymed.2021.153694

Yang, B., Qin, Q., Xu, L., Lv, X., Liu, Z., Song, E., et al. (2020). Polychlorinated Biphenyl Quinone Promotes Atherosclerosis through Lipid Accumulation and Endoplasmic Reticulum Stress via CD36. *Chem. Res. Toxicol.* 33 (6), 1497–1507. doi:10.1021/acs.chemrestox.0c00123

Yaron, J. R., Gangaraju, S., Rao, M. Y., Kong, X., Zhang, L., Su, F., et al. (2015). K+ Regulates Ca2+ to Drive Inflammasome Signaling: Dynamic Visualization of Ion Flux in Live Cells. *Cel Death Dis* 6, e1954. doi:10.1038/cddis.2015.277

Yin, H., Guo, Q., Li, X., Tang, T., Li, C., Wang, H., et al. (2018). Curcumin Suppresses IL-1β Secretion and Prevents Inflammation through Inhibition of the NLRP3 Inflammasome. *J.I.* 200 (8), 2835–2846. doi:10.4049/jimmunol.1701495

Yu, J.-W., and Lee, M.-S. (2016). Mitochondria and the NLRP3 Inflammasome: Physiological and Pathological Relevance. *Arch. Pharm. Res.* 39 (11), 1503–1518. doi:10.1007/s12272-016-0827-4

Yu, W., Li, S., Wu, H., Hu, P., Chen, L., Zeng, C., et al. (2021). Endothelial Nox4 Dysfunction Aggravates Atherosclerosis by Inducing Endoplasmic Reticulum Stress and Soluble Epoxide Hydrolase. *Free Radic. Biol. Med.* 164, 44–57. doi:10.1016/j.freeradbiomed.2020.12.450

Yue, L., Wang, L., Du, Y., Zhang, W., Hamada, K., Matsumoto, Y., et al. (2020). Type 3 Inositol 1,4,5-Trisphosphate Receptor Is a Crucial Regulator of Calcium Dynamics Mediated by Endoplasmic Reticulum in HEK Cells. *Cells* 9 (2), 275. doi:10.3390/cells9020275

Zhang, S., Zou, J., Li, P., Zheng, X., and Feng, D. (2018). Curcumin Protects against Atherosclerosis in Apolipoprotein E-Knockout Mice by Inhibiting Toll-like Receptor 4 Expression. *J. Agric. Food Chem.* 66 (2), 449–456. doi:10.1021/acs.jafc.7b04260

Zhao, C. C., Wu, X. Y., Yi, H., Chen, R., and Fan, G. (2021a). The Therapeutic Effects and Mechanisms of Salidroside on Cardiovascular and Metabolic Diseases: An Updated Review. *Chem. Biodiversity* 18 (7), e2100033. doi:10.1002/cbdv.202100033

Zhao, Z., Wang, X., Zhang, R., Ma, B., Niu, S., Di, X., et al. (2021b). Melatonin Attenuates Smoking-Induced Atherosclerosis by Activating the Nrf2 Pathway via NLRP3 Inflammasomes in Endothelial Cells. *Aging* 13 (8), 11363–11380. doi:10.18632/aging.202829

Zheng, D., Kern, L., and Elinav, E. (2021). The NLRP6 Inflammasome. *Immunology* 162 (3), 281–289. doi:10.1111/imm.13293

Zhong, Z., Liang, S., Sanchez-Lopez, E., He, F., Shalapour, S., Lin, X.-j., et al. (2018). New Mitochondrial DNA Synthesis Enables NLRP3 Inflammasome Activation. *Nature* 560 (7717), 198–203. doi:10.1038/s41586-018-0372-z

Zhou, R., Tardivel, A., Thorens, B., Choi, I., and Tschopp, J. (2010). Thioredoxin-interacting Protein Links Oxidative Stress to Inflammasome Activation. *Nat. Immunol.* 11 (2), 136–140. doi:10.1038/ni.1831

Zhou, Y., Tong, Z., Jiang, S., Zheng, W., Zhao, J., and Zhou, X. (2020). The Roles of Endoplasmic Reticulum in NLRP3 Inflammasome Activation. *Cells* 9 (5), 1219. doi:10.3390/cells9051219

Zhu, X., Zhang, J., Sun, H., Jiang, C., Dong, Y., Shan, Q., et al. (2014). Ubiquitination of Inositol-Requiring Enzyme 1 (IRE1) by the E3 Ligase CHIP Mediates the IRE1/TRAF2/JNK Pathway. *J. Biol. Chem.* 289 (44), 30567–30577. doi:10.1074/jbc.M114.562868

Zhuang, Y., Yasinta, M., Hu, C., Yang, L., Wangi, R., Huang, S., et al. (2015). Mitochondrial Dysfunction Confers Albumin-Induced NLRP3 Inflammasome Activation and Renal Tubular Injury. *Am. J. Physiology-Renal Physiol.* 308 (8), F857–F866. doi:10.1152/ajprenal.00203.2014

Conflict of Interest: The authors declare that the research was conducted in the absence of any commercial or financial relationships that could be construed as a potential conflict of interest.

Publisher's Note: All claims expressed in this article are solely those of the authors and do not necessarily represent those of their affiliated organizations, or those of the publisher, the editors and the reviewers. Any product that may be evaluated in this article, or claim that may be made by its manufacturer, is not guaranteed or endorsed by the publisher.

frontiers | Frontiers in Cell and Developmental Biology

REVIEW
published: 01 June 2022
doi: 10.3389/fcell.2022.853451

Exosomal Composition, Biogenesis and Profiling Using Point-of-Care Diagnostics—Implications for Cardiovascular Disease

Denise Burtenshaw[1†], Brian Regan[2†], Kathryn Owen[3,4], David Collins[2], David McEneaney[3], Ian L. Megson[5], Eileen M. Redmond[6] and Paul Aidan Cahill[1]*

[1]Vascular Biology and Therapeutics, School of Biotechnology, Dublin City University, Dublin, Ireland, [2]School of Biotechnology, Dublin City University, Dublin, Ireland, [3]Southern Health and Social Care Trust, Craigavon Area Hospital, Craigavon, United Kingdom, [4]Nanotechnology and Integrated Bioengineering Centre (NIBEC), Ulster University, Belfast, United Kingdom, [5]Division of Biomedical Sciences, Centre for Health Science, UHI Institute of Health Research and Innovation, Inverness, United Kingdom, [6]Department of Surgery, University of Rochester, Rochester, NY, United States

OPEN ACCESS

Edited by:
Yang Shen,
Sichuan University, China

Reviewed by:
Aleksandra Leszczynska,
University of California, San Diego, United States
Mingyi Wang,
National Institutes of Health (NIH), United States

***Correspondence:**
Paul Aidan Cahill
paul.cahill@dcu.ie

[†]These authors have contributed equally to this work

Specialty section:
This article was submitted to Molecular and Cellular Pathology, a section of the journal Frontiers in Cell and Developmental Biology

Received: 12 January 2022
Accepted: 26 April 2022
Published: 01 June 2022

Citation:
Burtenshaw D, Regan B, Owen K, Collins D, McEneaney D, Megson IL, Redmond EM and Cahill PA (2022) Exosomal Composition, Biogenesis and Profiling Using Point-of-Care Diagnostics—Implications for Cardiovascular Disease. Front. Cell Dev. Biol. 10:853451. doi: 10.3389/fcell.2022.853451

Arteriosclerosis is an important age-dependent disease that encompasses atherosclerosis, in-stent restenosis (ISR), pulmonary hypertension, autologous bypass grafting and transplant arteriosclerosis. Endothelial dysfunction and the proliferation of vascular smooth muscle cell (vSMC)-like cells is a critical event in the pathology of arteriosclerotic disease leading to intimal-medial thickening (IMT), lipid retention and vessel remodelling. An important aspect in guiding clinical decision-making is the detection of biomarkers of subclinical arteriosclerosis and early cardiovascular risk. Crucially, relevant biomarkers need to be good indicators of injury which change in their circulating concentrations or structure, signalling functional disturbances. Extracellular vesicles (EVs) are nanosized membraneous vesicles secreted by cells that contain numerous bioactive molecules and act as a means of intercellular communication between different cell populations to maintain tissue homeostasis, gene regulation in recipient cells and the adaptive response to stress. This review will focus on the emerging field of EV research in cardiovascular disease (CVD) and discuss how key EV signatures in liquid biopsies may act as early pathological indicators of adaptive lesion formation and arteriosclerotic disease progression. EV profiling has the potential to provide important clinical information to complement current cardiovascular diagnostic platforms that indicate or predict myocardial injury. Finally, the development of fitting devices to enable rapid and/or high-throughput exosomal analysis that require adapted processing procedures will be evaluated.

Keywords: exosome (vesicle), atheroscelorsis, stem cell repair mechanisms, endothelial (dys)function, point of care diagnosis

INTRODUCTION

Human arteriosclerotic disease is a complex systemic inflammatory disorder characterized by key interactions between several different biological modifiers. These include various lipids, enzymes, endothelial cells (ECs), vascular smooth muscle cells (vSMCs), cytokines and both circulating and resident vascular stem cells and mononuclear cells (Bennett et al., 2016). Initial endothelial dysfunction leads to intimal medial thickening (IMT) and lipid retention resulting in inflammatory and fibroproliferative responses that culminate in cellular infiltration, deposition of extracellular matrix (ECM), and the formation of atherosclerotic plaques. Consequently, unstable atherosclerotic plaques can lead to MI or ischaemic stroke.

Numerous pathologic observations suggest that early adaptive "transitional" lesions enriched with vSMC-like cells are commonly associated with atherosclerotic-prone regions of arteries. These adaptive lesions have been identified prior to pathologic intimal thickening, lipid accumulation and the presence of a developed plaque (Nakagawa and Nakashima, 2018). Similarly, endothelial dysfunction due to aberrant blood flow is associated with adaptive atheroprone lesion formation (Halcox et al., 2009), while the embryological origin of the arterial SMCs within the vessel wall may dictate lesion localisation and progression (Cheung et al., 2012). The progression of these adaptive lesions is an important therapeutic target and can be modelled *in vivo* using wildtype mice following flow restriction due to carotid artery ligation (Korshunov and Berk, 2003) and can further progress into advanced lesions using *ApoE* gene-deficient mice concurrently fed on a western diet (Nam et al., 2009; Liu et al., 2011).

It is widely recognised that vSMC-like cells are primarily responsible for the majority of neointimal cells in arteriosclerotic lesions following vessel injury in murine models [balloon angioplasty, coronary artery by-pass grafting (CABG), transplant arteriosclerosis, pulmonary hypertension and in-stent restenosis (ISR)] (Bennett et al., 2016). This vascular fibrosis and IMT is characterized by a reduced lumen diameter due to excessive deposition of ECM, inhibition of matrix degradation and the accumulation of neointimal cells (mostly vSMC-like cells and macrophages) (Lan et al., 2013).

Sonographic measurement of carotid intima-media thickness (cIMT) is widely used as an indicator of not only local, but generalised atherosclerosis, even in asymptomatic individuals (Touboul et al., 2005). Indeed, cIMT is not only an important surrogate marker for disease synonymous with subclinical atherosclerosis, but can also result from non-atherosclerotic processes such as vascular ageing (Qu and Qu, 2015), whereby an increase in IMT is observed even in populations with a low incidence of lipid driven atherosclerosis (Al Rifai et al., 2018). IMT increases threefold between ages 20–90 years and may at a given age predict future outcomes that can be accelerated in the presence of known CVD risk factors such as Low density lipoprotein (LDL). Hence, IMT typical of adaptive lesions in early subclinical atherosclerosis provides an important substrate for lipoprotein retention leading to accelerated atherosclerotic plaque formation and acute coronary syndrome (ACS) (Nakashima et al., 2008). When combined with elevated fasting remnant cholesterol levels, cIMT has also recently been successfully deployed in stratifying patients with ischemic stroke and optimal LDL cholesterol levels (Qian et al., 2021). Thus, sonographic detection and evaluation of atherosclerosis through cIMT and more recently, femoral plaque assessment, is fast-becoming critical to clinical decision-making in diagnostic evaluation of at-risk and symptomatic atherosclerotic patients.

Pre 2015 studies reveal little standardisation relating to the methods used for cIMT measurement, which gave rise to a disparity in the ability of cIMT to predict risk classification (van den Oord et al., 2013). From 2015 onwards, an industry-standard method was commonly adopted, with the measurement acquired at a plaque-free site >0.5 mm at the distal end near the carotid bifurcation (Ûygarden, 2017). Since this methodology became established results, have consistently found cIMT to be a reliable biomarker for CAD. More recently, several extensive studies have considered the inclusion of plaque measurements, which proved to be a helpful addition to traditional risk factors, giving the ability to predominantly reclassify the intermediate-risk patient group (Amato et al., 2017). However, as with the early cIMT studies, a defined methodology needs to be established, as plaque measurement techniques have been inconsistent.

Chronic coronary artery disease typical of AMI is usually associated with a rupture of atherosclerotic plaque, thrombus formation and obstruction of blood flow leading to necrosis of myocardium. However, in some patients with AMI, there are no significant lesions present in coronary arteries interrogated by angiography, thus confounding early identification of atherosclerosis. ST-segment elevation myocardial infarction (STEMI), non-ST-segment elevation myocardial infarction (NSTEMI), unstable angina and stable coronary artery disease (CAD) all carry significant morbidity and mortality (Dong et al., 2015). As a result, prompt diagnosis and appropriate treatment is essential in preventing adverse outcomes. Electrocardiogram (ECG) analysis and morphological features suggest STEMI have smaller lumen areas, greater plaque burden, and are more prone to plaque rupture compared with lesions causing NSTEMI/unstable angina or stable CAD (Dong et al., 2015).

The origin of the neointimal cells that cause IMT has attracted much debate and controversy with numerous animal studies raising two major possibilities for their proliferation: *1*) partial somatic cell reprogramming following de-differentiation (and in some cases within calcified lesions, trans-differentiation) of mature differentiated vSMCs or endothelial-mesenchymal transition (EndoMT) of ECs to vSMC-like cells (Nemenoff et al., 2011; Chappell et al., 2016; Cooley et al., 2014; Evrard et al., 2017), *2*) partial differentiation of immature multipotent "mesenchymal-like" vascular stem cells (MVSCs) that reside within the vessel wall or migrate from the circulation (Tang et al., 2012; Tang et al., 2020; Kramann et al., 2016; Wan et al., 2012). Several initial studies have provided important evidence for the involvement of a discrete subpopulation of differentiated medial SMCs in progressing IMT (Chappell et al., 2016; Dobnikar et al., 2018). However, lineage tracing analysis studies have also implicated glioma-associated oncogene-1 (Gli1) adventitial

progenitors (Baker and Péault, 2016) SRY-related HMG-box 10 (Sox10) and S100β adventitial and medial vascular stem cells (Yuan et al., 2017; Di Luca et al., 2021; Molony et al., 2021), in addition to Nestin MSC-like cells (Wan et al., 2012), in contributing to vascular fibrosis and the generation of intimal lesions following injury. Importantly, recent studies also suggest that some of these adventitial progenitors may be derived from a parent Myh11 SMC population (Majesky et al., 2017).

Myocardial infarction with non-obstructive coronary arteries (MINOCA) also involves a heterogenous group of atherosclerotic and non-atherosclerotic patients resulting in myocardial damage that is not due to obstructive coronary artery disease (Singh et al., 2021). While there are many sources of neointimal vSMC-like cells, in order to truly elaborate on the pathological events that occur during the onset of SMC de-differentiation, phenotypic modulation and/or stem cell differentiation, an understanding of the pivotal role of the vascular endothelium as the primary responder to injury in dictating disease progression is essential. Composed of a single layer of cells, the endothelium acts as the front line of defence by maintaining homeostasis and the release of anti-atherogenic protective molecules in addition to protecting the internal layers of the artery from circulating atherogenic molecules in the bloodstream. It is widely accepted that the endothelium is the primary responder to known risk factors associated with CVD, including diabetes, high-fat diets, physical inactivity along with several other metabolic disorders. Endothelial dysfunction (ED) marks the initiation of a cascade of events of primary importance to the pathogenesis of vascular disease (Cahill and Redmond, 2016).

EXTRACELLULAR VESICLES, THE CELLULAR POSTMEN!

Initially thought to be merely a disposal mechanism for cellular waste, extracellular vesicles (EVs) have recently become a focal point of research due to their multifunctional role in many biological processes, including cell-cell communication (Bang and Thum, 2012), protein clearance (Johnstone et al., 1987), regulation of immune response (Bobrie et al., 2011), cancer (Muralidharan-Chari et al., 2010) and development of many vascular disease (Jansen et al., 2017). Various biological mechanisms constitutively release these heterogeneous population of phospholipid bilayer-enclosed EVs from discrete cell types including, immune cells, tumour cells, neurons, and ECs. The molecular constituents found within circulating EVs include a variety of proteins, DNA and microRNAs (miRNAs). These are released into the extracellular environment where they are captured and internalised by neighbouring cells. Alternatively, they can potentially travel through the systemic circulation to access neighbouring tissues. This unique mode of intercellular communication between cells and tissues within the body facilitated by EVs constitutes their potential use as novel pathological circulating biomarkers in the discovery of and development of clinical diagnostic tools.

Characterisation of Extracellular Vesicles

Apoptotic Bodies

EVs are released in various shapes and forms by mammalian and non-mammalian cells. Due to their small size, differentiation between EVs of different origin proves challenging; however, they can be characterised to some extent by their size, content, and sub-cellular origin (Colombo et al., 2014). There are three main mechanisms by which extracellular vesicles may arise, resulting in three distinct subpopulations of vesicles (van der Pol et al., 2012). The first and most widely studied involves cell fragmentation during a programmed cell death process known as apoptosis. During this process, the cell undergoes several morphological changes resulting in membrane blebbing, membrane protrusion and subsequent release of apoptotic bodies. Apoptotic bodies are the largest sub-population of EVs and range between 1 and 5 μm in diameter (Kerr et al., 1972). Additionally, they consist of membrane-bound cytoplasm with tightly packed organelle and nuclear debris from the host cell. Once secreted into the extracellular space, these vesicles undergo phagocytosis by neighbouring immune cells (Arandjelovic and Ravichandran, 2015).

Microvesicles

The second method of EV generation involves the shedding of membrane-bound sacs, known as microvesicles, from various cell types. During this process, small cytoplasmic vesicles protrude from the host cell membrane, which then detaches through a blebbing process. The mechanism that drives this process is not fully understood; however, the rate of the shedding process is known to be dramatically increased by a rise in cytosolic concentrations of calcium ions. The increase of calcium ions activates scramblase and calpain, resulting in a loss of membrane phospholipid symmetry and degradation of various proteins, thus facilitating outward budding of microvesicles from the cellular membrane (Yuana et al., 2013). These EVs can vary widely in size, but generally fall between 100 nm and 1 μm in diameter. The cargo packaged within these cells includes proteins, DNA, and microRNA's (miR's); however, not all microvesicles will carry the same messages. The proteins carried within are indicative of the host cell from which they have departed (Del Conde et al., 2005).

Exosomes

As the smallest subset of EVs, exosomes range between 30 and 100 nm in size. These endosomal derived microvesicles first came to light in the 1980s when researchers Pan, Stahl, and Johnstone reported their existence in the extracellular space while studying the maturation of reticulocytes to erythrocytes *via* exosomal secretion of transferrin receptors in the bloodstream (Harding and Stahl, 1983). These vesicles are double-layered, with the lipid bilayer corresponding to that of the cells from which they are released. The release of exosomes from cells was initially considered to cellular waste secreted as a function of cellular homeostasis and bearing no significant impact on neighbouring cells and tissues.

Interestingly, however, in the past decade, it has been widely accepted that these vesicles are functional vehicles carrying a variety of membrane-bound complex cargo of lipids (Vidal et al.,

1989), proteins (Simpson et al., 2009), DNA, mRNA and miR's (Valadi et al., 2007). This unique process enables the delivery of these cargos to proximal and distal cells and tissues initiating a response, thus representing a mode of intercellular communication. Although initial discoveries indicated the release of exosomes from blood cells, the process has since been recognised to be a feature of almost all eukaryotic cells within the body including, but not limited to, various immune cells (dendritic cells, T-cells, B-cells, astrocytes) (Peters et al., 1989; Zitvogel et al., 1998) tumour cells (Verma et al., 2015), epithelial and resident vascular cells (cardiomyocytes, vSMCs, vascular progenitor cells, ECs) (Hergenreider et al., 2012; Zhao et al., 2017). Moreover, it is well established that their cargo may differ significantly and be dependent on the cell source. With this in mind, exosomes and their cargo may offer a potential insight into cell-cell communication as well as a prognostic information in various diseases such as cancers [94], neurodegenerative diseases [95], chronic inflammation [96], renal and CVD [97, 98].

Exosome Biogenesis

Upon their discovery in the 1980s, the production of exosomes was reported to be *via* an intracellular process in the endosomal compartment of the cell. This process is initiated by an inward membrane budding of an early endosome into the luminal compartment, leading to the formation of multivesicular bodies (MVBs). Following this, invagination of late endosomal membranes results in the formation of intraluminal vesicles (ILVs) within large MVB's (Pan et al., 1985; Johnstone et al., 1987).

It is at this stage that various proteins along with cytosolic compounds from the host cell are incorporated into the invaginating membrane-bound ILVs. There are two distinct pathways in which MVBs are generated—*1*) fusion to the plasma membrane and *2*) fusion with lysosomes and the degradation and recycling of their content (Babst, 2011).

The Endosomal Sorting Complex Required for Transport-Dependent Pathway

There are currently several proposed models associated with the mechanism by which exosomes are formed in MVBs (Fabrikant et al., 2009; Falguières et al., 2009; Hurley and Hanson, 2010). However, the most robust system for eukaryotic cells is the utilization of the established endosomal sorting complex required for transport (ESCRT) system and possibly additional ESCRT-independent pathways (Colombo et al., 2013) (**Figure 1**). ILV formation requires integration of two distinct pathways. The first involves endosomal enrichment for tetraspanins CD9 and CD63, along with membrane reorganization (Pols and Klumperman, 2009), while the second involves recruitment of the ESCRT complex to the site of ILV formation. The ESCRT pathway consists of approximately 20 proteins sorted into four soluble multi-protein complexes (ESCRTs 0, I, II, and III) that work together to facilitate MVB formation, vesicle budding, and protein cargo sorting (Christ et al., 2017) through ubiquitin-binding subunits. Initiation of the pathway begins with recognition and sequential binding of ESCRT-0 to ubiquitylated proteins in the endosomal membrane (Meister et al., 2017). ESCRT-I complex is then recruited to the cytosolic side of the early endosomes by way of various stimuli, including tsg101, phosphatidylinositol 3-phosphate (PIP3) and hepatocyte growth factor-regulated tyrosine kinase substrate (HRS), which then activates the ESCRT-II (Fernandez-Borja et al., 1999; Bache et al., 2003; Tamai et al., 2010) and initiates the oligomerization and formation of the ESCRT-III complex to promote the budding processes before budding formation and cleavage. The ESCRT-111 complex then separates from the MVB membrane *via* the sorting protein Vps4 and is disassembled by AAA-ATPase suppressor-of-potassium-transport-growth-defect-1 protein (SKD1) (Liégeois et al., 2006). In summary, following endosomal membrane reorganization, ESCRT-I and -II initiate and drive intraluminal budding of the MVB, while ESCRT-III completes the budding and cleavage process resulting in the formation of ILVs ready for secretion.

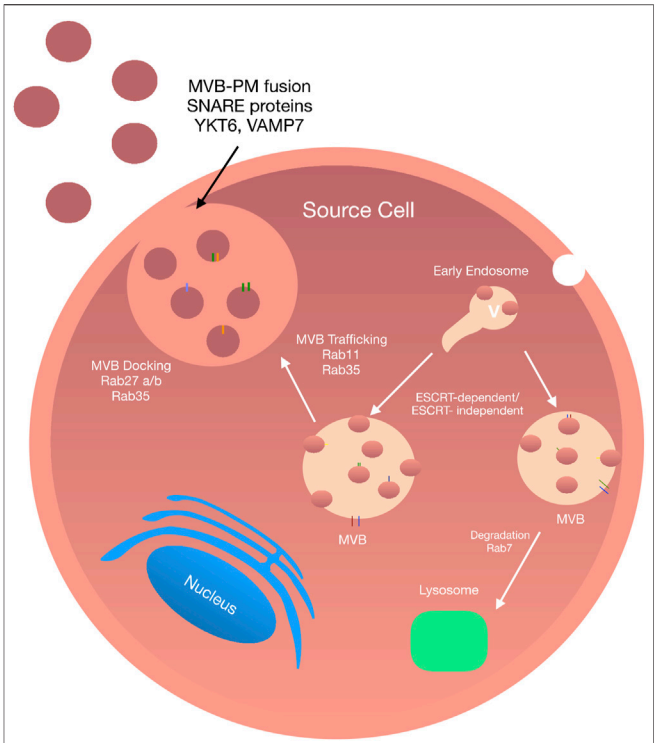

FIGURE 1 | Exosome Biogenesis: Exosomes biogenesis is a complex process and can be conducted in an ESCRT-dependent and -independent manner. The internalisation of the plasma membrane initiates the formation of exosomes by endocytosis. The fusion of early endosomes results in the production of multivesicular bodies. Upon maturation, MVBs are directed to the plasma membrane *via* a tightly Rab GTPase dependent multistep process where they undergo a SNARE-mediated plasma membrane fusion event followed by secretion into the extracellular space.

Endosomal Sorting Complex Required for Transport-Independent Pathway

Exosomes can also be formed in an ESCRT-independent manner. There are several ESCRT-independent mechanisms which

demonstrate the successful generation of ILVs in MVBs following complete disruption of ESCRT function (Stuffers et al., 2009). Although ESCRT-independent biogenesis of exosomes does not disrupt the general formation of ILVs, the formation of specific ILV populations may be hindered (Edgar et al., 2014). The discovery of a ceramide-based mechanism of ILV biogenesis initiated the hypothesis that exosome formation was not ESCRT dependent. Trajkovic et al. (2008) have shown that exosome biogenesis requires the generation of ceramide, a cone-shaped lipid produced during the hydrolysis of sphingomyelin by the enzyme sphingomyelinase. Production of ceramide may then facilitate the generation of membrane domains by membrane invagination due to its cone-like structure and further induce ILV curvature. Further studies have shown that MVBs loaded with CD63-positive ILVs were formed following depletion of components essential for ESCRT complexes. In addition to this, several other ESCRT-independent generation of ILVs have been reported that involve tetraspanin-mediated organization of cellular proteins for endosomal sorting and release (Escola et al., 1998). Interestingly, it is possible that different pathways may act together, or even in parallel to promote ILV formation and release. This hypothesis was proposed by Baietti et al. (2012) during the discovery of an alternative ESCRT pathway involving the syndecan syntenin-ALIX.

The leading players facilitating vesicle formation, loading of proteins and exosome biogenesis include heparinase, syndecan heparan sulfate proteoglycans, phospholipase D_2, ADP ribosylation factor 6, and syntenin. The formation of ILVs is dictated by the association of syntenin with ALIX and relies on the bioavailability of heparan sulfate, syndecans, ALIX, and ESCRTs (Baietti et al., 2012). A further study carried out by Hoshiono et al. (2013) investigating the growth of cancer cells, reported that ESCRTs and function in unisonwith ceramide to facilitate the formation of ILVs. To date, proteomic analysis of EVs suggests that a cell type can release mixed vesicles populations at any given time (Kowal et al., 2016). Therefore, it is not surprising that exosomal biogenesis may involve both ESCRT-dependent and independent pathways. However, despite the predominance of the ESCRT pathway as a primary driver of exosome biogenesis, a major challenge for the future is to gain a further understanding into how different regulators of exosome biogenesis interact with one another and the effect of each mediator on the production of diverse ILV populations.

Exosome Structure and the Cargo Within

Since their discovery in the 1980s, exosomes have been regarded to be a miniature version of the host cell in which they originate. This concept predominantly originated from the complex nature of exosomes in terms of structure and content which is highly dependent on that of the parent cell. In general, exosomes are heavily loaded with a diverse range of bioactive materials such as proteins, lipids, and nucleic acids. In recent years extensive research has been carried out in a bid to identify and characterise exosomal content. This has led to the establishment of three main publicly accessible databases: EVpedia, Vesiclepedia, and Exocarta which include useful information such as protein, lipid and nucleic acid content, as well as isolation and purification procedures (Mathivanan and Simpson, 2009; Kalra et al., 2012; Kim et al., 2013).

Although exosomes contain a comprehensive and heterozygous range of molecules, there are some aspects of exosome structure that are generally conserved across many populations. Scattered amongst their lipid bilayer is a cohort of proteins with various functions. Amongst these proteins are the tetraspanin family, typically CD9, CD37, CD63, CD81 and CD82 that are involved in multiple functions such as cell penetration, invasion, and fusion (Escola et al., 1998) (**Figure 2**).

Although CD9 was the first of the family of tetraspanins discovered in dendritic cells, several studies have reported an abundance of CD63 and CD81 expressed across a broad range of exosomes; these proteins are therefore considered to be robust markers for exosome detection. Also present within exosomes are small heat shock proteins (HSP27, HSP60, HSP70 and HSP90) that control the cellular response and antigen presentation during cellular stress, in addition to assisting protein folding and trafficking (Srivastava, 2002). Multivesicular body formation proteins involved in exosomes formation and release, Alix, TSG101, Rab GTPases such as RAB11B, RAB27A and ARF6, are also abundant within exosomes. Interestingly, endoplasmic reticulum, Golgi apparatus and nuclear proteins have not been detected in exosomal fractions; however, numerous studies have shown the presence of key transcription factors involved in Notch, Wnt and Hedgehog signalling in exosomes (Kalra et al., 2012; McGough and Vincent, 2016). While these proteins are commonly encapsulated in exosomes, it has been suggested that they are not uniformly distributed in all subpopulations, therefore highlighting that even the same cell can release structurally homogeneous vesicles containing heterogeneous contents.

Exosome Secretion and Release

Exosomes are released during physiological and pathological conditions by many cell types. There are two main pathways by which exosomes are released and secreted from their host MVB: the constitutive release pathway, associated with general physiological secretion of exosomes (Kalluri and LeBleu, 2020); and/or the inducible release pathway, initiated by stimuli such as heat shock, hypoxia, DNA damage, increased intracellular calcium release and lipopolysaccharide. The initiation of exosome release begins with the transport of MVBs to the plasma membrane, with this process depending on their interaction with actin and the microtubule cytoskeleton (Sinha et al., 2016).

There are many mediators involved during membrane trafficking of ILVs (including vesicle budding, membrane fusion, and transport along actin and tubulin) (Giannitsis et al., 2019). The most important of which are Rab guanosine triphosphatases (Rab GTPase), the largest family of small GTPases composed of approximately 70 distinct proteins (Stenmark, 2009). Among these are Rab11 and Rab35, that control trafficking membrane cargo to and from recycling endosomes on the way to the plasma membrane. Rab27A, promotes docking of MVBs and fusion to the plasma

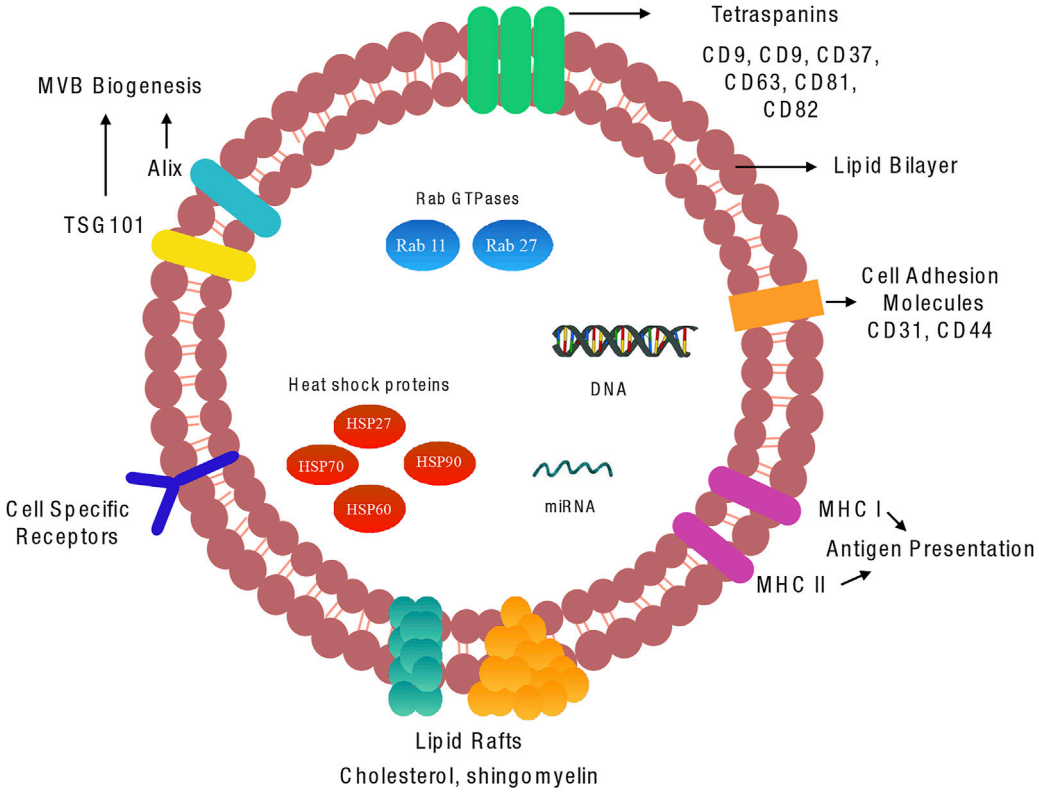

FIGURE 2 | Molecular components of vascular exosome: Exosomes are composed of a plasma membrane-derived phospholipid bilayer containing cytosol components from the cell of origin. The composition of the exosomes is dependent on the cell type of origin, the state of health of the source cell, and extracellular stimuli. There are various proteins, lipids, and miRNAs that are common to the majority of exosomes.

membrane while Rab27B facilitates vesicle transfer from the Golgi to MVBs (Ostrowski et al., 2010). In 2002 Savina et al. (2002) were the first to show the role of the Rab GTPase, Rab11 in exosomes secretion in human leukaemic K562 cells using ectopic expression of a dominant-negative Rab11 mutant to inhibit exosome release. Similarly, Rab11 depletion in *drosophila* S2 cells attenuated exosome secretion (Koles et al., 2012). Furthermore, shRNA knockdown of Rab2b, Rab GTPases in HeLa cells revealed that depletion of Rab27a and Rab27b reduced the ability of MVBs to dock onto the plasma membrane (Ostrowski et al., 2010) while Rab35 controls MVB docking and membrane fusion in oligodendrocytes (Hsu et al., 2010). By contrast, there are several GTPase independent pathways involved in exosome release, including through hypoxia-inducible factor 1α (King et al., 2012), glycan synthase kinase 3 (Hooper et al., 2012) and activation of p53 (Lespagnol et al., 2008).

Once transported to the plasma membrane, MVBs undergo a fusion event followed by exosome secretion into the extracellular space. In order to allow these coordinated multilevel changes in cytoskeletal plasma, membrane interactions have to be overcome. The first such interaction involves energy reduction of the membrane through protein-protein and protein-lipid interactions and enzymatic activation of membrane fusion machinery. Soluble *N*-ethylmaleimide-sensitive factor attachment protein receptors (SNAREs), tethering factors, Rabs, and other Ras GTPases facilitate MVBs fusion with the plasma membrane. To date, the exact molecular requirements for MVB membrane fusion are not well established; however, many studies have reported the crucial role of SNARE proteins and synaptotagmin family members (Jahn and Scheller, 2006). The primary function of SNARE proteins and their associated complexes is to facilitate vesicle fusion to the plasma membrane while providing specificity for membrane trafficking *via* the formation of a SNARE complex. Members of this family of proteins are classified into two categories, R or Q SNAREs. The formation of the SNARE complex involved in membrane fusion includes one R-SNARE, vesicle-associated membrane protein 7 (VAMP7) and three Q-SNAREs forming four coiled-coil helices (Pfeffer, 2007). RSNARE proteins VAMP7 and YKT6 have been reported as a necessity during exosome fusion of leukemic K562 cell lines and HEK293 cells, respectively (Fader et al., 2009).

During membrane fusion, vesicle SNAREs localized on MVBs interact directly with the target SNAREs to form a SNARE complex. Once this complex is formed, the MVB successfully fuses with the plasma membrane. Importantly, it has been shown that exosome secretion can be initiated independent of Rab GTPases through increases in intracellular calcium levels (Ca^{2+}). Increased levels of intracellular calcium following

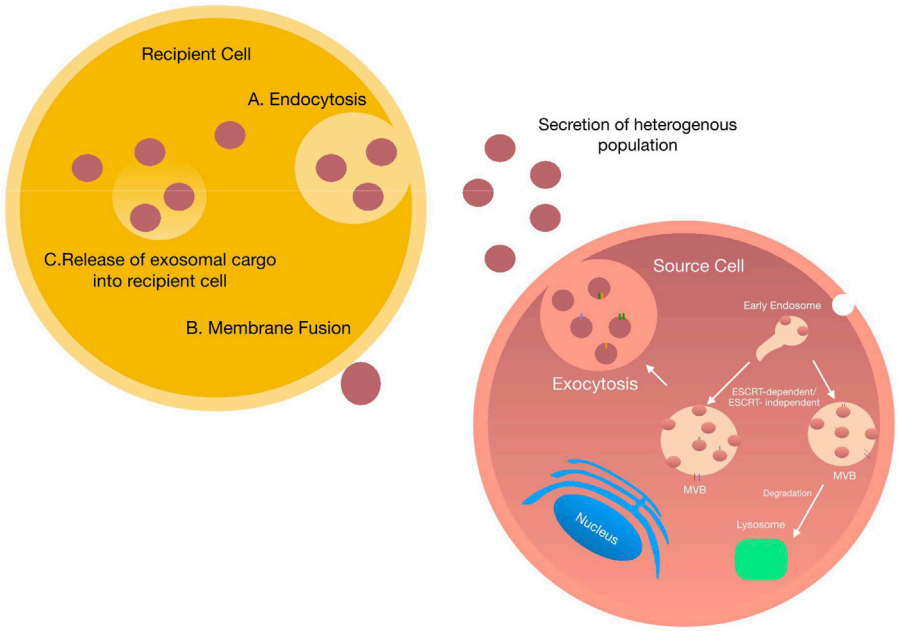

FIGURE 3 | Exosome uptake by neighbouring cells: Schematic representation of exosome uptake by neighbouring cells. Once secreted into the extracellular space, exosomes can be taken up by neighbouring cells *via* two main processes i) exosomes are engulphed into the target cell *via* endocytosis. Once endocytosed exosomes fuse with the endocytic compartment delivering various cargo ii) exosomes dock onto the plasma membrane of the target cell and directly deliver their cargo into the cytoplasm of the target cell.

monensin or calcium ionophore A23187 increases exosome secretion in human erythroleukemia K562 cells (Savina et al., 2003). Similarly, Fauré et al. reported that following potassium-induced depolarisation of critical neurons, subsequent influx of intracellular calcium led to an increase in exosome secretion. Comparable findings have since emerged for oligodendrocytes and breast carcinoma cell lines (Messenger et al., 2018). It is also noteworthy that some proteins, such as the synaptotagmin family, function as calcium sensors controlling exosomes secretion whereby knockdown of synaptotagmin-7 reduces the rate of exosome secretion (Hoshino et al., 2013). Regardless of the mechanism by which they are released from MVBs, exosomes remain close to their host cell interacting with neighbouring cells or are transported through bodily fluids to distant target cells.

Exosome Uptake and Function

On release, exosomes arrive at their target cell and present their contents to initiate functional responses, and/or promote phenotypic changes affecting the physiological or pathological status of the cell. Current research suggests that successful delivery of exosomal cargo can occur by two main mechanisms—*1*) endocytosis or *2*) direct fusion with the target cell (**Figure 3**). Exosomal endocytosis is a multi-step process that begins with exosome docking onto the plasma membrane of the recipient cell *via* receptor-ligand binding. Although the precise mechanisms for specific targeting of recipient cells are not clearly defined, several mediators are known, including specific lipids, lectins, tetraspanins, various extracellular matrix components and heparan sulfate proteoglycans. For example, uptake of tumour and non-tumour derived exosomes is substantially reduced in following the block of heparan sulfate proteoglycans (Atai et al., 2013; Svensson et al., 2013). Similarly, presentation of integrins on exosomes interact with cell adhesion molecules at the surface of recipient cells facilitating stable docking and attachment.

Irrespective of the mechanism by which exosomes dock to the recipient cell, once bound they either remain attached to the plasma membrane or become internalised (Denzer et al., 2000; Buschow et al., 2009). The method by which the exosomes become internalised differs depending on the cell type. Multiple mechanisms of endocytosis have been shown; for example, phagocytosis and clatherin-mediated endocytosis in neurons, macro-pinocytosis by microglia, caveolin-mediated endocytosis in epithelial cells and lastly lipid-raft endocytosis in tumour cells (Barrès et al., 2010; Feng et al., 2010; Fitzner et al., 2011; Nanbo et al., 2013).

Alternatively, exosomal uptake can occur *via* a direct membrane fusion event; however, this requires insertion of fusogenic proteins into the plasma membrane, followed by lipid reorganisation, protein reconstruction and membrane dimpling. Following interaction and uptake by recipient cells, exosomes may fuse with internal cytoplasmic endosomes resulting in the transfer of bioactive materials or possible degradation. However, it is currently unclear exactly how the cargo transfer takes place (Abels and Breakefield, 2016). Once internalised by the recipient cell, exosomes can initiate a diverse array of biological functions in both physiological and pathological conditions. Intercellular communication, immune modulation, coagulation and thrombosis and protection against cellular stress and death all represent mechanisms initiated in

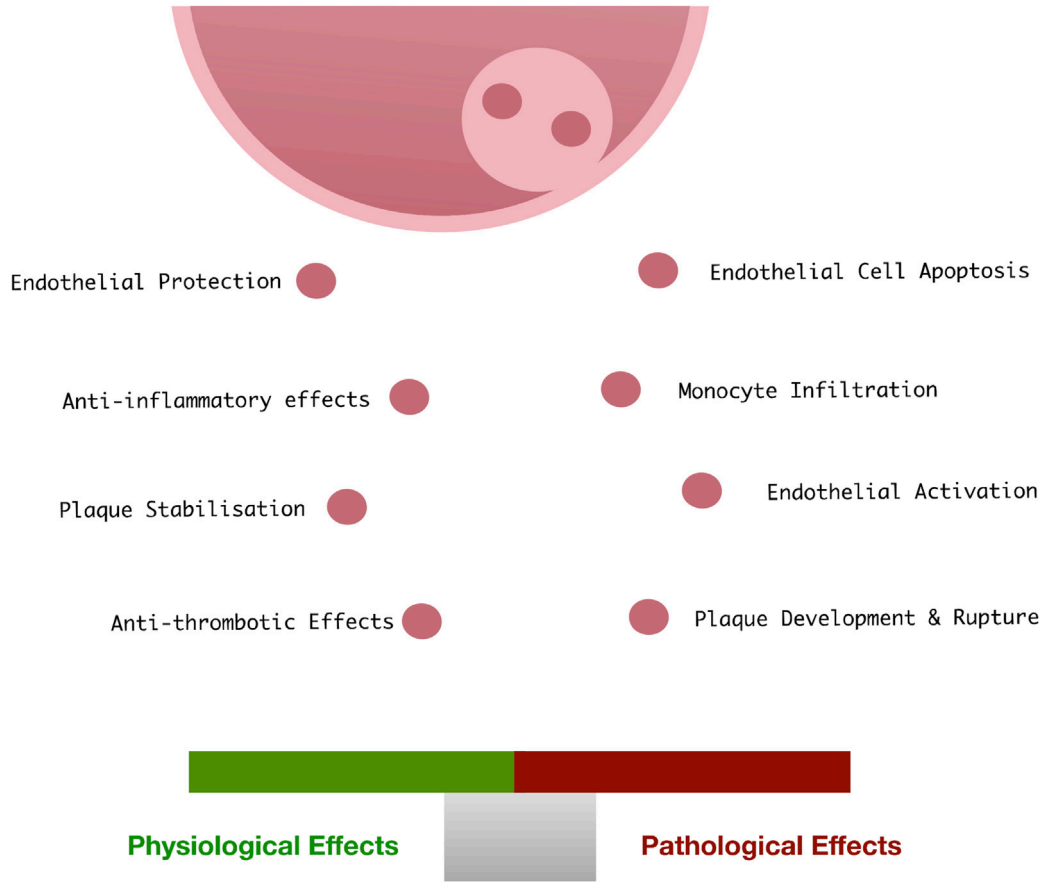

FIGURE 4 | Endothelial exosomes in vascular health and disease: Under physiological conditions, endothelial cells release exosomes at low concentrations which facilitate the protection and vascular homeostasis. When exposed to pathological vascular stimuli, the content of these exosomes changes, resulting in a loss of vascular homeostasis, apoptosis, monocyte infiltration, and subsequent facilitation of the development of CVD.

physiological conditions (Peters et al., 1989; Zitvogel et al., 1998; Valadi et al., 2007; Verma et al., 2015).

ENDOTHELIAL EXOSOMES

Like most cells in the body, vascular ECs retain the ability to release exosomes into the extracellular space in response to cellular activation or apoptosis. Vascular endothelial-derived exosomes play a role in physiological processes maintaining vascular homeostasis (Ridger et al., 2017), vascular development (Sheldon et al., 2010), endothelial regeneration and vascular cell protection, as well as the pathological progression of vascular disease (Bellin et al., 2019) (**Figure 4**). They are characterised by expression of various EC specific surface markers (CD31, CD55, CD144 and von Willebrand factor).

Endothelial Exosomes in Cardiovascular Disease

It is widely accepted that when exposed to cellular stress or oxidative damage, ECs release growth factors and cytokines which render change amongst neighbouring vascular cells (Haller et al., 2020). Invariably, ED leading to EC apoptosis drives maladaptive responses by favouring the release of atherogenic factors leading to perturbation of vascular homeostasis and vessel remodelling (Choy et al., 2001). Whether these bioactive materials are packaged into an exosome and secreted to impact other cells remains under active investigation. Nevertheless, it has recently been reported that circulating EC-EVs may differentiate STEMI from NSTEMI patients (Galeano-Otero et al., 2020; Haller et al., 2020). As guardians of vascular homeostasis, vascular ECs secrete low concentrations of exosomes into the bloodstream under physiological conditions. However, upon induction of ED, the concentration and content of EC-derived exosomes may change significantly whereby exosome mediated cell-cell communication is thought to drive vascular pathology (Migneault et al., 2020). Their biological effects are extremely complex and depend on the dysfunctional state of the releasing EC, their protein and nucleic acid content, and the diverse nature of the recipient cells (SMCs, ECs, macrophages/monocytes, stem cells).

Many studies have shown an increase in exosome content during the onset and progression of diabetes mellitus,

atherosclerosis and MI (Mallat et al., 2000; Bernal-Mizrachi et al., 2003). The release of exosomes from dysfunctional ECs mediate important repercussions on overall vascular function and pathology [cellular senescence, apoptosis and vascular calcification (VC)] due to their inherent capacity to easily access the bloodstream, resist degradation and significantly impact neighbouring cells within the vessel wall. Despite multiple studies demonstrating an association between endothelial release of circulating EVs and CVD, the understanding and functional implications of exosome secretion and cargo content are less well known. Indeed, the uptake of EC-derived exosomes from dysfunctional ECs containing various transcription factor proteins, lipids and miRNAs initiates a functional response in neighbouring cells. Quantitative proteomic analyses reveal that exosomes derived from ECs under different culture conditions have unique cargo (de Jong et al., 2012). *In vitro,* EC-EVs can be induced by TNFα, IL-1β, thrombin, lipopolysaccharide (LPS), C-reactive protein, and plasminogen activator-1 (Hromada et al., 2017). In addition, laminar shear stress, hyperglycaemia, and hypoxia are strong inducers of EC-EV generation (Hromada et al., 2017). Using *in vivo* models of ischemia–reperfusion injury, the release of exosomes from dysfunctional ECs within the circulation has also been demonstrated (Dieudé et al., 2015). These EVs, termed ApoExo's are released by human and murine ECs *in vitro* and characterized by the expression of an active 20 S proteasome core complex regulating their immunogenic activity to induce a pro-inflammatory response in naïve and transplanted mice (Dieudé et al., 2015; Migneault et al., 2020). Exosomes derived from dysfunctional ECs may also promote anti-apoptotic events in neighbouring cells through NF-κB activation thereby mediating a pro-survival, pro-migratory and anti-angiogenic phenotype in ECs consistent with changes to endothelial phenotype of potential importance in vascular response to injury (Migneault et al., 2020). In addition, KLF4-induced secretion of exosomes from human umbilical vein endothelial cells (HUVECs) harbours miR-143 and miR-145 enriched cargo which, upon uptake by vascular SMCs, regulate their phenotype through changes in vascular de-differentiation genes such as ELK1, KLF4, CAMK2d, and SHH2. Furthermore, exosomes derived from ECs expressing KLF4 also induced the formation of atherosclerotic lesions (Hergenreider et al., 2012). Exosome secretion is also particularly important in senescent ECs. Exposure of young ECs to exosomes from senescent ECs decreased the expression of inter-endothelial adherens junction proteins, VE-cadherin and beta-catenin (Takasugi, 2018) leading to altered endothelial junctional communication including suppressed cell growth, proliferation and migration of ECs that disrupt the endothelial barrier integrity (Wong et al., 2019).

A similar cross-talk mechanism exists between vascular ECs and circulating monocyte/macrophages, promoting the formation of atherosclerotic plaque. Exosomes secreted by LPS/interferon-alpha activated monocytes are endocytosed by human endothelial cells resulting in the expression of ICAM-1 and pro-inflammatory cytokines. This process results in ED *via* the Toll-like 4 (TLR4) and nuclear factor kappa-light-chain-enhancer of activated B cells (NF-κB) pathways contributing to the development of heart disease and potentially other chronic diseases (Tang et al., 2016). This exosome-dependent monocyte to endothelial crosstalk is also operational between monocytes and ECs and visa-versa in response to high glucose through modulation of the expression of surface proteins such as intercellular adhesion molecule 1 (ICAM-1) (Sáez et al., 2019). These findings support previous data showing that circulating EVs from newly diagnosed diabetes type 2 patients are enriched with proteins responsible for cell activation, i.e., ICAM-1 (Mallia et al., 2020). It has also been shown that transcription factors as components of the Notch and Wnt signalling pathways, such as delta-like 4 (Dll-4), are transported *via* exosomes to manage angiogenesis, a fundamental process in CVD (Gross et al., 2012; McGough and Vincent, 2016). Dll-4 is present in exosomes secreted by vascular ECs and is taken-up by neighbouring ECs to promote angiogenesis though inhibition of the Notch signalling pathway (Ushio-Fukai and Urao, 2009).

Numerous studies have shown that exosomes share many characteristics of matrix vesicles (MVs), which are unique extracellular membrane-bound microparticles that serve as initial sites for mineral formation (Qin et al., 2021). Exosomes are important transporters of molecules that drive vascular calcification (VC). VC is the abnormal deposition of calcium, phosphorus, and other minerals within the vessel wall and is closely associated with lesion formation and increased mortality due to pathological cardiovascular events. Both exosomes and MVs are enriched in calcified vascular walls and may promote the occurrence of VC through mineral deposition, and the reduced expression of fetuin-A (a known calcification inhibitor) in secreted exosomes (Qin et al., 2021). The current understanding on the origin and functions of osteoblast-like and osteoclast-like cells in the development and progression of calcified vascular lesions has been recently reviewed (Jiang et al., 2021). While smooth muscle trans-differentiation leading to VC in atherosclerosis is widely cited, recent focus on circulating and resident progenitor cells in the vasculature and their role in atherogenesis and VC has emerged (Leszczynska and Mary Murphy, 2018). When exposed to inflammatory stimuli, pericytes in particular, may turn into mesenchymal stromal progenitors and develop into osteoblasts and chondrocytes and produce large nodules containing type I collagen, osteopontin, matrix Gla protein (MGP), and osteocalcin to promote arterial calcification (Canfield et al., 2000; Leszczynska and Mary Murphy, 2018). The molecular mechanisms and balance between osteoblast-like and osteoclast-like cells in driving vascular calcification appears decisive (Zhang et al., 2018). Changes of miRNAs in exosomes can regulate osteogenic differentiation by promoting the expression of Runx2 and activating related signalling pathways, for example, the Wnt/β-catenin pathways (Leszczynska and Mary Murphy, 2018). Studies have shown that miRNAs with increased expression in the VC process can promote the osteogenic transformation of pericytes and SMCs by targeting anti-calcification proteins or contractility markers, while miRNAs with decreased expression can inhibit the osteogenic transformation by targeting osteogenic transcription factors (Zhang et al., 2018). Indeed, exosomes released from glucose-treated human ECs contain Notch3, an important

receptor in cell differentiation, and are able to promote vascular calcification through the mammalian target of rapamycin signalling pathway (Lin et al., 2019).

Other important mechanisms driving exosomal control of VC include regulation on cell autophagy (Dai et al., 2013) and oxidative stress (Chang et al., 2008). The autophagy pathway is a key regulator of cellular metabolism and EC homeostasis, and plays a critical role in maintaining normal vascular cell function (Phadwal et al., 2020). Emerging evidence suggests that autophagy directly protects against VC where endosomes, dysfunctional mitochondria, autophagic vesicles and Ca2+ and phosphate (Pi) enriched matrix laden EVs may work collectively to underpin the pathogenesis of VC. Excess ROS-induced stress has emerged as a critical mediator promoting VC through several mechanisms, including phosphate balance, phenotypic modulation of vSMCs, inflammation, DNA damage, and extracellular matrix remodelling (Hu et al., 2021).

In summary, a large body of research provides substantial evidence in favour of the active involvement of endothelium-derived exosomes in the development and progression of associated vascular diseases. Moreover, as endothelial exosomes efficiently deliver their cargo into recipient vascular cells to change function, they represent an important potential biomarker for disease detection and a therapeutic agent to effectively treat disease.

Exosomes and Their Diagnostic Potential

As exosomes are remarkably stable in biofluids, such as plasma and urine, and can be isolated for clinical evaluation even in the early stages of the disease, exosome-based biomarkers have quickly become adopted in the clinical arena with the first exosome RNA-based prostate cancer test introduced for early prostate cancer detection (Yu et al., 2021). Currently, circulating biomarkers of CVDs, such as total cholesterol levels and LDL, and MI prognostic biomarkers, including high-sensitivity C-reactive protein, high-sensitivity cardiac troponin and creatine kinase MB evaluate the risk of the occurrence and progression of the disease but fail to precisely predict whether the process starts or develops (Howard et al., 2000).

In the past decade, several studies have shown an association between elevated numbers of EVs, including exosomes, and prediction and development of CVD. Circulating EVs have been described during the development of atherosclerotic plaques (Aikawa, 2016; Kapustin and Shanahan, 2016), peripheral arterial disease (Badimon et al., 2016) and are associated with the Framingham risk assessment score (FRS) to determine a patient's 10-year risk of developing CVD. Currently, classical biomarkers used to diagnose acute pathologies associated with CVDs, such as myocardial infarction, are cardiac troponin I (cTnI) and isoenzyme creatine kinase MB. These biomarkers generally peak 12 h from the onset of an acute myocardial event, and their circulating levels are directly proportional to the scale of the infarct event (Adams et al., 1994). MiRNAs are the most widely studied element of exosome cargo. The importance of upregulation of two cardiac-specific miRNAs, miR-1 and miR-133a has been highlighted is studies using serum from patients diagnosed with an acute coronary event (Kuwabara et al., 2011). The levels of miR-1, mi-R133a, as well as mi-R208b and miR-499 were significantly increased in these patients compared to healthy volunteers. However, when compared to cardiac troponin T (cTnT), the four miRNAs were inferior for the diagnosis of AMI. By contrast, circulating miR-208a, which was undetectable in healthy patients, was elevated in 100% of patients presenting with MI and was detected within 4 h from the onset of chest pain, reaching its peak earlier than that of cardiac troponin (cTn) (Wang et al., 2010). Despite the identification of many other miRNAs as possible diagnostic biomarkers of atherosclerosis has-mi-R-192 and has-miR034a have shown the greatest promise as an early prognostic marker of disease. These miRs are upregulated in serum samples from AMI and ACS patients that experienced acute cardiovascular events within a year of their detection and support a role for exosome encapsulated miRs as biomarkers for both CVD and the prediction of adverse health outcomes.

Liquid biopsy-based exosomal profiling offers a promising platform to assist clinical diagnosis and prediction more accurately. In particular, exosomal miRNAs possess promising protective functions in CVD while circulating exosomes have shown great potential for diagnosis and risk assessment in CVD. In particular, substantial progress has been made in identifying the therapeutic role of circulating EC-derived EV miRNAs, particularly miR-92a-3p, in regulating the phenotype of ECs and SMCs under atherosclerotic conditions (Liu et al., 2019). Furthermore, miR-939-5p is downregulated in serum-based exosomes from patients with MI (Li et al., 2018).

Apart from miRNAs, exosomal proteins may also play a significant role in CVD diagnostics. P-selectin-expressing microparticles, CD3/CD45, SMA-α circulating exosome levels, and exosomal cystatin C, Serpin F2, CD14 levels are all significantly correlated with a high risk for incident CVD and mortality (Kanhai et al., 2013). In all, 252 upregulated EV proteins including apolipoprotein C-III, apolipoprotein D, platelet glycoprotein Ib alpha chain, complement C1q subcomponent subunit A, and complement C5 have been identified after MI using liquid chromatography coupled to tandem mass spectrometry and present an important opportunity for an EV diagnostic panel for the early diagnosis of MI (Cheow et al., 2016).

Similar studies have been performed in heart failure patients where miR-22, miR-320a, miR-423-5p, and miR-92b levels in both serum and serum exosomes present as potential specific biomarkers for the diagnosis and prognosis of systolic HF (Goren et al., 2012). Several serum-based exosomes containing p53-responsive miRNAs, such as miR-34a, miR-192, and miR-194 are also upregulated in HF patients within 1 year of acute MI onset (Matsumoto et al., 2013). Furthermore, an increased ratio of endothelial apoptotic microparticles ($CD31^+$/Annexin V^+) to mononuclear progenitor cells is elated to adverse clinical outcome in patients with acutely decompensated chronic HF (Berezin et al., 2015).

CARDIOVASCULAR DIAGNOSTICS

The measurement of biomarkers is a familiar feature of cardiovascular assessments that often dictates the provision of

additional diagnostic procedures and subsequent therapy. Their evaluation is integral to the rule-in/rule-out of AMI and they are frequently utilised to generate a cardiovascular risk score, which can increase the efficiency of the screening procedure (Papendick et al., 2017; Giannitsis et al., 2019), and consequently promote cost savings (Riley et al., 2017). Biomarkers are also finding utility in companion diagnostics and precision medicine, aligning with specific therapies and combining with molecular data to direct clinical decision-making (Currie and Delles, 2018; Hampel et al., 2019; Welcher, 2019). Their expanding applicability has accelerated research to further understand their relationship with cardiovascular injury and has promoted the pursuit for novel biomarkers of CVDs. Crucially, incorporating exosome measurement within diagnostic assessments in clinical settings will depend upon the development of fitting devices to enable rapid and/or high-throughput analysis, potentially demanding adapted processing procedures.

Currently, EVs are enriched and recovered using techniques such as centrifugation (ultracentrifugation, differential and gradient centrifugation), polymer-based precipitation, immunoaffinity, chromatography and filtration and are often chemically lysed after isolation (Doyle and Wang, 2019). Moreover, subsequent analysis can be conducted to recognise the released biomarker and accurately measure its presence—the exact manner of which depends upon the specific analyte. As a result, the entire analytical process can last several hours. This illustrates the resource intensive nature of measuring exosomes and their contents, suggesting this general approach is inherently unsuited to clinically urgent applications. Furthermore, although some exosomes may indicate pathological changes attributed to a CVD, to justify incorporation among current diagnostic techniques, their analysis should support the recognition of CVDs and ultimately improve patient management.

Point-of-Care Testing

Hospitals and clinics rely heavily on central laboratories to analyse patient samples and deliver accurate and timely results. This common operational model places the vast majority of blood/sample analysis responsibility on the central laboratory, irrespective of the relative exigency of the test. However, the layout of this model, in which sample transport and handling contribute to delays, is unfavourable for streamlining the triage process and ensuring critical needs are fulfilled. By contrast, point-of-care-testing (POCT) requires conducting a diagnostic test in a patient's proximity and incorporates the use of a compact device to facilitate rapid biomarker measurement. Unlike central laboratories in which a variety of sophisticated instruments and measurement equipment are routinely utilised, a point-of-care (POC) platform is generally robust, with the capacity to perform measurements in a range of test environments and without the need for highly specialised training.

This diagnostic approach is ideally suited to cardiovascular assessments in which immediate action is a priority. For instance, minimising the system delay—which is the time period between emergency department presentation and insertion of a catheter—correlates with reduced infarct size and improved left ventricular function following myocardial injury (Lonborg et al., 2012). A prominent characteristic of POC testing (POCT) is the ability to accommodate rapid analysis, ideally generating a response within 20 min of sample application. This rapid response has been shown to contribute towards reduced turnaround times (TATs), with one study demonstrating that the implementation of POCT for cTnI, the primary biomarker of AMI, reduced the length of stay by over 25% in emergency departments, thus shortening the system delay (Singer et al., 2005). This is one of many facets of POCT that rely on key characteristics for implementation . However, several criteria are identified including *1*) "laboratory testing is performed in the direct proximity of the patient," *2*) "results available quickly" and *3*) "results lead to a rapid diagnosis or consequences for treatment." Evidently, they all relate to improving patient management and the efficiency of the process. As a result, this format of diagnostic testing is ideally placed to positively impact cardiovascular assessments due to the critical need to triage patients without delay.

The development of compact and user-friendly platforms that can accommodate exosome analysis, whilst adhering to quality assurance and compliance with accreditation standards, in addition to the aforementioned recommendations, requires a combination of meticulous design and careful consideration of both the isolation and measurement processes (**Figure 5**). Moreover, the simplistic operation of these devices is made possible by the miniaturisation and automation of sequential tasks often associated with laboratory assays. Importantly, some processes are naturally more suited to POCT and are somewhat unrestricted by technological limitations. These are key factors to contemplate when assessing the feasibility of exosome measurement for POCT as current isolation processes and measurement techniques may be inherently unsuited for POCT.

EXOSOME DETECTION FOR CARDIOVASCULAR DISEASE DIAGNOSTICS

The isolation of pure exosomes is a critical step in developing exosomal profiling for clinical diagnostic application in CVD. There is a lack of consensus regarding the most appropriate approach for exosome isolation and characterization, both important issues for their effective clinical translation. A major challenge is the identification of a standard technique to isolate intact exosomes from bodily fluids with high reproducibility and purity. The various isolation platforms have been recently reviewed and include: *1*) Ultracentrifugation, *2*) Size-Based Isolation Methods *3*) Immuno-Affinity Purification *4*) Polymer-Based Precipitation and *5*) Microfluidics-Based Isolation Techniques (Zarà et al., 2020) (**Table 1**). Conventional exosome isolation processes such as centrifugation (most widely implemented) (Gardiner et al., 2016) and some polymer precipitation methods can take over 12 h to perform and are often reported to produce low recovery rates and result in an impure extract (Patel et al., 2019). Exosome purity and yield can be affected by several factors including rotor type, *g*-force and centrifugation times thus compromising

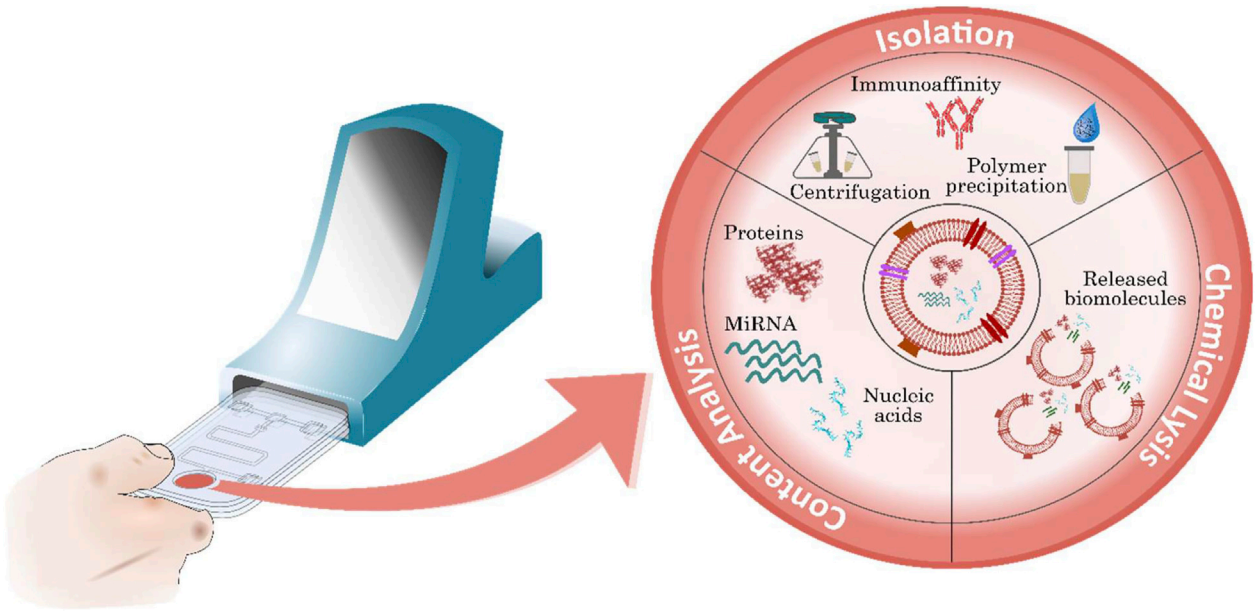

FIGURE 5 | Exosome-derived biomarkers for the diagnosis of CVD. Exosomes contain key potential biomarkers including various surface proteins, miRNAs and nucleic acids. Following isolation, exosomes can be measured, or further processed using exosome lysis before biomarker recognition to analyse contents.

centrifugation as a recognised standard for clinical exosome isolation (Cvjetkovic et al., 2014). Moreover, the purity of the exosome product is entirely dependent upon the isolation technique with a combination of ultrafiltration and chromatography producing much higher purity exosome yields than centrifugation (Shu et al., 2020), although this may only exemplify the challenges facing standardisation in practical applications.

Electrokinetic Separation

There are alternative isolation methods which not only offer improved performances but are more suited to POCT for CVD diagnostics. Dielectrophoresis (DEP), for instance, is a technique that enables controlled manipulation of particles in a fluid and can separate particles based on their dielectric properties, shape, size and the properties of the surrounding fluid using a non-uniform electrical field to induce a dipole moment in the targeted particles (Pethig, 2017). Moreover, it is ideally suited to separate EVs from bodily fluid samples and is widely utilised in a variety of microfluidic devices (Zhang et al., 2019a) and rapidly isolates exosomes from conditioned cell culture media, plasma, serum and urine in 20 min (Shi et al., 2019). This approach can be improved using insulator-based DEP to squeeze the electric field and avoids common electrode fouling and electrolysis problems associated with electrode-based DEP (Crowther and Hayes, 2017). Another DEP-based isolation device contains a microelectrode array to isolate exosomes from plasma samples and concentrate them at the microelectrode edges (Ibsen et al., 2017). Importantly, the microelectrode array consisted of a hydrogel coating to minimize fouling and reduce bubble formation, thus preserving the integrity of the electrode surfaces. A slightly different approach, which also utilises an electrical field for particle manipulation, is ion concentration polarization (ICP). Here, the electric field effectively drives the transportation of particles to the interface of an ion-exchange membrane at a rate dependent on the particle's electrophoretic mobility in a particular fluid (Fu et al., 2018). However, as this technique alone does not strictly discriminate between EVs and other biological fluid particles, ICP is often implemented in conjunction with complementary separation techniques (Marczak et al., 2018). This technique concentrates exosomes from serum within 10 min to a factor of 15 and could produce yields of approximately 70% in 20 min. Although, one potential limitation of this device is that the entire buffer solution must be exchanged frequently during operation. Another approach is to incorporate multiple separation mechanisms to enhance the recovery efficiency of isolation techniques. The development of an ICP-based microfluidic device that consists of 3D printed microtraps to assist exosome capture (Cheung et al., 2018) results in a 100-fold increase in the exosome concentration within the microchannel in 30 min.

Affinity-Based Isolation

Employing antibodies to target specific surface proteins is one of the more common approaches frequently reported for exosome isolation. Several studies detail the development of microfluidic-based EV enrichment using antibodies and demonstrate performance enhancement techniques such as; magnetic nanoparticle (Zhao et al., 2016) or magnetic nanowire conjugation of antibodies for improved particle manipulation (Lim et al., 2019), optimised microfluidic design to maximise sample mixing (Zhang et al., 2016; Dorayappan et al., 2019) and the use of microstructures (Zhang et al., 2019b) and

TABLE 1 | Performance characteristics of highly specific exosome isolation techniques.

Isolation technique	Property of separation	Specimen type	Sample volume capacity (µl)	Isolation time (min)	Particle size (nm)	Recovery rate
Dielectrophoresis (Shi et al., 2019)	Dielectric properties shape and size of particles in fluid	Plasma (filtered), serum and saliva (centrifuged and pre-concentrated)	200	20	50–150	NA
Dielectrophoresis (Ibsen et al., 2017)	Dielectric properties shape and size of particles in fluid	Plasma	30–50	30	50–150	NA
Microfluidic gel electrophoresis and ion-selective separation (Marczak et al., 2018)	Surface properties and particle size	Serum	25–50	10–20	130–260	60–80%
Ion concentration polarization with 3D-printed microtrap (Cheung et al., 2018)	Electrophoretic mobility of EVs, particle size/immunoaffinity and hydrophobic interactions (aldehyde)	EVs in PBS	30	30	Average size ≈50–75	Concentrate 100-fold
Acoustic trapping (Ku et al., 2018)	Particle size, density and compressibility of particles and fluid	Plasma and urine	300	30	154.2 (mean)	2.4*10⁸ particles/ml
Immunomagnetic (Zhao et al., 2016)	Immunoaffinity	Plasma	10—10,000	20	79.7% < 150	72%
Immunocapture (Zhang et al., 2019b)	Immunoaffinity	Plasma	2–125	40 for 20 µl sample (0.5 µl/min)	40–160	80–85%
Fe_3O_4@TiO_2 particle enrichment (Pang et al., 2020)	Affinity of phosphate head to TiO_2 and particle size	Serum (filtered)	4	5	30–200	NA
TiO_2 particle enrichment (Gao et al., 2019)	Affinity of phosphate head to TiO_2	Serum (filtered)	1–100	5	65–235	93.4
Tim4- phosphatidylserine affinity (Nakai et al., 2016)	Affinity of Tim4 protein towards phosphatidylserine	Cell culture supernatant (filtered)	50—4,000	Overnight	219 (mean)	15—20%
Nanostructure- functionalized lipid nanoprobe (Wan et al., 2019)	Affinity and particle size	Plasma (filtered)	1,000—2,000	100–200 (10 µl/min)	50–200	28.8%

Many of the techniques selected display favourable features for adaption within compact microfluidic-based cartridges. Bodily fluid sample often filtered to remove cellular debris and large extracellular vesicles. Fe_3O_4, Iron oxide, TiO_2, Titanium dioxide.

nanomaterials (Fang et al., 2017) to optimise the antibody loading capacity by increasing the overall surface area. However, EVs display other distinctive properties which can support alternative affinity-based interactions. These include the attraction between phospholipids and TiO_2 to facilitate EV isolation. Fe_3O_4@TiO_2 core-shell nanoparticles were synthesised, in which the outer TiO_2 shell supported binding of serum exosomes, whereas the Fe_3O_4 core enabled particle manipulation by magnetic separation from the sample and hence, exhibits some favourable characteristics for POCT (Li et al., 2017; Pang et al., 2020). Synthesis of TiO_2 -containing microspheres to facilitate TiO_2-based isolation of exosomes from buffer solutions and serum within 5 min has also been reported (Gao et al., 2019). However, a potential limitation of TiO_2 exosome isolation is the lack of specificity which may produce low purity extracts as serum proteins have also been shown to interact with TiO_2 nanomaterials (Zaqout et al., 2011; Kulkarni et al., 2015). Hence, the purity of the exosome extract might be compromised, thus possibly affecting downstream analysis. Nonetheless, both TiO_2-based isolation techniques were shown to achieve significantly improved performances in comparison to ultracentrifugation, with the second group performing proteomic analysis to demonstrate increased purity of the extract compared to samples processed by ultracentrifugation. Similar affinity-based approaches have also been reported, with one such technique immobilizing T-cell immunoglobulin domain mucin domain-containing protein 4 (Tim4) on the surface of magnetic beads to bind to phosphatidylserine (Nakai et al., 2016; Lea et al., 2017), a phospholipid typically found internally within the phospholipid membrane of vesicles. This technique has the distinct advantage of simple exosome release following enrichment due to the dependency of phosphatidylserine on the presence of Ca^{2+} (Tietjen et al., 2014). Although, the purity of the extracted exosomes acquired was higher (78.1%) than both ultracentrifugation (66%) and polymer precipitation (21.8%), one key limitation is that the exosome sample remains in the Tim4 protein overnight to initiate capture, an evident deficiency if to be considered for POCT.

The development of devices that incorporate lipid nanoprobes in conjunction with silica nanostructures to selectively isolate exosomes has also shown great promise (Wan et al., 2019). Reactive ion etching was employed to produce nanostructures in silica substrate correlating to EVs in the size range of approximately 120 nm, which also serves to increase the overall surface area available for lipid nanoprobe grafting. The lipid nanoprobe non-covalently interacts with the lipid membranes of the exosomes and thus together with the tailored nanostructures, offers an effective method for isolation. The microfluidic chip developed for the recovery of exosomes included a herringbone micromixer to stimulate increased interaction with the lipid nanoprobe functionalised nanostructures.

TABLE 2 | Platforms for isolating exosomes directly from bodily fluid samples that are routinely collected in clinical settings.

Isolation technique	On-chip pre-treatment	Property of separation	Specimen type	Sample volume (μl)	Isolation time (min)	Particle size (nm)	Recovery rate
Tilted-angle standing surface acoustic wave (Reátegui et al., 2018)	None	Particle size, density and compressibility of particles and fluid	Whole blood	100	25	75–125	82.4%
On-disc AAO membrane filtration (Sunkara et al., 2019)	Centrifugal disc plasma separation	Particle size	Whole blood	30–600	36	100–350	76–88%
Standing surface acoustic waves (Wang et al., 2020)	None	Particle size, density and compressibility of particles and fluid	Saliva	NA	10–20	20–250	NA
DC electrophoresis-assisted filtration (Davies et al., 2012)	None	Size and electrophoretic mobility	Whole blood	240	120	NA	1.5%
Immunoaffinity (Chen et al., 2019)	Size exclusion membrane filtration	Affinity	Whole blood	20	500	50–200	45%
Immunoaffinity (Zhou et al., 2020)	Inertial separation	Affinity	Whole blood	75	78	50–200	NA
DEP (Lewis et al., 2018)	None	Dielectric properties, shape and size of particles in fluid	Whole blood	25	20	NA	NA

Automated on-chip pre-treatment involved removing components of whole blood to simplify recovery of exosomes. Isolation time includes any required pre-treatment. AAO, Anodic aluminium oxide; DC, Direct current.

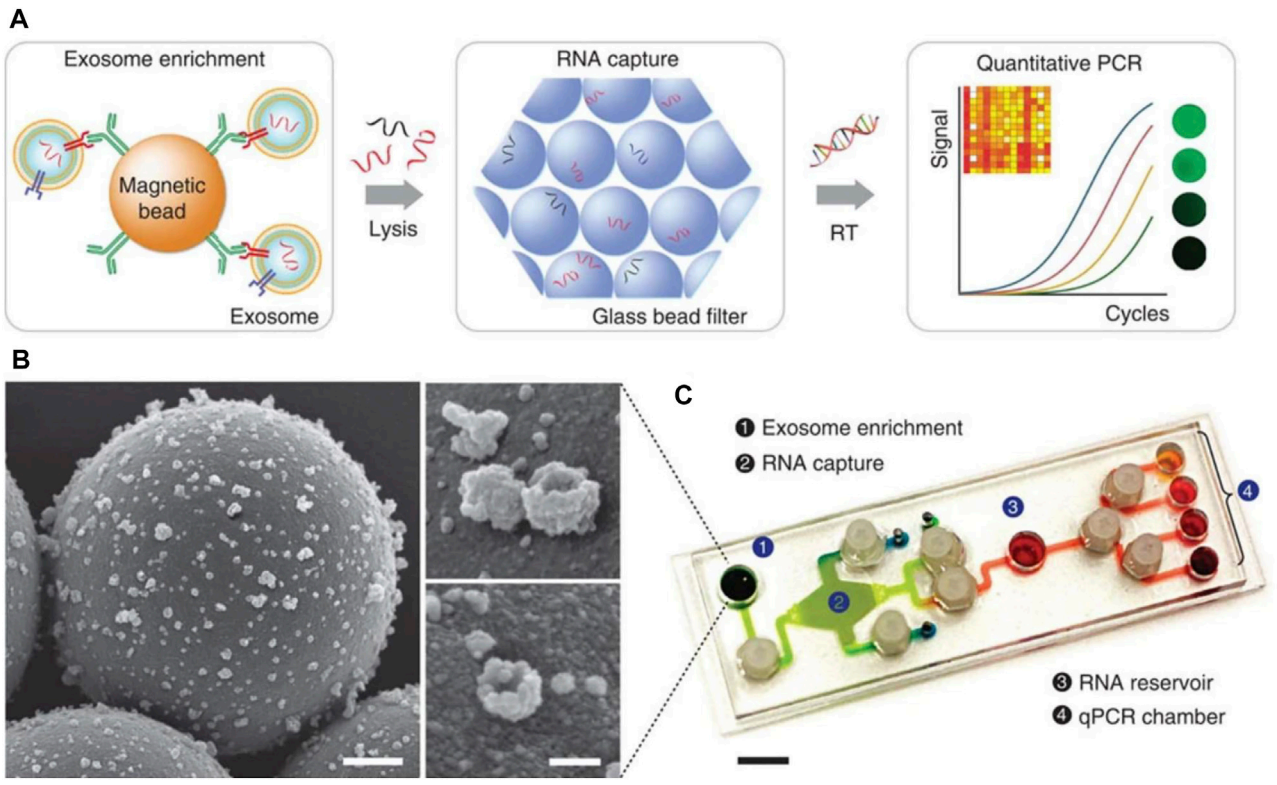

FIGURE 6 | Diagram of key steps/approaches for measuring exosome for the prediction of CVD. **(A)** Magnetic microbeads coated with specific antibodies enabled exosome isolation and addition of guanidine-based lysis buffer released the contents of enriched exosomes. Torque-actuated valves and permanent magnets were used to control the process. RNA is adsorbed on a glass-bead filter *via* electrostatic interactions and reagents are loaded to prepare for qPCR. **(B)** Images from scanning electron microscope of exosomes captured on antibody-coated magnetic microbeads. Scale bars 500 and 100 nm (inset) **(C)** Photograph of PDMS iMER cartridge. RT—Reverse transcription (Shao et al., 2015). Source: Reprinted in its original form under CC BY license. License access: https://creativecommons.org/licenses/by/4.0/legalcode.

Characteristics of Recent Isolation Techniques

The growing variety of highly specific EV isolation techniques provides an indication of the rate at which tailored approaches to EV isolation are emerging. Notably, many of these methods provide superior exosome yields compared to traditional isolation techniques and require less time to attain an enriched extract. A selection of EV isolation techniques and performance characteristics which are particularly relevant for POCT are summarised in **Table 2**. For instance, having the capacity to process small sample sizes is often a desired pre-requisite of POCT which permits the use of minimally invasive collection methods suitable for acquiring small sample volumes. On the contrary, processing larger amounts of sample may provide superior diagnostic value for exosome analysis. Nevertheless, performing sample analysis from small sample volumes with a short TATs are key characteristics of POC assays and are particularly relevant in acute care settings for CVDs. It is evident that the isolation techniques listed offer reduced processing time in comparison to the regularly employed standard approaches (**Table 2**). These techniques have been purposely developed to accommodate the separation of EVs from bodily fluids by targeting unique EV properties, with some implementing affinity–based approaches and others facilitating enrichment by particle size. However, the majority employ a combination of separation mechanisms which essentially augments the performance of these techniques, illustrating to an extent the existing inadequacies of traditional techniques due to their forced adaption for a process in which they are inherently constrained.

The ability to recover a large quantity of exosomes from a sample is a fundamental aspect of an exosome isolation technique. This recovery rate (the ratio between extracted exosomes and total sample exosomes) is a key metric that can be assessed to validate the proficiency of an enrichment technique and thus support the direct comparison of different approaches. However, the recovery rate was not determined in several studies, thus restricting direct comparison with other approaches. The apparent lack of cohesion between reported performance characteristics of these exosome isolation techniques increases uncertainty regarding the most promising methods. Moreover, determining the purity of the enriched exosomes is quite important as it can assist in confirming that a biomarker has originated from EVs and not just been co-isolated with the exosomes (Webber and Clayton, 2013). The co-isolation of contaminating factors may inhibit accurate detection of the EVs and/or their contents, although, some consider the purity of the EV extract less important for diagnostic purposes, inferring that the yield is a primary concern (Quek et al., 2017; Konoshenko et al., 2018). Beyond diagnostic applications, exosome enrichment might be required for therapeutic purposes or biomarker discovery and therefore, a lack of cohesion between reported characteristics may only serve to delay the adoption of a recognised standard for exosome isolation.

Exosomal Analysis for Point-of-Care-testing

A crucial aspect of adapting analytical techniques for POCT is the ability to refine and compartmentalise standard laboratory procedures to simplify the measurement process. A POC assay for instance, should measure biomarkers directly from samples without manual pre-treatment, thus eliminating the need for ancillary instrumentation and preventing inter-operator variability. Bodily fluid samples can be quite complex, however, often requiring pre-treatment to support accurate measurements. Whole blood, for example, comprises a multitude of biomolecules, cells and cellular debris which can be challenging to process. Therefore, plasma or serum are often the media of choice as red and white blood cells are removed, the main distinction between plasma and serum is that serum lacks the blood clotting agent fibrinogen. Crucially, before processing whole blood for serum extraction, the collected blood must be left to clot for approximately 30 min, whereas plasma separation can begin immediately, and can be complete within a few minutes. Various analytical approaches incorporate automated on-board plasma extraction prior to exosome isolation (*see* **Table 2**). These platforms permit exosome recovery from whole blood or saliva and can employ pre-treatment mechanisms to acquire plasma which minimises operator interaction and produces an enriched extract for subsequent biochemical analysis.

Centrifugal microfluidic lab-on-a-disc (LoaD) platforms are particularly suited to plasma extraction from whole blood with one group incorporating on-disc filtration to extract EVs from separated plasma (Sunkara et al., 2019). Whole blood samples were loaded onto the Exodisc-B LoaD platform and separated into individual constituents which enabled plasma to be collected for subsequent processing. This automated approach incorporated two filters that separated larger particles and smaller biomolecules from EVs within the plasma. The remaining EVs were collected in an elution chamber with a reported recovery efficiency that exceeded ultracentrifugation and a processing time (35–40 min), including plasma separation.

An alternative automated microfluidic-based plasma separation approach that involves an inertial separation structure has been reported (Zhou et al., 2020). Fundamental to the plasma collection reliability of this device is the flowrate at which whole blood was propelled through the inertial separation channels. Whole blood was actuated using a peristaltic pump which might not be entirely suited to POCT as cross-contamination could occur between assays if appropriate measures such as internal washing using pre-loaded buffers between assays or intermediary liquids to propel whole blood samples for example, are not employed. Therefore, if this approach was adapted for POCT, either on-chip micropumps or features such as diaphragms controlled by the system analyser may be required. Nevertheless, following plasma separation, this platform isolated exosomes using an antibody that recognised a specific tetraspanin and introduced an HRP-labelled detection antibody to quantify the concentration of bound EVs from small sample volumes.

Several of the platforms excluded pre-treatment methods, with one group developing an acousto-fluidic device to isolate exosomes directly from saliva by generating standing surface acoustic waves (sSAW) (Wang et al., 2020). Surface acoustic wave (SAW) technologies are frequently employed to control and manipulate particles in fluids and are particularly fitting for microfluidic devices. The sSAW method utilised two pairs of interdigital electrode transducers, the first of which forced larger particles (micrometre) towards a waste channel and the second pair removed remaining sub-micrometre particles larger than exosomes (>150 μm). This device demonstrated superior exosome yields in comparison with differential centrifugation and the extracted exosomes were consequently processed for the analysis of viral DNA using a droplet digital PCR assay performed on an external system.

Other groups report the recovery of sample EVs using tailored microfluidic-based devices, such as the nPLEX (Im et al., 2014) and iMER (Shao et al., 2015) platforms, which also support on-chip biochemical analysis. The basic operation principle of the iMER platform involves the recovery of sample exosomes, on-chip lysis, RNA enrichment and subsequent analysis of captured RNA. A complementary customised PCR system, including a thermal cycler and a fluorescence detector, facilitated RNA detection (**Figure 6**). The iMER platform required approximately 100 μl serum to measure exosome-derived RNA within 2 h; although this is a substantial improvement compared to laboratory-based techniques, to warrant adaption for POCT, the TAT would have to be reduced. Hence, this approach is possibly more suited to high-throughput laboratory analysis.

It must be emphasised that embedding multiple stepwise operations within a microfluidic device to isolate exosomes and measure their contents requires extended periods of time to accommodate the analytical process. Combining some of the more rapid exosome enrichment microfluidic-based techniques with emerging accelerated PCR assays may prove to support shorter TATs and permit integration within rapid sample-to-answer POC platforms (Bustin, 2017). Although, this would require further investigation to establish the exact configuration of a suitable exosome enrichment POC assay, its economic feasibility and justification of its development for a particular application. Conversely, exosome-derived RNA can be measured without employing a time-consuming exosome isolation process using a bespoke SPR-based exosome lysis platform (Ramshani et al., 2019). Reverse transcription PCR (RT-qPCR) was conducted to measure free-floating RNA in plasma samples. Remaining plasma was subjected to SAW to lyse sample exosomes and prepare for further RNA measurement. The difference between the RNA concentration before and after the lysis of the exosomes could be attributed to the release of EV-bound RNA. This complete approach required 1 h, with 30 min allocated for each RT-qPCR assay. If this approach was performed simultaneously, i.e., free-floating and lysed total RNA measured concurrently, in addition to adopting a rapid PCR assay (Chan et al., 2016; Eboigbodin et al., 2017), this method could enable rapid measurement of exosome-derived RNA. Crucially, this strategy may not be suitable for certain exosome-derived biomarkers, specifically proteins. However fundamentally, it illustrates the premise by which exosome-derived RNA could be measured in a manner that is fitting for POCT.

CONCLUSION

It is well established that endothelial dysfunction is a key atherosclerotic mechanism that without the balanced presence of corresponding athero-protective factors, leads to intimal thickening and progression of arteriosclerotic disease. Currently, cIMT is regarded as one of the primary surrogate indices of atherosclerosis. However, in some AMI patients, interrogation by angiography reveals no significant lesions within surveyed coronary beds. Fundamental to individual risk profiling and the diagnosis of ACS is the measurement of biomarkers, typically from collected whole blood specimens. Endothelial exosomes found in liquid biopsies may present as ideal cardiac biomarkers because they are involved in the progression of atherosclerosis and enhanced secretion has been demonstrated during periods of cellular stress.

Performing liquid biopsies is a potentially minimally-invasive route to elucidating underlying functional disturbances; however, the prospect of exploiting exosomes as diagnostic biomarkers of CVD is intrinsically dependent on the efficiency at which they can be acquired for analysis. Currently, isolating exosomes requires laborious processes that are conducted in laboratory settings and exhibit differing capabilities in attaining consistent yields and extract purity. Many of these approaches offer suboptimal performances and are inherently unsuited to POCT or efficient high-throughput measurements. Hence, tailored microfluidic-based devices favour adaption of exosomal analysis for diagnostic platforms and provide greatly reduced processing times. These devices—some of which incorporate automated pre-treatment—can efficiently enrich exosomes from whole blood, perform lysis and supply a nucleic acid, protein and lipid rich extract for subsequent analysis. The significance of exosomes and the cargo they harbour remains in its infancy, yet it is anticipated that greater detail will be revealed regarding their role in CVD and how best to interpret their fluctuating presence during disease progression. Ultimately, their clinical value for predicting CVD will be defined by a combination of diagnostic insight which they afford, therapeutic strategies which they permit and the ease at which they can be reliably and consistently isolated from samples.

AUTHOR CONTRIBUTIONS

The review was researched by DB, BR, and KO before DC, DM, IM, and ER made significant edits to the content. The final versions was edited by PC. The Figures were prepared by DB and BR.

FUNDING

This work was funded through the Eastern Corridor Medical Engineering Centre (ECME) Project, Number 88, eMS Ref No: 5034 by the European Union's INTERREG VA Programme and managed by the Special EU Programmes Body (SEUPB).

REFERENCES

Abels, E. R., and Breakefield, X. O. (2016). Introduction to Extracellular Vesicles: Biogenesis, RNA Cargo Selection, Content, Release, and Uptake. *Cell Mol. Neurobiol.* 36, 301–312. doi:10.1007/s10571-016-0366-z

Adams, J. E., Schechtman, K. B., Landt, Y., Ladenson, J. H., and Jaffe, A. S. (1994). Comparable Detection of Acute Myocardial Infarction by Creatine Kinase MB Isoenzyme and Cardiac Troponin I. *Clin. Chem.* 40, 1291–1295. doi:10.1093/clinchem/40.7.1291

Aikawa, E. (2016). Extracellular Vesicles in Cardiovascular Disease: Focus on Vascular Calcification. *J. Physiol.* 594, 2877–2880. doi:10.1113/JP272112

Al Rifai, M., Martin, S. S., McEvoy, J. W., Nasir, K., Blankstein, R., Yeboah, J., et al. (2018). The Prevalence and Correlates of Subclinical Atherosclerosis Among Adults with Low-Density Lipoprotein Cholesterol. *Atherosclerosis* 274, 61–66. doi:10.1016/j.atherosclerosis.2018.04.021

Amato, M., Veglia, F., de Faire, U., Giral, P., Rauramaa, R., Smit, A. J., et al. (2017). Carotid Plaque-Thickness and Common Carotid IMT Show Additive Value in Cardiovascular Risk Prediction and Reclassification. *Atherosclerosis* 263, 412–419. doi:10.1016/j.atherosclerosis.2017.05.023

Arandjelovic, S., and Ravichandran, K. S. (2015). Phagocytosis of Apoptotic Cells in Homeostasis. *Nat. Immunol.* 16, 907–917. doi:10.1038/ni.3253

Atai, N. A., Balaj, L., Van Veen, H., Breakefield, X. O., Jarzyna, P. A., Van Noorden, C. J. F., et al. (2013). Heparin Blocks Transfer of Extracellular Vesicles between Donor and Recipient Cells. *J. Neurooncol* 115, 343–351. doi:10.1007/s11060-013-1235-y

Babst, M. (2011). MVB Vesicle Formation: ESCRT-dependent, ESCRT-independent and Everything in between. *Curr. Opin. Cell Biol.* 23, 452–457. doi:10.1016/j.ceb.2011.04.008

Bache, K. G., Brech, A., Mehlum, A., and Stenmark, H. (2003). Hrs Regulates Multivesicular Body Formation via ESCRT Recruitment to Endosomes. *J. Cell Biol.* 162, 435–442. doi:10.1083/jcb.200302131

Badimon, L., Suades, R., Fuentes, E., Palomo, I., and Padró, T. (2016). Role of Platelet-Derived Microvesicles as Crosstalk Mediators in Atherothrombosis and Future Pharmacology Targets: A Link between Inflammation, Atherosclerosis, and Thrombosis. *Front. Pharmacol.* 7, 293. doi:10.3389/fphar.2016.00293

Baietti, M. F., Zhang, Z., Mortier, E., Melchior, A., Degeest, G., Geeraerts, A., et al. (2012). Syndecan-syntenin-ALIX Regulates the Biogenesis of Exosomes. *Nat. Cell Biol.* 14, 677–685. doi:10.1038/ncb2502

Baker, A. H., and Péault, B. (2016). A Gli(1)ttering Role for Perivascular Stem Cells in Blood Vessel Remodeling. *Cell Stem Cell* 19, 563–565. doi:10.1016/j.stem.2016.10.011

Bang, C., and Thum, T. (2012). Exosomes: New Players in Cell-Cell Communication. *Int. J. Biochem. Cell Biol.* 44, 2060–2064. doi:10.1016/j.biocel.2012.08.007

Barrès, C., Blanc, L., Bette-Bobillo, P., André, S., Mamoun, R., Gabius, H. J., et al. (2010). Galectin-5 Is Bound onto the Surface of Rat Reticulocyte Exosomes and Modulates Vesicle Uptake by Macrophages. *Blood* 115, 696–705. doi:10.1182/blood-2009-07-231449

Bellin, G., Gardin, C., Ferroni, L., Chachques, J. C., Rogante, M., Mitrečić, D., et al. (2019). Exosome in Cardiovascular Diseases: A Complex World Full of Hope. *Cells* 8, 166. doi:10.3390/cells8020166

Bennett, M. R., Sinha, S., and Owens, G. K. (2016). Vascular Smooth Muscle Cells in Atherosclerosis. *Circ. Res.* 118, 692–702. doi:10.1161/CIRCRESAHA.115.306361

Berezin, A. E., Kremzer, A. A., Samura, T. A., Martovitskaya, Y. V., Malinovskiy, Y. V., Oleshko, S. V., et al. (2015). Predictive Value of Apoptotic Microparticles to Mononuclear Progenitor Cells Ratio in Advanced Chronic Heart Failure Patients. *J. Cardiol.* 65, 403–411. doi:10.1016/J.JJCC.2014.06.014

Bernal-Mizrachi, L., Jy, W., Jimenez, J. J., Pastor, J., Mauro, L. M., Horstman, L. L., et al. (2003). High Levels of Circulating Endothelial Microparticles in Patients with Acute Coronary Syndromes. *Am. Heart J.* 145, 962–970. doi:10.1016/S0002-8703(03)00103-0

Bobrie, A., Colombo, M., Raposo, G., and Théry, C. (2011). Exosome Secretion: Molecular Mechanisms and Roles in Immune Responses. *Traffic* 12, 1659–1668. doi:10.1111/j.1600-0854.2011.01225.x

Buschow, S. I., Nolte-'t Hoen, E. N. M., van Niel, G., Pols, M. S., ten Broeke, T., Lauwen, M., et al. (2009). MHC II in Dendritic Cells Is Targeted to Lysosomes or T Cell-Induced Exosomes via Distinct Multivesicular Body Pathways. *Traffic* 10, 1528–1542. doi:10.1111/j.1600-0854.2009.00963.x

Bustin, S. A. (2017). How to Speed up the Polymerase Chain Reaction. *Biomol. Detect Quantif.* 12, 10–14. doi:10.1016/j.bdq.2017.05.002

Cahill, P. A., and Redmond, E. M. (2016). Vascular Endothelium - Gatekeeper of Vessel Health. *Atherosclerosis* 248, 97–109. doi:10.1016/j.atherosclerosis.2016.03.007

Canfield, A. E., Doherty, M. J., Wood, A. C., Farrington, C., Ashton, B., Begum, N., et al. (2000). Role of Pericytes in Vascular Calcification: A Review. *Z Kardiol.* 89, 20–27. doi:10.1007/s003920070096

Chan, K., Weaver, S. C., Wong, P. Y., Lie, S., Wang, E., Guerbois, M., et al. (2016). Rapid, Affordable and Portable Medium-Throughput Molecular Device for Zika Virus. *Sci. Rep.* 6, 1–12. doi:10.1038/srep38223

Chang, H. B., Javed, A., Dai, Q., Kappes, J. C., Clemens, T. L., Darley-Usmar, V. M., et al. (2008). Oxidative Stress Induces Vascular Calcification through Modulation of the Osteogenic Transcription Factor Runx2 by AKT Signaling. *J. Biol. Chem.* 283, 15319–15327. doi:10.1074/jbc.M800021200

Chappell, J., Harman, J. L., Narasimhan, V. M., Yu, H., Foote, K., Simons, B. D., et al. (2016). Extensive Proliferation of a Subset of Differentiated, yet Plastic, Medial Vascular Smooth Muscle Cells Contributes to Neointimal Formation in Mouse Injury and Atherosclerosis Models. *Circ. Res.* 119, 1313–1323. doi:10.1161/CIRCRESAHA.116.309799

Chen, Y. S., Ma, Y. D., Chen, C., Shiesh, S. C., and Lee, G. B. (2019). An Integrated Microfluidic System for On-Chip Enrichment and Quantification of Circulating Extracellular Vesicles from Whole Blood. *Lab. Chip* 19, 3305–3315. doi:10.1039/c9lc00624a

Cheow, E. S. H., Cheng, W. C., Lee, C. N., De Kleijn, D., Sorokin, V., and Sze, S. K. (2016). Plasma-derived Extracellular Vesicles Contain Predictive Biomarkers and Potential Therapeutic Targets for Myocardial Ischemic (MI) Injury. *Mol. Cell Proteomics* 15, 2628–2640. doi:10.1074/mcp.M115.055731

Cheung, C., Bernardo, A. S., Trotter, M. W. B., Pedersen, R. A., and Sinha, S. (2012). Generation of Human Vascular Smooth Muscle Subtypes Provides Insight into Embryological Origin-dependent Disease Susceptibility. *Nat. Biotechnol.* 30, 165–173. doi:10.1038/nbt.2107

Cheung, L. S., Sahloul, S., Orozaliev, A., and Song, Y. A. (2018). Rapid Detection and Trapping of Extracellular Vesicles by Electrokinetic Concentration for Liquid Biopsy on Chip. *Micromachines* 9, 306. doi:10.3390/mi9060306

Choy, J. C., Granville, D. J., Hunt, D. W. C., and McManus, B. M. (2001). Endothelial Cell Apoptosis: Biochemical Characteristics and Potential Implications for Atherosclerosis. *J. Mol. Cell Cardiol.* 33, 1673–1690. doi:10.1006/JMCC.2001.1419

Christ, L., Raiborg, C., Wenzel, E. M., Campsteijn, C., and Stenmark, H. (2017). Cellular Functions and Molecular Mechanisms of the ESCRT Membrane-Scission Machinery. *Trends Biochem. Sci.* 42, 42–56. doi:10.1016/j.tibs.2016.08.016

Colombo, M., Moita, C., van Niel, G., Kowal, J., Vigneron, J., Benaroch, P., et al. (2013). Analysis of ESCRT Functions in Exosome Biogenesis, Composition and Secretion Highlights the Heterogeneity of Extracellular Vesicles. *J. Cell Sci.* 126, 5553–5565. doi:10.1242/jcs.128868

Colombo, M., Raposo, G., and Théry, C. (2014). Biogenesis, Secretion, and Intercellular Interactions of Exosomes and Other Extracellular Vesicles. *Annu. Rev. Cell Dev. Biol.* 30, 255–289. doi:10.1146/annurev-cellbio-101512-122326

Cooley, B. C., Nevado, J., Mellad, J., Yang, D., Hilaire, St. C., Negro, A., et al. (2014). TGF-β Signaling Mediates Endothelial-To-Mesenchymal Transition (EndMT) during Vein Graft Remodeling. *Sci. Transl. Med.* 6, 227ra34. doi:10.1126/scitranslmed.3006927

Crowther, C. V., and Hayes, M. A. (2017). Refinement of Insulator-Based Dielectrophoresis. *Analyst* 142, 1608–1618. doi:10.1039/c6an02509a

Currie, G., and Delles, C. (2018). Precision Medicine and Personalized Medicine in Cardiovascular Disease. *Adv. Exp. Med. Biol.* 1065, 589–605. doi:10.1007/978-3-319-77932-4_36

Cvjetkovic, A., Lötvall, J., and Lässer, C. (2014). The Influence of Rotor Type and Centrifugation Time on the Yield and Purity of Extracellular Vesicles. *J. Extracell. Vesicles* 3, 1. doi:10.3402/jev.v3.23111

Dai, X. Y., Zhao, M. M., Cai, Y., Guan, Q. C., Zhao, Y., Guan, Y., et al. (2013). Phosphate-induced Autophagy Counteracts Vascular Calcification by Reducing Matrix Vesicle Release. *Kidney Int.* 83, 1042–1051. doi:10.1038/ki.2012.482

Davies, R. T., Kim, J., Jang, S. C., Choi, E. J., Gho, Y. S., and Park, J. (2012). Microfluidic Filtration System to Isolate Extracellular Vesicles from Blood. *Lab. Chip* 12, 5202–5210. doi:10.1039/c2lc41006k

de Jong, O. G., Verhaar, M. C., Chen, Y., Vader, P., Gremmels, H., Posthuma, G., et al. (2012). Cellular Stress Conditions Are Reflected in the Protein and RNA Content of Endothelial Cell-Derived Exosomes. *J. Extracell. Vesicles* 1, 1. doi:10.3402/jev.v1i0.18396

Del Conde, I., Shrimpton, C. N., Thiagarajan, P., and López, J. A. (2005). Tissue-factor-bearing Microvesicles Arise from Lipid Rafts and Fuse with Activated Platelets to Initiate Coagulation. *Blood* 106, 1604–1611. doi:10.1182/blood-2004-03-1095

Denzer, K., van Eijk, M., Kleijmeer, M. J., Jakobson, E., de Groot, C., and Geuze H, J. (2000). Follicular Dendritic Cells Carry MHC Class II-Expressing Microvesicles at Their Surface. *J. Immunol.* 165, 1259–1265. doi:10.4049/jimmunol.165.3.1259

Di Luca, M., Fitzpatrick, E., Burtenshaw, D., Liu, W., Helt, J. C., Hakimjavadi, R., et al. (2021). The Calcium Binding Protein S100β Marks Hedgehog-Responsive Resident Vascular Stem Cells within Vascular Lesions. *npj Regen. Med.* 6, 10. doi:10.1038/s41536-021-00120-8

Dieudé, M., Bell, C., Turgeon, J., Beillevaire, D., Pomerleau, L., Yang, B., et al. (2015). The 20S Proteasome Core, Active within Apoptotic Exosome-like Vesicles, Induces Autoantibody Production and Accelerates Rejection. *Sci. Transl. Med.* 7, 318ra200. doi:10.1126/scitranslmed.aac9816

Dobnikar, L., Taylor, A. L., Chappell, J., Oldach, P., Harman, J. L., Oerton, E., et al. (2018). Disease-relevant Transcriptional Signatures Identified in Individual Smooth Muscle Cells from Healthy Mouse Vessels. *Nat. Commun.* 9, 1. doi:10.1038/s41467-018-06891-x

Dong, L., Mintz, G. S., Witzenbichler, B., Metzger, D. C., Rinaldi, M. J., Duffy, P. L., et al. (2015). Comparison of Plaque Characteristics in Narrowings with ST-Elevation Myocardial Infarction (STEMI), Non-STEMI/unstable Angina Pectoris and Stable Coronary Artery Disease (From the ADAPT-DES IVUS Substudy). *Am. J. Cardiol.* 115, 860–866. doi:10.1016/j.amjcard.2015.01.008

Dorayappan, K. D. P., Gardner, M. L., Hisey, C. L., Zingarelli, R. A., Smith, B. Q., Lightfoot, M. D. S., et al. (2019). A Microfluidic Chip Enables Isolation of Exosomes and Establishment of Their Protein Profiles and Associated Signaling Pathways in Ovarian Cancer. *Cancer Res.* 79, 3503–3513. doi:10.1158/0008-5472.CAN-18-3538

Doyle, L. M., and Wang, M. Z. (2019). Overview of Extracellular Vesicles, Their Origin, Composition, Purpose, and Methods for Exosome Isolation and Analysis. *Cells* 8, 727. doi:10.3390/cells8070727

Eboigbodin, K. E., Moilanen, K., Elf, S., and Hoser, M. Rapid and Sensitive Real-Time Assay for the Detection of Respiratory Syncytial Virus Using RT-SIBA®. *BMC Infect. Dis.* (2017) 17:134. doi:10.1186/s12879-017-2227-x

Edgar, J. R., Eden, E. R., and Futter, C. E. (2014). Hrs- and CD63-dependent Competing Mechanisms Make Different Sized Endosomal Intraluminal Vesicles. *Traffic* 15, 197–211. doi:10.1111/tra.12139

Escola, J. M., Kleijmeer, M. J., Stoorvogel, W., Griffith, J. M., Yoshie, O., and Geuze, H. J. (1998). Selective Enrichment of Tetraspan Proteins on the Internal Vesicles of Multivesicular Endosomes and on Exosomes Secreted by Human B-Lymphocytes. *J. Biol. Chem.* 273, 20121–20127. doi:10.1074/jbc.273.32.20121

Evrard, S. M., Lecce, L., Michelis, K. C., Nomura-Kitabayashi, A., Pandey, G., Purushothaman, K. R., et al. (2017). Corrigendum: Endothelial to Mesenchymal Transition Is Common in Atherosclerotic Lesions and Is Associated with Plaque Instability. *Nat. Commun.* 8, 14710. doi:10.1038/ncomms14710

Fabrikant, G., Lata, S., Riches, J. D., Briggs, J. A. G., Weissenhorn, W., and Kozlov, M. M. (2009). Computational Model of Membrane Fission Catalyzed by ESCRT-III. *PLoS Comput. Biol.* 5, e1000575. doi:10.1371/journal.pcbi.1000575

Fader, C. M., Sánchez, D. G., Mestre, M. B., and Colombo, M. I. (2009). TI-VAMP/VAMP7 and VAMP3/cellubrevin: Two V-SNARE Proteins Involved in Specific Steps of the Autophagy/multivesicular Body Pathways. *Biochim. Biophys. Acta - Mol. Cell Res.* 1793, 1901–1916. doi:10.1016/j.bbamcr.2009.09.011

Falguières, T., Luyet, P. P., and Gruenberg, J. (2009). Molecular Assemblies and Membrane Domains in Multivesicular Endosome Dynamics. *Exp. Cell Res.* 315, 1567–1573. doi:10.1016/j.yexcr.2008.12.006

Fang, S., Tian, H., Li, X. X., Jin, D., Li, X. X., Kong, J., et al. (2017). Clinical Application of a Microfluidic Chip for Immunocapture and Quantification of Circulating Exosomes to Assist Breast Cancer Diagnosis and Molecular Classification. *PLoS One* 12, e0175050. doi:10.1371/journal.pone.0175050

Feng, D., Zhao, W. L., Ye, Y. Y., Bai, X. C., Liu, R. Q., Chang, L. F., et al. (2010). Cellular Internalization of Exosomes Occurs through Phagocytosis. *Traffic* 11, 675–687. doi:10.1111/j.1600-0854.2010.01041.x

Fernandez-Borja, M., Wubbolts, R., Calafat, J., Janssen, H., Divecha, N., Dusseljee, S., et al. (1999). Multivesicular Body Morphogenesis Requires Phosphatidylinositol 3-kinase Activity. *Curr. Biol.* 9, 55–58. doi:10.1016/S0960-9822(99)80048-7

Fitzner, D., Schnaars, M., Van Rossum, D., Krishnamoorthy, G., Dibaj, P., Bakhti, M., et al. (2011). Selective Transfer of Exosomes from Oligodendrocytes to Microglia by Macropinocytosis. *J. Cell Sci.* 124, 447–458. doi:10.1242/jcs.074088

Fu, L-M., Hou, H-H., Chiu, P-H., and Yang, R-J. (2018). Sample Preconcentration from Dilute Solutions on Micro/nanofluidic Platforms: A Review. *Electrophoresis* 39, 289–310. doi:10.1002/elps.201700340

Galeano-Otero, I., Del Toro, R., Guisado, A., Díaz, I., Mayoral-González, I., Guerrero-Márquez, F., et al. (2020). Circulating miR-320a as a Predictive Biomarker for Left Ventricular Remodelling in STEMI Patients Undergoing Primary Percutaneous Coronary Intervention. *J. Clin. Med.* 9, 1051. doi:10.3390/jcm9041051

Gao, F., Jiao, F., Xia, C., Zhao, Y., Ying, W., Xie, Y., et al. (2019). A Novel Strategy for Facile Serum Exosome Isolation Based on Specific Interactions between Phospholipid Bilayers and TiO 2. *Chem. Sci.* 10, 1579–1588. doi:10.1039/c8sc04197k

Gardiner, C., Vizio, D. Di., Sahoo, S., Théry, C., Witwer, K. W., Wauben, M., et al. (2016). Journal of Extracellular Vesicles Techniques Used for the Isolation and Characterization of Extracellular Vesicles: Results of a Worldwide Survey. *J. Extracell. Vesicles* 5, 32945. doi:10.3402/jev.v5.32945

Giannitsis, E., Clifford, P., Slagman, A., Ruedelstein, R., Liebetrau, C., Hamm, C., et al. (2019). Multicentre Cross-Sectional Observational Registry to Monitor the Safety of Early Discharge after Rule-Out of Acute Myocardial Infarction by Copeptin and Troponin: The Pro-core Registry. *BMJ Open* 9, e028311. doi:10.1136/bmjopen-2018-028311

Goren, Y., Kushnir, M., Zafrir, B., Tabak, S., Lewis, B. S., and Amir, O. (2012). Serum Levels of microRNAs in Patients with Heart Failure. *Eur. J. Heart Fail* 14, 147–154. doi:10.1093/eurjhf/hfr155

Gross, J. C., Chaudhary, V., Bartscherer, K., and Boutros, M. (2012). Active Wnt Proteins Are Secreted on Exosomes. *Nat. Cell Biol.* 14, 1036–1045. doi:10.1038/ncb2574

Halcox, J. P. J., Donald, A. E., Ellins, E., Witte, D. R., Shipley, M. J., Brunner, E. J., et al. (2009). Endothelial Function Predicts Progression of Carotid Intima-Media Thickness. *Circulation* 119, 1005–1012. doi:10.1161/CIRCULATIONAHA.108.765701

Haller, P. M., Jäger, B., Piackova, E., Sztulman, L., Wegberger, C., Wojta, J., et al. (2020). Changes in Circulating Extracellular Vesicles in Patients with St-Elevation Myocardial Infarction and Potential Effects of Remote Ischemic Conditioning-A Randomized Controlled Trial. *Biomedicines* 8, 218. doi:10.3390/BIOMEDICINES8070218

Hampel, H., Goetzl, E. J., Kapogiannis, D., Lista, S., and Vergallo, A. (2019). Biomarker-Drug and Liquid Biopsy Co-development for Disease Staging and Targeted Therapy: Cornerstones for Alzheimer's Precision Medicine and Pharmacology. *Front. Pharmacol.* 10, 310. doi:10.3389/fphar.2019.00310

Harding, C., and Stahl, P. (1983). Transferrin Recycling in Reticulocytes: pH and Iron Are Important Determinants of Ligand Binding and Processing. *Biochem. Biophys. Res. Commun.* 113, 650–658. doi:10.1016/0006-291X(83)91776-X

Hergenreider, E., Heydt, S., Tréguer, K., Boettger, T., Horrevoets, A. J. G., Zeiher, A. M., et al. (2012). Atheroprotective Communication between Endothelial Cells and Smooth Muscle Cells through miRNAs. *Nat. Cell Biol.* 14, 249–256. doi:10.1038/ncb2441

Hooper, C., Sainz-Fuertes, R., Lynham, S., Hye, A., Killick, R., Warley, A., et al. (2012). Wnt3a Induces Exosome Secretion from Primary Cultured Rat Microglia. *BMC Neurosci.* 13, 144. doi:10.1186/1471-2202-13-144

Hoshino, D., Kirkbride, K. C., Costello, K., Clark, E. S., Sinha, S., Grega-Larson, N., et al. (2013). Exosome Secretion Is Enhanced by Invadopodia and Drives Invasive Behavior. *Cell Rep.* 5, 1159–1168. doi:10.1016/j.celrep.2013.10.050

Howard, B. V., Robbins, D. C., Sievers, M. L., Lee, E. T., Rhoades, D., Devereux, R. B., et al. (2000). LDL Cholesterol as a Strong Predictor of Coronary Heart Disease in Diabetic Individuals with Insulin Resistance and Low LDL: The Strong Heart Study. *Arterioscler. Thromb. Vasc. Biol.* 20, 830–835. doi:10.1161/01.ATV.20.3.830

Hromada, C., Mühleder, S., Grillari, J., Redl, H., and Holnthoner, W. (2017). Endothelial Extracellular Vesicles-Promises and Challenges. *Front. Physiol.* 8, 275. doi:10.3389/fphys.2017.00275

Hsu, C., Morohashi, Y., Yoshimura, S. I., Manrique-Hoyos, N., Jung, S. Y., Lauterbach, M. A., et al. (2010). Regulation of Exosome Secretion by Rab35 and its GTPase-Activating Proteins TBC1D10A-C. *J. Cell Biol.* 189, 223–232. doi:10.1083/jcb.200911018

Hu, C. T., Shao, Y. D., Liu, Y. Z., Xiao, X., Cheng, Z. Bin., Qu, S. L., et al. (2021). Oxidative Stress in Vascular Calcification. *Clin. Chim. Acta* 519, 101–110. doi:10.1016/j.cca.2021.04.012

Hurley, J. H., and Hanson, P. I. (2010). Membrane Budding and Scission by the ESCRT Machinery: It's All in the Neck. *Nat. Rev. Mol. Cell Biol.* 11, 556–566. doi:10.1038/nrm2937

Ibsen, S. D., Wright, J., Lewis, J. M., Kim, S., Ko, S. Y., Ong, J., et al. (2017). Rapid Isolation and Detection of Exosomes and Associated Biomarkers from Plasma. *ACS Nano* 11, 6641–6651. doi:10.1021/acsnano.7b00549

Im, H., Shao, H., Park, Y. Il., Peterson, V. M., Castro, C. M., Weissleder, R., et al. (2014). Label-free Detection and Molecular Profiling of Exosomes with a Nano-Plasmonic Sensor. *Nat. Biotechnol.* 32, 490–495. doi:10.1038/nbt.2886

Jahn, R., and Scheller, R. H. (2006). SNAREs - Engines for Membrane Fusion. *Nat. Rev. Mol. Cell Biol.* 7, 631–643. doi:10.1038/nrm2002

Jansen, F., Nickenig, G., and Werner, N. (2017). Extracellular Vesicles in Cardiovascular Disease. *Circ. Res.* 120, 1649–1657. doi:10.1161/CIRCRESAHA.117.310752

Jiang, W., Zhang, Z., Li, Y., Chen, C., Yang, H., Lin, Q., et al. (2021). The Cell Origin and Role of Osteoclastogenesis and Osteoblastogenesis in Vascular Calcification. *Front. Cardiovasc Med.* 8, 639740. doi:10.3389/fcvm.2021.639740

Johnstone, R. M., Adam, M., Hammond, J. R., Orr, L., and Turbide, C. (1987). Vesicle Formation during Reticulocyte Maturation. Association of Plasma Membrane Activities with Released Vesicles (Exosomes). *J. Biol. Chem.* 262, 9412–9420. doi:10.1016/s0021-9258(18)48095-7

Kalluri, R., and LeBleu, V. S. (2020). The Biology, Function, and Biomedical Applications of Exosomes. *Science* 367, eaau6977. doi:10.1126/science.aau6977

Kalra, H., Simpson, R. J., Ji, H., Aikawa, E., Altevogt, P., Askenase, P., et al. (2012). Vesiclepedia: A Compendium for Extracellular Vesicles with Continuous Community Annotation. *PLoS Biol.* 10, e1001450. doi:10.1371/journal.pbio.1001450

Kanhai, D. A., Visseren, F. L. J., Van Der Graaf, Y., Schoneveld, A. H., Catanzariti, L. M., Timmers, L., et al. (2013). Microvesicle Protein Levels Are Associated with Increased Risk for Future Vascular Events and Mortality in Patients with Clinically Manifest Vascular Disease. *Int. J. Cardiol.* 168, 2358–2363. doi:10.1016/j.ijcard.2013.01.231

Kapustin, A. N., and Shanahan, C. M. (2016). Emerging Roles for Vascular Smooth Muscle Cell Exosomes in Calcification and Coagulation. *J. Physiol.* 594, 2905–2914. doi:10.1113/JP271340

Kerr, J. F. R., Wyllie, A. H., and Currie, A. R. (1972). Apoptosis: A Basic Biological Phenomenon with Wide-Ranging Implications in Tissue Kinetics. *Br. J. Cancer* 26, 239–257. doi:10.1038/bjc.1972.33

Kim, D. K., Kang, B., Kim, O. Y., Choi, D. S., Lee, J., Kim, S. R., et al. (2013). EVpedia: An Integrated Database of High-Throughput Data for Systemic Analyses of Extracellular Vesicles. *J. Extracell. Vesicles* 2, 1. doi:10.3402/jev.v2i0.20384

King, H. W., Michael, M. Z., Gleadle, J. M., and King, H. W. (2012). Hypoxic Enhancement of Exosome Release by Breast Cancer Cells. *BMC Cancer* 12, 421. doi:10.1186/1471-2407-12-421

Koles, K., Nunnari, J., Korkut, C., Barria, R., Brewer, C., Li, Y., et al. (2012). Mechanism of Evenness Interrupted (Evi)-Exosome Release at Synaptic Boutons. *J. Biol. Chem.* 287, 16820–16834. doi:10.1074/jbc.M112.342667

Konoshenko, M. Y., Lekchnov, E. A., Vlassov, A. V., and Laktionov, P. P. (2018). Isolation of Extracellular Vesicles: General Methodologies and Latest Trends. *Biomed. Res. Int.* 2018, 8545347. doi:10.1155/2018/8545347

Korshunov, V. A., and Berk, B. C. (2003). Flow-Induced Vascular Remodeling in the Mouse. *Atvb* 23, 2185–2191. doi:10.1161/01.ATV.0000103120.06092.14

Kowal, J., Arras, G., Colombo, M., Jouve, M., Morath, J. P., Primdal-Bengtson, B., et al. (2016). Proteomic Comparison Defines Novel Markers to Characterize Heterogeneous Populations of Extracellular Vesicle Subtypes. *Proc. Natl. Acad. Sci.* 113, E968–E977. doi:10.1073/pnas.1521230113

Kramann, R., Goettsch, C., Wongboonsin, J., Iwata, H., Schneider, R. K., Kuppe, C., et al. (2016). Adventitial MSC-like Cells Are Progenitors of Vascular Smooth Muscle Cells and Drive Vascular Calcification in Chronic Kidney Disease. *Cell Stem Cell* 19, 628–642. doi:10.1016/j.stem.2016.08.001

Ku, A., Lim, H. C., Evander, M., Lilja, H., Laurell, T., Scheding, S., et al. (2018). Acoustic Enrichment of Extracellular Vesicles from Biological Fluids. *Anal. Chem.* 90, 8011–8019. doi:10.1021/acs.analchem.8b00914

Kulkarni, M., Flašker, A., Lokar, M., Mrak-Poljšak, K., Mazare, A., Artenjak, A., et al. (2015). Binding of Plasma Proteins to Titanium Dioxide Nanotubes with Different Diameters. *Int. J. Nanomedicine* 10, 1359–1373. doi:10.2147/IJN.S77492

Kuwabara, Y., Ono, K., Horie, T., Nishi, H., Nagao, K., Kinoshita, M., et al. (2011). Increased microRNA-1 and microRNA-133a Levels in Serum of Patients with Cardiovascular Disease Indicate Myocardial Damage. *Circ. Cardiovasc Genet.* 4, 446–454. doi:10.1161/CIRCGENETICS.110.958975

Lan, T.-H., Huang, X.-Q., and Tan, H.-M. (2013). Vascular Fibrosis in Atherosclerosis. *Cardiovasc. Pathol.* 22, 401–407. doi:10.1016/j.carpath.2013.01.003

Lea, J., Sharma, R., Yang, F., Zhu, H., Sally Ward, E., Schroit, A. J., et al. (2017). Detection of Phosphatidylserine-Positive Exosomes as a Diagnostic Marker for Ovarian Malignancies: a Proof of Concept Study. *Oncotarget* 8, 14395–14407. doi:10.18632/oncotarget.14795

Lespagnol, A., Duflaut, D., Beekman, C., Blanc, L., Fiucci, G., Marine, J-C. C., et al. (2008). Exosome Secretion, Including the DNA Damage-Induced P53-dependent Secretory Pathway, Is Severely Compromised in TSAP6/Steap3-Null Mice. *Cell Death Differ.* 15, 1723–1733. doi:10.1038/cdd.2008.104

Leszczynska, A., and Mary Murphy, J. (2018). Vascular Calcification: Is it rather a Stem/progenitor Cells Driven Phenomenon? *Front. Bioeng. Biotechnol.* 6, 639740. doi:10.3389/fbioe.2018.00010

Lewis, J. M., Vyas, A. D., Qiu, Y., Messer, K. S., White, R., and Heller, M. J. (2018). Integrated Analysis of Exosomal Protein Biomarkers on Alternating Current Electrokinetic Chips Enables Rapid Detection of Pancreatic Cancer in Patient Blood. *ACS Nano* 12, 3311–3320. doi:10.1021/acsnano.7b08199

Li, H., Liao, Y., Gao, L., Zhuang, T., Huang, Z., Zhu, H., et al. (2018). Coronary Serum Exosomes Derived from Patients with Myocardial Ischemia Regulate Angiogenesis through the miR-939-Mediated Nitric Oxide Signaling Pathway. *Theranostics* 8, 2079–2093. doi:10.7150/thno.21895

Li, J. F., Zhang, Y. J., Ding, S. Y., Panneerselvam, R., and Tian, Z. Q. (2017). Core-shell Nanoparticle-Enhanced Raman Spectroscopy. *Chem. Rev.* 117, 5002–5069. doi:10.1021/acs.chemrev.6b00596

Liégeois, S., Benedetto, A., Garnier, J. M., Schwab, Y., and Labouesse, M. (2006). The V0-ATPase Mediates Apical Secretion of Exosomes Containing Hedgehog-Related Proteins in Caenorhabditis elegans. *J. Cell Biol.* 173, 949–961. doi:10.1083/jcb.200511072

Lim, J., Choi, M., Lee, H., Kim, Y. H., Han, J. Y., Lee, E. S., et al. (2019). Direct Isolation and Characterization of Circulating Exosomes from Biological Samples Using Magnetic Nanowires. *J. Nanobiotechnology* 17, 1–12. doi:10.1186/s12951-018-0433-3

Lin, X., Li, S., Wang, Y. J., Wang, Y., Zhong, J. Y., He, J. Y., et al. (2019). Exosomal Notch3 from High Glucose-Stimulated Endothelial Cells Regulates Vascular Smooth Muscle Cells Calcification/aging. *Life Sci.* 232, 116582. doi:10.1016/J.LFS.2019.116582

Liu, W., Redmond, E. M., Morrow, D., and Cullen, J. P. (2011). Differential Effects of Daily-Moderate versus Weekend-Binge Alcohol Consumption on Atherosclerotic Plaque Development in Mice. *Atherosclerosis* 219, 448–454. doi:10.1016/j.atherosclerosis.2011.08.034

Liu, Y., Li, Q., Hosen, M. R., Zietzer, A., Flender, A., Levermann, P., et al. (2019). Atherosclerotic Conditions Promote the Packaging of Functional MicroRNA-92a-3p into Endothelial Microvesicles. *Circ. Res.* 124, 575–587. doi:10.1161/CIRCRESAHA.118.314010

Lonborg, J., Schoos, M. M., Kelbæk, H., Holmvang, L., Steinmetz, J., Vejlstrup, N., et al. (2012). Impact of System Delay on Infarct Size, Myocardial Salvage Index, and Left Ventricular Function in Patients with ST-Segment Elevation

Myocardial Infarction. *Am. Heart J.* 164, 538–546. doi:10.1016/j.ahj.2012.07.021

Majesky, M. W., Horita, H., Ostriker, A., Lu, S., Regan, J. N., Bagchi, A., et al. (2017). Differentiated Smooth Muscle Cells Generate a Subpopulation of Resident Vascular Progenitor Cells in the Adventitia Regulated by Klf4. *Circ. Res.* 120, 296–311. doi:10.1161/CIRCRESAHA.116.309322

Mallat, Z., Benamer, H., Hugel, B., Benessiano, J., Steg, P. G., Freyssinet, J. M., et al. (2000). Elevated Levels of Shed Membrane Microparticles with Procoagulant Potential in the Peripheral Circulating Blood of Patients with Acute Coronary Syndromes. *Circulation* 101, 841–843. doi:10.1161/01.CIR.101.8.841

Mallia, A., Gianazza, E., Zoanni, B., Brioschi, M., Barbieri, S. S., and Banfi, C. (2020). Proteomics of Extracellular Vesicles: Update on Their Composition, Biological Roles and Potential Use as Diagnostic Tools in Atherosclerotic Cardiovascular Diseases. *Diagnostics* 10, 843. doi:10.3390/diagnostics10100843

Marczak, S., Richards, K., Ramshani, Z., Smith, E., Senapati, S., Hill, R., et al. (2018). Simultaneous Isolation and Preconcentration of Exosomes by Ion Concentration Polarization. *Electrophoresis* 39, 2029–2038. doi:10.1002/elps.201700491

Mathivanan, S., and Simpson, R. J. (2009). ExoCarta: A Compendium of Exosomal Proteins and RNA. *Proteomics* 9, 4997–5000. doi:10.1002/pmic.200900351

Matsumoto, S., Sakata, Y., Suna, S., Nakatani, D., Usami, M., Hara, M., et al. (2013). Circulating P53-Responsive MicroRNAs Are Predictive Indicators of Heart Failure after Acute Myocardial Infarction. *Circ. Res.* 113 (3), 322–326. doi:10.1161/CIRCRESAHA.113.301209

McGough, I. J., and Vincent, J-P. P. (2016). Exosomes in Developmental Signalling. *Development* 143, 2482–2493. doi:10.1242/dev.126516

Meister, M., Bänfer, S., Gärtner, U., Koskimies, J., Amaddii, M., Jacob, R., et al. (2017). Regulation of Cargo Transfer between ESCRT-0 and ESCRT-I Complexes by Flotillin-1 during Endosomal Sorting of Ubiquitinated Cargo. *Oncogenesis* 6, e344. doi:10.1038/oncsis.2017.47

Messenger, S. W., Woo, S. S., Sun, Z., and Martin, T. F. J. J. (2018). A Ca2+-Stimulated Exosome Release Pathway in Cancer Cells Is Regulated by Munc13-4. *J. Cell Biol.* 217, 2877–2890. doi:10.1083/jcb.201710132

Migneault, F., Dieudé, M., Turgeon, J., Beillevaire, D., Hardy, M. P., Brodeur, A., et al. (2020). Apoptotic Exosome-like Vesicles Regulate Endothelial Gene Expression, Inflammatory Signaling, and Function through the NF-Kb Signaling Pathway. *Sci. Rep.* 10, 1–15. doi:10.1038/s41598-020-69548-0

Molony, C., King, D., Di Luca, M., Kitching, M., Olayinka, A., Hakimjavadi, R., et al. (2021). Disease-Relevant Single Cell Photonic Signatures Identify S100β Stem Cells and Their Myogenic Progeny in Vascular Lesions. *Stem Cell Rev. Rep.* 17, 1713–1740. doi:10.1007/S12015-021-10125-X/FIGURES/10

Muralidharan-Chari, V., Clancy, J. W., Sedgwick, A., and D'Souza-Schorey, C. (2010). Microvesicles: Mediators of Extracellular Communication during Cancer Progression. *J. Cell Sci.* 123, 1603–1611. doi:10.1242/jcs.064386

Nakagawa, K., and Nakashima, Y. (2018). Pathologic Intimal Thickening in Human Atherosclerosis Is Formed by Extracellular Accumulation of Plasma-Derived Lipids and Dispersion of Intimal Smooth Muscle Cells. *Atherosclerosis* 274, 235–242. doi:10.1016/j.atherosclerosis.2018.03.039

Nakai, W., Yoshida, T., Diez, D., Miyatake, Y., Nishibu, T., Imawaka, N., et al. (2016). A Novel Affinity-Based Method for the Isolation of Highly Purified Extracellular Vesicles. *Sci. Rep.* 6, 1–11. doi:10.1038/srep33935

Nakashima, Y., Wight, T. N., and Sueishi, K. (2008). Early Atherosclerosis in Humans: Role of Diffuse Intimal Thickening and Extracellular Matrix Proteoglycans. *Cardiovasc Res.* 79, 14–23. doi:10.1093/cvr/cvn099

Nam, D., Ni, C.-W., Rezvan, A., Suo, J., Budzyn, K., Llanos, A., et al. (2009). Partial Carotid Ligation Is a Model of Acutely Induced Disturbed Flow, Leading to Rapid Endothelial Dysfunction and Atherosclerosis. *Am. J. Physiology-Heart Circulatory Physiology* 297, H1535–H1543. doi:10.1152/ajpheart.00510.2009

Nanbo, A., Kawanishi, E., Yoshida, R., and Yoshiyama, H. (2013). Exosomes Derived from Epstein-Barr Virus-Infected Cells Are Internalized via Caveola-dependent Endocytosis and Promote Phenotypic Modulation in Target Cells. *J. Virol.* 87, 10334–10347. doi:10.1128/jvi.01310-13

Nemenoff, R. A., Horita, H., Ostriker, A. C., Furgeson, S. B., Simpson, P. A., Vanputten, V., et al. (2011). SDF-1α Induction in Mature Smooth Muscle Cells by Inactivation of PTEN Is a Critical Mediator of Exacerbated Injury-Induced Neointima Formation. *Arterioscler. Thromb. Vasc. Biol.* 31, 1300–1308. doi:10.1161/ATVBAHA.111.223701

Ostrowski, M., Carmo, N. B., Krumeich, S., Fanget, I., Raposo, G., Savina, A., et al. (2010). Rab27a and Rab27b Control Different Steps of the Exosome Secretion Pathway. *Nat. Cell Biol.* 12, 19–30. doi:10.1038/ncb2000

Pan, B. T., Teng, K., Wu, C., Adam, M., and Johnstone, R. M. (1985). Electron Microscopic Evidence for Externalization of the Transferrin Receptor in Vesicular Form in Sheep Reticulocytes. *J. Cell Biol.* 101, 942–948. doi:10.1083/jcb.101.3.942

Pang, Y., Shi, J., Yang, X., Wang, C., Sun, Z., and Xiao, R. (2020). Personalized Detection of Circling Exosomal PD-L1 Based on Fe3O4@TiO2 Isolation and SERS Immunoassay. *Biosens. Bioelectron.* 148, 1–9. doi:10.1016/j.bios.2019.111800

Papendick, C., Blyth, A., Seshadri, A., Edmonds, M. J. R., Briffa, T., Cullen, L., et al. (2017). A Randomized Trial of a 1-hour Troponin T Protocol in Suspected Acute Coronary Syndromes: Design of the Rapid Assessment of Possible ACS in the Emergency Department with High Sensitivity Troponin T (RAPID-TnT) Study. *Am. Heart J.* 190, 25–33. doi:10.1016/j.ahj.2017.05.004

Patel, G. K., Khan, M. A., Zubair, H., Srivastava, S. K., Khushman, M., Singh, S., et al. (2019). Comparative Analysis of Exosome Isolation Methods Using Culture Supernatant for Optimum Yield, Purity and Downstream Applications. *Sci. Rep.* 9, 5335. doi:10.1038/s41598-019-41800-2

Peters, P. J., Geuze, H. J., Van Donk, H. A. D., Slot, J. W., Griffith, J. M., Stam, N. J., et al. (1989). Molecules Relevant for T Cell-target Cell Interaction Are Present in Cytolytic Granules of Human T Lymphocytes. *Eur. J. Immunol.* 19, 1469–1475. doi:10.1002/eji.1830190819

Pethig, R. (2017). "How Does Dielectrophoresis Differ from Electrophoresis?," in *Dielectrophoresis Theory, Methodology and Biological Applications* (UK: John Wiley & Sons), 31–48. doi:10.1002/9781118671443.ch2

Pfeffer, S. R. (2007). Unsolved Mysteries in Membrane Traffic. *Annu. Rev. Biochem.* 76, 629–645. doi:10.1146/annurev.biochem.76.061705.130002

Phadwal, K., Feng, D., Zhu, D., and MacRae, V. E. (2020). Autophagy as a Novel Therapeutic Target in Vascular Calcification. *Pharmacol. Ther.* 206, 107430. doi:10.1016/j.pharmthera.2019.107430

Pols, M. S., and Klumperman, J. (2009). Trafficking and Function of the Tetraspanin CD63. *Exp. Cell Res.* 315, 1584–1592. doi:10.1016/j.yexcr.2008.09.020

Qian, S., You, S., Sun, Y., Wu, Q., Wang, X., Tang, W., et al. (2021). Remnant Cholesterol and Common Carotid Artery Intima-Media Thickness in Patients with Ischemic Stroke. *Circ. Cardiovasc Imaging* 14, e010953. doi:10.1161/circimaging.120.010953

Qin, Z., Liao, R., Xiong, Y., Jiang, L., Li, J., Wang, L., et al. (2021). A Narrative Review of Exosomes in Vascular Calcification. *Ann. Transl. Med.* 9, 579. doi:10.21037/atm-20-7355

Qu, B., and Qu, T. (2015). Causes of Changes in Carotid Intima-Media Thickness: a Literature Review. *Cardiovasc Ultrasound* 13, 46. doi:10.1186/s12947-015-0041-4

Quek, C., Bellingham, S. A., Jung, C. H., Scicluna, B. J., Shambrook, M. C., Sharples, R. A., et al. (2017). Defining the Purity of Exosomes Required for Diagnostic Profiling of Small RNA Suitable for Biomarker Discovery. *RNA Biol.* 14, 245–258. doi:10.1080/15476286.2016.1270005

Ramshani, Z., Zhang, C., Richards, K., Chen, L., Xu, G., Stiles, B. L., et al. (2019). Extracellular Vesicle microRNA Quantification from Plasma Using an Integrated Microfluidic Device. *Commun. Biol.* 2, 1–9. doi:10.1038/s42003-019-0435-1

Reátegui, E., Van Der Vos, K. E., Lai, C. P., Zeinali, M., Atai, N. A., Aldikacti, B., et al. (2018). Engineered Nanointerfaces for Microfluidic Isolation and Molecular Profiling of Tumor-specific Extracellular Vesicles. *Nat. Commun.* 9, 175. doi:10.1038/s41467-017-02261-1

Ridger, V. C., Boulanger, C. M., Angelillo-Scherrer, A., Badimon, L., Blanc-Brude, O., Bochaton-Piallat, M. L., et al. (2017). Microvesicles in Vascular Homeostasis and Diseases Position Paper of the European Society of Cardiology (ESC) Working Group on Atherosclerosis and Vascular Biology. *Thromb. Haemost.* 117, 1296–1316. doi:10.1160/TH16-12-0943

Riley, R. F., Miller, C. D., Russell, G. B., Harper, E. N., Hiestand, B. C., Hoekstra, J. W., et al. (2017). Cost Analysis of the History, ECG, Age, Risk Factors, and Initial Troponin (HEART) Pathway Randomized Control Trial. *Am. J. Emerg. Med.* 35, 77–81. doi:10.1016/j.ajem.2016.10.005

Sáez, T., de Vos, P., Kuipers, J., Sobrevia, L., and Faas, M. M. (2019). Exosomes Derived from Monocytes and from Endothelial Cells Mediate Monocyte and

Endothelial Cell Activation under High D-Glucose Conditions. *Immunobiology* 224, 325–333. doi:10.1016/j.imbio.2019.02.004

Savina, A., Furlán, M., Vidal, M., and Colombo, M. I. (2003). Exosome Release Is Regulated by a Calcium-dependent Mechanism in K562 Cells. *J. Biol. Chem.* 278, 20083–20090. doi:10.1074/jbc.M301642200

Savina, A., Vidal, M., and Colombo, M. I. (2002). The Exosome Pathway in K562 Cells Is Regulated by Rab11. *J. Cell Sci.* 115, 2505–2515. doi:10.1242/jcs.115.12.2505

Shao, H., Chung, J., Lee, K., Balaj, L., Min, C., Carter, B. S., et al. (2015). Chip-based Analysis of Exosomal mRNA Mediating Drug Resistance in Glioblastoma. *Nat. Commun.* 6, 1–9. doi:10.1038/ncomms7999

Sheldon, H., Heikamp, E., Turley, H., Dragovic, R., Thomas, P., Oon, C. E., et al. (2010). New Mechanism for Notch Signaling to Endothelium at a Distance by Delta-like 4 Incorporation into Exosomes. *Blood* 116, 2385–2394. doi:10.1182/blood-2009-08-239228

Shi, L., Kuhnell, D., Borra, V. J., Langevin, S. M., Nakamura, T., and Esfandiari, L. (2019). Rapid and Label-free Isolation of Small Extracellular Vesicles from Biofluids Utilizing a Novel Insulator Based Dielectrophoretic Device. *Lab. Chip* 19, 3726–3734. doi:10.1039/c9lc00902g

Shu, S. La., Yang, Y., Allen, C. L., Hurley, E., Tung, K. H., Minderman, H., et al. (2020). Purity and Yield of Melanoma Exosomes Are Dependent on Isolation Method. *J. Extracell. Vesicles* 9, 1692401. doi:10.1080/20013078.2019.1692401

Üygarden, H. (2017). Carotid Intima-MediacThickness and Prediction of Cardiovascular Disease. *J. Amer. Heart. Assoc.* 6(1), e005313. doi:10.1161/JAHA.116.005313

Simpson, R. J., Lim, J. W. E., Moritz, R. L., and Mathivanan, S. (2009). Exosomes: Proteomic Insights and Diagnostic Potential. *Expert Rev. Proteomics* 6, 267–283. doi:10.1586/epr.09.17

Singer, A. J., Ardise, J., Gulla, J., and Cangro, J. (2005). Point-of-care Testing Reduces Length of Stay in Emergency Department Chest Pain Patients. *Ann. Emerg. Med.* 45, 587–591. doi:10.1016/j.annemergmed.2004.11.020

Singh, T., Chapman, A. R., Dweck, M. R., Mills, N. L., and Newby, D. E. (2021). MINOCA: A Heterogenous Group of Conditions Associated with Myocardial Damage. *Heart* 107 (18), 1458–1464. doi:10.1136/heartjnl-2020-318269

Sinha, S., Hoshino, D., Hong, N. H., Kirkbride, K. C., Grega-Larson, N. E., Seiki, M., et al. (2016). Cortactin Promotes Exosome Secretion by Controlling Branched Actin Dynamics. *J. Cell Biol.* 214, 197–213. doi:10.1083/jcb.201601025

Srivastava, P. (2002). Interaction of Heat Shock Proteins with Peptides and Antigen Presenting Cells: Chaperoning of the Innate and Adaptive Immune Responses. *Annu. Rev. Immunol.* 20, 395–425. doi:10.1146/annurev.immunol.20.100301.064801

Stenmark, H. (2009). Rab GTPases as Coordinators of Vesicle Traffic. *Nat. Rev. Mol. Cell Biol.* 10, 513–525. doi:10.1038/nrm2728

Stuffers, S., Sem Wegner, C., Stenmark, H., and Brech, A. (2009). Multivesicular Endosome Biogenesis in the Absence of ESCRTs. *Traffic* 10, 925–937. doi:10.1111/j.1600-0854.2009.00920.x

Sunkara, V., Kim, C. J., Park, J., Woo, H. K., Kim, D., Ha, H. K., et al. (2019). Fully Automated, Label-free Isolation of Extracellular Vesicles from Whole Blood for Cancer Diagnosis and Monitoring. *Theranostics* 9, 1851–1863. doi:10.7150/thno.32438

Svensson, K. J., Christianson, H. C., Wittrup, A., Bourseau-Guilmain, E., Lindqvist, E., Svensson, L. M., et al. (2013). Exosome Uptake Depends on ERK1/2-Heat Shock Protein 27 Signaling and Lipid Raft-Mediated Endocytosis Negatively Regulated by Caveolin-1. *J. Biol. Chem.* 288, 17713–17724. doi:10.1074/jbc.M112.445403

Takasugi, M. (2018). Emerging Roles of Extracellular Vesicles in Cellular Senescence and Aging. *Aging Cell* 17, e12734. doi:10.1111/acel.12734

Tamai, K., Tanaka, N., Nakano, T., Kakazu, E., Kondo, Y., Inoue, J., et al. (2010). Exosome Secretion of Dendritic Cells Is Regulated by Hrs, an ESCRT-0 Protein. *Biochem. Biophys. Res. Commun.* 399, 384–390. doi:10.1016/j.bbrc.2010.07.083

Tang, J., Wang, H., Huang, X., Li, F., Zhu, H., Li, Y., et al. (2020). Arterial Sca1+ Vascular Stem Cells Generate De Novo Smooth Muscle for Artery Repair and Regeneration. *Cell Stem Cell* 26, 81–96. e4. doi:10.1016/j.stem.2019.11.010

Tang, N., Sun, B., Gupta, A., Rempel, H., and Pulliam, L. (2016). Monocyte Exosomes Induce Adhesion Molecules and Cytokines via Activation of NF-Kb in Endothelial Cells. *FASEB J.* 30, 3097–3106. doi:10.1096/fj.201600368RR

Tang, Z., Wang, A., Yuan, F., Yan, Z., Liu, B., Chu, J. S., et al. (2012). Differentiation of Multipotent Vascular Stem Cells Contributes to Vascular Diseases. *Nat. Commun.* 3, 875. doi:10.1038/ncomms1867

Tietjen, G. T., Gong, Z., Chen, C-H. H., Vargas, E., Crooks, J. E., Cao, K. D., et al. (2014). Molecular Mechanism for Differential Recognition of Membrane Phosphatidylserine by the Immune Regulatory Receptor Tim4. *Proc. Natl. Acad. Sci. U. S. A.* 111, E1463–E1472. doi:10.1073/pnas.1320174111

Touboul, P.-J., Labreuche, J., Vicaut, E., Amarenco, P., and Genic Investigators (2005). Carotid Intima-Media Thickness, Plaques, and Framingham Risk Score as Independent Determinants of Stroke Risk. *Stroke* 36, 1741–1745. doi:10.1161/01.STR.0000174490.23495.57

Trajkovic, K., Hsu, C., Chiantia, S., Rajendran, L., Wenzel, D., Wieland, F., et al. (2008). Ceramide Triggers Budding of Exosome Vesicles into Multivesicular Endosomes. *Science* 319, 1244–1247. doi:10.1126/science.1153124

Ushio-Fukai, M., and Urao, N. (2009). Novel Role of NADPH Oxidase in Angiogenesis and Stem/Progenitor Cell Function. *Antioxid. Redox Signal* 11, 2517–2533. doi:10.1089/ars.2009.2582

Valadi, H., Ekström, K., Bossios, A., Sjöstrand, M., Lee, J. J., and Lötvall, J. O. (2007). Exosome-mediated Transfer of mRNAs and microRNAs Is a Novel Mechanism of Genetic Exchange between Cells. *Nat. Cell Biol.* 9, 654–659. doi:10.1038/ncb1596

van den Oord, S. C. H., Sijbrands, E. J. G., ten Kate, G. L., van Klaveren, D., van Domburg, R. T., van der Steen, A. F. W., et al. (2013). Carotid Intima-Media Thickness for Cardiovascular Risk Assessment: Systematic Review and Meta-Analysis. *Atherosclerosis* 228, 1–11. doi:10.1016/j.atherosclerosis.2013.01.025

van der Pol, E., Boing, A. N., Harrison, P., Sturk, A., Nieuwland, R., Böing, A. N., et al. (2012). Classification, Functions, and Clinical Relevance of Extracellular Vesicles. *Pharmacol. Rev.* 64, 676–705. doi:10.1124/pr.112.005983

Verma, M., Lam, T. K., Hebert, E., and Divi, R. L. (2015). Extracellular Vesicles: Potential Applications in Cancer Diagnosis, Prognosis, and Epidemiology. *BMC Clin. Pathol.* 15, 6. doi:10.1186/s12907-015-0005-5

Vidal, M., Sainte-Marie, J., Philippot, J. R., and Bienvenue, A. (1989). Asymmetric Distribution of Phospholipids in the Membrane of Vesicles Released during In Vitro Maturation of guinea Pig Reticulocytes: Evidence Precluding a Role for "Aminophospholipid Translocase. *J. Cell Physiol.* 140, 455–462. doi:10.1002/jcp.1041400308

Wan, M., Li, C., Zhen, G., Jiao, K., He, W., Jia, X., et al. (2012). Injury-activated Transforming Growth Factor β Controls Mobilization of Mesenchymal Stem Cells for Tissue Remodeling. *Stem Cells* 30, 2498–2511. doi:10.1002/stem.1208

Wan, Y., Maurer, M., He, H. Z., Xia, Y. Q., Hao, S. J., Zhang, W. L., et al. (2019). Enrichment of Extracellular Vesicles with Lipid Nanoprobe Functionalized Nanostructured Silica. *Lab. Chip* 19, 2346–2355. doi:10.1039/c8lc01359d

Wang, G. K., Zhu, J. Q., Zhang, J. T., Li, Q., Li, Y., He, J., et al. (2010). Circulating microRNA: A Novel Potential Biomarker for Early Diagnosis of Acute Myocardial Infarction in Humans. *Eur. Heart J.* 31, 659–666. doi:10.1093/eurheartj/ehq013

Wang, Z., Li, F., Rufo, J., Chen, C., Yang, S., Li, L., et al. (2020). Acoustofluidic Salivary Exosome Isolation: A Liquid Biopsy Compatible Approach for Human Papillomavirus–Associated Oropharyngeal Cancer Detection. *J. Mol. Diagn.* 22, 50–59. doi:10.1016/j.jmoldx.2019.08.004

Webber, J., and Clayton, A. (2013). How Pure Are Your Vesicles? *J. Extracell. Vesicles* 2, 19861. doi:10.3402/jev.v2i0.19861

Welcher, R. (2019). Use of Companion Diagnostics (CDx) and Predictive Biomarkers for Cancer Targeted Therapy: Clinical Applications in Precision Medicine. *Predict. Biomarkers Oncol.* 49, 539–551. doi:10.1007/978-3-319-95228-4_49

Wong, P. F., Tong, K. L., Jamal, J., Khor, E. S., Lai, S. L., and Mustafa, M. R. (2019). Senescent HUVECs-Secreted Exosomes Trigger Endothelial Barrier Dysfunction in Young Endothelial Cells. *EXCLI J.* 18, 764. doi:10.17179/EXCLI2019-1505

Yu, W., Hurley, J., Roberts, D., Chakrabortty, S. K., Enderle, D., Noerholm, M., et al. (2021). Exosome-based Liquid Biopsies in Cancer: Opportunities and Challenges. *Ann. Oncol. Off. J. Eur. Soc. Med. Oncol.* 32, 466. doi:10.1016/J.ANNONC.2021.01.074

Yuan, F., Wang, D., Xu, K., Wang, J., Zhang, Z., Yang, L., et al. (2017). Contribution of Vascular Cells to Neointimal Formation. *PLoS One* 12, e0168914. doi:10.1371/journal.pone.0168914

Yuana, Y., Sturk, A., and Nieuwland, R. (2013). Extracellular Vesicles in Physiological and Pathological Conditions. *Blood Rev.* 27, 31–39. doi:10.1016/j.blre.2012.12.002

Zaqout, M. S. K. K., Sumizawa, T., Igisu, H., Higash, T., Myojo, T., Higashi, T., et al. (2011). Binding of Human Serum Proteins to Titanium Dioxide Particles In Vitro. *J. Occup. Health* 53 (2), 75–83. doi:10.1539/joh.L10034

Zarà, M., Amadio, P., Campodonico, J., Sandrini, L., and Barbieri, S. S. (2020). Exosomes in Cardiovascular Diseases. *Diagnostics* 10, 943. doi:10.3390/diagnostics10110943

Zhang, C., Zhang, K., Huang, F., Feng, W., Chen, J., Zhang, H., et al. (2018). Exosomes, the Message Transporters in Vascular Calcification. *J. Cell Mol. Med.* 22, 4024–4033. doi:10.1111/jcmm.13692

Zhang, H., Chang, H., and Neuzil, P. (2019). DEP-on-a-chip: Dielectrophoresis Applied to Microfluidic Platforms. *Micromachines* 10, 423. doi:10.3390/mi10060423

Zhang, P., He, M., and Zeng, Y. (2016). Ultrasensitive Microfluidic Analysis of Circulating Exosomes Using a Nanostructured Graphene Oxide/polydopamine Coating. *Lab. Chip* 16, 3033–3042. doi:10.1039/c6lc00279j

Zhang, P., Zhou, X., He, M., Shang, Y., Tetlow, A. L., Godwin, A. K., et al. (2019). Ultrasensitive Detection of Circulating Exosomes with a 3D-Nanopatterned Microfluidic Chip. *Nat. Biomed. Eng.* 3, 438–451. doi:10.1038/s41551-019-0356-9

Zhao, L., Luo, H., Li, X., Li, T., He, J., Qi, Q., et al. (2017). Exosomes Derived from Human Pulmonary Artery Endothelial Cells Shift the Balance between Proliferation and Apoptosis of Smooth Muscle Cells. *Cardiol* 137, 43–53. doi:10.1159/000453544

Zhao, Z., Yang, Y., Zeng, Y., and He, M. (2016). A Microfluidic ExoSearch Chip for Multiplexed Exosome Detection towards Blood-Based Ovarian Cancer Diagnosis. *Lab. Chip* 16, 489–496. doi:10.1039/c5lc01117e

Zhou, S., Hu, T., Zhang, F., Tang, D., Li, D., Cao, J., et al. (2020). Integrated Microfluidic Device for Accurate Extracellular Vesicle Quantification and Protein Markers Analysis Directly from Human Whole Blood. *Anal. Chem.* 92, 1574–1581. doi:10.1021/acs.analchem.9b04852

Zitvogel, L., Regnault, A., Lozier, A., Wolfers, J., Flament, C., Tenza, D., et al. (1998). Eradication of Established Murine Tumors Using a Novel Cell-free Vaccine: Dendritic Cell-Derived Exosomes. *Nat. Med.* 4, 594–600. doi:10.1038/nm0598-594

Conflict of Interest: The authors declare that the research was conducted in the absence of any commercial or financial relationships that could be construed as a potential conflict of interest.

Publisher's Note: All claims expressed in this article are solely those of the authors and do not necessarily represent those of their affiliated organizations, or those of the publisher, the editors and the reviewers. Any product that may be evaluated in this article, or claim that may be made by its manufacturer, is not guaranteed or endorsed by the publisher.

Advantages of publishing in Frontiers

OPEN ACCESS
Articles are free to read for greatest visibility and readership

FAST PUBLICATION
Around 90 days from submission to decision

HIGH QUALITY PEER-REVIEW
Rigorous, collaborative, and constructive peer-review

TRANSPARENT PEER-REVIEW
Editors and reviewers acknowledged by name on published articles

Frontiers
Avenue du Tribunal-Fédéral 34
1005 Lausanne | Switzerland

Visit us: www.frontiersin.org
Contact us: frontiersin.org/about/contact

REPRODUCIBILITY OF RESEARCH
Support open data and methods to enhance research reproducibility

DIGITAL PUBLISHING
Articles designed for optimal readership across devices

FOLLOW US
@frontiersin

IMPACT METRICS
Advanced article metrics track visibility across digital media

EXTENSIVE PROMOTION
Marketing and promotion of impactful research

LOOP RESEARCH NETWORK
Our network increases your article's readership